PEOPLE'S DEMOCRATIC REPUBLIC OF ALGERIA
MINISTRY OF HIGHER EDUCATION AND SCIENTIFIC RESEARCH

ABOU-BEKR BELKAID UNIVERSITY – TLEMCEN

THESIS

Presented at:

FACULTY OF SCIENCES – DEPARTMENT DE CHEMISTRY

For the award of the degree of:

LMD DOCTORATE

Specialty: Physical chemistry

By:

Mrs. Djazia BELHADJ

Topic

Thermodynamic and thermophysical properties of chemicals of industrial and environmental interest Measurement and modeling

---

Defended publicly on April 20th, 2024 before the jury composed of:

Pr. Amina NEGADI	University of Tlemcen	President
Pr. Latifa NEGADI	University of Tlemcen	Supervisor
Pr. Indra BAHADUR	University of North-West Afrique du Sud	Examiner
Pr. Zahia ZIZI	University of Sidi Belabbes	Examiner
Pr. Abdelhak BOUSSAID	University of Tlemcen	Examiner

Laboratory of Applied Thermodynamics and Molecular Modeling

PEOPLE'S DEMOCRATIC REPUBLIC OF ALGERIA
MINISTRY OF HIGHER EDUCATION AND SCIENTIFIC RESEARCH

ABOU-BEKR BELKAID UNIVERSITY – TLEMCEN

THESIS

Presented at:

FACULTY OF SCIENCES – DEPARTMENT DE CHEMISTRY

For the award of the degree of:

LMD DOCTORATE

Specialty: Physical chemistry

By:

Mrs. Djazia BELHADJ

Topic

Thermodynamic and thermophysical properties of chemicals of industrial and environmental interest Measurement and modeling

---

Defended publicly on April 20th, 2024 before the jury composed of:

Pr. Amina NEGADI	University of Tlemcen	President
Pr. Latifa NEGADI	University of Tlemcen	Supervisor
Pr. Indra BAHADUR	University of North-West Afrique du Sud	Examiner
Pr. Zahia ZIZI	University of Sidi Belabbes	Examiner
Pr. Abdelhak BOUSSAID	University of Tlemcen	Examiner

Laboratory of Applied Thermodynamics and Molecular Modeling

Acknowledgement

First and foremost, I would like to thank the Almighty God for His grace throughout my academic journey to this extent, and for the successful completion of this doctoral study.

I would like to express my gratitude and warmest thanks to my supervisor, Professor Latifa NEGADI for her invaluable support, encouragement, and guidance at every stage of this work. Her effort in the provision of equipment and materials, organizing the meetings to give directions as well as her presence at every progress, detailed review of manuscript and valuable contributions is much appreciated. It has been a great pleasure to have her as my supervisor.

I gratefully acknowledge and thank the President of the jury Pr. Amina NEGADI and I also would like to extend my sincere gratitude and appreciation to the members of the jury Pr. Indra BAHADUR and Pr. Zahia ZIZI as well as Pr. Abdelhak BOUSSAID.

I learned a lot about VLE measurement at Laboratoire des Multimatériaux et Interfaces of the University of Claude Bernard, Lyon 1. (France). My deepest thanks go to Dr. Ilham MOKBEL and Pr. Jacques JOSE for giving me this opportunity to not only learn from them but as well as for their assistance and guidance.

I wish to also express my sincere thanks to team members and my colleagues from the research laboratory of Thermodynamique Appliquée et Modélisation Moléculaire of the University of Abou Bekr Belkaid Tlemcen, especially Dr. Nouria BABA AHMED, Dr. Faiza OUAAR and Mrs Badra FEDDAL for their assistance.

Finally, special thanks to my family for their kind support. To my dear father, Abdelhalim BELHADJ (gone but not forgotten), your love and support for my education has made me this far in life. To my beloved mother, Mrs. Fatiha MAMMAD for her kind support and encouragement in all my academic endeavours. To all my siblings and aunts, for their moral support and encouragement throughout this journey. I say thank a big thank you to you all.

Table of contents

List of tables

List of figures

Acronyms

22MEE	2-(2-methoxyethoxy)ethanol
DMSO	Dimethyl sulfoxide
ρ	Density
u	Speed of sound
n_D	Refractive index
κ_s	Isentropic compressibility
L_f	Intermolecular free length
Z	Specific acoustic impedance
R_A	Relative association
r	Relaxation strength
R	Rao's molar sound function
CAS	Chemical Abstracts Service
κ_{jacob}	Jacobson's temperature-dependent constant
M	Molecular weight
V_m^E	Excess molar volume
σ	Standard deviation
VLE	Vapor-liquid equilibrium
P	Vapor pressure
p_i	Vapor pressure of pure component
T	Temperature
R	Ideal gas constant
f	Fugacity
ϕ	Fugacity coefficient
i	Component
x	Mole fraction in the liquid phase
y	Mole fraction in the vapor phase
γ	Liquid phase activity coefficient
V	Molar volume
G^E	Molar excess Gibbs functions
τ	Interaction parameter
G	Interaction parameter
α	The non-random parameter
z	Coordination number
Φ	Segment fraction
θ	Area fraction
SSQ	Sum of squared relative error

General introduction

The global energy sector is changing rapidly. Each year, the worldwide demand for primary energy rises by 1.3% to 2040 (Megía et al., 2021) with an increasing demand for energy services as a consequence of the global economic growth, the increase in the population, and advances in technology. In this sense, fossil fuels (oil, natural gas, and coal) have been widely used for energy production and are projected to remain the dominant energy source until at least 2050 (Megía et al., 2021). Apart from the economic matters, the widespread use of fossil fuels is responsible for a long-term environmental problem. Energy production, conversion, and utilization results in the emission of greenhouse gases, such as carbon dioxide, nitrogen oxides, and other volatile compounds, and solid particles into the atmosphere, contributing to global climate change and global warming (Kulik, 2020). Globally, the largest source of greenhouse gases emissions is carbon dioxide (CO_2) from the combustion of fossil fuels. Total world CO_2 emissions from the consumption of petroleum, naturel gas, and coal, and the flaring of naturel gas increased from 5.892 million metric tons of carbon equivalent in 1992 to 6.568 million metric tons in 2001 (Balat, 2007). In addition, petroleum derived plastics also contribute to environmental issues particularly in aquatic life because of their duration more than hundreds years in the nature. On the other hand, there are limited sources of fossil-based fuels as a sustainable energy since they have a regeneration cycle time less than their usage ratio, which makes them non-renewable resources (Alma, 2013).

For all of these reasons, and the need to minimize environmental impact caused by the use of fossil energy and also the depletion of their reserves have increased the need for renewable energy sources. Countries have to determine a rational policy that requires the use of new and renewable own energy and eco-friendly fuel and material technologies that would meet the basic principles of green chemistry, as defined by (Anastas and Warner, 2000). For the sustainable production of green energy, biofuels for transportation, electricity, heat and various chemicals and materials, biomass is the most attractive source among the alternative resources with huge potentials. Economic, abundance, easy accessibility, carbon neutrality, eco-friendly features of biomass make it a good alternative to solve the problems of fossil energy and their products (Alma, 2013).

Biomass is the name given to all the earth's living matter (Garg et al., 1998). It is a general term for material derived from growing plants or from animal manure. Biomass is the term used to describe all biological produced matter. This includes wood and woody wastes, agricultural crops and their waste byproducts, municipal solid waste, animal wastes, waste from food processing, and aquatic plants and algae (Demirbas, 2004). Biomass consists of complex polymers of carbon (C), hydrogen (H) and oxygen (O), also significant amounts of trace elements can be found in some types of biomass. According to origin, function and final products, biomass is classified in two ways: categorization based on types of biomass existing in nature and categorization based on the use and application of biomass as feedstock. The former is the most used classification splitting biomass into different groups: wood and woody biomass, herbaceous biomass, aquatic biomass, animal and human waste biomass and biomass mixtures (Tursi, 2019).

The composition of biomass is largely diverse, it contains varying amounts of cellulose, hemicellulose, lignin and small amounts of lipids, proteins, simple sugars and starches. Biomass also contains inorganic constituents and a fraction of water. Among these compounds, cellulose, hemicellulose, and lignin are the three main constituents. The combination of cellulose, hemicelluloses, and ligninis are called lignocellulose, which comprises around half of the plant matter produced by photosynthesis and represents the most abundant renewable organic resource on earth (Saidur, 2011).

In the present work, we focus more specifically on lignocellulosic biomass from agricultural or forestry origin. The composition of lignocellulose biomass highly depends on its source. There is a significant variation of the cellulose, hemicellulose and lignin content of lignocellulose depending on whether it is derived from hardwood or softwood. Generally, the contents of cellulose, hemicellulose, and lignin are between 30.42 to 49.85 %, 18.00 to 35.00 %, and 7.00 to 36.02 %, respectively, for the agricultural residues. The contents of cellulose, hemicellulose, and lignin are generally between 23.70 to 59.70 %, 13.00 to 39.00 %, and 18.10 to 34.00 %, respectively, for the forest residues (Ruan, 2019). Lignocellulose biomass can be converted into energy through treatment and conversion processes, the processes involved are commonly classified as follows (Tursi, 2019):

Thermo-chemical conversion: in thermo-chemical conversion processes, energy is produced by applying heat and chemical processes. There are four thermo-chemical conversion processes: combustion, pyrolysis, gasification, and liquefaction.

Biochemical conversion: biochemical conversion processes allow the decomposition of biomass to available carbohydrates, which could be converted into liquid fuels and biogas, as well as different types of bio-products, using biological agents such as bacteria, enzymes. The most used biochemical technologies include anaerobic digestion and fermentation.

Physico-chemical conversion: the physico-chemical conversion processes of biomass lead to the production of high-density biofuels. More specifically, various types of vegetable oil ad animal fats are converted into biodiesel through esterification and/or transesterification processes.

Lignocellulosic biomasses are considered as prospective resources for biofuels not only because they are available on a renewable basis but also, they have no net increase in CO_2 release into the atmosphere. Consequently, biofuels are regarded as carbon neutral and basically free from detrimental compounds such as sulphur and aromatics (Nanda, 2014). On the other hand, Biofuels can be used in pure form or blended with gasoline (Demirbas, 2004). Biofuels have been classified by some researchers into three groups depending on the feedstock sources and generation technologies: the first-generation biofuels are derived from edible feedstocks like wheat, palm, corn, maize, soybean, sugarcane, rapeseed, oil crops, sugar beet, etc. Lignocellulosic feedstocks are included in the second-generation biofuels. The third-generation biofuels are mainly derived from algae feedstocks (Ruan, 2019).

The present work is part of our general program of research concerning the thermophysical and thermodynamic properties of binary mixtures containing molecules of industrial and environmental interest carried out in the research Laboratory of Thermodyamique Appliquée et Modélisation Moléculaire (LATA2M) of the University of Abou Bekr Belkaid Tlemcen.

This dissertation reports the results obtained from the study of volumetric, acoustic and optical properties of binary mixtures containing 2-(2-methoxyethoxy)ethanol (22MEE) , furfural and 1-hexene with alcohols (methanol, ethanol, propan-1-ol, propan-2-ol, butan-1-ol and butan-2-ol), dimethyl sulfoxide (DMSO), acetonitrile, sulfolane and alkoxyethanols (2-methoxyethanol, 2-ethoxyethanol and 2-butoxyethanol) and also the study of vapor-liquid equilibrium of three binary systems composed of N,N-dimethylacetamide with 1,3,5-trimethylbenzene or propan-2-ol or DMSO.

Alkoxyethanols (glycol ethers) are very interesting class of molecules from a practical point of view, as oxygenated compounds are increasingly used as additives to gasoline owing to their octane enhancing and pollution-reducing properties as well as in various applications in petroleum, cosmetics, textile, pharmaceutical, and the other industries (Belhadj et al., 2020; Zéberg-Mikkelsen et al., 2006; Csikos, 1976). The addition of the oxygenated compounds to diesel fuel improves diesel fuel combustion in engines, which would reduce pollutant emissions (CO, NOx, unburned hydrocarbons and smoke) and increase engine efficiency. Some authors assigned the decrease of particulate emissions to the blend oxygen percentage (Gómez-Cuenca, 2011). Several researchers studied blends of some glycol ethers with diesel fuel, a decrease in CO, hydrocarbons or particulate mater emissions being found. Moreover, these results showed that oxygen addition by glycol ether addition was more effective than oxygen addition by alcohols. (Gómez-Cuenca, 2011). Alkoxyethanols are also of great importance in view of the presence of the (−O− and −OH groups) in the same molecule, which allow self-association via both inter and intra molecular hydrogen bonds. The long hydrocarbon chain present in alkoxyethanols resists solubility in water, while ether or alcohol groups promoted hydrophilic solubility. This type of structure provides the ability to couple the unlike phase as well as the compatibility between water and the number of organic solvents (Belhadj et al., 2020; Barbés et al., 1994; Buckley et al., 1972).

2-(2-methoxyethoxy)ethanol has been selected as alkoxyethanols for thermophysical and thermodynamic study with six alcohols (methanol, ethanol, propan-1-ol, propan-2-ol, butan-1-ol and butan-2-ol) and this within the cooperation between LATA2M and University of Burgos in Spain. Densities of binary mixture containing {ethyl tert-butyl ether + 2-(2-methoxyethoxy)ethanol} have been measured by (Kinart et al., 2005) at (293.15, 298.15, 303.15, 308.15, and 313.15) K. Also, (Douhéret et al., 1995) have measured densities and speed of sound of aqueous mixture of 2-(2-methoxyethoxy)ethanol at 298.15 K. Excess molar enthalpies and excess molar volumes have been also reported by (Kim and Kim, 2006) for binary mixture {1,2-dichloropropane + 2-(2-methoxyethoxy)ethanol} at 298.15 K. Excess molar volumes and viscosities have been also measured by (Pal and Kumar 2001) at atmospheric pressure and 298.15 K for binary mixture {2-(2-methoxyethoxy)ethanol + pyrrolidin-2-one}. Additionally, (Mozo et al., 2007) have measured densities and speed of sound of {2-(2-methoxyethoxy)ethanol + butan-1-ol} at (293.15, 298.15 and 303.15) K and atmospheric pressure. More recently, (Lifi et al., 2020) have measured excess molar enthalpy at atmospheric pressure and temperatures of (298.15 and 313.15) K for {2-(2-methoxyethoxy)ethanol + 1-hexene} and {2-(2-methoxyethoxy)ethanol + cyclohexane.

Furfural is produced from hemicellulose contained in the structural components of plants. Its exceptional physical properties make it a selective extractant for removing aromatics from lubricating oils and diesel fuels (Hoydonckx, 2000).
Furfural is employed as the raw material for the synthesis of other chemicals (Schay, 2010). Furfural is an intermediate product in the manufacture and production of furan resins which among other uses finds application as a binding agent in foundry technologies. Furfural also finds use in the production of specialist adhesives, plastics, nylons, flavourants, pesticides and paints. Furfural is also used as a butadiene extractant and a refining solvent in the manufacture of synthetic rubber. Furfural's usefulness also lies in its physical strength and corrosion resistance (Schay, 2010). Reference has also been made to its use in cigar manufacture, perfume and even as a food preservative (Schay, 2010).
Despite the great range of application of furfural, its thermophysical and thermodynamic properties and especially its mixtures are not enough studied. Densities and speed of sounds of (furfural + ethanol or butan-1-ol or butan-2-ol) have been measured by (Bendiaf et al., 2015) at (283.15, 293.15, 303.15, and 313.15) K. (Naorem and Suri, 1988) have determined densities and speed of sounds of (furfural + benzene or toluene or ethylbenzene or o-xylene or m-xylene or p-xylene) at 308.15 K. Also, densities and speed of sounds of (furfural + toluene) were measured by (Zaoui-Djelloul-Daouadji et al., 2015) in the temperature range (283.15 K to 313.15) K. Additionally, excess thermodynamic properties of furfural and alkyl esters have been studied by (Rajalakshmi et al., 2019) at (303.15, 308.15, 313.15 and 318.15) K. Furthermore, the isothermal vapor-liquid equilibrium data were measured by (Tai et al., 2014) for (furan + furfural) at (353.2, 373.2 and 408.2) K. Also, the isobaric vapor-liquid equilibrium data for binary systems (furfural + 2-acetylfuran or 5-methylfurfural) were experimentally measured at 3.60 and 5.18 kPa by (Zheng et al., 2018). Vapor-liquid equilibrium data were also measured by (Cabezas et al., 1991) at 760 mmHg for binary systems (furfural + dichloromethane or 1,2-dichloroethane or trichloroethylene or tetrachloroethylene). In addition, (Bendiaf et al., 2014) were measured the isothermal vapor-liquid equilibrium data for binary system (furfural + toluene) at temperatures between (283.15 to 343.15) K. More recently, (Simić et al., 2021) have presented data on density, speed of sound and refractive index in the temperature range (288.15 to 345.15) K for the binary system (furfural + furfuryl alcohol).

1-hexene is one of short-chain olefins readily available from biomass sources. It can be derived from bioethanol by dehydration to ethylene followed by selective trimerization (Morris et al., 2019). 1-hexene is a compelling sustainable alkene for biofuel development which can be converted into synthetic paraffinic kerosene by catalytic routes (Morris et al., 2019). 1-hexene properties and characteristics make it a renewable C_6 platform for fuel synthesis. With a boiling point of 63 °C, 1-hexene can be stored and transported in a similar condition to gasoline. 1-hexene is also used with ethylene for the generation of linear low-density polyethylene (Harvey et al., 2014). Additionally, 1-hexene has a variety of applications including the generation of plasticizers, surfactants, detergents, and lubricants (Agapie, 2011).
Once 1-hexene has many applications, investigation of its properties in different mixtures is important. Excess enthalpy, density, speed of sound, and refractive index for {2-(2-ethoxyethoxy)ethanol + 1-hexene} have been determined by (Lifi et al., 2021) at 0.1 MPa

and (298.15 and 313.15) K. (Vega-Maza et al., 2013) were measured the isobaric heat capacities and densities for the binary mixtures (ethanol + 1-hexane) and (cyclohexane + 1-hexene) over the range (250 to 400) K and (0 to 20) MPa. Also, excess molar enthalpies have been reported by (Wang et al., 2004) for the four binary systems formed by (1-hexene + cyclohexane or methylcyclohexane or benzene or toluene) at 298.15 K. In addition, excess molar enthalpies at 298.15 K are reported for (1-hexene + 2-methyltetrahydrofuran or methyl tert-butyl ether or di-isopropyl ether or di-n-butyl ether) by (Wang et al., 2004). Densities and refractive indices were also measured by (Tojo and Diaz, 1995) at 298.15 K for binary mixtures of (1-hexene + o-xylene or m-xylene or p-xylene or ethylbenzene). Furthermore, isobaric vapor-liquid equilibrium data were determined by (Marrufo et al., 2009) for the binary systems (1-hexene + n-hexane or cyclohexane or cyclohexene) at 30, 60 and 101.3 kPa. Experimental data of vapor-liquid equilibria and excess enthalpies were also reported for binary systems (1-pentanol + 1-hexene) and (2-pentanol + 1-hexene) by (Moreau et al., 2018) *at* 313.15 K. Additionally, vapor pressures of (propyl ethanoate + 1-hexene) were measured by (Negadi et al., 2007) at temperatures between 263 and 363 K. (Gmehling, 1983) have also studied isothermal vapor-liquid equilibrium of binary mixtures (methyl acetate + 1-hexene) at 50 K and (1-hexene + ethyl acetate) at 60 K.

Alkylamides are a group of bioactive compounds that can be obtained from different plant families (Elufioye et al., 2020; Zaitseva et al., 2019). Interest in alkylamides as a class of compound has grown tremendously in recent years. This interest is due to the many presumed benefits in food, pesticides, batteries, polymer fibers, cosmetics, and medicine (Elufioye et al., 2020). Many articles have been published on alkylamides, these publications date back to 1952.

(Aihara, 1952) has reported vapor pressure of acetamide and N-methylacetamide. Vapor pressures of some mono and di-alkyl substituted aliphatic amides at different temperatures have been studied by (Gopal et al., 1968). Vapor Pressure of 3-Methoxypropylamine and Six Substituted Amides have been measured by (Vasil'eva et al., 1983). Also, isobaric vapor-liquid equilibrium data of cyclohexanone + N-methylacetamide system have been reported by (Aucejo et al., 1993) at 6.66, 13.33, and 26.66 kPa. Furthermore, vapor-liquid equilibrium of binary systems containing monosubstituted amides and hydrocarbons was measured in the temperature range from 363 to 423 K by (Schmelzer et al., 1995). Additionally, (Zaitseva et al., 2019) have determined vapor pressures and enthalpies of vaporization of N-methylacetamide, N-ethylacetamide, N-n-propylacetamide and N-tert-butylacetamide at temperature of 298.15 K.

In order to extend the database of this family of molecules and provide new reliable thermodynamic properties of industrial solvents, N,N-dimethylacetamide (DMA) has been selected as one of the methylated derivatives of acetamide for a thermodynamic study in different binary mixtures and this within the framework of the Tassili Project (21 MDU 318). N,N-dimethylacetamide is a commodity chemical which is used in large quantities in many industries. Its high solubility in water and its excellent solvent power for high molecular weight polymers and resins make DMA a desirable solvent in fiber and polyurethane production. It is also a good reaction medium for the production of pharmaceuticals and cosmetics (Dinçer et al., 2010). At the same time the structure of N,N-dimethylacetamide

make it less volatile than many common organic solvents despite its low molar masses and enable more effective recuperation within industrial processes (Zaitseva et al., 2019).
From a literature search, isothermal vapor-liquid equilibrium of binary mixtures formed by N,N-dimethylacetamide with 1-chlorobutane or 1-chlorohexane or 1-chlorooctane have been reported by (Garcia-Gimenez et al., 2007) at 313.15, 323.15 and 333.15 K. (Gill et al., 2009) have measured the isobaric vapor-liquid equilibrium of N,N-dimethylacetamide with cumene at 97.3 kPa. Also, isobaric vapor-liquid equilibrium of 2-isopropoxypropane with N,N-dimethylacetamide and 2-propanol with N,N-dimethylacetamide have been determined by (Zhang et al., 2013) at 101.3 kPa. In addition, (Mi et al., 2015) have presented the vapor-liquid equilibrium of N,N-dimethylacetamide with cyclohexene or cyclohexane or benzene at atmospheric pressure. Furthermore, the isobaric vapor-liquid equilibrium of acetic acid with N,N-dimethylacetamide has been reported by (Lin et al., 2016) at 7 and 12 kPa. Then, (Zehioua et al., 2016) have studied the vapor-liquid equilibrium of 1,1,1,2-tetrafluoroethane with N,N-dimethylacetamide at temperatures varying between 303 and 353 K. Additionally, vapor-liquid equilibrium of binary mixtures containing 1-butanol or Methyl isobutyl ketone with N,N-dimethylacetamide have been also measured by (Wang et al., 2019) at 101.3 kPa. The most recent study of vapor pressures of N,N-dimethylacetamide has been reported by (Štejfa et al., 2020) over a wide temperature range.

There is a huge amount of available data for pure compounds, but the thermophysical and thermodynamic properties of binary mixtures are different from those of pure compounds. There is scarce or no data available in the literature for the selected binary mixtures. The study of thermophysical and thermodynamic properties of binary liquid mixtures can be contributed to clarification of the various intermolecular interactions existing between the different species found in solution. Obviously, the reliable knowledge of these properties of pure compounds and mixtures is of great importance in many fields of research as well as in industrial practice. Studying the concentration and temperature dependence of thermophysical and thermodynamics properties contributes to our understanding of intermolecular interactions in liquids, liquid mixtures and solutions. Intermolecular interactions in binary mixtures modify the structural arrangements which lead to change the shape of the molecule. The investigation of molecular interactions is therefore crucial in elucidation of the structural changes in the mixtures (Belhadj et al., 2021). Also, reliable experimental data is necessary to develop physical models, and industrial design development process. The main step in the design of any production plant is the processes simulation. The reliability of simulation process depends mainly on the thermodynamic models used to describe the physical behavior of the molecules implicated (Reddy et al., 2012).

This dissertation is divided into two (02) chapters in order to describe the work developed through the research with main introduction, and conclusion.

Chapter 1 presents the collected experimental data of density, speed of sound and refractive index of pure chemicals and binary mixtures:

- 2-(2-methoxyethoxy)ethanol (1) + Methanol (2)
- 2-(2-methoxyethoxy)ethanol (1) + Ethanol (2)

- 2-(2-methoxyethoxy)ethanol (1) + Propan-1-ol (2)
- 2-(2-methoxyethoxy)ethanol (1) + Propan-2-ol (2)
- 2-(2-methoxyethoxy)ethanol (1) + Butan-1-ol (2)
- 2-(2-methoxyethoxy)ethanol (1) + Butan-2-ol (2)
- Furfural (1) + DMSO (2)
- Furfural (1) + Acetonitrile (2)
- Furfural (1) + Sulfolane (2)
- 1-Hexene (1) + 2-Methoxyethanol (2)
- 1-Hexene (1) + 2-Ethoxyethanol (2)
- 1-Hexene (1) + 2-Butoxyethanol (2)

The experimental data have been used to determine various excess/derived properties at different temperatures and over the whole composition range. Excess properties were fitted to the Redlich−Kister polynomial equation. Apparatus and procedure used for the measurements of density, speed of sound and refractive index have been also described in this chapter.

Chapter 2 contains vapor-liquid equilibrium (VLE) data of N,N-dimethylacetamide with 1,3,5-trimethylbenzene or propan-2-ol or DMSO measured using a static apparatus. Barker's method has been used to evaluate the excess Gibbs function G^E, the vapor phase composition y_i and the activity coefficients γ_1 and γ_2. Additionally, the experimental data were correlated by using NRTL, UNIQUAC and Modified UNIFAC (Dortmund) models.

References

Megía, P. J., Vizcaíno, A. J., Calles, J. A., & Carrero, A. (2021). Hydrogen production technologies: from fossil fuels toward renewable sources. A mini review. Energy & Fuels, 35(20), 16403-16415.

Kulik, A. C. (2020). Experimental study of thermodynamic properties of liquid mixtures with interest as biofuels: binary systems: 2-Propanol, DIPE and 1 Hexene (Doctoral dissertation).

Balat, M. (2007). Status of fossil energy resources: A global perspective. Energy Sources, Part B: Economics, Planning, and Policy, 2(1), 31-47.

Alma, M. H., & Karaoğul, T. S. A. (2013, June). Liquefaction Processes of Biomass for the Production of Valuable Chemicals and Biofuels: A Review. In FPS 67th International Convention and SWST 56th International Convention, Texas, USA.

Anastas, P. T., & Warner, J. C. (2000). Tools of green chemistry. Green Chemistry: Theory and Practice; Oxford University Press: New York, NY, USA.

Demirbas, A. (2004). The importance of biomass. Energy sources, 26(4), 361-366.

Garg, H. P., & Datta, G. (1998, May). Global status on renewable energy. In Solar energy heating and cooling methods in building, international workshop: Iran University of Science and Technology (pp. 19-20).

Tursi, A. (2019). A review on biomass: importance, chemistry, classification, and conversion. Biofuel Research Journal, 6(2), 962.

Saidur, R., Abdelaziz, E. A., Demirbas, A., Hossain, M. S., & Mekhilef, S. (2011). A review on biomass as a fuel for boilers. Renewable and sustainable energy reviews, 15(5), 2262-2289.

Ruan, R., Zhang, Y., Chen, P., Liu, S., Fan, L., Zhou, N., ... & Li, B. (2019). Biofuels: introduction. In Biofuels: Alternative feedstocks and conversion processes for the production of liquid and gaseous biofuels (pp. 3-43). Academic Press.

Nanda, S., Mohammad, J., Reddy, S. N., Kozinski, J. A., & Dalai, A. K. (2014). Pathways of lignocellulosic biomass conversion to renewable fuels. Biomass Conversion and Biorefinery, 4, 157-191.

Belhadj, D., Bahadur, I., Negadi, A., Muñoz-Rujas, N., Montero, E., & Negadi, L. (2020). Thermodynamic, Ultrasonic, and Transport Study of Binary Mixtures Containing 2-(2-Methoxyethoxy) ethanol and Alcohols at (293.15–323.15) K. Journal of Chemical & Engineering Data, 65(11), 5192-5209.

Zéberg-Mikkelsen, C. K., Lugo, L., García, J., & Fernández, J. (2006). " Volumetric properties under pressure for the binary system ethanol plus toluene"(vol 235, pg 139, 2005). Fluid Phase Equilibria, 240(2), 229-229.

Csikos, R. (1976). Low-Lead Fuel with MTBE and C4 Alcohols.

Gómez-Cuenca, F., Gómez-Marín, M., & Folgueras-Díaz, M. B. (2011). Effects of ethylene glycol ethers on diesel fuel properties and emissions in a diesel engine. Energy conversion and management, 52(8-9), 3027-3033.

Barbés, B., García, I., González, J. A., Cobos, J. C., & Casanova, C. (1994). Excess properties of (an n-alkoxyethanol+ an organic solvent) VI. VEm {xCH3 (CH2) v-1O (CH2) 2O (CH2) 2OH+(1-x) C6H5CH3} for v= 1, 2, and 4 at the temperature 298.15 K. The Journal of Chemical Thermodynamics, 26(8), 791-795.

Buckley, P., & Brochu, M. (1972). Microwave Spectrum, Dipole Moment, and Intramolecular Hydrogen Bond of 2-Methoxyethanol. Canadian Journal of Chemistry, 50(8), 1149-1156.

Kinart, C. M., Nowak, K., & Kinart, W. J. (2005). Volumetric properties of binary mixtures of alkoxyethanols with ethyl tert-butyl ether at various temperatures. The Journal of Chemical Thermodynamics, 37(5), 423-429.

Douhéret, G., Lajoie, P., Davis, M. I., Ratliff, J. L., Ulloa, J., & Høiland, H. (1995). Volumetric properties of binary mixtures of water with methoxy (ethoxy) n ethanols. Journal of the Chemical Society, Faraday Transactions, 91(15), 2291-2298.

Kim, J., & Kim, M. (2006). Excess Molar Enthalpies and Excess Molar Volumes for the Binary Mixtures {1, 2-dichloropropane+ 2-(2-methoxyethoxy) ethanol, and+ 2-(2-ethoxyethoxy) ethanol} at 298.15 K. Korean Chemical Engineering Research, 44(5), 444-452.

Pal, A., & Kumar, H. (2001). Excess molar volumes and viscosities of binary mixtures of some n-alkoxyethanols with pyrrolidin-2-one at 298.15 K. Journal of molecular liquids, 94(2), 163-177.

Mozo, I., García de la Fuente, I., González, J. A., & Cobos, J. C. (2007). Thermodynamics of mixtures containing alkoxyethanols. XXIV. Densities, excess molar volumes, and speeds of sound at (293.15, 298.15, and 303.15) K and isothermal compressibilities at 298.15 K for 2-(2-alkoxyethoxy) ethanol+ 1-butanol systems. Journal of Chemical & Engineering Data, 52(5), 2086-2090.

Lifi, M., Muñoz-Rujas, N., Montero, E. A., Negadi, L., Aguilar, F., & Alaoui, F. E. M. H. (2020). Excess molar enthalpy measurement and modelling of (oxygenated compounds+ hydrocarbon) mixtures: Binary and ternary mixtures containing 2-(2-methoxyethoxy) ethanol, 1-hexene and cyclohexane at (298.15 and 313.15) K. The Journal of Chemical Thermodynamics, 149, 106171.

Hoydonckx, H. E., Van Rhijn, W. M., Van Rhijn, W., De Vos, D. E., & Jacobs, P. A. (2000). Furfural and derivatives. Ullmann's encyclopedia of industrial chemistry.

Schay, S. R. (2010). The production of furfural from sunflower husks using the s-suprayield process (Doctoral dissertation).

Bendiaf, L., Bahadur, I., Negadi, A., Naidoo, P., Ramjugernath, D., & Negadi, L. (2015). Effects of alkyl group and temperature on the interactions between furfural and alcohol: Insight from density and sound velocity studies. Thermochimica acta, 599, 13-22.

Naorem, H., & Suri, S. K. (1988). Excess molar volumes, speeds of sound, and isentropic compressibilities of binary mixtures of furfural with some aromatic hydrocarbons. Canadian journal of chemistry, 66(5), 1295-1298.

Zaoui-Djelloul-Daouadji, M., Bendiaf, L., Bahadur, I., Negadi, A., Ramjugernath, D., Ebenso, E. E., & Negadi, L. (2015). Volumetric and acoustic properties of binary systems (furfural or furfuryl alcohol+ toluene) and (furfuryl alcohol+ ethanol) at different temperatures. Thermochimica Acta, 611, 47-55.

Rajalakshmi, R., Ravikumar, S., Sivakumar, K., & Pandiyan, V. (2019). Excess thermodynamic properties of intermolecular interactions in binary liquid mixtures of furfural with alkyl acetates (C1-C5) at different temperatures. Chemical Data Collections, 24, 100299.

Tai, W. P., Lee, H. Y., & Lee, M. J. (2014). Isothermal vapor–liquid equilibrium for binary mixtures containing furfural and its derivatives. Fluid Phase Equilibria, 384, 134-142.

Zheng, H., Luo, X., Yin, G., Chen, J., & Zhao, S. (2018). Vapor pressure and isobaric vapor–liquid equilibrium for binary systems of furfural, 2-acetylfuran, and 5-methylfurfural at 3.60 and 5.18 kPa. Journal of Chemical & Engineering Data, 63(1), 49-56.

Cabezas, J. L., Beltrán, S., & Coca, J. (1991). Isobaric vapor—liquid equilibrium data for furfural with chlorinated hydrocarbons. Fluid phase equilibria, 62(1-2), 163-172.

Bendiaf, L., Negadi, A., Mokbel, I., & Negadi, L. (2014). Isothermal vapor–liquid equilibria of binary systems containing green solvents derived from biomass:(Furfuryl alcohol+ toluene),(furfuryl alcohol+ ethanol), or (furfural+ toluene). Fuel, 122, 247-253.

Simić, Z. V., Kijevčanin, M. L., Radović, I. R., Grilc, M., & Ivaniš, G. R. (2021). Thermodynamic and transport properties of biomass-derived furfural, furfuryl alcohol and their mixtures. Energies, 14(22), 7769.

Morris, D. M., Quintana, R. L., & Harvey, B. G. (2019). High-performance jet fuels derived from bio-based alkenes by iron-catalyzed [2+ 2] cycloaddition. ChemSusChem, 12(8), 1646-1652.

Harvey, B. G., & Meylemans, H. A. (2014). 1-Hexene: a renewable C6 platform for full-performance jet and diesel fuels. Green Chemistry, 16(2), 770-776.

Agapie, T. (2011). Selective ethylene oligomerization: Recent advances in chromium catalysis and mechanistic investigations. Coordination Chemistry Reviews, 255(7-8), 861-880.

Lifi, M., Lorenzo, J., Aguilar, F., Muñoz-Rujas, N., Montero, E. A., Chhiti, Y., & Alaoui, F. E. M. H. (2021). Excess enthalpy, density, speed of sound and refractive index of binary mixtures {2-(2-ethoxyethoxy) ethanol+ 1-hexene, or cyclohexane, or methylcyclohexane at (298.15 and 313.15) K: Application of the PPR-78 cubic equation of state, NRTL and UNIQUAC models. The Journal of Chemical Thermodynamics, 153, 106306.

Vega-Maza, D., Martín, M. C., Trusler, J. M., & Segovia, J. J. (2013). Heat capacities and densities of the binary mixtures containing ethanol, cyclohexane or 1-hexene at high pressures. The Journal of Chemical Thermodynamics, 57, 550-557.

Wang, Z., Benson, G. C., & Lu, B. C. Y. (2004). Excess molar enthalpies of binary mixtures of 1-hexene with some cyclic and aromatic hydrocarbons at 298.15 K. Thermochimica acta, 414(1), 31-33.

Wang, Z., Benson, G. C., & Lu, B. C. Y. (2004). Excess enthalpies of binary mixtures of 1-hexene with some ethers at 25° C. Journal of solution chemistry, 33, 143-147.

Tojo, J., & Diaz, C. (1995). Densities and refractive-indexes for 1-hexene plus o-xylene, plus m-xylene, plus p-xylene, and plus ethylbenzene. Journal of Chemical and Engineering Data, 40(1), 96-98.

Marrufo, B., Aucejo, A., Sanchotello, M., & Loras, S. (2009). Isobaric vapor–liquid equilibrium for binary mixtures of 1-hexene+ n-hexane and cyclohexane+ cyclohexene at 30, 60 and 101.3 kPa. Fluid phase equilibria, 279(1), 11-16.

Moreau, A., Segovia, J. J., Bermejo, M. D., & Martín, M. C. (2018). Vapor-liquid equilibria and excess enthalpies of the binary systems 1-pentanol or 2-pentanol and 1-hexene or 1, 2, 4-trimethylbenzene for the development of biofuels. Fluid Phase Equilibria, 460, 85-94.

Negadi, L., Belabbaci, A., Ait Kaci, A., & Jose, J. (2007). Isothermal Vapor− Liquid Equilibria and Excess Enthalpies of (Propyl Ethanoate+ Heptane), (Propyl Ethanoate+ Cyclohexane), and (Propyl Ethanoate+ 1-Hexene). Journal of Chemical & Engineering Data, 52(1), 47-55.

Gmehling, J. (1983). Isothermal vapor-liquid equilibriums in binary systems formed by esters with alkenes. Journal of Chemical and Engineering Data, 28(1), 27-30.

Elufioye, T. O., Habtemariam, S., & Adejare, A. (2020). Chemistry and pharmacology of alkylamides from natural origin. Revista brasileira de farmacognosia, 30(5), 622-640.

Zaitseva, K. V., Varfolomeev, M. A., & Verevkin, S. P. (2019). Vapour pressures and enthalpies of vaporisation of N-alkyl acetamides. Journal of Molecular Liquids, 293, 111453.

Aihara, Studies on hydrogen bonding by measuring vapor pressure. I. Vapor pres-sure of acetamide andNmethylacetamide, J. Chem. Soc. Jpn. Pure Chem. Sect. 73(1952) 855–857.

Gopal. R, Rizvi. S.A, Vapour pressures of some mono- and di-alkyl substituted ali-phatic amides at different temperatures, J. Indian Chem. Soc. 45 (1968) 13–16.

Vasil'eva. T.F, Vapor pressure of 3 -methoxypropylamine and six substituted amides in Teplofiz Svoistva Uglevodororov Nefteprod, G.I. Cherednichenko, ed(s)., Ts NIIT Eneftekhim, Moscow, 1983, 85 -94

Aucejo. A, Monton. J.B, Munoz. R, Sanchotello. M, Isobaric vapor-liquid equilibriumdata for the cyclohexanone +Nmethylacetamide system, J. Chem. Eng. Data 38(1993) 160–162.

Schmelzer. J, Pusch. J, Phase equilibria in binary systems containingNmonosubstituted amides and hydrocarbons, Fluid Phase Equilib. 110 (1995)183–196

Dinçer, N. E., & Erkey, C. (2010). Measurement and thermodynamic modeling of partition coefficients in N, N-dimethylacetamide–water–carbon dioxide system. The Journal of Supercritical Fluids, 55(2), 690-695.

Garcia-Gimenez, P., Embid, J. M., Velasco, I., & Otin, S. (2007). (Vapour+ liquid) equilibria and excess molar enthalpies for binary mixtures containing N, N-dialkylamides and 1-chloroalkanes. The Journal of Chemical Thermodynamics, 39(9), 1264-1271.

Gill, B. K., Rattan, V. K., & Kapoor, S. (2009). Vapor− Liquid Equilibrium Data for N-Methylacetamide and N, N-Dimethylacetamide with Cumene at 97.3 kPa. Journal of Chemical & Engineering Data, 54(4), 1175-1178.

Zhang, Z., Yang, L., Xing, Y., & Li, W. (2013). Vapor–Liquid Equilibrium for Ternary and Binary Mixtures of 2-Isopropoxypropane, 2-Propanol, and N, N-Dimethylacetamide at 101.3 kPa. Journal of Chemical & Engineering Data, 58(2), 357-363.

Mi, W., Tong, R., Hua, C., Yue, K., Jia, D., Lu, P., & Bai, F. (2015). Vapor–liquid equilibrium data for binary systems of N, N-dimethylacetamide with cyclohexene, cyclohexane, and benzene separately at atmospheric pressure. Journal of Chemical & Engineering Data, 60(11), 3063-3068.

Lin, R., Cui, X., Yu, X., Zhang, Y., Feng, T., Li, X., ... & Jie, H. (2016). Isobaric vapor–liquid equilibrium of acetic acid+ N, N-dimethylacetamide+ 1-butyl-3-methylimidazolium Bis [(trifluoromethyl) sulfonyl]-imide. Fluid Phase Equilibria, 410, 1-8.

Zehioua, R., Coquelet, C., & Meniai, A. H. (2016). p–T–x Measurements for 1, 1, 1, 2-Tetrafluoroethane (R134a) + N, N-Dimethylacetamide (DMA) and N-Methyl-2-pyrrolidone (NMP). Journal of Chemical & Engineering Data, 61(2), 912-919.

Wang, Y., Zhang, H., Zhang, W., Liu, Y., Cui, P., Yang, J., ... & Xu, D. (2019). Vapor–liquid equilibrium for binary of 1-butanol+ n, n-dimethylacetamide and methyl isobutyl ketone+ n, n-dimethylacetamide at 101.3 kPa. Journal of Chemical & Engineering Data, 64(9), 4142-4147.

Štejfa, V., Chun, S., Pokorný, V., Fulem, M., & Růžička, K. (2020). Thermodynamic study of acetamides. Journal of Molecular Liquids, 319, 114019.

Belhadj, D., Negadi, A., Venkatesu, P., Bahadur, I., & Negadi, L. (2021). Density, speed of sound, refractive index and related derived/excess properties of binary mixtures (furfural+ dimethyl sulfoxide), (furfural+ acetonitrile) and (furfural+ sulfolane) at different temperatures. Journal of Molecular Liquids, 330, 115436.

Reddy, K. R., Kumar, D. B. K., Rao, G. S., Sri, P. S., & Rambabu, C. (2012). Vapor–liquid equilibria and excess molar volumes of N-methyl-2-pyrrolidone with 2-alkoxyethanols. Fluid phase equilibria, 336, 52-58.

Chapter 1: Volumetric, acoustic, and optical properties

1.1 Introduction

In this chapter the experimental densities (ρ), speeds of sound (u) and refractive indices (n_D) were determined for binary mixtures containing 2-(2-methoxyethoxy)ethanol, furfural and 1-hexene in different solvents. Density, speed of sound and refractive index have been reported at different temperatures and at pressure of 0.1 MPa using an Anton Paar DSA 5000M digital vibrating tube densimeter and a digital refractometer Abbemat 300.
The obtained data were used to calculate isentropic compressibility (κ_s), intermolecular free length (L_f), specific acoustic impedance (Z), relative association (R_A), relaxation strength (r) and Rao's molar sound function (R). The excess/deviation properties on mixing were also derived from values of measured properties for all studied mixtures under the same experimental conditions. Excess/deviation properties were fitted to the Redlich−Kister equation to estimate the coefficients. The standard deviation of the fit was calculated between the predicted and the experimental quantities to ensure the accuracy of the experimental data.

1.2 Chemicals

The chemicals used in this study were supplied by specialized companies, with a high purity. Table 1.1 summarizes the specifications of chemicals, including the chemical name, CAS number and the purities provided by their respective suppliers. Purity of chemicals has been verified in Table 1.2 by comparing measured values of density, speed of sound, and refractive index with reliable literature data, a good agreement was observed between both set of data.

Table 1.1: Purities, CAS #, Molar Mass, and Suppliers of Chemicals Used in This Study

Chemical name	Purity (as stated by the supplier)	CAS #	Molar mass/(g.mole^{-1})	Supplier
22MEE	≥ 0.99	111-77-3	120.15	TCI
Methanol	≥ 0.997	67-56-1	32.04	Sigma-Aldrich
Ethanol	≥ 0.998	64-17-5	46.07	Honeywell
Propan-1-ol	≥ 0.99	71-23-8	60.10	Sigma-Aldrich
Propan-2-ol	≥ 0.998	67-63-0	60.10	Sigma-Aldrich
Butan-1-ol	≥ 0.995	71-36-3	74.12	Biochem Chemopharma
Butan-2-ol	≥ 0.99	78-92-2	74.12	Sigma-Aldrich
Furfural	99.0	98-01-1	96.08	Sigma-Aldrich
DMSO	99.5	67-68-5	78.13	Sigma-Aldrich
Acetonitrile	99.9	75-05-8	41.05	Sigma-Aldrich
Sulfolane	99.0	126-33-0	120.17	Sigma-Aldrich
1-Hexene	97.0	592-41-6	84.16	Sigma-Aldrich
2-Methoxyethanol	≥ 0.995	109-86-4	76.09	Sigma-Aldrich
2-Ethoxyethanol	≥ 0.990	110-80-5	90.12	TCI
2-Butoxyethanol	≥ 0.990	111-76-2	118.18	TCI

Table 1.2: Comparison of experimental densities, ρ, speeds of sound, u, and refractive indices, n_D, of the pure components with the corresponding literature values at different temperatures and at pressure of 0.1 MPa.

Component	T/(K)	ρ / (g.cm^{-3})		u / (m.s^{-1})		n_D	
		Exp.	Lit.	Exp.	Lit.	Exp.	Lit.
22MEE	293.15	1.0196	1.019810 [1] 1.02080 [3]	1433.62	1432.37 [1]	1.4262	1.42632 [2] 1.42640 [4]
	298.15	1.0152	1.01501 [2] 1.0154 [6]	1416.05	1415.5 [5] 1415.98 [7]	1.4245	1.4245 [4] 1.4243 [8]
	303.15	1.0108	1.010908 [1] 1.01183 [3]	1398.97	1397.93 [1]	1.4225	-
	313.15	1.0019	1.00322 [3] 1.00260 [9]	1365.06	-	1.4187	-
	323.15	0.9929	-	1331.34	-	1.4148	-
Methanol	293.15	0.7916	0.791 [10] 0.7913 [12]	1120.60	1119.6 [10] 1119 [13]	1.3287	1.329 [11] 1.32843 [13]
	298.15	0.7869	0.787 [11] 0.7869 [14]	1103.99	1104 [11] 1102.81 [15]	1.3266	1.327 [11] 1.3266 [16]
	303.15	0.7822	0.782 [10] 0.78218 [17]	1087.55	1086.6 [10] 1086 [13]	1.3247	1.325 [11] 1.3247 [18]
	313.15	0.7726	0.772 [10] 0.77267 [17]	1055.13	1054.2 [10] 1054 [13]	1.3207	1.321 [11] 1.3207 [18]
	323.15	0.7630	0.763 [11] 0.76302 [17]	1023.02	1022 [11] 1024.00 [19]	1.3167	1.317 [11] 1.3165 [18]
Ethanol	293.15	0.7898	0.790 [10] 0.7894 [18]	1162.46	1162.3 [10] 1161.78 [19]	1.3615	1.361 [20] 1.3615 [18]
	298.15	0.7855	0.785 [20] 0.7854 [21]	1144.95	1144 [20] 1142 [13]	1.3595	1.359 [20] 1.3593 [18]
	303.15	0.7812	0.781 [10] 0.7815 [12]	1127.91	1128.2 [10] 1127.58 [19]	1.3575	1.357 [20] 1.3573 [18]
	313.15	0.7724	0.772 [10] 0.7722 [22]	1094.28	1094.5 [10] 1094.07 [19]	1.3535	1.353 [20] 1.3533 [18]
	323.15	0.7635	0.763 [20] 0.7635 [22]	1060.90	1060 [20] 1061.20 [19]	1.3493	1.349 [20] 1.3491 [18]
Propan-1-ol	293.15	0.8042	0.803756 [23] 0.80410 [24]	1225.30	1223.89 [23] 1223.22 [19]	1.3851	1.385100 [23] 1.3850 [18]

	298.15	0.8001	0.799748 [23] 0.7995 [18]	1208.03	1206.85 [23] 1206 [13]	1.3831	1.383110 [23] 1.38307 [13]
	303.15	0.7961	0.795709 [23] 0.79586 [24]	1190.90	1189.76 [23] 1189 [13]	1.3811	1.381120 [23] 1.3811 [24]
	313.15	0.7879	0.787518 [23] 0.7873 [13]	1157.04	1155.93 [23] 1155 [13]	1.3771	1.377060 [23] 1.3774 [18]
	323.15	0.7795	0.779137 [23] 0.7792 [25]	1123.41	1122.34 [23] 1121.00 [19]	1.3729	1.372930 [23] 1.3732 [18]
Propan-2-ol	293.15	0.7857	0.785296 [23] 0.7851 [25]	1159.32	1157.49 [23] 1156 [13]	1.3772	1.377100 [23] 1.37702 [13]
	298.15	0.7815	0.781090 [23] 0.7813 [26]	1141.33	1140.12 [23] 1139 [13]	1.3751	1.375020 [23] 1.37521 [13]
	303.15	0.7772	0.776811 [23] 0.7767 [25]	1123.71	1122.56 [23] 1122 [13]	1.3730	1.372900 [23] 1.37261 [13]
	313.15	0.7684	0.768011 [23] 0.7680 [22]	1088.43	1087.34 [23] 1086 [13]	1.3686	1.368580 [23] 1.36821 [13]
	323.15	0.7592	0.758829 [23] 0.7591 [25]	1052.76	1051.73 [23] -	1.3641	1.364080 [23] -
Butan-1-ol	293.15	0.8107	0.809937 [23] 0.81034 [24]	1260.37	1258.13 [23] 1257.66 [19]	1.3992	1.399250 [23] 1.3994 [24]
	298.15	0.8069	0.806119 [23] 0.8059 [13]	1243.32	1241.32 [23] 1241 [13]	1.3972	1.397260 [23] 1.3972 [24]
	303.15	0.8030	0.802272 [23] 0.803155 [27]	1226.42	1224.47 [23] 1224 [13]	1.3952	1.395280 [23] 1.39521 [13]
	313.15	0.7952	0.794474 [23] 0.7940 [18]	1192.97	1191.12 [23] 1190.28 [19]	1.3913	1.391330 [23] 1.39090 [13]
	323.15	0.7872	0.786505 [23] 0.7864 [28]	1159.74	1158.00 [23] 1157.19 [19]	1.3872	1.387270 [23] 1.3867 [18]
Butan-2-ol	293.15	0.8067	0.806 [29] 0.8067 [13]	1230.52	1230.1 [29] 1230 [13]	1.3973	1.397 [29] 1.39722 [13]
	298.15	0.8025	0.802 [29] 0.8024 [14]	1212.49	1212.1 [29] 1212 [13]	1.3952	1.395 [29] 1.3951 [14]
	303.15	0.7983	0.798 [29] 0.7984 [13]	1194.41	1194.1 [29] 1195 [13]	1.3930	1.393 [29] 1.39288 [13]
	313.15	0.7896	0.789 [29]	1157.98	1157.7 [29]	1.3886	1.389 [29]

			0.78956 [30]		1157.12 [30]		1.38818 [13]
	323.15	0.7805	0.780 [29] 0.78047 [30]	1120.98	1120.7 [29] 1120.16 [30]	1.3840	1.384 [29] -
Furfural	293.15	1.1600	1.15933 [31] 1.160128 [32]	1458.20	1458.8 [31] 1458.52 [32]	1.5264	1.526168 [32]
	298.15	1.1547	1.154805 [32]	1440.17	1440.19 [32]	1.5237	1.523577 [32]
	303.15	1.1493	1.14869 [31] 1.149478 [32]	1422.02	1422.5 [31] 1422.05 [32]	1.5212	1.520969 [32]
	313.15	1.1387	1.13801 [31] 1.138793 [32]	1386.01	1386.5 [31] 1385.97 [32]	1.5162	1.515740 [32]
	323.15	1.1279	1.128061 [32]	1350.29	1350.20 [32]	1.5111	1.510486 [32]
DMSO	293.15	1.1003	1.100 [33] 1.10073 [34]	1503.63	1504.7 [33]	1.4783	1.479 [33]
	298.15	1.0953	1.095 [35] 1.09574 [34]	1486.81	1486.8 [35]	1.4769	1.477 [35] 1.4768 [34]
	303.15	1.0903	1.090 [33] 1.09074 [34]	1469.88	1471.0 [33]	1.4749	1.475 [33] 1.4733 [34]
	313.15	1.0803	1.080 [33] 1.08075 [34]	1436.28	1437.4 [33]	1.4703	1.470 [33] 1.4694 [34]
	323.15	1.0702	1.070 [35] 1.07019 [36]	1403.00	1403.0 [35]	1.4661	1.466 [35] 1.4659 [36]
Acetonitrile	293.15	0.7820	0.782 [33] 0.7821 [25]	1299.20	1299.7 [33] 1299 [37]	1.3439	1.344 [33] 1.3436 [38]
	298.15	0.7766	0.7766 [25]	1279.40	1284 [37]	1.3415	1.3411 [38]
	303.15	0.7711	0.771 [33] 0.7710 [25]	1259.27	1258.8 [33] 1268 [37]	1.3391	1.339 [33] 1.3390 [38]
	313.15	0.7602	0.760 [33] 0.7602 [25]	1218.56	1218.4 [33] 1229 [37]	1.3342	1.334 [33] 1.3348 [39]
	323.15	0.7491	0.7491 [25]	1178.67	1189 [37]	1.3293	1.3297 [39]
Sulfolane	303.15	1.2617	1.2618 [40]	1583.52	1588 [40]	1.4817	1.4814 [41]
	313.15	1.2529	1.2532 [41]	1552.30	1558 [40]	1.4782	1.47800 [41]
	323.15	1.2442	1.2442 [41]	1520.73	-	1.4748	1.47440 [41]

1-Hexene	293.15	0.6735	0.6732 [42]	1088.81	-	1.3880	1.3879 [42]
	298.15	0.6688	0.6684 [42]	1066.46	1066.06 [43]	1.3852	1.3850 [42]
	303.15	0.6640	-	1044.01	-	1.3824	-
2-Methoxyethanol	293.15	0.9646	0.9646 [44]	1359.64	1358 [44]	1.4023	1.4020 [44]
	298.15	0.9600	0.9603 [45]	1342.49	1340.2 [45]	1.4004	1.4002 [45]
	303.15	0.9554	0.9553 [44]	1325.15	1322 [44]	1.3984	1.3970 [44]
2-Ethoxyethanol	293.15	0.9294	0.930 [20] 0.9296 [44]	1319.87	1321 [20] 1328 [44]	1.4080	1.408 [20] 1.4080 [44]
	298.15	0.9249	0.925 [20] 0.9258 [46]	1302.33	1303 [20] 1300 [46]	1.4059	1.406 [20] 1.4056 [46]
	303.15	0.9204	0.920 [20] 0.9210 [46]	1284.61	1286 [20] 1286 [44]	1.4039	1.404 [20] 1.4037 [46]
2-Butoxyethanol	293.15	0.9004	0.90119 [47]	1322.98	1323.9 [47]	1.4196	1.4196 [48]
	298.15	0.8962	0.8966 [45]	1306.11	1303.4 [45]	1.4176	1.4176 [45]
	303.15	0.8920	0.89235 [47]	1289.04	1290.6 [47]	1.4156	1.4157 [48]

[1] [Mozo et al., 2007]
[2] [Kim et al., 2006]
[3] [Kinart et al., 2005]
[4] [Riddick et al., 1986]
[5] [Pal et al., 1996]
[6] [Carmona et al., 1999]
[7] [Douhéret et al., 1995]
[8] [Comelli et al., 2000]
[9] [Francesconi et al., 1999]
[10] [Negadi et al., 2017]
[11] [Benkelfat-Seladji et al., 2021]
[12] [Gong et al., 2012]
[13] [Rodriguez et al., 2001]
[14] [Aralaguppi et al., 1999]
[15] [Varfolomeev et al., 2014]
[16] [Ritzoulis et al., 2000]
[17] [Wu et al., 2015]
[18] [Ortega et al., 1982]
[19] [Wilson et al., 1964]
[20] [Benkelfat-Seladji et al., 2022]
[21] [Nikam et al., 1995]
[22] [Lee et al., 1995]
[23] [Ouaar et al., 2020]
[24] [Jiménez et al., 2001]
[25] [Paez et al., 1989]
[26] [Nikam et al., 1996]
[27] [Dubey et al., 2008]
[28] [Mokhtarani et al., 2009]
[29] [Makhlouf et al., 2019]
[30] [Papari et al., 2013]
[31] [Bendiaf et al., 2015]
[32] [Lomba et al., 2011]
[33] [Ouaar et al., 2017]
[34] [Ciocirlan et al., 2008]
[35] [Ouaar et al., 2018]
[36] [Ciocirlan et al., 2009]
[37] [Chen et al., 2015]
[38] [Iloukhani et al., 2009]
[39] [Yang et al., 2016]
[40] [Patwari et al., 2009]
[41] [Vahidi et al., 2013]
[42] [Mears et al., 1950]
[43] [Tardajos et al., 1986]
[44] [Singh et al., 2013]
[45] [Sarkar et al., 2009]
[46] [Aralaguppi et al., 1996]
[47] [Cwiklinska et al., 2011]
[48] [Chiou et al., 2010]

1.3 Apparatus and procedure

Binary mixtures of various compositions were prepared by syringing weighed amounts of the pure liquids into bottles with airtight stoppers. The weighing was done on an OHAUS, EX124 US analytical balance with a standard uncertainty of 0.0001 g. The average uncertainty in the mole fraction of the mixtures was estimated to be less than 0.0007.

Density and speed of sound measurements of the pure components and their mixtures were carried out at different temperatures and at pressure of 0.1 MPa using a digital vibrating tube densimeter and sound velocity analyzer Anton Paar (DSA 5000M) with a temperature accuracy of ±0.02 K. The instrument can measure simultaneously density in the range from 0 to 3×10^3 kg m^{-3} and sound velocity from 1000 to 2000 m s^{-1} in a temperature range from 273.15 to 343.15K with pressure variation from 0 to 0.3×10^5 Pa. The sound velocity is measured using a propagation time technique (Fortin et al., 2013). The sample is sandwiched between two piezoelectric ultrasound transducers. One transducer emits sound waves through the sample-filled cavity (frequency around 3 MHz) and the second transducer receives those waves. Thus, the sound velocity is obtained by dividing the known distance between transmitter and receiver by the measured propagation time of the sound waves (Fortin et al., 2013).

The combined expanded uncertainty in experimental measurements has been found to be 0.005 g.cm^{-3} for the density and 1.35 m.s^{-1} for the speed of sound.

Measurement of refractive index of pure components and binary mixtures were gotten by a digital refractometer (Anton Paar Abbemat 300) with an uncertainty in the experimental measurements of ± 0.006. Abbemat refractometer determine the refractive index within a measuring range of 1.26 n_D to 1.72 n_D and a temperature range from 4 °C to 125 °C.

The refractometer was calibrated with water before each temperature and each series of measurements and checked for pure liquids with known refractive indices. Reproducibility of the results was confirmed by performing a minimum five independent readings for each sample. All measurements were performed at the specified temperature range with a temperature accuracy of ±0.02 K.

Each experimental device used in this study was validated by measuring the data of pure components and the data were compared to literature values given in Table 1.2. The difference between the experimental and literature data was within the experimental error.

1.4 Calculations of the empirical equations

From the experimental data of density, speed of sound and refractive indices, various thermodynamic acoustical and optical properties were calculated using the following relations employed in previous studies.

The isentropic compressibility (κ_S) is calculated directly from the measured values of u and the ρ using Newton–Laplace equation as: (Awasthi et al., 2004; Azhagiri et al., 2009; Ion et al., 2013; Dash et al., 2012)

$$\kappa_s = 1/(\rho u^2) \tag{1.1}$$

Where ρ and u are the density and speed of sound of the mixtures respectively.

The u and the ρ of the medium using Newton–Laplace equation give the intermolecular free length (L_f) as: (Rastogi et al., 2003; Awasthi et al., 2003; Azhagiri et al., 2009)

$$L_f = \kappa_{jacob} \times (\kappa_s)^{1/2} \quad (1.2)$$

Where, κ_{jacob} is the Jacobson's temperature-dependent constant which is equal to

κ_{jacob} = (93.875 + 0.375 T) × 10^{-8} (Thanuja et al., 2012)

The specific acoustic impedance was calculated using the following relation: (Awasthi et al., 2004; Azhagiri et al., 2009; Ion et al., 2013; Dash et al., 2012)

$$Z = \rho \times u \quad (1.3)$$

The relative association (R_A) is given by: (Azhagiri et al., 2009)

$$R_A = (\rho/\rho_0) \times (u_0/u)^{1/3} \quad (1.4)$$

Where ρ_0 and u_0 are the density and speed of sound of the pure solvents, respectively.

The relaxation strength (r) was calculated according to the following equation: (Azhagiri et al., 2009; Ion et al., 2013)

$$r = 1 - (u/u_\infty)^2 \quad (1.5)$$

Where u_∞ is speed of sound at infinity and its value is 1600 $m.s^{-1}$.

Rao's molar sound function (R) is given by: (Rastogi et al., 2003; Bagchi et al., 1986)

$$R = (M/\rho) \times u^{1/3} \quad (1.6)$$

Where M is the molecular weight of the mixture.

Thermodynamic excess functions are very sensitive toward mutual interactions between the component molecules of the binary mixtures. The sign and the extent of deviation of the functions from ideality depend on the strength of interactions between unlike molecules (Sandhu et al., 1986; García et al., 1996). Excess molar volume (V_m^E), deviations in isentropic compressibility ($\Delta\kappa_s$), deviations in intermolecular free length (ΔL_f), deviations in acoustic impedance (ΔZ), deviations in speed of sound (Δu) and deviation of refractive index (Δn_D) are calculated using the general relation:

$$Y^E = Y - (x_1 Y_1 + x_2 Y_2) \quad (1.7)$$

Where Y represents V_m , κ_s , L_f, Z, u or n_D of the mixture. x is the mole fraction, subscript 1 refers to 2-(2-methoxyethoxy)ethanol or furfural or 1-hexene and subscript 2 refers to methanol, ethanol, propan-1-ol, propan-2-ol, butan-1-ol, butan-2-ol, DMSO, acetonitrile, sulfolane, 2-methoxyethanol, 2-ethoxyethanol or 2-butoxyethanol.

1.5 Results and discussion

Study of volumetric, acoustic, and optical properties has been devoted for the following binary mixtures:

a) 2-(2-Methoxyethoxy)ethanol

2-(2-methoxyethoxy)ethanol (1) + Methanol (2)
2-(2-methoxyethoxy)ethanol (1) + Ethanol (2)
2-(2-methoxyethoxy)ethanol (1) + Propan-1-ol (2)
2-(2-methoxyethoxy)ethanol (1) + Propan-2-ol (2)
2-(2-methoxyethoxy)ethanol (1) + Butan-1-ol (2)
2-(2-methoxyethoxy)ethanol (1) + Butan-2-ol (2)

b) Furfural

Furfural (1) + DMSO (2)
Furfural (1) + Acetonitrile (2)
Furfural (1) + Sulfolane (2)

c) 1-Hexene

1-Hexene (1) + 2-Methoxyethanol (2)
1-Hexene (1) + 2-Ethoxyethanol (2)
1-Hexene (1) + 2-Butoxyethanol (2)

1.5.1 Thermophysical and optical properties

1.5.1.1 Density

The experimentally determined densities ρ at (293.15, 303.15, 313.15 and 323.15) K and at pressure p = 0.1 MPa for the binary mixtures (22MEE + methanol or ethanol or propan-1-ol or propan-2-ol or butan-1-ol or butan-2-ol), over the complete composition range expressed by mole fraction x_1 of 22MEE are presented in Table A1.3 and plotted in Figures 1.1 (a-f). The experimental data of the binary mixtures of 22MEE with methanol, ethanol, propan-2-ol and butan-2-ol measured here cannot be compared to data in the literature because, to the best of our knowledge, these systems apparently were not previously measured.

In Figures 1.2 (a-c), the experimental density values for the binary system (22MEE + propan-1-ol) at temperature of (293.15, 303.15, 313.15 and 323.15) K and those reported by (Pal et al., 2004) at temperature of (298.15, 308.15 and 318.15) K are compared and show a good agreement.

In Figure 1.3, the experimental density values for the binary mixture (22MEE + butan-1-ol) at temperature of (293.15 and 303.15) K and those reported by (Mozo et al., 2007) at temperature of (293.15 and 303.15) K are compared and show a good agreement.

The values of density ρ for the binary mixtures (furfural + DMSO) and (furfural + acetonitrile) have been measured at (293.15, 303.15, 313.15 and 323.15) K and at pressure of 0.1 MPa and for (furfural + sulfolane) at (303.15, 313.15 and 323.15) K. The results are listed as a function of the mole fraction of furfural in Table A1.4 The plots of density at investigated temperatures are represented in Figures 1.4 (a-c).

Densities for binary mixtures containing 1-hexene with 2-methoxyethanol, 2-ethoxyethanol or 2-butoxyethanol have been determined at temperatures of (293.15, 298.15 and 303.15) K and at pressure p = 0.1 MPa over the whole composition range. Density data are listed in Table A1.5 and plotted against the mole fraction of 1-hexene in Figures 1.5 (a-c).
No literature data are available to compare density results of binary systems containing furfural or 1-hexene.

It is evident from the results reported in Tables 1.3, 1.4 and 1.5 and figures that the density ρ values decrease by increasing the temperature for all the studied binary systems at the same concentration. This can be explained by the molecular agitations in binary mixtures with increase in temperature which causes weakened molecular interactions resulting in decreasing ρ values (Umapathi et al., 2020). Also, the ρ values increase with composition for all binary mixtures containing 22MEE, (furfural + DMSO) and (furfural + acetonitrile) systems whereas decrease for the (furfural + sulfolane) system and all binary mixtures containing 1-hexene.

Figure 1.1 (a)

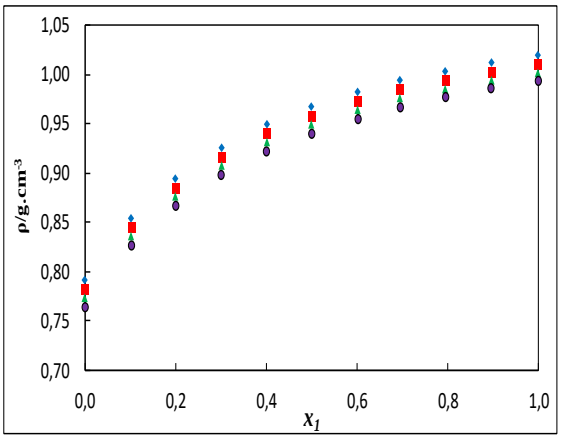

Figure 1.1 (b)

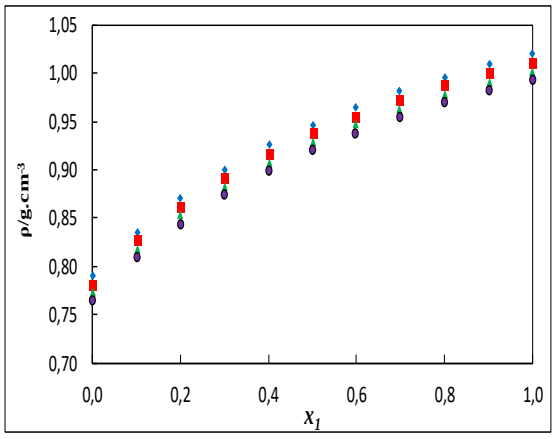

Figure 1.1 (c)

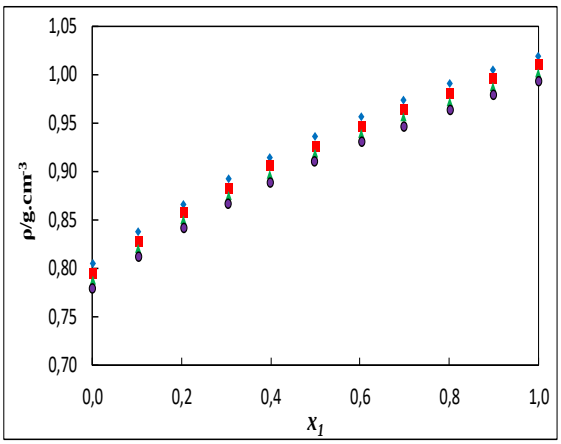

Figure 1.1 (d)

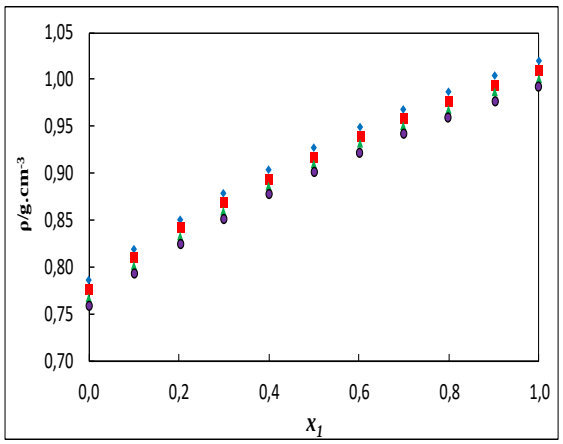

Figure 1.1 (e)

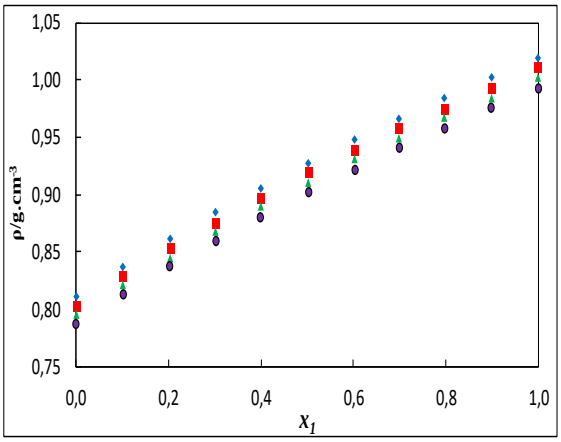

Figure 1.1 (f)

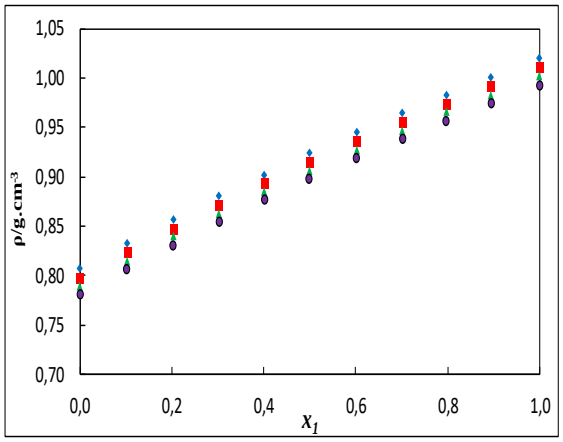

Figure 1.1: Plot of density (ρ) for the binary mixtures: (a) {22MEE (1) + methanol (2)}, (b) {22MEE (1) + ethanol (2)}, (c) {22MEE (1) + propan-1-ol (2)}, (d) {22MEE (1) + propan-2-ol (2)}, (e) {22MEE (1) + butan-1-ol (2)}, and (f) {22MEE (1) + butan-2-ol (2)} as function of the composition expressed in the mole fraction of 22MEE at 293.15 K (◆), 303.15 K (■), 313.15 K (▲) and 323.15K (●).

Figure 1.2 (a)

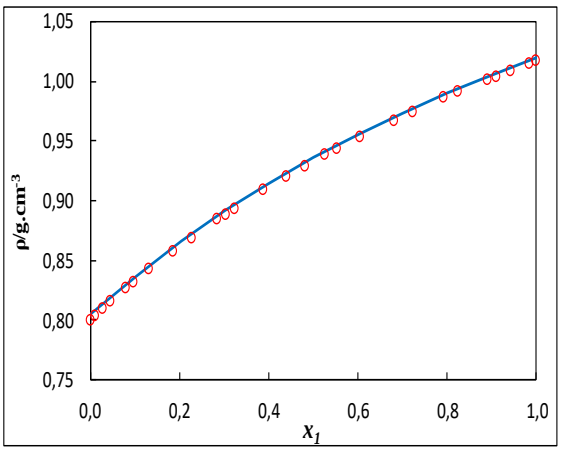

Figure 1.2 (b)

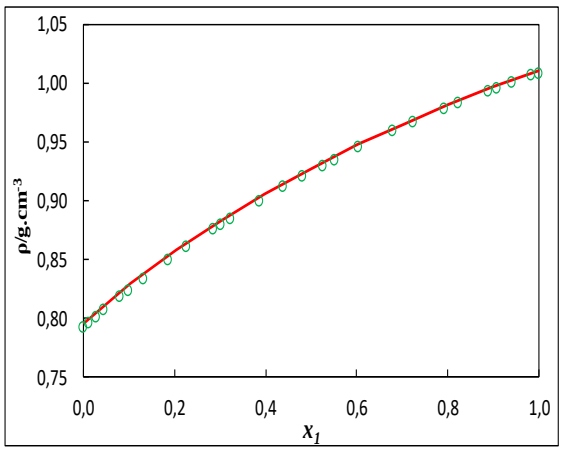

Figure 1.2 (c)

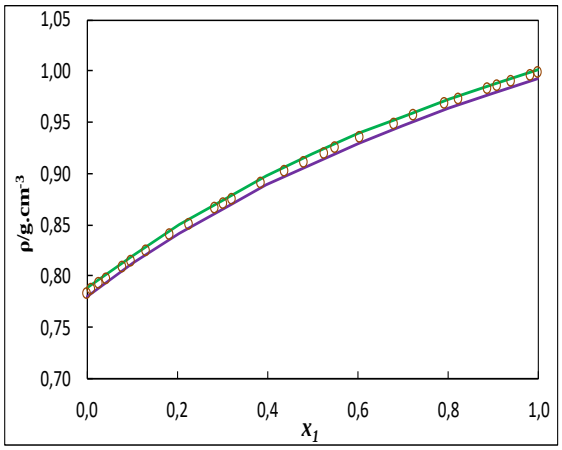

Figure 1.2: Plot of density (ρ) for the binary system {22MEE (1) + propan-1-ol (2)} as function of the composition expressed in the mole fraction of 22MEE at temperature of (a) 293.15 K (—), (b) 303.15 K (—), (c) 313.15 K (—) and 323.15 K (—) together with those reported by Pal et al. (2004) at (a) 298.15 K (o), (b) 308.15 K (o) and (c) 318.15 K (o).

Figure 1.3 (a) **Figure 1.3 (b)**

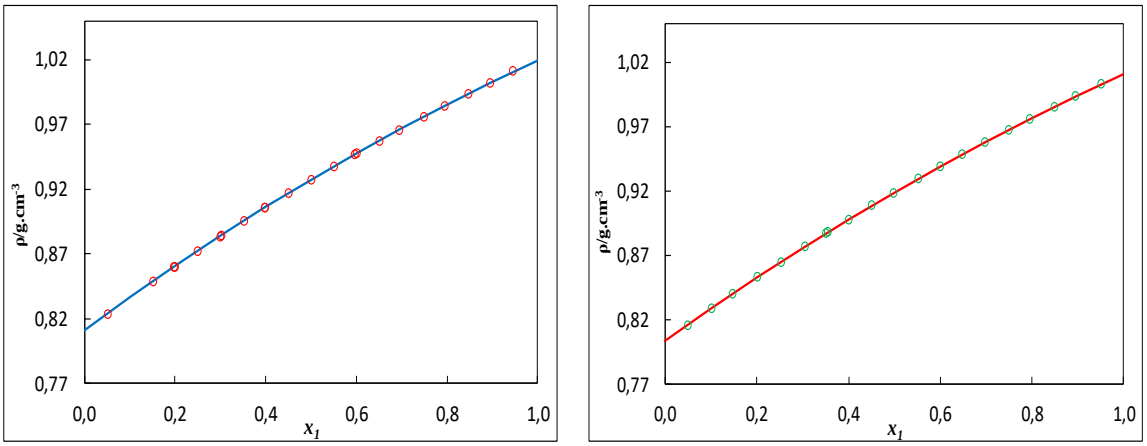

Figure 1.3: Plot of density (ρ) for the binary system {22MEE (1) + butan-1-ol (2)} as function of the composition expressed in the mole fraction of 22MEE at temperature of (a) 293.15 K (—) and (b) 303.15 K (—) together with those reported by Mozo et al. (2007) at (a) 293.15 K (O) and (b) 303.15 K (O).

Figure 1.4 (a) **Figure 1.4 (b)**

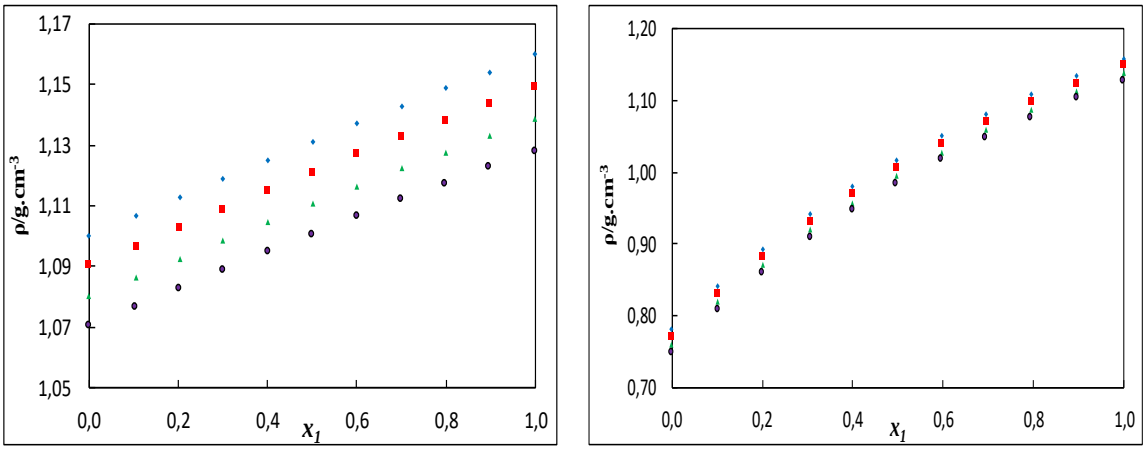

Figure 1.4 (c)

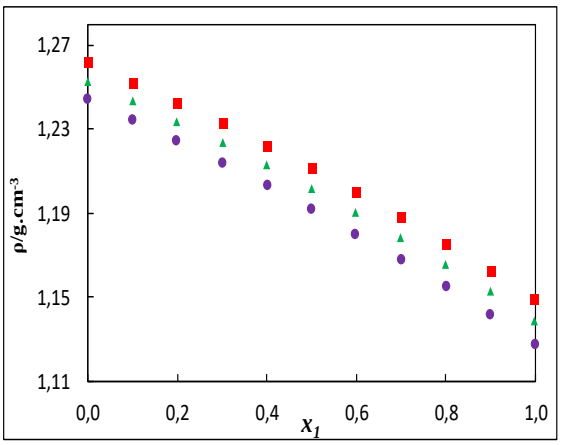

Figure 1.4: Plot of density (ρ) for the binary mixtures: (a) {furfural (1) + DMSO (2), (b) {furfural (1) + acetonitrile (2)}, (c) {furfural (1) + sulfolane (2)} as function of the composition expressed in the mole fraction of furfural at 293.15 K (◆), 303.15 K (■), 313.15 K (▲) and 323.15 K (●).

Figure 1.5 (a)

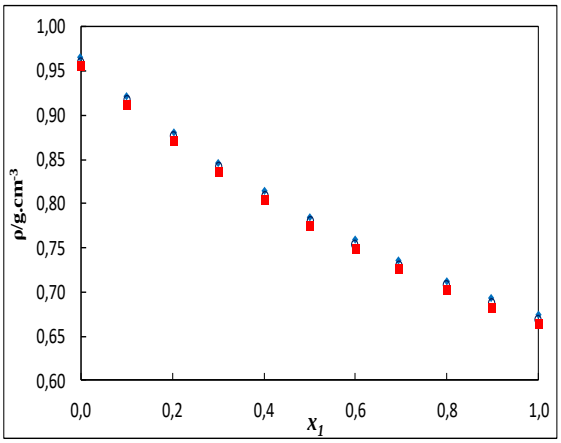

Figure 1.5 (b)

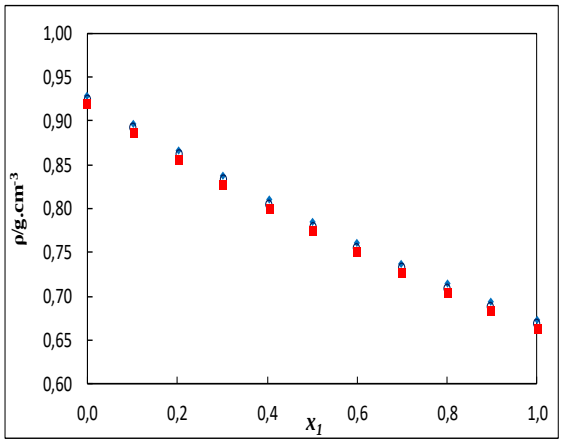

Figure 1.5 (c)

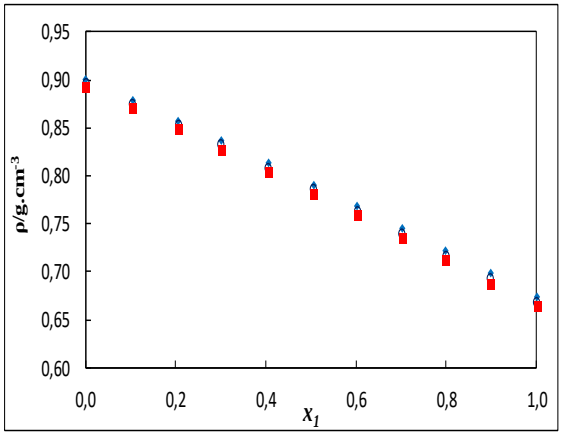

Figure 1.5: Plot of density (ρ) for the binary mixtures: (a) {1-hexene (1) + 2-methoxyethanol (2)}, (b) {1-hexene (1) + 2-ethoxyethanol (2)}, (c) {1-hexene (1) + 2-butoxyethanol (2)} as function of the composition expressed in the mole fraction of 1-hexene at 293.15 K (◆), 298.15 K (○), and 303.15 K (■).

1.5.1.2 Speed of sound

Speed of sound u results for 22MEE binary mixtures measured at the same conditions are summarized in Table A1.3 and the plots are in Figures 1.6 (a-f). Speed of sound, u, for the binary mixture (22MEE + butan-1-ol) at temperature of (293.15 and 303.15) K together with literature data reported by (Mozo et al., 2007) at (293.15 and 303.15) K were plotted in Figure 1.7 for the comparison purpose. From Figure 1.7, it can be seen that the experimental, u, values are in a good accordance with those reported by (Mozo et al., 2007).

Figure 1.6 (a)

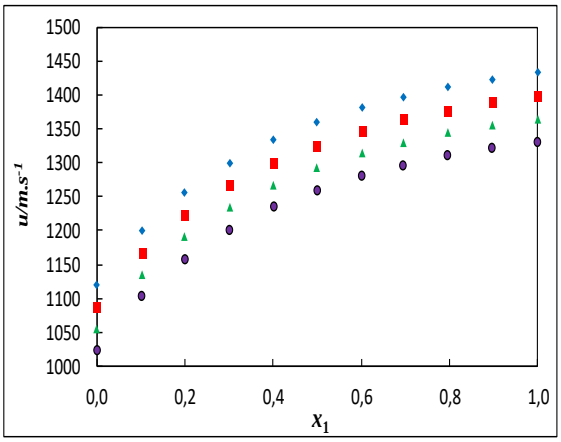

Figure 1.6 (b)

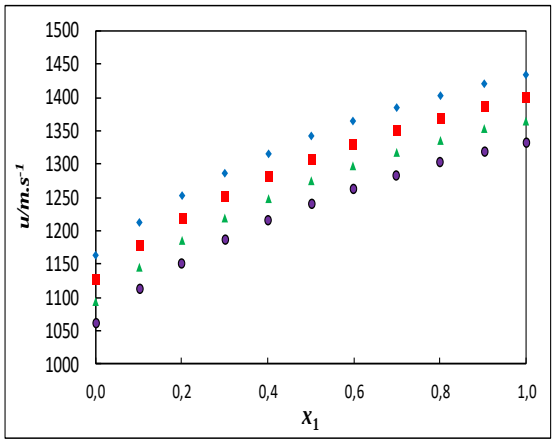

Figure 1.6 (c)

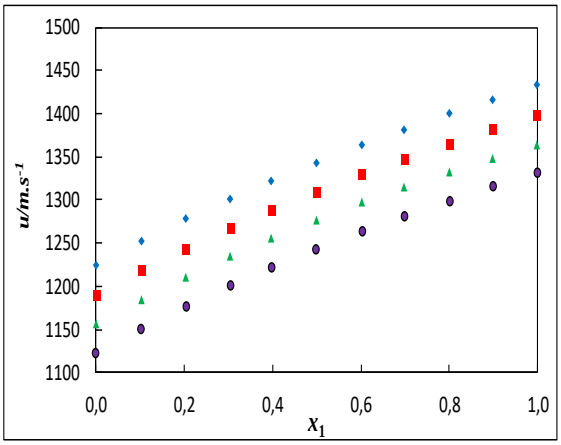

Figure 1.6 (d)

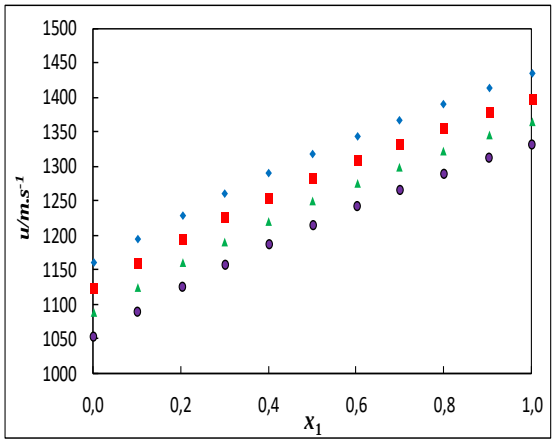

Figure 1.6 (e)

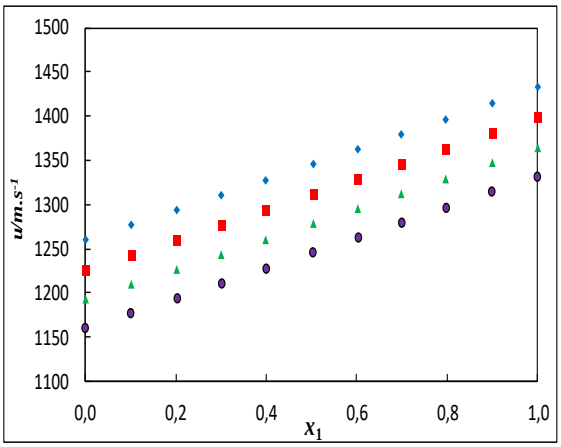

Figure 1.6 (f)

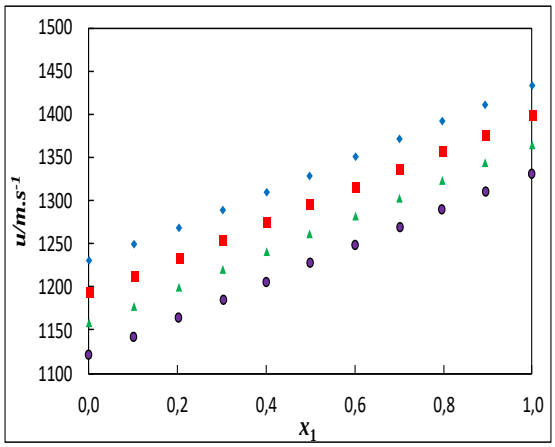

Figure 1.6: Plot of speed of sound (u) for the binary mixtures: (a) {22MEE (1) + methanol (2)}, (b) {22MEE (1) + ethanol (2)}, (c) {22MEE (1) + propan-1-ol (2)}, (d) {22MEE (1) + propan-2-ol (2)}, (e) {22MEE (1) + butan-1-ol (2)}, and (f) {22MEE (1) + butan-2-ol (2)} as function of the composition expressed in the mole fraction of 22MEE at 293.15 K (◆), 303.15 K (■), 313.15 K (▲) and 323.15K (●).

Figure 1.7 (a) **Figure 1.7 (b)**

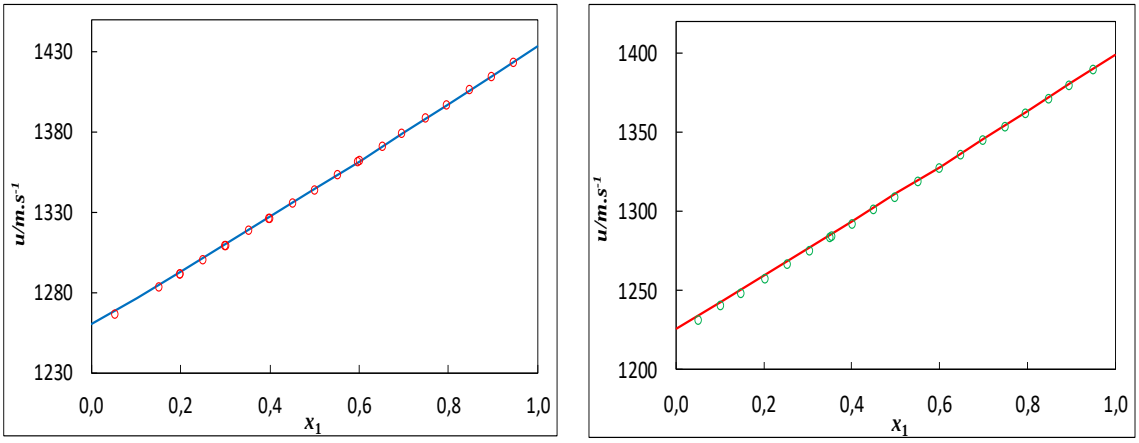

Figure 1.7: Plot of speed of sound (u) for the binary mixtures: {22MEE (1) + butan-1-ol (2)} as function of the composition expressed in the mole fraction of 22MEE at temperature of (a) 293.15 K (—) and (b) 303.15 K (—) together with those reported by Mozo et al. (2007) at (a) 293.15 K (o) and (b) 303.15 K (o).

Speed of sound u results at the same conditions cited above of binary mixtures containing furfural or 1-hexene are listed in Tables 1.4 and 1.5 respectively and the curves are shown in Figures 1.8 (a-c) and 1.9 (a-c).
No literature data are available to compare speed of sound results of binary systems containing furfural or 1-hexene.

Speed of sound u data provides information about (solvent + solvent), (solute + solvent) and (solute + solute) interactions in mixtures (Roy et al., 2011). Tables 1.3, 1.4 and 1.5 reveal that the u values decrease with an increase in temperature for all the studied binary mixtures which can be explained by the fact that with an increase in the temperature, the free spaces in molecules increase (Umapathi et al., 2020). With increasing temperature, the thermal energy causes the breaking of the bonds and it weakens the molecular forces which decrease the speed of sound (Riddick et al., 1970). The decrease in u signifies that the interaction between solute and solvent is becoming less dominant (Thanuja et al., 2012). The values of u were found to increase with increasing composition x_1 for all binary mixtures containing 22MEE and (furfural + acetonitrile) system whereas this decreases with increasing composition x_1 for (furfural + DMSO), (furfural + sulfolane) systems and all binary mixtures containing 1-hexene at the investigated temperatures.

Figure 1.8 (a)

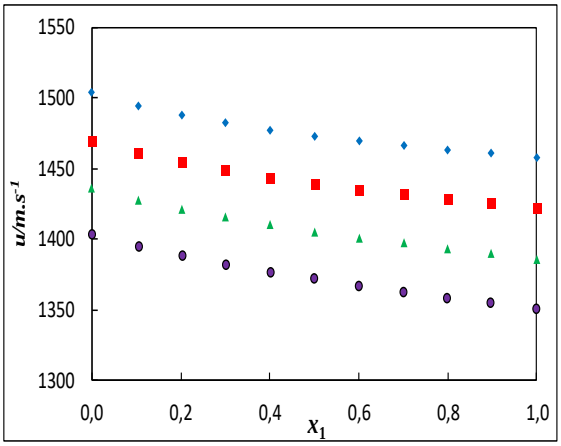

Figure 1.8 (b)

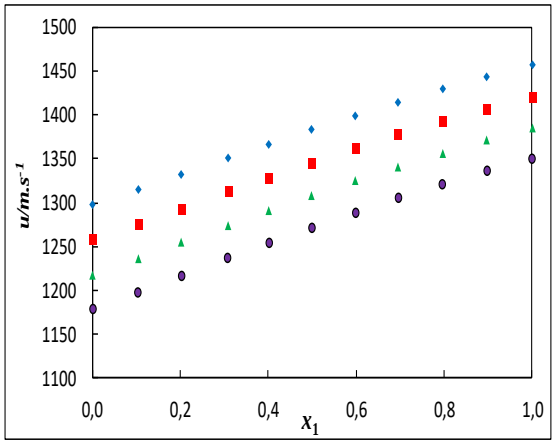

Figure 1.8 (c)

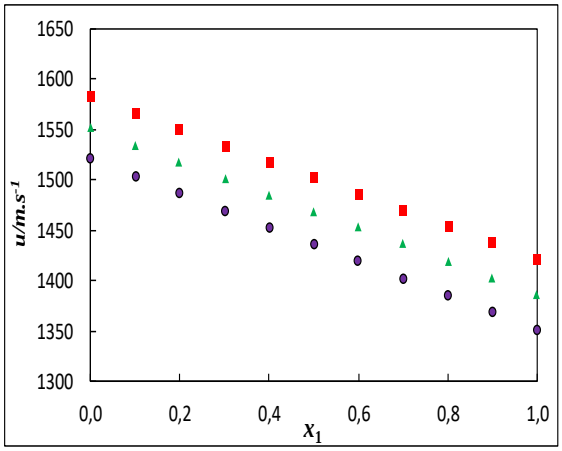

Figure 1.8: Plot of speed of sound (u) for the binary mixtures: (a) {furfural (1) + DMSO (2)}, (b) {furfural (1) + acetonitrile (2)}, (c) {furfural (1) + sulfolane (2)} as function of the composition expressed in the mole fraction of furfural at 293.15 K (◆), 303.15 K (■), 313.15 K (▲) and 323.15 K (●).

Figure 1.9 (a)

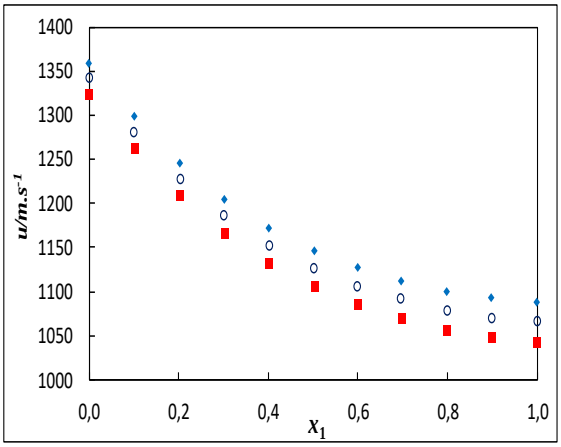

Figure 1.9 (b)

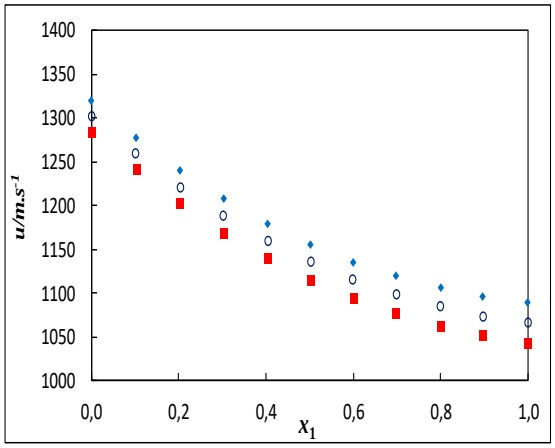

Figure 1.9 (c)

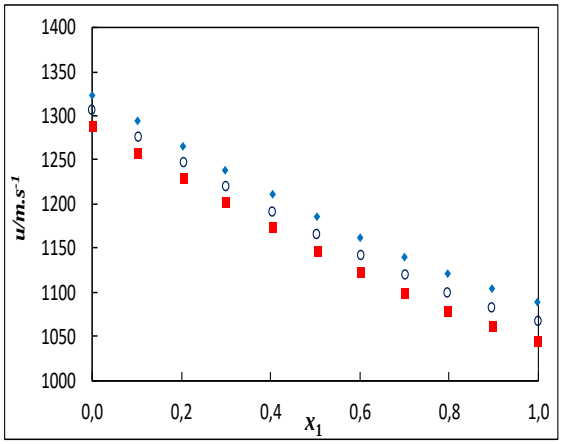

Figure 1.9: Plot of speed of sound (u) for the binary mixtures: (a) {1-hexene (1) + 2-methoxyethanol (2)}, (b) {1-hexene (1) + 2-ethoxyethanol (2)}, (c) {1-hexene (1) + 2-butoxyethanol (2)} as function of the composition expressed in the mole fraction of 1-hexene at 293.15 K (◆), 298.15 K (○), and 303.15 K (■).

1.5.1.3 Refractive index

Refractive indices n_D were measured for all the studied mixtures at the same experimental conditions and are included in Tables 1.3, 1.4 and 1.5 and presented in Figures 1.10 (a-f), 1.11 (a-c) and 1.12 (a-c). As the results show, increasing temperature leads to the decrease of refractive index values for all the studied systems. In addition, the elevation of concentration increases the refractive index values for 22MEE and furfural mixtures whereas this decreases for 1-hexene binary mixtures.

The experimentally determined n_D values for the studied systems at the investigated temperatures cannot be compared to data in the literature because these systems apparently are not reported previously.

Figure 1.10 (a)

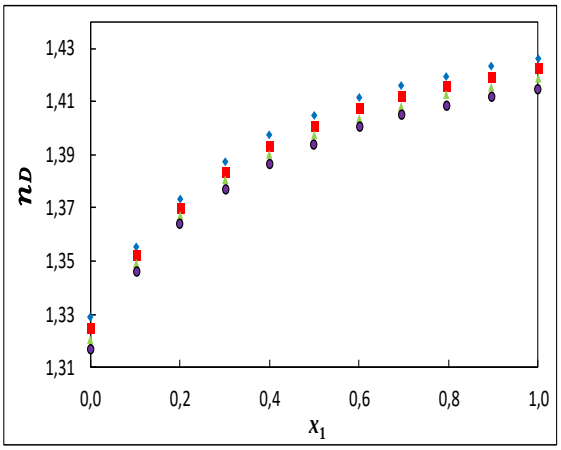

Figure 1.10 (b)

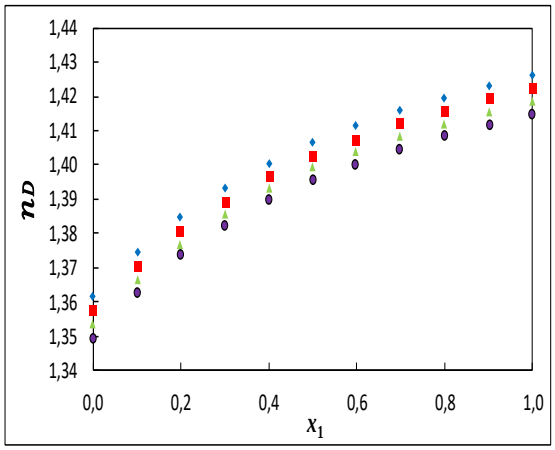

Figure 1.10 (c)

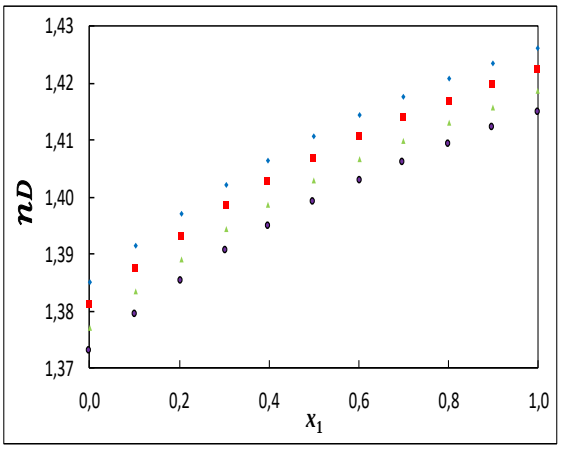

Figure 1.10 (d)

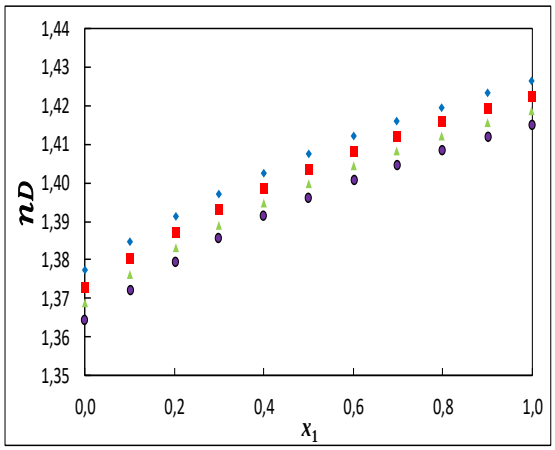

Figure 1.10 (e)

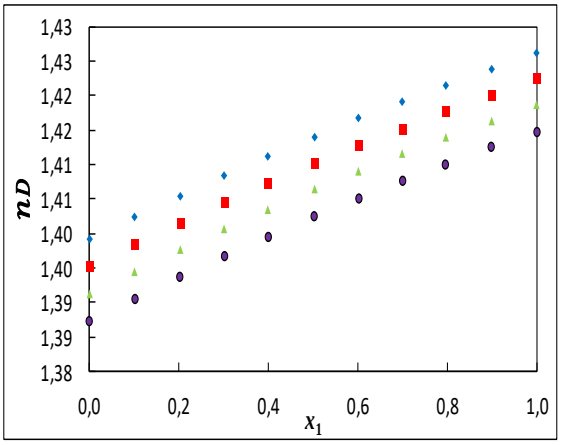

Figure 1.10 (f)

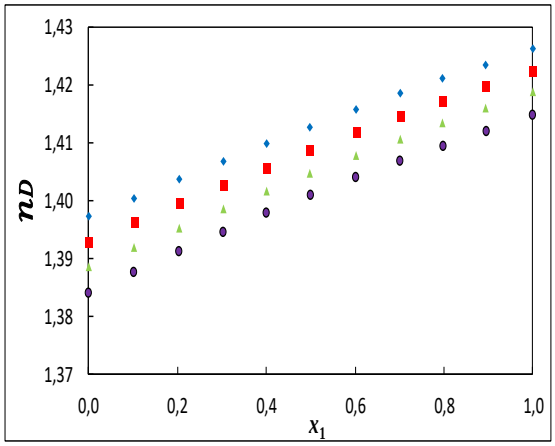

Figure 1.10: Plot of refractive index (n_D) for the binary mixtures: (a) {22MEE (1) + methanol (2)}, (b) {22MEE (1) + ethanol (2)}, (c) {22MEE (1) + propan-1-ol (2)}, (d) {22MEE (1) + propan-2-ol (2)}, (e) {22MEE (1) + butan-1-ol (2)}, and (f) {22MEE (1) + butan-2-ol (2)} as function of the composition expressed in the mole fraction of 22MEE at 293.15 K (◆), 303.15 K (■), 313.15 K (▲) and 323.15K (●).

Figure 1.11 (a)

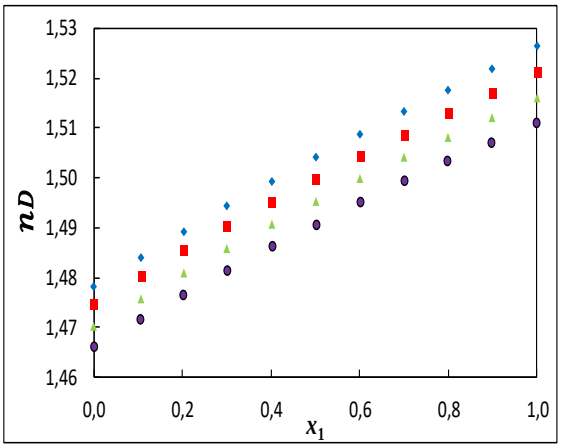

Figure 1.11 (b)

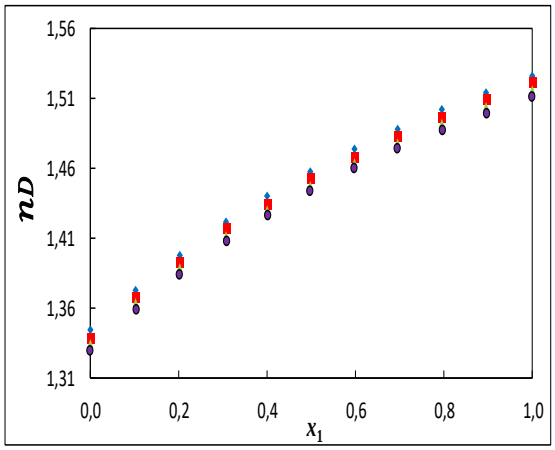

Figure 1.11 (c)

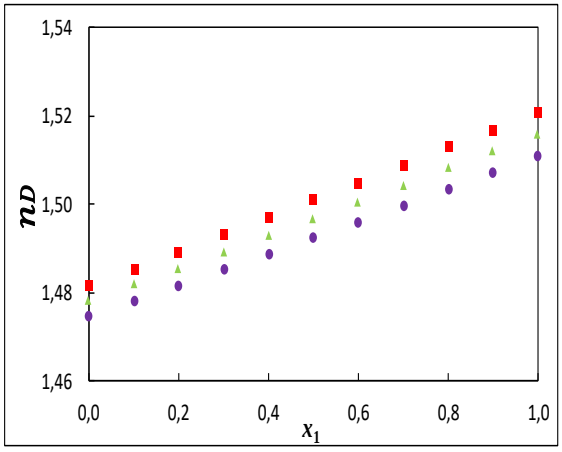

Figure 1.11: Plot of refractive index (n_D) for the binary mixtures: (a) {furfural (1) + DMSO (2)}, (b) {furfural (1) + acetonitrile (2)}, (c) {furfural (1) + sulfolane (2)} as function of the composition expressed in the mole fraction of furfural at 293.15 K (◆), 303.15 K (■), 313.15 K (▲) and 323.15 K (●).

Figure 1.12 (a)

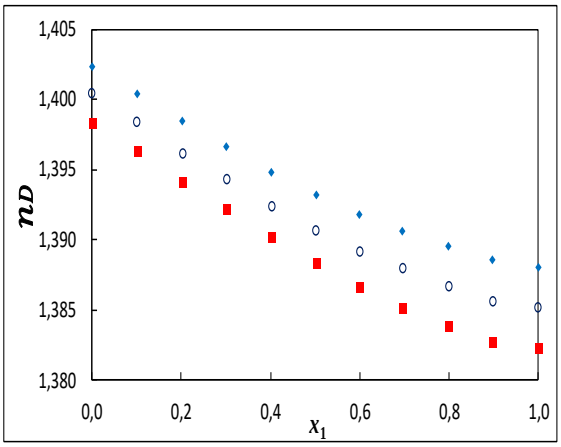

Figure 1.12 (b)

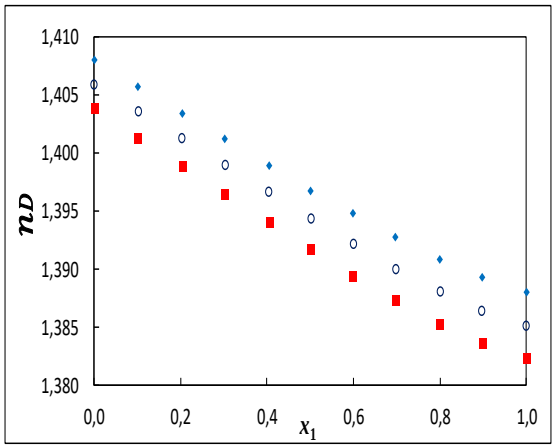

Figure 1.12 (c)

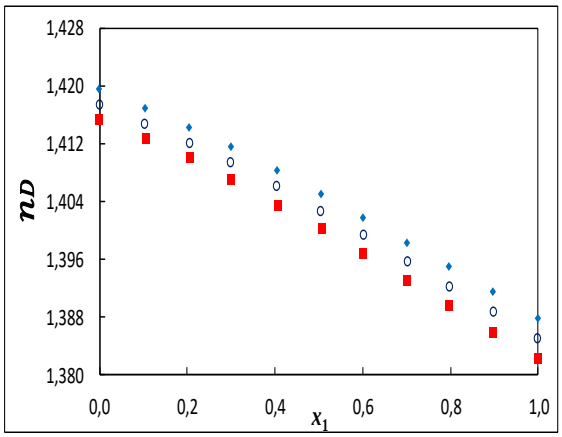

Figure 1.12: Plot of refractive index (n_D) for the binary mixtures: (a) {1-hexene (1) + 2-methoxyethanol (2)}, (b) {1-hexene (1) + 2-ethoxyethanol (2)}, (c) {1-hexene (1) + 2-butoxyethanol (2)} as function of the composition expressed in the mole fraction of 1-hexene at 293.15 K (◆), 298.15 K (○), and 303.15 K (■).

1.5.2 Derived properties

The calculated data of isentropic compressibility (κ_s), intermolecular free length (L_f), specific acoustic impedance (Z), relative association (R_A), relaxation strength (r) and Rao's molar sound function (R) for 22MEE, furfural or 1-hexene binary mixtures at the investigated temperatures are provided in Tables 1.6, 1.7 and 1.8 respectively. The plots of these properties are presented in Figures 1.13(a-f), 1.14(a-c), 1.15(a-c), 1.16(a-f), 1.17(a-c), 1.18(a-c), 1.19(a-f), 1.20(a-c), 1.21(a-c), 1.22(a-f), 1.23(a-c), 1.24(a-c), 1.25(a-f), 1.26(a-c), 1.27(a-c), 1.28(a-f), 1.29(a-c), 1.30(a-c).

1.5.2.1 Isentropic compressibility

As shown in Figures 1.13(a-f), 1.14(a-c), 1.15(a-c), the isentropic compressibility κ_s increases with an increase in temperature at a fixed composition for all investigated systems. An increase in isentropic compressibility κ_s indicates a change in the arrangement of the solvent molecules around the solute molecule undergoing conformational change, which results in weakening of the solute/solvent interactions (Thanuja et al., 2012). This makes the solution more compressible (Bendiaf et al., 2015). Also, κ_s decreases with increase in concentration for all binary mixtures containing 22MEE and (furfural + acetonitrile) system which is an indicative of the fact that intermolecular forces are increasing which conducts the molecules to a closer packing resulting into a decrease in intermolecular free length (Pandey et al., 2013). As the concentration is increasing, κ_s increases for the (furfural + sulfolane) system and all binary mixtures containing 1-hexene inversely to (furfural + DMSO) which is not really affected by the concentration.

Figure 1.13 (a)

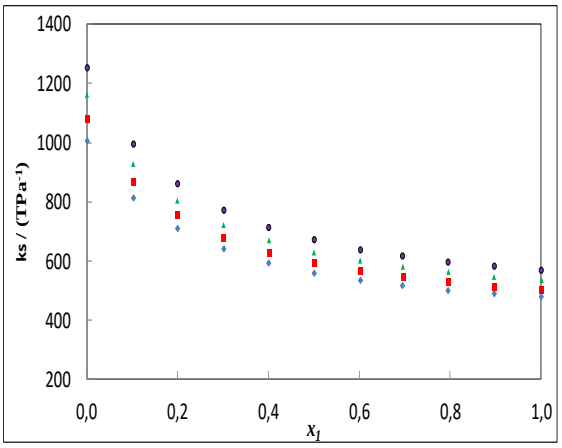

Figure 1.13 (b)

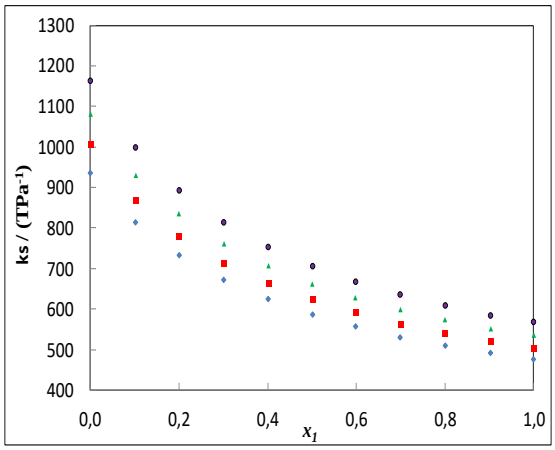

Figure 1.13 (c)

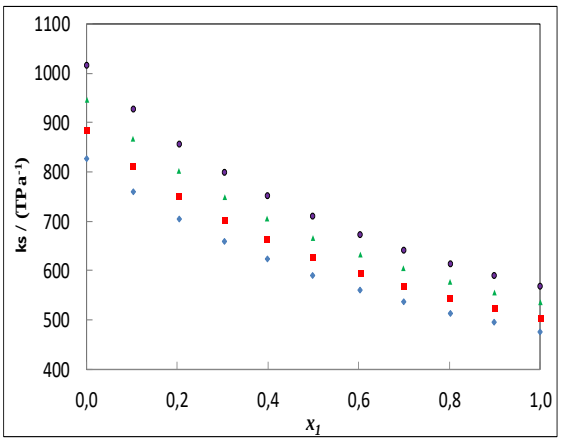

Figure 1.13 (d)

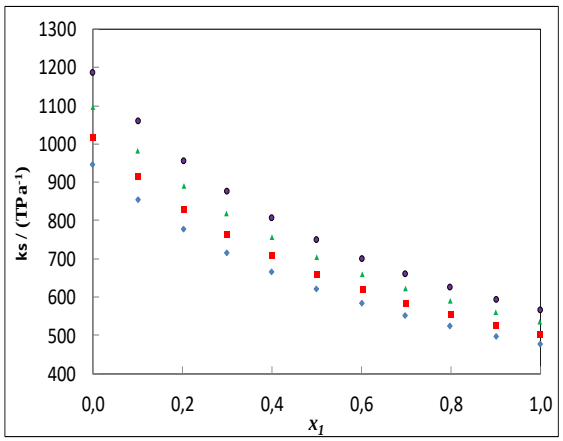

Figure 1.13 (e)

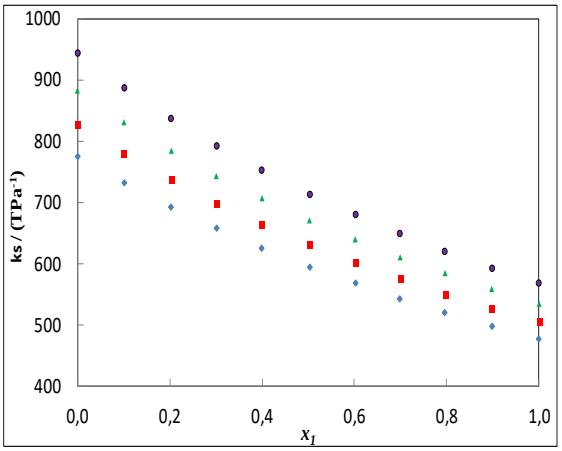

Figure 1.13 (f)

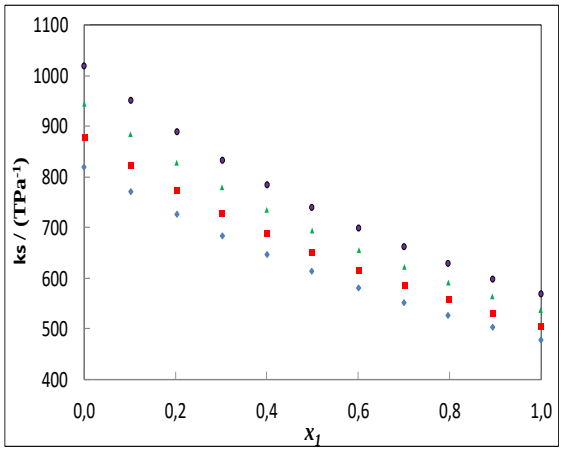

Figure 1.13: Plot of isentropic compressibility (κ_s) for the binary mixtures: (a) {22MEE (1) + methanol (2)}, (b) {22MEE (1) + ethanol (2)}, (c) {22MEE (1) + propan-1-ol (2)}, (d) {22MEE (1) + propan-2-ol (2)}, (e) {22MEE (1) + butan-1-ol (2)}, and (f) {22MEE (1) + butan-2-ol (2)} as function of the composition expressed in the mole fraction of 22MEE at 293.15 K (◆), 303.15 K (■), 313.15 K (▲) and 323.15K (●).

Figure 1.14 (a)

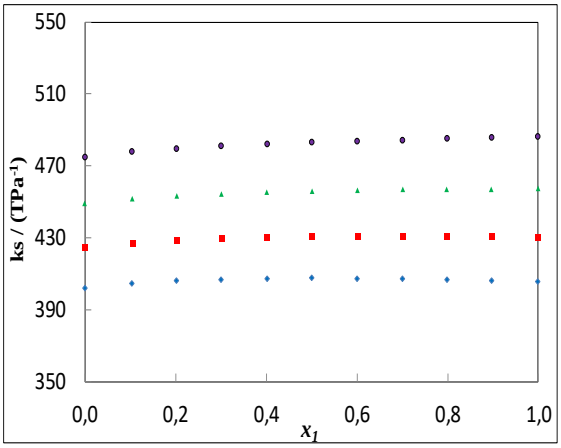

Figure 1.14 (b)

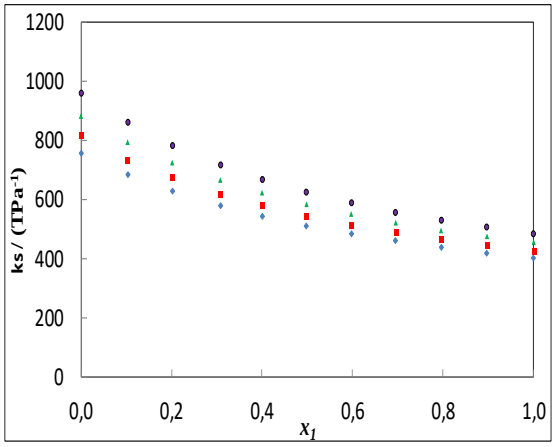

Figure 1.14 (c)

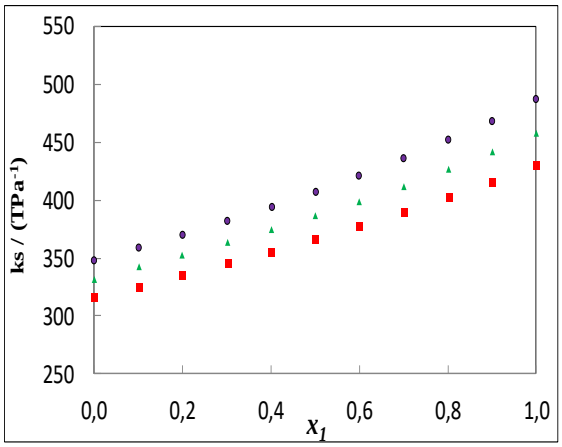

Figure 1.14: Plot of isentropic compressibility (κ_S) for the binary mixtures: (a) {furfural (1) + DMSO (2)}, (b) {furfural (1) + acetonitrile (2)}, (c) {furfural (1) + sulfolane (2)} as function of the composition expressed in the mole fraction of furfural at 293.15 K (◆), 303.15 K (■), 313.15 K (▲) and 323.15 K (●).

Figure 1.15 (a)

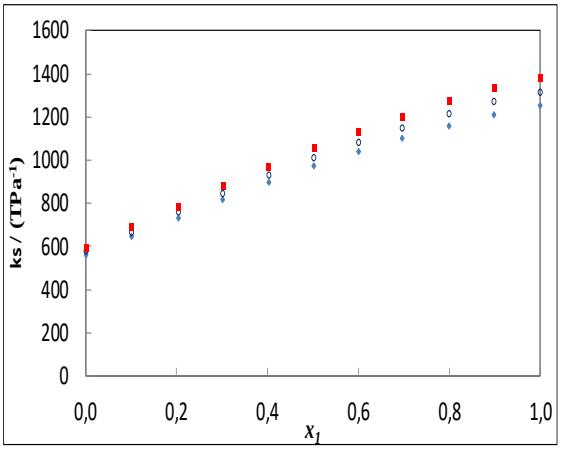

Figure 1.15 (b)

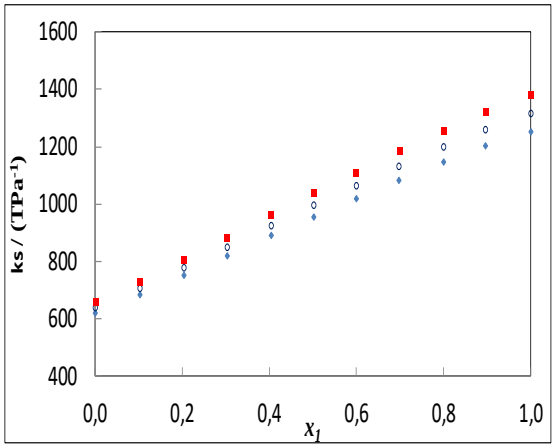

Figure 1.15 (c)

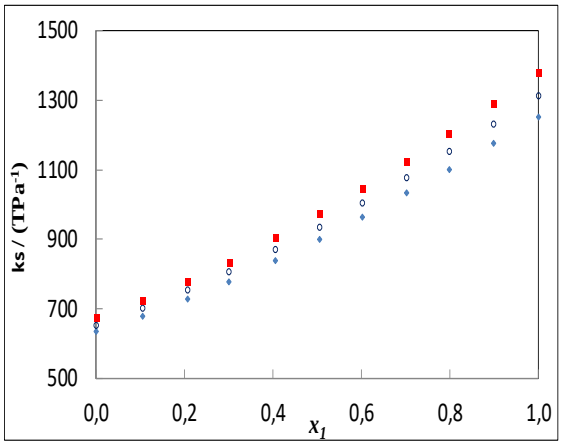

Figure 1.15: Plot of isentropic compressibility (κ_s) for the binary mixtures: (a) {1-hexene (1) + 2-methoxyethanol (2)}, (b) {1-hexene (1) + 2-ethoxyethanol (2)}, (c) {1-hexene (1) + 2-butoxyethanol (2)} as function of the composition expressed in the mole fraction of 1-hexene at 293.15 K (◆), 298.15 K (○), and 303.15 K (■).

1.5.2.2 Intermolecular free length

Figures 1.16(a-f), 1.17(a-c), 1.18(a-c) show the variation of intermolecular free length L_f with mole fraction for all investigated systems. From these figures, it is clear that L_f gives a similar behavior as reflected by κ_s for each mixture at the investigated temperatures. Intermolecular free length and isentropic compressibility are directly related to each other.

Hence, the isentropic compressibility increases with an increase in intermolecular free length. The stronger intermolecular interactions result in a tightly packed liquid structure which leads to the decrease in isentropic compressibility and intermolecular free length (Thanuja et al., 2012). The formation of weaker intermolecular interaction leads to an increase in isentropic compressibility and intermolecular free length.

Moreover, intermolecular free length is a predominant factor in determining the variation of speed of sound in solutions. The inter dependence of L_f and u has been evolved from a model for sound propagation proposed by (Eyring and Kincaid., 1938), speed of sound should decrease if the intermolecular free length increases and vice versa as a result of mixing of components.

Figure 1.16 (a)

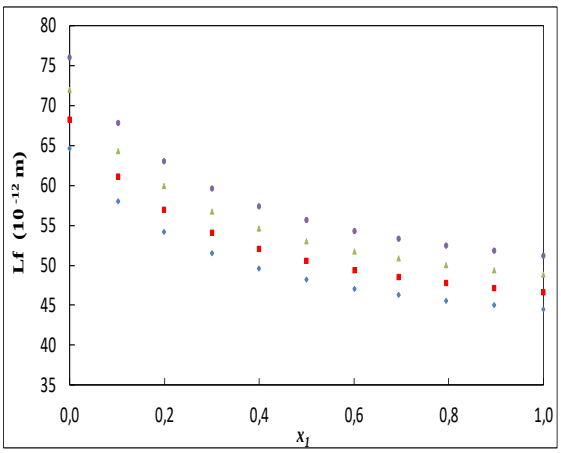

Figure 1.16 (b)

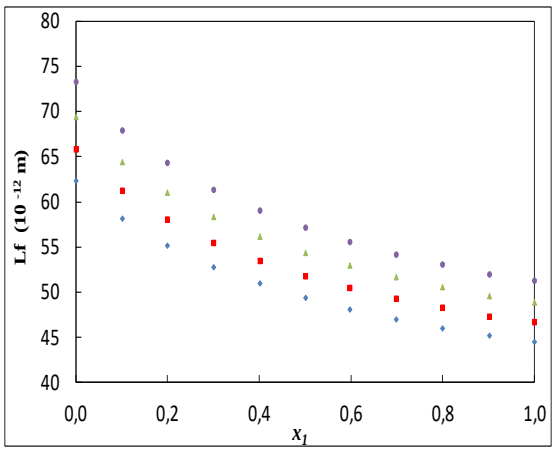

Figure 1.16 (c)

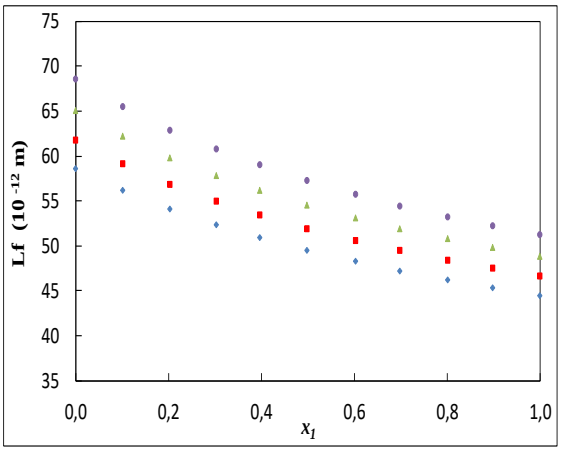

Figure 1.16 (d)

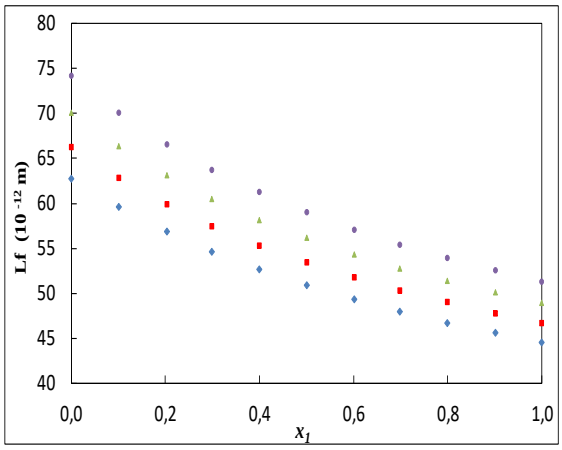

Figure 1.16 (e)

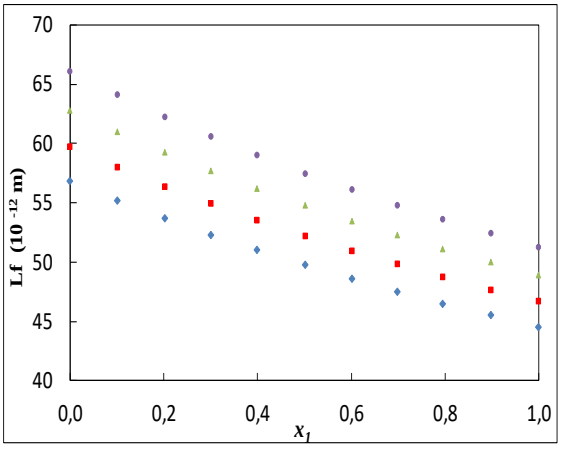

Figure 1.16 (f)

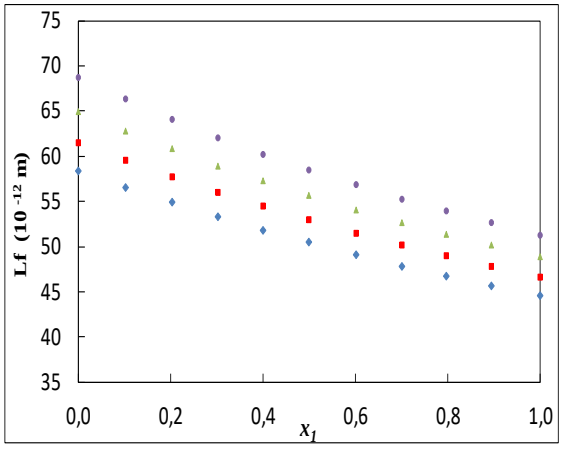

Figure 1.16: Plot of intermolecular free length (L_f) for the binary mixtures: (a) {22MEE (1) + methanol (2)}, (b) {22MEE (1) + ethanol (2)}, (c) {22MEE (1) + propan-1-ol (2)}, (d) {22MEE (1) + propan-2-ol (2)}, (e) {22MEE (1) + butan-1-ol (2)}, and (f) {22MEE (1) + butan-2-ol (2)} as function of the composition expressed in the mole fraction of 22MEE at 293.15 K (◆), 303.15 K (■), 313.15 K (▲) and 323.15K (●).

Figure 1.17 (a)

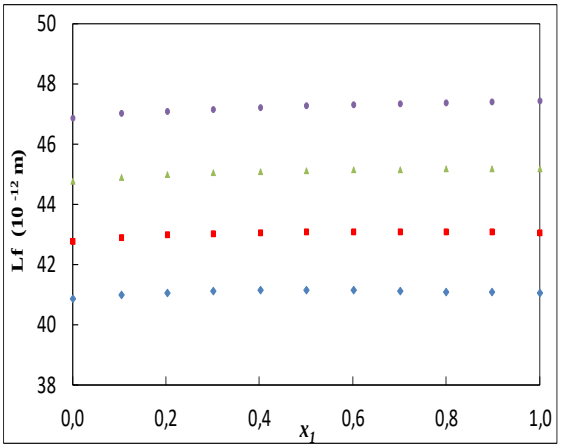

Figure 1.17 (b)

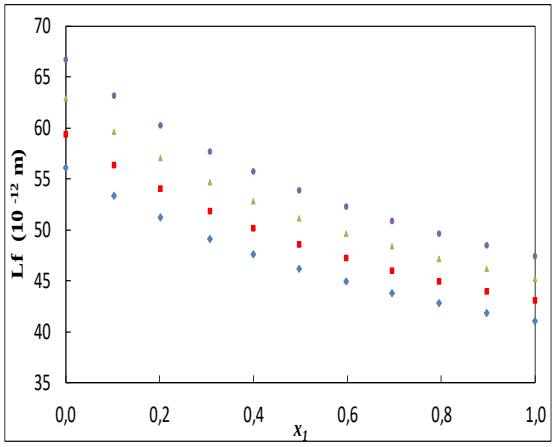

Figure 1.17 (c)

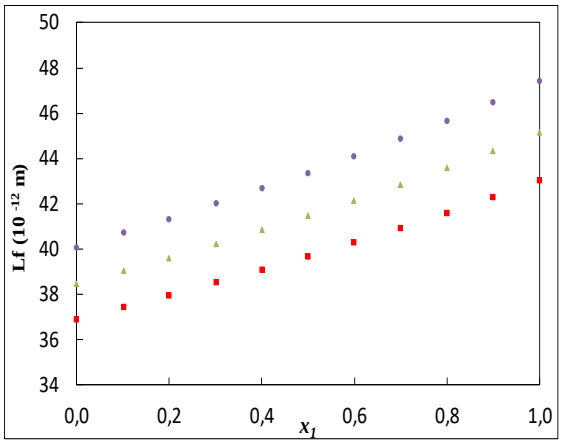

Figure 1.17: Plot of intermolecular free length (L_f) for the binary mixtures: (a) {furfural (1) + DMSO (2)}, (b) {furfural (1) + acetonitrile (2)}, (c) {furfural (1) + sulfolane (2)} as function of the composition expressed in the mole fraction of furfural at 293.15 K (◆), 303.15 K (■), 313.15 K (▲) and 323.15 K (●).

Figure 1.18 (a)

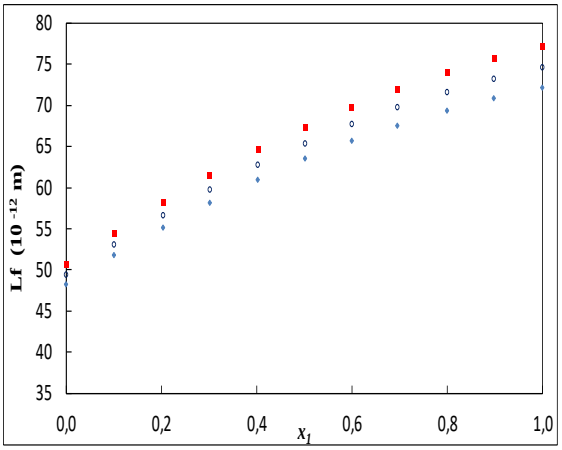

Figure 1.18 (b)

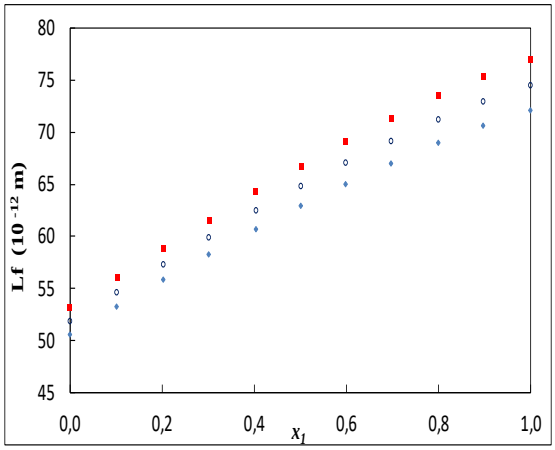

Figure 1.18 (c)

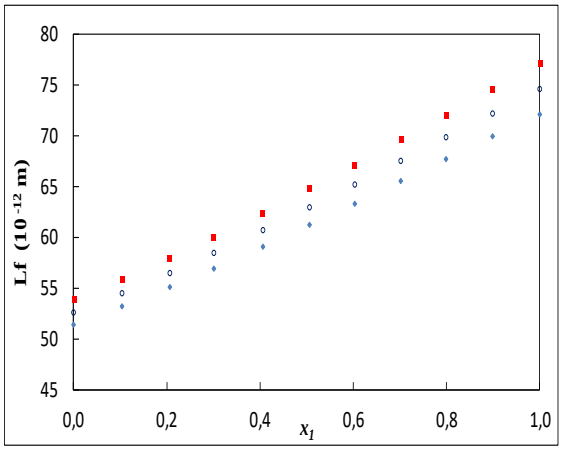

Figure 1.18: Plot of intermolecular free length (L_f) for the binary mixtures: (a) {1-hexene (1) + 2-methoxyethanol (2)}, (b) {1-hexene (1) + 2-ethoxyethanol (2)}, (c) {1-hexene (1) + 2-butoxyethanol (2)} as function of the composition expressed in the mole fraction of 1-hexene at 293.15 K (◆), 298.15 K (○), and 303.15 K (■).

1.5.2.3 Specific acoustic impedance

The specific acoustic impedance Z is the parameter related to the inertial and elastic properties of the medium (Awasthi et al., 2003). Therefore, it is important to analyze specific acoustic impedance in relation to concentration and temperature. The dependence of Z on the concentration of 22MEE or furfural or 1-hexene is shown graphically in Figures 1.19(a-f), 1.20(a-c), 1.21(a-c). As figures shown, the specific acoustic impedance of 22MEE mixtures and the two binary systems (furfural + DMSO) and (furfural + acetonitrile) increases by increasing the concentration and decreases for (furfural + sulfolane) and all 1-hexene mixtures. The specific acoustic impedance Z exhibits a decreasing trend with temperature for all investigated mixtures.

Figure 1.19 (a)

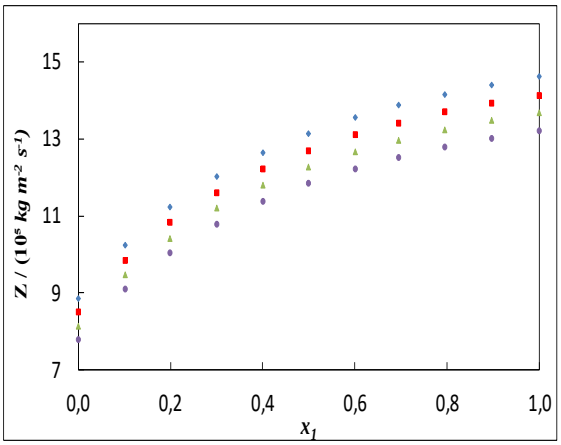

Figure 1.19 (b)

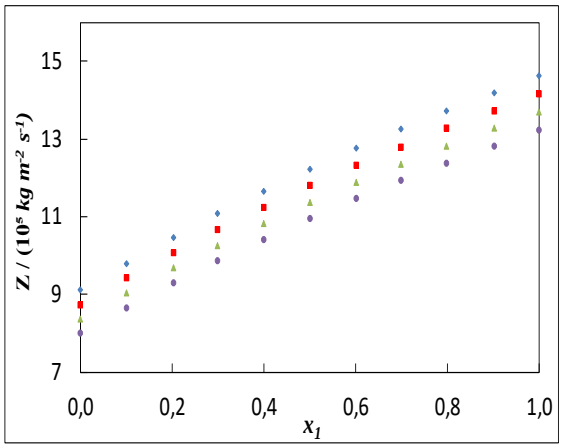

Figure 1.19 (c)

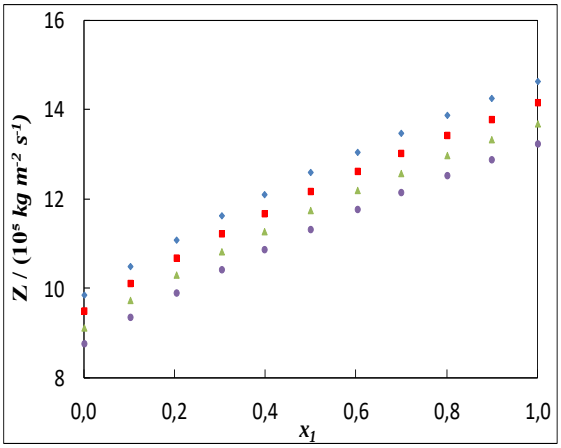

Figure 1.19 (d)

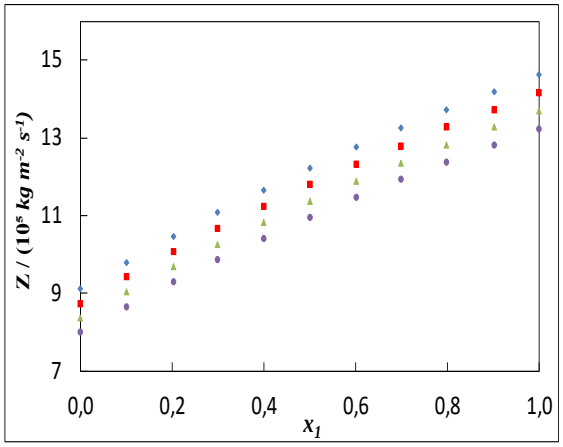

Figure 1.19 (e)

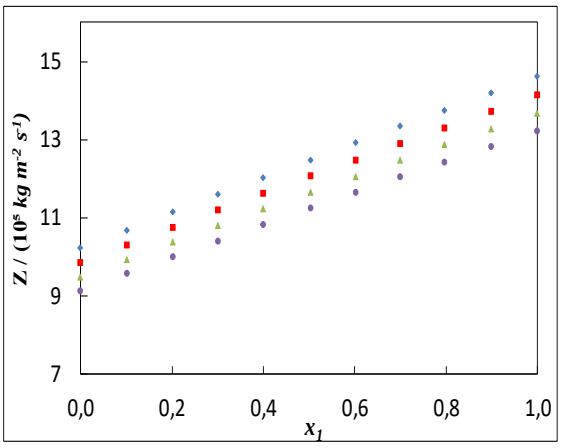

Figure 1.19 (f)

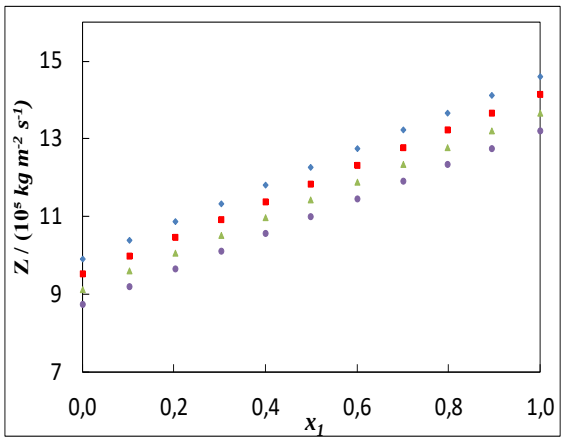

Figure 1.19: Plot of specific acoustic impedance (Z) for the binary mixtures: (a) {22MEE (1) + methanol (2)}, (b) {22MEE (1) + ethanol (2)}, (c) {22MEE (1) + propan-1-ol (2)}, (d) {22MEE (1) + propan-2-ol (2)}, (e) {22MEE (1) + butan-1-ol (2)}, and (f) {22MEE (1) + butan-2-ol (2)} as function of the composition expressed in the mole fraction of 22MEE at 293.15 K (◆), 303.15 K (■), 313.15 K (▲) and 323.15K (●).

Figure 1.20 (a)

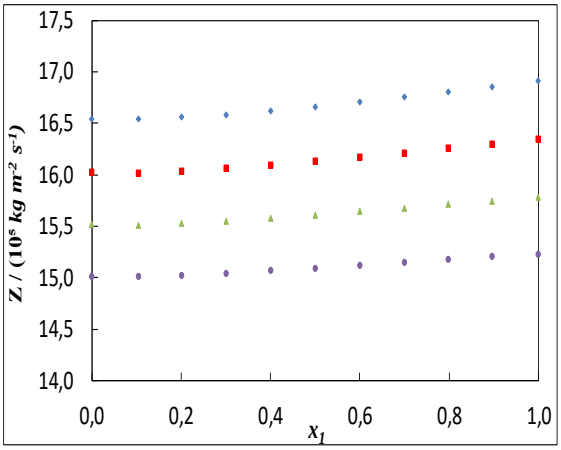

Figure 1.20 (b)

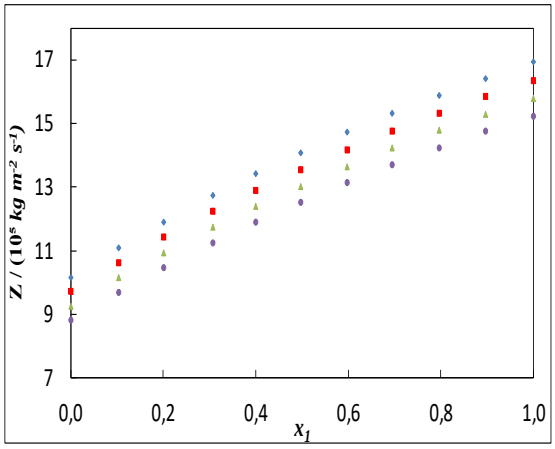

Figure 1.20 (c)

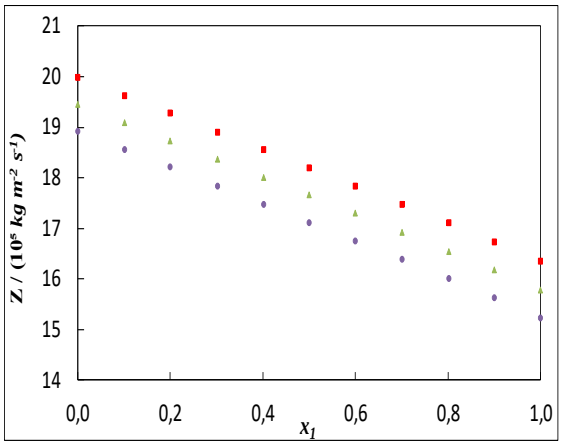

Figure 1.20: Plot of specific acoustic impedance (Z) for the binary mixtures: (a) {furfural (1) + DMSO (2)}, (b) {furfural (1) + acetonitrile (2)}, (c) {furfural (1) + sulfolane (2)} as function of the composition expressed in the mole fraction of furfural at 293.15 K (◆), 303.15 K (■), 313.15 K (▲) and 323.15 K (●).

Figure 1.21 (a)

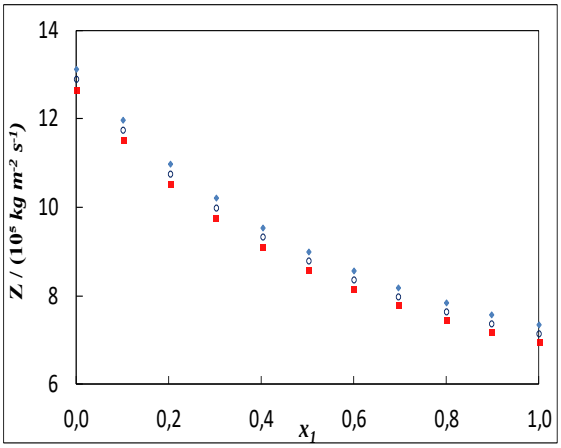

Figure 1.21 (b)

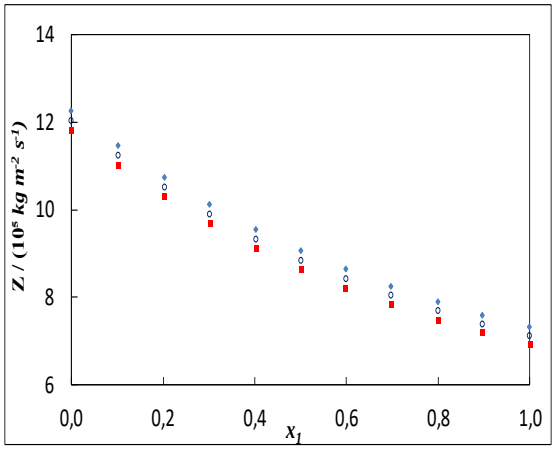

Figure 1.21 (c)

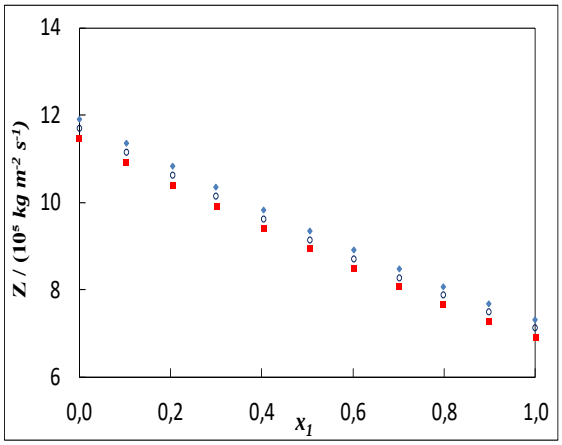

Figure 1.21: Plot of specific acoustic impedance (Z) for the binary mixtures: (a) {1-hexene (1) + 2-methoxyethanol (2)}, (b) {1-hexene (1) + 2-ethoxyethanol (2)}, (c) {1-hexene (1) + 2-butoxyethanol (2)} as function of the composition expressed in the mole fraction of 1-hexene at 293.15 K (◆), 298.15 K (○), and 303.15 K (■).

1.5.2.4 Relative association

Relative association R_A is defined as a measure of the extent of interaction between the component molecules in a real mixture relative to that in an ideal one (Ali et al., 2002).The variation of relative association R_A for all binary mixtures is presented in Figures 1.22(a-f), 1.23(a-c), 1.24(a-c), The plots indicate that the relative association R_A is not affected by temperature for all studied systems. Additionally, R_A increases with the increase of concentration for 22MEE mixtures, (furfural + DMSO) and (furfural + acetonitrile) systems inversely to (furfural + sulfolane) and all 1-hexene mixtures which reveals a decrease in R_A values.

Figure 1.22 (a)

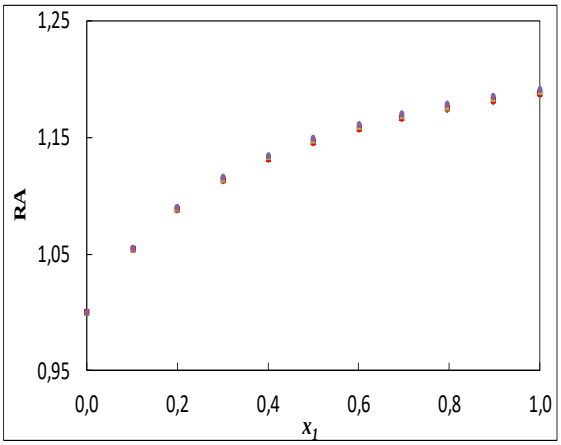

Figure 1.22 (b)

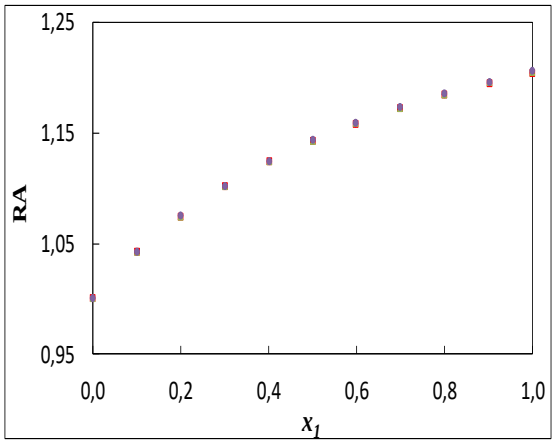

Figure 1.22 (c)

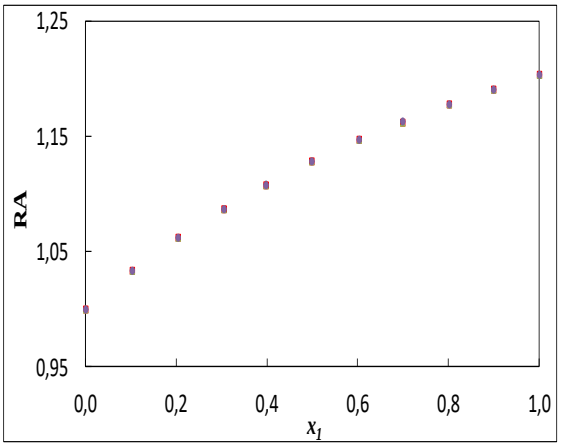

Figure 1.22 (d)

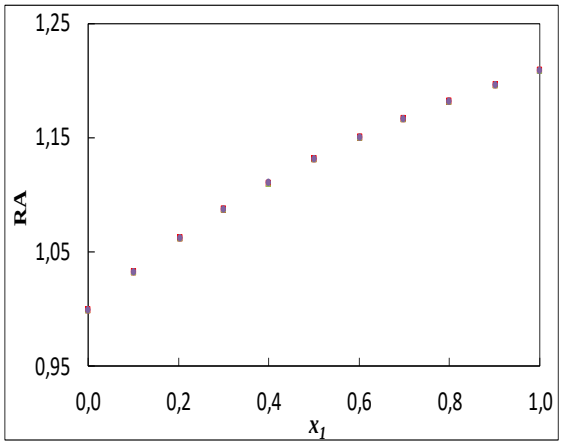

Figure 1.22 (e)

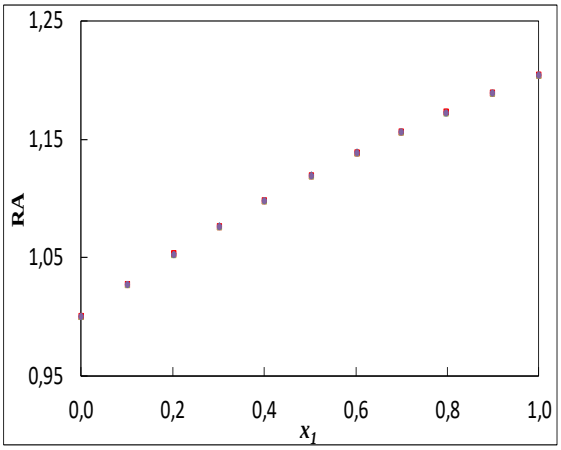

Figure 1.22 (f)

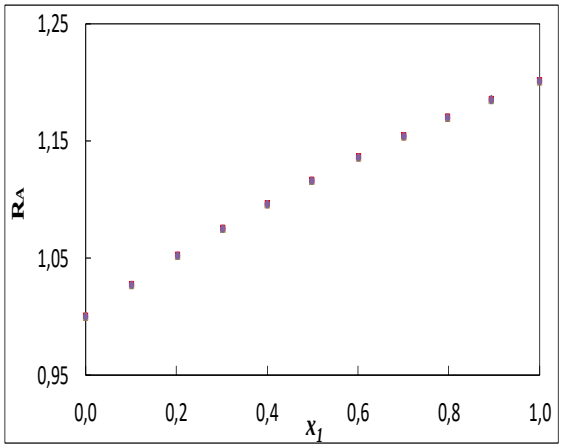

Figure 1.22: Plot of relative association (R_A) for the binary mixtures: (a) {22MEE (1) + methanol (2)}, (b) {22MEE (1) + ethanol (2)}, (c) {22MEE (1) + propan-1-ol (2)}, (d) {22MEE (1) + propan-2-ol (2)}, (e) {22MEE (1) + butan-1-ol (2)}, and (f) {22MEE (1) + butan-2-ol (2)} as function of the composition expressed in the mole fraction of 22MEE at 293.15 K (◆), 303.15 K (■), 313.15 K (▲) and 323.15K (●).

Figure 1.23 (a)

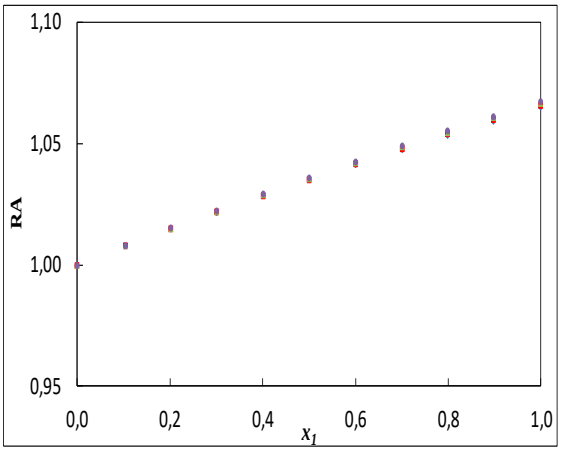

Figure 1.23 (b)

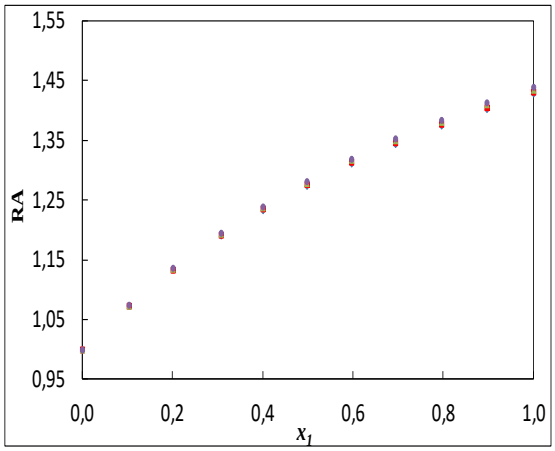

Figure 1.23 (c)

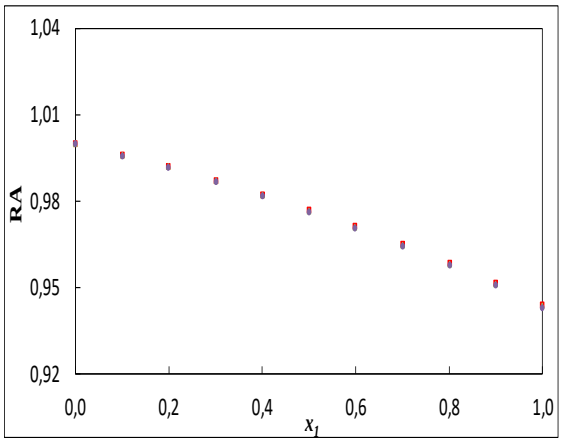

Figure 1.23: Plot of relative association (R_A) for the binary mixtures: (a) {furfural (1) + DMSO (2)}, (b) {furfural (1) + acetonitrile (2)}, (c) {furfural (1) + sulfolane (2)} as function of the composition expressed in the mole fraction of furfural at 293.15 K (◆), 303.15 K (■), 313.15 K (▲) and 323.15 K (●).

Figure 1.24 (a)

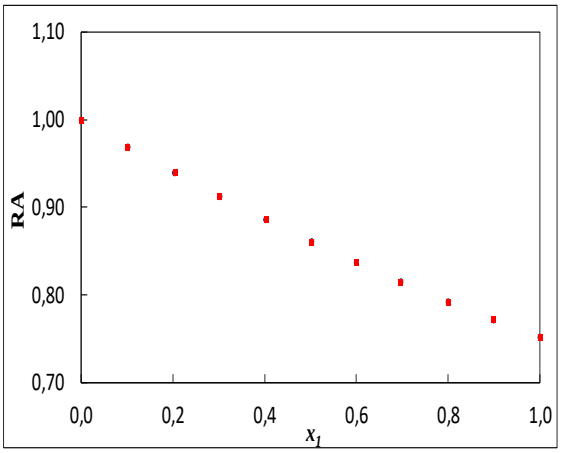

Figure 1.24 (b)

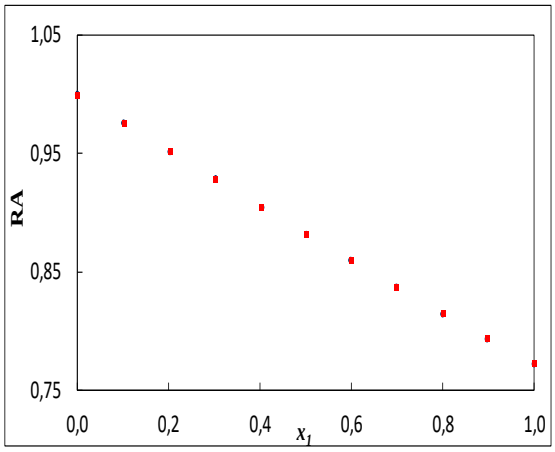

Figure 1.24 (c)

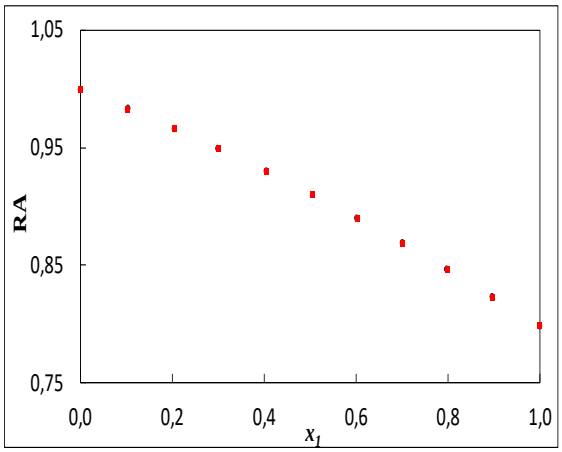

Figure 1.24: Plot of relative association (R_A) for the binary mixtures: (a) {1-hexene (1) + 2-methoxyethanol (2)}, (b) {1-hexene (1) + 2-ethoxyethanol (2)}, (c) {1-hexene (1) + 2-butoxyethanol (2)} as function of the composition expressed in the mole fraction of 1-hexene at 293.15 K (◆), 298.15 K (○), and 303.15 K (■).

1.5.2.5 Relaxation strength

The dependence of the relaxation strength r on the concentration of the solute at the investigated temperatures for all studied mixtures is shown graphically in Figures 1.25(a-f), 1.26(a-c), 1.27(a-c). Relaxation strength is found to decrease with increase in concentration for 22MEE mixtures and (furfural + acetonitrile) system and increase for both systems (furfural + DMSO), (furfural + sulfolane) and all mixtures containing 1-hexene. At a fixed concentration, it increases with temperature. The increase in r suggests the predominance of solute-solute interactions whereas the decrease in r values confirms the presence of solute-solvent interactions (Azhagiri et al., 2009; Baluja et al., 2002).

Figure 1.25 (a)

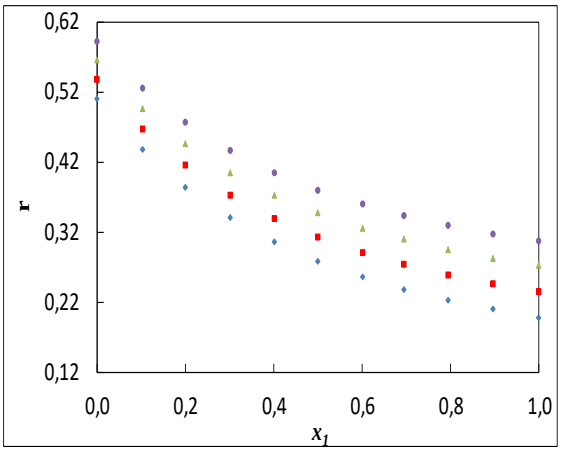

Figure 1.25 (b)

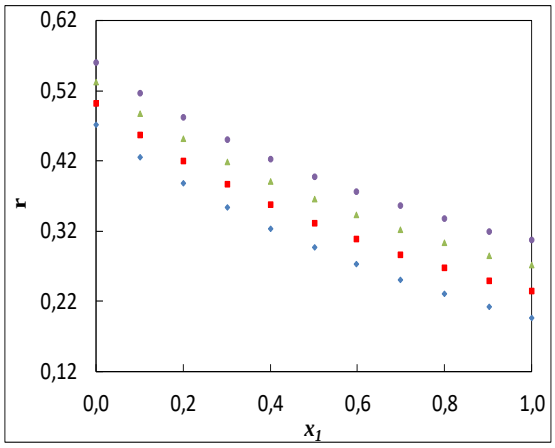

Figure 1.25 (c)

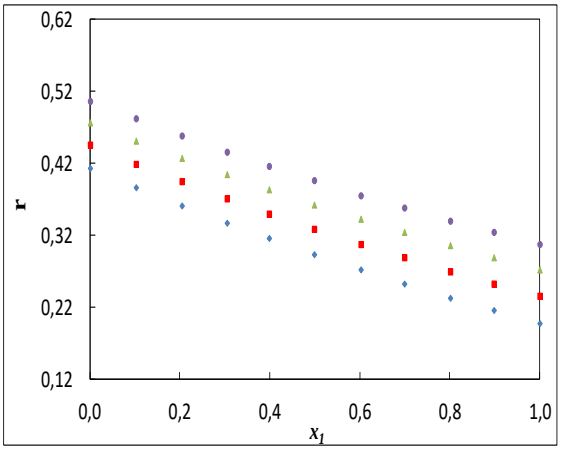

Figure 1.25 (d)

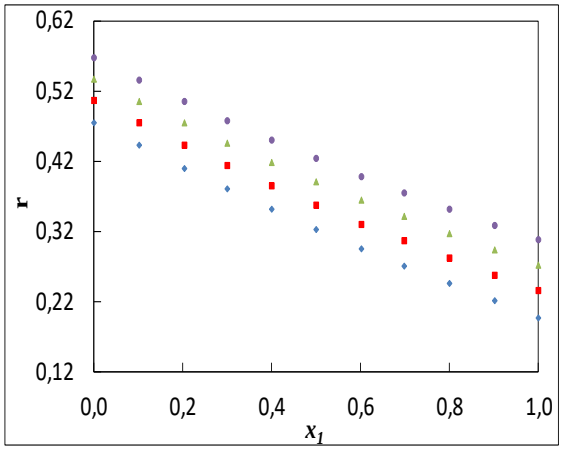

Figure 1.25 (e)

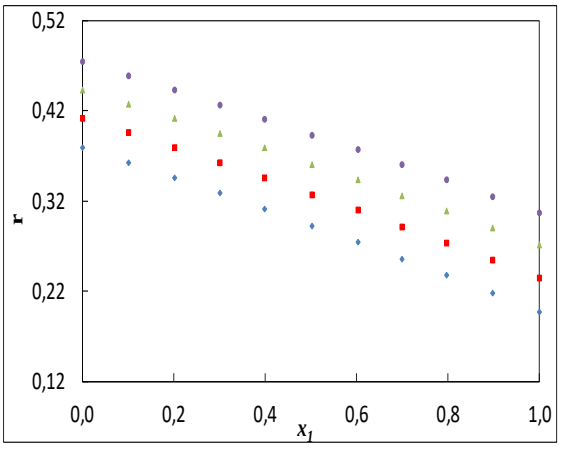

Figure 1.25 (f)

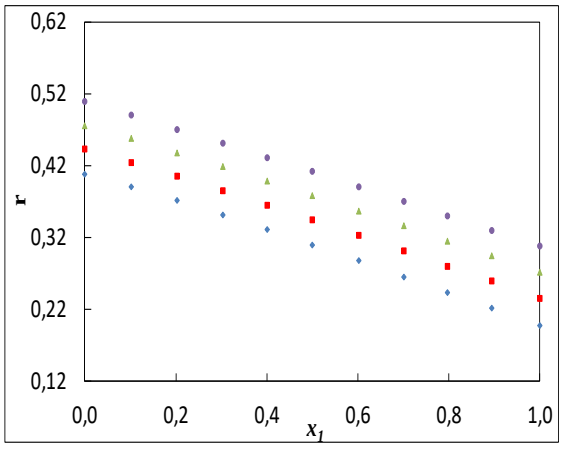

Figure 1.25: Plot of relaxation strength (r) for the binary mixtures: (a) {22MEE (1) + methanol (2)}, (b) {22MEE (1) + ethanol (2)}, (c) {22MEE (1) + propan-1-ol (2)}, (d) {22MEE (1) + propan-2-ol (2)}, (e) {22MEE (1) + butan-1-ol (2)}, and (f) {22MEE (1) + butan-2-ol (2)} as function of the composition expressed in the mole fraction of 22MEE at 293.15 K (◆), 303.15 K (■), 313.15 K (▲) and 323.15K (●).

Figure 1.26 (a)

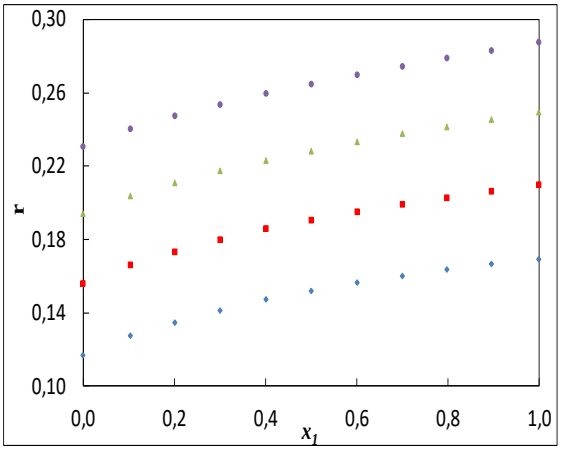

Figure 1.26 (b)

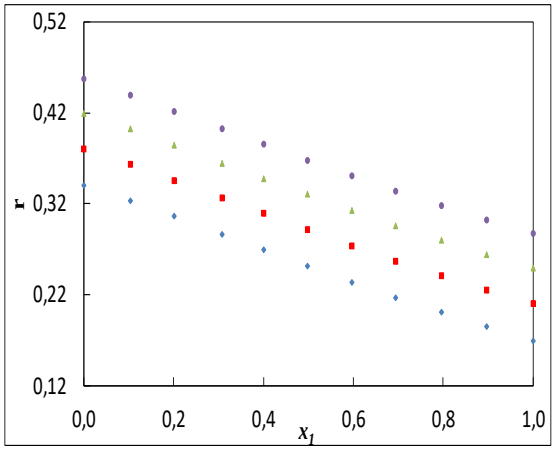

Figure 1.26 (c)

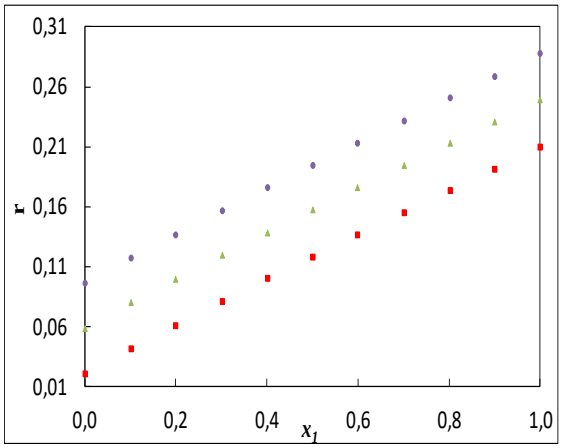

Figure 1.26: Plot of relaxation strength (r) for the binary mixtures: (a) {furfural (1) + DMSO (2)}, (b) {furfural (1) + acetonitrile (2)}, (c) {furfural (1) + sulfolane (2)} as function of the composition expressed in the mole fraction of furfural at 293.15 K (◆), 303.15 K (■), 313.15 K (▲) and 323.15 K (●).

Figure 1.27 (a)

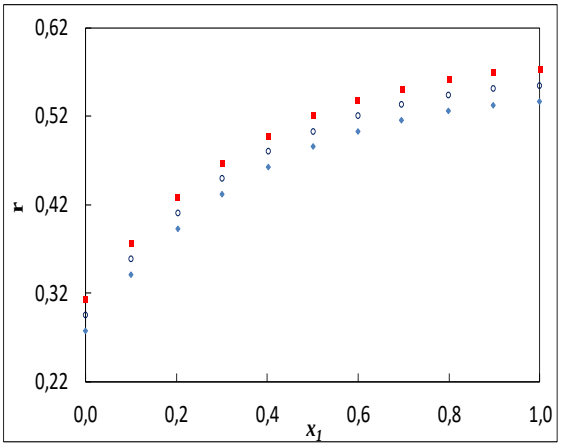

Figure 1.27 (b)

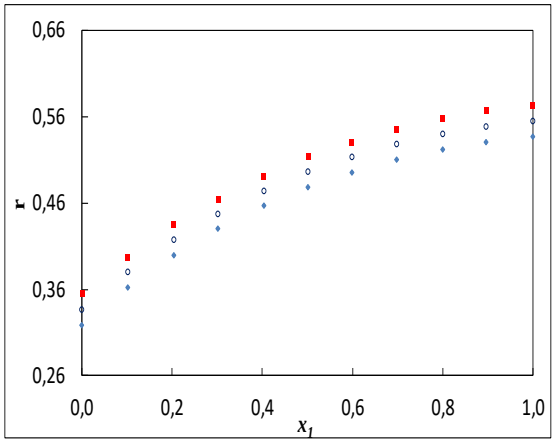

Figure 1.27 (c)

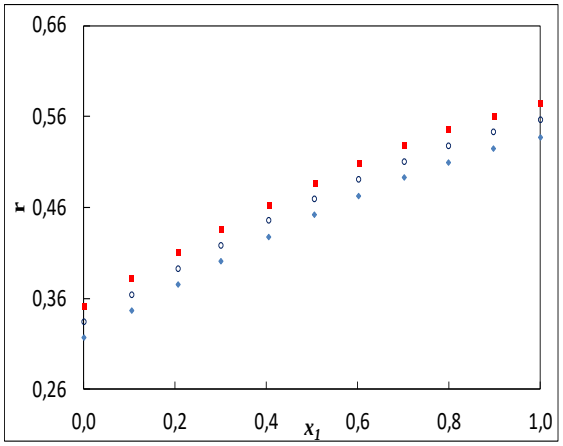

Figure 1.27: Plot of relaxation strength (r) for the binary mixtures: (a) {1-hexene (1) + 2-methoxyethanol (2)}, (b) {1-hexene (1) + 2-ethoxyethanol (2)}, (c) {1-hexene (1) + 2-butoxyethanol (2)} as function of the composition expressed in the mole fraction of 1-hexene at 293.15 K (◆), 298.15 K (○), and 303.15 K (■).

1.5.2.6 Rao's molar sound function

Figures 1.28(a-f), 1.29(a-c), 1.30(a-c) present the results of Rao's molar sound function R for all investigated systems at different temperatures. It can be seen that the variation in R is linearly increasing with the concentration for 22MEE mixtures, (furfural + acetonitrile), (furfural + DMSO), (1-hexene + 2-methoxyethanol) and (1-hexene + 2-ethoxyethanol) systems and decreasing for (furfural + sulfolane) and (1-hexene + 2-butoxyethanol) systems. Also, the R values are independent of temperature for all studied mixtures.

Figure 1.28 (a)

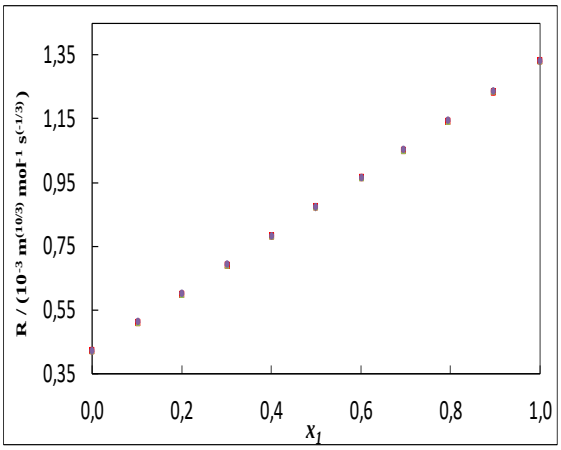

Figure 1.28 (b)

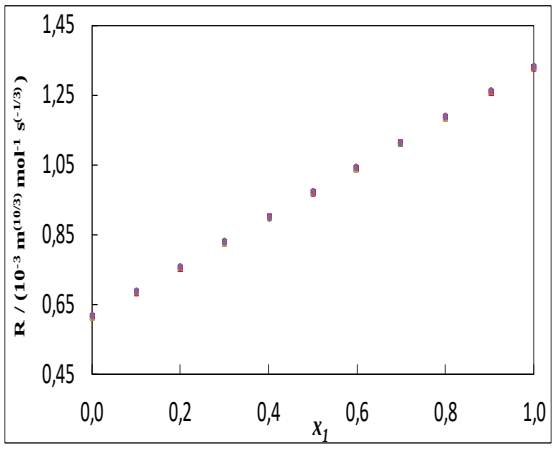

Figure 1.28 (c)

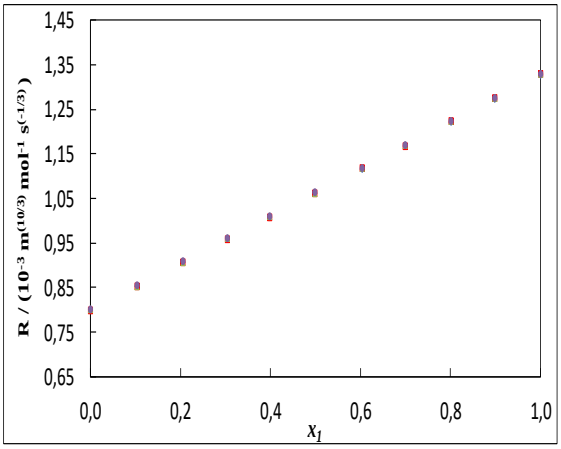

Figure 1.28 (d)

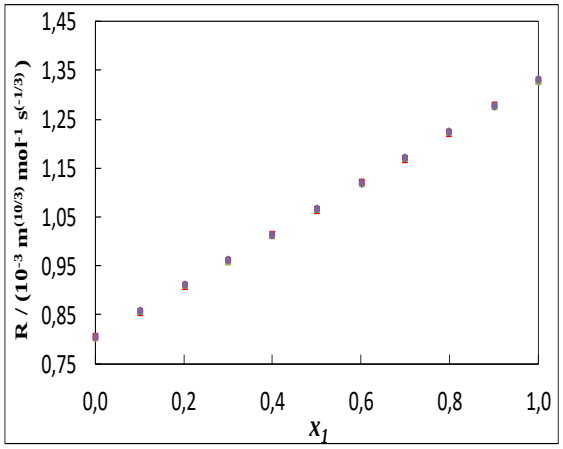

Figure 1.28 (e)

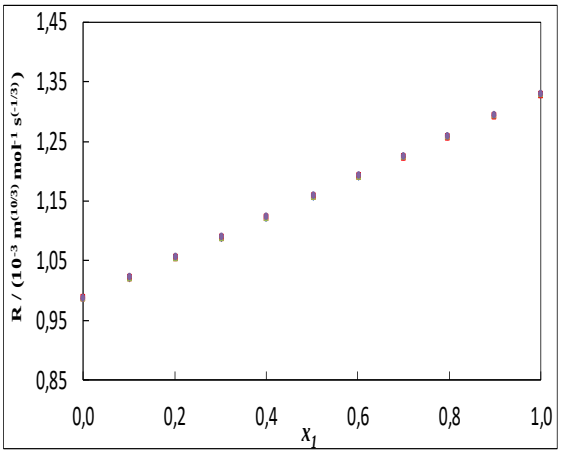

Figure 1.28 (f)

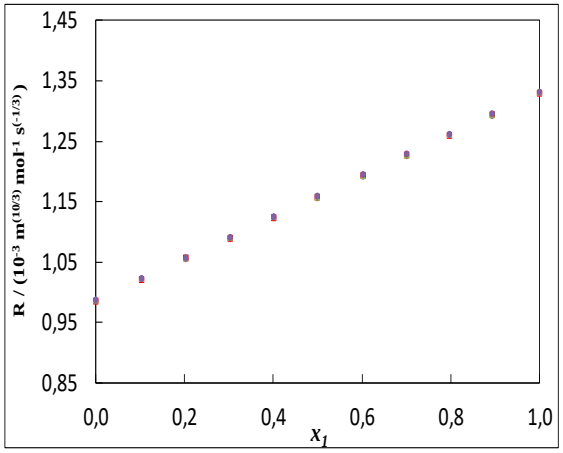

Figure 1.28: Plot of Rao's molar sound function (R) for the binary mixtures: (a) {22MEE (1) + methanol (2)}, (b) {22MEE (1) + ethanol (2)}, (c) {22MEE (1) + propan-1-ol (2)}, (d) {22MEE (1) + propan-2-ol (2)}, (e) {22MEE (1) + butan-1-ol (2)}, and (f) {22MEE (1) + butan-2-ol (2)} as function of the composition expressed in the mole fraction of 22MEE at 293.15 K (◆), 303.15 K (■), 313.15 K (▲) and 323.15K (●).

Figure 1.29 (a)

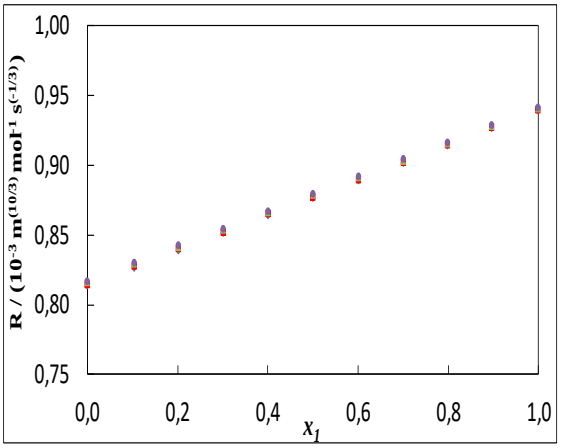

Figure 1.29 (b)

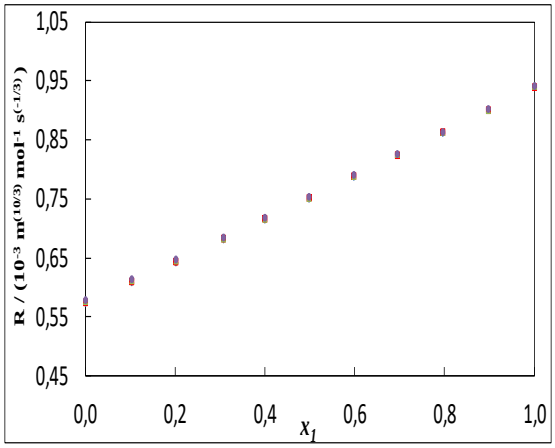

Figure 1.29 (c)

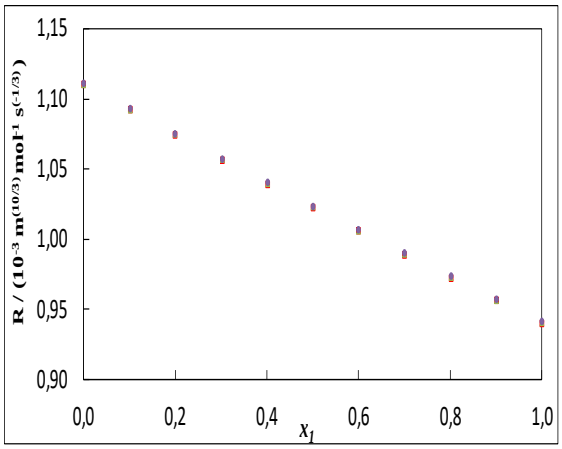

Figure 1.29: Plot of Rao's molar sound function (R) for the binary mixtures: (a) {furfural (1) + DMSO (2)}, (b) {furfural (1) + acetonitrile (2)}, (c) {furfural (1) + sulfolane (2)} as function of the composition expressed in the mole fraction of furfural at 293.15 K (◆), 303.15 K (■), 313.15 K (▲) and 323.15 K (●).

Figure 1.30 (a)

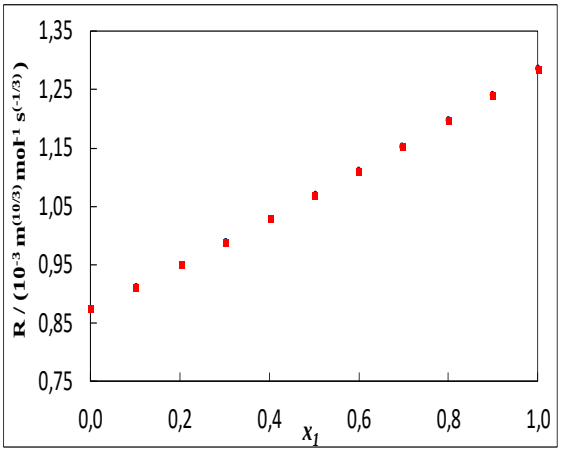

Figure 1.30 (b)

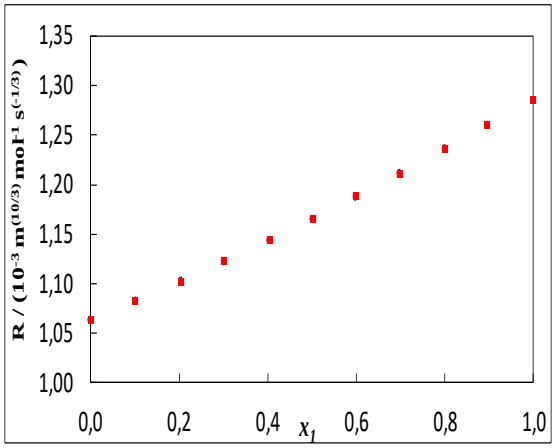

Figure 1.30 (c)

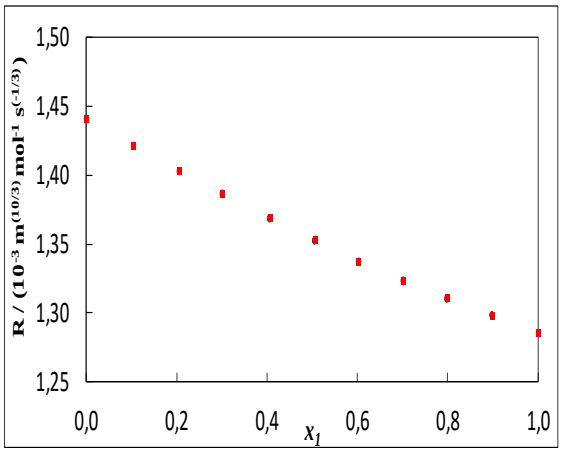

Figure 1.30: Plot of Rao's molar sound function (R) for the binary mixtures: (a) {1-hexene (1) + 2-methoxyethanol (2)}, (b) {1-hexene (1) + 2-ethoxyethanol (2)}, (c) {1-hexene (1) + 2-butoxyethanol (2)} as function of the composition expressed in the mole fraction of 1-hexene at 293.15 K (◆), 298.15 K (○), and 303.15 K (■).

1.5.3 Excess properties

The deviations in excess functions from ideality provide a relatively better tool to assess the strength of interactions between the component molecules of the binary mixtures. Excess values of molar volume (V_m^E), deviations in isentropic compressibility ($\Delta\kappa_s$), deviations in intermolecular free length (ΔL_f), deviations in acoustic impedance (ΔZ), deviations in speed of sound (Δu) and changes in refractive index (Δn_D) were evaluated from the experimental data for all the studied mixtures at same experimental conditions and given in Tables 1.9, 1.10 and 1.11. The variations of the above mentioned properties with the mole fraction of 22MEE or furfural or 1-hexene are presented graphically in Figures 1.31(a-f), 1.34(a-c), 1.35(a-c), 1.36(a-f), 1.37(a-c), 1.38(a-c), 1.39(a-f), 1.40(a-c), 1.41(a-c), 1.42(a-f), 1.43(a-c), 1.44(a-c), 1.45(a-f), 1.46(a-c), 1.47(a-c), 1.48(a-f), 1.49(a-c), 1.50(a-c).

1.5.3.1 Excess molar volume

The excess molar volumes, V_m^E, for the studied systems were calculated from densities of the pure liquids and their mixtures using standard equation given above.

The corresponding V_m^E values of 22MEE mixtures measured at different temperatures are presented in Table A1.9 and plotted against mole fraction of 22MEE in Figure 1.31(a-f). For the binary mixtures of (22MEE + methanol or + ethanol or + propan-1-ol), the negative values of V_m^E are observed. The V_m^E values of the (22MEE + methanol) mixture are more negative than those observed for the (22MEE + ethanol) and (22MEE + propan-1-ol) mixtures. For the mixtures of (22MEE with butan-1-ol or butan-2-ol), the positive V_m^E values increase systematically in the order stated for the liquids. Both positive and negative V_m^E values are observed for the (22MEE + propan-2-ol) system, which has a sinusoidal shape.

The molecules of the alkoxyalkanols are self-associated as the alcohols (Barbés et al., 1994). The effect of the simultaneous presence of etheric and alcoholic oxygen atoms in the same molecule of alkoxyalkanol and the presence of the etheric oxygen improve the ability of the -OH group (Buckley and Brochu, 1972) to form hydrogen bonds in the alkoxyalkanol molecules. As already mentioned below, the V_m^E values are negative over the complete composition range in the case of methanol, ethanol and propan-1-ol systems and positive for the butan-1-ol and butan-2-ol systems. These results may be explained by the depolymerisation of self-associated alkoxyalkanols by the alcohols and self-associated alcohols by the alkoxyalkanols which contributes to the expansion of volume and the hydrogen bond formation between alkoxyalkanols and alcohols which leads to volume contraction (Ramana et al., 1996). According to V_m^E results, we can suggest that expansion of volume is dominant in butan-1-ol and butan-2-ol systems while the contraction in volume is dominant in methanol, ethanol and propan-1-ol systems. The positive deviations are mostly due to H-bond breaking while negative could be due to weak specific interactions between unlike molecules (Ramana et al., 1996). The V_m^E values decrease with an increase of temperature for (22MEE + methanol, or + ethanol, or + propan-2-ol, or + butan-2-ol) binary mixtures may be due to a decrease of packing efficiency between 22MEE and methanol, or + ethanol, or + propan-2-ol, or + butan-2-ol and vice versa for (22MEE + propan-1-ol, or + butan-1-ol) binary mixtures where increases.

Also, excess molar volumes, V_m^E, values increase as the chain length of alcohol increases at the same temperature. However, 22MEE interacts more strongly with methanol.

The excess molar volumes, V_m^E, for the binary mixtures {22MEE (1) + butan-1-ol (2) at temperature of (293.15, 303.15, 313.15 and 323.15) K together with literature data reported by (Mozo et al., 2007) at (293.15 and 303.15) K and those reported by (Cobos et al., 1988) at 298.15 K were plotted in Figures 1.32 and 1.33 respectively for the comparison purpose. From these figures, it can be observed that the experimental, V_m^E, values are in a good accordance with literature data reported by (Mozo et al., 2007) and by (Cobos et al., 1988) respectively.

Inspection of Figure 1.34(a-c) reveals that the excess molar volume $V_m{}^E$ values are positive over the complete composition range for the system (furfural + DMSO) and negative for both (furfural + acetonitrile) and (furfural + sulfolane) systems. It's well known that the furfural molecules are dipolar associate in the pure state (Kulnevich et al., 1972), these dipolar associates are breaking by the addition of polar solvents. The positive values of $V_m{}^E$ are due to mutual breaking of hydrogen-bonding structures in the mixtures resulting in expansion in volume (Ali et al., 2005).The predominance of hydrogen bond interactions between the unlike molecules over the dissociation effects in the mixtures is indicated by the negative values of $V_m{}^E$ (Radojković at al., 1977; Homer et al., 1973; Grolier et al., 1975). The magnitudes of $V_m{}^E$ values follow the sequence: (furfural + DMSO) > (furfural + sulfolane) > (furfural + acetonitrile), from these results it's clear that the interaction of furfural with acetonitrile is stronger than furfural with sulfolane than furfural with DMSO.

The calculated data of $V_m{}^E$ for the three binary systems containing 1-hexene at different temperatures are presented in Table A1.11, and the representative curves are shown in Figure 1.35(a-c). Both positive and negative $V_m{}^E$ values are observed for all the studied mixtures at all temperatures. Positive values of $V_m{}^E$ are due to H-bond breaking while negative are mostly because of weak specific interactions between the mixing components (Shi et al., 2019; Sarkar et al., 2009). Alkoxyalkanols molecules are self-associated, the presence of etheric and alcoholic oxygen atoms in the same molecule and the presence of the etheric oxygen lead to hydrogen bonds formation in the alkoxyalkanols molecules (Barbés et al., 1994; Buckley et al., 1972). For the binary mixtures (1-hexene + 2-methoxyethanol or 2-ethoxyethanol) $V_m{}^E$ values shifted from negative to positive at lower concentration of 1-hexene while the binary mixture (1-hexene + 2-butoxyethanol) shows negative values at all temperatures and over the whole range of mole fractions of 1-hexene except at $x_1 = 0.9$. The negative $V_m{}^E$ values of lower and higher concentration of 1-hexene for (1-hexene + 2-methoxyethanol or 2-ethoxyethanol) and (1-hexene + 2-butoxyethanol) suggest a minimal interaction between alkoxyalkanols with 1-hexene depending on the amount of each constituent is available in the solution.

Figure 1.31 (a)

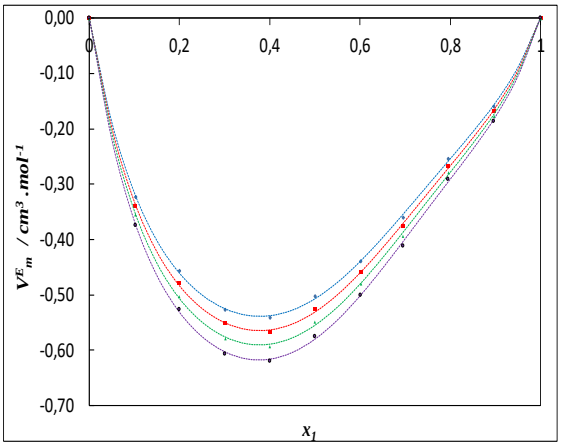

Figure 1.31 (b)

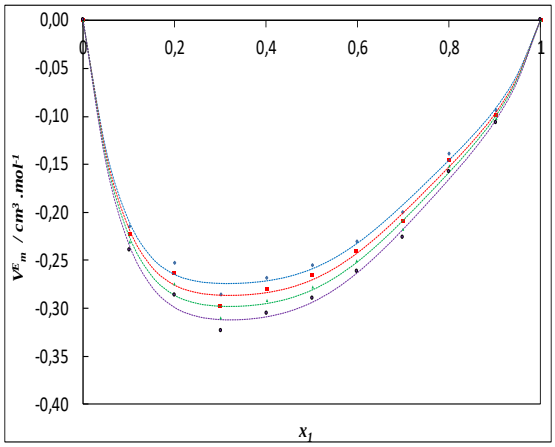

Figure 1.31 (c)

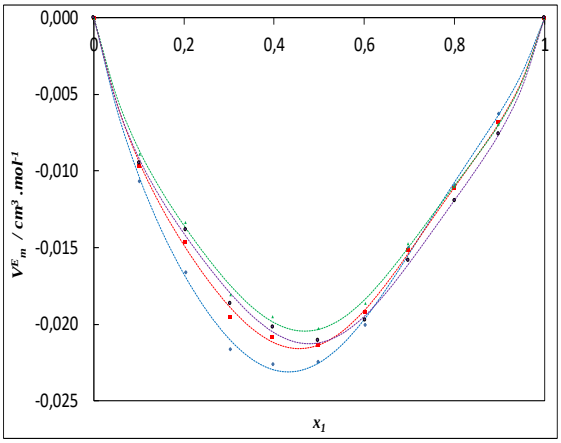

Figure 1.31 (d)

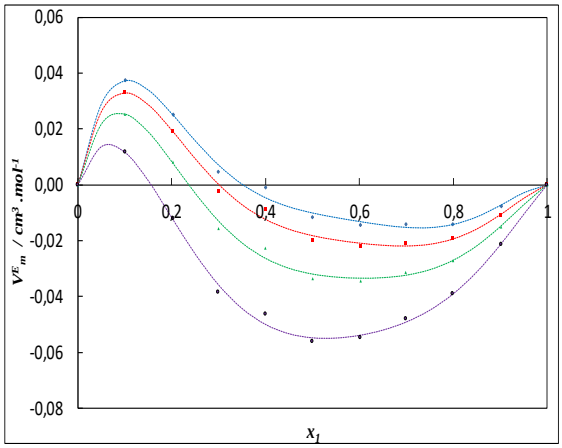

Figure 1.31 (e)

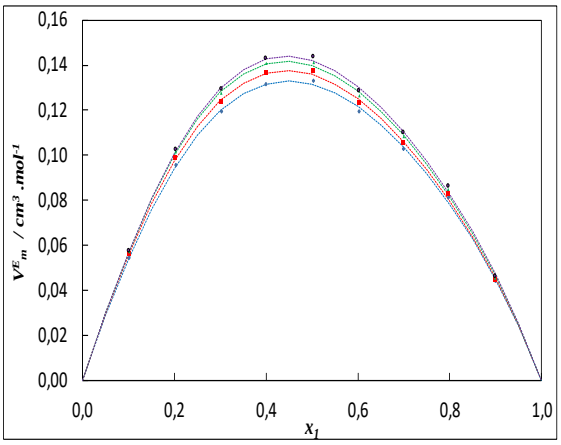

Figure 1.31 (f)

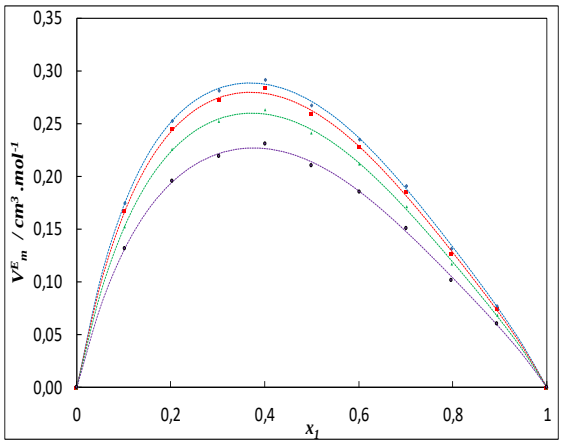

Figure 1.31: Plot of excess molar volumes V_m^E for the binary mixtures: (a) {22MEE (1) + methanol (2)}, (b) {22MEE (1) + ethanol (2)}, (c) {22MEE (1) + propan-1-ol (2)}, (d) {22MEE (1) + propan-2-ol (2)}, (e) {22MEE (1) + butan-1-ol (2)}, and (f) {22MEE (1) + butan-2-ol (2)} as function of the composition expressed in the mole fraction of 22MEE at 293.15 K (◆), 303.15 K (■), 313.15 K (▲) and 323.15K (●). The dotted lines were generated using Redlich-Kister polynomial curve-fitting.

Figure 1.32 (a) **Figure 1.32 (b)**

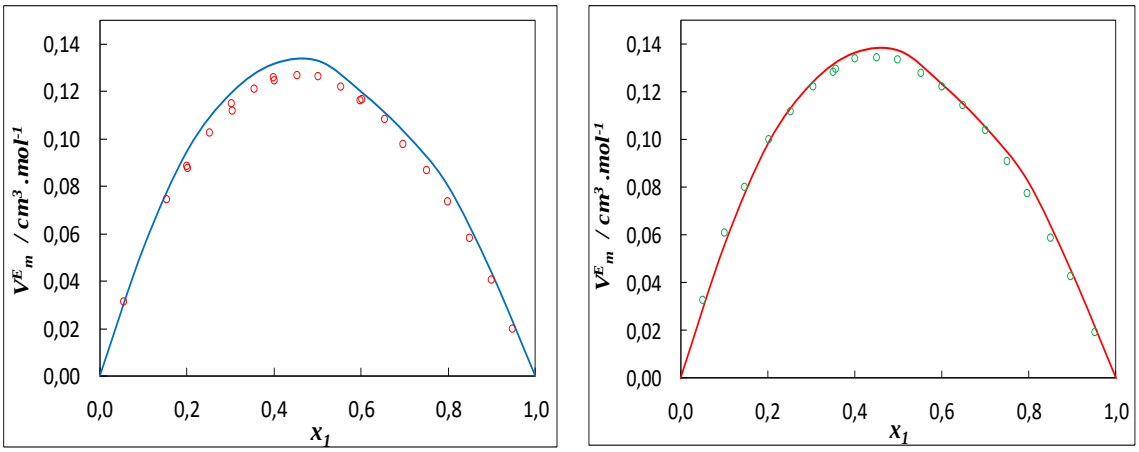

Figure 1.32: Plot of excess molar volumes, V_m^E, for the binary mixtures {22MEE (1) + butan-1-ol (2)} at (a) 293.15 K (—) and (b) 303.15 K (—) together with those reported by Mozo et al. (2007) at (a) 293.15 K (o) and (b) 303.15 K (o).

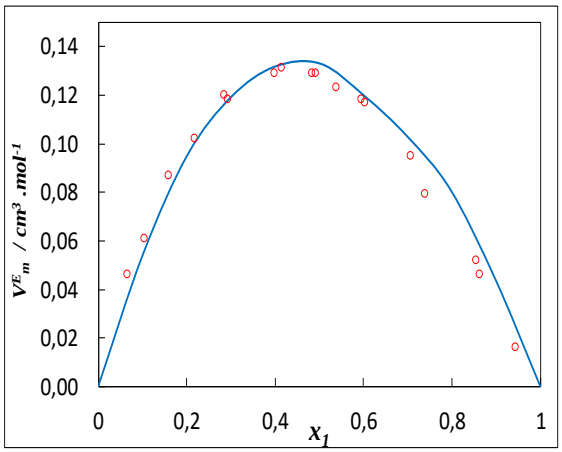

Figure 1.33: Plot of excess molar volumes, V_m^E, for the binary mixtures {22MEE (1) + butan-1-ol (2)} at 293.15 K (—) together with those reported by Cobos et al. (1988) at 298.15 K (o).

Figure 1.34 (a)

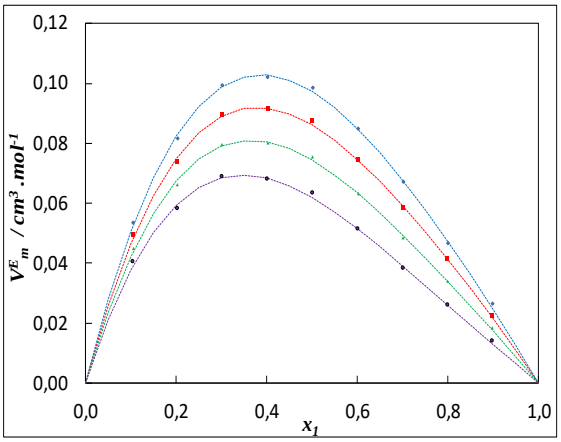

Figure 1.34 (b)

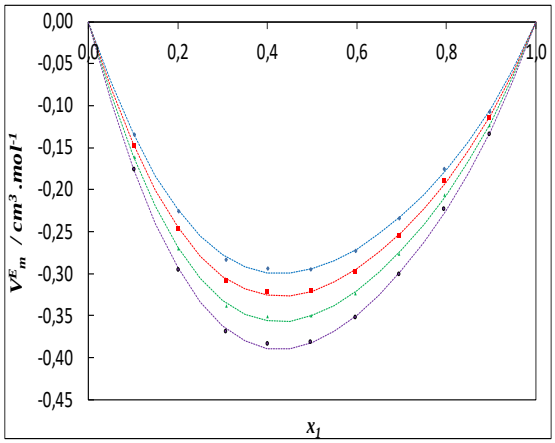

Figure 1.34 (c)

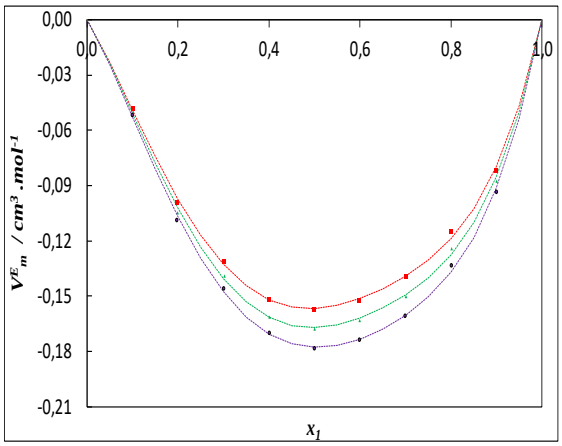

Figure 1.34: Plot of excess molar volumes V_m^E for the binary mixtures: (a) {furfural (1) + DMSO (2)}, (b) {furfural (1) + acetonitrile (2)}, (c) {furfural (1) + sulfolane (2)} as function of the composition expressed in the mole fraction of furfural at 293.15 K (◆), 303.15 K (■), 313.15 K (▲) and 323.15 K (●). The dotted lines were generated using Redlich-Kister polynomial curve-fitting.

Figure 1.35 (a)

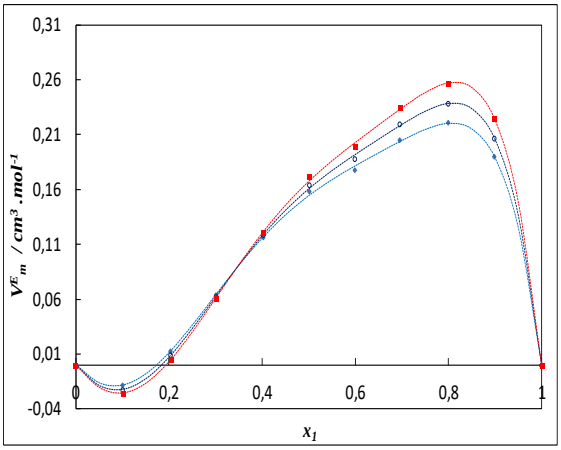

Figure 1.35 (b)

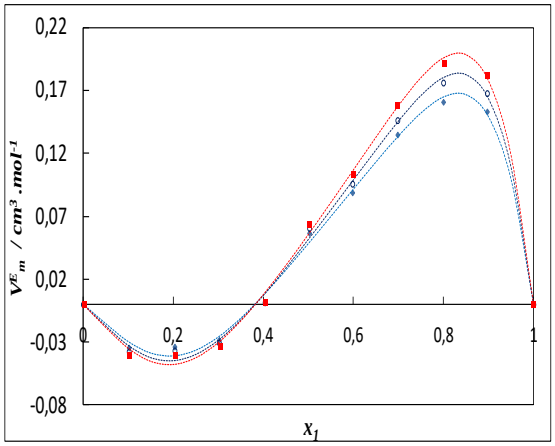

Figure 1.35 (c)

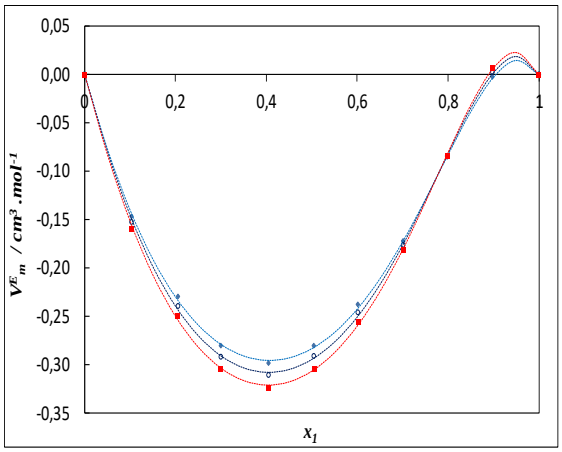

Figure 1.35: Plot of excess molar volumes V_m^E for the binary mixtures: (a) {1-hexene (1) + 2-methoxyethanol (2)}, (b) {1-hexene (1) + 2-ethoxyethanol (2)}, (c) {1-hexene (1) + 2-butoxyethanol (2)} as function of the composition expressed in the mole fraction of 1-hexene at 293.15 K (◆), 298.15 K (○), and 303.15 K (■). The dotted lines were generated using Redlich-Kister polynomial curve-fitting.

1.5.3.2 Deviation in isentropic compressibility

The deviation in isentropic compressibility $\Delta\kappa_s$ over the entire composition range for all studied mixtures is included in Tables 1.9, 1.10 and 1.11 and the plots are presented in Figures 1.36(a-f), 1.37(a-c), 1.38(a-c).

As the results show in Figure 1.36(a-f), the $\Delta\kappa_s$ values are negative over the entire mole fraction range and become more negative with increasing temperatures for all binary mixtures containing 22MEE.

It can be seen from Figure 1.37(a-c) that $\Delta\kappa_s$ values are positive for (furfural + DMSO) mixture and negative for (furfural + acetonitrile) and (furfural + sulfolane) systems. Increasing temperature for all furfural mixtures leads to a decrease in $\Delta\kappa_s$ values.

Isentropic compressibility for 1-hexene mixtures is presented in Figure 1.38(a-c). From Figure 1.38(a-c), it can be seen that $\Delta\kappa_s$ values are all positive for the first and the second binary mixtures (1-hexene + 2-methoxyethanol) and (1-hexene + 2-ethoxyethanol) at all temperatures except at the mole fraction $x_1 = 0.1$ of the second binary mixtures where the $\Delta\kappa_s$ values are negative at 298.15 and 303.15 K. For the third binary mixture (1-hexene + 2-butoxyethanol), the values of $\Delta\kappa_s$ are all negative at all temperatures.

The observed negative deviations in isentropic compressibility can be explained in terms of specific interactions between molecules in mixtures which provides decreasing in the free-space (Choudary et al., 1982; Dharmaraju et al., 1982; Benson et al., 1981). Positive deviation indicates weak interactions between component molecules resulting from the disruption of molecular association (Thanuja et al., 2012).

Figure 1.36 (a)

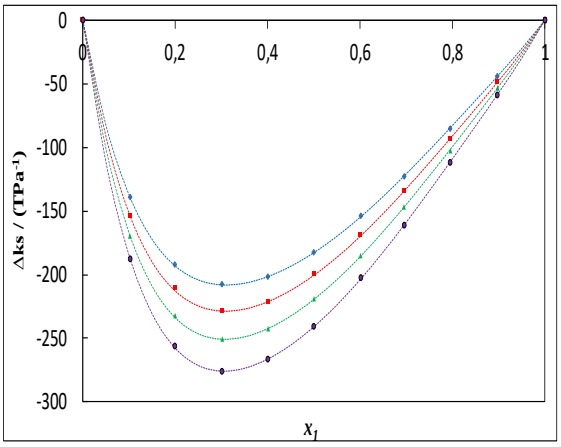

Figure 1.36 (b)

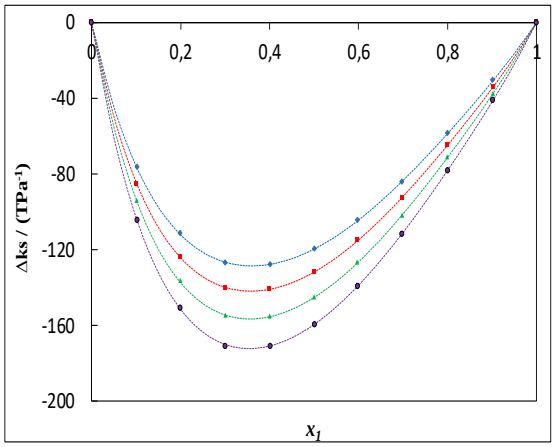

Figure 1.36 (c)

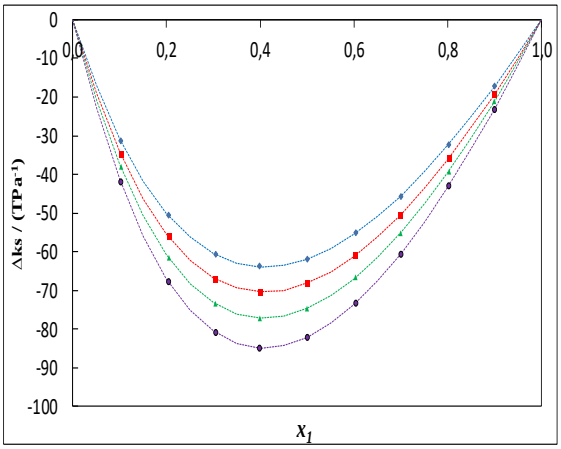

Figure 1.36 (d)

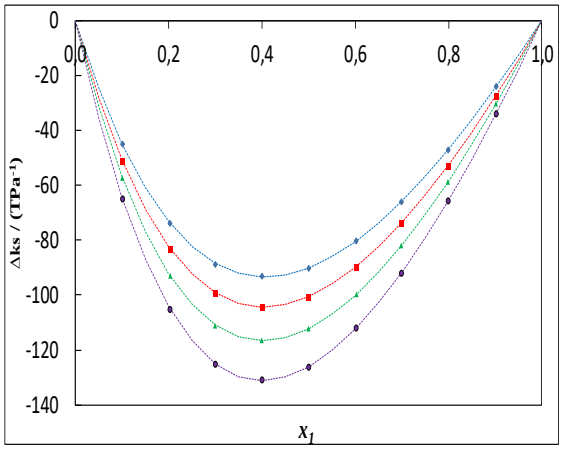

Figure 1.36 (e)

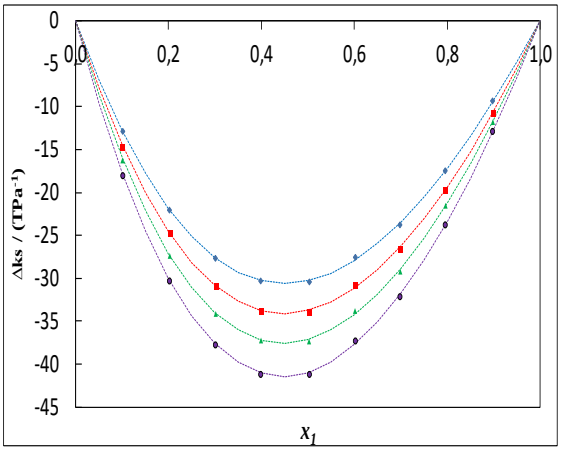

Figure 1.36 (f)

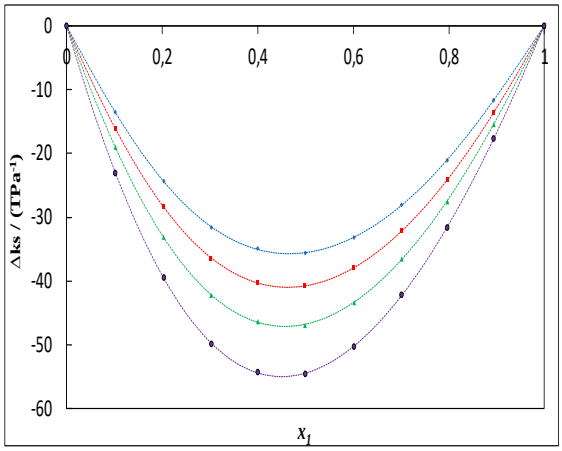

Figure 1.36: Plot of deviations in isentropic compressibility $\Delta\kappa_s$ for the binary mixtures: (a) {22MEE (1) + methanol (2)}, (b) {22MEE (1) + ethanol (2)}, (c) {22MEE (1) + propan-1-ol (2)}, (d) {22MEE (1) + propan-2-ol (2)}, (e) {22MEE (1) + butan-1-ol (2)}, and (f) {22MEE (1) + butan-2-ol (2)} as function of the composition expressed in the mole fraction of 22MEE at 293.15 K (◆), 303.15 K (■), 313.15 K (▲) and 323.15K (●). The dotted lines were generated using Redlich-Kister polynomial curve-fitting.

Figure 1.37 (a)

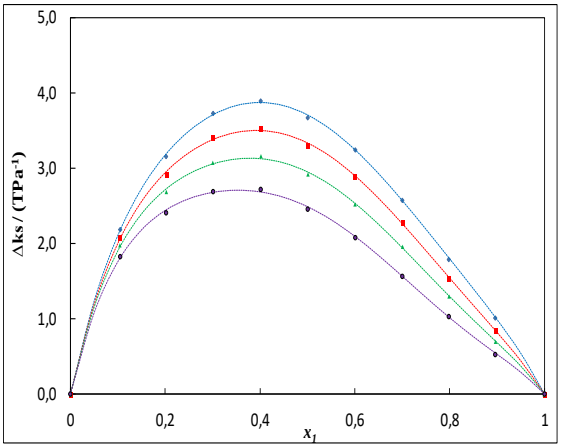

Figure 1.37 (b)

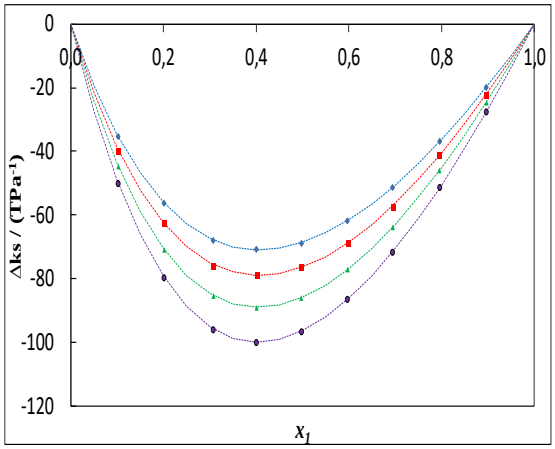

Figure 1.37 (c)

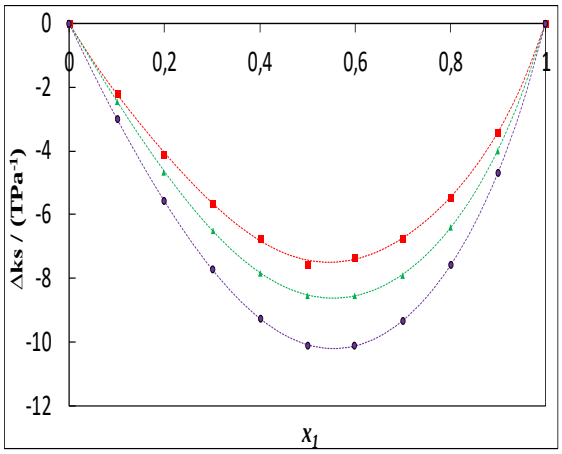

Figure 1.37: Plot of deviations in isentropic compressibility $\Delta\kappa_s$ for the binary mixtures: (a) {furfural (1) + DMSO (2)}, (b) {furfural (1) + acetonitrile (2)}, (c) {furfural (1) + sulfolane (2)} as function of the composition expressed in the mole fraction of furfural at 293.15 K (◆), 303.15 K (■), 313.15 K (▲) and 323.15 K (●). The dotted lines were generated using Redlich-Kister polynomial curve-fitting.

Figure 1.38 (a)

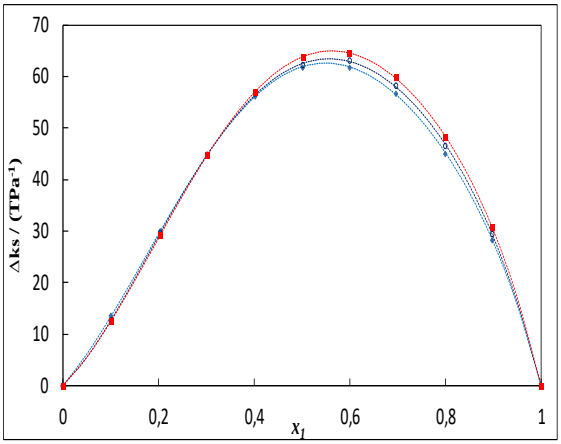

Figure 1.38 (b)

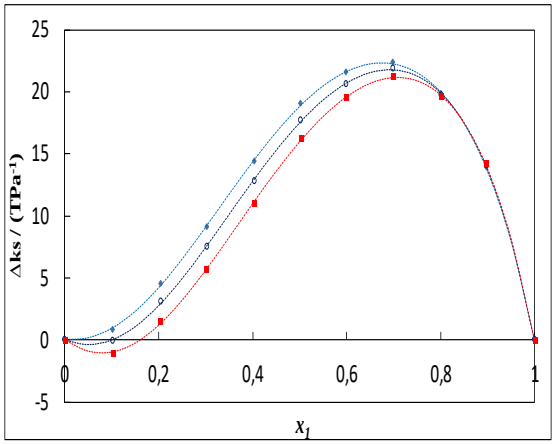

Figure 1.38 (c)

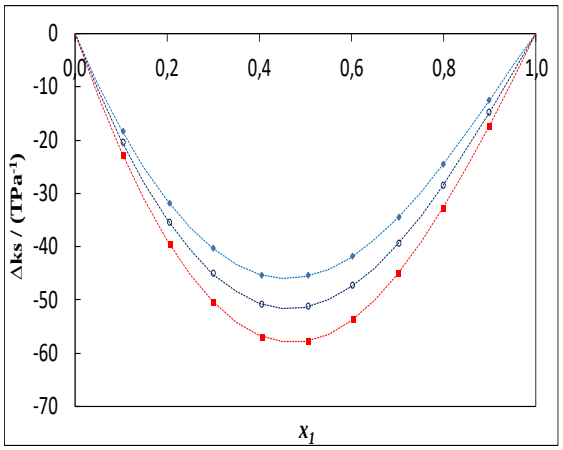

Figure 1.38: Plot of deviations in isentropic compressibility $\Delta\kappa_s$ for the binary mixtures: (a) {1-hexene (1) + 2-methoxyethanol (2)}, (b) {1-hexene (1) + 2-ethoxyethanol (2)}, (c) {1-hexene (1) + 2-butoxyethanol (2)} as function of the composition expressed in the mole fraction of 1-hexene at 293.15 K (◆), 298.15 K (○), and 303.15 K (■). The dotted lines were generated using Redlich-Kister polynomial curve-fitting.

1.5.3.3 Deviation in intermolecular free length

Figures 1.39(a-f), 1.40(a-c), 1.41(a-c) present data of deviation in intermolecular free length ΔL_f over the whole mole fraction range for all investigated systems. The results show that ΔL_f values are negative for all 22MEE mixtures, (furfural + acetonitrile), (furfural + sulfolane) and (1-hexene + 2-butoxyethanol) systems inversely to (furfural + DMSO), (1-hexene + 2-methoxyethanol) and (1-hexene + 2-ethoxyethanol) systems which reveal positive values. Increasing temperature at a fixed composition leads to a decrease in ΔL_f values for all studied mixtures except (1-hexene + 2-methoxyethanol) and (1-hexene + 2-ethoxyethanol) which reveal an increase in ΔL_f values.

The negative values of ΔL_f suggest that either a strong intermolecular interaction or a change in conformation or orientation of molecules taking place in solution, resulting in the formation of a more compact structure due to hydrogen bonding between unlike molecules (Thanuja et al., 2012). Physical interaction due to dispersion forces or weak dipole–dipole interaction (Misra et al., 2007) are indicated by positive values of ΔL_f .

Figure 1.39 (a)

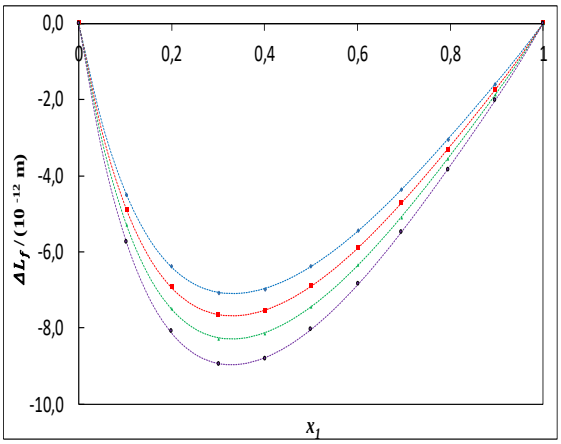

Figure 1.39 (b)

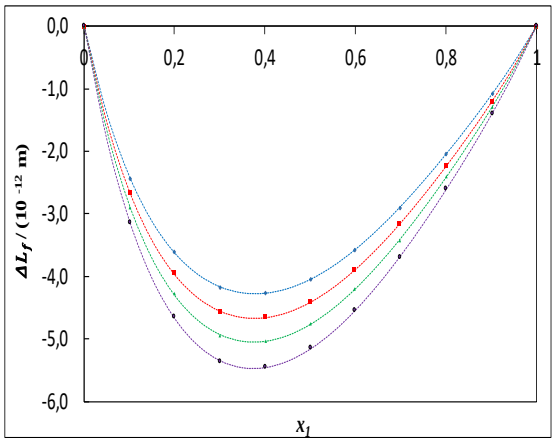

Figure 1.39 (c)

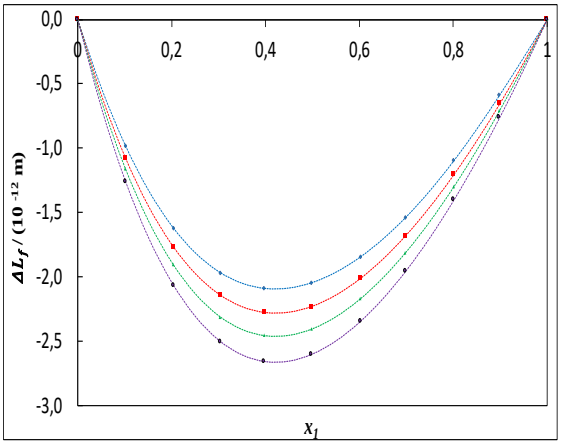

Figure 1.39 (d)

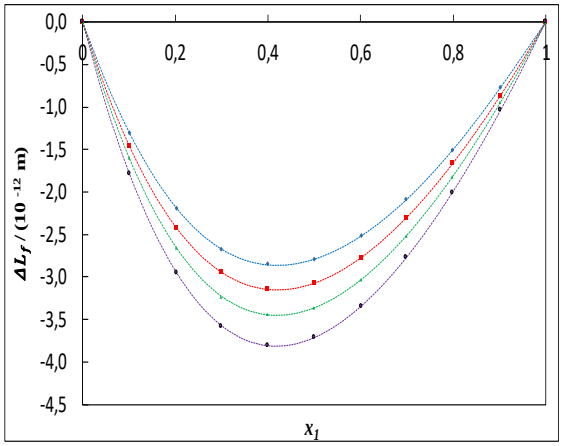

Figure 1.39 (e)

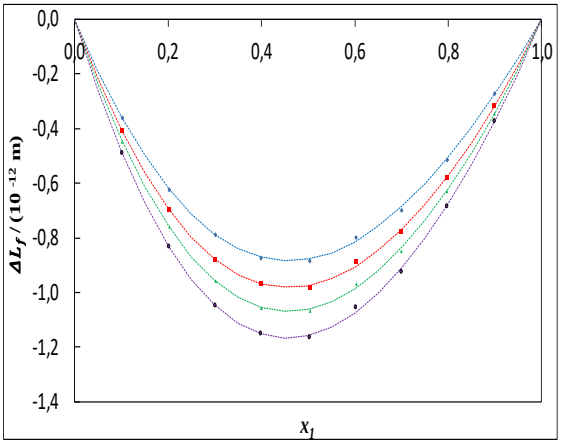

Figure 1.39 (f)

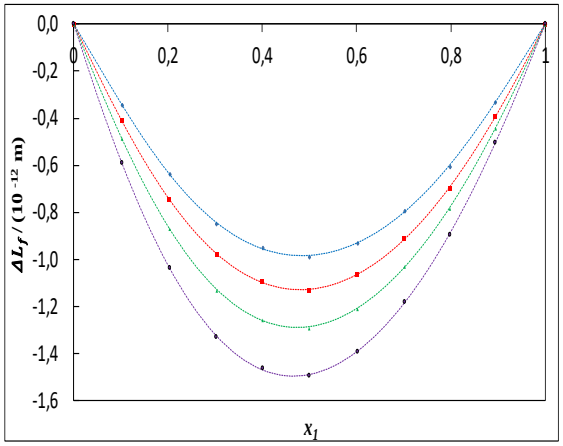

Figure 1.39: Plot of deviations in intermolecular free length ΔL_f for the binary mixtures: (a) {22MEE (1) + methanol (2)}, (b) {22MEE (1) + ethanol (2)}, (c) {22MEE (1) + propan-1-ol (2)}, (d) {22MEE (1) + propan-2-ol (2)}, (e) {22MEE (1) + butan-1-ol (2)}, and (f) {22MEE (1) + butan-2-ol (2)} as function of the composition expressed in the mole fraction of 22MEE at 293.15 K (◆), 303.15 K (■), 313.15 K (▲) and 323.15K (●). The dotted lines were generated using Redlich-Kister polynomial curve-fitting.

Figure 1.40 (a)

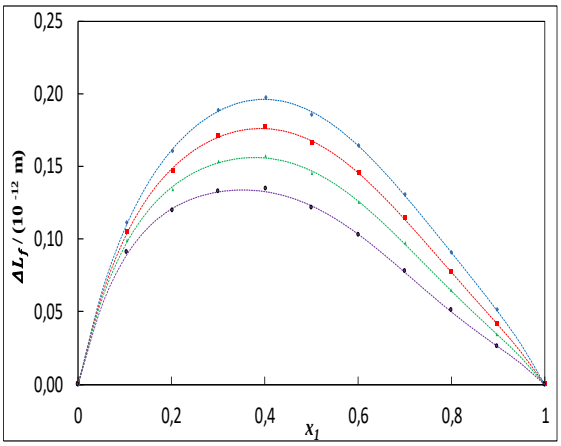

Figure 1.40 (b)

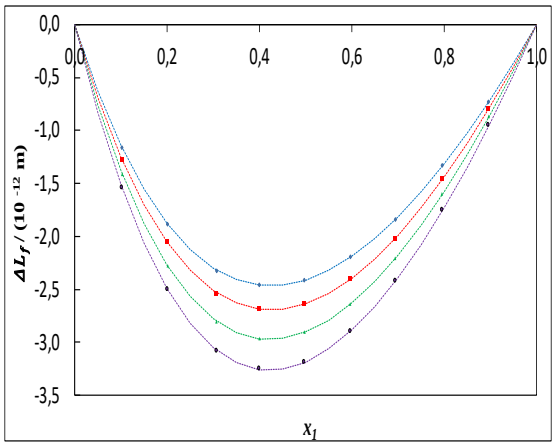

Figure 1.40 (c)

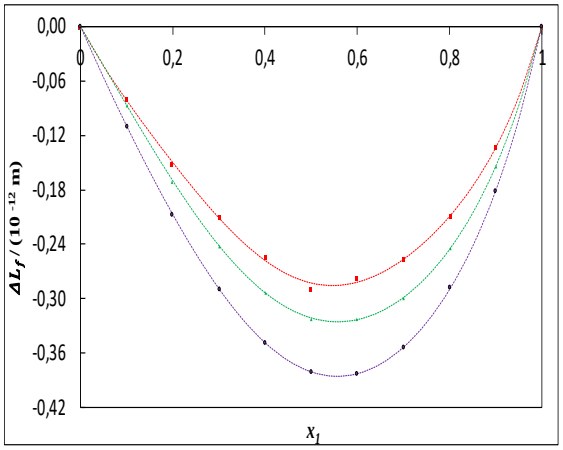

Figure 1.40: Plot of deviations in intermolecular free length ΔL_f for the binary mixtures: (a) {furfural (1) + DMSO (2)}, (b) {furfural (1) + acetonitrile (2)}, (c) {furfural (1) + sulfolane (2)} as function of the composition expressed in the mole fraction of furfural at 293.15 K (◆), 303.15 K (■), 313.15 K (▲) and 323.15 K (●). The dotted lines were generated using Redlich-Kister polynomial curve-fitting.

Figure 1.41 (a) **Figure 1.41 (b)**

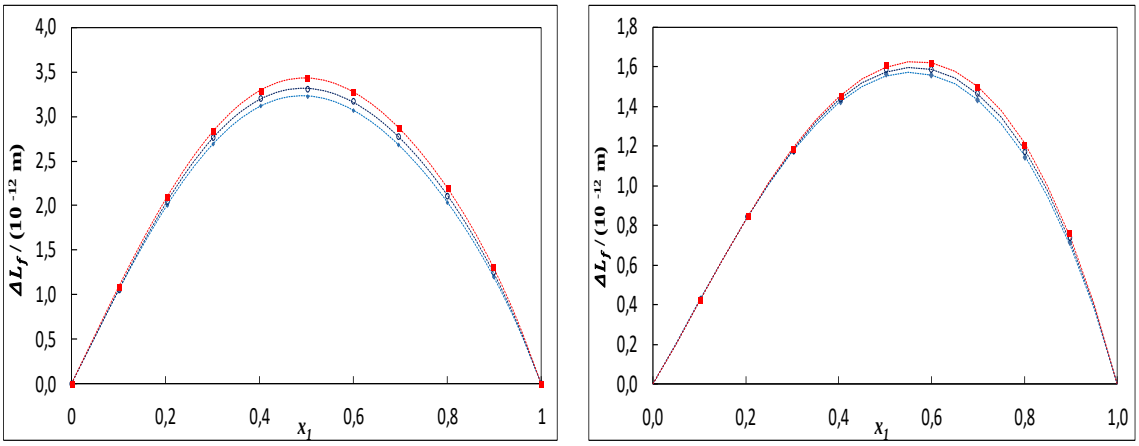

Figure 1.41 (c)

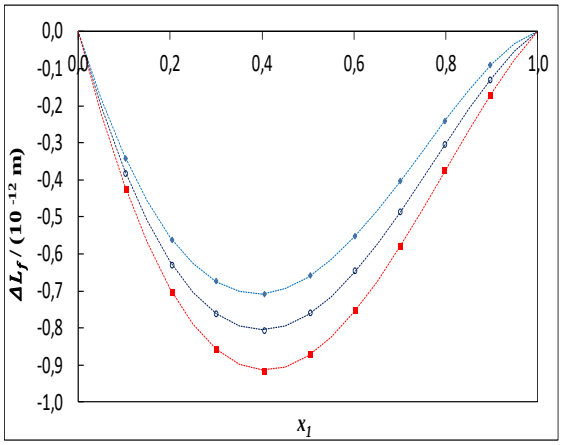

Figure 1.41: Plot of deviations in intermolecular free length ΔL_f for the binary mixtures: (a) {1-hexene (1) + 2-methoxyethanol (2)}, (b) {1-hexene (1) + 2-ethoxyethanol (2)}, (c) {1-hexene (1) + 2-butoxyethanol (2)} as function of the composition expressed in the mole fraction of 1-hexene at 293.15 K (◆), 298.15 K (○), and 303.15 K (■). The dotted lines were generated using Redlich-Kister polynomial curve-fitting.

1.5.3.4 Deviation in acoustic impedance

The results of deviation in acoustic impedance ΔZ are shown in Figures 1.42(a-f), 1.43(a-c), 1.44(a-c) for all studied mixtures. These Figures indicate that ΔZ values are positive for (22MEE + methanol), (22MEE + ethanol), (22MEE + propan-1-ol), (22MEE + propan-2-ol), (22MEE + butan-1-ol), (furfural + acetonitrile) and (furfural + sulfolane) mixtures, negative for (furfural + DMSO) and all mixtures containing 1-hexene. Both positive and negative values are observed for (22MEE + butan-2-ol). In general, positive deviations in ΔZ are in accordance with the presence of strong interactions and negative deviations in ΔZ indicate weak interactions between the unlike molecules in the mixture (Tiwari et al., 1995).

Figure 1.42 (a)

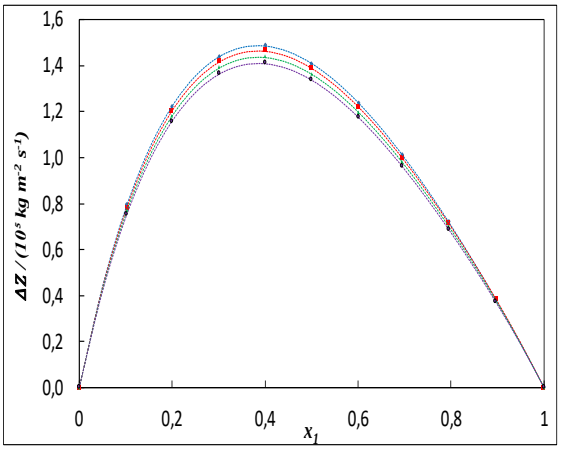

Figure 1.42 (b)

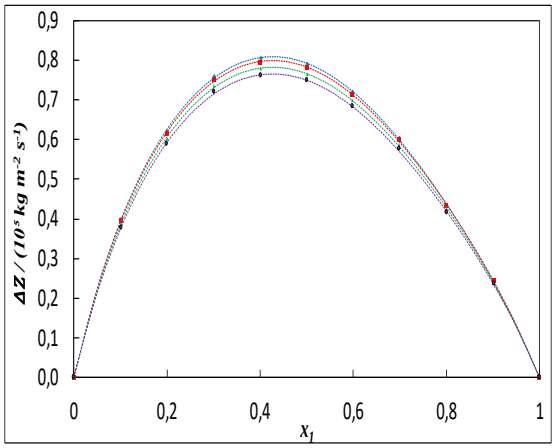

Figure 1.42 (c)

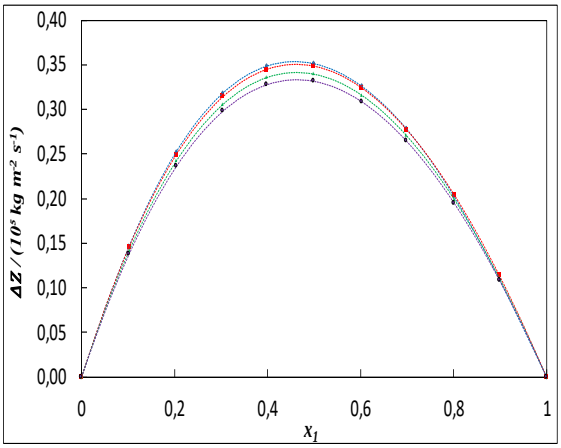

Figure 1.42 (d)

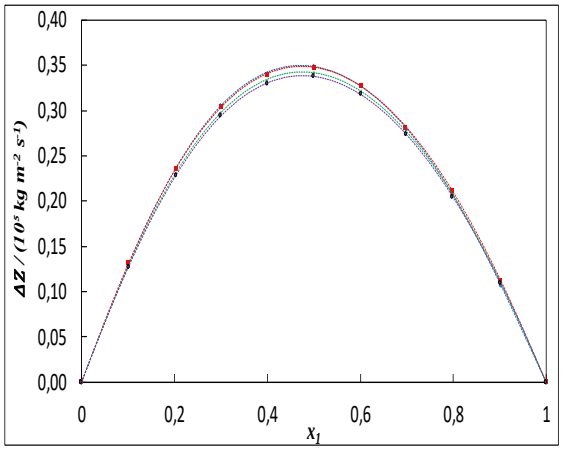

Figure 1.42 (e)

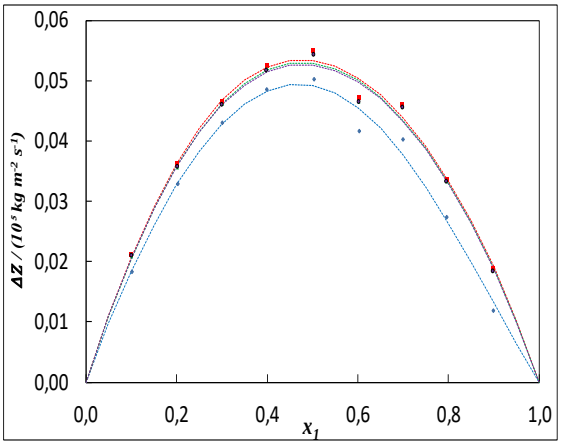

Figure 1.42 (f)

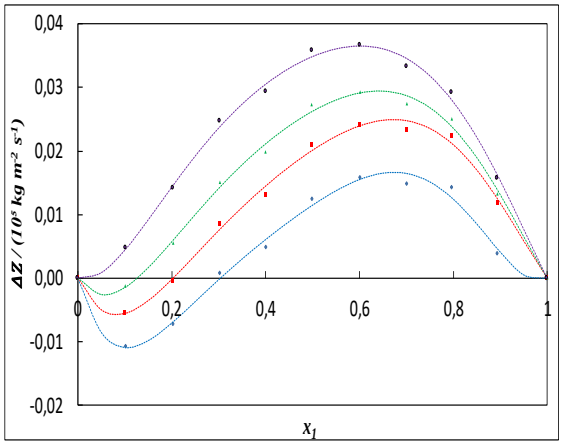

Figure 1.42: Plot of deviations in acoustic impedance ΔZ for the binary mixtures: (a) {22MEE (1) + methanol (2)}, (b) {22MEE (1) + ethanol (2)}, (c) {22MEE (1) + propan-1-ol (2)}, (d) {22MEE (1) + propan-2-ol (2)}, (e) {22MEE (1) + butan-1-ol (2)}, and (f) {22MEE (1) + butan-2-ol (2)} as function of the composition expressed in the mole fraction of 22MEE at 293.15 K (◆), 303.15 K (■), 313.15 K (▲) and 323.15K (●). The dotted lines were generated using Redlich-Kister polynomial curve-fitting.

Figure 1.43 (a)

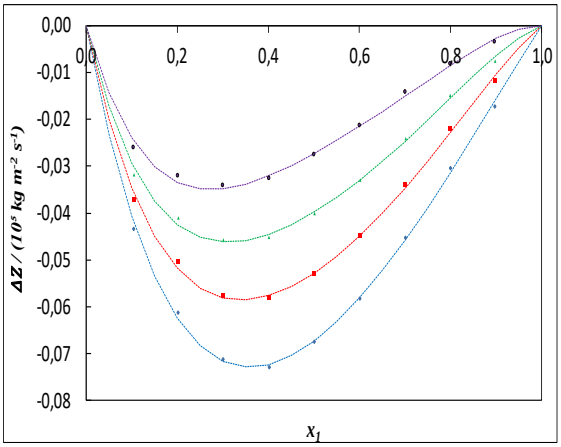

Figure 1.43 (b)

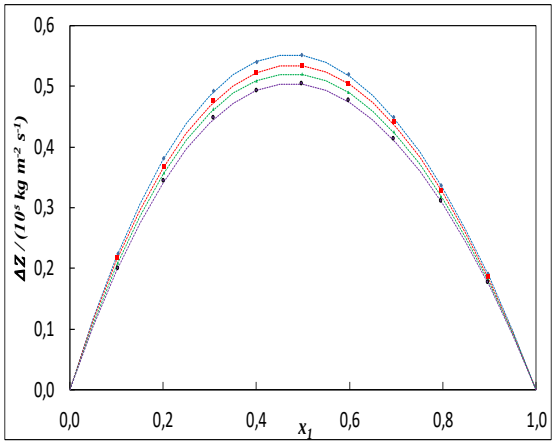

Figure 1.43 (c)

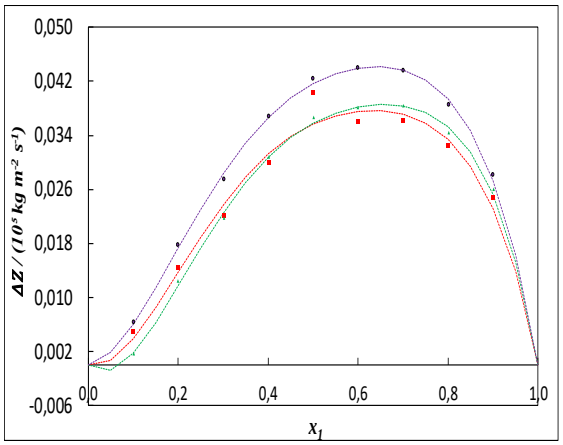

Figure 1.43: Plot of deviations in acoustic impedance ΔZ for the binary mixtures: (a) {furfural (1) + DMSO (2)}, (b) {furfural (1) + acetonitrile (2)}, (c) {furfural (1) + sulfolane (2)} as function of the composition expressed in the mole fraction of furfural at 293.15 K (◆), 303.15 K (■), 313.15 K (▲) and 323.15 K (●). The dotted lines were generated using Redlich-Kister polynomial curve-fitting.

Figure 1.44 (a)

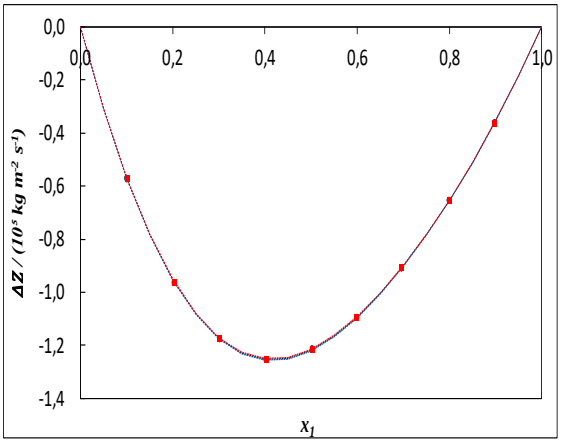

Figure 1.44 (b)

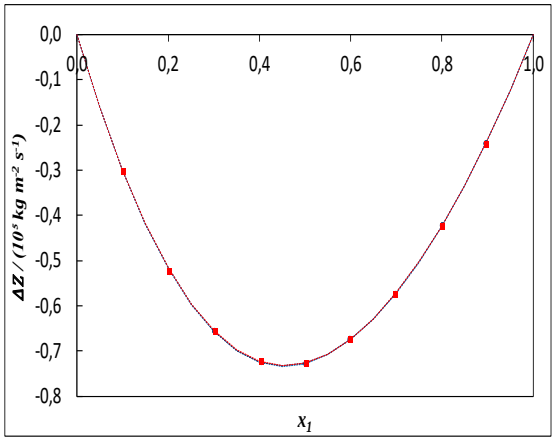

Figure 1.44 (c)

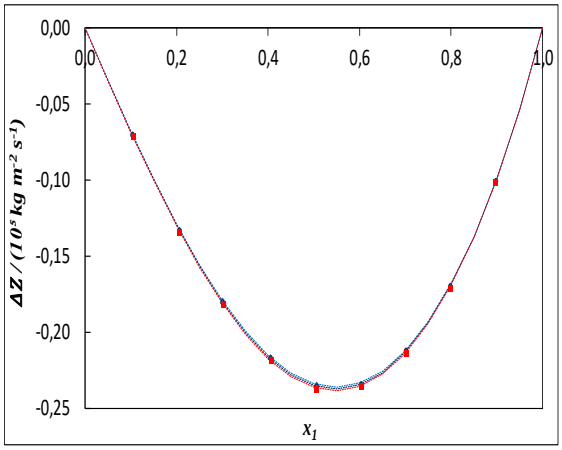

Figure 1.44: Plot of deviations in acoustic impedance ΔZ for the binary mixtures: (a) {1-hexene (1) + 2-methoxyethanol (2)}, (b) {1-hexene (1) + 2-ethoxyethanol (2)}, (c) {1-hexene (1) + 2-butoxyethanol (2)} as function of the composition expressed in the mole fraction of 1-hexene at 293.15 K (◆), 298.15 K (○), and 303.15 K (■). The dotted lines were generated using Redlich-Kister polynomial curve-fitting.

1.5.3.5 Deviation in speed of sound

The dependence of deviations in speed of sound Δu on mole fraction of 22MEE or furfural or 1-hexene is presented in Figures 1.45(a-f), 1.46(a-c), 1.47(a-c). The Δu values are positive for (22MEE + methanol), (22MEE + ethanol), (22MEE + propan-1-ol), (22MEE + propan-2-ol) and (furfural + acetonitrile) and negative for (22MEE + butan-1-ol), (furfural + DMSO) and all mixtures containing 1-hexene. Both positive and negative values are observed for (22MEE + butan-2-ol) and (furfural + sulfolane) systems.

Figure 1.45 (a)

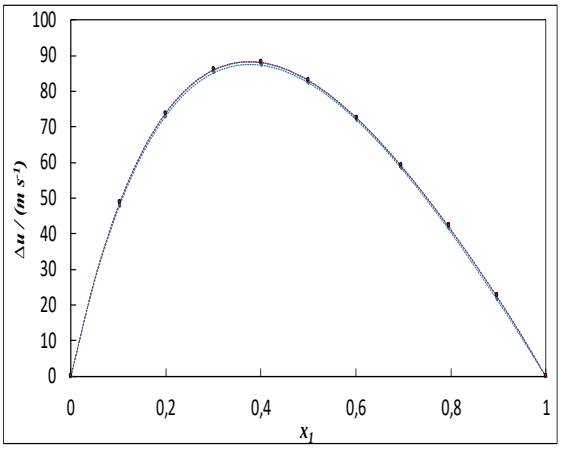

Figure 1.45 (b)

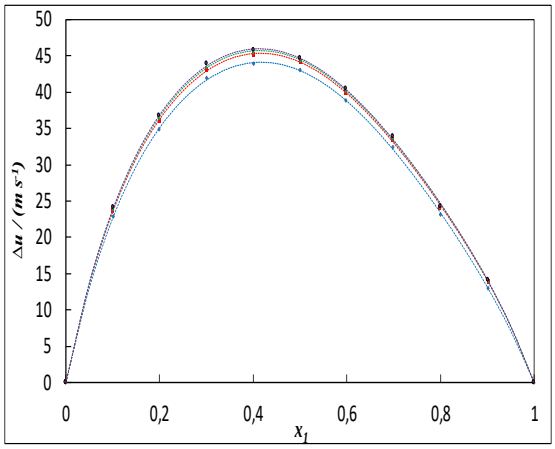

Figure 1.45 (c)

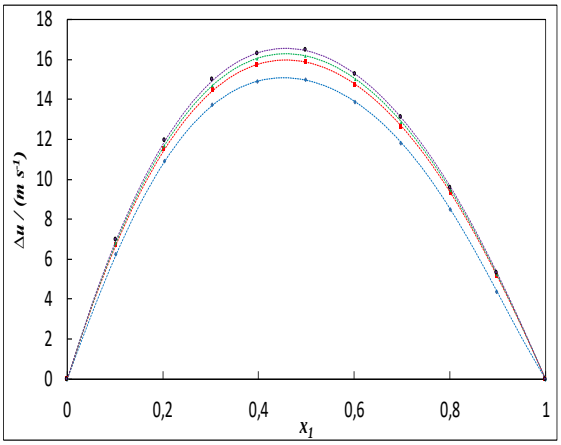

Figure 1.45 (d)

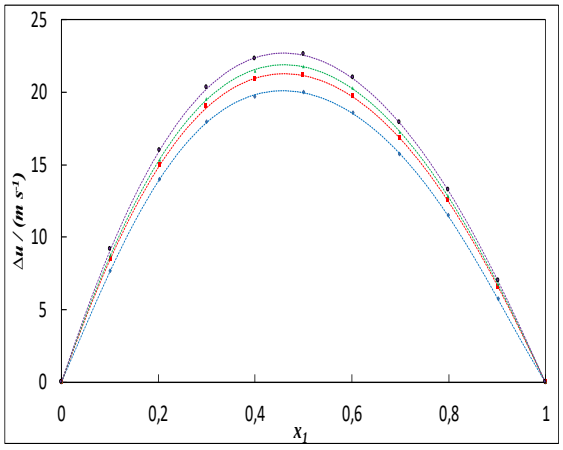

Figure 1.45 (e)

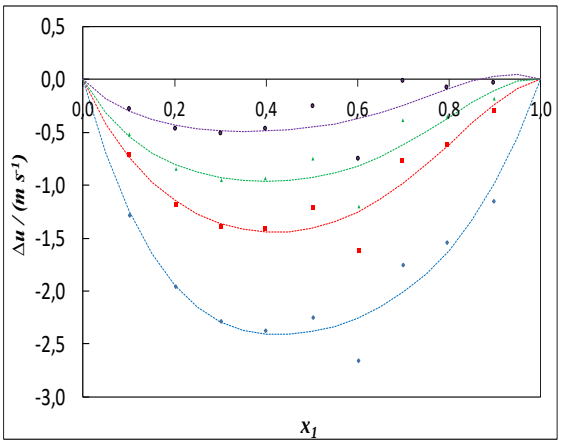

Figure 1.45 (f)

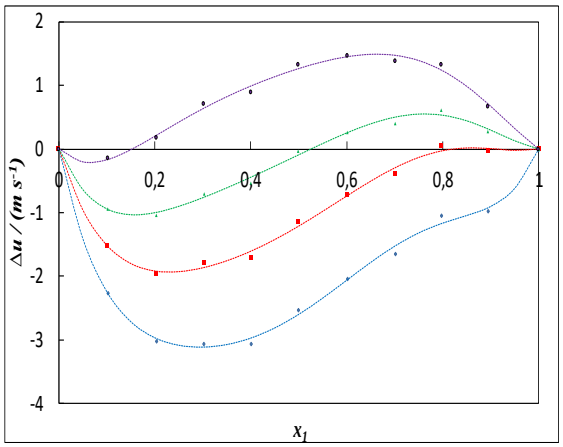

Figure 1.45: Plot of deviations in speed of sound Δu for the binary mixtures: (a) {22MEE (1) + methanol (2)}, (b) {22MEE (1) + ethanol (2)}, (c) {22MEE (1) + propan-1-ol (2)}, (d) {22MEE (1) + propan-2-ol (2)}, (e) {22MEE (1) + butan-1-ol (2)}, and (f) {22MEE (1) + butan-2-ol (2)} as function of the composition expressed in the mole fraction of 22MEE at 293.15 K (◆), 303.15 K (■), 313.15 K (▲) and 323.15K (●). The dotted lines were generated using Redlich-Kister polynomial curve-fitting.

Figure 1.46 (a)

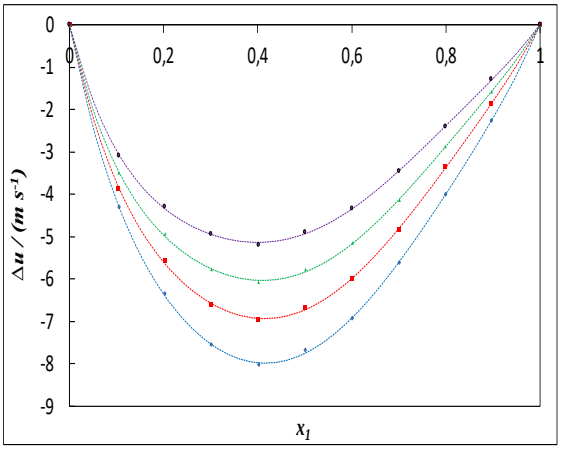

Figure 1.46 (b)

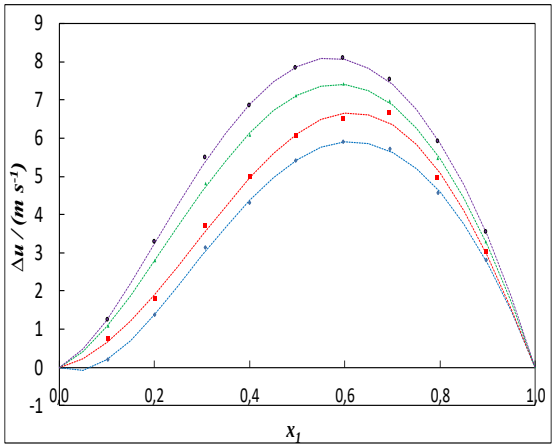

Figure 1.46 (c)

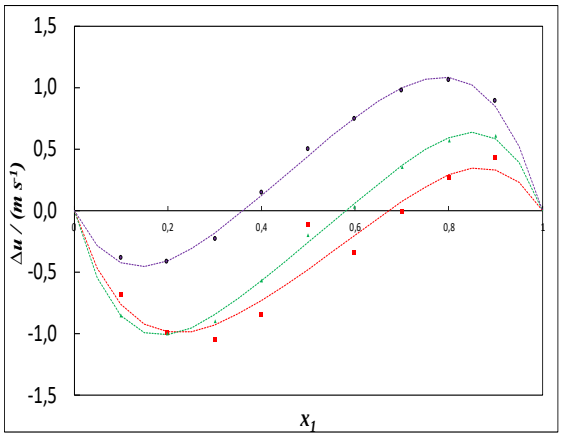

Figure 1.46: Plot of deviations in speed of sound Δu for the binary mixtures: (a) {furfural (1) + DMSO (2)}, (b) {furfural (1) + acetonitrile (2)}, (c) {furfural (1) + sulfolane (2)} as function of the composition expressed in the mole fraction of furfural at 293.15 K (◆), 303.15 K (■), 313.15 K (▲) and 323.15 K (●). The dotted lines were generated using Redlich-Kister polynomial curve-fitting.

Figure 1.47 (a)

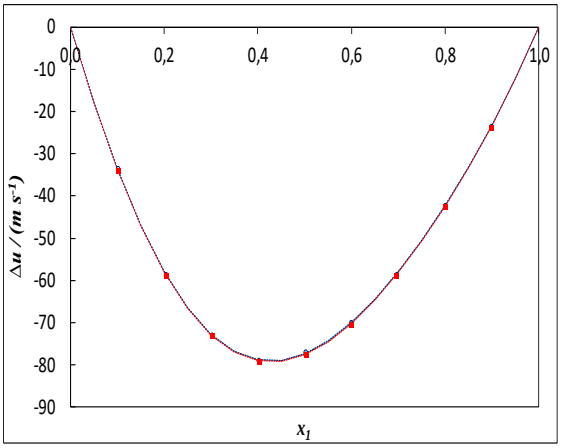

Figure 1.47 (b)

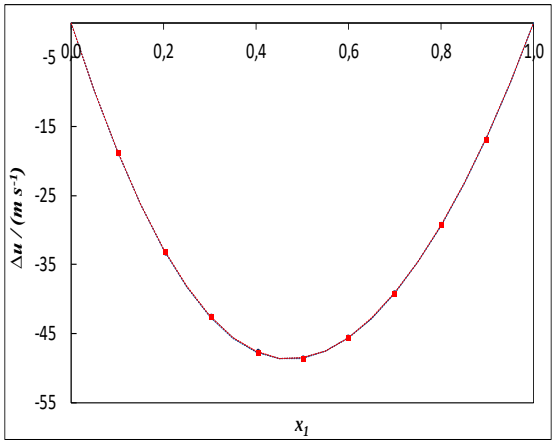

Figure 1.47 (c)

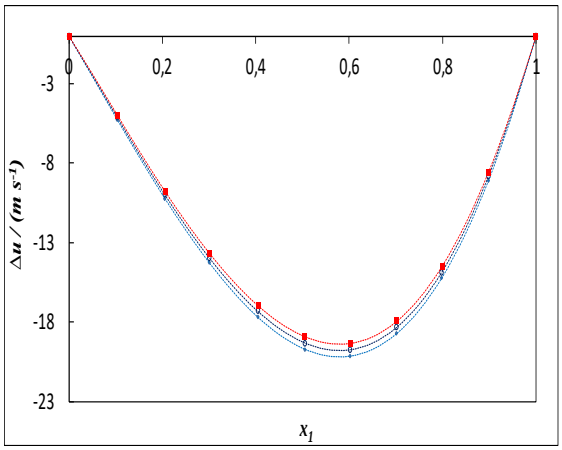

Figures 1.47: Plot of deviations in speed of sound Δu for the binary mixtures: (a) {1-hexene (1) + 2-methoxyethanol (2)}, (b) {1-hexene (1) + 2-ethoxyethanol (2)}, (c) {1-hexene (1) + 2-butoxyethanol (2)} as function of the composition expressed in the mole fraction of 1-hexene at 293.15 K (◆), 298.15 K (○), and 303.15 K (■). The dotted lines were generated using Redlich-Kister polynomial curve-fitting.

1.5.3.6 Deviation in refractive index

Data of deviation in refractive index (Δn_D) for all investigated mixtures are plotted in Figures 1.48(a-f), 1.49(a-c), 1.50(a-c). it's clear from the plots that the changes in the refractive index of mixtures containing 22MEE, (furfural + DMSO), (furfural + acetonitrile) and (1-hexene + 2-butoxyethanol) systems are positive throughout the entire composition range. In the case of binary systems (furfural + sulfolane), (1-hexene + 2-methoxyethanol) and (1-hexene + 2-ethoxyethanol), the results show negative values over the whole range of composition and at all the temperatures.

Figure 1.48 (a)

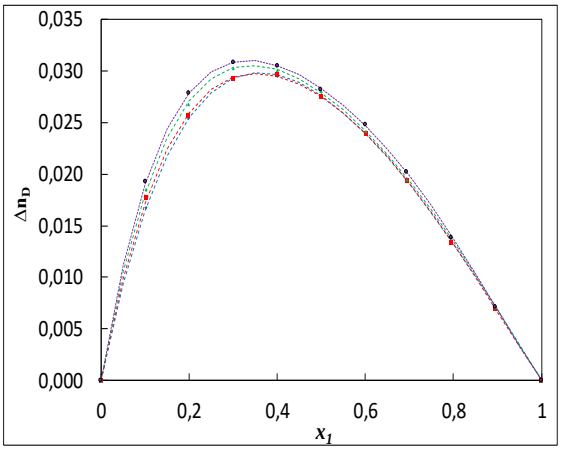

Figure 1.48 (b)

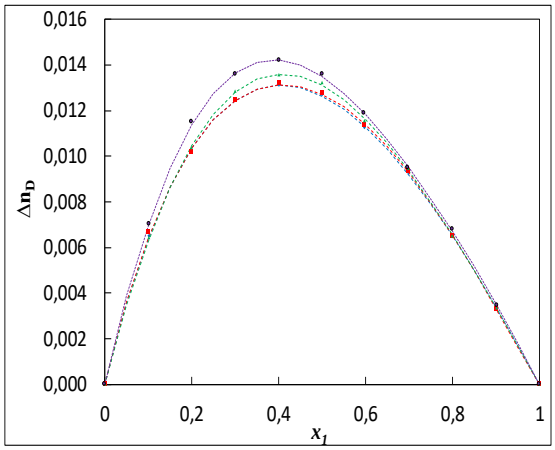

Figure 1.48 (c)

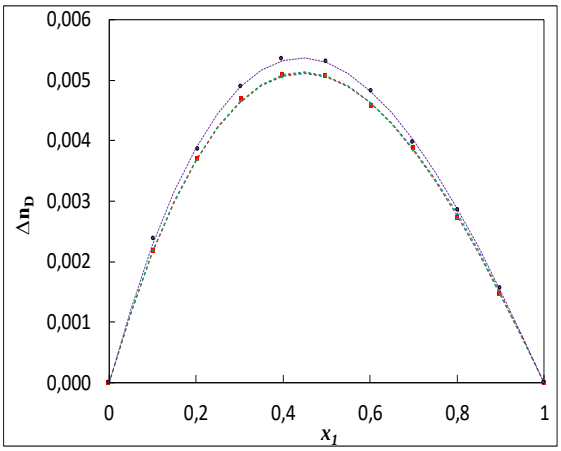

Figure 1.48 (d)

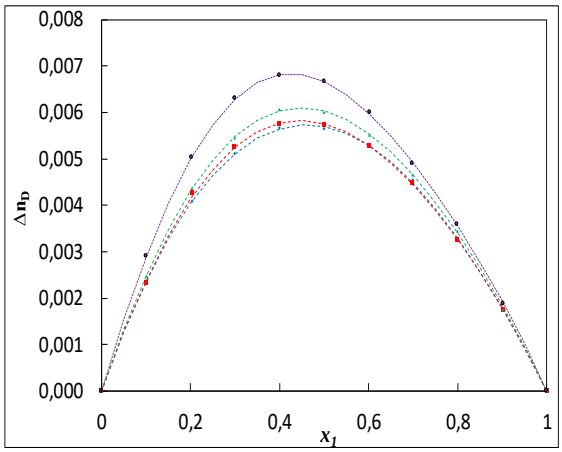

Figure 1.48 (e)

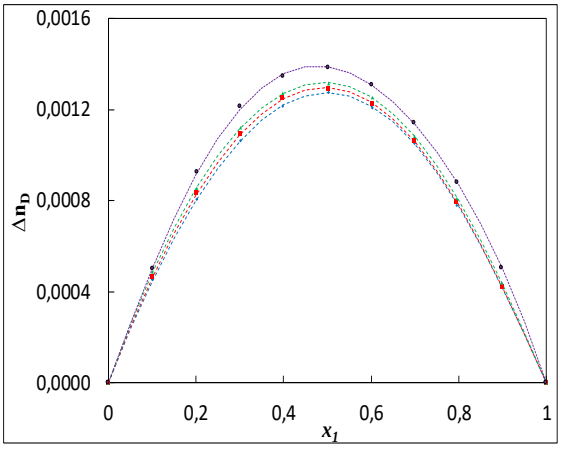

Figure 1.48 (f)

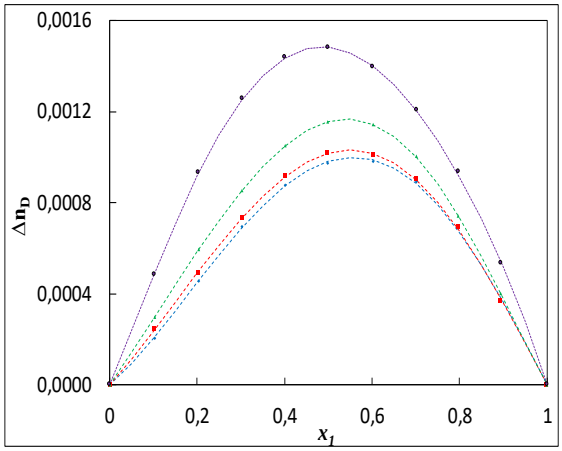

Figure 1.48: Plot of changes of refractive index Δn_D for the binary mixtures: (a) {22MEE (1) + methanol (2)}, (b) {22MEE (1) + ethanol (2)}, (c) {22MEE (1) + propan-1-ol (2)}, (d) {22MEE (1) + propan-2-ol (2)}, (e) {22MEE (1) + butan-1-ol (2)}, and (f) {22MEE (1) + butan-2-ol (2)} as function of the composition expressed in the mole fraction of 22MEE at 293.15 K (◆), 303.15 K (■), 313.15 K (▲) and 323.15K (●). The dotted lines were generated using Redlich-Kister polynomial curve-fitting.

Figure 1.49 (a)

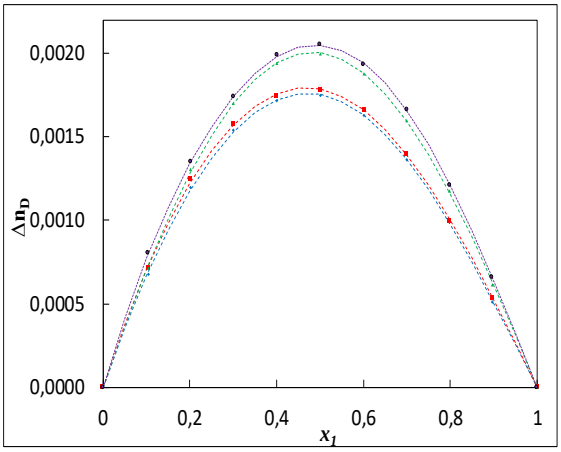

Figure 1.49 (b)

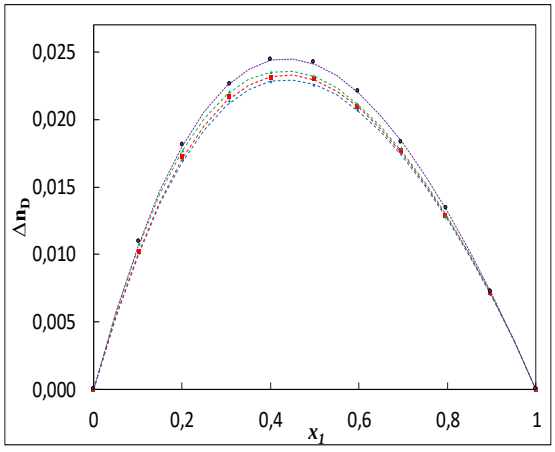

Figure 1.49 (c)

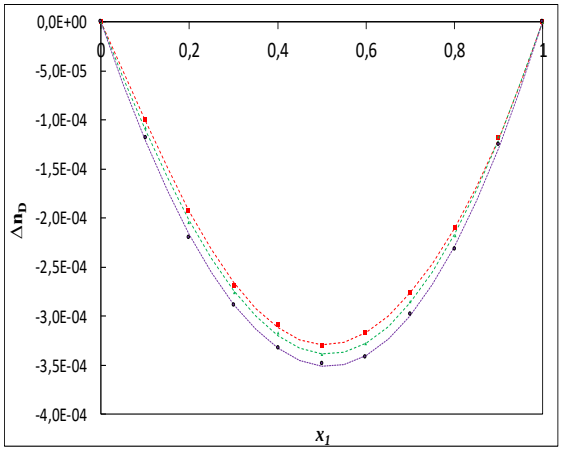

Figure 1.49: Plot of changes of refractive index Δn_D for the binary mixtures: (a) {furfural (1) + DMSO (2)}, (b) {furfural (1) + acetonitrile (2)}, (c) {furfural (1) + sulfolane (2)} as function of the composition expressed in the mole fraction of furfural at 293.15 K (◆), 303.15 K (■), 313.15 K (▲) and 323.15 K (●). The dotted lines were generated using Redlich-Kister polynomial curve-fitting.

Figure 1.50 (a)

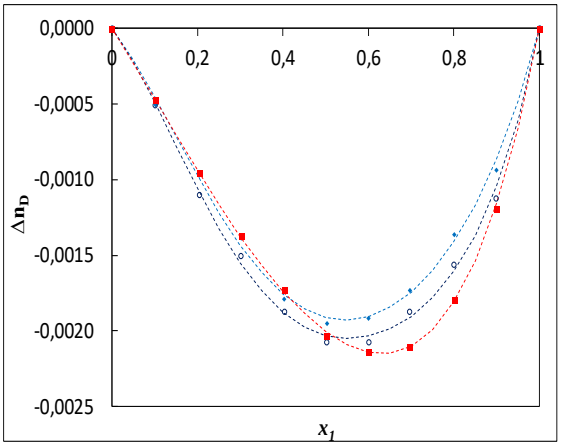

Figure 1.50 (b)

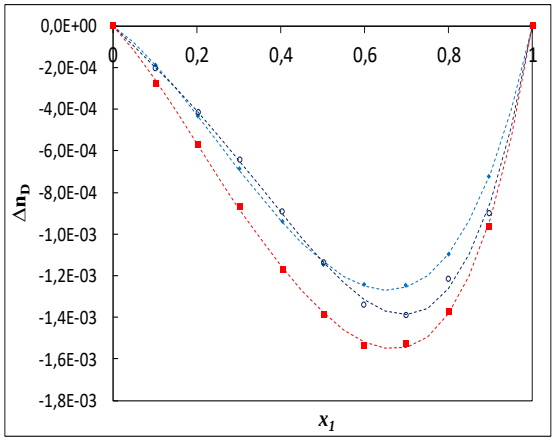

Figure 1.50 (c)

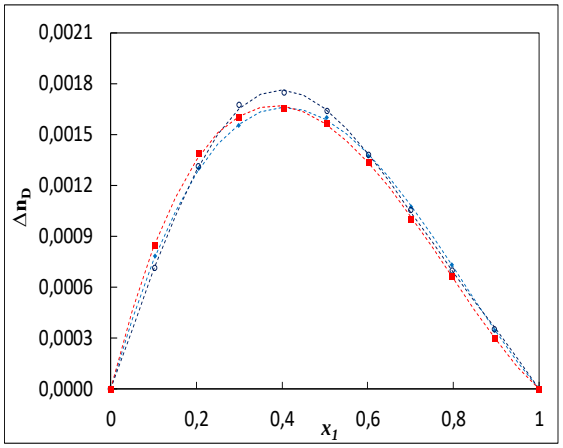

Figure 1.50: Plot of changes of refractive index Δn_D for the binary mixtures: (a) {1-hexene (1) + 2-methoxyethanol (2)}, (b) {1-hexene (1) + 2-ethoxyethanol (2)}, (c) {1-hexene (1) + 2-butoxyethanol (2)} as function of the composition expressed in the mole fraction of 1-hexene at 293.15 K (◆), 298.15 K (○), and 303.15 K (■). The dotted lines were generated using Redlich-Kister polynomial curve-fitting.

1.5.4 Correlation of derived properties

The excess functions V_m^E , $\Delta\kappa_s$, ΔL_f , ΔZ, Δu and Δn_D of all studied mixtures were fitted to Redlich–Kister (Redlich and Kister, 1948) polynomial equation of the type

$$X = x_1 x_2 \sum_{i=1}^{k} A_i (1 - 2x_1)^{i-1} \quad (1.8)$$

where $X = V_m^E$ or $\Delta\kappa_s$ or ΔL_f or ΔZ or Δu or Δn_D.

A_i are the fitting parameters obtained by least-square method.
In each case, the optimum number of coefficients was ascertained from an examination of the variation of standard deviation, σ, with:

$$\sigma(X) = \left[\frac{\sum_{i=1}^{N}(X_{expt} - X_{calc})^2}{(N-k)}\right]^{1/2} \quad (1.9)$$

where $X_{expt.}$ and $X_{calc.}$ are the experimental and calculated values of the property X, respectively, and N and k are the number of experimental points and number of coefficients used in the Redlich-Kister equation.
Tables 1.12, 1.13 and 1.14 present the values of the fitting parameters A_i together with the standard deviation, σ, for the binary mixtures containing 22MEE or furfural or 1-hexene respectively. The values of V_m^E , $\Delta\kappa_s$, ΔL_f , ΔZ, Δu and Δn_D as well as the plots of the Redlich-Kister model are displayed in Figures 1.31(a-f), 1.34(a-c), 1.35(a-c), 1.36(a-f), 1.37(a-c), 1.38(a-c), 1.39(a-f), 1.40(a-c), 1.41(a-c), 1.42(a-f), 1.43(a-c), 1.44(a-c), 1.45(a-f), 1.46(a-c), 1.47(a-c), 1.48(a-f), 1.49(a-c), 1.50(a-c).
The agreement between the experimental data and those calculated using Redlich–Kister equation was satisfactory at the investigated temperatures for all the systems.
It may be concluded that Redlich-Kister equation allowed us to calculate with a very good accuracy excess molar volume (V_m^E), deviations in isentropic compressibility ($\Delta\kappa_s$), deviations in intermolecular free length (ΔL_f), deviations in acoustic impedance (ΔZ), deviations in speed of sound (Δu) and changes in refractive index (Δn_D).

1.6 Conclusion

Densities, speeds of sound and refractive indices of twelve (12) binary mixtures containing 22MEE or furfural or 1-hexene have been studied at different temperatures and at pressure of 0.1 MPa using an Anton Paar DSA 5000M digital vibrating tube densimeter and a digital refractometer Abbemat 300. From experimental measurements, several derived and excess properties have been determined. These properties include isentropic compressibility (κ_s), intermolecular free length (L_f), specific acoustic impedance (Z), relative association (R_A), relaxation strength (r), Rao's molar sound function (R), excess molar volume (V_m^E), deviations in isentropic compressibility ($\Delta\kappa_s$), deviations in intermolecular free length (ΔL_f), deviations in acoustic impedance (ΔZ), deviations in speed of sound (Δu) and changes in refractive index (Δn_D). All the experimental data measured and those calculated were presented, both numerically and graphically, the results were discussed from the thermodynamic point of view and compared with the currently literature available and Redlich-Kister polynomial with good results.

References

Fortin, T. J., Laesecke, A., Freund, M., & Outcalt, S. (2013). Advanced calibration, adjustment, and operation of a density and sound speed analyzer. The Journal of Chemical Thermodynamics, 57, 276-285.

Awasthi, A., Rastogi, M., & Shukla, J. P. (2004). Ultrasonic and IR study of molecular association process through hydrogen bonding in ternary liquid mixtures. Fluid phase equilibria, 215(2), 119-127.

Azhagiri, S., Jayakumar, S., Padmanaban, R., Gunasekaran, S., & Srinivasan, S. (2009). Acoustic and thermodynamic properties of binary liquid mixtures of benzaldehyde in hexane and cyclohexane. Journal of solution Chemistry, 38(4), 441-448.

Ion, I., Sirbu, F., & Ion, A. C. (2013). Density, refractive index, and ultrasound speed in mixtures of active carbon and exfoliated graphite nanoplatelets dispersed in N, N-dimethylformamide at temperatures from (293.15 to 318.15) K. Journal of Chemical & Engineering Data, 58(5), 1212-1222.

Dash, S. K., Pradhan, S. K., Dalai, B., Moharana, L., & Swain, B. B. (2012). Studies on molecular interaction in binary mixtures of diethyl ether with some alkanols–an acoustic approach. Physics and Chemistry of Liquids, 50(6), 735-749.

Rastogi, M., Awasthi, A., Gupta, M., & Shukla, J. P. (2003). Molecular association of aliphatic ketones and phenol in a nonpolar solvent-ultrasonic and IR study. Journal of Molecular liquids, 107(1-3), 185-204.

Awasthi, A., & Shukla, J. P. (2003). Ultrasonic and IR study of intermolecular association through hydrogen bonding in ternary liquid mixtures. Ultrasonics, 41(6), 477-486.

Thanuja, B., Nithya, G., & Kanagam, C. C. (2012). Ultrasonic studies of intermolecular interactions in binary mixtures of 4-methoxy benzoin with various solvents: excess molar functions of ultrasonic parameters at different concentrations and in different solvents. Ultrasonics sonochemistry, 19(6), 1213-1220.

Bagchi, S., Nema, S. K., & Singh, R. P. (1986). Ultrasonic and viscometric investigation of ISRO polyol in various solvents and its compatibility with polypropylene glycol. European polymer journal, 22(10), 851-857.

Sandhu, J. S., Sharma, A. K., & Wadi, R. K. (1986). Excess molar volumes of n-alkanol (C1-C5) binary mixtures with acetonitrile. Journal of Chemical and Engineering Data, 31(2), 152-154.

García, B., Alcalde, R., Leal, J. M., & Matos, J. S. (1996). Formamide–(C 1–C 5) alkan-1-ols solvent systems. Journal of the Chemical Society, Faraday Transactions, 92(18), 3347-3352.

Pal, A., & Kumar, A. (2004). Excess molar volumes and viscosities of binary liquid mixtures of 1-propanol plus ethylene glycol monomethyl ether, plus diethylene glycol monomethyl ether, and plus triethylene glycol monomethyl ether at (298.15, 308.15 and 318.15) K. Journal of the Indian Chemical Society, 81(5), 375-383.

Mozo, I., García de la Fuente, I., González, J. A., & Cobos, J. C. (2007). Thermodynamics of mixtures containing alkoxyethanols. XXIV. Densities, excess molar volumes, and speeds of sound at (293.15, 298.15, and 303.15) K and isothermal compressibilities at 298.15 K for 2-(2-alkoxyethoxy) ethanol+ 1-butanol systems. Journal of Chemical & Engineering Data, 52(5), 2086-2090.

Umapathi, R., Rao, C. N., Naidoo, P., Bahadur, I., Ramjugernath, D., & Venkatesu, P. (2020). Effect of temperature on molecular interactions between tri (butyl) methylphosphonium methylsulfate and furfural. The Journal of Chemical Thermodynamics, 149, 106150.

Roy, M. N., Ekka, D., & Dewan, R. (2011). Physico-chemical studies of some bio-active solutes in pure methanoic acid. Acta Chim. Slov, 58(4), 792-796.

JA Riddick and WB Bunger, (1970). vol. II of Techniques of Organic Chemistry. Solvents, Organic.,.

Bendiaf, L., Bahadur, I., Negadi, A., Naidoo, P., Ramjugernath, D., & Negadi, L. (2015). Effects of alkyl group and temperature on the interactions between furfural and alcohol: Insight from density and sound velocity studies. Thermochimica acta, 599, 13-22.

Pandey, P. K., Awasthi, A., & Awasthi, A. (2013). Intermolecular interactions in binary mixtures of 2-Chloroethanol with 2-Dimethylaminoethanol and 2-Diethylaminoethanol at different temperatures. Chemical Physics, 423, 119-126.

Kincaid, J. F., & Eyring, H. (1938). Free volumes and free angle ratios of molecules in liquids. The Journal of Chemical Physics, 6(10), 620-629.

Ali, A., Hyder, S., & Nain, A. K. (2002). molecular interaction in binary mixtures of benzyl alcohol with ethanol, propan-1-ol and octan-1-ol at 303 K: an ultrasonic and viscometric study. Collection of Czechoslovak chemical communications, 67(8), 1125-1140.

Baluja, S., & Oza, S. (2002). Ultrasonic studies of some derivatives of sulphonamide in dimethylformamide. Fluid Phase Equilibria, 200(1), 11-18.

Barbés, B., García, I., González, J. A., Cobos, J. C., & Casanova, C. (1994). Excess properties of (an n-alkoxyethanol+ an organic solvent) VI. VEm {xCH3 (CH2) v-1O (CH2) 2O (CH2) 2OH+(1-x) C6H5CH3} for v= 1, 2, and 4 at the temperature 298.15 K. The Journal of Chemical Thermodynamics, 26(8), 791-795.

Buckley, P., & Brochu, M. (1972). Microwave Spectrum, Dipole Moment, and Intramolecular Hydrogen Bond of 2-Methoxyethanol. Canadian Journal of Chemistry, 50(8), 1149-1156.

Ramana Reddy, K. V., Rambabu, K., Devarajulu, T., & Krishnaiah, A. (1996). Excess volumes of (2-ethoxyethanol+ alcohols) at 308.15 K. Physics and Chemistry of Liquids, 31(1), 9-13.

Cobos, J. C., Garcia, I., Casanova, C., Roux-Desgranges, G., & Grolier, J. P. E. (1988). Excess properties of mixtures of some n-alkoxyethanols with organic solvents: III. VE and CEp with butan-1-ol at 298.15 K. Thermochimica acta, 131, 73-78.

Kulnevich, V. G., & Shapiro, Y. M. (1972). Electronic spectroscopy of solutions of heterocyclic-compounds in H2SO4. 1. Study of stability of furan compounds in H2SO4. Khimiya Geterotsiklicheskikh Soedinenii, (12), 1594-1596.

Ali, A., Nain, A. K., Chand, D., & Ahmad, R. (2005). Volumetric, ultrasonic and viscometric studies of molecular interactions in binary mixtures of aromatic+ aliphatic alcohols at different temperatures. Physics and Chemistry of Liquids, 43(2), 205-224.

Radojković, N., Tasić, A., Grozdanić, D., Djordjević, B., & Malić, D. (1977). Excess volumes of acetone+ benzene, acetone+ cyclohexane, and acetone+ benzene+ cyclohexane at 298.15 K. The Journal of Chemical Thermodynamics, 9(4), 349-356.

Homer, J., & Cooke, M. C. (1973). Molecular complexes. Part 9. Studies by a phase distribution procedure which employs nuclear magnetic resonance spectroscopy for quantitative measurements. Journal of the Chemical Society, Faraday Transactions 1: Physical Chemistry in Condensed Phases, 69, 1990-1994.

Grolier, J. P., Benson, G. C., & Picker, P. (1975). Enthalpies of mixing of organic liquids measured directly as a function of composition by means of scanning dynamic flow microcalorimetry. The Journal of Chemical Thermodynamics, 7(1), 89-95.

Shi, X., Li, C., Guo, H., & Shen, S. (2019). Density, viscosity, and excess properties of binary mixtures of 2-(methylamino) ethanol with 2-methoxyethanol, 2-ethoxyethanol, and 2-butoxyethanol from 293.15 to 353.15 K. Journal of Chemical & Engineering Data, 64(9), 3960-3970.

Sarkar, L., & Roy, M. N. (2009). Density, viscosity, refractive index, and ultrasonic speed of binary mixtures of 1, 3-dioxolane with 2-methoxyethanol, 2-ethoxyethanol, 2-butoxyethanol, 2-propylamine, and cyclohexylamine. Journal of Chemical & Engineering Data, 54(12), 3307-3312.

Choudary, N., & Naidu, P. (1982). Sound velocities and isentropic compressibilities of mixtures of 1, 2-dichloroethane with alkanols. Chem. Scr, 19(2), 89-92.

Dharmaraju, G., Venkateswarlu, P., & Raman, G. K. (1982). Ultrasonic studies in binary-liquid mixtures of associated liquids (cyclohexylamine+ alcohol). Chem. Scripta, 19, 140-142.

Benson, G. C., & Handa, Y. P. (1981). Ultrasonic speeds and isentropic compressibilities for (decan-1-ol+ n-alkane) at 298.15 K. The Journal of Chemical Thermodynamics, 13(9), 887-896.

Misra, V. K., Vibhu, I., Singh, R., Gupta, M., & Shukla, J. P. (2007). Ultrasonic velocity, viscosity, density and excess properties of binary mixture of dimethyl sulphoxide with propanoic acid and n-butyric acid. Journal of molecular liquids, 135(1-3), 166-169.

Tiwari, K., Patra, C., & Chakravortty, V. (1995). Molecular interaction study on binary mixtures of dimethyl sulphoxide with benzene, carbon tetrachloride and toluene from the excess properties of ultrasonic velocity, viscosity and density. Acoustics letters, 19(3), 53-59.

Redlich, O., & Kister, A. T. (1948). Algebraic representation of thermodynamic properties and the classification of solutions. Industrial & Engineering Chemistry, 40(2), 345-348.

Chapter 2: Vapor-liquid equilibrium of binary mixtures Measurement and modeling

2.1 Introduction

In this chapter, vapor-liquid equilibrium (VLE) of three binary mixtures composed of N,N-dimethylacetamide with 1,3,5-trimethylbenzene or propan-2-ol or DMSO have been measured by means of a static apparatus at several temperatures. The obtained data were correlated with the Antoine equation. From these data, the excess Gibbs function G^E and the vapor phase composition y_i were evaluated for several constant temperatures and fitted to Redlich–Kister equation using the Barker's method. The activity coefficients γ_1 and γ_2 of the components in binary mixtures were also estimated. Additionally, the experimental data were correlated by using three activity coefficient models NRTL, UNIQUAC and Modified UNIFAC (Dortmund).

2.2 Chemicals

The chemicals used for VLE measurements are N,N-dimethylacetamide, 1,3,5-trimethylbenzene, propan-2-ol and dimethyl sulfoxide (DMSO), they were supplied by Acros Organics, Aldrich, VWR Chemicals and Carlo Erba Reagents respectively. The detailed information of the chemicals such as abstracts registry number (CAS number), the stated purity by the suppliers and sources are given in Table 2.1. All chemicals were used without further purification owing to their high purity grade, which was more than 0.98.

Table 2.1: Purities, CAS #, Molar Mass, and Suppliers of Chemicals Used for VLE measurements.

Chemicals name	Purity (as stated by the supplier	CAS #	Molar mass/(g.mole^{-1})	Supplier
N,N-dimethylacetamide	99.5	127-19-5	87.12	Acros Organics
1,3,5-trimethylbenzene	≥ 98	108-67-8	120.20	Aldrich
Propan-2-ol	100	67-63-0	60.10	VWR Chemicals
DMSO	≥ 99.9	67-68-5	78.13	Carlo Erba Reagents

2.3 Apparatus and procedure

2.3.1 Apparatus description

The vapor pressure measurements for the pure chemicals and binary systems were carried out using a static apparatus. The apparatus description and the successive improvements carried out have already been published (Sasse et al., 1988), (Kasehgari et al., 1993) and (Mokbel et al., 1995). These improvements of the static device allow reliable measurements in a large pressure range between 0.5 Pa and 200 kPa (temperature range: -70 to 190 °C).

The static apparatus shown in Figure 2.1 consists mainly of a degassing system (shown in Figure 2.2), the measurement cell, the differential manometer (Datametrics MKS, type 670, model 616A), and the absolute pressure gage (Rosemount).

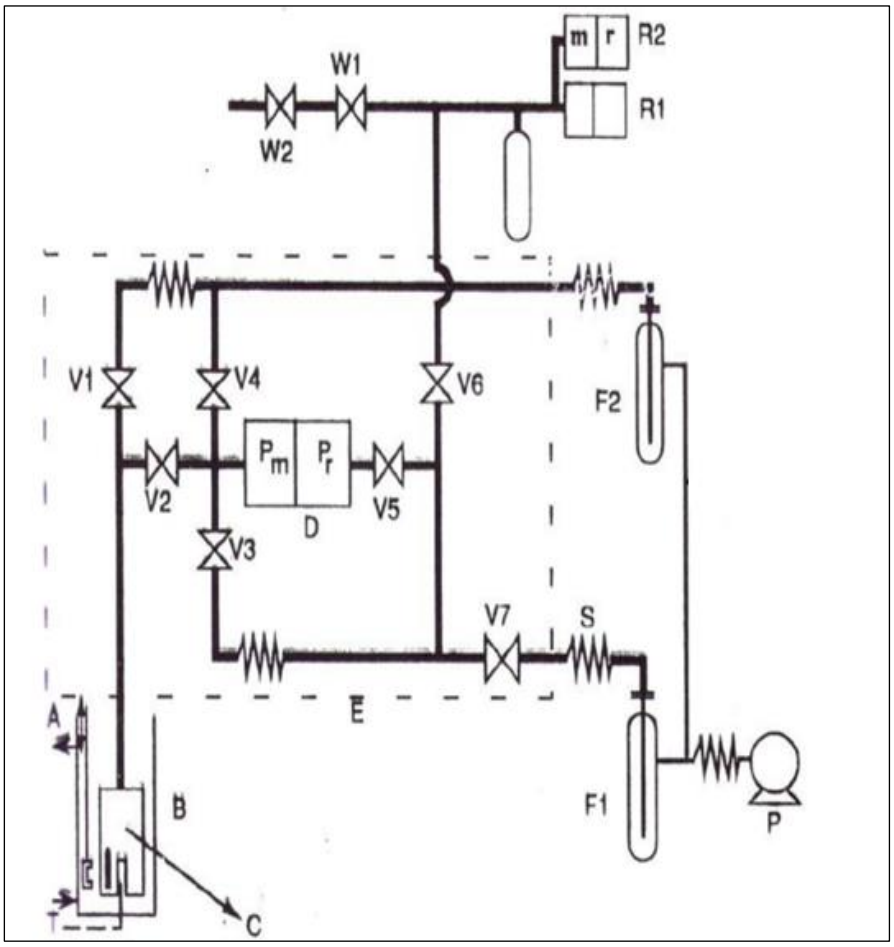

Figure 2.1: Static apparatus for vapor pressure measurement (P_m: measurement side; P_r: reference side). A: Magnetic stirrer; B: Thermostatic bath; C: Measuring cell; D: differential pressure sensor (Datametrics MKS); E: thermoregulated enclosure; F1 and F2: liquid nitrogen traps; P: vacuum pumps; R1: absolute pressure gauge (Rosemount 1); R2: differential pressure gauge (Rosemount 2); S: flexible; T: Copper-constantan thermocouple; $V_{1,2,3,4,5,6,7}$ and $W_{1,2}$: valves.

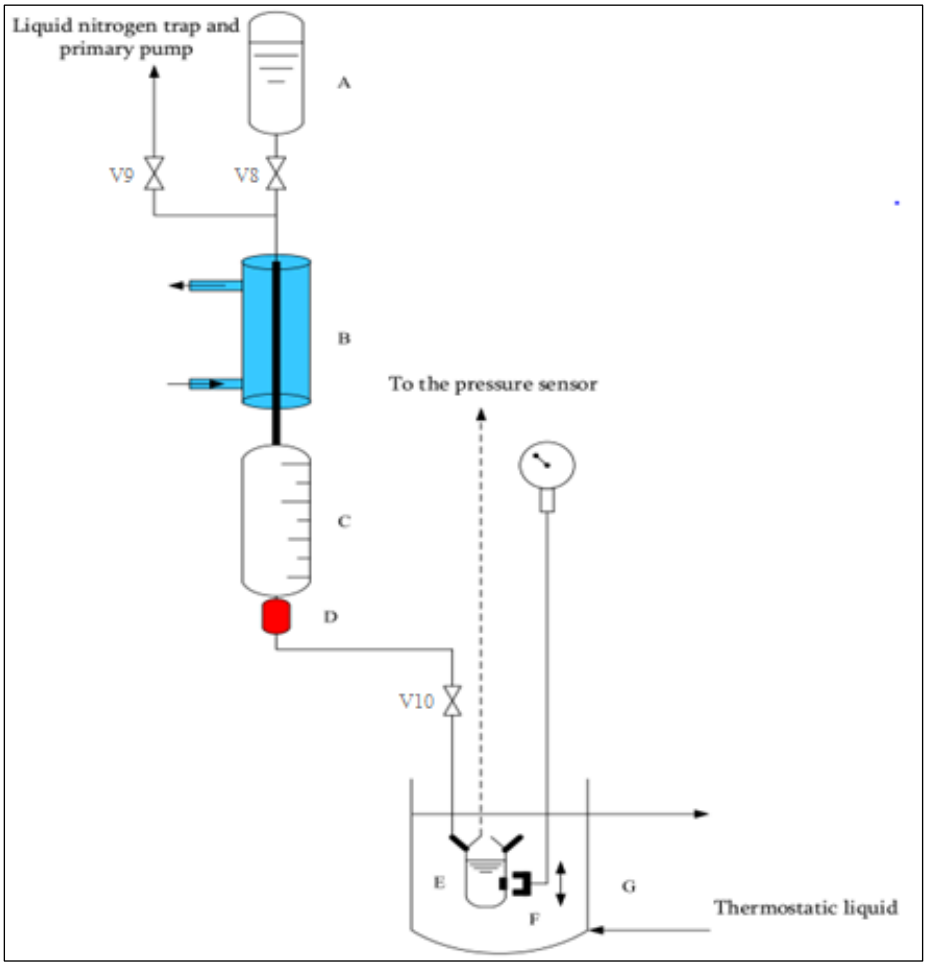

Figure 2.2: Schematic diagram of degassing system. A: Mixing preparation vial; B: refrigerant supplied with chilled water; C: degassing bulb; D: heated glass-to-metal welding; E: measuring cell; F: magnetic stirrer; G: thermostatically controlled bath; V8 and V10: valves; and V9: solenoid valve.

The measurement cell is constituted of two parts in order to permit rapid mounting and removal: the upper part is connected in permanence to the rest of the device, a condensation coil is welded on this part. The lower part constitutes the sample reservoir. When degassing, the lower part of the cell is heated and the coil is traversed by cold water (for heavy hydrocarbons) or by N_2 liquid (for volatile compounds such as cyclopentane) so as to minimize losses of the compound during vapor ventings.

Temperature measurements were carried out using a copper-constantan thermocouple calibrated against a 25 Ω platinum resistance standard thermometer (±0.001 K, IPTS 90) and a Leeds & Northrup bridge ($\pm 10^{-4}$ Ω). Calibration consists of measuring the electromotive force E delivered by the thermocouple as a function of the temperature t (°C) detected by the platinum resistance thermometer. During measurement, the stability of the temperature is ± 0.02 K.

The apparatus is equipped with three pressure gauge which give a possibility to measure in different regimes depending on the vapor pressure of the sample investigated.

a) Pressure range $0.5 \leq P\ (Pa) \leq 1300$

A differential manometer from Datametrics D, Wilmington, MA (model 1173) is used for measurements in the pressure range from 0.5 to 1300 Pa with a permanent dynamic pumping on its reference side P_r. The pressure measurement consists on applying the vapor pressure of the sample on the measurements side P_m of the gauge D by opening the valve V2 (V1, V3 and V4 closed). The vapor pressure is given by the following expression:

$$P = P_m - P_r \tag{2.1}$$

The residual pressure in the reference side P_r is about 10^{-4} Pa and therefore can be neglected.

b) Pressure range $1.3 \leq P\ (kPa) \leq 40$

The measurements are carried out by introducing air into the reference side P_r by opening V6 (V5, W1, W2 are opened and V7 closed). The absolute pressure gauge $R1$ allows the measurements of this back pressure P_{abs}.
The vapor pressure is given by:

$$P = (P_m - P_r)_{Datametrics} - P_{abs_{(Rosemount1)}} \tag{2.2}$$

c) Pressure range $40 \leq P\ (kPa) \leq 200$

In this case, the air back pressure is measured with the differential pressure gauge $R2$. First, the reference side of the gauge $R2$ is maintained at 0.1 Pa using a rotary pump. In this case, vapor pressure is calculated as follow:

$$P = (P_m - P_r)_{Datametrics} + (P_r - PR2)_{(Rosemount2)} \tag{2.3}$$

When the vapor pressure exceeds atmospheric pressure, nitrogen under pressure is introduced into the reference side of the gauge D and the reference side of the gauge $R2$ is at atmospheric pressure. Atmospheric pressure is measured by the gauge $R2$.
Vapor pressure is given by:

$$P = (P_m - P_r)_{Datametrics} + (P_r - PR2)_{(Rosemount2)} + P_{atm} \tag{2.4}$$

The pressure gages were calibrated against a U-manometer filled with mercury or apiezon K oil depending on the pressure range. The calibration was then checked by measuring the vapor and the sublimation pressures of water and naphthalene (Bassil et al., 2020; Sarraute et al., 2006).

The estimated uncertainties on our measurements of temperature and pressure are as follow:

- 0.02 °C for the temperature range $-70 \leq t\ (°C) \leq 190$
- 3% for pressures lower than 600 Pa
- 1% for the pressure range: $600 < P(Pa) < 1300$
- 0.3% for pressures over 1300 Pa

2.3.2 Degassing procedure and vapor pressure measurement

Degassing of pure chemicals and their binary mixtures is performed using a degassing system of the apparatus shown in Figure 2.2. This system allows to carry out the degassing and to limit as much as possible the change of composition of the binary mixtures.

First, 110 ml of the binary mixture is prepared in the mixing preparation vial A by weighing. A quantity of 3 cm^3 of this mixture is stored in a refrigerator and is used as a standard for gas chromatography. The remaining quantity is used for the vapor pressure measurements after being thoroughly degassed to remove the dissolved air.

The sample is transferred to the glass degassing bulb C by opening valve V8 (valve V10 is closed). The degassing process is carried out by boiling the sample under vacuum. An electric valve, opened for a few seconds, evacuates the dissolved air in the sample. The refrigerant placed above the degassing bulb and maintained at 0 °C minimizes the loss of the sample and the change of its composition. After degassing, the sample is slowly transferred into the measurement cell E, by opening V10. The measurement cell is immersed in a constant-temperature bath and is stirred during the experiment.

Once thermodynamic equilibrium is reached, the vapor is released by opening V1 during 10 seconds to 2 minutes according to the pressure. Opening V2, pressure is transmitted to the pressure gauge. The apparatus is provided with V4 which allows vapor evacuation into the trap F2 after measurement. Once the vapor pressures measurements were carried out, melting ice is used to condensate the vapor in the measurement cell. After that, the sample is collected from the measurement cell in order to determine its composition by gas chromatography.

2.3.3 Determination of mole fraction in liquid phase

Mole fraction of mixture after vapor pressure measurements have been determined by gas chromatography. Before degassing, 3 cm^3 of the sample are taken to serve as a reference for determining the mole fraction of liquid mixture which is calculated as follow:

$$\left(\frac{x_1}{x_2}\right)_{after} = \left(\frac{x_1}{x_2}\right)_{before} \frac{\left(\frac{S_1}{S_2}\right)_{after}}{\left(\frac{S_1}{S_2}\right)_{before}} \quad (2.5)$$

Where: $x_1 + x_2 = 1$

S: Chromatography peak area « before » and « after » vapor pressure measurement.
The chromatographic conditions are as follow:

- Gas chromatography apparatus: « GC Agilent 6890 plus » with automatic injector and autosampler.
- Column: RTX amines, length 30 m, diameter 320 µm, film thickness 1 µm.
- Carrier gas : H_2, 40 mL/min
- Detector: flame ionization detector FID, 250°C

- Injected volume : 1 µL
- Injection: split =10, injector set at 250 °C

Figure 2.3 (a)

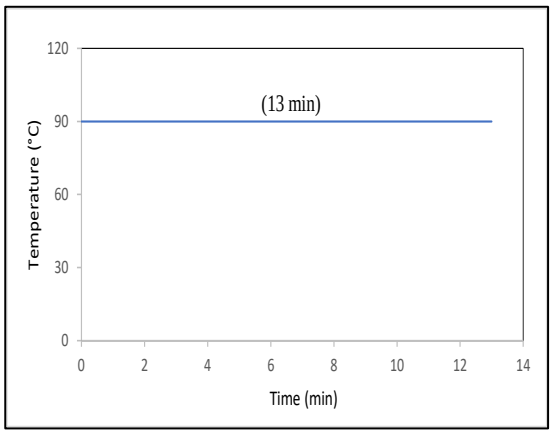

Figure 2.3 (b)

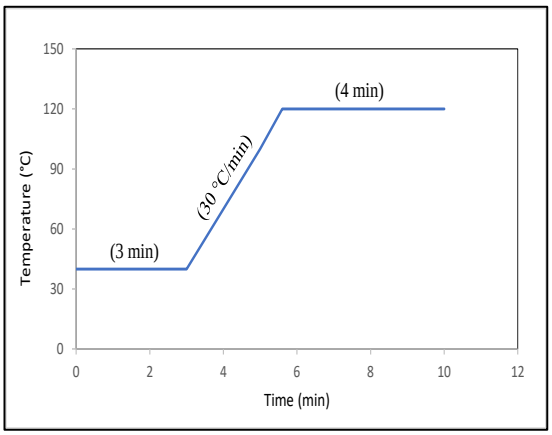

Figure 2.3 (c)

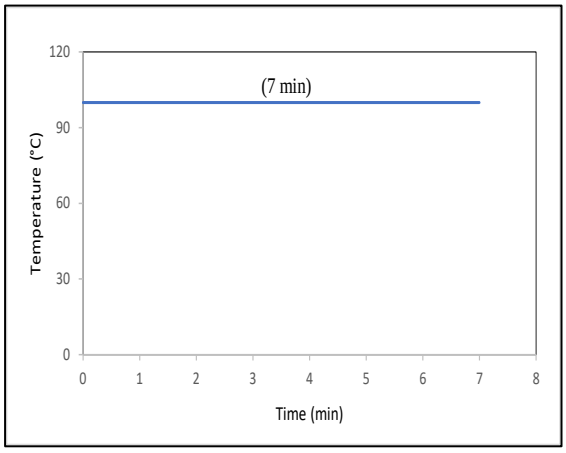

Figure 2.3: Oven temperature programming for (a): 1,3,5-trimethylbenzene, (b): propan-2-ol and (c): DMSO binary mixtures.

Figure 2.4 (a)

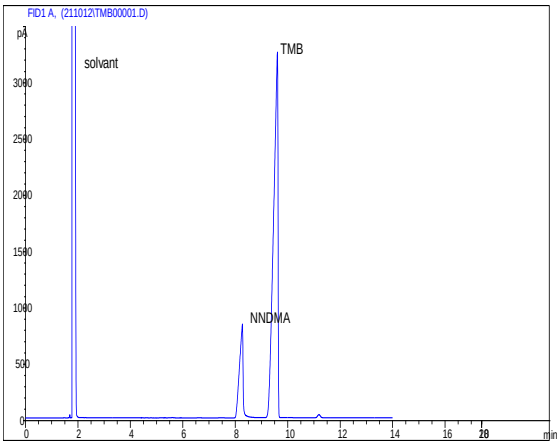

Figure 2.4 (b)

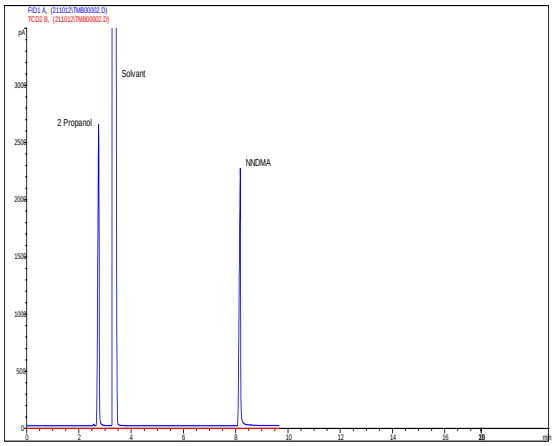

Figure 2.4 (c)

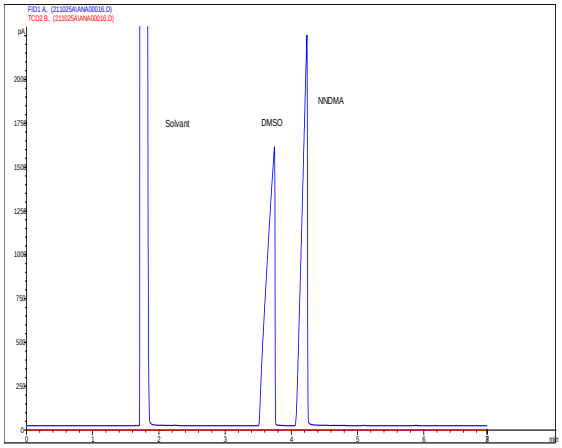

Figure 2.4: Examples of gas chromatography analyses for (a): 1,3,5-trimethylbenzene, (b): propan-2-ol and (c): DMSO binary mixtures.

2.4 Theoretical part

2.4.1 Antoine equation

Many different formulas and representations have been presented for the vapor pressure-temperature relationship for pure liquids and their mixtures. This is due not only to the importance of this physical property itself but also to its relation to other thermodynamic properties. Antoine's equation (Antoine, 1888) is one of the most common equations used for interpolation of pressures at the temperatures under consideration of pure liquids and their mixtures. The equation in its simplified form is given by:

$$\log_{10} P\ (Pa) = A\ - \frac{B}{T\ (K)+C} \tag{2.6}$$

where P is the vapor pressure, T is the temperature.
$A,\ B$ and C are constants, different for each component.

The constants $A,\ B$ and C have been obtained by minimizing the following objective function:

$$Q = \sum \left(\frac{P_{calc} - P_{exp}}{P_{exp}} \right)^2 \tag{2.7}$$

The overall mean relative deviation in pressure is:

$$\frac{\delta P}{P}\ \% \ = \ \frac{100}{n} \sum_{i=1}^{n} \left(\frac{P_{calc}\ - P_{exp}}{P_{exp}} \right) \tag{2.8}$$

Where n is the total number of experimental values.

2.4.2 Barker Method

Barker's method application is required in the study of vapor-liquid equilibrium of multi-component system. It is more efficient in systems comprising two solvents than using other classical methods of parameter estimation because it eliminates the need to experimentally draw vapor phase compositions, which generally have high experimental errors. Instead, total pressure and liquid mole fraction data are used to obtain the activity coefficient model and parameters and hence to calculate vapor phase mole fraction that were not directly measured (Jain, 2021). Also, Barker method have been used to determine the molar excess Gibbs functions G^E from the Redlich-Kister equation (Barker, 1953).

Vapor-liquid equilibrium is described by equality of fugacities. At equilibrium, at system temperature T and pressure P, the fugacity of each component i in vapor phase is equal to the fugacity of the same component in liquid phase:

$$f_i^v \ = \ f_i^l \tag{2.9}$$

f_i^v, f_i^l: fugacity of component i in vapor and liquid phase respectively.

For the vapor phase, the composition is nearly always expressed by the mole fraction y. To relate f_i^v to temperature, pressure and mole fraction, it is useful to introduce the vapor phase fugacity coefficient ϕ_i^v :

$$f_i^v = y_i \, \phi_i \, P \tag{2.10}$$

The liquid phase fugacity of component i is related to its mole fraction x_i in the liquid phase by:

$$f_i^l = x_i \, \gamma_i f_i^{0\,L} \tag{2.11}$$

Here γ_i is the liquid phase activity coefficient of component i.
$f_i^{0\,L}$ is the fugacity of liquid component i at system temperature and pressure at a defined standard state.

The fugacity $f_i^{0\,L}$ of the pure liquid is related to its vapor pressure p_i :

$$f_i^{0\,L} = p_i \, \phi_i^0 \, exp\left[\int_{P_i}^{P} \frac{V_i}{RT} dP\right] \tag{2.12}$$

Here the expression $exp\left[\int_{P_i}^{P} \frac{V_i}{RT} dP\right]$ is the so-called Poynting correction which allows for the influence of the change of pressure on fugacity from P to p_i.

ϕ_i^0: is the fugacity coefficient for the pure component at the pressure p_i.

By combining equations (2.9), (2.10) and (2.11) one obtains the following equation for equilibrium between vapor and liquid at the temperature T and the pressure P:

$$y_i \, \phi_i P = x_i \, \gamma_i \, p_i \, \phi_i^0 \, exp\left[\int_{P_i}^{P} \frac{V_i}{RT} dP\right] \tag{2.13}$$

P: total equilibrium pressure
p_i: vapor pressure of pure component i
y_i: mole fraction in vapor phase of component i
ϕ_i: vapor phase fugacity coefficient
x_i: mole fraction in liquid phase of component i
γ_i: activity coefficient of component i in the liquid phase
V_i: molar volume of pure liquid i

At low pressures, equation (2.13) can be simplified, because the fugacity coefficients tend towards 1 and Poynting corrections usually are very close to unity.

Neglecting these corrections leads to:

$$y_i \, P = x_i \, \gamma_i \, p_i \tag{2.14}$$

The total pressure for binary system is calculated by the following expression:

$$P = \gamma_1 x_1 p_1 + \gamma_2 x_2 p_2 \tag{2.15}$$

Where:
P: total equilibrium pressure
x_i: mole fraction in liquid phase of component i
γ_i: activity coefficient of component i in the liquid phase
p_i: vapor pressure of pure component i

$$p_1 = P\ exp\left[\frac{(V_1^L - B_{11})(P - P_1) - P\delta_{12}y_2^2}{RT}\right] \tag{2.16}$$

$$p_2 = P\ exp\left[\frac{(V_2^L - B_{22})(P - P_2) - P\delta_{12}y_1^2}{RT}\right] \tag{2.17}$$

In which is defined by: $\delta_{12} = 2B_{12} - B_{11} - B_{22} = 2B_{12}^E$

B_{ii}: second virial coefficient of pure component i
y_i : mole fraction in vapor phase of component i
V_i^L: liquid molar volume of component i
B_{12}: second virial cross coefficient
B_{12}^E: excess second virial cross coefficient

The molar excess Gibbs functions G^E were estimated from the Redlich-Kister equation using Barker's method (Barker, 1953):

$$G^E = x_1\,(1 - x_1)\sum_{j=1}^{m} RTG_j(x_1 - x_2)^{j-1} \tag{2.18}$$

Where: m is number of parameters G_j .
$x_1\ and\ x_2$: mole fractions of component 1 and 2, respectively.

With:

$$G^E = x_1\overline{G_1}^E + x_2\overline{G_2}^E \tag{2.19}$$

$$\overline{G_i}^E = RT\ln\gamma_i = \frac{\delta[(n_1+n_2)G^E]}{\delta n_i} \tag{2.20}$$

The derivation indicated above leads to the following expressions:

$$\ln\gamma_1 = x_2^2\sum_{j=1}^{m}\{G_i(x_1 - x_2)^{j-2}[(2j-1)x_1 - x_2]\} \tag{2.21}$$

$$\ln\gamma_2 = x_1^2\sum_{j=1}^{m}\{G_i(x_1 - x_2)^{j-2}[x_1 - (2j-1)x_2]\} \tag{2.22}$$

$$x_1 d\ln\gamma_1 + x_2 d\ln\gamma_2 = 0 \qquad (T, P\ x = Constants)$$

Using the experimental results (x, P), the coefficients G_j were determined by regression through minimization of the sum of deviations in vapor pressures.

$$\sum_{i=1}^{n} \left| \frac{P_{exp} - P_{calc}}{P_{exp}} \right|^2 \tag{2.23}$$

The vapor phase composition is calculated using equation (2.14) and the activity coefficients values obtained from equations (2.21) and (2.22):

$$y_i = \frac{x_i \gamma_i}{P} P_i \tag{2.24}$$

2.5 Results and discussions

2.5.1 Experimental vapor pressures of pure compounds

Experimental vapor pressures of the pure compounds measured between 273.15 and 363.15 K for N,N-dimethylacetamide and 1,3,5-trimethylbenzene, between 273.15 and 357.15 K for propan-2-ol and between 293.15 and 363.15 K for DMSO are given in Tables 2.3 to 2.6. The presentation plots of vapor pressures are compared in Figures 2.5, 2.6, 2.7 and 2.8 with the literature data for all pure compounds.

For pure N,N-dimethylacetamide, our vapor pressures data are in good agreement with those reported by (Štejfa et al., 2020) in the temperature range (238.15 to 308.15) K and (Zhang et al., 2013) in the temperature range (378.79 to 440.31) K as presented in Figure 2.5.

Figure 2.5 (a) **Figure 2.5 (b)**

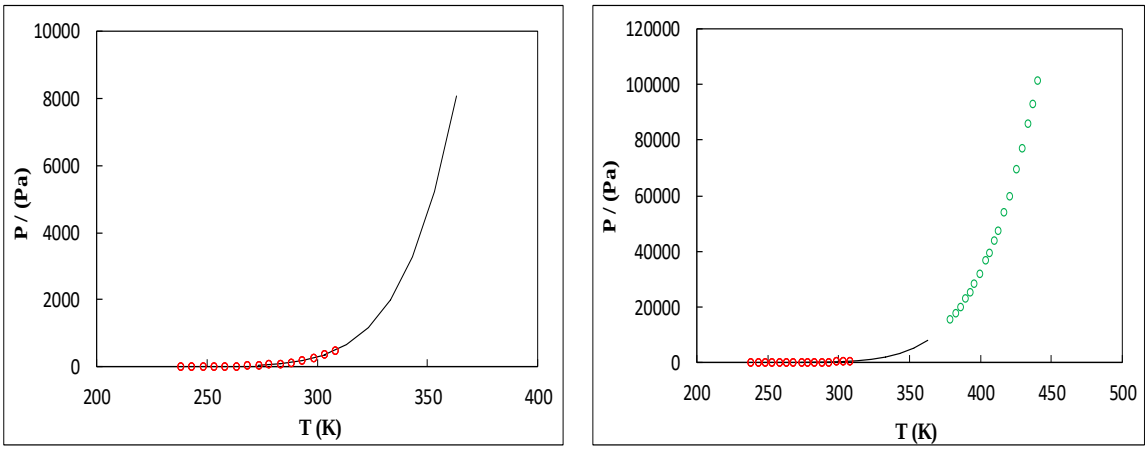

Figure 2.5: Vapor pressures of N,N-dimethylacetamide (—) together with literature (a) Štejfa et al.(2020) (o) and (b) Štejfa et al.(2020) (o) and Zhang et al.(2013) (o).

As indicated in Figure 2.6, our experimental vapor pressures for 1,3,5-trimethylbenzene show an excellent agreement with the literature data (Khelidj et al., 2020) in the temperature range (273.15 to 363.15) K. Also, our experimental results agree with those reported by (Kassel et al., 1936) in the same temperature range.

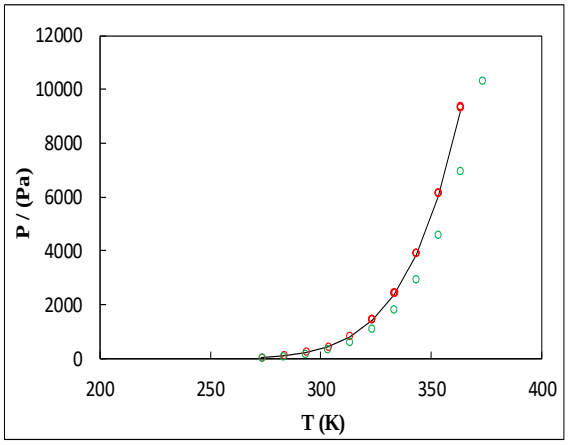

Figure 2.6: Vapor pressures of 1,3,5-trimethylbenzene (—) together with literature Khelidj et al. (2020) (o) and Kassel et al. (1936) (o).

In Figure 2.7 experimental vapor pressures for propan-2-ol fit perfectly to literature values reported by (Nasirzadeh et al., 2004); (Zhang et al., 2013) and (Dejoz et al., 1996) in the temperature range (298.15 to 355.42) K.

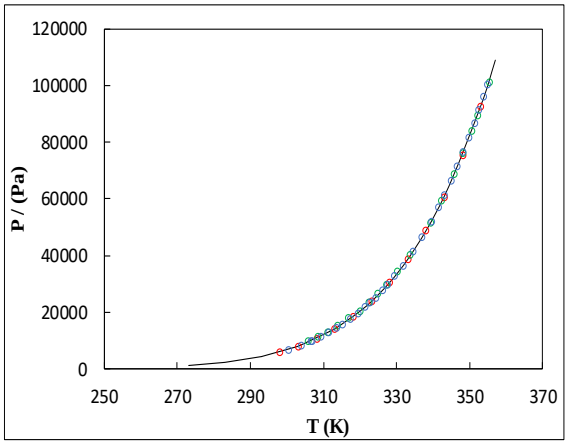

Figure 2.7: Vapor pressures of propan-2-ol (—) together with literature Nasirzadeh et al. (2004) (o) Zhang et al. (2013) (o) and Dejoz et al. (1996) (o).

In Figure 2.8 comparison of the data indicates no systematic discrepancy between experimental vapor pressures of DMSO and literature values reported by (Negadi et al., 2002). The comparison is favorable in the temperature range (293.15 to 363.15) K.

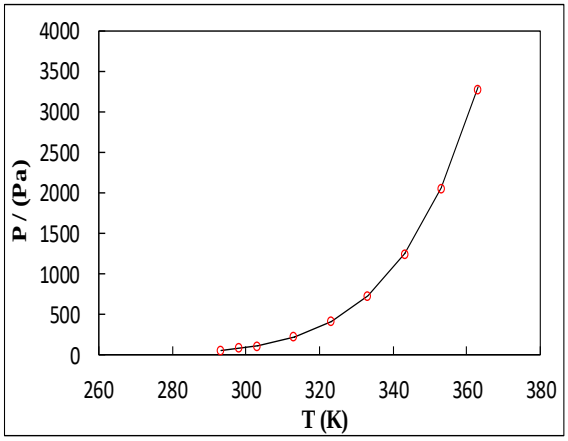

Figure 2.8: Vapor pressures of DMSO (—) together with literature Negadi et al. (2002) (o).

As mentioned above, experimental vapor pressures for pure components were fitted to the Antoine equation and the evaluated constants A, B, C are summarized in Table 2.2 together with the overall mean relative deviations in pressure. We observed that the Antoine equation fits our experimental results with standard deviations 0.12% for N,N-dimethylacetamide, 0.11% for 1,3,5-trimethylbenzene, 0.28% for propan-2-ol and 0.09% for DMSO.

Table 2.2: Coefficients A, B, and C and overall mean relative deviation in pressure of the Antoine equation

Components	A (σ_A)	B (σ_B)	C (σ_C)	$\delta P/P$ (%)
N,N-dimethylacetamide $0 \leq T\ (°C) \leq 90$	7.608 (0.015)	1846 (8.260)	227.0 (0.593)	0.12
1,3,5-trimethylbenzene $0 \leq T\ (°C) \leq 90$	7.496 (0.019)	1807 (10.40)	229.4 (0.769)	0.11
propan-2-ol $0 \leq T\ (°C) \leq 84$	8.196 (0.035)	1600 (17.74)	219.0 (1.404)	0.28
DMSO $20 \leq T\ (°C) \leq 90$	7.837 (0.027)	2092 (15.24)	234.8 (1.041)	0.09

2.5.2 Vapor-liquid equilibrium of binary mixtures

The VLE data of binary systems were measured at temperature ranging from 273.15 to 363.15 K for {N,N-dimethylacetamide (1) + 1,3,5-trimethylbenzene (2)}, from 273.15 to 353.15 K for {N,N-dimethylacetamide (1) + propan-2-ol (2)} and from 293.15 to 363.15 K for {N,N-dimethylacetamide (1) + DMSO (2)}. The obtained results were fitted to the Antoine equation at constant composition. Then, the experimental data were reduced according to the Barker method (Barker, 1953). The molar excess Gibbs functions G^E were estimated from the Redlich-Kister equation.

a) N,N-dimethylacetamide (1) + 1,3,5-trimethylbenzene (2)

The Antoine parameters A, B, C for this binary mixture are given in Table A2.8 for each composition. The relative error between the experimental and the calculated values are between 0.05 and 1.19 %.
The constants of the Redlich-Kister expansion and the pressure standard deviations for {N,N-dimethylacetamide (1) + 1,3,5-trimethylbenzene (2)} are listed in Table A2.7. A three-parameter expansion have been used for data of this mixture.
The experimental $x - P$ data, calculated y_i, $G^E$and activity coefficients γ_i for the {N,N-dimethylacetamide (1) + 1,3,5-trimethylbenzene (2)} binary system at 273.15 to 363.15 K are summarized in Table A2.11. From Figure 2.9, it can be seen that our experimental pressures are in a good agreement with those estimated using Barker's method. This system shows positive azeotropic behavior for the whole investigated temperatures (273.15 to 363.15 K). The azeotropic composition vary approximatively from 0.3000 at T = 273.15 K to 0.4000 at T = 363.15 K. To the best of our knowledge, there are no *(T-P-x)* data found in the open literature for comparison at the investigated temperature range for all the mixtures.

The excess Gibbs energies G^E for {N,N-dimethylacetamide (1) + 1,3,5-trimethylbenzene (2)} binary system are shown in Figure 2.10. This system exhibits positive deviations in G^E values over the whole composition range. G^E values decrease with increasing temperature at a fixed composition for low mole fraction N,N-dimethylacetamide (compositions x_1 between 0.1 to 0.4). For high mole fraction N,N-dimethylacetamide, the variation of G^E is as follow: at $x_1 = 0.6$, G^E increase then decrease with temperature inversely to $x_1 = 0.8\ or\ 0.9$ where G^E decrease then increase with temperature. Increasing temperature from 273.15 to 363.15 K leads to an increase in G^E for $x_1 = 0.7$. The equimolar G^E of this system increases with increasing temperature from 821.6 J.mol^{-1} at T = 273.15 K to 822.2 J.mol^{-1} at T = 283.15 K then decrease to 782.4 J.mol^{-1} at 363.15 K.

Figure 2.9 (a) **Figure 2.9 (b)**

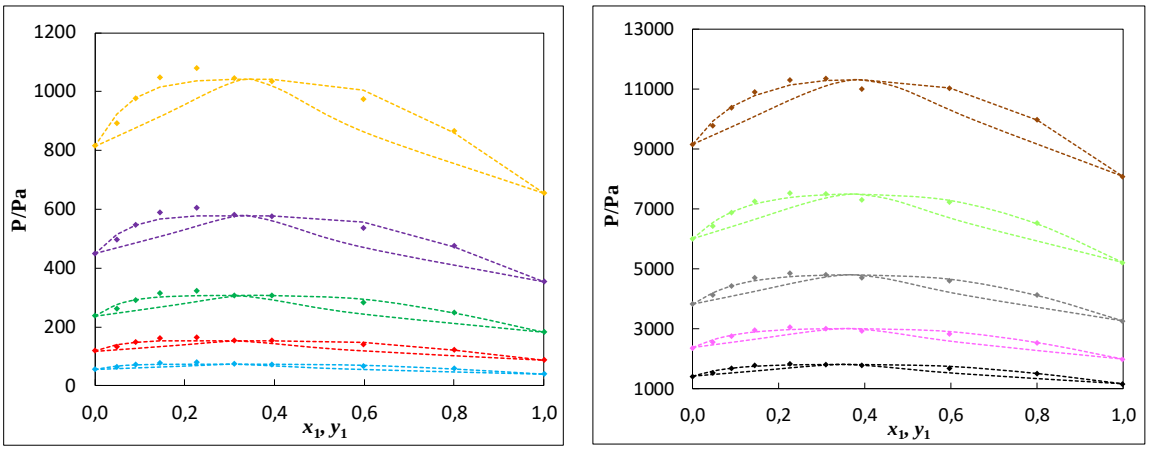

Figure 2.9: Plot of the experimental and calculated values of P against mole fraction x, y for the binary mixture {N,N-dimethylacetamide (1) + 1,3,5-trimethylbenzene (2)} at different temperatures (a): 273.15 K (◆), 283.15 K (◆), 293.15 K (◆), 303.15 K (◆), 313.15 K (◆), (b): 323.15 K (◆), 333.15 K (◆), 343.15 K (◆), 353.15 K (◆), 363.15 K (◆). The dotted lines are the calculated values using Barker method.

Figure 2.10 (a) **Figure 2.10 (b)**

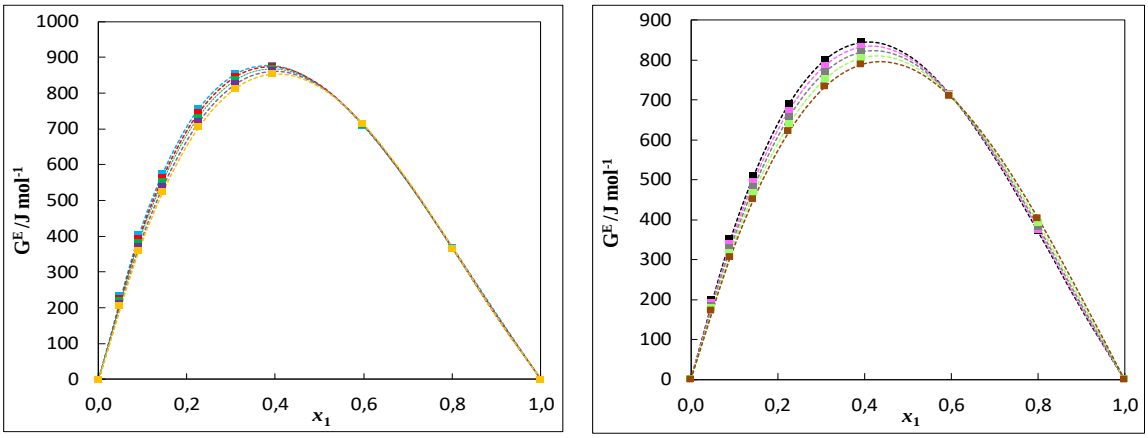

Figure 2.10: Plot of excess Gibbs energies G^E calculated using Barker Method against mole fraction x for the binary mixture {N,N-dimethylacetamide (1) + 1,3,5-trimethylbenzene (2)} at different temperatures (a): 273.15 K (■), 283.15 K (■), 293.15 K (■), 303.15 K (■), 313.15 K (■), (b): 323.15 K (■), 333.15 K (■), 343.15 K (■), 353.15 K (■), 363.15 K (■).

b) N,N-dimethylacetamide (1) + propan-2-ol (2)

Table A2.9 summarizes the Antoine parameters A, B, C at constant composition for {N,N-dimethylacetamide (1) + propan-2-ol (2)} binary system. The relative error between the experimental and the calculated values is less than 1 %.
The constants of the Redlich-Kister expansion and the pressure standard deviations for {N,N-dimethylacetamide (1) + propan-2-ol (2)} are given in Table A2.7. A four-parameter expansion have been used for this system.
The experimental $x - P$ data, calculated y_i, $G^E$and activity coefficients γ_i for the {N,N-dimethylacetamide (1) + propan-2-ol (2)} binary system at 273.15 to 353.15 K are presented in Table A2.11 and the plots of the experimental and calculated pressures are shown in Figure 2.11. From Figure 2.11, it is noticeable that the experimental pressures are in a good accordance with those estimated using Barker's method.

Figure 2.12 represent the change in the excess Gibbs energies G^E for the {N,N-dimethylacetamide (1) + propan-2-ol (2)} mixture. The G^E data exhibit negative values over the entire range of composition at all investigated temperatures. The increase of temperature leads to a decrease in G^E values in propan-2-ol rich region. For the N,N-dimethylacetamide rich region, we observe a decrease in the excess Gibbs energies G^E values at low temperatures followed by an increase at high temperatures. The equimolar G^E of this system decreases with increasing temperature from -262 J.mol^{-1} at T = 273.15 K to -439.5 J.mol^{-1} at T = 353.15 K.

Figure 2.11 (a) **Figure 2.11 (b)**

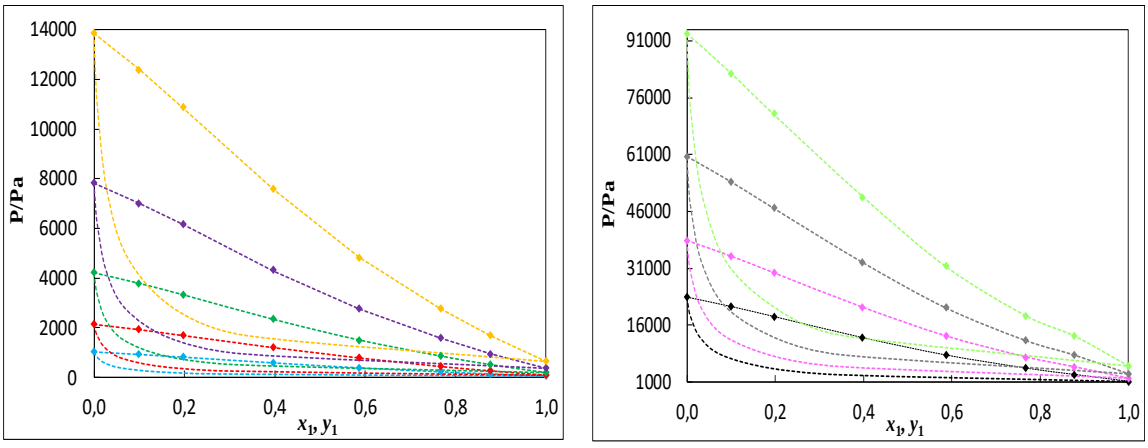

Figure 2.11: Plot of the experimental and calculated values of P against mole fraction x, y for the binary mixture {N,N-dimethylacetamide (1) + propan-2-ol (2)} at different temperatures (a): 273.15 K (◆), 283.15 K (◆), 293.15 K (◆), 303.15 K (◆), 313.15 K (◆), (b): 323.15 K (◆), 333.15 K (◆), 343.15 K (◆), 353.15 K (◆). The dotted lines are the calculated values using Barker method.

Figure 2.12 (a) **Figure 2.12 (b)**

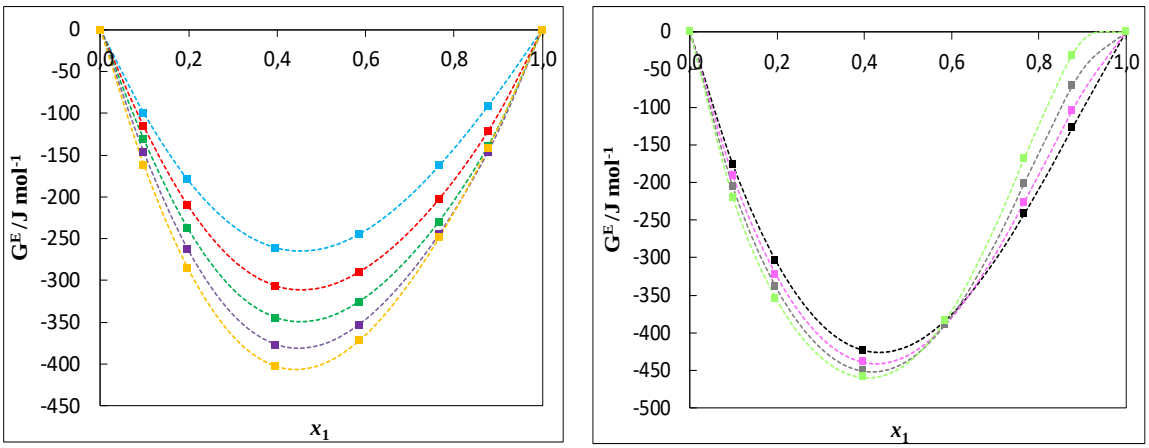

Figure 2.12: Plot of excess Gibbs energies G^E calculated using Barker Method against mole fraction x for the binary mixture {N,N-dimethylacetamide (1) + propan-2-ol (2)} at different temperatures (a): 273.15 K (■), 283.15 K (■), 293.15 K (■), 303.15 K (■), 313.15 K (■), (b): 323.15 K (■), 333.15 K (■), 343.15 K (■), 353.15 K (■).

c) N,N-dimethylacetamide (1) + DMSO (2)

The Antoine parameters A, B, C for {N,N-dimethylacetamide (1) + DMSO (2)} system are given in Table A2.10. The relative error between our experimental data and the calculated values is less than 0.18 %.

Table A2.7 reports the constants of the Redlich-Kister expansion and the pressure standard deviations of this system where a three-parameter expansion have been used.

The experimental $x - P$ data, calculated y_i, G^E and activity coefficients γ_i for the {N,N-dimethylacetamide (1) + DMSO (2)} binary mixture at 293.15 to 363.15 K are listed in Table A2.11 and the plots of the experimental pressures and those calculated using Barker's method are shown in Figure 2.13. As observed, the estimated pressures are in a good agreement with our experimental values.

Figure 2.13 (a) **Figure 2.13 (b)**

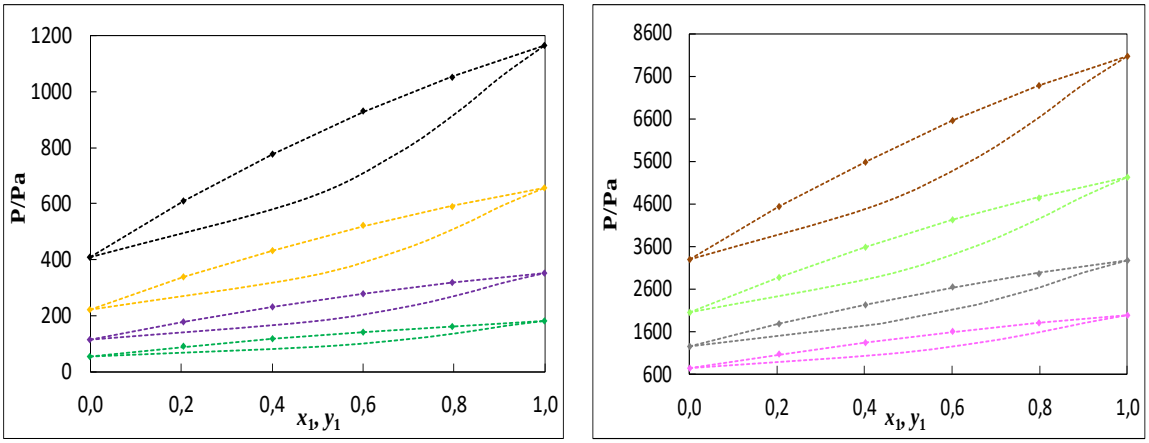

Figure 2.13: Plot of the experimental and calculated values of P against mole fraction x, y for the binary mixture {N,N-dimethylacetamide (1) + DMSO (2)} at different temperatures (a): 293.15 K (◆), 303.15 K (◆), 313.15 K (◆), 323.15 K (◆), (b): 333.15 K (◆), 343.15 K (◆), 353.15 K (◆), 363.15 K (◆). The dotted lines are the calculated values using Barker method.

The excess Gibbs energies G^E values are presented in Figures 2.14 for {N,N-dimethylacetamide (1) + DMSO (2)} mixture. Positive deviation is observed in G^E values at all temperatures and over the entire composition range. Increasing temperature from 293.15 to 363.15 K leads to a decrease in G^E values at fixed composition. The equimolar G^E of {N,N-dimethylacetamide (1) + DMSO (2)} decreases with increasing temperature from 201.7 J.mol^{-1} at T = 293.15 K to 174.7 J.mol^{-1} at T = 363.15 K.

Figure 2.14 (a) **Figure 2.14 (b)**

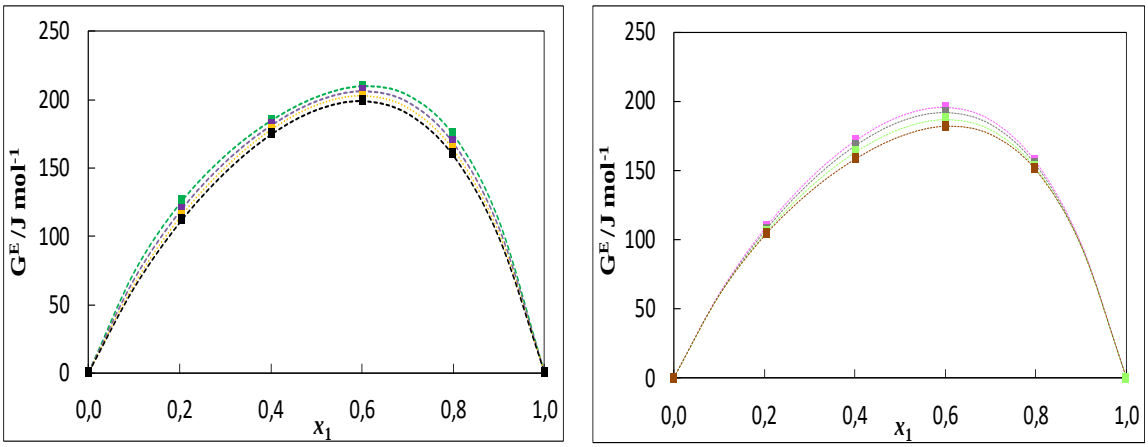

Figure 2.14: Plot of excess Gibbs energies G^E calculated using Barker Method against mole fraction x for the binary mixture {N,N-dimethylacetamide (1) + DMSO (2)} at different temperatures (a): 293.15 K (■), 303.15 K (■), 313.15 K (■), 323.15 K (■), (b): 333.15 K (■), 343.15 K (■), 353.15 K (■), 363.15 K (■).

2.6 Modeling of vapor-liquid equilibrium

In this part the NRTL (non-random two-liquid), UNIQUAC (universal quasi-chemical) and modified UNIFAC (Dortmund) models have been applied in order to model the phase equilibria of the studied binary mixtures. The simulation software used for this purpose is SIMULIS THERMODYNAMICS marketed by the company PROSIM (France).

2.6.1 Activity coefficient models

2.6.1.1 NRTL model (Non-Random Two Liquid)

The nonrandom two-liquid model was an empirical equation proposed by (Renon and Prausnitz,1968) based on the local composition representation of the excess Gibbs energy G^E of liquid mixtures. The NRTL expression for the Gibbs energy is:

$$\frac{G^E}{RT} = \sum_i x_i \frac{\sum_j \tau_{ji} G_{ji} x_j}{\sum_k G_{ki} x_k} \tag{2.25}$$

The NRTL model is utilized widely in phase equilibria calculations and employs three adjustable parameters (two interaction parameters and the non-randomness factor) that are determined through regression of experimental data for a specific binary vapor–liquid equilibrium (VLE) system.

For binary mixtures, NRTL equation is given as follow:

$$\frac{G^E}{RT} = x_1 x_2 \left(\frac{\tau_{21} G_{21}}{x_1 + x_2 G_{21}} + \frac{\tau_{12} G_{12}}{x_1 G_{12} + x_2} \right) \tag{2.26}$$

Where

$$\tau_{21} = \frac{g_{21} - g_{11}}{RT} \tag{2.27}$$

$$\tau_{12} = \frac{g_{12} - g_{22}}{RT} \tag{2.28}$$

$$G_{12} = exp(-\alpha_{12}\tau_{12}) \tag{2.29}$$

$$G_{21} = exp(-\alpha_{12}\tau_{21}) \tag{2.30}$$

The two interaction parameters $(g_{12} - g_{22})$ and $(g_{21} - g_{11})$ are temperature-dependent parameters, inversely to the non-randomness parameter α_{12} which, to a good approximation, does not depend on temperature and can often be estimated with sufficient accuracy from the nature of components 1 and 2 (Renon and Prausnitz,1968).

From (2.26) the activity coefficients γ_1 and γ_2 of component 1 and 2 in a binary mixture are obtained by differentiation:

$$\ln \gamma_1 = x_2^2 \left[\tau_{21} \left(\frac{G_{21}}{x_1 + x_2\, G_{21}}\right)^2 + \frac{\tau_{12} G_{12}}{(x_1 G_{12} + x_2)^2}\right] \tag{2.31}$$

$$\ln \gamma_2 = x_1^2 \left[\tau_{12} \left(\frac{G_{12}}{x_1 G_{12} + x_2}\right)^2 + \frac{\tau_{21} G_{21}}{(x_1 + x_2 G_{21})^2}\right] \tag{2.32}$$

The NRTL equation is readily generalized to multicomponent mixtures, the result for such mixtures contains only binary parameters.

2.6.1.2 UNIQUAC model (Universal Quasi Chemical)

The UNIQUAC equation gives a good representation of vapor–liquid equilibria (VLE) using only two adjustable interaction parameters which describe the energy of interaction between molecules i and j, for each binary pair. The UNIQUAC equation has been proposed by (Abrams and Prausnitz,1975), it consists of a combinatorial part that attempts to describe the dominant entropic contribution, and a residual part that is due primarily to intermolecular forces that are responsible for the enthalpy of mixing. The combinatorial part is determined only by the composition and by the sizes and shapes of the molecules, it requires only pure component data. The residual part, however, depends also on intermolecular forces, the two adjustable binary parameters, therefore, appear only the residual part (Prausnitz et al., 1998).

The UNIQUAC equation for binary systems is:

$$g^E = g^E_{(combinatorial)} + g^E_{(residual)} \tag{2.33}$$

$$\frac{g^E_{(combinatorial)}}{RT} = x_1 \ln \frac{\Phi_1}{x_1} + x_2 \ln \frac{\Phi_2}{x_2} + \frac{z}{2}\left(q_1 x_1 \ln \frac{\theta_1}{\Phi_1} + q_2 x_2 \ln \frac{\theta_2}{\Phi_2}\right) \tag{2.34}$$

$$\frac{g^E_{(residual)}}{RT} = -q_1 x_1 \ln(\theta_1 + \theta_2 \tau_{21}) - q_2 x_2 \ln(\theta_2 + \theta_1 \tau_{12}) \tag{2.35}$$

Where the coordination number is set equal to 10 and segment fraction Φ and area fraction θ are given by:

$$\Phi_1 = \frac{x_1 r_1}{x_1 r_1 + x_2 r_2} \tag{2.36}$$

$$\theta_1 = \frac{x_1 q_1}{x_1 q_1 + x_2 q_2} \tag{2.37}$$

The parameters r and q are pure-component molecular-structure constants depending on molecular size and external surface areas.

For each binary combination in a multicomponent mixture, there are two adjustable parameters τ_{21} and τ_{12}. These, in turn are given in terms of characteristic energies Δu_{21} and Δu_{12} by:

$$\ln \tau_{21} = -\frac{\Delta u_{21}}{RT} \tag{2.38}$$

$$\ln \tau_{12} = -\frac{\Delta u_{12}}{RT} \tag{2.39}$$

In a multicomponent mixture, the UNIQUAC equation for the activity coefficient of component i is:

$$\ln \gamma_i = \ln \gamma_i^C + \ln \gamma_i^R \tag{2.40}$$

The combinatorial part is given by:

$$\ln \gamma_i^C = \ln \frac{\Phi_i}{x_i} + \frac{z}{2} q_i \ln \frac{\theta_i}{\Phi_i} + l_i - \frac{\Phi_i}{x_i} \sum_j x_j l_j \tag{2.41}$$

$$l_i = \frac{z}{2}(r_i - q_i) - (r_i - 1) \tag{2.42}$$

The residual part is given by:

$$\ln \gamma_i^R = q_i - q_i \ln \left(\sum_{j=1}^{n} \theta_j \tau_{ji} \right) - q_i \sum_{j=1}^{n} \frac{\theta_j \tau_{ij}}{\sum_{k=1}^{n} \theta_k \tau_{kj}} \tag{2.43}$$

2.6.1.3 Original UNIFAC model (Universal Functional Activity Coefficient)

The original UNIFAC model that combines the functional group concept with a model for activity coefficients based on an extension of the quasi-chemical theory of liquid mixtures (UNIQUAC) was proposed by (Fredenslund et al., in 1975). This model can be applied at infinite dilution and finite concentrations and was the most widely used before several revisions and extensions were developed. The activity coefficient is expressed as a function of composition and temperature. The model has a combinatorial contribution to the activity coefficient, $\ln \gamma_i^C$, essentially due to differences in size and shape of the molecules, and a residual contribution, γ_i^R, essentially due to energetic interactions.

$$\ln \gamma_i = \ln \gamma_i^C + \ln \gamma_i^R \tag{2.44}$$

Combinatorial Part:

$$\ln \gamma_i^C = \ln \frac{\Phi_i}{x_i} + \frac{z}{2} q_i \ln \frac{\theta_i}{\Phi_i} + l_i - \frac{\Phi_i}{x_i} \sum_j x_j l_j \tag{2.45}$$

$$\Phi_i = \frac{r_i x_i}{\sum_j x_j r_j} \tag{2.46}$$

$$\theta_i = \frac{q_i x_i}{\sum_j q_j x_j} \tag{2.47}$$

The pure component parameters r_i and q_i are, respectively, relative to molecular van der Waals volumes and molecular surface areas. They are calculated as the sum of the group volume and group area parameters, R_k and Q_k:

$$r_i = \sum_k v_k^{(i)} R_k \tag{2.48}$$

$$q_i = \sum_k v_k^{(i)} Q_k \tag{2.49}$$

where $v_k^{(i)}$, always an integer, is the number of groups of type k in molecule i. The group parameters R_k and Q_k are normally obtained from van der Waals group volumes and surface areas, v_k and A_k, given by (Bondi, 1968):

$$R_k = \frac{v_k}{15.17} \tag{2.50}$$

$$Q_k = \frac{A_k}{2.5 \times 10^9} \tag{2.51}$$

Residual Part:

$$\ln \gamma_i^R = \sum_k v_k^{(i)} \left[\ln \Gamma_k - \ln \Gamma_k^{(i)} \right] \tag{2.52}$$

Γ_k is the group residual activity coefficient, and $\Gamma_k^{(i)}$ is the residual activity coefficient of group k in a reference solution containing only molecules of type i.

$$\ln \Gamma_k = Q_k \left[1 - \ln \left(\sum_m \theta_m \Psi_{mk} \right) - \sum_m \left(\theta_m \Psi_{km} \Big/ \sum_n \theta_n \Psi_{nm} \right) \right] \tag{2.53}$$

$$\theta_m = \frac{Q_m X_m}{\sum_n Q_n X_n} \tag{2.54}$$

$$X_m = \frac{\sum_i v_m^{(i)} x_i}{\sum_i \sum_k v_k^{(i)} x_i} \tag{2.55}$$

X_m is the fraction of group m in the mixture. The group interaction parameters Ψ_{nm} and Ψ_{mn} are defined by:

$$\Psi_{nm} = exp\left[-\left(\frac{a_{nm}}{T}\right)\right] \tag{2.56}$$

$$\Psi_{mn} = exp\left[-\left(\frac{a_{mn}}{T}\right)\right] \tag{2.57}$$

The parameters a_{nm} and a_{mn} characterize the interaction between groups n and m.

2.6.1.4 Modified UNIFAC model (Dortmund)

Modified UNIFAC **(**Dortmund) has been proposed by (Weidlich et al., 1987). In the modified UNIFAC (Dortmund) model, as in the original UNIFAC model, the activity coefficient is the sum of a combinatorial and a residual part:

$$\ln \gamma_i = \ln \gamma_i^C + \ln \gamma_i^R \tag{2.58}$$

The combinatorial part was changed in an empirical way to make it possible to deal with compounds very different in size:

$$\ln \gamma_i^C = \ln \frac{\Phi_i^{'}}{x_i} + 1 - \frac{\Phi_i^{'}}{x_i} - \frac{z}{2} q_i \left(1 - \frac{\Phi_i}{\theta_i} + \ln \frac{\Phi_i}{\theta_i}\right) \tag{2.59}$$

With:

$$\Phi_i^{'} = \frac{r_i^{3/4} x_i}{\sum_j r_j^{3/4} x_j} \tag{2.60}$$

All other parameters are calculated in the same way as for the original UNIFAC model

In comparison to the original UNIFAC method, the temperature-dependent parameters were introduced to permit a better description of the real behavior (activity coefficients) as a function of temperature.

$$\Psi_{nm} = exp\left[-\left(\frac{a_{nm}+b_{nm}T+c_{nm}T^2}{T}\right)\right] \tag{2.61}$$

2.6.2 Modeling results for N,N-dimethylacetamide (1) + 1,3,5-trimethylbenzene (2) system

Experimental vapor-liquid equilibrium data of this system have been modeled using NRTL, UNIQUAC and Modified UNIFAC (Do) models. The binary interactions parameters for the NRTL and UNIQUAC models and sum of squared relative error (SSQ) for the three models are respectively given in Tables 2.12 and 2.13.

Figure 2.15 shows the graphical representation of the three activity coefficient models to (*P, x, y)* data for this system. Regarding the results, it can be observed that the experimental data and those correlated using the NRTL and UNIQUAC models are almost superimposable over the entire composition range. Modeling using the Modified UNIFAC (Do) model shows deviations from experimental data for all temperatures.

Figure 2.15 (a) **Figure 2.15 (b)**

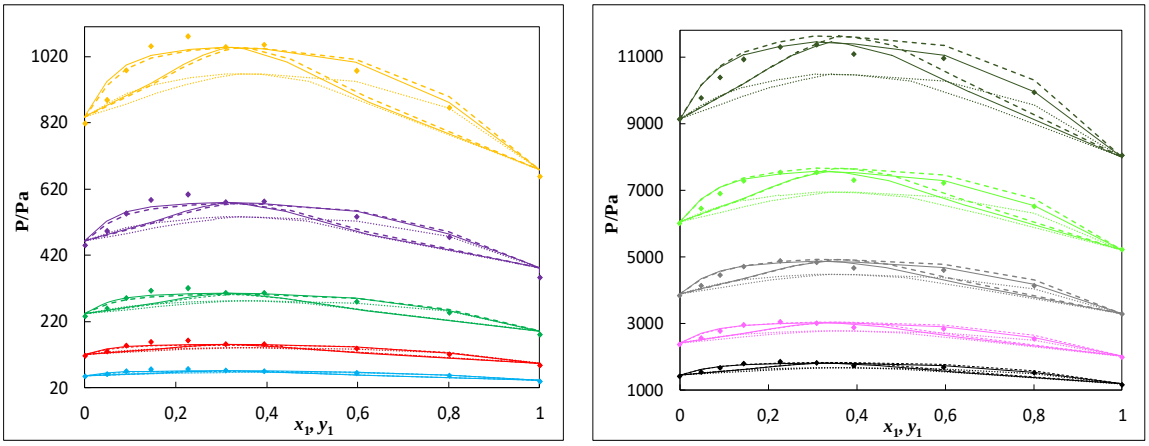

Figure 2.15: Comparison between experimental and calculated (*P, x, y)* using NRTL (—), UNIQUAC (-----) and Modified UNIFAC (……) models for the binary mixture {N,N-dimethylacetamide (1) +1,3,5-trimethylbenzene (2)} at different temperatures (a): 273.15 K (◆), 283.15 K (◆), 293.15 K (◆), 303.15 K (◆), 313.15 K (◆), (b): 323.15 K (◆), 333.15 K (◆), 343.15 K (◆), 353.15 K (◆), 363.15 K (◆).

2.6.3 Modeling results for N,N-dimethylacetamide (1) + propan-2-ol (2) system

This system has been also modeled using the three activity coefficient models NRTL, UNIQUAC and Modified UNIFAC (Do). The binary interactions parameters for the NRTL and UNIQUAC models and sum of squared relative error (SSQ) for the three models are respectively given in Tables 2.12 and 2.13.

Figure 2.16 is the illustrative plots of the three activity coefficient models to (*P, x, y)* data for this system. As shown on the plots, the experimental data are well represented by the NRTL, UNIQUAC and Modified UNIFAC (Do) models.

Figure 2.16 (a) **Figure 2.16 (b)**

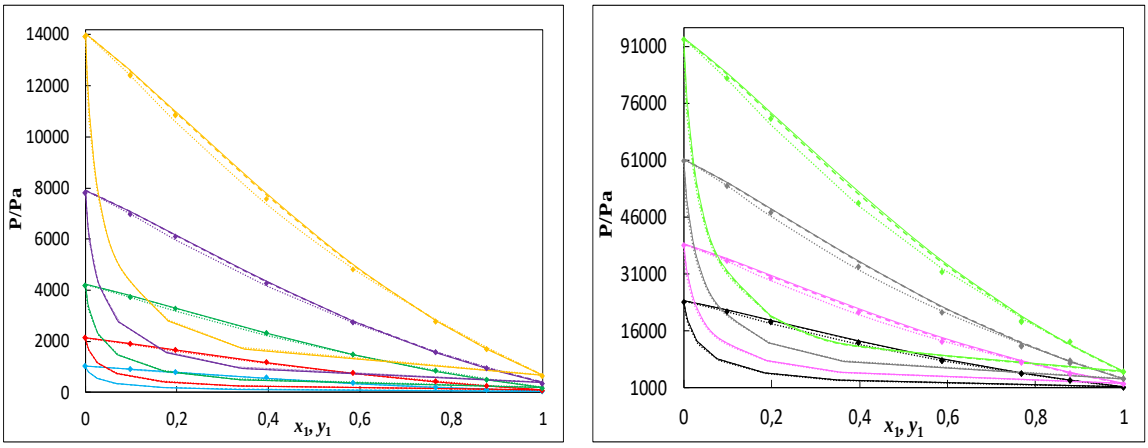

Figure 2.16: Comparison between experimental and calculated (*P, x, y)* using NRTL (—), UNIQUAC (-----) and Modified UNIFAC (……) models for the binary mixture {N,N-dimethylacetamide (1) + propan-2-ol (2) } at different temperatures (a): 273.15 K (◆), 283.15 K (◆), 293.15 K (◆), 303.15 K (◆), 313.15 K (◆), (b): 323.15 K (◆), 333.15 K (◆), 343.15 K (◆), 353.15 K (◆).

2.6.4 Modeling results for N,N-dimethylacetamide (1) + DMSO (2) system

The three activity coefficient models NRTL, UNIQUAC and Modified UNIFAC (Do) have been also used to model this system. The binary interactions parameters for the NRTL and UNIQUAC models and sum of squared relative error (SSQ) for the three models are respectively presented in Tables 2.12 and 2.13.

The graphical representation of the three activity coefficient models to (*P, x, y)* data for this system is shown in Figure 2.17. As shown on the plots, the NRTL, UNIQUAC and Modified UNIFAC (Do) models provide a good fit to the isothermal VLE data.

Figure 2.17 (a) **Figure 2.17 (b)**

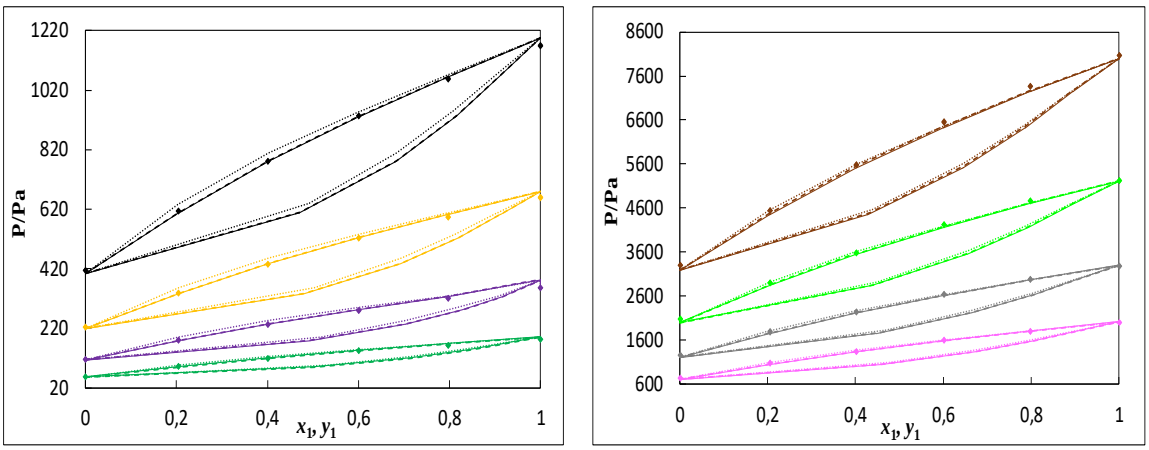

Figure 2.17: Comparison between experimental and calculated (*P, x, y)* using NRTL (—), UNIQUAC (-----) and Modified UNIFAC (……) models for the binary mixture {N,N-dimethylacetamide (1) + DMSO (2)} at different temperatures (a): 293.15 K (◆), 303.15 K (◆), 313.15 K (◆), 323.15 K (◆), (b): 333.15 K (◆), 343.15 K (◆), 353.15 K (◆), 363.15 K (◆).

2.7 Conclusion

In this chapter, vapor pressures of pure components, N,N-dimethylacetamide, 1,3,5-trimethylbenzene, propan-2-ol and DMSO, and their binary mixtures composed of N,N-dimethylacetamide with 1,3,5-trimethylbenzene or propan-2-ol or DMSO were measured using a static apparatus at different temperatures. The experimental results of pure components are in good agreement with the literature data. No data in the open literature were found to be compared for the studied binary mixtures. The obtained data were correlated with the Antoine equation. From these data, the excess Gibbs function G^E, the vapor phase composition y_i and the activity coefficients γ_1 and γ_2 were evaluated. The experimental data generated for the three mixtures were correlated with the NRTL, UNIQUAC and Modified UNIFAC (Do) models. The application of NRTL and UNIQUAC models were found suitable for representing the experimental results. Modeling using the Modified UNIFAC (Do) model shows deviations from experimental data for {N,N-dimethylacetamide (1) + 1,3,5-trimethylbenzene (2)} system.

References

Sasse, K., Jose, J., & Merlin, J. C. (1988). A static apparatus for measurement of low vapor pressures. Experimental results on high molecular-weight hydrocarbons. Fluid phase equilibria, 42, 287-304.

Kasehgari, H., Mokbel, I., Viton, C., & Jose, J. (1993). Vapor pressure of 11 alkylbenzenes in the range 10− 3–280 torr, correlation by equation of state. Fluid phase equilibria, 87(1), 133-152.

Mokbel, I., Rauzy, E., Loiseleur, H., Berro, C., & Jose, J. (1995). Vapor pressures of 12 alkylcyclohexanes, cyclopentane, butylcyclopentane and trans-decahydronaphthalene down to 0.5 Pa. Experimental results, correlation and prediction by an equation of state. Fluid phase equilibria, 108(1-2), 103-120.

Bassil, G., Aoun, M., Saab, J., Goutaudier, C., Jose, J., & Mokbel, I. (2020). Liquid–(Liquid)–Vapor Equilibrium of Solvents (P-Xylene, Methyl Hexadecanoate, and Methyl Oleate), Binary Systems (Water+ Solvents), and Ternary Systems (Water+ Methyl Hexadecanoate+ Model Molecule of Tar) Issued from the Biomass Gasification Process. Journal of Chemical & Engineering Data, 65(4), 1669-1678.

Sarraute, S., Mokbel, I., Gomes, M. F. C., Majer, V., Delepine, H., & Jose, J. (2006). Vapour pressures, aqueous solubility, Henry's law constants and air/water partition coefficients of 1, 8-dichlorooctane and 1, 8-dibromooctane. Chemosphere, 64(11), 1829-1836.

Antoine, C., C. R. Séan. Acad. Sci. 107 (1888) 681–684. 778–780, 836–837

Jain, V. (2021). A Barker Type Approach for Measuring and Interpreting VLE of Polymer Mixed Solvent Systems (Doctoral dissertation, University of South Florida).

Barker, J. A. (1953). Determination of activity coefficients from total pressure measurements. Australian Journal of Chemistry, 6(3), 207-210.

Štejfa, V., Chun, S., Pokorný, V., Fulem, M., & Růžička, K. (2020). Thermodynamic study of acetamides. Journal of Molecular Liquids, 319, 114019.

Zhang, Z., Yang, L., Xing, Y., & Li, W. (2013). Vapor–Liquid Equilibrium for Ternary and Binary Mixtures of 2-Isopropoxypropane, 2-Propanol, and N, N-Dimethylacetamide at 101.3 kPa. Journal of Chemical & Engineering Data, 58(2), 357-363.

Khelidj, O., Mokbel, I., Negadi, L., Jose, J., & Prausnitz, J. M. (2020). Recovery of Butanol from a Bioreactor. Phase Equilibria for Extracting Butanol from a Dilute Aqueous Solution Using Dodecane or 1, 3, 5-Trimethylbenzene. Journal of Chemical & Engineering Data, 66(1), 234-242.

Kassel, L. S. (1936). Vapor pressures of the xylenes and mesitylene1. Journal of the American Chemical Society, 58(4), 670-671.

Nasirzadeh, K., Zimin, D., Neueder, R., & Kunz, W. (2004). Vapor-pressure measurements of liquid solutions at different temperatures: Apparatus for use over an

extended temperature range and some new data. Journal of Chemical & Engineering Data, 49(3), 607-612.

Dejoz, A., González-Alfaro, V., Miguel, P. J., & Vázquez, M. I. (1996). Isobaric Vapor− Liquid Equilibria of Tetrachloroethylene+ 1-Propanol and+ 2-Propanol at 20 and 100 kPa. Journal of Chemical & Engineering Data, 41(6), 1361-1365.

Negadi, L., Kaci, A. A., & Jose, J. (2002). Thermodynamic properties of dimethyl sulfoxide+ benzene or+ isopropylbenzene mixtures. In Int. Conf. Distill. Absorpt. (Vol. 6, pp. 1-15).

Renon, H., & Prausnitz, J. M. (1968). Local compositions in thermodynamic excess functions for liquid mixtures. AIChE journal, 14(1), 135-144.

Abrams, D. S., & Prausnitz, J. M. (1975). Statistical thermodynamics of liquid mixtures: a new expression for the excess Gibbs energy of partly or completely miscible systems. AIChE Journal, 21(1), 116-128.

Prausnitz, J.M., Lichtenhalter, R. N. & Azevedo, E. G. (1998). Molecular Thermodynamics of Fluid-Phase Equilibria. Pearson Education, New York City, New York. pp 263.

Fredenslund, A., Jones, R. L., & Prausnitz, J. M. (1975). Group-contribution estimation of activity coefficients in nonideal liquid mixtures. AIChE Journal, 21(6), 1086-1099.

Bondi, A., Wiley.J and Sons. Physical Properties of Molecular Crystals, Liquids and Gases. 1968.

Weidlich, U., & Gmehling, J. (1987). A modified UNIFAC model. 1. Prediction of VLE, hE, and. gamma. infin. Industrial & engineering chemistry research, 26(7), 1372-1381.

General conclusion

The work presented in this thesis is part of our general program of research concerning the thermophysical and thermodynamic properties of binary mixtures containing molecules of industrial and environmental interest carried out in the research laboratory of Applied Thermodynamics and Molecular Modeling of the University of Abou Bekr Belkaid Tlemcen.

This dissertation reported the results obtained from the study of volumetric, acoustic and optical properties of twelve (12) binary mixtures and also the study of vapor-liquid equilibrium of three binary systems. The results were published in three class "A" specialty journals.

Density, speed of sound and refractive index of binary mixtures containing 2-(2-methoxyethoxy)ethanol (22MEE) , furfural and 1-hexene with alcohols (methanol, ethanol, propan-1-ol, propan-2-ol, butan-1-ol and butan-2-ol), dimethyl sulfoxide (DMSO), acetonitrile, sulfolane and alkoxyethanols (2-methoxyethanol, 2-ethoxyethanol and 2-butoxyethanol) have been measured over the whole composition range at different temperatures and at pressure of 0,1 MPa using an Anton Paar DSA 5000M digital vibrating tube densimeter and a digital refractometer Abbemat 300. Experimental data of densities, speeds of sound and refractive indices have been used to calculate isentropic compressibility (κ_s), intermolecular free length (L_f), specific acoustic impedance (Z), relative association (R_A), relaxation strength (r) and Rao's molar sound function (R). Excess values of molar volume ($V_{\mathrm{m}}^{\mathrm{E}}$), deviations in isentropic compressibility ($\Delta\kappa_s$), deviations in intermolecular free length (ΔL_f), deviations in acoustic impedance (ΔZ), deviations in speed of sound (Δu) and changes in refractive index (Δn_D) have been also evaluated from values of measured properties for all studied mixtures under the same experimental conditions. Excess/deviation properties have been fitted to the Redlich−Kister polynomial equation. All the experimental, derived and excess data have been presented both numerically and graphically and discussed from the thermodynamic point of view.

Furthermore, vapor-liquid equilibrium of three binary systems composed of N,N-dimethylacetamide with 1,3,5-trimethylbenzene or propan-2-ol or DMSO have been measured at several temperatures by means of a static apparatus. The obtained data were correlated with the Antoine equation. From these data, the excess Gibbs function G^E and the vapor phase composition y_i were evaluated for several constant temperatures and fitted to Redlich–Kister equation using the Barker's method. The activity coefficients γ_1 and γ_2 of the components in binary mixtures were also estimated. Additionally, the experimental data have been used to estimate the binary interactions parameters of NRTL and UNIQUAC models. Modified UNIFAC (Do) model have been also applied to correlate the vapor-liquid equilibrium data of the studied mixtures.

In conclusion, this work is of practical interest because it overcomes the lack of thermophysical and thermodynamic data of the selected compounds, and a fundamental interest in the correlation of experimental data using various equation and models.
This thesis has enabled us to extend the database of the studied molecules in order to make available to the scientific community a large number of original experimental data.

However, the work presented is only the beginning of a study overview of mixtures of compounds having the same interest, namely the contribution to the diminution of pollution and industrial development. For the continuation of this research program, the obtained data will be completed by the study of excess molar enthalpies, heat capacity, viscosity of the binary mixtures and also the application of other thermodynamic model COSMO-RS and equations of state (PSRK, PC-SAFT, …).

Annexes

Annexes 1

Table A1.3: Densities, ρ, speed of sound, u, and refractive indices, n_D, for the binary systems (22MEE + methanol or ethanol or propan-1-ol or propan-2-ol or butan-1-ol or butan-2-ol) at (293.15, 303.15, 313.15 and 323.15) K and at pressure p = 0.1 MPa.

x_1	ρ /(g.cm^{-3})	u / (m.s^{-1})	n_D
	{22MEE (1) + methanol (2)}		
	T = 293.15 K		
0.0000	0.7916	1120.60	1.3287
0.1022	0.8540	1200.39	1.3554
0.1994	0.8948	1255.85	1.3736
0.3011	0.9261	1300.11	1.3874
0.4004	0.9493	1333.37	1.3973
0.4997	0.9674	1359.33	1.4050
0.6013	0.9823	1380.72	1.4114
0.6949	0.9935	1396.62	1.4159
0.7951	1.0036	1410.96	1.4196
0.8964	1.0124	1422.78	1.4233
1.0000	1.0196	1433.62	1.4262
	T = 303.15 K		
0.0000	0.7822	1087.55	1.3247
0.1022	0.8448	1167.77	1.3524
0.1994	0.8856	1223.10	1.3700
0.3011	0.9170	1267.25	1.3835
0.4004	0.9403	1300.36	1.3936
0.4997	0.9584	1326.11	1.4011
0.6013	0.9733	1347.29	1.4075
0.6949	0.9846	1363.11	1.4122
0.7951	0.9947	1377.30	1.4159
0.8964	1.0035	1389.24	1.4194
1.0000	1.0108	1398.97	1.4225
	T = 313.15 K		
0.0000	0.7726	1055.13	1.3207
0.1022	0.8354	1135.34	1.3493
0.1994	0.8763	1190.52	1.3671
0.3011	0.9079	1234.49	1.3805
0.4004	0.9312	1267.43	1.3901
0.4997	0.9494	1292.95	1.3978
0.6013	0.9643	1313.96	1.4038
0.6949	0.9757	1329.62	1.4083
0.7951	0.9858	1343.64	1.4125
0.8964	0.9947	1355.46	1.4157
1.0000	1.0019	1365.06	1.4187
	T = 323.15 K		
0.0000	0.7630	1023.02	1.3167
0.1022	0.8259	1103.27	1.3461
0.1994	0.8670	1158.24	1.3642
0.3011	0.8986	1201.98	1.3772
0.4004	0.9221	1234.71	1.3866
0.4997	0.9403	1260.03	1.3940
0.6013	0.9553	1280.86	1.4006
0.6949	0.9666	1296.34	1.4052
0.7951	0.9768	1310.20	1.4086
0.8964	0.9857	1321.87	1.4119
1.0000	0.9929	1331.34	1.4148

{22MEE (1) + ethanol (2)}

T = 293.15 K

0.0000	0.7898	1162.46	1.3615
0.1014	0.8353	1212.88	1.3746
0.1994	0.8699	1251.46	1.3847
0.3004	0.8999	1285.89	1.3934
0.4011	0.9250	1315.20	1.4006
0.5009	0.9464	1341.32	1.4066
0.5978	0.9646	1363.40	1.4115
0.6984	0.9811	1384.30	1.4160
0.8001	0.9956	1402.53	1.4198
0.9024	1.0088	1420.18	1.4233
1.0000	1.0196	1433.62	1.4262

T = 303.15 K

0.0000	0.7812	1127.91	1.3575
0.1014	0.8266	1179.12	1.3707
0.1994	0.8611	1218.03	1.3806
0.3004	0.8912	1252.50	1.3895
0.4011	0.9162	1281.77	1.3968
0.5009	0.9376	1307.76	1.4028
0.5978	0.9557	1329.86	1.4077
0.6984	0.9723	1350.67	1.4123
0.8001	0.9868	1368.80	1.4160
0.9024	1.0000	1386.45	1.4195
1.0000	1.0108	1398.97	1.4225

T = 313.15 K

0.0000	0.7724	1094.28	1.3535
0.1014	0.8177	1145.68	1.3665
0.1994	0.8523	1184.68	1.3769
0.3004	0.8823	1219.20	1.3859
0.4011	0.9073	1248.39	1.3932
0.5009	0.9287	1274.29	1.3994
0.5978	0.9468	1296.32	1.4041
0.6984	0.9634	1317.07	1.4085
0.8001	0.9779	1335.10	1.4122
0.9024	0.9911	1352.65	1.4157
1.0000	1.0019	1365.06	1.4187

T = 323.15 K

0.0000	0.7635	1060.90	1.3493
0.1014	0.8088	1112.46	1.3630
0.1994	0.8433	1151.53	1.3739
0.3004	0.8733	1186.06	1.3826
0.4011	0.8983	1215.18	1.3898
0.5009	0.9197	1241.01	1.3957
0.5978	0.9378	1262.97	1.4004
0.6984	0.9544	1283.65	1.4046
0.8001	0.9689	1301.58	1.4085
0.9024	0.9821	1319.05	1.4119
1.0000	0.9929	1331.34	1.4148

{22MEE (1) + propan-1-ol (2)}

T = 293.15 K

0.0000	0.8042	1225.30	1.3851

0.1021	0.8370	1252.83	1.3915
0.2041	0.8664	1278.72	1.3972
0.3039	0.8922	1302.35	1.4023
0.3978	0.9143	1323.09	1.4065
0.4989	0.9360	1344.22	1.4107
0.6028	0.9563	1364.74	1.4145
0.6986	0.9735	1382.66	1.4177
0.8015	0.9905	1400.78	1.4208
0.8987	1.0053	1416.88	1.4236
1.0000	1.0196	1433.62	1.4262
	T = 303.15 K		
0.0000	0.7961	1190.90	1.3811
0.1021	0.8288	1218.88	1.3875
0.2041	0.8580	1244.87	1.3933
0.3039	0.8837	1268.59	1.3984
0.3978	0.9058	1289.39	1.4027
0.4989	0.9274	1310.57	1.4069
0.6028	0.9476	1331.06	1.4107
0.6986	0.9647	1348.91	1.4139
0.8015	0.9817	1366.97	1.4170
0.8987	0.9965	1383.05	1.4198
1.0000	1.0108	1398.97	1.4225
	T = 313.15 K		
0.0000	0.7879	1157.04	1.3771
0.1021	0.8205	1185.12	1.3835
0.2041	0.8495	1211.20	1.3893
0.3039	0.8752	1234.97	1.3944
0.3978	0.8971	1255.82	1.3987
0.4989	0.9187	1276.98	1.4029
0.6028	0.9389	1297.43	1.4068
0.6986	0.9559	1315.24	1.4100
0.8015	0.9729	1333.21	1.4132
0.8987	0.9876	1349.22	1.4160
1.0000	1.0019	1365.06	1.4187
	T = 323.15 K		
é0.0000	0.7795	1123.41	1.3729
0.1021	0.8119	1151.60	1.3796
0.2041	0.8409	1177.78	1.3853
0.3039	0.8665	1201.58	1.3906
0.3978	0.8883	1222.44	1.3950
0.4989	0.9098	1243.60	1.3992
0.6028	0.9300	1264.03	1.4030
0.6986	0.9471	1281.76	1.4062
0.8015	0.9639	1299.65	1.4094
0.8987	0.9787	1315.61	1.4122
1.0000	0.9929	1331.34	1.4148

{22MEE (1) + propan-2-ol (2)}

T = 293.15 K

0.0000	0.7857	1159.32	1.3772
0.1010	0.8198	1194.71	1.3845
0.2032	0.8514	1229.03	1.3912
0.2995	0.8785	1259.44	1.3970
0.4001	0.9042	1288.78	1.4025
0.5002	0.9277	1316.52	1.4074

0.6022	0.9495	1343.07	1.4120
0.6987	0.9686	1366.70	1.4160
0.7989	0.9869	1389.96	1.4196
0.9023	1.0043	1412.53	1.4232
1.0000	1.0196	1433.62	1.4262
	T = 303.15 K		
0.0000	0.7772	1123.71	1.3730
0.1010	0.8113	1160.01	1.3803
0.2032	0.8428	1194.58	1.3873
0.2995	0.8698	1225.16	1.3931
0.4001	0.8955	1254.71	1.3986
0.5002	0.9189	1282.58	1.4035
0.6022	0.9408	1309.21	1.4081
0.6987	0.9598	1332.86	1.4121
0.7989	0.9781	1356.12	1.4158
0.9023	0.9955	1378.66	1.4194
1.0000	1.0108	1398.97	1.4225
	T = 313.15 K		
0.0000	0.7684	1088.43	1.3686
0.1010	0.8024	1125.11	1.3762
0.2032	0.8339	1159.99	1.3832
0.2995	0.8610	1190.84	1.3891
0.4001	0.8866	1220.58	1.3947
0.5002	0.9101	1248.60	1.3997
0.6022	0.9319	1275.29	1.4043
0.6987	0.9509	1299.00	1.4083
0.7989	0.9692	1322.25	1.4121
0.9023	0.9866	1344.78	1.4156
1.0000	1.0019	1365.06	1.4187
	T = 323.15 K		
0.0000	0.7592	1052.76	1.364130
0.1010	0.7933	1090.03	1.372160
0.2032	0.8249	1125.35	1.379470
0.2995	0.8519	1156.51	1.385620
0.4001	0.8776	1186.52	1.391210
0.5002	0.9010	1214.71	1.396160
0.6022	0.9229	1241.52	1.400660
0.6987	0.9419	1265.30	1.404460
0.7989	0.9602	1288.57	1.408230
0.9023	0.9776	1311.11	1.411770
1.0000	0.9929	1331.34	1.414840

{22MEE (1) + butan-1-ol (2)}

	T = 293.15 K		
0.0000	0.8107	1260.37	1.3992
0.1013	0.8367	1276.63	1.4024
0.2024	0.8614	1293.49	1.4055
0.3016	0.8844	1310.33	1.4084
0.3992	0.9059	1327.15	1.4112
0.5031	0.9278	1345.28	1.4141
0.6025	0.9478	1362.09	1.4167
0.6993	0.9664	1379.77	1.4192
0.7966	0.9844	1396.84	1.4215
0.8986	1.0024	1414.90	1.4239
1.0000	1.0196	1433.62	1.4262

T = 303.15 K

0.0000	0.8030	1226.42	1.3952
0.1013	0.8289	1243.18	1.3985
0.2024	0.8533	1260.17	1.4016
0.3016	0.8762	1277.06	1.4046
0.3992	0.8976	1293.88	1.4074
0.5031	0.9194	1312.01	1.4103
0.6025	0.9393	1328.76	1.4129
0.6993	0.9579	1346.32	1.4154
0.7966	0.9757	1363.26	1.4178
0.8986	0.9937	1381.17	1.4202
1.0000	1.0108	1398.97	1.4225

T = 313.15 K

0.0000	0.7952	1192.97	1.3913
0.1013	0.8209	1209.88	1.3945
0.2024	0.8452	1226.96	1.3977
0.3016	0.8679	1243.92	1.4007
0.3992	0.8892	1260.73	1.4035
0.5031	0.9109	1278.80	1.4064
0.6025	0.9308	1295.45	1.4091
0.6993	0.9492	1312.93	1.4116
0.7966	0.9670	1329.71	1.4140
0.8986	0.9848	1347.43	1.4164
1.0000	1.0019	1365.06	1.4187

T = 323.15 K

0.0000	0.7872	1159.74	1.3872
0.1013	0.8127	1176.84	1.3905
0.2024	0.8369	1194.01	1.3937
0.3016	0.8595	1210.98	1.3968
0.3992	0.8808	1227.77	1.3996
0.5031	0.9023	1245.81	1.4025
0.6025	0.9221	1262.38	1.4052
0.6993	0.9404	1279.72	1.4077
0.7966	0.9581	1296.36	1.4101
0.8986	0.9759	1313.90	1.4125
1.0000	0.9929	1331.34	1.4148

{22MEE (1) + butan-2-ol (2)}

T = 293.15 K

0.0000	0.8067	1230.52	1.3973
0.1021	0.8322	1248.99	1.4004
0.2032	0.8569	1268.76	1.4036
0.3026	0.8803	1288.92	1.4067
0.4006	0.9024	1308.82	1.4098
0.4992	0.9238	1329.37	1.4127
0.6015	0.9450	1350.66	1.4157
0.7012	0.9648	1371.29	1.4185
0.7973	0.9832	1391.41	1.4211
0.8943	1.0010	1411.18	1.4235
1.0000	1.0196	1433.62	1.4262

T = 303.15 K

0.0000	0.7983	1194.41	1.3930
0.1021	0.8239	1213.77	1.3963
0.2032	0.8485	1234.00	1.3995
0.3026	0.8718	1254.52	1.4027

0.4006	0.8938	1274.66	1.4058
0.4992	0.9152	1295.37	1.4088
0.6015	0.9364	1316.75	1.4118
0.7012	0.9561	1337.46	1.4146
0.7973	0.9745	1357.57	1.4172
0.8943	0.9922	1377.32	1.4198
1.0000	1.0108	1398.97	1.4225
	T = 313.15 K		
0.0000	0.7896	1157.98	1.3886
0.1021	0.8153	1178.18	1.3920
0.2032	0.8399	1199.02	1.3953
0.3026	0.8632	1219.95	1.3986
0.4006	0.8852	1240.41	1.4017
0.4992	0.9065	1261.33	1.4048
0.6015	0.9276	1282.81	1.4079
0.7012	0.9474	1303.60	1.4107
0.7973	0.9657	1323.71	1.4134
0.8943	0.9833	1343.45	1.4160
1.0000	1.0019	1365.06	1.4187
	T = 323.15 K		
0.0000	0.7805	1120.98	1.3840
0.1021	0.8063	1142.30	1.3877
0.2032	0.8310	1163.89	1.3912
0.3026	0.8543	1185.35	1.3946
0.4006	0.8763	1206.15	1.3978
0.4992	0.8976	1227.32	1.4009
0.6015	0.9188	1248.98	1.4040
0.7012	0.9385	1269.87	1.4068
0.7973	0.9568	1290.03	1.4095
0.8943	0.9744	1309.78	1.4121
1.0000	0.9929	1331.34	1.4148

Table A1.4: Densities, ρ, speed of sound, u, and refractive indices, n_D, for the binary systems (furfural + DMSO, or acetonitrile) at (293.15, 303.15, 313.15 and 323.15) K and for (furfural + sulfolane) at (303.15, 313.15 and 323.15) K and at pressure of 0.1 MPa.

x_1	ρ /(g.cm^{-3})	u / (m.s^{-1})	n_D
	{Furfural (1) + DMSO (2)}		
	T= 293.15 K		
0.0000	1.1003	1503.63	1.4783
0.1047	1.1067	1494.58	1.4840
0.2024	1.1127	1488.10	1.4892
0.3008	1.1188	1482.42	1.4943
0.4017	1.1250	1477.36	1.4993
0.5009	1.1311	1473.20	1.5041
0.6011	1.1371	1469.41	1.5088
0.7008	1.1430	1466.18	1.5134
0.7989	1.1487	1463.35	1.5177
0.8971	1.1543	1460.62	1.5219
1.0000	1.1600	1458.20	1.5264
	T= 303.15 K		
0.0000	1.0903	1469.88	1.4749
0.1047	1.0966	1461.00	1.4805
0.2024	1.1027	1454.62	1.4856
0.3008	1.1087	1448.88	1.4904
0.4017	1.1149	1443.67	1.4953
0.5009	1.1209	1439.24	1.4999
0.6011	1.1269	1435.13	1.5044
0.7008	1.1327	1431.50	1.5088
0.7989	1.1383	1428.28	1.5129
0.8971	1.1437	1425.09	1.5170
1.0000	1.1493	1422.02	1.5212
	T= 313.15 K		
0.0000	1.0803	1436.28	1.4703
0.1047	1.0866	1427.53	1.4758
0.2024	1.0926	1421.18	1.4809
0.3008	1.0986	1415.40	1.4858
0.4017	1.1048	1410.01	1.4907
0.5009	1.1107	1405.33	1.4953
0.6011	1.1166	1400.92	1.4998
0.7008	1.1223	1396.91	1.5040
0.7989	1.1278	1393.25	1.5081
0.8971	1.1332	1389.62	1.5121
1.0000	1.1387	1386.01	1.5162
	T= 323.15 K		
0.0000	1.0702	1403.00	1.4661
0.1047	1.0766	1394.40	1.4716
0.2024	1.0826	1388.04	1.4765
0.3008	1.0885	1382.20	1.4814
0.4017	1.0946	1376.63	1.4862
0.5009	1.1005	1371.71	1.4907
0.6011	1.1063	1366.99	1.4951
0.7008	1.1119	1362.61	1.4993
0.7989	1.1173	1358.48	1.5033

0.8971	1.1226	1354.43	1.5071
1.0000	1.1279	1350.29	1.5111

{Furfural (1) + Acetonitrile (2)}

T= 293.15 K

0.0000	0.7820	1299.20	1.3439
0.1030	0.8420	1315.78	1.3727
0.2016	0.8931	1332.62	1.3976
0.3079	0.9422	1351.28	1.4214
0.4006	0.9804	1367.19	1.4397
0.4978	1.0170	1383.78	1.4572
0.5975	1.0509	1400.10	1.4736
0.6949	1.0811	1415.41	1.4882
0.7961	1.1097	1430.35	1.5019
0.8969	1.1358	1444.61	1.5145
1.0000	1.1600	1458.20	1.5264

T= 303.15 K

0.0000	0.7711	1259.27	1.3391
0.1030	0.8311	1276.77	1.3680
0.2016	0.8822	1293.85	1.3930
0.3079	0.9313	1313.08	1.4168
0.4006	0.9696	1329.44	1.4351
0.4978	1.0061	1346.35	1.4527
0.5975	1.0401	1363.01	1.4688
0.6949	1.0704	1379.03	1.4833
0.7961	1.0990	1393.79	1.4969
0.8969	1.1252	1408.26	1.5096
1.0000	1.1493	1422.02	1.5212

T= 313.15 K

0.0000	0.7602	1218.56	1.3342
0.1030	0.8201	1236.90	1.3637
0.2016	0.8712	1255.10	1.3886
0.3079	0.9203	1274.92	1.4123
0.4006	0.9586	1291.72	1.4306
0.4978	0.9952	1309.03	1.4480
0.5975	1.0293	1326.02	1.4641
0.6949	1.0595	1341.88	1.4785
0.7961	1.0882	1357.33	1.4918
0.8969	1.1144	1372.02	1.5046
1.0000	1.1387	1386.01	1.5162

T= 323.15 K

0.0000	0.7491	1178.67	1.3293
0.1030	0.8090	1197.59	1.3590
0.2016	0.8600	1216.54	1.3841
0.3079	0.9092	1236.99	1.4079
0.4006	0.9475	1254.25	1.4266
0.4978	0.9842	1271.95	1.4440
0.5975	1.0183	1289.30	1.4600
0.6949	1.0486	1305.44	1.4740
0.7961	1.0774	1321.19	1.4875
0.8969	1.1036	1336.12	1.4996
1.0000	1.1279	1350.29	1.5111

{Furfural (1) + Sulfolane (2)}

	T= 303.15 K		
0.0000	1.2617	1583.52	1.4817
0.1012	1.2522	1566.49	1.4856
0.1990	1.2429	1550.40	1.4894
0.3018	1.2326	1533.72	1.4934
0.4013	1.2221	1517.87	1.4973
0.5005	1.2113	1502.57	1.5012
0.5991	1.2000	1486.42	1.5051
0.7006	1.1880	1470.37	1.5091
0.8014	1.1757	1454.36	1.5132
0.9002	1.1631	1438.56	1.5172
1.0000	1.1493	1422.02	1.5212
	T= 313.15 K		
0.0000	1.2529	1552.30	1.4782
0.1012	1.2433	1534.62	1.4820
0.1990	1.2338	1518.22	1.4856
0.3018	1.2233	1501.21	1.4894
0.4013	1.2127	1485.00	1.4931
0.5005	1.2016	1468.87	1.4969
0.5991	1.1902	1452.71	1.5006
0.7006	1.1780	1436.16	1.5045
0.8014	1.1654	1419.61	1.5084
0.9002	1.1526	1403.21	1.5123
1.0000	1.1387	1386.01	1.5162
	T= 323.15 K		
0.0000	1.2442	1520.73	1.4748
0.1012	1.2343	1503.09	1.4783
0.1990	1.2247	1486.40	1.4818
0.3018	1.2140	1469.05	1.4855
0.4013	1.2032	1452.48	1.4890
0.5005	1.1920	1435.92	1.4926
0.5991	1.1804	1419.36	1.4962
0.7006	1.1680	1402.30	1.4999
0.8014	1.1552	1385.20	1.5037
0.9002	1.1421	1368.18	1.5074
1.0000	1.1279	1350.29	1.5111

Table A1.5: Densities, ρ, speed of sound, u, and refractive indices, n_D, for the binary systems (1-hexene + 2-methoxyethanol, or 2-ethoxyethanol, or 2-butoxyethanol) at (293.15, 298.15 and 303.15) K and at pressure p = 0.1 MPa.

x_1	ρ /(g.cm^{-3})	u / (m.s^{-1})	n_D
	{1-hexene (1) + 2-methoxyethanol (2)}		
	T = 293.15 K		
0.0000	0.9646	1359.64	1.4023
0.1008	0.9209	1298.49	1.4004
0.2037	0.8805	1245.87	1.3984
0.3016	0.8458	1205.08	1.3966
0.4023	0.8134	1171.85	1.3948
0.5020	0.7843	1146.55	1.3932
0.5995	0.7585	1127.34	1.3918
0.6960	0.7350	1112.70	1.3906
0.7996	0.7119	1100.96	1.3895
0.8980	0.6919	1092.84	1.3885
1.0000	0.6735	1088.81	1.3880
	T = 298.15 K		
0.0000	0.9600	1342.49	1.4004
0.1008	0.9162	1281.10	1.3983
0.2037	0.8758	1227.58	1.3962
0.3016	0.8410	1186.26	1.3943
0.4023	0.8086	1152.50	1.3924
0.5020	0.7795	1126.96	1.3907
0.5995	0.7537	1106.93	1.3892
0.6960	0.7302	1091.79	1.3879
0.7996	0.7070	1079.51	1.3867
0.8980	0.6870	1070.96	1.3856
1.0000	0.6688	1066.46	1.3852
	T = 303.15 K		
0.0000	0.9554	1325.15	1.3984
0.1008	0.9116	1262.89	1.3963
0.2037	0.8710	1209.12	1.3942
0.3016	0.8362	1167.25	1.3922
0.4023	0.8037	1132.96	1.3902
0.5020	0.7746	1106.59	1.3883
0.5995	0.7488	1086.35	1.3866
0.6960	0.7252	1070.72	1.3851
0.7996	0.7021	1057.94	1.3838
0.8980	0.6822	1048.95	1.3828
1.0000	0.6640	1044.01	1.3824
	{1-hexene (1) + 2-ethoxyethanol (2)}		
	T = 293.15 K		
0.0000	0.9294	1319.87	1.4080
0.1018	0.8971	1277.43	1.4058
0.2034	0.8663	1239.53	1.4035
0.3022	0.8380	1207.40	1.4013
0.4038	0.8101	1178.77	1.3990
0.5018	0.7845	1155.22	1.3968
0.5989	0.7604	1135.79	1.3948
0.6981	0.7369	1119.27	1.3928

0.8004	0.7140	1105.67	1.3909
0.8970	0.6935	1095.68	1.3893
1.0000	0.6735	1088.81	1.3880
	T = 298.15 K		
0.0000	0.9249	1302.33	1.4059
0.1018	0.8925	1259.45	1.4036
0.2034	0.8617	1221.08	1.4013
0.3022	0.8333	1188.47	1.3990
0.4038	0.8054	1159.36	1.3967
0.5018	0.7797	1135.32	1.3944
0.5989	0.7556	1115.43	1.3922
0.6981	0.7321	1098.40	1.3901
0.8004	0.7092	1084.30	1.3881
0.8970	0.6887	1073.86	1.3864
1.0000	0.6688	1066.46	1.3852
	T = 303.15 K		
0.0000	0.9204	1284.61	1.4039
0.1018	0.8879	1241.27	1.4014
0.2034	0.8570	1202.44	1.3990
0.3022	0.8285	1169.36	1.3965
0.4038	0.8006	1139.77	1.3940
0.5018	0.7748	1115.27	1.3917
0.5989	0.7507	1094.88	1.3895
0.6981	0.7272	1077.39	1.3873
0.8004	0.7043	1062.81	1.3853
0.8970	0.6839	1051.93	1.3836
1.0000	0.6640	1044.01	1.3824

{1-hexene (1) + 2-butoxyethanol (2)}

	T = 293.15 K		
0.0000	0.9004	1322.98	1.4196
0.1038	0.8788	1293.40	1.4171
0.2055	0.8571	1264.62	1.4144
0.3001	0.8364	1238.41	1.4117
0.4053	0.8130	1210.36	1.4084
0.5053	0.7902	1184.92	1.4052
0.6023	0.7678	1161.75	1.4019
0.7017	0.7445	1139.94	1.3985
0.7980	0.7216	1120.85	1.3951
0.8977	0.6977	1103.64	1.3916
1.0000	0.6735	1088.81	1.3880
	T = 298.15 K		
0.0000	0.8962	1306.11	1.4176
0.1038	0.8746	1276.11	1.4150
0.2055	0.8527	1246.86	1.4123
0.3001	0.8320	1220.21	1.4096
0.4053	0.8085	1191.66	1.4062
0.5053	0.7857	1165.68	1.4029
0.6023	0.7632	1142.00	1.3995
0.7017	0.7399	1119.63	1.3959
0.7980	0.7169	1099.98	1.3924
0.8977	0.6930	1082.14	1.3888
1.0000	0.6688	1066.46	1.3852
	T = 303.15 K		
0.0000	0.8920	1289.04	1.4156

0.1038	0.8703	1258.64	1.4130
0.2055	0.8484	1228.93	1.4102
0.3001	0.8276	1201.85	1.4072
0.4053	0.8040	1172.79	1.4038
0.5053	0.7812	1146.30	1.4004
0.6023	0.7586	1122.12	1.3969
0.7017	0.7352	1099.19	1.3933
0.7980	0.7122	1078.96	1.3897
0.8977	0.6882	1060.51	1.3861
1.0000	0.6640	1044.01	1.3824

Table A1.6: Isentropic compressibility (κ_s), intermolecular free length (L_f), specific acoustic impedance (Z), relative association (R_A), relaxation strength (r) and Rao's molar sound function (R) for the binary systems (22MEE + methanol or ethanol or propan-1-ol or propan-2-ol or butan-1-ol or butan-2-ol) at (293.15, 303.15, 313.15 and 323.15) K and at pressure p = 0.1 MPa.

x_1	κ_s / (TPa^{-1})	L_f/ (10 $^{-12}$ m)	Z / (10^5 kg m^{-2} s^{-1})	R_A	r	R / (10^{-3} m$^{(10/3)}$ mol^{-1} s$^{(-1/3)}$)
			{22MEE (1) + methanol (2)}			
			T= 293.15 K			
0.0000	1006.0	64.642	8.8706	1.0000	0.5095	0.4204
0.1022	812.61	58.098	10.252	1.0544	0.4371	0.5108
0.1994	708.63	54.254	11.237	1.0882	0.3839	0.5982
0.3011	638.82	51.512	12.040	1.1134	0.3397	0.6902
0.4004	592.48	49.608	12.658	1.1318	0.3055	0.7805
0.4997	559.43	48.205	13.150	1.1459	0.2782	0.8710
0.6013	534.02	47.098	13.562	1.1575	0.2553	0.9638
0.6949	516.01	46.297	13.876	1.1663	0.2381	1.0494
0.7951	500.52	45.596	14.160	1.1741	0.2223	1.1410
0.8964	487.96	45.020	14.404	1.1811	0.2093	1.2334
1.0000	477.20	44.521	14.617	1.1865	0.1972	1.3287
			T= 303.15 K			
0.0000	1080.9	68.240	8.5064	1.0000	0.5380	0.4213
0.1022	868.06	61.152	9.8649	1.0547	0.4673	0.5116
0.1994	754.82	57.024	10.832	1.0888	0.4156	0.5991
0.3011	679.03	54.085	11.621	1.1142	0.3727	0.6911
0.4004	628.91	52.051	12.228	1.1327	0.3395	0.7814
0.4997	593.31	50.556	12.710	1.1470	0.3131	0.8720
0.6013	566.00	49.379	13.114	1.1587	0.2909	0.9647
0.6949	546.59	48.525	13.422	1.1676	0.2742	1.0503
0.7951	529.97	47.782	13.700	1.1755	0.2590	1.1419
0.8964	516.31	47.162	13.942	1.1825	0.2461	1.2344
1.0000	505.51	46.666	14.140	1.1882	0.2355	1.3294
			T= 313.15 K			
0.0000	1162.6	72.047	8.1523	1.0000	0.5651	0.4222
0.1022	928.64	64.393	9.4847	1.0552	0.4965	0.5125
0.1994	805.11	59.957	10.433	1.0895	0.4464	0.6000
0.3011	722.76	56.808	11.208	1.1151	0.4047	0.6921
0.4004	668.48	54.633	11.803	1.1338	0.3725	0.7823
0.4997	630.07	53.040	12.275	1.1483	0.3470	0.8729
0.6013	600.62	51.786	12.671	1.1601	0.3256	0.9656
0.6949	579.75	50.878	12.973	1.1691	0.3094	1.0512
0.7951	561.90	50.089	13.245	1.1771	0.2948	1.1428
0.8964	547.21	49.430	13.482	1.1842	0.2823	1.2353
1.0000	535.64	48.905	13.676	1.1900	0.2721	1.3303
			T= 323.15 K			
0.0000	1252.3	76.105	7.8054	1.0000	0.5912	0.4231
0.1022	994.68	67.826	9.1124	1.0556	0.5245	0.5135
0.1994	859.79	63.059	10.042	1.0903	0.4760	0.6010

0.3011	770.24	59.685	10.801	1.1162	0.4356	0.6930
0.4004	711.39	57.360	11.385	1.1351	0.4045	0.7832
0.4997	669.86	55.660	11.848	1.1497	0.3798	0.8738
0.6013	638.07	54.324	12.236	1.1616	0.3591	0.9666
0.6949	615.60	53.358	12.531	1.1708	0.3436	1.0521
0.7951	596.40	52.519	12.798	1.1788	0.3294	1.1437
0.8964	580.61	51.819	13.030	1.1861	0.3174	1.2361
1.0000	568.20	51.263	13.219	1.1920	0.3076	1.3312

{22MEE (1) + ethanol (2)}

T= 293.15 K

0.0000	936.97	62.385	9.1811	1.0000	0.4721	0.6133
0.1014	813.85	58.142	10.131	1.0427	0.4254	0.6841
0.1994	734.03	55.217	10.886	1.0746	0.3882	0.7538
0.3004	672.02	52.834	11.572	1.1017	0.3541	0.8256
0.4011	625.01	50.952	12.165	1.1239	0.3243	0.8977
0.5009	587.27	49.390	12.695	1.1425	0.2972	0.9692
0.5978	557.73	48.131	13.151	1.1581	0.2739	1.0387
0.6984	531.89	47.003	13.581	1.1720	0.2515	1.1111
0.8001	510.60	46.053	13.964	1.1841	0.2316	1.1843
0.9024	491.50	45.183	14.326	1.1948	0.2121	1.2582
1.0000	477.20	44.521	14.617	1.2038	0.1972	1.3287

T= 303.15 K

0.0000	1006.2	65.839	8.8111	1.0000	0.5031	0.6139
0.1014	870.18	61.227	9.7462	1.0425	0.4569	0.6848
0.1994	782.74	58.069	10.489	1.0744	0.4205	0.7546
0.3004	715.30	55.511	11.162	1.1016	0.3872	0.8265
0.4011	664.35	53.498	11.743	1.1239	0.3582	0.8986
0.5009	623.60	51.831	12.262	1.1425	0.3319	0.9701
0.5978	591.62	50.485	12.710	1.1581	0.3092	1.0396
0.6984	563.78	49.282	13.132	1.1721	0.2874	1.1120
0.8001	540.87	48.270	13.507	1.1843	0.2681	1.1853
0.9024	520.25	47.341	13.864	1.1949	0.2491	1.2592
1.0000	505.51	46.666	14.140	1.2043	0.2355	1.3294

T= 313.15 K

0.0000	1081.1	69.479	8.4527	1.0000	0.5322	0.6146
0.1014	931.65	64.497	9.3688	1.0426	0.4873	0.6856
0.1994	836.02	61.097	10.097	1.0745	0.4518	0.7554
0.3004	762.50	58.349	10.757	1.1018	0.4194	0.8273
0.4011	707.22	56.194	11.326	1.1241	0.3912	0.8994
0.5009	663.09	54.412	11.835	1.1428	0.3657	0.9710
0.5978	628.49	52.974	12.274	1.1585	0.3436	1.0405
0.6984	598.39	51.690	12.688	1.1725	0.3224	1.1129
0.8001	573.69	50.612	13.056	1.1848	0.3037	1.1861
0.9024	551.48	49.622	13.406	1.1955	0.2853	1.2600
1.0000	535.64	48.905	13.676	1.2049	0.2721	1.3303

T= 323.15 K

0.0000	1163.7	73.361	8.1002	1.0000	0.5603	0.6154
0.1014	999.09	67.976	8.9972	1.0426	0.5166	0.6865
0.1994	894.29	64.312	9.7107	1.0747	0.4820	0.7562
0.3004	814.02	61.358	10.358	1.1020	0.4505	0.8282
0.4011	753.89	59.048	10.916	1.1244	0.4232	0.9003
0.5009	705.98	57.141	11.414	1.1432	0.3984	0.9719

0.5978	668.47	55.602	11.845	1.1590	0.3769	1.0414
0.6984	635.88	54.230	12.251	1.1731	0.3563	1.1138
0.8001	609.21	53.081	12.611	1.1854	0.3382	1.1870
0.9024	585.22	52.025	12.954	1.1962	0.3204	1.2609
1.0000	568.20	51.263	13.219	1.2057	0.3076	1.3312

{22MEE (1) + propan-1-ol (2)}

T= 293.15 K

0.0000	828.27	58.655	9.8534	1.0000	0.4135	0.7997
0.1021	761.16	56.228	10.487	1.0332	0.3869	0.8530
0.2041	705.91	54.149	11.078	1.0621	0.3613	0.9065
0.3039	660.81	52.391	11.620	1.0872	0.3375	0.9590
0.3978	624.79	50.943	12.097	1.1082	0.3162	1.0085
0.4989	591.28	49.558	12.582	1.1285	0.2942	1.0619
0.6028	561.45	48.292	13.051	1.1472	0.2725	1.1170
0.6986	537.34	47.244	13.460	1.1627	0.2532	1.1679
0.8015	514.55	46.231	13.874	1.1779	0.2335	1.2226
0.8987	495.50	45.367	14.244	1.1910	0.2158	1.2744
1.0000	477.20	44.521	14.617	1.2033	0.1972	1.3287

T= 303.15 K

0.0000	885.69	61.770	9.4808	1.0000	0.4460	0.8002
0.1021	812.13	59.149	10.102	1.0331	0.4197	0.8536
0.2041	752.08	56.920	10.681	1.0619	0.3946	0.9072
0.3039	703.12	55.037	11.211	1.0869	0.3714	0.9597
0.3978	664.08	53.487	11.679	1.1080	0.3506	1.0093
0.4989	627.81	52.006	12.154	1.1283	0.3291	1.0627
0.6028	595.62	50.655	12.613	1.1470	0.3079	1.1178
0.6986	569.67	49.539	13.013	1.1625	0.2892	1.1688
0.8015	545.14	48.461	13.419	1.1777	0.2701	1.2235
0.8987	524.63	47.540	13.782	1.1908	0.2528	1.2754
1.0000	505.51	46.666	14.140	1.2033	0.2355	1.3294

T= 313.15 K

0.0000	948.05	65.062	9.1163	1.0000	0.4771	0.8008
0.1021	867.81	62.248	9.7233	1.0330	0.4514	0.8543
0.2041	802.41	59.856	10.289	1.0619	0.4270	0.9079
0.3039	749.20	57.838	10.808	1.0869	0.4042	0.9605
0.3978	706.81	56.178	11.266	1.1079	0.3840	1.0101
0.4989	667.54	54.595	11.731	1.1282	0.3630	1.0636
0.6028	632.75	53.153	12.181	1.1470	0.3425	1.1187
0.6986	604.73	51.963	12.573	1.1625	0.3243	1.1696
0.8015	578.30	50.815	12.970	1.1778	0.3057	1.2244
0.8987	556.21	49.835	13.325	1.1909	0.2889	1.2762
1.0000	535.64	48.905	13.676	1.2034	0.2721	1.3303

T= 323.15 K

0.0000	1016.5	68.565	8.7571	1.0000	0.5070	0.8015
0.1021	928.71	65.538	9.3502	1.0330	0.4820	0.8550
0.2041	857.30	62.968	9.9038	1.0619	0.4581	0.9087
0.3039	799.37	60.803	10.411	1.0869	0.4360	0.9613
0.3978	753.30	59.025	10.859	1.1080	0.4163	1.0109
0.4989	710.68	57.331	11.315	1.1283	0.3959	1.0644
0.6028	672.98	55.790	11.755	1.1471	0.3759	1.1196
0.6986	642.71	54.520	12.139	1.1627	0.3582	1.1705
0.8015	614.18	53.297	12.528	1.1780	0.3402	1.2253

0.8987	590.33	52.252	12.876	1.1911	0.3239	1.2771
1.0000	568.20	51.263	13.219	1.2037	0.3076	1.3312

{22MEE (1) + propan-2-ol (2)}

T= 293.15 K

0.0000	946.98	62.717	9.1087	1.0000	0.4750	0.8036
0.1010	854.59	59.579	9.7945	1.0330	0.4424	0.8564
0.2032	777.56	56.831	10.464	1.0628	0.4100	0.9096
0.2995	717.62	54.596	11.064	1.0877	0.3804	0.9598
0.4001	665.83	52.589	11.654	1.1110	0.3512	1.0124
0.5002	621.93	50.826	12.213	1.1317	0.3230	1.0649
0.6022	583.84	49.245	12.753	1.1507	0.2954	1.1185
0.6987	552.73	47.915	13.238	1.1670	0.2704	1.1693
0.7989	524.49	46.675	13.717	1.1823	0.2453	1.2221
0.9023	499.04	45.529	14.186	1.1968	0.2206	1.2767
1.0000	477.20	44.521	14.617	1.2090	0.1972	1.3287

T= 303.15 K

0.0000	1019.0	66.255	8.7333	1.0000	0.5067	0.8040
0.1010	916.05	62.820	9.4106	1.0328	0.4744	0.8570
0.2032	831.50	59.850	10.068	1.0625	0.4426	0.9103
0.2995	765.91	57.441	10.657	1.0874	0.4137	0.9605
0.4001	709.32	55.279	11.236	1.1107	0.3850	1.0132
0.5002	661.52	53.384	11.786	1.1314	0.3574	1.0657
0.6022	620.16	51.688	12.317	1.1504	0.3305	1.1194
0.6987	586.48	50.264	12.793	1.1667	0.3060	1.1702
0.7989	555.95	48.939	13.264	1.1820	0.2816	1.2230
0.9023	528.50	47.715	13.724	1.1965	0.2575	1.2777
1.0000	505.51	46.666	14.140	1.2090	0.2355	1.3294

T= 313.15 K

0.0000	1098.6	70.037	8.3632	1.0000	0.5372	0.8046
0.1010	984.46	66.300	9.0283	1.0329	0.5055	0.8576
0.2032	891.17	63.080	9.6735	1.0625	0.4744	0.9110
0.2995	819.04	60.473	10.253	1.0874	0.4461	0.9613
0.4001	757.04	58.140	10.822	1.1107	0.4180	1.0140
0.5002	704.83	56.099	11.363	1.1314	0.3910	1.0665
0.6022	659.82	54.278	11.884	1.1504	0.3647	1.1202
0.6987	623.22	52.751	12.352	1.1667	0.3409	1.1711
0.7989	590.15	51.333	12.815	1.1821	0.3171	1.2239
0.9023	560.47	50.025	13.268	1.1966	0.2936	1.2785
1.0000	535.64	48.905	13.676	1.2091	0.2721	1.3303

T= 323.15 K

0.0000	1188.5	74.140	7.9924	1.0000	0.5671	0.8053
0.1010	1060.9	70.047	8.6475	1.0329	0.5359	0.8583
0.2032	957.30	66.539	9.2824	1.0626	0.5053	0.9117
0.2995	877.62	63.710	9.8525	1.0875	0.4775	0.9621
0.4001	809.38	61.183	10.413	1.1108	0.4501	1.0148
0.5002	752.16	58.980	10.945	1.1316	0.4236	1.0674
0.6022	702.99	57.020	11.458	1.1506	0.3979	1.1210
0.6987	663.12	55.380	11.918	1.1669	0.3746	1.1719
0.7989	627.22	53.859	12.373	1.1824	0.3514	1.2248
0.9023	595.03	52.459	12.818	1.1969	0.3285	1.2794
1.0000	568.20	51.263	13.219	1.2095	0.3076	1.3312

{22MEE (1) + butan-1-ol (2)}

T= 293.15 K

0.0000	776.47	56.791	10.218	1.0000	0.3795	0.9875
0.1013	733.30	55.190	10.682	1.0277	0.3634	1.0214
0.2024	693.88	53.686	11.142	1.0533	0.3464	1.0554
0.3016	658.58	52.303	11.588	1.0768	0.3293	1.0889
0.3992	626.72	51.022	12.023	1.0983	0.3120	1.1220
0.5031	595.55	49.737	12.482	1.1198	0.2931	1.1574
0.6025	568.66	48.601	12.910	1.1392	0.2753	1.1912
0.6993	543.51	47.514	13.335	1.1566	0.2563	1.2246
0.7966	520.65	46.504	13.750	1.1733	0.2378	1.2581
0.8986	498.32	45.496	14.183	1.1897	0.2180	1.2933
1.0000	477.20	44.521	14.617	1.2048	0.1972	1.3287

T= 303.15 K

0.0000	827.92	59.721	9.8486	1.0000	0.4125	0.9880
0.1013	780.63	57.991	10.304	1.0275	0.3963	1.0220
0.2024	737.93	56.382	10.754	1.0531	0.3797	1.0561
0.3016	699.81	54.907	11.190	1.0765	0.3629	1.0897
0.3992	665.45	53.542	11.614	1.0980	0.3460	1.1228
0.5031	631.86	52.173	12.063	1.1195	0.3276	1.1583
0.6025	602.96	50.966	12.481	1.1389	0.3103	1.1921
0.6993	575.97	49.812	12.896	1.1563	0.2920	1.2255
0.7966	551.48	48.742	13.301	1.1729	0.2740	1.2590
0.8986	527.56	47.673	13.724	1.1893	0.2548	1.2943
1.0000	505.51	46.666	14.140	1.2047	0.2355	1.3294

T= 313.15 K

0.0000	883.61	62.812	9.4865	1.0000	0.4441	0.9886
0.1013	832.21	60.958	9.9317	1.0275	0.4282	1.0226
0.2024	785.91	59.238	10.370	1.0530	0.4119	1.0568
0.3016	744.61	57.660	10.796	1.0763	0.3956	1.0904
0.3992	707.51	56.206	11.211	1.0979	0.3791	1.1236
0.5031	671.30	54.748	11.649	1.1193	0.3612	1.1591
0.6025	640.21	53.466	12.057	1.1387	0.3445	1.1929
0.6993	611.17	52.239	12.462	1.1561	0.3266	1.2264
0.7966	584.90	51.104	12.858	1.1728	0.3093	1.2599
0.8986	559.27	49.972	13.270	1.1892	0.2908	1.2951
1.0000	535.64	48.905	13.676	1.2046	0.2721	1.3303

T= 323.15 K

0.0000	944.48	66.092	9.1295	1.0000	0.4746	0.9892
0.1013	888.41	64.100	9.5647	1.0274	0.4590	1.0234
0.2024	838.09	62.258	9.9932	1.0529	0.4431	1.0576
0.3016	793.34	60.573	10.409	1.0763	0.4272	1.0913
0.3992	753.20	59.021	10.814	1.0978	0.4112	1.1245
0.5031	714.06	57.467	11.241	1.1192	0.3937	1.1600
0.6025	680.54	56.102	11.640	1.1387	0.3775	1.1938
0.6993	649.29	54.799	12.035	1.1561	0.3603	1.2273
0.7966	621.05	53.594	12.421	1.1728	0.3435	1.2608
0.8986	593.54	52.393	12.823	1.1892	0.3257	1.2960
1.0000	568.20	51.263	13.219	1.2046	0.3076	1.3312

{22MEE (1) + butan-2-ol (2)}

T= 293.15 K

0.0000	818.72	58.316	9.9261	1.0000	0.4085	0.9846
0.1021	770.28	56.564	10.394	1.0266	0.3906	1.0200
0.2032	724.96	54.875	10.872	1.0515	0.3712	1.0546
0.3026	683.78	53.293	11.346	1.0746	0.3510	1.0885

0.4006	646.93	51.838	11.810	1.0959	0.3309	1.1220
0.4992	612.55	50.441	12.280	1.1161	0.3097	1.1557
0.6015	580.06	49.085	12.764	1.1357	0.2874	1.1909
0.7012	551.18	47.848	13.231	1.1537	0.2655	1.2252
0.7973	525.33	46.713	13.681	1.1700	0.2437	1.2583
0.8943	501.66	45.648	14.126	1.1855	0.2221	1.2919
1.0000	477.20	44.521	14.617	1.2012	0.1972	1.3287
			T= 303.15 K			
0.0000	878.02	61.502	9.5354	1.0000	0.4427	0.9851
0.1021	823.88	59.575	10.000	1.0265	0.4245	1.0205
0.2032	773.96	57.742	10.470	1.0513	0.4052	1.0552
0.3026	728.79	56.032	10.937	1.0743	0.3852	1.0892
0.4006	688.57	54.464	11.394	1.0956	0.3653	1.1228
0.4992	651.17	52.964	11.855	1.1158	0.3445	1.1565
0.6015	615.95	51.512	12.330	1.1354	0.3227	1.1917
0.7012	584.68	50.187	12.788	1.1533	0.3013	1.2260
0.7973	556.79	48.976	13.229	1.1697	0.2801	1.2592
0.8943	531.29	47.841	13.666	1.1852	0.2590	1.2928
1.0000	505.51	46.666	14.140	1.2011	0.2355	1.3294
			T= 313.15 K			
0.0000	944.42	64.937	9.1440	1.0000	0.4762	0.9857
0.1021	883.64	62.813	9.6053	1.0265	0.4578	1.0211
0.2032	828.19	60.810	10.070	1.0513	0.4384	1.0558
0.3026	778.40	58.954	10.531	1.0743	0.4186	1.0899
0.4006	734.25	57.258	10.980	1.0956	0.3990	1.1235
0.4992	693.40	55.642	11.434	1.1157	0.3785	1.1573
0.6015	655.09	54.083	11.900	1.1353	0.3572	1.1925
0.7012	621.15	52.664	12.350	1.1533	0.3362	1.2269
0.7973	590.99	51.369	12.783	1.1696	0.3155	1.2600
0.8943	563.44	50.158	13.211	1.1851	0.2950	1.2936
1.0000	535.64	48.905	13.676	1.2011	0.2721	1.3303
			T= 323.15 K			
0.0000	1019.5	68.668	8.7497	1.0000	0.5091	0.9864
0.1021	950.45	66.300	9.2107	1.0266	0.4903	1.0218
0.2032	888.33	64.097	9.6719	1.0514	0.4708	1.0566
0.3026	833.06	62.071	10.127	1.0744	0.4512	1.0907
0.4006	784.40	60.231	10.570	1.0956	0.4317	1.1243
0.4992	739.59	58.485	11.017	1.1158	0.4116	1.1582
0.6015	697.74	56.806	11.475	1.1354	0.3906	1.1934
0.7012	660.79	55.282	11.917	1.1534	0.3701	1.2277
0.7973	628.05	53.895	12.343	1.1697	0.3499	1.2609
0.8943	598.22	52.600	12.763	1.1853	0.3299	1.2945
1.0000	568.20	51.263	13.219	1.2012	0.3076	1.3312

Table A1.7: Isentropic compressibility (κ_s), intermolecular free length (L_f), specific acoustic impedance (Z), relative association (R_A), relaxation strength (r) and Rao's molar sound function (R) for the binary systems (furfural + DMSO, or acetonitrile) at (293.15, 303.15, 313.15 and 323.15) K and for (furfural + sulfolane) at (303.15, 313.15 and 323.15) K and at pressure of 0.1 MPa.

x_1	κ_s / (TPa^{-1})	L_f / (10^{-12} m)	Z / (10^5 kg m^{-2} s^{-1})	R_A	r	R / (10^{-3} m$^{(10/3)}$ mol^{-1} s$^{(-1/3)}$)
			{furfural (1) + DMSO (2)}			
			T= 293.15 K			
0.0000	401.97	40.862	16.545	1.0000	0.1168	0.8135
0.1047	404.52	40.991	16.540	1.0078	0.1274	0.8266
0.2024	405.83	41.057	16.558	1.0148	0.1350	0.8389
0.3008	406.74	41.103	16.585	1.0216	0.1416	0.8513
0.4017	407.26	41.129	16.621	1.0285	0.1474	0.8640
0.5009	407.37	41.135	16.663	1.0350	0.1522	0.8764
0.6011	407.29	41.131	16.709	1.0414	0.1566	0.8890
0.7008	406.97	41.115	16.759	1.0476	0.1603	0.9016
0.7989	406.52	41.092	16.810	1.0535	0.1635	0.9139
0.8971	406.09	41.070	16.859	1.0592	0.1666	0.9263
1.0000	405.43	41.037	16.915	1.0651	0.1694	0.9393
			T= 303.15 K			
0.0000	424.51	42.764	16.026	1.0000	0.1560	0.8148
0.1047	427.20	42.900	16.022	1.0079	0.1662	0.8279
0.2024	428.60	42.970	16.040	1.0149	0.1735	0.8402
0.3008	429.65	43.022	16.064	1.0218	0.1800	0.8525
0.4017	430.36	43.058	16.096	1.0287	0.1859	0.8651
0.5009	430.70	43.075	16.132	1.0353	0.1909	0.8776
0.6011	430.87	43.083	16.172	1.0418	0.1955	0.8901
0.7008	430.83	43.081	16.215	1.0481	0.1995	0.9025
0.7989	430.65	43.072	16.258	1.0541	0.2031	0.9149
0.8971	430.51	43.065	16.299	1.0599	0.2067	0.9272
1.0000	430.27	43.053	16.344	1.0659	0.2101	0.9401
			T= 313.15 K			
0.0000	448.74	44.762	15.516	1.0000	0.1942	0.8160
0.1047	451.60	44.905	15.512	1.0079	0.2040	0.8291
0.2024	453.13	44.981	15.528	1.0150	0.2110	0.8413
0.3008	454.35	45.041	15.550	1.0220	0.2174	0.8536
0.4017	455.29	45.087	15.577	1.0290	0.2234	0.8662
0.5009	455.88	45.117	15.609	1.0357	0.2285	0.8786
0.6011	456.33	45.139	15.643	1.0423	0.2334	0.8911
0.7008	456.60	45.152	15.678	1.0486	0.2378	0.9035
0.7989	456.77	45.161	15.713	1.0547	0.2417	0.9157
0.8971	456.99	45.172	15.747	1.0606	0.2457	0.9280
1.0000	457.17	45.180	15.782	1.0666	0.2496	0.9408
			T= 323.15 K			
0.0000	474.69	46.855	15.015	1.0000	0.2311	0.8173
0.1047	477.73	47.005	15.012	1.0080	0.2405	0.8303
0.2024	479.44	47.089	15.027	1.0152	0.2474	0.8425
0.3008	480.86	47.159	15.046	1.0222	0.2537	0.8548

0.4017	482.06	47.217	15.069	1.0293	0.2597	0.8673
0.5009	482.95	47.261	15.095	1.0360	0.2650	0.8796
0.6011	483.72	47.299	15.123	1.0427	0.2701	0.8920
0.7008	484.36	47.330	15.152	1.0491	0.2747	0.9044
0.7989	484.96	47.360	15.179	1.0553	0.2791	0.9166
0.8971	485.59	47.390	15.204	1.0613	0.2834	0.9288
1.0000	486.26	47.423	15.230	1.0674	0.2878	0.9415

{furfural (1) + acetonitrile (2)}

T= 293.15 K

0.0000	757.64	56.098	10.159	1.0000	0.3407	0.5728
0.1030	686.01	53.380	11.079	1.0722	0.3237	0.6080
0.2016	630.51	51.176	11.901	1.1325	0.3063	0.6425
0.3079	581.26	49.137	12.732	1.1892	0.2867	0.6805
0.4006	545.66	47.608	13.404	1.2327	0.2698	0.7142
0.4978	513.51	46.184	14.073	1.2735	0.2520	0.7500
0.5975	485.40	44.902	14.714	1.3109	0.2343	0.7870
0.6949	461.70	43.792	15.302	1.3437	0.2174	0.8234
0.7961	440.45	42.773	15.873	1.3744	0.2008	0.8616
0.8969	421.87	41.861	16.408	1.4021	0.1848	0.8998
1.0000	405.43	41.037	16.915	1.4274	0.1694	0.9393

T= 303.15 K

0.0000	817.77	59.354	9.711	1.0000	0.3806	0.5749
0.1030	738.11	56.389	10.611	1.0728	0.3632	0.6098
0.2016	677.14	54.010	11.414	1.1337	0.3461	0.6441
0.3079	622.78	51.797	12.228	1.1910	0.3265	0.6819
0.4006	583.56	50.139	12.890	1.2348	0.3096	0.7155
0.4978	548.30	48.601	13.546	1.2760	0.2919	0.7512
0.5975	517.50	47.216	14.177	1.3137	0.2743	0.7881
0.6949	491.27	46.004	14.761	1.3466	0.2571	0.8245
0.7961	468.39	44.920	15.318	1.3778	0.2412	0.8625
0.8969	448.15	43.939	15.845	1.4057	0.2253	0.9006
1.0000	430.27	43.053	16.344	1.4313	0.2101	0.9401

T= 313.15 K

0.0000	885.91	62.894	9.263	1.0000	0.4200	0.5768
0.1030	797.03	59.655	10.144	1.0734	0.4024	0.6115
0.2016	728.69	57.041	10.934	1.1348	0.3847	0.6456
0.3079	668.51	54.634	11.733	1.1925	0.3651	0.6833
0.4006	625.21	52.835	12.382	1.2367	0.3482	0.7168
0.4978	586.38	51.168	13.028	1.2783	0.3306	0.7523
0.5975	552.56	49.671	13.648	1.3164	0.3132	0.7891
0.6949	524.16	48.377	14.218	1.3497	0.2966	0.8254
0.7961	498.78	47.192	14.771	1.3810	0.2803	0.8634
0.8969	476.68	46.135	15.290	1.4092	0.2647	0.9014
1.0000	457.17	45.180	15.782	1.4349	0.2496	0.9408

T= 323.15 K

0.0000	960.89	66.664	8.829	1.0000	0.4573	0.5789
0.1030	861.91	63.137	9.688	1.0742	0.4398	0.6133
0.2016	785.65	60.279	10.463	1.1361	0.4219	0.6472
0.3079	718.80	57.657	11.247	1.1943	0.4023	0.6847
0.4006	670.86	55.702	11.885	1.2390	0.3855	0.7181
0.4978	628.01	53.893	12.519	1.2809	0.3680	0.7535
0.5975	590.76	52.271	13.129	1.3193	0.3507	0.7902

0.6949	559.57	50.872	13.689	1.3530	0.3343	0.8263
0.7961	531.74	49.591	14.234	1.3845	0.3181	0.8643
0.8969	507.56	48.450	14.746	1.4130	0.3026	0.9022
1.0000	486.26	47.423	15.230	1.4390	0.2878	0.9415
			{furfural (1) + sulfolane (2)}			
			T= 303.15 K			
0.0000	316.08	36.901	19.979	1.0000	0.0205	1.1101
0.1012	325.43	37.442	19.616	0.9961	0.0414	1.0919
0.1990	334.71	37.973	19.270	0.9921	0.0610	1.0744
0.3018	344.91	38.547	18.904	0.9874	0.0811	1.0563
0.4013	355.15	39.115	18.550	0.9824	0.1000	1.0391
0.5005	365.67	39.690	18.200	0.9770	0.1181	1.0223
0.5991	377.16	40.309	17.837	0.9714	0.1369	1.0056
0.7006	389.33	40.954	17.469	0.9652	0.1555	0.9887
0.8014	402.13	41.622	17.098	0.9586	0.1738	0.9720
0.9002	415.47	42.306	16.731	0.9518	0.1916	0.9559
1.0000	430.27	43.053	16.344	0.9442	0.2101	0.9401
			T= 313.15 K			
0.0000	331.23	38.457	19.449	1.0000	0.0587	1.1105
0.1012	341.53	39.051	19.080	0.9961	0.0801	1.0923
0.1990	351.63	39.624	18.732	0.9921	0.0996	1.0748
0.3018	362.74	40.245	18.364	0.9873	0.1197	1.0568
0.4013	373.94	40.861	18.008	0.9823	0.1386	1.0396
0.5005	385.71	41.500	17.650	0.9769	0.1572	1.0228
0.5991	398.13	42.162	17.290	0.9712	0.1756	1.0062
0.7006	411.56	42.868	16.918	0.9649	0.1943	0.9893
0.8014	425.77	43.601	16.545	0.9583	0.2128	0.9727
0.9002	440.62	44.355	16.174	0.9514	0.2309	0.9566
1.0000	457.17	45.180	15.782	0.9438	0.2496	0.9408
			T= 323.15 K			
0.0000	347.55	40.092	18.920	1.0000	0.0966	1.1107
0.1012	358.59	40.724	18.553	0.9960	0.1175	1.0926
0.1990	369.57	41.343	18.204	0.9919	0.1370	1.0752
0.3018	381.70	42.016	17.834	0.9870	0.1570	1.0572
0.4013	393.95	42.685	17.476	0.9820	0.1759	1.0401
0.5005	406.89	43.380	17.116	0.9766	0.1946	1.0233
0.5991	420.54	44.101	16.753	0.9708	0.2131	1.0067
0.7006	435.39	44.874	16.379	0.9645	0.2319	0.9899
0.8014	451.15	45.679	16.002	0.9578	0.2505	0.9733
0.9002	467.73	46.510	15.626	0.9509	0.2688	0.9573
1.0000	486.26	47.423	15.230	0.9432	0.2878	0.9415

Table A1.8: Isentropic compressibility (κ_s), intermolecular free length (L_f), specific acoustic impedance (Z), relative association (R_A), relaxation strength (r) and Rao's molar sound function (R) for the binary systems (1-hexene + 2-methoxyethanol, or 2-ethoxyethanol, or 2-butoxyethanol) at (293.15, 298.15 and 303.15) K and at pressure p = 0.1 MPa.

x_1	κ_s / (TPa^{-1})	L_f/ (10 $^{-12}$ m)	Z / (10^5 kg m^{-2} s^{-1})	R_A	r	R / (10^{-3} m$^{(10/3)}$ mol^{-1} s$^{(-1/3)}$)
			{1-hexene (1) + 2-methoxyethanol (2)}			
			T= 293.15 K			
0.0000	560.80	48.264	13.115	1.0000	0.2779	0.8739
0.1008	644.04	51.722	11.958	0.9695	0.3414	0.9111
0.2037	731.68	55.129	10.970	0.9398	0.3937	0.9500
0.3016	814.19	58.154	10.192	0.9128	0.4327	0.9880
0.4023	895.30	60.982	9.5315	0.8861	0.4636	1.0284
0.5020	969.85	63.470	8.9930	0.8607	0.4865	1.0694
0.5995	1037.3	65.641	8.5514	0.8371	0.5036	1.1104
0.6960	1098.9	67.560	8.1786	0.8147	0.5164	1.1519
0.7996	1158.9	69.382	7.8375	0.7918	0.5265	1.1973
0.8980	1210.2	70.901	7.5609	0.7714	0.5335	1.2407
1.0000	1252.5	72.129	7.3328	0.7519	0.5369	1.2856
			T= 298.15 K			
0.0000	577.97	49.448	12.888	1.0000	0.2960	0.8744
0.1008	665.00	53.040	11.738	0.9694	0.3589	0.9116
0.2037	757.71	56.617	10.751	0.9399	0.4113	0.9504
0.3016	844.99	59.789	9.9763	0.9129	0.4503	0.9884
0.4023	931.13	62.762	9.3186	0.8862	0.4811	1.0288
0.5020	1010.1	65.370	8.7847	0.8607	0.5039	1.0699
0.5995	1082.9	67.683	8.3427	0.8372	0.5214	1.1108
0.6960	1149.0	69.719	7.9717	0.8148	0.5344	1.1523
0.7996	1213.7	71.656	7.6323	0.7920	0.5448	1.1976
0.8980	1269.0	73.271	7.3579	0.7716	0.5520	1.2410
1.0000	1314.7	74.579	7.1320	0.7522	0.5557	1.2857
			T= 303.15 K			
0.0000	596.06	50.673	12.660	1.0000	0.3141	0.8748
0.1008	687.83	54.435	11.512	0.9696	0.3770	0.9119
0.2037	785.28	58.163	10.532	0.9400	0.4289	0.9507
0.3016	877.76	61.493	9.7602	0.9130	0.4678	0.9888
0.4023	969.35	64.621	9.1056	0.8863	0.4986	1.0291
0.5020	1054.3	67.392	8.5717	0.8610	0.5217	1.0701
0.5995	1131.6	69.822	8.1343	0.8374	0.5390	1.1111
0.6960	1202.7	71.981	7.7653	0.8150	0.5522	1.1526
0.7996	1272.5	74.041	7.4280	0.7922	0.5628	1.1979
0.8980	1332.3	75.759	7.1556	0.7719	0.5702	1.2413
1.0000	1381.7	77.152	6.9323	0.7525	0.5742	1.2858
			{1-hexene (1) + 2-ethoxyethanol (2)}			
			T= 293.15 K			
0.0000	617.61	50.649	12.267	1.0000	0.3195	1.0636
0.1018	683.08	53.266	11.460	0.9758	0.3626	1.0826

0.2034	751.27	55.862	10.739	0.9518	0.3998	1.1024
0.3022	818.59	58.311	10.118	0.9288	0.4305	1.1223
0.4038	888.36	60.745	9.5496	0.9051	0.4572	1.1437
0.5018	955.22	62.990	9.0622	0.8823	0.4787	1.1654
0.5989	1019.4	65.072	8.6367	0.8601	0.4961	1.1876
0.6981	1083.2	67.077	8.2481	0.8376	0.5106	1.2111
0.8004	1145.6	68.983	7.8946	0.8149	0.5225	1.2361
0.8970	1201.0	70.631	7.5991	0.7940	0.5310	1.2601
1.0000	1252.5	72.129	7.3328	0.7726	0.5369	1.2856
			T= 298.15 K			
0.0000	637.46	51.930	12.046	1.0000	0.3375	1.0640
0.1018	706.33	54.664	11.241	0.9758	0.3804	1.0831
0.2034	778.32	57.382	10.522	0.9519	0.4176	1.1028
0.3022	849.64	59.953	9.9032	0.9288	0.4483	1.1227
0.4038	923.77	62.514	9.3373	0.9052	0.4750	1.1441
0.5018	995.07	64.882	8.8517	0.8824	0.4965	1.1658
0.5989	1063.7	67.082	8.4282	0.8602	0.5140	1.1879
0.6981	1132.2	69.207	8.0413	0.8378	0.5287	1.2115
0.8004	1199.4	71.231	7.6896	0.8150	0.5407	1.2364
0.8970	1259.1	72.983	7.3961	0.7941	0.5495	1.2604
1.0000	1314.7	74.579	7.1320	0.7728	0.5557	1.2857
			T= 303.15 K			
0.0000	658.41	53.258	11.823	1.0000	0.3554	1.0644
0.1018	730.96	56.115	11.022	0.9758	0.3981	1.0834
0.2034	807.02	58.963	10.305	0.9519	0.4352	1.1032
0.3022	882.66	61.664	9.6885	0.9289	0.4659	1.1230
0.4038	961.51	64.359	9.1249	0.9053	0.4925	1.1444
0.5018	1037.6	66.857	8.6416	0.8825	0.5141	1.1661
0.5989	1111.1	69.187	8.2198	0.8603	0.5317	1.1882
0.6981	1184.6	71.438	7.8350	0.8379	0.5466	1.2118
0.8004	1257.0	73.587	7.4854	0.8151	0.5588	1.2367
0.8970	1321.4	75.449	7.1941	0.7943	0.5678	1.2607
1.0000	1381.7	77.152	6.9323	0.7731	0.5742	1.2858

{1-hexene (1) + 2-butoxyethanol (2)}

			T= 303.15 K			
0.0000	634.55	51.339	11.912	1.0000	0.3163	1.4409
0.1038	680.18	53.153	11.367	0.9835	0.3465	1.4214
0.2055	729.58	55.049	10.839	0.9663	0.3753	1.4029
0.3001	779.57	56.904	10.358	0.9496	0.4009	1.3862
0.4053	839.64	59.056	9.8399	0.9301	0.4277	1.3685
0.5053	901.29	61.186	9.3637	0.9105	0.4515	1.3523
0.6023	964.98	63.310	8.9201	0.8905	0.4728	1.3375
0.7017	1033.6	65.524	8.4870	0.8690	0.4924	1.3232
0.7980	1103.1	67.689	8.0881	0.8470	0.5093	1.3104
0.8977	1176.7	69.910	7.7006	0.8232	0.5242	1.2980
1.0000	1252.5	72.129	7.3328	0.7982	0.5369	1.2856
			T= 313.15 K			
0.0000	654.08	52.603	11.705	1.0000	0.3336	1.4414
0.1038	702.13	54.501	11.161	0.9835	0.3639	1.4219
0.2055	754.31	56.490	10.632	0.9663	0.3927	1.4034
0.3001	807.23	58.438	10.152	0.9497	0.4184	1.3867
0.4053	870.98	60.701	9.6348	0.9302	0.4453	1.3689

0.5053	936.65	62.948	9.1589	0.9106	0.4692	1.3527
0.6023	1004.6	65.193	8.7161	0.8906	0.4906	1.3379
0.7017	1078.2	67.538	8.2837	0.8690	0.5103	1.3236
0.7980	1152.8	69.836	7.8858	0.8471	0.5274	1.3108
0.8977	1232.2	72.201	7.4994	0.8233	0.5426	1.2984
1.0000	1314.7	74.579	7.1320	0.7984	0.5557	1.2857
			T= 323.15 K			
0.0000	674.68	53.912	11.498	1.0000	0.3509	1.4419
0.1038	725.30	55.898	10.954	0.9835	0.3812	1.4223
0.2055	780.46	57.984	10.426	0.9664	0.4101	1.4038
0.3001	836.52	60.031	9.9466	0.9497	0.4358	1.3871
0.4053	904.25	62.414	9.4296	0.9302	0.4627	1.3692
0.5053	974.24	64.784	8.9544	0.9107	0.4867	1.3530
0.6023	1046.9	67.157	8.5124	0.8907	0.5081	1.3382
0.7017	1125.8	69.641	8.0810	0.8691	0.5280	1.3239
0.7980	1206.2	72.084	7.6840	0.8472	0.5453	1.3110
0.8977	1291.9	74.602	7.2989	0.8234	0.5607	1.2986
1.0000	1381.7	77.152	6.9323	0.7986	0.5742	1.2858

Table A1.9: Excess molar volume (V_m^E), deviations in isentropic compressibility ($\Delta\kappa_s$), deviations in intermolecular free length (ΔL_f), deviations in acoustic impedance (ΔZ), deviations in speed of sound (Δu) and changes of refractive index (Δn_D) for the binary systems (22MEE + methanol or ethanol or propan-1-ol or propan-2-ol or butan-1-ol or butan-2-ol) at (293.15, 303.15, 313.15 and 323.15) K and at pressure p = 0.1 MPa.

x_1	V_m^E / (cm^3 mol^{-1})	$\Delta\kappa_s$/ (TPa^{-1})	ΔL_f / (10 $^{-12}$ m)	ΔZ/ (10^5 kg m^{-2} s^{-1})	Δu / (m s^{-1})	Δn_D
			{22MEE (1) + methanol (2)}			
			T= 293.15 K			
0.0000	0.0000	0.0000	0.0000	0.0000	0.0000	0.0000
0.1022	-0.3219	-139.35	-4.4883	0.7938	47.805	0.0168
0.1994	-0.4562	-191.90	-6.3756	1.2200	72.822	0.0254
0.3011	-0.5266	-207.96	-7.0720	1.4395	85.261	0.0294
0.4004	-0.5410	-201.80	-6.9779	1.4868	87.445	0.0296
0.4997	-0.5015	-182.33	-6.3829	1.4079	82.317	0.0276
0.6013	-0.4382	-154.00	-5.4458	1.2362	71.901	0.0240
0.6949	-0.3602	-122.50	-4.3628	1.0117	58.492	0.0194
0.7951	-0.2542	-85.048	-3.0485	0.7203	41.492	0.0134
0.8964	-0.1588	-44.013	-1.5849	0.3817	21.585	0.0071
1.0000	0.0000	0.0000	0.0000	0.0000	0.0000	0.0000
			T= 303.15 K			
0.0000	0.0000	0.0000	0.0000	0.0000	0.0000	0.0000
0.1022	-0.3384	-154.09	-4.8833	0.7828	48.398	0.0177
0.1994	-0.4788	-211.36	-6.9132	1.2016	73.441	0.0257
0.3011	-0.5522	-228.66	-7.6587	1.4184	85.933	0.0293
0.4004	-0.5666	-221.65	-7.5511	1.4656	88.125	0.0297
0.4997	-0.5252	-200.10	-6.9033	1.3882	82.947	0.0275
0.6013	-0.4587	-168.94	-5.8884	1.2195	72.483	0.0239
0.6949	-0.3770	-134.47	-4.7223	1.0000	59.144	0.0195
0.7951	-0.2667	-93.474	-3.3058	0.7143	42.154	0.0134
0.8964	-0.1681	-48.808	-1.7389	0.3848	22.529	0.0070
1.0000	0.0000	0.0000	0.0000	0.0000	0.0000	0.0000
			T= 313.15 K			
0.0000	0.0000	0.0000	0.0000	0.0000	0.0000	0.0000
0.1022	-0.3555	-169.85	-5.2899	0.7679	48.541	0.0186
0.1994	-0.5021	-232.42	-7.4750	1.1790	73.578	0.0269
0.3011	-0.5784	-251.03	-8.2712	1.3921	86.042	0.0303
0.4004	-0.5927	-243.08	-8.1486	1.4389	88.212	0.0301
0.4997	-0.5493	-219.22	-7.4428	1.3626	82.951	0.0281
0.6013	-0.4793	-184.97	-6.3455	1.1972	72.469	0.0242
0.6949	-0.3938	-147.15	-5.0867	0.9816	59.109	0.0195
0.7951	-0.2783	-102.23	-3.5588	0.7009	42.099	0.0139
0.8964	-0.1767	-53.373	-1.8721	0.3780	22.505	0.0071
1.0000	0.0000	0.0000	0.0000	0.0000	0.0000	0.0000
			T= 323.15 K			
0.0000	0.0000	0.0000	0.0000	0.0000	0.0000	0.0000
0.1022	-0.3743	-187.74	-5.7405	0.7538	48.745	0.0193
0.1994	-0.5270	-256.10	-8.0912	1.1566	73.729	0.0279
0.3011	-0.6062	-276.10	-8.9398	1.3657	86.126	0.0309
0.4004	-0.6203	-267.03	-8.7989	1.4117	88.246	0.0305

0.4997	-0.5745	-240.61	-8.0312	1.3369	82.946	0.0282
0.6013	-0.5010	-202.89	-6.8437	1.1748	72.447	0.0248
0.6949	-0.4114	-161.31	-5.4831	0.9632	59.058	0.0202
0.7951	-0.2906	-112.01	-3.8346	0.6877	42.049	0.0139
0.8964	-0.1857	-58.461	-2.0167	0.3710	22.468	0.0072
1.0000	0.0000	0.0000	0.0000	0.0000	0.0000	0.0000

{22MEE (1) + ethanol (2)}

T= 293.15 K

0.0000	0.0000	0.0000	0.0000	0.0000	0.0000	0.0000
0.1014	-0.2152	-76.500	-2.4317	0.3983	22.924	0.0065
0.1994	-0.2530	-111.26	-3.6055	0.6208	34.927	0.0103
0.3004	-0.2856	-126.82	-4.1848	0.7578	41.968	0.0125
0.4011	-0.2688	-127.53	-4.2674	0.8035	43.970	0.0131
0.5009	-0.2555	-119.40	-4.0472	0.7907	43.035	0.0127
0.5978	-0.2310	-104.40	-3.5749	0.7201	38.845	0.0113
0.6984	-0.2004	-83.964	-2.9052	0.6036	32.456	0.0093
0.8001	-0.1393	-58.508	-2.0392	0.4333	23.115	0.0065
0.9024	-0.0940	-30.597	-1.0823	0.2399	13.038	0.0034
1.0000	0.0000	0.0000	0.0000	0.0000	0.0000	0.0000

T= 303.15 K

0.0000	0.0000	0.0000	0.0000	0.0000	0.0000	0.0000
0.1014	-0.2229	-85.276	-2.6683	0.3947	23.724	0.0066
0.1994	-0.2638	-123.64	-3.9468	0.6150	36.067	0.0102
0.3004	-0.2980	-140.50	-4.5679	0.7496	43.158	0.0125
0.4011	-0.2807	-141.02	-4.6504	0.7945	45.130	0.0132
0.5009	-0.2668	-131.81	-4.4041	0.7815	44.075	0.0128
0.5978	-0.2411	-115.28	-3.8932	0.7132	39.915	0.0114
0.6984	-0.2092	-92.738	-3.1660	0.5992	33.446	0.0093
0.8001	-0.1459	-64.737	-2.2283	0.4322	24.015	0.0065
0.9024	-0.0988	-34.152	-1.1967	0.2438	13.948	0.0033
1.0000	0.0000	0.0000	0.0000	0.0000	0.0000	0.0000

T= 313.15 K

0.0000	0.0000	0.0000	0.0000	0.0000	0.0000	0.0000
0.1014	-0.2308	-94.160	-2.8953	0.3864	23.942	0.0064
0.1994	-0.2748	-136.33	-4.2788	0.6024	36.403	0.0104
0.3004	-0.3103	-154.75	-4.9487	0.7348	43.572	0.0128
0.4011	-0.2924	-155.10	-5.0317	0.7784	45.492	0.0136
0.5009	-0.2778	-144.80	-4.7606	0.7655	44.375	0.0132
0.5978	-0.2510	-126.56	-4.2061	0.6988	40.172	0.0116
0.6984	-0.2175	-101.76	-3.4197	0.5874	33.671	0.0095
0.8001	-0.1517	-71.000	-2.4059	0.4239	24.169	0.0065
0.9024	-0.1025	-37.432	-1.2915	0.2393	14.031	0.0033
1.0000	0.0000	0.0000	0.0000	0.0000	0.0000	0.0000

T= 323.15 K

0.0000	0.0000	0.0000	0.0000	0.0000	0.0000	0.0000
0.1014	-0.2394	-104.19	-3.1445	0.3779	24.137	0.0070
0.1994	-0.2868	-150.64	-4.6429	0.5896	36.701	0.0115
0.3004	-0.3237	-170.75	-5.3645	0.7194	43.914	0.0136
0.4011	-0.3055	-170.92	-5.4487	0.7620	45.799	0.0142
0.5009	-0.2900	-159.42	-5.1511	0.7495	44.645	0.0136
0.5978	-0.2618	-139.23	-4.5487	0.6843	40.405	0.0119
0.6984	-0.2267	-111.90	-3.6971	0.5756	33.869	0.0095

0.8001	-0.1582	-78.026	-2.5998	0.4154	24.301	0.0068
0.9024	-0.1067	-41.123	-1.3956	0.2349	14.118	0.0034
1.0000	0.0000	0.0000	0.0000	0.0000	0.0000	0.0000

{22MEE (1) + propan-1-ol (2)}

T= 293.15 K

0.0000	0.0000	0.0000	0.0000	0.0000	0.0000	0.0000
0.1021	-0.0106	-31.266	-0.9834	0.1467	6.2564	0.0022
0.2041	-0.0166	-50.709	-1.6210	0.2527	10.902	0.0037
0.3039	-0.0216	-60.782	-1.9692	0.3187	13.748	0.0047
0.3978	-0.0226	-63.830	-2.0897	0.3486	14.922	0.0051
0.4989	-0.0224	-61.856	-2.0461	0.3517	14.997	0.0051
0.6028	-0.0200	-55.205	-1.8438	0.3260	13.869	0.0046
0.6986	-0.0150	-45.676	-1.5377	0.2783	11.833	0.0039
0.8015	-0.0109	-32.349	-1.0965	0.2026	8.5170	0.0028
0.8987	-0.0062	-17.263	-0.5861	0.1090	4.3631	0.0015
1.0000	0.0000	0.0000	0.0000	0.0000	0.0000	0.0000

T= 303.15 K

0.0000	0.0000	0.0000	0.0000	0.0000	0.0000	0.0000
0.1021	-0.0097	-34.737	-1.0783	0.1455	6.7319	0.0022
0.2041	-0.0146	-56.012	-1.7667	0.2492	11.503	0.0037
0.3039	-0.0196	-67.040	-2.1436	0.3144	14.464	0.0047
0.3978	-0.0208	-70.373	-2.2748	0.3443	15.721	0.0051
0.4989	-0.0214	-68.221	-2.2295	0.3485	15.872	0.0051
0.6028	-0.0192	-60.901	-2.0106	0.3238	14.740	0.0046
0.6986	-0.0151	-50.433	-1.6796	0.2776	12.657	0.0039
0.8015	-0.0111	-35.847	-1.2039	0.2041	9.3074	0.0027
0.8987	-0.0068	-19.396	-0.6558	0.1136	5.1578	0.0015
1.0000	0.0000	0.0000	0.0000	0.0000	0.0000	0.0000

T= 313.15 K

0.0000	0.0000	0.0000	0.0000	0.0000	0.0000	0.0000
0.1021	-0.0089	-38.130	-1.1644	0.1413	6.8370	0.0022
0.2041	-0.0133	-61.471	-1.9081	0.2423	11.703	0.0037
0.3039	-0.0181	-73.535	-2.3147	0.3060	14.719	0.0047
0.3978	-0.0195	-77.189	-2.4572	0.3357	16.031	0.0051
0.4989	-0.0202	-74.774	-2.4069	0.3399	16.167	0.0051
0.6028	-0.0186	-66.711	-2.1697	0.3160	15.000	0.0046
0.6986	-0.0147	-55.227	-1.8122	0.2710	12.882	0.0039
0.8015	-0.0110	-39.219	-1.2978	0.1992	9.4475	0.0027
0.8987	-0.0069	-21.212	-0.7068	0.1109	5.2328	0.0015
1.0000	0.0000	0.0000	0.0000	0.0000	0.0000	0.0000

T= 323.15 K

0.0000	0.0000	0.0000	0.0000	0.0000	0.0000	0.0000
0.1021	-0.0095	-42.003	-1.2605	0.1374	6.9562	0.0024
0.2041	-0.0138	-67.695	-2.0660	0.2360	11.931	0.0039
0.3039	-0.0186	-80.899	-2.5044	0.2982	14.986	0.0049
0.3978	-0.0202	-84.863	-2.6574	0.3272	16.317	0.0054
0.4989	-0.0211	-82.172	-2.6026	0.3316	16.462	0.0053
0.6028	-0.0197	-73.289	-2.3460	0.3086	15.284	0.0048
0.6986	-0.0158	-60.618	-1.9578	0.2646	13.095	0.0040
0.8015	-0.0119	-43.018	-1.4012	0.1944	9.5896	0.0029
0.8987	-0.0076	-23.279	-0.7639	0.1085	5.3336	0.0016
1.0000	0.0000	0.0000	0.0000	0.0000	0.0000	0.0000

{22MEE (1) + propan-2-ol (2)}

T= 293.15 K

0.0000	0.0000	0.0000	0.0000	0.0000	0.0000	0.0000
0.1010	0.0375	-44.948	-1.3003	0.1294	7.6856	0.0024
0.2032	0.0251	-73.968	-2.1893	0.2362	13.978	0.0041
0.2995	0.0047	-88.685	-2.6721	0.3062	17.979	0.0051
0.4001	-0.0009	-93.208	-2.8483	0.3411	19.721	0.0057
0.5002	-0.0116	-90.062	-2.7892	0.3491	19.993	0.0056
0.6022	-0.0143	-80.257	-2.5151	0.3271	18.576	0.0053
0.6987	-0.0140	-65.990	-2.0875	0.2799	15.714	0.0045
0.7989	-0.0140	-47.205	-1.5062	0.2079	11.513	0.0032
0.9023	-0.0075	-24.072	-0.7709	0.1072	5.7203	0.0018
1.0000	0.0000	0.0000	0.0000	0.0000	0.0000	0.0000

T= 303.15 K

0.0000	0.0000	0.0000	0.0000	0.0000	0.0000	0.0000
0.1010	0.0331	-51.072	-1.4570	0.1312	8.4986	0.0023
0.2032	0.0193	-83.162	-2.4248	0.2357	14.943	0.0043
0.2995	-0.0023	-99.309	-2.9476	0.3043	19.021	0.0053
0.4001	-0.0088	-104.24	-3.1395	0.3395	20.877	0.0057
0.5002	-0.0198	-100.62	-3.0729	0.3481	21.183	0.0057
0.6022	-0.0220	-89.629	-2.7715	0.3272	19.748	0.0053
0.6987	-0.0211	-73.719	-2.3028	0.2813	16.813	0.0045
0.7989	-0.0191	-52.842	-1.6674	0.2109	12.517	0.0033
0.9023	-0.0110	-27.193	-0.8651	0.1125	6.5941	0.0017
1.0000	0.0000	0.0000	0.0000	0.0000	0.0000	0.0000

T= 313.15 K

0.0000	0.0000	0.0000	0.0000	0.0000	0.0000	0.0000
0.1010	0.0254	-57.252	-1.6027	0.1285	8.7402	0.0025
0.2032	0.0081	-93.020	-2.6629	0.2308	15.355	0.0044
0.2995	-0.0156	-110.96	-3.2352	0.2985	19.571	0.0055
0.4001	-0.0227	-116.32	-3.4427	0.3333	21.479	0.0061
0.5002	-0.0337	-112.16	-3.3676	0.3421	21.798	0.0060
0.6022	-0.0343	-99.779	-3.0337	0.3215	20.283	0.0055
0.6987	-0.0314	-82.010	-2.5196	0.2766	17.276	0.0047
0.7989	-0.0270	-58.717	-1.8224	0.2074	12.832	0.0035
0.9023	-0.0151	-30.194	-0.9450	0.1106	6.7580	0.0018
1.0000	0.0000	0.0000	0.0000	0.0000	0.0000	0.0000

T= 323.15 K

0.0000	0.0000	0.0000	0.0000	0.0000	0.0000	0.0000
0.1010	0.0117	-64.953	-1.7824	0.1272	9.1333	0.0029
0.2032	-0.0120	-105.16	-2.9524	0.2281	15.989	0.0050
0.2995	-0.0384	-125.12	-3.5793	0.2948	20.327	0.0063
0.4001	-0.0462	-130.95	-3.8045	0.3294	22.308	0.0068
0.5002	-0.0562	-126.06	-3.7161	0.3381	22.602	0.0067
0.6022	-0.0547	-111.98	-3.3440	0.3178	21.009	0.0060
0.6987	-0.0481	-91.939	-2.7749	0.2735	17.883	0.0049
0.7989	-0.0389	-65.749	-2.0049	0.2050	13.264	0.0036
0.9023	-0.0214	-33.795	-1.0395	0.1095	6.9986	0.0019
1.0000	0.0000	0.0000	0.0000	0.0000	0.0000	0.0000

{22MEE (1) + butan-1-ol (2)}

T= 293.15 K

0.0000	0.0000	0.0000	0.0000	0.0000	0.0000	0.0000

0.1013	0.0545	-12.868	-0.3590	0.0183	-1.2827	0.0005
0.2024	0.0955	-22.011	-0.6215	0.0330	-1.9516	0.0008
0.3016	0.1193	-27.634	-0.7882	0.0431	-2.2880	0.0011
0.3992	0.1317	-30.297	-0.8720	0.0487	-2.3730	0.0012
0.5031	0.1329	-30.369	-0.8819	0.0503	-2.2463	0.0013
0.6025	0.1196	-27.500	-0.7976	0.0417	-2.6597	0.0012
0.6993	0.1029	-23.687	-0.6971	0.0404	-1.7485	0.0011
0.7966	0.0811	-17.412	-0.5125	0.0274	-1.5426	0.0008
0.8986	0.0440	-9.2388	-0.2701	0.0119	-1.1459	0.0004
1.0000	0.0000	0.0000	0.0000	0.0000	0.0000	0.0000
			T= 303.15 K			
0.0000	0.0000	0.0000	0.0000	0.0000	0.0000	0.0000
0.1013	0.0561	-14.640	-0.4086	0.0212	-0.7118	0.0005
0.2024	0.0989	-24.720	-0.6961	0.0362	-1.1799	0.0008
0.3016	0.1238	-30.881	-0.8775	0.0466	-1.3969	0.0011
0.3992	0.1365	-33.778	-0.9684	0.0525	-1.4136	0.0012
0.5031	0.1373	-33.868	-0.9807	0.0550	-1.2141	0.0013
0.6025	0.1230	-30.714	-0.8898	0.0471	-1.6179	0.0012
0.6993	0.1054	-26.494	-0.7798	0.0461	-0.7590	0.0011
0.7966	0.0829	-19.603	-0.5796	0.0337	-0.6150	0.0008
0.8986	0.0444	-10.654	-0.3174	0.0190	-0.2969	0.0004
1.0000	0.0000	0.0000	0.0000	0.0000	0.0000	0.0000
			T= 313.15 K			
0.0000	0.0000	0.0000	0.0000	0.0000	0.0000	0.0000
0.1013	0.0572	-16.166	-0.4461	0.0209	-0.5152	0.0005
0.2024	0.1015	-27.263	-0.7590	0.0357	-0.8468	0.0009
0.3016	0.1274	-34.061	-0.9576	0.0462	-0.9481	0.0011
0.3992	0.1408	-37.209	-1.0554	0.0521	-0.9300	0.0013
0.5031	0.1413	-37.263	-1.0675	0.0545	-0.7427	0.0013
0.6025	0.1263	-33.755	-0.9675	0.0466	-1.2008	0.0013
0.6993	0.1082	-29.119	-0.8482	0.0459	-0.3773	0.0011
0.7966	0.0848	-21.517	-0.6295	0.0334	-0.3485	0.0008
0.8986	0.0455	-11.668	-0.3437	0.0186	-0.1736	0.0004
1.0000	0.0000	0.0000	0.0000	0.0000	0.0000	0.0000
			T= 323.15 K			
0.0000	0.0000	0.0000	0.0000	0.0000	0.0000	0.0000
0.1013	0.0573	-17.971	-0.4903	0.0211	-0.2756	0.0005
0.2024	0.1025	-30.223	-0.8319	0.0358	-0.4676	0.0009
0.3016	0.1292	-37.660	-1.0464	0.0459	-0.5104	0.0012
0.3992	0.1428	-41.085	-1.1517	0.0517	-0.4644	0.0013
0.5031	0.1434	-41.127	-1.1648	0.0543	-0.2562	0.0014
0.6025	0.1283	-37.235	-1.0555	0.0465	-0.7456	0.0013
0.6993	0.1098	-32.066	-0.9234	0.0456	-0.0147	0.0011
0.7966	0.0860	-23.681	-0.6850	0.0332	-0.0782	0.0009
0.8986	0.0461	-12.827	-0.3735	0.0184	-0.0333	0.0005
1.0000	0.0000	0.0000	0.0000	0.0000	0.0000	0.0000

{22MEE (1) + butan-2-ol (2)}

			T= 293.15 K			
0.0000	0.0000	0.0000	0.0000	0.0000	0.0000	0.0000
0.1021	0.1750	-13.579	-0.3434	-0.0107	-2.2595	0.0002
0.2032	0.2534	-24.375	-0.6381	-0.0072	-3.0210	0.0005
0.3026	0.2815	-31.595	-0.8478	0.0008	-3.0593	0.0007
0.4006	0.2921	-34.968	-0.9515	0.0049	-3.0676	0.0009
0.4992	0.2681	-35.685	-0.9881	0.0125	-2.5351	0.0010

0.6015	0.2355	-33.221	-0.9321	0.0158	-2.0332	0.0010
0.7012	0.1914	-28.054	-0.7945	0.0148	-1.6505	0.0009
0.7973	0.1320	-21.085	-0.6044	0.0143	-1.0439	0.0007
0.8943	0.0773	-11.625	-0.3307	0.0040	-0.9759	0.0004
1.0000	0.0000	0.0000	0.0000	0.0000	0.0000	0.0000
			T= 303.15 K			
0.0000	0.0000	0.0000	0.0000	0.0000	0.0000	0.0000
0.1021	0.1672	-16.128	-0.4124	-0.0054	-1.5185	0.0002
0.2032	0.2448	-28.387	-0.7456	-0.0005	-1.9676	0.0005
0.3026	0.2728	-36.505	-0.9802	0.0085	-1.7911	0.0007
0.4006	0.2837	-40.214	-1.0942	0.0132	-1.7025	0.0009
0.4992	0.2596	-40.896	-1.1316	0.0210	-1.1539	0.0010
0.6015	0.2281	-37.992	-1.0655	0.0242	-0.7115	0.0010
0.7012	0.1849	-32.127	-0.9111	0.0234	-0.3943	0.0009
0.7973	0.1267	-24.218	-0.6970	0.0224	0.0620	0.0007
0.8943	0.0740	-13.584	-0.3926	0.0119	-0.0316	0.0004
1.0000	0.0000	0.0000	0.0000	0.0000	0.0000	0.0000
			T= 313.15 K			
0.0000	0.0000	0.0000	0.0000	0.0000	0.0000	0.0000
0.1021	0.1531	-19.056	-0.4879	-0.0012	-0.9357	0.0003
0.2032	0.2261	-33.184	-0.8699	0.0056	-1.0295	0.0006
0.3026	0.2525	-42.320	-1.1317	0.0151	-0.6937	0.0009
0.4006	0.2641	-46.404	-1.2565	0.0199	-0.5321	0.0011
0.4992	0.2414	-46.967	-1.2920	0.0273	-0.0219	0.0012
0.6015	0.2123	-43.430	-1.2096	0.0292	0.2626	0.0011
0.7012	0.1722	-36.621	-1.0311	0.0275	0.4086	0.0010
0.7973	0.1173	-27.506	-0.7851	0.0251	0.6228	0.0007
0.8943	0.0687	-15.400	-0.4413	0.0133	0.2747	0.0004
1.0000	0.0000	0.0000	0.0000	0.0000	0.0000	0.0000
			T= 323.15 K			
0.0000	0.0000	0.0000	0.0000	0.0000	0.0000	0.0000
0.1021	0.1316	-23.033	-0.5913	0.0048	-0.1505	0.0005
0.2032	0.1958	-39.524	-1.0350	0.0142	0.1741	0.0009
0.3026	0.2196	-49.909	-1.3301	0.0247	0.7138	0.0013
0.4006	0.2311	-54.326	-1.4641	0.0293	0.8938	0.0014
0.4992	0.2106	-54.653	-1.4944	0.0358	1.3308	0.0015
0.6015	0.1857	-50.305	-1.3916	0.0366	1.4596	0.0014
0.7012	0.1510	-42.257	-1.1810	0.0333	1.3786	0.0012
0.7973	0.1019	-31.634	-0.8957	0.0292	1.3276	0.0009
0.8943	0.0604	-17.680	-0.5027	0.0157	0.6714	0.0005
1.0000	0.0000	0.0000	0.0000	0.0000	0.0000	0.0000

Table A1.10: Excess molar volume (V_m^E), deviations in isentropic compressibility ($\Delta\kappa_s$), deviations in intermolecular free length (ΔL_f), deviations in acoustic impedance (ΔZ), deviations in speed of sound (Δu) and changes of refractive index (Δn_D) for the binary systems (furfural + DMSO or acetonitrile) at (293.15, 303.15, 313.15 and 323.15) K and for (furfural + sulfolane) at (303.15, 313.15 and 323.15) K and at pressure of 0.1 MPa.

x_1	V_m^E / (cm^3 mol^{-1})	$\Delta\kappa_s$/ (TPa^{-1})	ΔL_f / (10 $^{-12}$ m)	ΔZ/ (10^5 kg m^{-2} s^{-1})	Δu / (m s^{-1})	Δn_D
			{furfural (1) + DMSO (2)}			
			T= 293.15 K			
0.0000	0.0000	0.0000	0.0000	0.0000	0.0000	0.0000
0.1047	0.0534	2.1902	0.1112	-0.0436	-4.2951	0.0007
0.2024	0.0816	3.1636	0.1604	-0.0614	-6.3330	0.0012
0.3008	0.0992	3.7279	0.1889	-0.0713	-7.5463	0.0015
0.4017	0.1021	3.8966	0.1973	-0.0730	-8.0190	0.0017
0.5009	0.0984	3.6712	0.1859	-0.0675	-7.6751	0.0017
0.6011	0.0849	3.2457	0.1643	-0.0584	-6.9127	0.0016
0.7008	0.0672	2.5802	0.1306	-0.0453	-5.6119	0.0014
0.7989	0.0467	1.7908	0.0907	-0.0305	-3.9862	0.0010
0.8971	0.0264	1.0144	0.0514	-0.0173	-2.2561	0.0005
1.0000	0.0000	0.0000	0.0000	0.0000	0.0000	0.0000
			T= 303.15 K			
0.0000	0.0000	0.0000	0.0000	0.0000	0.0000	0.0000
0.1047	0.0491	2.0871	0.1050	-0.0374	-3.8708	0.0007
0.2024	0.0739	2.9184	0.1467	-0.0505	-5.5710	0.0012
0.3008	0.0894	3.4087	0.1712	-0.0578	-6.6055	0.0016
0.4017	0.0912	3.5298	0.1772	-0.0582	-6.9828	0.0017
0.5009	0.0874	3.3038	0.1658	-0.0531	-6.6679	0.0018
0.6011	0.0744	2.8953	0.1452	-0.0451	-5.9820	0.0017
0.7008	0.0581	2.2798	0.1143	-0.0342	-4.8389	0.0014
0.7989	0.0414	1.5380	0.0771	-0.0221	-3.3649	0.0010
0.8971	0.0226	0.8387	0.0421	-0.0118	-1.8562	0.0005
1.0000	0.0000	0.0000	0.0000	0.0000	0.0000	0.0000
			T= 313.15 K			
0.0000	0.0000	0.0000	0.0000	0.0000	0.0000	0.0000
0.1047	0.0449	1.9831	0.0989	-0.0318	-3.4886	0.0007
0.2024	0.0662	2.6893	0.1340	-0.0412	-4.9231	0.0013
0.3008	0.0794	3.0786	0.1533	-0.0457	-5.7606	0.0017
0.4017	0.0800	3.1620	0.1573	-0.0452	-6.0746	0.0019
0.5009	0.0755	2.9221	0.1453	-0.0402	-5.7708	0.0020
0.6011	0.0632	2.5239	0.1255	-0.0330	-5.1434	0.0019
0.7008	0.0484	1.9576	0.0973	-0.0241	-4.1400	0.0016
0.7989	0.0341	1.3015	0.0647	-0.0149	-2.8695	0.0012
0.8971	0.0184	0.6944	0.0345	-0.0076	-1.5643	0.0006
1.0000	0.0000	0.0000	0.0000	0.0000	0.0000	0.0000
			T= 323.15 K			
0.0000	0.0000	0.0000	0.0000	0.0000	0.0000	0.0000
0.1047	0.0403	1.8322	0.0905	-0.0261	-3.0832	0.0008
0.2024	0.0582	2.4134	0.1192	-0.0322	-4.2892	0.0013
0.3008	0.0688	2.6906	0.1328	-0.0343	-4.9468	0.0017
0.4017	0.0678	2.7247	0.1345	-0.0328	-5.1943	0.0020

0.5009	0.0632	2.4625	0.1215	-0.0277	-4.8887	0.0021
0.6011	0.0514	2.0811	0.1027	-0.0215	-4.3268	0.0019
0.7008	0.0381	1.5677	0.0774	-0.0144	-3.4500	0.0017
0.7989	0.0258	1.0333	0.0510	-0.0082	-2.4102	0.0012
0.8971	0.0140	0.5271	0.0260	-0.0037	-1.2855	0.0007
1.0000	0.0000	0.0000	0.0000	0.0000	0.0000	0.0000

{furfural (1) + acetonitrile (2)}

T= 293.15 K

0.0000	0.0000	0.000	0.0000	0.0000	0.0000	0.0000
0.1030	-0.1344	-35.350	-1.1663	0.2235	0.2013	0.0101
0.2016	-0.2261	-56.134	-1.8866	0.3805	1.3721	0.0169
0.3079	-0.2837	-67.937	-2.3246	0.4924	3.1283	0.0213
0.4006	-0.2942	-70.893	-2.4572	0.5391	4.3001	0.0228
0.4978	-0.2947	-68.787	-2.4162	0.5505	5.4240	0.0225
0.5975	-0.2733	-61.793	-2.1969	0.5186	5.8992	0.0207
0.6949	-0.2347	-51.205	-1.8405	0.4489	5.7283	0.0175
0.7961	-0.1757	-36.801	-1.3356	0.3358	4.5749	0.0127
0.8969	-0.1072	-19.875	-0.7291	0.1902	2.8068	0.0070
1.0000	0.0000	0.000	0.0000	0.0000	0.0000	0.0000

T= 303.15 K

0.0000	0.0000	0.000	0.0000	0.0000	0.0000	0.0000
0.1030	-0.1475	-39.740	-1.2856	0.2172	0.7350	0.0102
0.2016	-0.2473	-62.531	-2.0587	0.3664	1.7763	0.0172
0.3079	-0.3097	-75.688	-2.5387	0.4756	3.7038	0.0216
0.4006	-0.3213	-78.988	-2.6851	0.5220	4.9779	0.0231
0.4978	-0.3210	-76.554	-2.6378	0.5333	6.0571	0.0230
0.5975	-0.2972	-68.740	-2.3982	0.5032	6.4986	0.0209
0.6949	-0.2549	-57.242	-2.0233	0.4408	6.6726	0.0177
0.7961	-0.1902	-40.902	-1.4575	0.3266	4.9597	0.0128
0.8969	-0.1151	-22.078	-0.7955	0.1852	3.0236	0.0071
1.0000	0.0000	0.000	0.0000	0.0000	0.0000	0.0000

T= 313.15 K

0.0000	0.0000	0.000	0.0000	0.0000	0.0000	0.0000
0.1030	-0.1616	-44.719	-1.4138	0.2089	1.0909	0.0108
0.2016	-0.2707	-70.803	-2.2829	0.3569	2.7890	0.0177
0.3079	-0.3386	-85.403	-2.8059	0.4629	4.8068	0.0220
0.4006	-0.3513	-88.959	-2.9629	0.5080	6.0853	0.0235
0.4978	-0.3502	-86.086	-2.9069	0.5193	7.1072	0.0232
0.5975	-0.3237	-77.185	-2.6395	0.4901	7.4104	0.0211
0.6949	-0.2767	-63.841	-2.2081	0.4248	6.9668	0.0178
0.7961	-0.2065	-45.818	-1.6007	0.3182	5.4681	0.0128
0.8969	-0.1241	-24.696	-0.8723	0.1804	3.2782	0.0072
1.0000	0.0000	0.000	0.0000	0.0000	0.0000	0.0000

T= 323.15 K

0.0000	0.0000	0.000	0.0000	0.0000	0.0000	0.0000
0.1030	-0.1766	-50.088	-1.5447	0.1991	1.2413	0.0109
0.2016	-0.2960	-79.576	-2.5064	0.3432	3.2785	0.0181
0.3079	-0.3698	-95.967	-3.0824	0.4467	5.4830	0.0226
0.4006	-0.3840	-99.909	-3.2547	0.4912	6.8349	0.0244
0.4978	-0.3822	-96.591	-3.1914	0.5028	7.8413	0.0242
0.5975	-0.3527	-86.542	-2.8967	0.4752	8.0889	0.0221
0.6949	-0.3018	-71.516	-2.4217	0.4124	7.5193	0.0183

0.7961	-0.2243	-51.311	-1.7556	0.3094	5.8985	0.0134
0.8969	-0.1342	-27.649	-0.9568	0.1758	3.5283	0.0072
1.0000	0.0000	0.000	0.0000	0.0000	0.0000	0.0000

{furfural (1) + sulfolane (2)}

T= 303.15 K

0.0000	0.0000	0.0000	0.0000	0.0000	0.0000	0.0000
0.1012	-0.0481	-2.2059	-0.0808	0.0048	-0.6840	-0.0001
0.1990	-0.0994	-4.0879	-0.1521	0.0142	-0.9886	-0.0002
0.3018	-0.1311	-5.6398	-0.2111	0.0220	-1.0524	-0.0003
0.4013	-0.1517	-6.7515	-0.2547	0.0299	-0.8417	-0.0003
0.5005	-0.1573	-7.5572	-0.2899	0.0402	-0.1175	-0.0003
0.5991	-0.1523	-7.3280	-0.2779	0.0360	-0.3442	-0.0003
0.7006	-0.1395	-6.7485	-0.2572	0.0362	-0.0102	-0.0003
0.8014	-0.1155	-5.4514	-0.2092	0.0324	0.2611	-0.0002
0.9002	-0.0816	-3.4042	-0.1329	0.0248	0.4293	-0.0001
1.0000	0.0000	0.0000	0.0000	0.0000	0.0000	0.0000

T= 313.15 K

0.0000	0.0000	0.0000	0.0000	0.0000	0.0000	0.0000
0.1012	-0.0500	-2.4420	-0.0869	0.0017	-0.8492	-0.0001
0.1990	-0.1045	-4.6552	-0.1710	0.0124	-0.9956	-0.0002
0.3018	-0.1388	-6.5016	-0.2416	0.0217	-0.8966	-0.0003
0.4013	-0.1612	-7.8250	-0.2936	0.0308	-0.5696	-0.0003
0.5005	-0.1677	-8.5462	-0.3223	0.0366	-0.2001	-0.0003
0.5991	-0.1629	-8.5499	-0.3227	0.0381	0.0355	-0.0003
0.7006	-0.1499	-7.8900	-0.2993	0.0384	0.3555	-0.0003
0.8014	-0.1240	-6.3843	-0.2437	0.0344	0.5697	-0.0002
0.9002	-0.0876	-3.9788	-0.1542	0.0260	0.6115	-0.0001
1.0000	0.0000	0.0000	0.0000	0.0000	0.0000	0.0000

T= 323.15 K

0.0000	0.0000	0.0000	0.0000	0.0000	0.0000	0.0000
0.1012	-0.0520	-3.0006	-0.1102	0.0063	-0.3892	-0.0001
0.1990	-0.1092	-5.5737	-0.2077	0.0177	-0.4199	-0.0002
0.3018	-0.1459	-7.7237	-0.2894	0.0274	-0.2339	-0.0003
0.4013	-0.1703	-9.2635	-0.3492	0.0368	0.1458	-0.0003
0.5005	-0.1787	-10.0891	-0.3813	0.0424	0.4970	-0.0003
0.5991	-0.1740	-10.1170	-0.3825	0.0439	0.7418	-0.0003
0.7006	-0.1609	-9.3324	-0.3539	0.0435	0.9728	-0.0003
0.8014	-0.1334	-7.5545	-0.2879	0.0385	1.0554	-0.0002
0.9002	-0.0936	-4.6903	-0.1810	0.0281	0.8875	-0.0001
1.0000	0.0000	0.0000	0.0000	0.0000	0.0000	0.0000

Table A1.11: Excess molar volume (V_m^E), deviations in isentropic compressibility ($\Delta\kappa_s$), deviations in intermolecular free length (ΔL_f), deviations in acoustic impedance (ΔZ), deviations in speed of sound (Δu) and changes of refractive index (Δn_D) for the binary systems (1-hexene + 2-methoxyethanol, or 2-ethoxyethanol, or 2-butoxyethanol) at (293.15, 298.15 and 303.15) K and at pressure p = 0.1 MPa.

x_1	V_m^E / (cm^3 mol^{-1})	$\Delta\kappa_s$/ (TPa^{-1})	ΔL_f / (10 $^{-12}$ m)	ΔZ/ (10^5 kg m^{-2} s^{-1})	Δu / (m s^{-1})	Δn_D
			{1-hexene (1) + 2-methoxyethanol (2)}			
			T= 293.15 K			
0.0000	0.0000	0.0000	0.0000	0.0000	0.0000	0.0000
0.1008	-0.0183	13.525	1.0528	-0.5745	-33.855	-0.0005
0.2037	0.0131	29.984	2.0038	-0.9672	-58.604	-0.0010
0.3016	0.0640	44.784	2.6931	-1.1792	-72.885	-0.0014
0.4023	0.1165	56.191	3.1162	-1.2570	-78.824	-0.0018
0.5020	0.1582	61.800	3.2258	-1.2192	-77.128	-0.0020
0.5995	0.1776	61.806	3.0688	-1.0969	-69.927	-0.0019
0.6960	0.2056	56.631	2.6861	-0.9119	-58.441	-0.0017
0.7996	0.2209	45.035	2.0356	-0.6541	-42.126	-0.0014
0.8980	0.1900	28.310	1.2075	-0.3619	-23.605	-0.0009
1.0000	0.0000	0.0000	0.0000	0.0000	0.0000	0.0000
			T= 298.15 K			
0.0000	0.0000	0.0000	0.0000	0.0000	0.0000	0.0000
0.1008	-0.0221	12.775	1.0596	-0.5698	-33.571	-0.0005
0.2037	0.0095	29.661	2.0500	-0.9645	-58.685	-0.0011
0.3016	0.0623	44.831	2.7623	-1.1759	-72.987	-0.0015
0.4023	0.1187	56.721	3.2033	-1.2535	-78.932	-0.0019
0.5020	0.1642	62.258	3.3058	-1.2137	-76.958	-0.0021
0.5995	0.1877	63.164	3.1684	-1.0944	-70.070	-0.0021
0.6960	0.2201	58.198	2.7795	-0.9101	-58.581	-0.0019
0.7996	0.2381	46.618	2.1135	-0.6532	-42.268	-0.0016
0.8980	0.2069	29.469	1.2564	-0.3615	-23.665	-0.0011
1.0000	0.0000	0.0000	0.0000	0.0000	0.0000	0.0000
			T= 303.15 K			
0.0000	0.0000	0.0000	0.0000	0.0000	0.0000	0.0000
0.1008	-0.0255	12.594	1.0929	-0.5711	-33.926	-0.0005
0.2037	0.0056	29.190	2.0964	-0.9617	-58.764	-0.0010
0.3016	0.0611	44.774	2.8344	-1.1728	-73.116	-0.0014
0.4023	0.1209	57.187	3.2946	-1.2502	-79.076	-0.0017
0.5020	0.1715	63.784	3.4261	-1.2131	-77.423	-0.0020
0.5995	0.1989	64.561	3.2739	-1.0919	-70.246	-0.0021
0.6960	0.2353	59.848	2.8789	-0.9083	-58.755	-0.0021
0.7996	0.2567	48.267	2.1954	-0.6523	-42.412	-0.0018
0.8980	0.2251	30.746	1.3094	-0.3612	-23.747	-0.0012
1.0000	0.0000	0.0000	0.0000	0.0000	0.0000	0.0000
			{1-hexene (1) + 2-ethoxyethanol (2)}			
			T= 293.15 K			
0.0000	0.0000	0.0000	0.0000	0.0000	0.0000	0.0000
0.1018	-0.0346	0.8355	0.4303	-0.3049	-18.918	-0.0002
0.2034	-0.0334	4.5180	0.8434	-0.5251	-33.341	-0.0004

0.3022	-0.0284	9.1143	1.1706	-0.6585	-42.643	-0.0007
0.4038	0.0016	14.377	1.4224	-0.7253	-47.798	-0.0009
0.5018	0.0566	19.024	1.5622	-0.7291	-48.706	-0.0011
0.5989	0.0884	21.590	1.5593	-0.6755	-45.705	-0.0012
0.6981	0.1345	22.349	1.4320	-0.5742	-39.289	-0.0012
0.8004	0.1609	19.862	1.1417	-0.4232	-29.261	-0.0011
0.8970	0.1532	13.957	0.7159	-0.2422	-16.940	-0.0007
1.0000	0.0000	0.0000	0.0000	0.0000	0.0000	0.0000
			T= 298.15 K			
0.0000	0.0000	0.0000	0.0000	0.0000	0.0000	0.0000
0.1018	-0.0374	-0.0770	0.4277	-0.3042	-18.868	-0.0002
0.2034	-0.0366	3.0942	0.8445	-0.5241	-33.273	-0.0004
0.3022	-0.0306	7.5046	1.1785	-0.6575	-42.580	-0.0006
0.4038	0.0018	12.816	1.4379	-0.7242	-47.726	-0.0009
0.5018	0.0603	17.751	1.5863	-0.7282	-48.653	-0.0011
0.5989	0.0957	20.635	1.5879	-0.6747	-45.644	-0.0013
0.6981	0.1460	21.872	1.4650	-0.5739	-39.261	-0.0014
0.8004	0.1763	19.801	1.1729	-0.4232	-29.242	-0.0012
0.8970	0.1675	14.108	0.7374	-0.2422	-16.906	-0.0009
1.0000	0.0000	0.0000	0.0000	0.0000	0.0000	0.0000
			T= 303.15 K			
0.0000	0.0000	0.0000	0.0000	0.0000	0.0000	0.0000
0.1018	-0.0402	-1.0852	0.4251	-0.3037	-18.847	-0.0003
0.2034	-0.0399	1.4893	0.8449	-0.5232	-33.231	-0.0006
0.3022	-0.0327	5.6672	1.1855	-0.6566	-42.540	-0.0009
0.4038	0.0020	11.029	1.4533	-0.7233	-47.686	-0.0012
0.5018	0.0642	16.231	1.6097	-0.7273	-48.609	-0.0014
0.5989	0.1040	19.573	1.6194	-0.6743	-45.642	-0.0015
0.6981	0.1585	21.267	1.4991	-0.5736	-39.248	-0.0015
0.8004	0.1920	19.648	1.2047	-0.4232	-29.226	-0.0014
0.8970	0.1825	14.225	0.7596	-0.2422	-16.873	-0.0010
1.0000	0.0000	0.0000	0.0000	0.0000	0.0000	0.0000

{1-hexene (1) + 2-butoxyethanol (2)}

T= 293.15 K

0.0000	0.0000	0.0000	0.0000	0.0000	0.0000	0.0000
0.1038	-0.1465	-18.487	-0.3432	-0.0698	-5.2834	0.0008
0.2055	-0.2295	-31.967	-0.5622	-0.1323	-10.237	0.0013
0.3001	-0.2798	-40.451	-0.6747	-0.1794	-14.287	0.0016
0.4053	-0.2983	-45.356	-0.7088	-0.2161	-17.715	0.0017
0.5053	-0.2804	-45.508	-0.6583	-0.2344	-19.737	0.0016
0.6023	-0.2378	-41.791	-0.5509	-0.2336	-20.181	0.0014
0.7017	-0.1723	-34.568	-0.4042	-0.2115	-18.713	0.0011
0.7980	-0.0854	-24.626	-0.2406	-0.1695	-15.254	0.0007
0.8977	-0.0020	-12.611	-0.0906	-0.1008	-9.1336	0.0003
1.0000	0.0000	0.0000	0.0000	0.0000	0.0000	0.0000
			T= 298.15 K			
0.0000	0.0000	0.0000	0.0000	0.0000	0.0000	0.0000
0.1038	-0.1523	-20.500	-0.3823	-0.0702	-5.1348	0.0007
0.2055	-0.2391	-35.542	-0.6295	-0.1331	-10.001	0.0013
0.3001	-0.2918	-45.142	-0.7611	-0.1804	-13.972	0.0017
0.4053	-0.3108	-50.864	-0.8083	-0.2171	-17.324	0.0017
0.5053	-0.2912	-51.257	-0.7589	-0.2357	-19.338	0.0016

0.6023	-0.2461	-47.378	-0.6468	-0.2346	-19.760	0.0014
0.7017	-0.1760	-39.496	-0.4869	-0.2124	-18.308	0.0011
0.7980	-0.0842	-28.479	-0.3046	-0.1699	-14.881	0.0007
0.8977	0.0025	-14.911	-0.1295	-0.1007	-8.8444	0.0004
1.0000	0.0000	0.0000	0.0000	0.0000	0.0000	0.0000
			T= 303.15 K			
0.0000	0.0000	0.0000	0.0000	0.0000	0.0000	0.0000
0.1038	-0.1589	-22.742	-0.4255	-0.0704	-4.9766	0.0008
0.2055	-0.2494	-39.521	-0.7035	-0.1339	-9.7557	0.0014
0.3001	-0.3044	-50.368	-0.8563	-0.1813	-13.648	0.0016
0.4053	-0.3241	-56.981	-0.9169	-0.2182	-16.943	0.0017
0.5053	-0.3032	-57.694	-0.8704	-0.2368	-18.930	0.0016
0.6023	-0.2550	-53.649	-0.7534	-0.2356	-19.330	0.0013
0.7017	-0.1803	-45.029	-0.5787	-0.2132	-17.902	0.0010
0.7980	-0.0838	-32.758	-0.3741	-0.1704	-14.537	0.0007
0.8977	0.0077	-17.459	-0.1714	-0.1007	-8.5750	0.0003
1.0000	0.0000	0.0000	0.0000	0.0000	0.0000	0.0000

Table A1.12: Coefficients A_i, and standard deviations, σ, obtained for the binary systems (22MEE + methanol or ethanol or propan-1-ol or propan-2-ol or butan-1-ol or butan-2-ol) at (293.15, 303.15, 313.15 and 323.15) K and at pressure p = 0.1 MPa for the Redlich–Kister equation.

	T (K)	A_1	A_2	A_3	A_4	A_5	σ
				{22MEE (1) + methanol (2)}			
V_m^E / (cm^3 mol^{-1})	293.15	-2.027	1.009	-0.154	0.184	-1.165	0.006
	303.15	-2.123	1.064	-0.159	0.178	-1.265	0.006
	313.15	-2.220	1.121	-0.161	0.183	-1.364	0.006
	323.15	-2.322	1.182	-0.166	0.195	-1.475	0.007
$\Delta\kappa_s$/ (TPa^{-1})	293.15	-729.9	473.3	-291.4	280.6	-202.0	0.7
	303.15	-801.2	521.4	-321.1	311.6	-241.4	0.8
	313.15	-877.9	574.3	-355.0	348.5	-271.8	0.9
	323.15	-963.6	633.2	-392.8	393.0	-309.3	1.0
ΔL_f / (10^{-12} m)	293.15	-25.55	15.30	-8.607	7.226	-4.904	0.018
	303.15	-27.64	16.59	-9.320	7.787	-5.986	0.020
	313.15	-29.80	17.98	-10.13	8.544	-6.619	0.022
	323.15	-32.16	19.48	-11.00	9.468	-7.411	0.025
ΔZ/ (10^5 $kg\ m^{-2}\ s^{-1}$)	293.15	5.636	-2.540	0.962	-0.474	0.327	0.002
	303.15	5.559	-2.498	0.927	-0.394	0.463	0.002
	313.15	5.457	-2.453	0.901	-0.378	0.464	0.002
	323.15	5.355	-2.404	0.875	-0.375	0.474	0.002
Δu / ($m\ s^{-1}$)	293.15	329.5	-157.3	62.34	-36.00	19.54	0.2
	303.15	332.0	-158.5	65.57	-30.77	27.28	0.2
	313.15	332.1	-159.4	66.01	-31.16	27.81	0.2
	323.15	332.1	-159.9	66.59	-32.87	29.05	0.2
Δn_D	293.15	0.111	-0.058	0.029	-0.014	-	0.000
	303.15	0.110	-0.056	0.034	-0.027	-	0.000
	313.15	0.112	-0.060	0.042	-0.029	-	0.000
	323.15	0.113	-0.059	0.047	-0.041	-	0.000
				{22MEE (1) + ethanol (2)}			
V_m^E / (cm^3 mol^{-1})	293.15	-1.036	0.384	-0.276	0.653	-1.134	0.010
	303.15	-1.081	0.406	-0.297	0.651	-1.158	0.010
	313.15	-1.126	0.427	-0.317	0.664	-1.173	0.011
	323.15	-1.175	0.452	-0.336	0.672	-1.195	0.011
$\Delta\kappa_s$/ (TPa^{-1})	293.15	-478.2	239.3	-116.1	106.0	-99.73	0.4
	303.15	-528.1	266.8	-133.8	118.4	-116.9	0.4
	313.15	-580.2	295.8	-150.7	131.9	-127.6	0.5
	323.15	-638.7	328.4	-169.4	147.6	-141.0	0.5
ΔL_f / (10^{-12} m)	293.15	-16.21	7.214	-3.129	2.799	-3.079	0.014
	303.15	-17.64	7.919	-3.587	3.003	-3.596	0.015
	313.15	-19.07	8.635	-3.990	3.266	-3.822	0.017
	323.15	-20.64	9.415	-4.409	3.570	-4.121	0.019

ΔZ/ *(10^5 kg m^{-2} s^{-1})*	293.15	3.166	-0.891	0.231	-0.234	0.541	0.004
	303.15	3.131	-0.879	0.252	-0.182	0.596	0.004
	313.15	3.067	-0.862	0.257	-0.169	0.569	0.004
	323.15	3.003	-0.843	0.256	-0.158	0.553	0.004
Δu / *(m s^{-1})*	293.15	172.1	-54.73	14.65	-17.36	42.69	0.3
	303.15	176.5	-56.62	18.13	-13.93	49.50	0.3
	313.15	177.8	-57.77	19.80	-13.50	47.81	0.3
	323.15	178.9	-58.66	20.83	-13.31	47.26	0.3
Δn_D	293.15	0.051	-0.019	0.006	-0.003	-	0.000
	303.15	0.051	-0.018	0.005	-0.005	-	0.000
	313.15	0.052	-0.021	0.002	0.001	-	0.000
	323.15	0.054	-0.025	0.007	0.002	-	0.000
{22MEE (1) + propan-1-ol (2)}							
V_m^E / *(cm^3 mol^{-1})*	293.15	-0.090	0.035	0.031	-0.010	-0.053	0.001
	303.15	-0.085	0.022	0.037	-0.007	-0.069	0.000
	313.15	-0.081	0.016	0.040	-0.006	-0.074	0.000
	323.15	-0.085	0.011	0.039	0.000	-0.080	0.000
$\Delta\kappa_s$/ (TPa^{-1})	293.15	-247.4	87.27	-29.61	12.12	-	0.1
	303.15	-272.6	96.01	-36.79	12.73	-	0.0
	313.15	-298.8	106.0	-40.35	13.85	-	0.0
	323.15	-328.4	117.4	-44.90	15.45	-	0.0
ΔL_f / (10^{-12} m)	293.15	-8.177	2.488	-0.934	0.312	0.462	0.001
	303.15	-8.910	2.685	-0.960	0.277	0.093	0.001
	313.15	-9.620	2.914	-1.024	0.291	0.097	0.001
	323.15	-10.40	3.169	-1.102	0.317	0.083	0.001
ΔZ/ *(10^5 kg m^{-2} s^{-1})*	293.15	1.406	-0.227	0.077	-0.037	-0.138	0.000
	303.15	1.393	-0.210	0.061	-0.004	-0.037	0.000
	313.15	1.359	-0.201	0.055	-0.003	-0.035	0.000
	323.15	1.326	-0.192	0.048	-0.002	-0.029	0.000
Δu / *(m s^{-1})*	293.15	59.90	-10.46	6.82	-3.24	-15.22	0.0
	303.15	63.43	-10.23	5.566	-0.446	-4.894	0.0
	313.15	64.63	-10.54	5.174	-0.282	-4.819	0.0
	323.15	65.82	-10.86	4.833	-0.191	-4.243	0.0
Δn_D	293.15	0.020	-0.004	0.000	0.000	-	0.000
	303.15	0.020	-0.005	-0.001	0.000	-	0.000
	313.15	0.020	-0.005	-0.001	0.000	-	0.000
	323.15	0.021	-0.005	0.000	0.000	-	0.000
{22MEE (1) + propan-2-ol (2)}							
V_m^E / *(cm^3 mol^{-1})*	293.15	-0.040	-0.073	0.066	-0.368	0.399	0.003
	303.15	-0.073	-0.074	0.073	-0.358	0.364	0.002
	313.15	-0.128	-0.060	0.069	-0.344	0.343	0.003
	323.15	-0.219	-0.028	0.054	-0.316	0.315	0.003
	293.15	-360.7	134.4	-40.19	7.28	-	0.2
	303.15	-402.6	151.0	-53.09	12.70	-	0.1

$\Delta\kappa_s$/ (TPa^{-1})	313.15	-448.8	170.7	-60.75	15.06	-	0.1
	323.15	-504.3	195.4	-71.94	19.43	-	0.1
ΔL_f / (10^{-12} m)	293.15	-11.15	3.488	-1.170	0.002	0.869	0.005
	303.15	-12.29	3.833	-1.220	0.107	0.303	0.005
	313.15	-13.47	4.253	-1.338	0.131	0.295	0.005
	323.15	-14.87	4.777	-1.513	0.199	0.246	0.005
ΔZ/ (10^5 kg m^{-2} s^{-1})	293.15	1.394	-0.159	0.030	0.048	-0.224	0.001
	303.15	1.391	-0.143	0.023	0.058	-0.111	0.001
	313.15	1.367	-0.136	0.015	0.056	-0.104	0.001
	323.15	1.351	-0.132	0.012	0.052	-0.091	0.001
Δu / (m s^{-1})	293.15	79.84	-13.16	4.729	1.553	-19.61	0.1
	303.15	84.66	-12.98	4.385	1.929	-8.017	0.1
	313.15	87.09	-13.56	3.913	2.102	-7.751	0.1
	323.15	90.32	-14.51	3.819	1.995	-6.902	0.1
Δn_D	293.15	0.023	-0.004	0.000	-0.001	-	0.000
	303.15	0.023	-0.005	0.000	0.002	-	0.000
	313.15	0.024	-0.005	0.000	0.001	-	0.000
	323.15	0.027	-0.009	0.000	0.003	-	0.000
{22MEE (1) + butan-1-ol (2)}							
V_m^E / (cm^3 mol^{-1})	293.15	0.526	-0.109	0.035	0.069	-	0.002
	303.15	0.544	-0.121	0.027	0.077	-	0.002
	313.15	0.560	-0.129	0.021	0.090	-	0.002
	323.15	0.569	-0.131	0.014	0.097	-	0.002
$\Delta\kappa_s$/ (TPa^{-1})	293.15	-121.2	24.67	-1.452	-0.261	-	0.2
	303.15	-135.0	27.39	-6.215	-0.535	-	0.2
	313.15	-148.5	30.83	-6.906	-0.593	-	0.2
	323.15	-163.9	34.62	-8.269	0.464	-	0.2
ΔL_f / (10^{-12} m)	293.15	-3.513	0.594	0.042	-0.009	-	0.008
	303.15	-3.898	0.642	-0.142	-0.051	-	0.008
	313.15	-4.245	0.717	-0.152	-0.055	-	0.009
	323.15	-4.630	0.795	-0.183	-0.020	-	0.010
ΔZ/ (10^5 kg m^{-2} s^{-1})	293.15	0.197	-0.028	-0.035	-0.014	-	0.002
	303.15	0.214	-0.019	0.011	0.013	-	0.002
	313.15	0.212	-0.018	0.010	0.012	-	0.002
	323.15	0.211	-0.017	0.011	0.005	-	0.002
Δu / (m s^{-1})	293.15	-9.541	1.602	-4.387	0.274	-	0.2
	303.15	-5.635	1.861	0.413	2.508	-	0.2
	313.15	-3.718	1.421	0.271	2.535	-	0.2
	323.15	-1.809	1.147	0.502	1.805	-	0.2
Δn_D	293.15	0.005	0.000	0.000	0.000	-	0.000
	303.15	0.005	0.000	0.000	0.000	-	0.000
	313.15	0.005	0.000	0.000	0.000	-	0.000
	323.15	0.006	-0.001	0.000	0.001	-	0.000

{22MEE (1) + butan-2-ol (2)}

V_m^E / *(cm³ mol⁻¹)*	293.15	1.085	-0.520	0.186	-0.270	0.388	0.004
	303.15	1.052	-0.513	0.176	-0.235	0.335	0.004
	313.15	0.979	-0.475	0.146	-0.198	0.303	0.004
	323.15	0.856	-0.414	0.110	-0.151	0.262	0.004
$\Delta\kappa_s$/ (TPa^{-1})	293.15	-142.4	19.55	-0.250	-5.902	17.25	0.1
	303.15	-163.2	24.45	-2.122	-6.743	11.72	0.1
	313.15	-187.4	32.04	-4.224	-6.094	11.60	0.1
	323.15	-218.1	42.96	-8.923	-4.247	11.47	0.1
ΔL_f / (10^{-12} m)	293.15	-3.938	0.258	0.065	-0.170	0.674	0.005
	303.15	-4.512	0.356	0.013	-0.233	0.436	0.005
	313.15	-5.151	0.538	-0.032	-0.214	0.429	0.005
	323.15	-5.959	0.806	-0.157	-0.163	0.427	0.006
ΔZ/ *(10⁵ kg m⁻² s⁻¹)*	293.15	0.046	0.098	-0.017	0.010	-0.176	0.002
	303.15	0.080	0.097	-0.007	0.037	-0.101	0.001
	313.15	0.105	0.082	-0.005	0.030	-0.091	0.001
	323.15	0.139	0.062	0.008	0.023	-0.084	0.001
Δu / *(m s⁻¹)*	293.15	-10.42	9.526	-1.755	-0.263	-14.54	0.1
	303.15	-4.858	8.950	-0.733	2.533	-7.511	0.1
	313.15	-0.370	7.149	-0.562	2.251	-6.972	0.1
	323.15	5.046	4.714	0.812	1.760	-6.786	0.1
Δn_D	293.15	0.004	0.001	-0.001	0.000	-	0.000
	303.15	0.004	0.001	-0.001	0.000	-	0.000
	313.15	0.005	0.001	-0.001	-0.001	-	0.000
	323.15	0.006	0.000	-0.001	0.001	-	0.000

Table A1.13: Coefficients A_i, and standard deviations, σ, obtained for the binary systems (furfural + DMSO, or acetonitrile) at (293.15, 303.15, 313.15 and 323.15) K and for (furfural + sulfolane) at (303.15, 313.15 and 323.15) K and at pressure of 0.1 MPa for the Redlich–Kister equation.

	T (K)	A_1	A_2	A_3	A_4	A_5	σ
			{Furfural (1) + DMSO (2)}				
V_m^E / (cm^3 mol^{-1})	293.15	0.389	-0.186	0.043	0.011	-	0.001
	303.15	0.345	-0.179	0.049	0.012	-	0.001
	313.15	0.298	-0.178	0.051	0.009	-	0.001
	323.15	0.248	-0.176	0.051	0.006	-	0.001
$\Delta\kappa_s$/ (TPa^{-1})	293.15	14.83	-6.448	-0.274	-2.080	6.170	0.031
	303.15	13.36	-6.136	-0.472	-3.286	6.381	0.036
	313.15	11.82	-6.026	-0.521	-3.848	7.032	0.035
	323.15	9.968	-6.007	-0.215	-3.993	7.009	0.035
ΔL_f / (10^{-12} m)	293.15	0.751	-0.327	-0.012	-0.107	0.313	0.002
	303.15	0.670	-0.309	-0.022	-0.167	0.321	0.002
	313.15	0.588	-0.301	-0.024	-0.193	0.350	0.002
	323.15	0.492	-0.297	-0.009	-0.198	0.345	0.002
ΔZ/ (10^5 $kg\ m^{-2}\ s^{-1}$)	293.15	-0.269	0.147	-0.068	0.043	-	0.001
	303.15	-0.211	0.129	-0.061	0.062	-	0.001
	313.15	-0.159	0.117	-0.061	0.066	-	0.001
	323.15	-0.109	0.107	-0.061	0.063	-	0.001
Δu / ($m\ s^{-1}$)	293.15	-30.99	10.79	0.128	4.134	-10.38	0.055
	303.15	-26.94	9.530	0.560	5.850	-10.05	0.060
	313.15	-23.30	8.645	0.582	6.264	-10.23	0.054
	323.15	-19.74	7.938	0.047	5.966	-9.276	0.050
Δn_D	293.15	0.007	-0.001	-0.001	-0.000	-	0.000
	303.15	0.007	-0.001	-0.001	-0.000	-	0.000
	313.15	0.008	-0.001	-0.001	0.000	-	0.000
	323.15	0.008	-0.000	-0.001	-0.001	-	0.000
			{Furfural (1) + acetonitrile (2)}				
V_m^E / (cm^3 mol^{-1})	293.15	-1.178	0.301	-0.205	-0.147	-	0.003
	303.15	-1.284	0.336	-0.218	-0.145	-	0.003
	313.15	-1.401	0.378	-0.233	-0.157	-	0.004
	323.15	-1.529	0.417	-0.247	-0.163	-	0.004
$\Delta\kappa_s$/ (TPa^{-1})	293.15	-274.6	97.87	-37.58	12.67	-	0.076
	303.15	-305.7	107.7	-43.57	20.12	-	0.172
	313.15	-343.7	126.2	-49.60	16.97	-	0.081
	323.15	-385.7	143.7	-54.98	15.74	-	0.086
ΔL_f / (10^{-12} m)	293.15	-9.649	2.832	-0.940	0.263	-	0.003
	303.15	-10.54	3.011	-1.076	0.530	-	0.007
	313.15	-11.61	3.502	-1.180	0.331	-	0.003
	323.15	-12.75	3.894	-1.246	0.226	-	0.004

ΔZ/ *(10^5 kg m^{-2} s^{-1})*	293.15	2.201	-0.250	0.055	0.022	-	0.001
	303.15	2.135	-0.201	0.057	-0.038	-	0.002
	313.15	2.077	-0.219	0.043	0.027	-	0.001
	323.15	2.012	-0.201	0.027	0.052	-	0.001
Δu / *(m s^{-1})*	293.15	21.77	15.76	-8.817	2.747	-	0.070
	303.15	24.51	17.86	-7.567	-3.572	-	0.195
	313.15	28.53	13.06	-7.841	2.519	-	0.058
	323.15	31.54	11.94	-8.718	5.177	-	0.066
Δn_D	293.15	0.090	-0.023	0.004	0.003	-	0.000
	303.15	0.092	-0.024	0.004	0.004	-	0.000
	313.15	0.093	-0.026	0.006	0.002	-	0.000
	323.15	0.096	-0.025	0.003	0.001	-	0.000
{Furfural (1) + Sulfolane (2)}							
V_m^E / *(cm^3 mol^{-1})*	303.15	-0.626	0.021	-0.134	-0.369	-	0.002
	313.15	-0.668	0.011	-0.137	-0.396	-	0.002
	323.15	-0.711	-0.011	-0.140	-0.406	-	0.003
$\Delta\kappa_s$/ (TPa^{-1})	303.15	-29.72	-6.009	2.933	-3.696	-8.312	0.088
	313.15	-34.11	-7.459	-0.196	-5.098	-3.315	0.027
	323.15	-40.33	-8.881	-0.906	-4.683	-4.180	0.022
ΔL_f / (10^{-12} m)	303.15	-1.132	-0.242	0.180	-0.188	-0.433	0.005
	313.15	-1.285	-0.299	0.016	-0.263	-0.153	0.001
	323.15	-1.523	-0.347	-0.011	-0.231	-0.205	0.001
ΔZ/ *(10^5 kg m^{-2} s^{-1})*	303.15	0.143	0.061	0.012	0.114	-	0.003
	313.15	0.143	0.071	0.010	0.144	-	0.001
	323.15	0.167	0.072	0.029	0.118	-	0.001
Δu / *(m s^{-1})*	303.15	-1.923	5.425	-0.771	3.411	-	0.201
	313.15	-1.040	6.320	-0.768	5.684	-	0.041
	323.15	1.787	6.420	0.879	3.751	-	0.045
Δn_D	303.15	-0.001	0.000	0.000	0.000	-	0.000
	313.15	-0.001	0.000	0.000	0.000	-	0.000
	323.15	-0.001	0.000	0.000	0.000	-	0.000

Table A1.14: Coefficients A_i, and standard deviations, σ, obtained for the binary systems (1-hexene + 2-methoxyethanol, or 2-ethoxyethanol, or 2-butoxyethanol) at (293.15, 298.15 and 303.15) K and at pressure p = 0.1 MPa for the Redlich–Kister equation.

	T (K)	A_1	A_2	A_3	A_4	A_5	σ
			{1-hexene (1) + 2-methoxyethanol (2)}				
V_m^E / (cm^3 mol^{-1})	293.15	0.618	0.638	0.012	1.254	0.784	0.003
	298.15	0.642	0.717	0.038	1.348	0.859	0.003
	303.15	0.670	0.802	0.049	1.445	0.971	0.003
$\Delta\kappa_s$/ (TPa^{-1})	293.15	247.4	58.65	-54.03	64.63	39.21	0.137
	298.15	250.2	66.43	-44.09	72.29	21.41	0.279
	303.15	255.2	76.85	-56.43	72.41	43.75	0.138
ΔL_f / (10^{-12} m)	293.15	12.92	-0.507	-1.351	2.321	0.812	0.004
	298.15	13.27	-0.412	-1.003	2.593	0.129	0.009
	303.15	13.72	-0.235	-1.417	2.557	0.860	0.004
ΔZ/ (10^5 $kg\ m^{-2}\ s^{-1}$)	293.15	-4.885	1.679	-0.404	-0.282	-	0.000
	298.15	-4.871	1.677	-0.401	-0.320	-	0.002
	303.15	-4.861	1.661	-0.409	-0.285	-	0.000
Δu / ($m\ s^{-1}$)	293.15	-309.2	93.94	-9.601	-32.96	-	0.070
	298.15	-309.5	94.45	-9.386	-36.80	-	0.197
	303.15	-310.4	93.31	-9.858	-32.83	-	0.065
Δn_D	293.15	-0.008	-0.002	0.001	-0.002	-	0.000
	298.15	-0.008	-0.002	-0.001	-0.004	-	0.000
	303.15	-0.008	-0.004	-0.002	-0.001	-	0.000
			{1-hexene (1) + 2-ethoxyethanol (2)}				
V_m^E / (cm^3 mol^{-1})	293.15	0.192	0.854	0.283	0.603	0.704	0.007
	298.15	0.206	0.926	0.331	0.675	0.751	0.008
	303.15	0.221	1.003	0.380	0.740	0.799	0.008
$\Delta\kappa_s$/ (TPa^{-1})	293.15	75.25	75.38	-8.227	19.78	25.77	0.182
	298.15	70.02	81.91	-6.611	21.06	25.93	0.191
	303.15	63.97	89.29	-5.089	21.51	26.41	0.189
ΔL_f / (10^{-12} m)	293.15	6.204	1.436	-0.055	0.683	-	0.008
	298.15	6.297	1.580	-0.037	0.718	-	0.008
	303.15	6.392	1.744	-0.021	0.724	-	0.008
ΔZ/ (10^5 $kg\ m^{-2}\ s^{-1}$)	293.15	-2.912	0.525	-0.096	-0.108	-	0.001
	298.15	-2.908	0.521	-0.097	-0.110	-	0.001
	303.15	-2.905	0.516	-0.098	-0.107	-	0.001
Δu / ($m\ s^{-1}$)	293.15	-194.5	21.96	-0.177	-10.40	-	0.080
	298.15	-194.3	21.73	0.038	-10.28	-	0.076
	303.15	-194.2	21.41	0.259	-9.679	-	0.067
Δn_D	293.15	-0.005	-0.003	-0.001	-0.001	-	0.000
	298.15	-0.005	-0.004	-0.002	0.000	-	0.000

	303.15	-0.006	-0.004	-0.002	-0.001	-	0.000
			{1-hexene (1) + 2-butoxyethanol (2)}				
V_m^E / *(cm³ mol⁻¹)*	293.15	-1.132	0.527	0.308	0.672	0.358	0.003
	298.15	-1.177	0.568	0.349	0.716	0.387	0.004
	303.15	-1.225	0.606	0.385	0.777	0.433	0.004
$\Delta\kappa_s$/ (TPa^{-1})	293.15	-182.5	33.05	22.74	8.751	-	0.043
	298.15	-205.5	31.82	22.65	7.345	-	0.051
	303.15	-231.2	30.00	22.89	6.820	-	0.069
ΔL_f / (10^{-12} m)	293.15	-2.652	1.575	0.496	0.193	-	0.001
	298.15	-3.055	1.605	0.482	0.144	-	0.002
	303.15	-3.501	1.627	0.476	0.124	-	0.002
ΔZ/ *(10⁵ kg m⁻² s⁻¹)*	293.15	-0.935	-0.190	0.017	-0.041	-	0.000
	298.15	-0.940	-0.190	0.021	-0.036	-	0.000
	303.15	-0.945	-0.190	0.025	-0.035	-	0.000
Δu / *(m s⁻¹)*	293.15	-78.66	-26.88	-0.469	0.029	2.155	0.021
	298.15	-77.02	-26.51	-0.266	1.010	3.621	0.026
	303.15	-75.35	-26.10	-0.241	1.495	5.125	0.030
Δn_D	293.15	0.006	-0.003	0.000	0.000	-	0.000
	298.15	0.007	-0.004	-0.001	0.002	-	0.000
	303.15	0.006	-0.003	0.000	-0.001	-	0.000

Annexes 2

Table A2.3: Experimental vapor pressures and deviations from values calculated by Antoine's equation of N,N-dimethylacetamide

T_{exp} (°C)	T_{exp} (K)	P_{exp} (mm Hg)	P_{exp} (kPa)	$\delta P/P$ (%)
- 0.05	273.10	0.295	0.039	- 0.32
- 0.05	273.10	0.296	0.039	- 0.02
9.98	283.13	0.655	0.087	0.23
9.99	283.14	0.655	0.087	0.06
20.01	293.16	1.358	0.181	0.25
20.03	293.18	1.358	0.181	0.09
30.06	303.21	2.658	0.354	0.11
30.06	303.21	2.655	0.354	0.00
40.08	313.23	4.932	0.658	- 0.12
40.08	313.23	4.936	0.658	- 0.03
50.10	323.25	8.758	1.168	-0.25
50.10	323.25	8.780	1.170	-0.01
60.07	333.22	14.941	1.992	-0.12
60.09	333.25	14.946	1.993	-0.19
70.06	343.21	24.649	3.286	0.14
70.07	343.22	24.612	3.281	- 0.06
80.02	353.17	39.185	5.224	0.07
80.02	353.17	39.209	5.227	0.13
89.95	363.10	60.477	8.063	0.08
89.97	363.12	60.463	8.061	- 0.03
	|Standard deviation|			**0.12**

Table A2.4: Experimental vapor pressures and deviations from values calculated by Antoine's equation of 1,3,5-trimethylbenzene

T_{exp} (°C)	T_{exp} (K)	P_{exp} (mm Hg)	P_{exp} (kPa)	$\delta P/P$ (%)
- 0.06	273.09	0.413	0.055	0.48
- 0.05	273.10	0.409	0.055	-0.57
9.99	283.14	0.881	0.117	0.04
10.00	283.15	0.883	0.118	0.24
20.03	293.18	1.773	0.236	0.01
20.04	293.19	1.771	0.236	-0.20
30.06	303.21	3.380	0.451	-0.02
30.07	303.22	3.382	0.451	-0.01
40.08	313.23	6.129	0.817	-0.16
40.09	313.24	6.142	0.819	-0.01
50.08	323.23	10.677	1.424	0.08
50.09	323.24	10.675	1.423	0.01
50.10	323.25	10.688	1.425	0.07
60.05	333.20	17.836	2.378	0.08
60.06	333.21	17.822	2.376	-0.04
70.06	343.21	28.842	3.845	0.07
70.06	343.21	28.819	3.842	-0.01
80.05	353.20	45.118	6.015	-0.06
80.05	353.20	45.155	6.020	0.02
89.98	363.13	68.613	9.148	0.03
89.99	363.14	68.581	9.143	-0.06
	|Standard deviation|			**0.11**

Table A2.5: Experimental vapor pressures and deviations from values calculated by Antoine's equation of propan-2-ol

T_{exp} (°C)	T_{exp} (K)	P_{exp} (mm Hg)	P_{exp} (kPa)	$\delta P/P$ (%)
-0.04	273.11	7.716	1.029	0.29
-0.04	273.11	7.722	1.030	0.38
9.99	283.14	16.042	2.139	-0.25
9.99	283.14	16.049	2.140	-0.21
20.01	293.16	31.458	4.194	-0.39
20.02	293.17	31.443	4.192	-0.50
30.03	303.18	58.638	7.818	-0.16
30.05	303.20	58.647	7.819	-0.27
40.06	313.21	104.468	13.928	0.29
40.06	313.21	104.465	13.928	0.28
40.08	313.23	104.574	13.942	0.28
40.08	313.13	104.379	13.916	0.09
50.06	323.21	177.180	23.622	0.24
60.04	333.19	289.441	38.589	0.32
70.06	343.21	456.930	60.919	0.19
80.06	353.21	697.145	92.945	-0.19
84.02	357.17	817.432	108.982	-0.38
	|Standard deviation|			**0.28**

Table A2.6: Experimental vapor pressures and deviations from values calculated by Antoine's equation of DMSO

T_{exp} (°C)	T_{exp} (K)	P_{exp} (mm Hg)	P_{exp} (kPa)	$\delta P/P$ (%)
20.02	293.17	0.419	0.056	-0.24
20.03	293.18	0.422	0.056	0.30
30.06	303.21	0.860	0.115	-0.09
30.07	303.22	0.862	0.115	0.05
40.08	313.23	1.670	0.223	-0.04
40.08	313.23	1.669	0.223	-0.09
50.08	323.23	3.094	0.412	0.06
50.09	323.24	3.095	0.413	0.04
60.09	333.24	5.486	0.731	-0.09
60.09	333.24	5.491	0.732	0.01
70.09	343.24	9.392	1.252	0.08
70.12	343.27	9.398	1.253	-0.02
80.08	353.23	15.529	2.070	0.20
80.10	353.25	15.507	2.067	-0.04
90.05	363.20	24.784	3.304	-0.03
90.06	363.21	24.777	3.303	-0.10
	|Standard deviation|			**0.09**

Table A2.7: Redlich–Kister expansion parameters and standard deviation for the studied binary mixtures

T (K)	G_1	σ	G_2	σ	G_3	σ	G_4	σ
N,N-dimethylacetamide (1) + 1,3,5-trimethylbenzene (2)								
273.15	1.4470	0.101	-0.7758	0.288	0.0973	0.475	-	-
283.15	1.3970	0.091	-0.7271	0.263	0.0379	0.442	-	-
293.15	1.3486	0.082	-0.6769	0.237	-0.0105	0.406	-	-
303.15	1.3015	0.073	-0.6255	0.211	-0.0485	0.368	-	-
313.15	1.2556	0.064	-0.5726	0.185	-0.0764	0.330	-	-
323.15	1.2105	0.055	-0.5184	0.160	-0.0943	0.292	-	-
333.15	1.1663	0.048	-0.4628	0.139	-0.1025	0.257	-	-
343.15	1.1226	0.042	-0.4058	0.120	-0.1011	0.228	-	-
353.15	1.0794	0.038	-0.3475	0.108	-0.0901	0.208	-	-
363.15	1.0365	0.037	-0.2879	0.103	-0.0700	0.201	-	-
N,N-dimethylacetamide (1) + propan-2-ol (2)								
273.15	-0.4615	0.005	0.0983	0.010	0.0460	0.017	-0.0273	0.031
283.15	-0.5243	0.008	0.0998	0.014	0.0101	0.024	-0.0810	0.044
293.15	-0.5691	0.008	0.1106	0.015	-0.0042	0.027	-0.0986	0.049
303.15	-0.5988	0.008	0.1292	0.015	0.0006	0.025	-0.0853	0.047
313.15	-0.6160	0.007	0.1544	0.012	0.0222	0.021	-0.0454	0.039
323.15	-0.6228	0.005	0.1851	0.010	0.0586	0.017	0.0170	0.031
333.15	-0.6212	0.006	0.2204	0.010	0.1079	0.018	0.0987	0.033
343.15	-0.6127	0.008	0.2595	0.016	0.1685	0.027	0.1968	0.051
353.15	-0.5987	0.013	0.3017	0.024	0.2389	0.043	0.3088	0.080
N,N-dimethylacetamide (1) + DMSO (2)								
293.15	0.3311	0.007	0.1078	0.018	0.1407	0.036	-	-
303.15	0.3157	0.008	0.1038	0.020	0.1083	0.042	-	-
313.15	0.3011	0.008	0.0996	0.021	0.0863	0.044	-	-
323.15	0.2870	0.008	0.0954	0.021	0.0731	0.043	-	-
333.15	0.2732	0.007	0.0915	0.019	0.0674	0.039	-	-
343.15	0.2593	0.006	0.0879	0.016	0.0680	0.034	-	-
353.15	0.2455	0.005	0.0848	0.013	0.0740	0.027	-	-
363.15	0.2314	0.004	0.0823	0.009	0.0846	0.020	-	-

Table A2.8: Antoine parameters A, B and C and standard deviations for the N,N-dimethylacetamide (1) + 1,3,5-trimethylbenzene (2) system

x_1	A (σ)	B (σ)	C (σ)	$\delta P/P$ (%)
0.0000	7.496 (0.019)	1807 (10.40)	229.4 (0.769)	0.11
0.0483	7.580 (0.007)	1853 (4.119)	234.4 (0.303)	0.05
0.0912	7.426 (0.015)	1769 (7.889)	229.6 (0.597)	0.10
0.1448	7.364 (0.011)	1731 (5.943)	227.6 (0.456)	0.08
0.2269	7.335 (0.013)	1701 (6.763)	224.7 (0.522)	0.09
0.3098	7.419 (0.008)	1727 (4.345)	224.7 (0.331)	0.07
0.3940	7.281 (0.144)	1669 (75.20)	221.1 (5.831)	1.19
0.5975	7.651 (0.058)	1845 (31.53)	231.8 (2.294)	0.38
0.8010	7.607 (0.014)	1832 (7.497)	229.7 (0.548)	0.10
1.0000	7.608 (0.015)	1846 (8.260)	227.0 (0.593)	0.12

Table A2.9: Antoine parameters A, B and C and standard deviations for the N,N-dimethylacetamide (1) + propan-2-ol (2) system

x_1	A (σ)	B (σ)	C (σ)	$\delta P/P$ (%)
0.0000	8.196 (0.035)	1600 (17.74)	219.0 (1.404)	0.28
0.0983	8.122 (0.043)	1591 (21.75)	218.5 (1.731)	0.31
0.1970	8.002 (0.041)	1563 (20.52)	216.6 (1.644)	0.27
0.3964	7.878 (0.050)	1591 (25.86)	219.8 (2.074)	0.33
0.5862	7.769 (0.025)	1640 (12.97)	224.1 (1.026)	0.18
0.7668	7.670 (0.020)	1706 (10.59)	228.5 (0.827)	0.16
0.8777	9.583 (0.242)	2894 (164.6)	301.4 (9.635)	1.00
1.0000	7.608 (0.015)	1846 (8.260)	227.0 (0.593)	0.12

Table A2.10: Antoine parameters A, B and C and standard deviations for the N,N-dimethylacetamide (1) + DMSO (2) system

x_1	A (σ)	B (σ)	C (σ)	$\delta P/P$ (%)
0.0000	7.837 (0.027)	2092 (15.24)	234.8 (1.041)	0.09
0.2048	7.708 (0.027)	2000 (15.68)	233.8 (1.116)	0.10
0.4018	7.601 (0.017)	1910 (9.741)	229.5 (0.715)	0.07
0.6007	7.638 (0.016)	1906 (9.326)	230.5 (0.688)	0.06
0.7977	7.713 (0.026)	1925 (14.25)	232.5 (1.002)	0.18
1.0000	7.608 (0.015)	1846 (8.260)	227.0 (0.593)	0.12

Table A2.11: Values of the liquid phase composition x_1 , vapor phase composition $y_{1,calc}$, vapor pressure P_{exp}, standard deviations $\delta P/P$, activity Coefficients γ_1 and γ_2 , and excess molar Gibbs Functions G^E for the studied binary mixtures

x_1	$y_{1,calc}$	P_{exp} (Pa)	$\delta P/P$ (%)	γ_1	γ_2	G^E(J.mol^{-1})
N,N-dimethylacetamide (1) + 1,3,5-trimethylbenzene (2)						
			T = 273.15 K			
0.0000	0.0000	55.0	0.00	10.177	1.0000	0.0
0.0483	0.2002	62.6	-5.63	6.9178	1.0095	232.5
0.0912	0.2635	70.2	0.16	5.1136	1.0325	404.0
0.1448	0.2938	76.4	5.94	3.6829	1.0786	575.8
0.2269	0.3044	77.5	6.57	2.4503	1.1830	756.9
0.3098	0.3046	72.1	-0.37	1.7964	1.3247	852.9
0.3940	0.3085	72.0	-0.42	1.4290	1.4987	876.2
0.5975	0.3677	65.6	-5.00	1.0700	1.9659	709.7
0.8010	0.5603	56.7	0.34	0.9984	2.2695	367.5
1.0000	1.0000	39.6	0.00	1.0000	2.1566	0.0
			T = 283.15 K			
0.0000	0.0000	117.5	0.00	8.6886	1.0000	0.0
0.0483	0.1874	131.9	-5.20	6.1636	1.0084	225.6
0.0912	0.2539	147.3	0.00	4.6967	1.0291	393.5
0.1448	0.2905	159.7	5.07	3.4836	1.0709	563.4
0.2269	0.3087	162.8	5.83	2.3885	1.1666	745.6
0.3098	0.3138	153.3	-0.12	1.7802	1.2986	845.2
0.3940	0.3202	152.8	-0.33	1.4265	1.4636	872.9
0.5975	0.3800	140.0	-4.72	1.0679	1.9220	711.5
0.8010	0.5727	122.1	0.45	0.9953	2.2218	365.2
1.0000	1.0000	87.3	0.00	1.0000	2.0296	0.0
			T = 293,15K			
0.0000	0.0000	235.9	0.00	7.5010	1.0000	0.0
0.0483	0.1757	262.0	-4.72	5.5292	1.0075	218.7
0.0912	0.2447	291.0	-0.09	4.3308	1.0261	382.8
0.1448	0.2866	314.5	4.32	3.3000	1.0640	550.6
0.2269	0.3121	321.9	5.14	2.3272	1.1517	733.4
0.3098	0.3220	306.3	0.04	1.7629	1.2746	836.3
0.3940	0.3311	304.5	-0.41	1.4236	1.4306	868.1
0.5975	0.3923	281.2	-4.32	1.0674	1.8774	712.9
0.8010	0.5844	247.1	0.54	0.9934	2.1759	364.1
1.0000	1.0000	180.5	0.00	1.0000	1.9370	0.0
			T = 303,15K			
0.0000	0.0000	449.0	0.00	6.5436	1.0000	0.0
0.0483	0.1650	494.3	-4.22	4.9913	1.0067	211.7
0.0912	0.2359	545.6	-0.15	4.0078	1.0233	372.0
0.1448	0.2824	587.4	3.66	3.1301	1.0577	537.3
0.2269	0.3146	603.4	4.48	2.2663	1.1382	720.1
0.3098	0.3293	579.6	0.17	1.7442	1.2524	825.9
0.3940	0.3413	574.6	-0.61	1.4202	1.3995	861.8
0.5975	0.4046	535.7	-3.84	1.0683	1.8324	713.9
0.8010	0.5955	473.7	0.61	0.9926	2.1315	364.6
1.0000	1.0000	352.6	0.00	1.0000	1.8731	0.0
			T = 313,15K			
0.0000	0.0000	814.6	0.00	5.7651	1.0000	0.0

0.0483	0.1553	890.3	-3.71	4.5325	1.0059	204.7
0.0912	0.2273	976.5	-0.17	3.7212	1.0209	361.0
0.1448	0.2778	1047.2	3.09	2.9722	1.0520	523.6
0.2269	0.3162	1078.8	3.88	2.2057	1.1258	705.9
0.3098	0.3357	1045.4	0.27	1.7242	1.2318	814.1
0.3940	0.3509	1032.7	-0.90	1.4163	1.3701	853.9
0.5975	0.4170	973.1	-3.28	1.0706	1.7869	714.5
0.8010	0.6062	865.2	0.65	0.9928	2.0883	366.5
1.0000	1.0000	655.2	0.00	1.0000	1.8341	0.0
			T = 323,15K			
0.0000	0.0000	1416.3	0.00	5.1274	1.0000	0.0
0.0483	0.1466	1538.5	-3.20	4.1389	1.0053	197.8
0.0912	0.2191	1676.2	-0.18	3.4657	1.0187	349.9
0.1448	0.2730	1790.7	2.59	2.8248	1.0470	509.5
0.2269	0.3171	1848.6	3.33	2.1453	1.1146	690.7
0.3098	0.3412	1806.1	0.36	1.7028	1.2128	800.9
0.3940	0.3598	1777.4	-1.25	1.4119	1.3422	844.4
0.5975	0.4295	1694.3	-2.68	1.0743	1.7408	714.6
0.8010	0.6165	1513.7	0.66	0.9941	2.0460	370.1
1.0000	1.0000	1164.1	0.00	1.0000	1.8181	0.0
			T = 333,15K			
0.0000	0.0000	2370.1	0.00	4.6022	1.0000	0.0
0.0483	0.1386	2561.6	-2.71	3.7997	1.0047	191.1
0.0912	0.2113	2771.9	-0.18	3.2371	1.0169	338.9
0.1448	0.2679	2949.9	2.16	2.6869	1.0425	495.1
0.2269	0.3172	3050.3	2.83	2.0849	1.1045	674.6
0.3098	0.3460	3003.0	0.45	1.6800	1.1953	786.2
0.3940	0.3682	2943.2	-1.63	1.4068	1.3158	833.2
0.5975	0.4423	2840.1	-2.03	1.0793	1.6943	714.2
0.8010	0.6266	2548.0	0.65	0.9965	2.0045	375.5
1.0000	1.0000	1987.2	0.00	1.0000	1.8238	0.0
			T = 343,15K			
0.0000	0.0000	3831.9	0.00	4.1676	1.0000	0.0
0.0483	0.1314	4124.6	-2.23	3.5063	1.0043	184.5
0.0912	0.2038	4432.6	-0.18	3.0318	1.0153	327.9
0.1448	0.2626	4699.2	1.78	2.5575	1.0386	480.5
0.2269	0.3166	4864.9	2.40	2.0244	1.0955	657.7
0.3098	0.3499	4823.6	0.55	1.6558	1.1791	770.1
0.3940	0.3760	4707.7	-2.03	1.4009	1.2907	820.2
0.5975	0.4552	4600.6	-1.37	1.0857	1.6472	713.3
0.8010	0.6364	4142.5	0.59	0.9999	1.9635	382.8
1.0000	1.0000	3272.3	0.00	1.0000	1.8510	0.0
			T = 353,15K			
0.0000	0.0000	6006.0	0.00	3.8066	1.0000	0.0
0.0483	0.1249	6443.1	-1.78	3.2517	1.0039	178.1
0.0912	0.1966	6876.6	-0.18	2.8468	1.0140	317.2
0.1448	0.2570	7262.7	1.45	2.4356	1.0353	465.7
0.2269	0.3152	7524.9	2.01	1.9639	1.0874	639.9
0.3098	0.3531	7510.8	0.68	1.6301	1.1641	752.5
0.3940	0.3833	7298.8	-2.44	1.3944	1.2669	805.5
0.5975	0.4684	7225.3	-0.69	1.0934	1.5998	711.9
0.8010	0.6461	6526.8	0.50	1.0043	1.9228	392.0
1.0000	1.0000	5216.1	0.00	1.0000	1.9000	0.0
			T = 363,15K			

0.0000	0.0000	9152.4	0.00	3.5059	1.0000	0.0
0.0483	0.1191	9791.7	-1.34	3.0299	1.0036	172.0
0.0912	0.1898	10378.8	-0.19	2.6797	1.0129	306.6
0.1448	0.2513	10921.2	1.15	2.3208	1.0326	450.8
0.2269	0.3133	11321.1	1.68	1.9034	1.0803	621.2
0.3098	0.3556	11370.4	0.83	1.6029	1.1504	733.4
0.3940	0.3900	11001.4	-2.83	1.3870	1.2442	789.0
0.5975	0.4819	11033.5	-0.02	1.1023	1.5521	710.0
0.8010	0.6557	9994.9	0.37	1.0096	1.8825	403.2
1.0000	1.0000	8073.6	0.00	1.0000	1.9712	0.0

N,N-dimethylacetamide (1) + propan-2-ol (2)

T = 273,15K

0.0000	0.0000	1028.9	0.00	0.6148	1.0000	0.0
0.0983	0.0028	923.8	-0.27	0.6647	0.9957	-100.0
0.1970	0.0070	814.5	-0.12	0.7276	0.9801	-179.0
0.3964	0.0232	582.8	0.27	0.8582	0.9142	-260.6
0.5862	0.0585	375.3	-0.24	0.9479	0.8318	-244.2
0.7668	0.1408	213.6	0.15	0.9886	0.7639	-162.5
0.8777	0.2732	126.9	-0.05	0.9976	0.7334	-90.9
1.0000	1.0000	39.6	0.00	1.0000	0.7085	0.0

T = 283,15K

0.0000	0.0000	2145.6	0.00	0.5868	1.0000	0.0
0.0983	0.0028	1924.0	-0.43	0.6289	0.9959	-116.0
0.1970	0.0070	1695.6	-0.13	0.6952	0.9785	-209.7
0.3964	0.0243	1203.4	0.36	0.8407	0.9034	-306.4
0.5862	0.0618	771.0	-0.33	0.9347	0.8174	-289.7
0.7668	0.1493	439.3	0.21	0.9776	0.7454	-202.3
0.8777	0.2943	258.2	-0.08	0.9923	0.6950	-120.8
1.0000	1.0000	87.3	0.00	1.0000	0.6093	0.0

T = 293,15K

0.0000	0.0000	4207.5	0.00	0.5569	1.0000	0.0
0.0983	0.0028	3768.0	-0.51	0.6021	0.9954	-131.7
0.1970	0.0072	3317.8	-0.11	0.6735	0.9760	-237.4
0.3964	0.0255	2339.1	0.37	0.8297	0.8942	-344.8
0.5862	0.0656	1493.4	-0.35	0.9285	0.8043	-325.6
0.7668	0.1584	852.4	0.22	0.9736	0.7295	-229.4
0.8777	0.3119	502.6	-0.08	0.9904	0.6727	-138.8
1.0000	1.0000	180.5	0.00	1.0000	0.5704	0.0

T = 303,15K

0.0000	0.0000	7816.4	0.00	0.5262	1.0000	0.0
0.0983	0.0029	6990.8	-0.53	0.5822	0.9943	-147.0
0.1970	0.0075	6148.1	-0.05	0.6601	0.9727	-262.3
0.3964	0.0268	4311.2	0.32	0.8240	0.8864	-376.8
0.5862	0.0697	2745.9	-0.31	0.9284	0.7922	-352.7
0.7668	0.1682	1571.2	0.20	0.9755	0.7156	-244.6
0.8777	0.3263	939.8	-0.08	0.9916	0.6629	-145.5
1.0000	1.0000	352.6	0.00	1.0000	0.5745	0.0

T = 313,15K

0.0000	0.0000	13842.4	0.00	0.4953	1.0000	0.0
0.0983	0.0029	12364.4	-0.51	0.5678	0.9927	-162.0
0.1970	0.0078	10858.0	0.04	0.6531	0.9688	-284.7
0.3964	0.0282	7580.5	0.21	0.8226	0.8798	-402.8
0.5862	0.0742	4821.2	-0.21	0.9332	0.7809	-371.9

0.7668	0.1787	2767.2	0.14	0.9827	0.7031	-248.7
0.8777	0.3377	1694.1	-0.06	0.9953	0.6632	-141.5
1.0000	1.0000	655.2	0.00	1.0000	0.6158	0.0
			T = 323,15K			
0.0000	0.0000	23494.3	0.00	0.4647	1.0000	0.0
0.0983	0.0030	20959.4	-0.44	0.5577	0.9907	-176.8
0.1970	0.0081	18374.9	0.16	0.6513	0.9645	-304.8
0.3964	0.0298	12783.1	0.04	0.8245	0.8742	-423.5
0.5862	0.0791	8124.3	-0.07	0.9424	0.7701	-383.9
0.7668	0.1898	4679.5	0.05	0.9944	0.6916	-242.5
0.8777	0.3464	2953.0	-0.02	1.0013	0.6719	-127.5
1.0000	1.0000	1164.1	0.00	1.0000	0.6962	0.0
			T = 333,15K			
0.0000	0.0000	38392.1	0.00	0.4350	1.0000	0.0
0.0983	0.0031	34207.9	-0.34	0.5510	0.9884	-191.5
0.1970	0.0086	29934.9	0.29	0.6539	0.9599	-323.0
0.3964	0.0314	20766.1	-0.17	0.8293	0.8694	-439.5
0.5862	0.0844	13196.5	0.12	0.9553	0.7597	-389.3
0.7668	0.2016	7630.3	-0.07	1.0102	0.6809	-226.8
0.8777	0.3528	4991.4	0.02	1.0093	0.6879	-104.2
1.0000	1.0000	1987.2	0.00	1.0000	0.8236	0.0
			T = 343,15K			
0.0000	0.0000	60639.8	0.00	0.4064	1.0000	0.0
0.0983	0.0033	53966.6	-0.21	0.5471	0.9858	-206.0
0.1970	0.0091	47134.7	0.45	0.6599	0.9549	-339.3
0.3964	0.0331	32623.6	-0.41	0.8364	0.8653	-451.2
0.5862	0.0902	20739.9	0.34	0.9715	0.7495	-388.9
0.7668	0.2141	12040.7	-0.21	1.0295	0.6706	-202.2
0.8777	0.3571	8201.9	0.08	1.0190	0.7104	-72.2
1.0000	1.0000	3272.3	0.00	1.0000	1.0123	0.0
			T = 353,15K			
0.0000	0.0000	92895.3	0.00	0.3790	1.0000	0.0
0.0983	0.0034	82577.0	-0.05	0.5454	0.9830	-220.4
0.1970	0.0096	71979.3	0.62	0.6689	0.9498	-354.2
0.3964	0.0349	49730.5	-0.69	0.8453	0.8618	-459.2
0.5862	0.0963	31640.1	0.60	0.9906	0.7394	-383.2
0.7668	0.2273	18446.6	-0.38	1.0522	0.6605	-169.4
0.8777	0.3597	13130.8	0.14	1.0302	0.7390	-31.9
1.0000	1.0000	5216.1	0.00	1.0000	1.2851	0.0

N,N-dimethylacetamide (1) + DMSO (2)

			T = 293,15K			
0.0000	0.0000	55.9	0.00	1.4390	1.0000	0.0
0.2048	0.4957	89.8	0.03	1.2032	1.0173	125.6
0.4018	0.7028	117.1	-0.11	1.1365	1.0416	184.7
0.6007	0.8302	143.0	0.23	1.0927	1.0854	209.6
0.7977	0.9143	162.9	-0.22	1.0369	1.2366	175.1
1.0000	1.0000	180.5	0.00	1.0000	1.7853	0.0
			T = 303,15K			
0.0000	0.0000	114.3	0.00	1.3775	1.0000	0.0
0.2048	0.4838	178.5	0.04	1.1954	1.0140	119.9
0.4018	0.6936	231.1	-0.13	1.1329	1.0372	181.4
0.6007	0.8231	280.2	0.26	1.0861	1.0839	206.2

0.7977	0.9110	318.1	-0.25	1.0327	1.2272	169.2
1.0000	1.0000	352.6	0.00	1.0000	1.6952	0.0
			T = 313,15K			
0.0000	0.0000	221.6	0.00	1.3336	1.0000	0.0
0.2048	0.4719	337.7	0.04	1.1873	1.0117	115.5
0.4018	0.6843	433.5	-0.14	1.1284	1.0339	178.3
0.6007	0.8163	522.4	0.26	1.0806	1.0816	202.8
0.7977	0.9079	591.2	-0.25	1.0297	1.2174	164.3
1.0000	1.0000	655.2	0.00	1.0000	1.6275	0.0
			T = 323,15K			
0.0000	0.0000	410.2	0.00	1.3031	1.0000	0.0
0.2048	0.4602	610.8	0.04	1.1786	1.0102	112.1
0.4018	0.6749	777.5	-0.13	1.1232	1.0314	175.1
0.6007	0.8098	931.5	0.25	1.0760	1.0785	199.3
0.7977	0.9050	1051.8	-0.24	1.0274	1.2072	160.3
1.0000	1.0000	1164.1	0.00	1.0000	1.5771	0.0
			T = 333,15K			
0.0000	0.0000	728.4	0.00	1.2828	1.0000	0.0
0.2048	0.4487	1061.0	0.03	1.1694	1.0094	109.4
0.4018	0.6654	1339.1	-0.12	1.1173	1.0295	171.6
0.6007	0.8037	1596.1	0.23	1.0721	1.0747	195.5
0.7977	0.9022	1798.8	-0.21	1.0259	1.1966	157.1
1.0000	1.0000	1987.2	0.00	1.0000	1.5404	0.0
			T = 343,15K			
0.0000	0.0000	1245.4	0.00	1.2705	1.0000	0.0
0.2048	0.4374	1777.2	0.03	1.1597	1.0092	107.4
0.4018	0.6560	2224.2	-0.10	1.1109	1.0281	167.8
0.6007	0.7979	2638.6	0.20	1.0690	1.0701	191.5
0.7977	0.8996	2969.1	-0.18	1.0251	1.1855	154.6
1.0000	1.0000	3272.3	0.00	1.0000	1.5147	0.0
			T = 353,15K			
0.0000	0.0000	2058.2	0.00	1.2644	1.0000	0.0
0.2048	0.4263	2880.7	0.02	1.1494	1.0095	105.8
0.4018	0.6466	3575.2	-0.08	1.1040	1.0270	163.5
0.6007	0.7925	4223.1	0.16	1.0664	1.0648	187.0
0.7977	0.8971	4746.2	-0.14	1.0248	1.1741	152.7
1.0000	1.0000	5216.1	0.00	1.0000	1.4982	0.0
			T = 363,15K			
0.0000	0.0000	3297.7	0.00	1.2633	1.0000	0.0
0.2048	0.4154	4532.2	0.02	1.1385	1.0101	104.4
0.4018	0.6374	5578.5	-0.06	1.0967	1.0261	158.6
0.6007	0.7873	6563.6	0.11	1.0644	1.0588	182.1
0.7977	0.8949	7369.3	-0.10	1.0250	1.1623	151.3
1.0000	1.0000	8073.6	0.00	1.0000	1.4894	0.0

Table A2.12: Binary interaction parameters for the NRTL and UNIQUAC models for the studied mixtures

	Cij^0 (J. mol^{-1})	Cji^0 (J. mol^{-1})	Cij^T (J/ mol. °C)	Cji^T (J/ mol. °C)	α
	N,N-dimethylacetamide (1) + 1,3,5-trimethylbenzene (2)				
	-238.311	1472.457	1.484	-4.455	0.3
NRTL	**N,N-dimethylacetamide (1) + propan-2-ol (2)**				
	-749.353	795.383	-3.136	1.195	0.3
	N,N-dimethylacetamide (1) + DMSO (2)				
	-49.178	108.426	7.722	-4.760	0.3
	Aij^0 (J. mol^{-1})	Aji^0 (J. mol^{-1})	Aij^T (J/ mol. °C)	Aji^T (J/ mol. °C)	-
	N,N-dimethylacetamide (1) + 1,3,5-trimethylbenzene (2)				
	-155.136	716.932	-0.554	0.123	-
UNIQUAC	**N,N-dimethylacetamide (1) + propan-2-ol (2)**				
	33.723	130.723	-0.902	0.073	-
	N,N-dimethylacetamide (1) + DMSO (2)				
	372.679	-361.124	-0.227	0.548	-

Table A2.13: Sum of squared relative error (SSQ) for the NRTL, UNIQUAC and Modified UNIFAC (Do) models for the studied mixtures

Model	SSQ
N,N-dimethylacetamide (1) + 1,3,5-trimethylbenzene (2)	
NRTL	0.202
UNIQUAC	0.213
Modified UNIFAC (Dortmund)	0.957
N,N-dimethylacetamide (1) + propan-2-ol (2)	
NRTL	0.113
UNIQUAC	0.115
Modified UNIFAC (Dortmund)	0.178
N,N-dimethylacetamide (1) + DMSO (2)	
NRTL	0.029
UNIQUAC	0.031
Modified UNIFAC (Dortmund)	0.106

$$SSQ = \sum \left(\frac{P_{calc} - P_{exp}}{P_{exp}} \right)^2$$

Publications

1- Djazia Belhadj, Indra Bahadur, Amina Negadi, Natalia Muñoz-Rujas, Eduardo Montero, and Latifa Negadi. Thermodynamic, Ultrasonic, and Transport Study of Binary Mixtures Containing 2-(2-Methoxyethoxy)ethanol and Alcohols at (293.15−323.15) K. Journal of Chemical and Engineering Data (2020), 65, 11, 5192–5209.

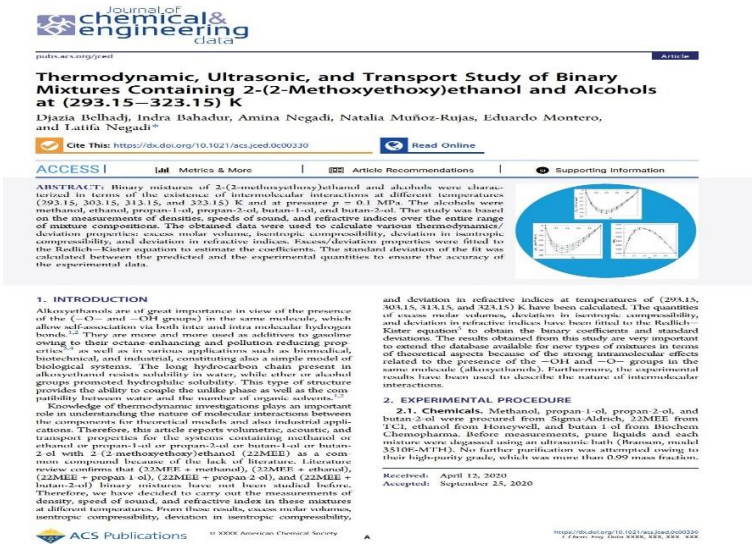
Journal of chemical & engineering data

pubs.acs.org/jced

Article

Thermodynamic, Ultrasonic, and Transport Study of Binary Mixtures Containing 2-(2-Methoxyethoxy)ethanol and Alcohols at (293.15−323.15) K

Djazia Belhadj, Indra Bahadur, Amina Negadi, Natalia Muñoz-Rujas, Eduardo Montero, and Latifa Negadi*

Cite This: https://dx.doi.org/10.1021/acs.jced.0c00330 Read Online

ACCESS | Metrics & More | Article Recommendations | Supporting Information

ABSTRACT: Binary mixtures of 2-(2-methoxyethoxy)ethanol and alcohols were characterized in terms of the existence of intermolecular interactions at different temperatures (293.15, 303.15, 313.15, and 323.15) K and at pressure p = 0.1 MPa. The alcohols were methanol, ethanol, propan-1-ol, propan-2-ol, butan-1-ol, and butan-2-ol. The study was based on the measurements of densities, speeds of sound, and refractive indices over the entire range of mixture compositions. The obtained data were used to calculate various thermodynamics/deviation properties: excess molar volume, isentropic compressibility, deviation in isentropic compressibility, and deviation in refractive indices. Excess/deviation properties were fitted to the Redlich−Kister equation to estimate the coefficients. The standard deviation of the fit was calculated between the predicted and the experimental quantities to ensure the accuracy of the experimental data.

1. INTRODUCTION

Alkoxyethanols are of great importance in view of the presence of the (−O− and −OH groups) in the same molecule, which allow self-association via both inter and intra molecular hydrogen bonds.[1,2] They are more and more used as additives to gasoline owing to their octane-enhancing and pollution reducing properties[3] as well as in various applications such as biomedical, biotechnical, and industrial, constituting also a simple model of biological systems. The long hydrocarbon chain present in alkoxyethanol resists solubility in water, while ether or alcohol groups promoted hydrophilic solubility. This type of structure provides the ability to couple the unlike phase as well as the compatibility between water and the number of organic solvents.[4]

Knowledge of thermodynamic investigations plays an important role in understanding the nature of molecular interactions between the components for theoretical models and also industrial applications. Therefore, this article reports volumetric, acoustic, and transport properties for the systems containing methanol or ethanol or propan-1-ol or propan-2-ol or butan-1-ol or butan-2-ol with 2-(2-methoxyethoxy)ethanol (2MEE) as a common compound because of the lack of literature. Literature review confirms that (2MEE + methanol), (2MEE + ethanol), (2MEE + propan 1 ol), (2MEE + propan 2 ol), and (2MEE + butan-2-ol) binary mixtures have not been studied before. Therefore, we have decided to carry out the measurements of density, speed of sound, and refractive index in these mixtures at different temperatures. From these results, excess molar volumes, isentropic compressibility, deviation in isentropic compressibility, and deviation in refractive indices at temperatures of (293.15, 303.15, 313.15, and 323.15) K have been calculated. The quantities of excess molar volumes, deviation in isentropic compressibility, and deviation in refractive indices have been fitted to the Redlich−Kister equation[5] to obtain the binary coefficients and standard deviations. The results obtained from this study are very important to extend the database available for new types of mixtures in terms of theoretical aspects because of the strong intramolecular effects related to the presence of the −OH and −O− groups in the same molecule (alkoxyethanols). Furthermore, the experimental results have been used to describe the nature of intermolecular interactions.

2. EXPERIMENTAL PROCEDURE

2.1. Chemicals. Methanol, propan-1-ol, propan-2-ol, and butan-2-ol were procured from Sigma-Aldrich, 2-2MEE from TCI, ethanol from Honeywell, and butan-1-ol from Biochem Chemopharma. Before measurements, pure liquids and each mixture were degassed using an ultrasonic bath (Branson, model 3510E-MTH). No further purification was attempted owing to their high-purity grade, which was more than 0.99 mass fraction.

Received: April 12, 2020
Accepted: September 25, 2020

ACS Publications © XXXX American Chemical Society

2. Djazia Belhadj, Amina Negadi, Pannuru Venkatesu, Indra Bahadur, Latifa Negadi. Density, speed of sound, refractive index and related derived/excess properties of binary mixtures (furfural + dimethyl sulfoxide), (furfural + acetonitrile) and (furfural + sulfolane) at different temperatures. Journal of Molecular Liquids (2021), 330, 115436.


Journal of Molecular Liquids 330 (2021) 115436

Contents lists available at ScienceDirect

Journal of Molecular Liquids

journal homepage: www.elsevier.com/locate/molliq

Density, speed of sound, refractive index and related derived/excess properties of binary mixtures (furfural + dimethyl sulfoxide), (furfural + acetonitrile) and (furfural + sulfolane) at different temperatures

Djazia Belhadj [a], Amina Negadi [a], Pannuru Venkatesu [b], Indra Bahadur [c], Latifa Negadi [a,d,e,*]

[a] LATA2M, Laboratoire de Thermodynamique Appliquée et Modélisation Moléculaire, University of Tlemcen, Post Office Box 119, Tlemcen 13000, Algeria
[b] Department of Chemistry, University of Delhi, Delhi 110 007, India
[c] Department of Chemistry, School of Physical and Chemical Sciences, Faculty of Natural and Agricultural Sciences, North-West University (Mafikeng Campus), Private Bag X2046, Mmabatho 2735, South Africa
[d] Thermodynamics Research Unit, School of Engineering, University of KwaZulu-Natal, Howard College Campus, King George V Avenue, 4041 Durban, South Africa

ARTICLE INFO

Article history:
Received 29 July 2020
Received in revised form 16 November 2020
Accepted 16 January 2021
Available online 22 January 2021

Keywords:
Thermodynamic properties
Furfural
DMSO
Acetonitrile
Sulfolane

ABSTRACT

In this work, experimental densities (ρ), speed of sound (u) and refractive indices (n_D) were measured over the entire composition range for the binary mixtures containing furfural with dimethyl sulfoxide (DMSO) or acetonitrile at (293.15, 303.15, 313.15 and 323.15) K whereas for sulfolane mixture at (303.15, 313.15 and 323.15) K and at pressure of 0.1 MPa. Further, the measured data has been utilized to compute isentropic compressibility (κ_S), intermolecular free length(L_f), specific acoustic impedance(Z), relative association(K_A), relaxation strength (r) and Rao's molar sound function(R). The excess/derived properties on mixing were also derived from values of measured properties for all studied mixtures under the same experimental conditions. The correlation of excess/derived properties was made by help of the Redlich-Kister polynomial equation and found to be satisfactory. The experimental and calculated results were interpreted from the viewpoint of intermolecular interactions that occur between the components of the investigated systems.

© 2021 Elsevier B.V. All rights reserved.

1. Introduction

Liquid mixtures have found applications in different fields rather than single liquid as they provide a wide choice of solvent mixtures with appropriate properties [1]. Thermophysical properties of binary liquid mixtures can be contributed to clarification of the various intermolecular interactions existing between the different species found in solution. Obviously, the reliable knowledge of these properties of pure compounds and mixtures is of great importance in many fields of research as well as in industrial practice [2–4]. Studying the concentration and temperature dependence of thermophysical and thermodynamics properties contributes to our understanding of intermolecular interactions in liquids, liquid mixtures and solutions [2–5]. Intermolecular interactions in binary mixtures modify the structural arrangements which lead to change the shape of the molecule [6]. The investigation of molecular interactions is therefore crucial in elucidation of the structural changes in the mixtures.

The present paper is focused on a study of thermophysical and thermodynamic properties of three binary systems formed by dimethyl sulfoxide (DMSO) or acetonitrile or sulfolane with furfural as a common compound. Furfural is one of the furan derivatives produced from the hemicellulosic fraction of lignocellulosics, which is considered a promising commodity bio-based chemical because of the possibility of its use in the production of several products as paints, fertilizers, fuel additives and many others products [5,7,8]. Once furfural has many applications, investigation of its properties in different mixtures is important. In this regard and as a continuation of our research program on thermodynamic and thermophysical properties of binary mixtures containing solvents derived from biomass [9–13], we report here experimental results of density (ρ), speed of sound (u) and refractive index (n_D) for the binary systems mentioned above over the whole miscibility range at different temperatures and at pressure of 0.1 MPa. These properties have been used to determine isentropic compressibility(κ_S), intermolecular free length(L_f), specific acoustic impedance(Z), relative association(K_A), relaxation strength (r) and Rao's molar sound function (R) and also the deviation parameters. The significance of these results has been

* Corresponding author at: LATA2M, Laboratoire de Thermodynamique Appliquée et Modélisation Moléculaire, University of Tlemcen, Post Office Box 119, Tlemcen 13000, Algeria.
E-mail address: latifa.negadi@univ-tlemcen.dz (L. Negadi).

https://doi.org/10.1016/j.molliq.2021.115436
0167-7322/© 2021 Elsevier B.V. All rights reserved.

3- Djazia Belhadj, Amina Negadi, Ariel Hernandez, Ilham Mokbel, Indra Bahadur, Latifa Negadi. A study on mixing properties of binary mixtures of 1-hexene with alkoxyethanols at different temperatures. The Journal of Chemical Thermodynamics (2022), 172, 106820.

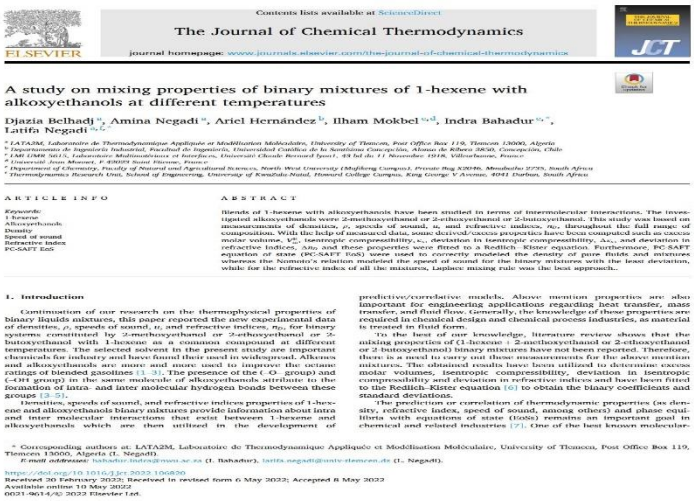
J. Chem. Thermodynamics 172 (2022) 106820

Contents lists available at ScienceDirect

The Journal of Chemical Thermodynamics

journal homepage: www.journals.elsevier.com/the-journal-of-chemical-thermodynamics

A study on mixing properties of binary mixtures of 1-hexene with alkoxyethanols at different temperatures

Djazia Belhadj [a], Amina Negadi [a], Ariel Hernández [b], Ilham Mokbel [c,d], Indra Bahadur [e,*], Latifa Negadi [a,f,*]

[a] LATA2M, Laboratoire de Thermodynamique Appliquée et Modélisation Moléculaire, University of Tlemcen, Post Office Box 119, Tlemcen 13000, Algeria
[b] Departamento de Ingeniería Industrial, Facultad de Ingeniería, Universidad Católica de la Santísima Concepción, Alonso de Ribera 3850, Concepción, Chile
[c] LMI, UMR 5615, Laboratoire de Multimatériaux et Interfaces, Université Claude Bernard Lyon1, 69 bd du 11 Novembre 1918, Villeurbanne, France
[d] Université Jean Monnet, 42023 Saint-Etienne, France
[e] Department of Chemistry, Faculty of Natural and Agricultural Sciences, North West University (Mafikeng Campus), Private Bag X2046, Mmabatho 2735, South Africa
[f] Thermodynamics Research Unit, School of Engineering, University of KwaZulu-Natal, Howard College Campus, King George V Avenue, 4041 Durban, South Africa

ARTICLE INFO

Keywords:
1-hexene
Alkoxyethanols
Density
Speed of sound
Refractive Index
PC-SAFT EoS

ABSTRACT

Blends of 1-hexene with alkoxyethanols have been studied in terms of intermolecular interactions. The investigated alkoxyethanols were 2-methoxyethanol or 2-ethoxyethanol or 2-butoxyethanol. This study was based on measurements of densities, ρ, speeds of sound, u, and refractive indices, n_D, throughout the full range of composition. With the help of measured data, some derived/excess properties have been computed such as excess molar volume, V_m^E, isentropic compressibility, κ_s, deviation in isentropic compressibility, $\Delta\kappa_s$, and deviation in refractive indices, Δn_D and these properties were fitted to a Redlich–Kister equation. Furthermore, PC-SAFT equation of state (PC-SAFT EoS) were used to correctly modelled the density of pure fluids and mixtures whereas the Nomoto's relation modeled the speed of sound for the binary mixtures with the least deviation, while for the refractive index of all the mixtures, Laplace mixing rule was the best approach.

1. Introduction

Continuation of our research on the thermophysical properties of binary liquids mixtures, this paper reported the new experimental data of densities, ρ, speeds of sound, u, and refractive indices, n_D, for binary systems constituted by 2-methoxyethanol or 2-ethoxyethanol or 2-butoxyethanol with 1-hexene as a common compound at different temperatures. The selected solvent in the present study are important chemicals for industry and have found their used in widespread. Alkenes and alkoxyethanols are more and more used to improve the octane ratings of blended gasolines [1–3]. The presence of the (−O− group) and (−OH group) in the same molecule of alkoxyethanols attribute to the formation of intra- and inter molecular hydrogen bonds between these groups [3–5].

Densities, speeds of sound, and refractive indices properties of 1-hexene and alkoxyethanols binary mixtures provide information about intra and inter molecular interactions that exist between 1-hexene and alkoxyethanols which are then utilized in the development of predictive/correlative models. Above mention properties are also important for engineering applications regarding heat transfer, mass transfer, and fluid flow. Generally, the knowledge of these properties are required in chemical design and chemical process industries, as material is treated in fluid form.

To the best of our knowledge, literature review shows that the mixing properties of (1-hexene + 2-methoxyethanol or 2-ethoxyethanol or 2-butoxyethanol) binary mixtures have not been reported. Therefore, there is a need to carry out these measurements for the above mention mixtures. The obtained results have been utilized to determine excess molar volumes, isentropic compressibility, deviation in isentropic compressibility and deviation in refractive indices and have been fitted to the Redlich–Kister equation [6] to obtain the binary coefficients and standard deviations.

The prediction or correlation of thermodynamic properties (as density, refractive index, speed of sound, among others) and phase equilibria with equations of state (EoSs) remains an important goal in chemical and related industries [7]. One of the best known molecular-

* Corresponding authors at: LATA2M, Laboratoire de Thermodynamique Appliquée et Modélisation Moléculaire, University of Tlemcen, Post Office Box 119, Tlemcen 13000, Algeria (L. Negadi).
E-mail addresses: bahadur.indra@nwu.ac.za (I. Bahadur), latifa.negadi@univ-tlemcen.dz (L. Negadi).

https://doi.org/10.1016/j.jct.2022.106820
Received 20 February 2022; Received in revised form 6 May 2022; Accepted 8 May 2022
Available online 10 May 2022
0021-9614/© 2022 Elsevier Ltd.

Communications

1- Djazia Belhadj, Amina Negadi, Pannuru Venkatesu, Indra Bahadur, Latifa Negadi.

Density, speed of sound, refractive index and related derived/excess properties of binary mixtures (furfural + dimethyl sulfoxide), (furfural + acetonitrile) and (furfural + sulfolane) at different temperatures.

10th Jubilees of the Rostocker International Conference: "Technical Thermodynamics: Thermophysical Properties and Energy Systems" (THERMAM 2021).

THERMAM 2021

ROSTOCK

CERTIFICATE OF PARTICIPATION

This is to certify that

Djazia BELHADJ

has participated

at the 10th ROSTOCKER INTERNATIONAL CONFERENCE: "TECHNICAL THERMODYNAMICS: THERMOPHYSICAL PROPERTIES AND ENERGY SYSTEMS", 09-10 September 2021, which was organized online by the University of Rostock with a poster presentation on the topic "Density, speed of sound, refractive index and related derived/excess properties of binary mixtures (furfural + dimethyl sulfoxide), (furfural + acetonitrile) and (furfural + sulfolane) at different temperatures".

Chair of the conference: Prof. Dr.-Ing. habil. Karsten Müller

2- Djazia Belhadj, Amina Negadi, Natalia Muñoz-Rujas, Eduardo Montero, Latifa Negadi.

Thermodynamic, Ultrasonic, and Transport Study of Binary Mixtures Containing 2-(2-Methoxyethoxy)ethanol and Alcohols at (293.15–323.15) K

2ème Séminaire international sur les sciences de la matière (physique et chimie) organisé par Algerian Journal of Engineering, Architecture and Urbanism 17 et 18 septembre 2021.

République Algérienne Démocratique et Populaire
Ministère de l'Enseignement Supérieur et de la Recherche Scientifique
Algerian Journal of Engineering, Architecture and Urbanism
https://www.aneau.org/ajeau/
ISSN : 2588-1760
Siège social : A.N.E.A.U. Association, Université USTO, Bir El Djir, Oran, 31000, Algeria

ATTESTATION

Cette attestation est délivrée :
Djazia Belhadj LATA2M, Laboratoire de Thermodynamique Appliquée et Modélisation Moléculaire, University of Tlemcen, Post Office Box 119, Tlemcen 13000, Algeria
Amina Negadi LATA2M, Laboratoire de Thermodynamique Appliquée et Modélisation Moléculaire, University of Tlemcen, Post Office Box 119, Tlemcen 13000, Algeria
Natalia Muñoz-Rujas Departamento de Ingeniería Electromecánica, Universidad de Burgos, Escuela Politécnica Superior, Avenida Cantabria s/n 09006 Burgos (Spain)
Eduardo Montero Departamento de Ingeniería Electromecánica, Universidad de Burgos, Escuela Politécnica Superior, Avenida Cantabria s/n 09006 Burgos (Spain)
Latifa Negadi LATA2M, Laboratoire de Thermodynamique Appliquée et Modélisation Moléculaire, University of Tlemcen, Post Office Box 119, Tlemcen 13000, Algeria Thermodynamics Research Unit, School of Engineering, University of KwaZulu- Natal, Howard College Campus, King George V Avenue, 4041 Durban, South Africa

Pour sa (leur) participation au **SÉMINAIRE INTERNATIONAL SUR LES SCIENCES DE LA MATIERE (PHYSIQUE ET CHIMIE)** en ligne (webinaire), organisé par Algerian Journal of Engineering, Architecture and Urbanism le 17 et 18 Septembre 2021, avec une **communication orale** intitulée:
Thermodynamic, Ultrasonic, and Transport Study of Binary Mixtures Containing 2-(2-Methoxyethoxy)ethanol and Alcohols at (293.15–323.15) K
Oran, Algerie
18/09/2021
Le Président du séminaire
Dr. HAMMA Walid

Journal of chemical & engineering data

pubs.acs.org/jced Article

Thermodynamic, Ultrasonic, and Transport Study of Binary Mixtures Containing 2-(2-Methoxyethoxy)ethanol and Alcohols at (293.15−323.15) K

Djazia Belhadj, Indra Bahadur, Amina Negadi, Natalia Muñoz-Rujas, Eduardo Montero, and Latifa Negadi*

Cite This: https://dx.doi.org/10.1021/acs.jced.0c00330 Read Online

ABSTRACT: Binary mixtures of 2-(2-methoxyethoxy)ethanol and alcohols were characterized in terms of the existence of intermolecular interactions at different temperatures (293.15, 303.15, 313.15, and 323.15) K and at pressure p = 0.1 MPa. The alcohols were methanol, ethanol, propan-1-ol, propan-2-ol, butan-1-ol, and butan-2-ol. The study was based on the measurements of densities, speeds of sound, and refractive indices over the entire range of mixture compositions. The obtained data were used to calculate various thermodynamics/deviation properties: excess molar volume, isentropic compressibility, deviation in isentropic compressibility, and deviation in refractive indices. Excess/deviation properties were fitted to the Redlich−Kister equation to estimate the coefficients. The standard deviation of the fit was calculated between the predicted and the experimental quantities to ensure the accuracy of the experimental data.

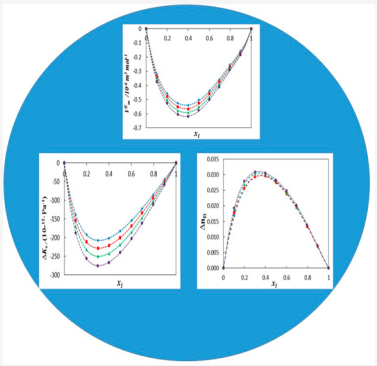

1. INTRODUCTION

Alkoxyethanols are of great importance in view of the presence of the (−O− and −OH groups) in the same molecule, which allow self-association via both inter and intra molecular hydrogen bonds.[1,2] They are more and more used as additives to gasoline owing to their octane-enhancing and pollution-reducing properties[3,4] as well as in various applications such as biomedical, biotechnical, and industrial, constituting also a simple model of biological systems. The long hydrocarbon chain present in alkoxyethanol resists solubility in water, while ether or alcohol groups promoted hydrophilic solubility. This type of structure provides the ability to couple the unlike phase as well as the compatibility between water and the number of organic solvents.[1,2]

Knowledge of thermodynamic investigations plays an important role in understanding the nature of molecular interactions between the components for theoretical models and also industrial applications. Therefore, this article reports volumetric, acoustic, and transport properties for the systems containing methanol or ethanol or propan-1-ol or propan-2-ol or butan-1-ol or butan-2-ol with 2-(2-methoxyethoxy)ethanol (22MEE) as a common compound because of the lack of literature. Literature review confirms that (22MEE + methanol), (22MEE + ethanol), (22MEE + propan-1-ol), (22MEE + propan-2-ol), and (22MEE + butan-2-ol) binary mixtures have not been studied before. Therefore, we have decided to carry out the measurements of density, speed of sound, and refractive index in these mixtures at different temperatures. From these results, excess molar volumes, isentropic compressibility, deviation in isentropic compressibility, and deviation in refractive indices at temperatures of (293.15, 303.15, 313.15, and 323.15) K have been calculated. The quantities of excess molar volumes, deviation in isentropic compressibility, and deviation in refractive indices have been fitted to the Redlich−Kister equation[5] to obtain the binary coefficients and standard deviations. The results obtained from this study are very important to extend the database available for new types of mixtures in terms of theoretical aspects because of the strong intramolecular effects related to the presence of the −OH and −O− groups in the same molecule (alkoxyethanols). Furthermore, the experimental results have been used to describe the nature of intermolecular interactions.

2. EXPERIMENTAL PROCEDURE

2.1. Chemicals. Methanol, propan-1-ol, propan-2-ol, and butan-2-ol were procured from Sigma-Aldrich, 22MEE from TCI, ethanol from Honeywell, and butan-1-ol from Biochem Chemopharma. Before measurements, pure liquids and each mixture were degassed using an ultrasonic bath (Branson, model 3510E-MTH). No further purification was attempted owing to their high-purity grade, which was more than 0.99 mass fraction.

Received: April 12, 2020
Accepted: September 25, 2020

Table 1. CAS #, Suppliers, Molar Mass, and Purities of Chemicals Used in This Study

chemical name	CAS #	supplier	lot #	water contents (ppm) (Karl Fisher analysis)	molar mass/(g·mol^{-1})	mass fraction purity (as statedby the supplier)	mass fraction purity GC analysis (final)
22MEE	111-77-3	TCI	T7MDIBJ	300	120.15	≥0.99	≥0.99
methanol	67-56-1	Sigma-Aldrich	STBF9892V	250	32.04	≥0.997	≥0.996
ethanol	64-17-5	Honeywell	SZBG2370H	200	46.07	≥0.998	≥0.995
propan-1-ol	71-23-8	Sigma-Aldrich	SZBF2320V	225	60.10	≥0.99	≥0.99
propan-2-ol	67-63-0	Sigma-Aldrich	STBF8249V	235	60.10	≥0.998	≥0.994
butan-1-ol	71-36-3	Biochem Chemopharma		260	74.12	≥0.995	≥0.992
butan-2-ol	78-92-2	Sigma-Aldrich	STBG2236V	280	74.12	≥0.99	≥0.99

Table 2. Comparison of Experimental Density, ρ, Speed of Sound, u, and Refractive Indices n_D of the Pure Component with the Corresponding Literature Values at (293.15, 298.15, 303.15, 313.15, and 323.15) K[a]

		ρ/(10^3 × kg m^{-3})		u/(m·s^{-1})		n_D	
component	T/(K)	exp.	lit.	exp.	lit.	exp.	lit.
22MEE	293.15	1.020	1.019810[7]	1433.62	1432.37[7]	1.426	1.42632[9]
			1.02080[10]				1.42640[11]
	298.15	1.015	1.015408[7]	1416.05	1415.21[7]	1.425	1.4245[11]
			1.01640[10]		1415.5[12]		1.4233[13]
			1.01501[9]		1417.1[14]		1.4243[15]
			1.01670[11]		1415.98[16]		
			1.0164[17]				
			1.01539[18]				
			1.0154[13]				
			1.01591[19]				
			1.0164[20]				
			1.01487[21]				
			1.0164[12]				
			1.01591[15]				
			1.0164[14]				
			1.01445[16]				
			1.0176[22]				
	303.15	1.011	1.010908[7]	1398.97	1397.93[7]	1.423	
			1.01183[10]				
	313.15	1.002	1.00322[10]	1365.06		1.419	
			1.00260[19]				
	323.15	0.993		1331.34		1.415	
methanol	293.15	0.792	0.7913[23]	1120.60	1119.6[24]	1.329	1.3284[25]
			0.79108[26]		1121.18[27]		1.32843[28]
			0.7911[29]		1119[28]		
			0.791[24]				
			0.7912[28]				
	298.15	0.787	0.78720[29]	1103.99	1108[30]	1.327	1.3278[30]
			0.7868[31]		1108[32]		1.3264[33]
			0.7867[34]		1102[28]		1.3267[25]
			0.7866[23]		1102.81[35]		1.3275[32]
			0.786671[36]				1.32645[28]
			0.78686[37]				1.32645[38]
			0.7863[39]				1.3266[40]
			0.78666[41]				
			0.7866[42]				
			0.7869[30]				
			0.78655[33]				
			0.7864[25]				
			0.7868[32]				
			0.7866[28]				
			0.7865[38]				
			0.78658[35]				
	303.15	0.782	0.78218[43]	1087.55	1086.6[24]	1.325	1.3247[25]
			0.7818[23]		1088.19[27]		1.3241[28]
			0.78196[41]		1086[28]		

https://dx.doi.org/10.1021/acs.jced.0c00330
J. Chem. Eng. Data XXXX, XXX, XXX−XXX

Table 2. continued

component	T/(K)	$\rho/(10^3 \times \text{kg m}^{-3})$ exp.	$\rho/(10^3 \times \text{kg m}^{-3})$ lit.	$u/(\text{m·s}^{-1})$ exp.	$u/(\text{m·s}^{-1})$ lit.	n_D exp.	n_D lit.
			0.78195[26]				
			0.7816[25]				
			0.78182[44]				
			0.782[24]				
			0.7818[28]				
	313.15	0.773	0.77267[43]	1055.13	1054.2[24]	1.321	1.3207[25]
			0.7723[23]		1055.88[27]		1.32048[28]
			0.77221[41]		1054[28]		
			0.77201[26]				
			0.7720[25]				
			0.772[24]				
			0.7726[28]				
	323.15	0.763	0.76302[43]	1023.02	1024.00[27]	1.317	1.3165[25]
			0.7626[23]				
ethanol	293.15	0.790	0.7901[23]	1162.46	1162.3[24]	1.362	1.3615[25]
			0.78824[26]		1161.78[27]		1.36125[28]
			0.7894[25]		1160[28]		1.3619[45]
			0.790[24]		1162.5[46]		1.3620[47]
			0.7893[28]				
			0.78999[45]				
			0.78999[47]				
			0.7890[48]				
			0.78999[46]				
	298.15	0.786	0.78546[29]	1144.95	1148[30]	1.360	1.3605[30]
			0.7854[31]		1152[32]		1.3593[33]
			0.7858[23]		1142[28]		1.3593[25]
			0.785339[36]				1.3608[32]
			0.78540[37]				1.35922[28]
			0.7849[39]				1.35922[38]
			0.78497[41]				1.3593[49]
			0.7850[42]				1.3597[40]
			0.7854[40]				
			0.78524[33]				
			0.7852[25]				
			0.7862[32]				
			0.7850[28]				
			0.7852[38]				
			0.78553[49]				
	303.15	0.781	0.7815[23]	1127.91	1128.2[24]	1.458	1.3573[25]
			0.78068[41]		1127.58[27]		1.35680[28]
			0.78073[26]		1126[28]		
			0.7807[25]		1128.3[46]		
			0.78074[44]				
			0.781[24]				
			0.7807[28]				
			0.7807[50]				
			0.7803[48]				
			0.78138[46]				
	313.15	0.772	0.7728[23]	1094.28	1094.5[24]	1.354	1.3533[25]
			0.77213[41]		1094.07[27]		1.35303[28]
			0.77198[26]		1093[28]		
			0.7718[25]		1094.6[46]		
			0.772[24]				
			0.7721[28]				
			0.7722[50]				
			0.7720[48]				
			0.77264[46]				
	323.15	0.764	0.7639[23]	1060.90	1061.20[27]	1.349	1.3491[25]
			0.7635[50]				

https://dx.doi.org/10.1021/acs.jced.0c00330
J. Chem. Eng. Data XXXX, XXX, XXX−XXX

Table 2. continued

component	T/(K)	$\rho/(10^3 \times \text{kg m}^{-3})$ exp.	$\rho/(10^3 \times \text{kg m}^{-3})$ lit.	$u/(\text{m·s}^{-1})$ exp.	$u/(\text{m·s}^{-1})$ lit.	n_D exp.	n_D lit.
			0.7630[48]				
propan-1-ol	293.15	0.804	0.80364[26]	1225.30	1224.3[51]	1.385	1.385[51]
			0.803[51]		1223.22[27]		1.3850[25]
			0.8036[52]		1223[28]		1.38494[28]
			0.8033[25]				1.385[53]
			0.8034[28]				1.3852[54]
			0.8036[48]				
			0.8032[53]				
			0.80410[54]				
			0.80428[55]				
	298.15	0.800	0.79991[37]	1208.03	1216[30]	1.383	1.3838[30]
			0.7996[39]		1207.3[51]		1.383[51]
			0.79958[41]		1216[32]		1.3838[33]
			0.7995[30]		1206[28]		1.3832[25]
			0.800[51]		1205.64[35]		1.3848[32]
			0.7996[52]		1205.69[56]		1.38307[28]
			0.79961[33]		1208.1[57]		1.38307[38]
			0.7995[25]				1.3830[49]
			0.8001[32]				1.38304[56]
			0.7995[28]				
			0.7995[38]				
			0.79947[35]				
			0.79962[49]				
			0.79975[56]				
			0.7995[57]				
			0.7996[58]				
	303.15	0.796	0.79548[41]	1190.90	1189.9[51]	1.381	1.381[51]
			0.79548[26]		1188.66[27]		1.3814[25]
			0.796[51]		1189[28]		1.38104[28]
			0.7956[52]		1192.6[57]		1.3811[54]
			0.7955[25]				
			0.79561[44]				
			0.7955[28]				
			0.7956[48]				
			0.7956[59]				
			0.79642[55]				
			0.7955[57]				
			0.79586[54]				
	313.15	0.788	0.78737[41]	1157.04	1156.0[51]	1.377	1.377[51]
			0.78702[26]		1154.72[27]		1.3774[25]
			0.788[51]		1155[28]		1.37676[28]
			0.7874[52]		1160.2[57]		
			0.7872[25]				
			0.7873[28]				
			0.7874[48]				
			0.7873[59]				
			0.78851[55]				
			0.7874[57]				
	323.15	0.780	0.780[51]	1123.41	1122.5[51]	1.373	1.373[51]
			0.7792[52]		1121.00[27]		1.3732[25]
			0.7791[48]				
			0.7786[59]				
			0.78102[55]				
propan-2-ol	293.15	0.786	0.785[51]	1159.32	1157.8[51]	1.377	1.377[51]
			0.7851[52]		1156[28]		1.37702[28]
			0.7849[28]				1.378[53]
			0.78535[55]				
			0.7872[53]				
	298.15	0.782	0.7818[31]	1141.33	1140.2[51]	1.375	1.375[51]

https://dx.doi.org/10.1021/acs.jced.0c00330
J. Chem. Eng. Data XXXX, XXX, XXX−XXX

Table 2. continued

component	T/(K)	$\rho/(10^3 \times \text{kg m}^{-3})$ exp.	$\rho/(10^3 \times \text{kg m}^{-3})$ lit.	$u/(\text{m·s}^{-1})$ exp.	$u/(\text{m·s}^{-1})$ lit.	n_D exp.	n_D lit.
			0.7813[39]		1139[28]		1.3751[33]
			0.78123[41]		1145.5[57]		1.3745[60]
			0.781[51]				1.37521[28]
			0.7809[52]				1.37496[61]
			0.78096[33]				1.37496[62]
			0.78098[60]				1.3752[40]
			0.7809[28]				1.37520[63]
			0.7810[61]				1.37515[64]
			0.7810[62]				
			0.7810[40]				
			0.78105[63]				
			0.78110[55]				
			0.7807[57]				
			0.7807[58]				
	303.15	0.777	0.77695[41]	1123.71	1122.6[51]	1.373	1.373[51]
			0.777[51]		1122[28]		1.37261[28]
			0.7767[52]		1126.3[57]		
			0.77659[44]				
			0.7766[28]				
			0.7768[50]				
			0.77712[55]				
			0.7765[57]				
			0.7772[65]				
	313.15	0.768	0.76798[41]	1088.43	1087.4[51]	1.369	1.369[51]
			0.768[51]		1086[28]		1.36821[28]
			0.7678[52]		1091.3[57]		
			0.7678[28]				
			0.7680[50]				
			0.76879[55]				
			0.7682[57]				
			0.7694[65]				
	323.15	0.759	0.759[51]	1052.76	1051.8[51]	1.364	1.364[51]
			0.7591[52]				
			0.7593[50]				
			0.75968[55]				
butan-1-ol	293.15	0.811	0.810[51]	1260.37	1258.4[51]	1.399	1.399[51]
			0.8089[25]		1257.66[27]		1.3988[25]
			0.80952[66]		1257[28]		1.3992[66]
			0.8095[28]		1257.5[46]		1.39924[28]
			0.8098[48]		1255.94[67]		1.3994[54]
			0.81034[54]				1.3997[68]
			0.80965[46]				
			0.80960[68]				
			0.80965[69]				
			0.80943[67]				
	298.15	0.807	0.8064[31]	1243.32	1244[30]	1.397	1.3984[30]
			0.80584[37]		1241.8[51]		1.397[51]
			0.8057[39]		1256[32]		1.3975[33]
			0.80576[41]		1241[28]		1.3973[70]
			0.8059[30]		1240.37[35]		1.3967[25]
			0.806[51]		1240.5[71]		1.3984[32]
			0.80577[34]		1240.2[72]		1.3972[66]
			0.805877[70]		1238.99[67]		1.39702[28]
			0.8054[25]		1239.2[73]		1.3973[49]
			0.8071[32]		1241.0[74]		1.3973[40]
			0.80558[66]				1.3972[54]
			0.8059[28]				
			0.80581[35]				
			0.80576[49]				

https://dx.doi.org/10.1021/acs.jced.0c00330
J. Chem. Eng. Data XXXX, XXX, XXX−XXX

Table 2. continued

component	T/(K)	$\rho/(10^3 \times \text{kg m}^{-3})$ exp.	$\rho/(10^3 \times \text{kg m}^{-3})$ lit.	$u/(\text{m·s}^{-1})$ exp.	$u/(\text{m·s}^{-1})$ lit.	n_D exp.	n_D lit.
			0.80576[72]				
			0.80562[67]				
	303.15	0.803	0.80201[41]	1226.42	1225.0[51]	1.395	1.395[51]
			0.802[51]		1223.55[27]		1.3947[25]
			0.8018[25]		1224[28]		1.3946[75]
			0.8019[75]		1223.6[46]		1.3963[66]
			0.80192[66]		1226.5[71]		1.39521[28]
			0.80191[44]		1223.25[76]		1.3953[54]
			0.8018[28]		1222.08[67]		
			0.8021[48]				
			0.80195[54]				
			0.80200[46]				
			0.80204[68]				
			0.803155[71]				
			0.80179[67]				
	313.15	0.795	0.79432[41]	1192.97	1191.8[51]	1.391	1.391[51]
			0.794[51]		1190.28[27]		1.3908[25]
			0.7940[25]		1190[28]		1.3920[66]
			0.79426[66]		1190.2[46]		1.39090[28]
			0.7941[28]		1189.92[76]		
			0.7943[48]		1189.9[72]		
			0.79421[46]		1188.6[73]		
			0.7967[65]		1189.5[74]		
			0.79431[68]				
			0.79423[76]				
			0.79422[72]				
			0.79416[73]				
			0.79420[74]				
	323.15	0.787	0.787[51]	1159.74	1158.7[51]	1.387	1.387[51]
			0.7864[48]		1157.19[27]		1.3867[25]
			0.78629[76]		1156.92[76]		
butan-2-ol	293.15	0.807	0.806[51]	1230.52	1230.1[51]	1.397	1.397[51]
			0.80554[66]		1230[28]		1.3971[66]
			0.8067[28]		1232.4[46]		1.39722[28]
			0.80734[46]		1228.38[67]		
			0.80648[67]				
	298.15	0.803	0.8024[30]	1212.49	1212.1[51]	1.395	1.3951[30]
			0.802[51]		1212[28]		1.395[51]
			0.80249[33]		1211.62[76]		1.3954[33]
			0.802362[70]		1212.2[72]		1.3948[70]
			0.80206[66]		1210.43[67]		1.3954[66]
			0.80256[60]		1211.5[73]		1.3948[60]
			0.8024[28]		1212.4[74]		1.39523[28]
			0.8028[65]				1.3951[77]
			0.80244[76]				1.39503[78]
			0.80241[72]				
			0.80239[67]				
			0.80220[73]				
			0.8027[77]				
			0.80241[78]				
	303.15	0.798	0.798[51]	1194.41	1194.1[51]	1.393	1.393[51]
			0.7988[75]		1195[28]		1.3903[75]
			0.79845[66]		1196.1[46]		1.3928[66]
			0.7984[28]		1193.54[76]		1.39288[28]
			0.79899[46]		1192.47[67]		
			0.7988[65]				
			0.79824[76]				
			0.79819[67]				
	313.15	0.790	0.789[51]	1157.98	1157.7[51]	1.389	1.389[51]

https://dx.doi.org/10.1021/acs.jced.0c00330
J. Chem. Eng. Data XXXX, XXX, XXX−XXX

Table 2. continued

component	T/(K)	$\rho/(10^3 \times \text{kg m}^{-3})$ exp.	$\rho/(10^3 \times \text{kg m}^{-3})$ lit.	$u/(\text{m·s}^{-1})$ exp.	$u/(\text{m·s}^{-1})$ lit.	n_D exp.	n_D lit.
			0.79007[66]		1157[28]		1.3890[66]
			0.7895[28]		1159.5[46]		1.38818[28]
			0.79028[46]		1157.12[76]		
			0.7911[65]		1157.5[72]		
			0.78956[76]		1157.1[73]		
			0.78963[72]		1155.3[72]		
			0.78959[73]				
			0.78941[74]				
	323.15	0.781	0.780[51]	1120.98	1120.7[51]	1.384	1.384[51]
			0.78047[76]		1120.16[76]		

[a]Standard uncertainties u are $u(T)$ = 0.02 K and $u(p)$ = 0.04 MPa and the combined expanded uncertainty U_c in mole fraction, density, speed of sound, and refractive index were $U_c(x)$ = 0.0006, $U_c(\rho)$ = 0.005 g·cm^{-3}, $U_c(u)$ = 1.33 m·s^{-1}, and $U_c(n)$ = 0.004, respectively (0.95 level of confidence).

Table 3. Densities, ρ, Speed of Sound, u, Isentropic Compressibility, κ_s, and Refractive Indices, n_D, for the Binary Systems (22MEE + Methanol or Ethanol or Propan-1-ol or Propan-2-ol or Butan-1-ol or Butan-2-ol) at (293.15, 303.15, 313.15, and 323.15) K and at Pressure p = 0.1 MPa[a]

x_1	$\rho/(10^3 \times \text{kg m}^{-3})$	$u/(\text{ms}^{-1})$	$\kappa_s/(10^{-12} \times \text{Pa}^{-1})$	n_D
		{22MEE (1) + Methanol (2)}		
		T = 293.15 K		
0.0000	0.792	1120.60	1006	1.329
0.1022	0.854	1200.39	813	1.355
0.1994	0.895	1255.85	709	1.374
0.3011	0.926	1300.11	639	1.387
0.4004	0.949	1333.37	592	1.397
0.4997	0.967	1359.33	559	1.405
0.6013	0.982	1380.72	534	1.411
0.6949	0.994	1396.62	516	1.416
0.7951	1.004	1410.96	501	1.420
0.8964	1.012	1422.78	488	1.423
1.0000	1.020	1433.62	477	1.426
		T = 303.15 K		
0.0000	0.782	1087.55	1081	1.325
0.1022	0.845	1167.77	868	1.352
0.1994	0.886	1223.10	755	1.370
0.3011	0.917	1267.25	679	1.384
0.4004	0.940	1300.36	629	1.394
0.4997	0.958	1326.11	593	1.401
0.6013	0.973	1347.29	566	1.407
0.6949	0.985	1363.11	547	1.412
0.7951	0.995	1377.30	530	1.416
0.8964	1.004	1389.24	516	1.419
1.0000	1.011	1398.97	506	1.423
		T = 313.15 K		
0.0000	0.773	1055.13	1163	1.321
0.1022	0.835	1135.34	929	1.349
0.1994	0.876	1190.52	805	1.367
0.3011	0.908	1234.49	723	1.381
0.4004	0.931	1267.43	668	1.390
0.4997	0.949	1292.95	630	1.398
0.6013	0.964	1313.96	601	1.404
0.6949	0.976	1329.62	580	1.408
0.7951	0.986	1343.64	562	1.413
0.8964	0.995	1355.46	547	1.416
1.0000	1.002	1365.06	536	1.419
		T = 323.15 K		
0.0000	0.763	1023.02	1252	1.317
0.1022	0.826	1103.27	995	1.346
0.1994	0.867	1158.24	860	1.364
0.3011	0.899	1201.98	770	1.377
0.4004	0.922	1234.71	711	1.387
0.4997	0.940	1260.03	670	1.394
0.6013	0.955	1280.86	638	1.401
0.6949	0.967	1296.34	616	1.405
0.7951	0.977	1310.20	596	1.409
0.8964	0.986	1321.87	581	1.412
1.0000	0.993	1331.34	568	1.415
		{22MEE (1) + Ethanol (2)}		
		T = 293.15 K		
0.0000	0.790	1162.46	937	1.361
0.1014	0.835	1212.88	814	1.375
0.1994	0.870	1251.46	734	1.385
0.3004	0.900	1285.89	672	1.393
0.4011	0.925	1315.20	625	1.401
0.5009	0.946	1341.32	587	1.407
0.5978	0.965	1363.40	558	1.412
0.6984	0.981	1384.30	532	1.416
0.8001	0.996	1402.53	511	1.420
0.9024	1.009	1420.18	491	1.423
1.0000	1.020	1433.62	477	1.426
		T = 303.15 K		
0.0000	0.781	1127.91	1006	1.357
0.1014	0.827	1179.12	870	1.371
0.1994	0.861	1218.03	783	1.381
0.3004	0.891	1252.50	715	1.389
0.4011	0.916	1281.77	664	1.397
0.5009	0.938	1307.76	624	1.403
0.5978	0.956	1329.86	592	1.408
0.6984	0.972	1350.67	564	1.412
0.8001	0.987	1368.80	541	1.416
0.9024	1.000	1386.45	520	1.420
1.0000	1.011	1398.97	506	1.423
		T = 313.15 K		
0.0000	0.772	1094.28	1081	1.353
0.1014	0.818	1145.68	932	1.367
0.1994	0.852	1184.68	836	1.377
0.3004	0.882	1219.20	763	1.386
0.4011	0.907	1248.39	707	1.393
0.5009	0.929	1274.29	663	1.399
0.5978	0.947	1296.32	628	1.404
0.6984	0.963	1317.07	598	1.409

https://dx.doi.org/10.1021/acs.jced.0c00330
J. Chem. Eng. Data XXXX, XXX, XXX−XXX

Table 3. continued

x_1	$\rho/(10^3 \times kg\ m^{-3})$	$u/(ms^{-1})$	$\kappa_s/(10^{-12} \times Pa^{-1})$	n_D
		T = 313.15 K		
0.8001	0.978	1335.10	574	1.412
0.9024	0.991	1352.65	551	1.416
1.0000	1.002	1365.06	536	1.419
		T = 323.15 K		
0.0000	0.764	1060.90	1164	1.349
0.1014	0.809	1112.46	999	1.363
0.1994	0.843	1151.53	894	1.374
0.3004	0.873	1186.06	814	1.383
0.4011	0.898	1215.18	754	1.390
0.5009	0.920	1241.01	706	1.396
0.5978	0.938	1262.97	668	1.400
0.6984	0.954	1283.65	636	1.405
0.8001	0.969	1301.58	609	1.409
0.9024	0.982	1319.05	585	1.412
1.0000	0.993	1331.34	568	1.415
		{22MEE (1) + Propan-1-ol (2)}		
		T = 293.15 K		
0.0000	0.804	1225.30	828	1.385
0.1021	0.837	1252.83	761	1.392
0.2041	0.866	1278.72	706	1.397
0.3039	0.892	1302.35	661	1.402
0.3978	0.914	1323.09	625	1.407
0.4989	0.936	1344.22	591	1.411
0.6028	0.956	1364.74	561	1.415
0.6986	0.974	1382.66	537	1.418
0.8015	0.991	1400.78	515	1.421
0.8987	1.005	1416.88	495	1.424
1.0000	1.020	1433.62	477	1.426
		T = 303.15 K		
0.0000	0.796	1190.90	886	1.381
0.1021	0.829	1218.88	812	1.388
0.2041	0.858	1244.87	752	1.393
0.3039	0.884	1268.59	703	1.398
0.3978	0.906	1289.39	664	1.403
0.4989	0.927	1310.57	628	1.407
0.6028	0.948	1331.06	596	1.411
0.6986	0.965	1348.91	570	1.414
0.8015	0.982	1366.97	545	1.417
0.8987	0.997	1383.05	525	1.420
1.0000	1.011	1398.97	506	1.423
		T = 313.15 K		
0.0000	0.788	1157.04	948	1.377
0.1021	0.821	1185.12	868	1.384
0.2041	0.850	1211.20	802	1.389
0.3039	0.875	1234.97	749	1.394
0.3978	0.897	1255.82	707	1.399
0.4989	0.919	1276.98	668	1.403
0.6028	0.939	1297.43	633	1.407
0.6986	0.956	1315.24	605	1.410
0.8015	0.973	1333.21	578	1.413
0.8987	0.988	1349.22	556	1.416
1.0000	1.002	1365.06	536	1.419
		T = 323.15 K		
0.0000	0.779	1123.41	1016	1.373
0.1021	0.812	1151.60	929	1.380
0.2041	0.841	1177.78	857	1.385
0.3039	0.867	1201.58	799	1.391
0.3978	0.888	1222.44	753	1.395
0.4989	0.910	1243.60	711	1.399
0.6028	0.930	1264.03	673	1.403
0.6986	0.947	1281.76	643	1.406
0.8015	0.964	1299.65	614	1.409
0.8987	0.979	1315.61	590	1.412
1.0000	0.993	1331.34	568	1.415
		{22MEE (1) + Propan-2-ol (2)}		
		T = 293.15 K		
0.0000	0.786	1159.32	947	1.377
0.1010	0.820	1194.71	855	1.385
0.2032	0.851	1229.03	778	1.391
0.2995	0.879	1259.44	718	1.397
0.4001	0.904	1288.78	666	1.403
0.5002	0.928	1316.52	622	1.407
0.6022	0.950	1343.07	584	1.412
0.6987	0.969	1366.70	553	1.416
0.7989	0.987	1389.96	524	1.420
0.9023	1.004	1412.53	499	1.423
1.0000	1.020	1433.62	477	1.426
		T = 303.15 K		
0.0000	0.777	1123.71	1019	1.373
0.1010	0.811	1160.01	916	1.380
0.2032	0.843	1194.58	831	1.387
0.2995	0.870	1225.16	766	1.393
0.4001	0.896	1254.71	709	1.399
0.5002	0.919	1282.58	662	1.404
0.6022	0.941	1309.21	620	1.408
0.6987	0.960	1332.86	586	1.412
0.7989	0.978	1356.12	556	1.416
0.9023	0.996	1378.66	529	1.419
1.0000	1.011	1398.97	506	1.423
		T = 313.15 K		
0.0000	0.768	1088.43	1099	1.369
0.1010	0.802	1125.11	984	1.376
0.2032	0.834	1159.99	891	1.383
0.2995	0.861	1190.84	819	1.389
0.4001	0.887	1220.58	757	1.395
0.5002	0.910	1248.60	705	1.399
0.6022	0.932	1275.29	660	1.404
0.6987	0.951	1299.00	623	1.408
0.7989	0.969	1322.25	590	1.412
0.9023	0.987	1344.78	560	1.416
1.0000	1.002	1365.06	536	1.419
		T = 323.15 K		
0.0000	0.759	1052.76	1188	1.364
0.1010	0.793	1090.03	1061	1.372
0.2032	0.825	1125.35	957	1.380
0.2995	0.852	1156.51	878	1.386
0.4001	0.878	1186.52	809	1.391
0.5002	0.901	1214.71	752	1.396
0.6022	0.923	1241.52	703	1.401
0.6987	0.942	1265.30	663	1.405
0.7989	0.960	1288.57	627	1.408
0.9023	0.978	1311.11	595	1.412
1.0000	0.993	1331.34	568	1.415
		{22MEE (1) + Butan-1-ol (2)}		
		T = 293.15 K		
0.0000	0.811	1260.37	776	1.399
0.1013	0.837	1276.63	733	1.402
0.2024	0.861	1293.49	694	1.406
0.3016	0.884	1310.33	659	1.408
0.3992	0.906	1327.15	627	1.411
0.5031	0.928	1345.28	596	1.414
0.6025	0.948	1362.09	569	1.417
0.6993	0.966	1379.77	544	1.419
0.7966	0.984	1396.84	521	1.422

https://dx.doi.org/10.1021/acs.jced.0c00330
J. Chem. Eng. Data XXXX, XXX, XXX−XXX

Table 3. continued

x_1	$\rho/(10^3 \times \text{kg m}^{-3})$	$u/(\text{ms}^{-1})$	$\kappa_s/(10^{-12} \times \text{Pa}^{-1})$	n_D
		T = 293.15 K		
0.8986	1.002	1414.90	498	1.424
1.0000	1.020	1433.62	477	1.426
		T = 303.15 K		
0.0000	0.803	1226.42	828	1.395
0.1013	0.829	1243.18	781	1.399
0.2024	0.853	1260.17	738	1.402
0.3016	0.876	1277.06	700	1.405
0.3992	0.898	1293.88	665	1.407
0.5031	0.919	1312.01	632	1.410
0.6025	0.939	1328.76	603	1.413
0.6993	0.958	1346.32	576	1.415
0.7966	0.976	1363.26	551	1.418
0.8986	0.994	1381.17	528	1.420
1.0000	1.011	1398.97	506	1.423
		T = 313.15 K		
0.0000	0.795	1192.97	884	1.391
0.1013	0.821	1209.88	832	1.395
0.2024	0.845	1226.96	786	1.398
0.3016	0.868	1243.92	745	1.401
0.3992	0.889	1260.73	708	1.404
0.5031	0.911	1278.80	671	1.406
0.6025	0.931	1295.45	641	1.409
0.6993	0.949	1312.93	611	1.412
0.7966	0.967	1329.71	585	1.414
0.8986	0.985	1347.43	559	1.416
1.0000	1.002	1365.06	536	1.419
		T = 323.15 K		
0.0000	0.787	1159.74	944	1.387
0.1013	0.813	1176.84	888	1.391
0.2024	0.837	1194.01	838	1.394
0.3016	0.860	1210.98	793	1.397
0.3992	0.881	1227.77	753	1.400
0.5031	0.902	1245.81	714	1.403
0.6025	0.922	1262.38	681	1.405
0.6993	0.940	1279.72	649	1.408
0.7966	0.958	1296.36	621	1.410
0.8986	0.976	1313.90	594	1.413
1.0000	0.993	1331.34	568	1.415
		{22MEE (1) + Butan-2-ol (2)}		
		T = 293.15 K		
0.0000	0.807	1230.52	819	1.397
0.1021	0.832	1248.99	770	1.400
0.2032	0.857	1268.76	725	1.404
0.3026	0.880	1288.92	684	1.407
0.4006	0.902	1308.82	647	1.410
0.4992	0.924	1329.37	613	1.413
0.6015	0.945	1350.66	580	1.416
0.7012	0.965	1371.29	551	1.419
0.7973	0.983	1391.41	525	1.421
0.8943	1.001	1411.18	502	1.424
1.0000	1.020	1433.62	477	1.426
		T = 303.15 K		
0.0000	0.798	1194.41	878	1.393
0.1021	0.824	1213.77	824	1.396
0.2032	0.849	1234.00	774	1.400
0.3026	0.872	1254.52	729	1.403
0.4006	0.894	1274.66	689	1.406
0.4992	0.915	1295.37	651	1.409
0.6015	0.936	1316.75	616	1.412
0.7012	0.956	1337.46	585	1.415
0.7973	0.975	1357.57	557	1.417
0.8943	0.992	1377.32	531	1.420
1.0000	1.011	1398.97	506	1.423
		T = 313.15 K		
0.0000	0.790	1157.98	944	1.389
0.1021	0.815	1178.18	884	1.392
0.2032	0.840	1199.02	828	1.395
0.3026	0.863	1219.95	778	1.399
0.4006	0.885	1240.41	734	1.402
0.4992	0.907	1261.33	693	1.405
0.6015	0.928	1282.81	655	1.408
0.7012	0.947	1303.60	621	1.411
0.7973	0.966	1323.71	591	1.413
0.8943	0.983	1343.45	563	1.416
1.0000	1.002	1365.06	536	1.419
		T = 323.15 K		
0.0000	0.781	1120.98	1020	1.384
0.1021	0.806	1142.30	950	1.388
0.2032	0.831	1163.89	888	1.391
0.3026	0.854	1185.35	833	1.395
0.4006	0.876	1206.15	784	1.398
0.4992	0.898	1227.32	740	1.401
0.6015	0.919	1248.98	698	1.404
0.7012	0.939	1269.87	661	1.407
0.7973	0.957	1290.03	628	1.410
0.8943	0.974	1309.78	598	1.412
1.0000	0.993	1331.34	568	1.415

[a]Standard uncertainties u are $u(T)$ = 0.02 K and $u(p)$ = 0.04 MPa and the combined expanded uncertainty U_c in mole fraction, density, speed of sound, and refractive index were $U_c(x)$ = 0.0006, $U_c(\rho)$ = 0.005 g·cm^{-3}, $U_c(u)$ = 1.33 m·s^{-1}, and $U_c(n)$ = 0.004, respectively (0.95 level of confidence).

The chemicals used in this work and their chemical abstract registry number (CAS number), suppliers, and the purities provided by their respective suppliers are included in Table 1. The water content was estimated before the experiments, and was found to be very low, which is also given in Table 1. This was accomplished by utilizing the Karl Fisher coulometer (756KF Coulometer Metrohm). Experimental values of density, speed of sound, and refractive index of the pure liquids are compared in Table 2 at (293.15, 298.15, 303.15, 313.15, and 323.15) K, and these values show good agreement with the published results.[7,9−78]

2.2. Apparatus and Procedure. Liquid solutions of various compositions of 22MEE with methanol, ethanol, propan-1-ol, propan-2-ol, butan-1-ol, and butan-2-ol were prepared by syringing weighed amounts of the pure liquids into bottles with airtight stoppers. The weighing was done on an OHAUS analytical balance with a standard uncertainty of 0.0001 g. The standard uncertainty in the mole fraction is 0.0006. Density and speed of sound measurements of the pure components and their mixtures were carried out using an Anton Paar DSA 5000M digital vibrating tube densimeter with a standard uncertainty of 0.02 K in temperature. The speed of sound values were measured using a propagation time technique.[79] The combined expanded uncertainty in experimental measurements has been found to be 0.005 g·cm^{-3} for the density and 1.33 m·s^{-1} for the speed of sound.

https://dx.doi.org/10.1021/acs.jced.0c00330
J. Chem. Eng. Data XXXX, XXX, XXX−XXX

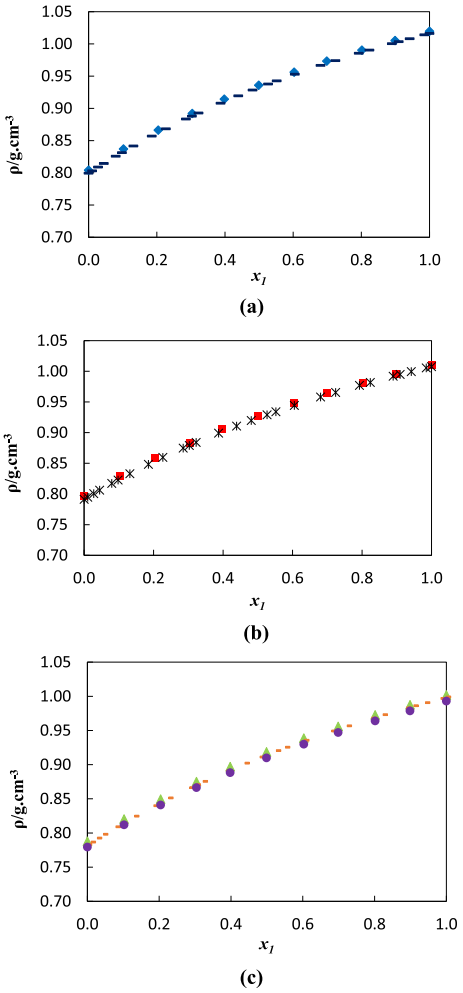

Figure 1. Plot of density for the binary system {22MEE (1) + propan-1-ol (2)} as a function of the composition expressed in the mole fraction of 22MEE at temperatures of (a) 293.15 K (blue ◆), (b) 303.15 K (red ■), and (c) 313.15 K (green ▲) and 323.15 K (violet ●) together with the literature[6] at (a) 298.15 K (dark blue —), (b) 308.15 K (black *), and (c) 318.15 K (brown -).

Refractive indices for the sodium D-line were determined using the digital refractometer Abbemat 300, Anton Paar with a standard uncertainty of 0.02 K in temperature. The combined expanded uncertainty has been found to be 0.004 for the refractive index. Ultrapure water supplied by SH Calibration Service GmbH Graz and dried air was used for the calibration of the Anton Paar DSA 5000M digital vibrating tube densimeter as well as digital refractometer Abbemat 300, Anton Paar at each temperature. Each experimental device used in this study was validated by measuring the data of pure components and the data were compared to literature values given in Table 2. The difference between the experimental and literature data was within the experimental error. The reported uncertainty values in the measured as well as derived thermodynamic parameters were calculated as per error propagation methods.[80]

3. RESULTS AND DISCUSSION

3.1. Density, Speed of Sound, and Refractive Indices. In the present work, the experimentally determined densities, speed of sound, and refractive indices at (293.15, 303.15, 313.15, and 323.15) K and at pressure p = 0.1 MPa for the binary mixtures (22MEE + methanol or ethanol or propan-1-ol or propan-2-ol or butan-1-ol or butan-2-ol), over the complete composition range expressed by mole fraction x_1 of 22MEE,

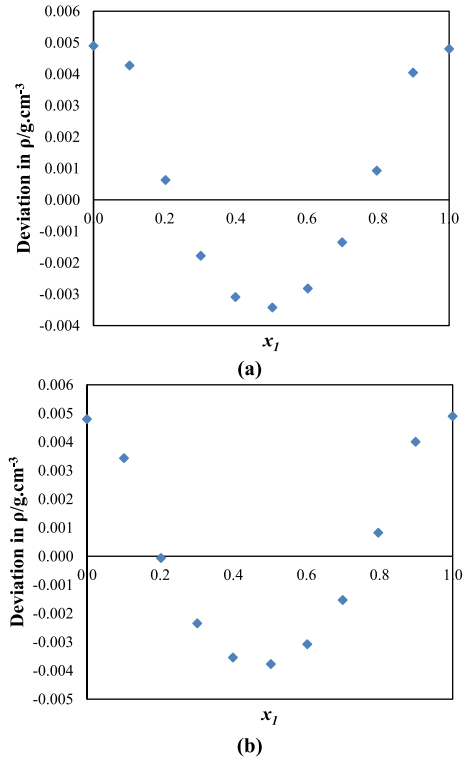

Figure 2. Plot of deviation in densities, ρ, of binary mixture {22MEE (1) + butan-1-ol (2)} with the literature data[7] at (a) 293.15 K (blue ◆) and (b) 303.15 K (blue ◆).

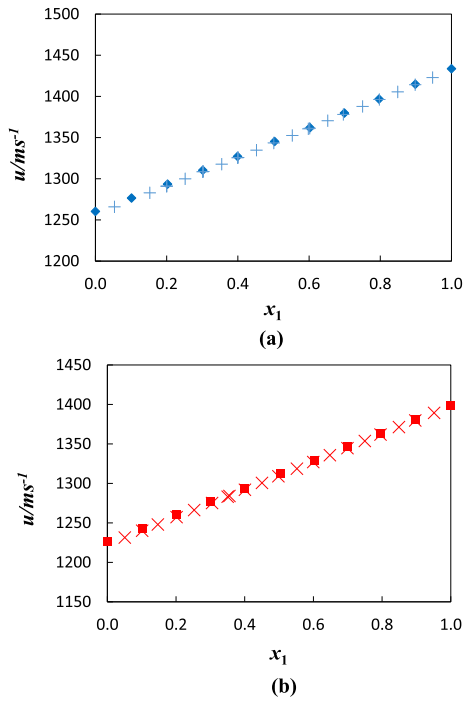

Figure 3. Plot of speed of sound for the binary system {22MEE (1) + butan-1-ol (2)} as a function of the composition expressed in the mole fraction of 22MEE at temperatures of (a) 293.15 K (blue ◆) and (b) 303.15 K (red ■) together with the literature data[7] at (a) 293.15 K (blue +) and (b) 303.15 K (blue ×).

https://dx.doi.org/10.1021/acs.jced.0c00330
J. Chem. Eng. Data XXXX, XXX, XXX−XXX

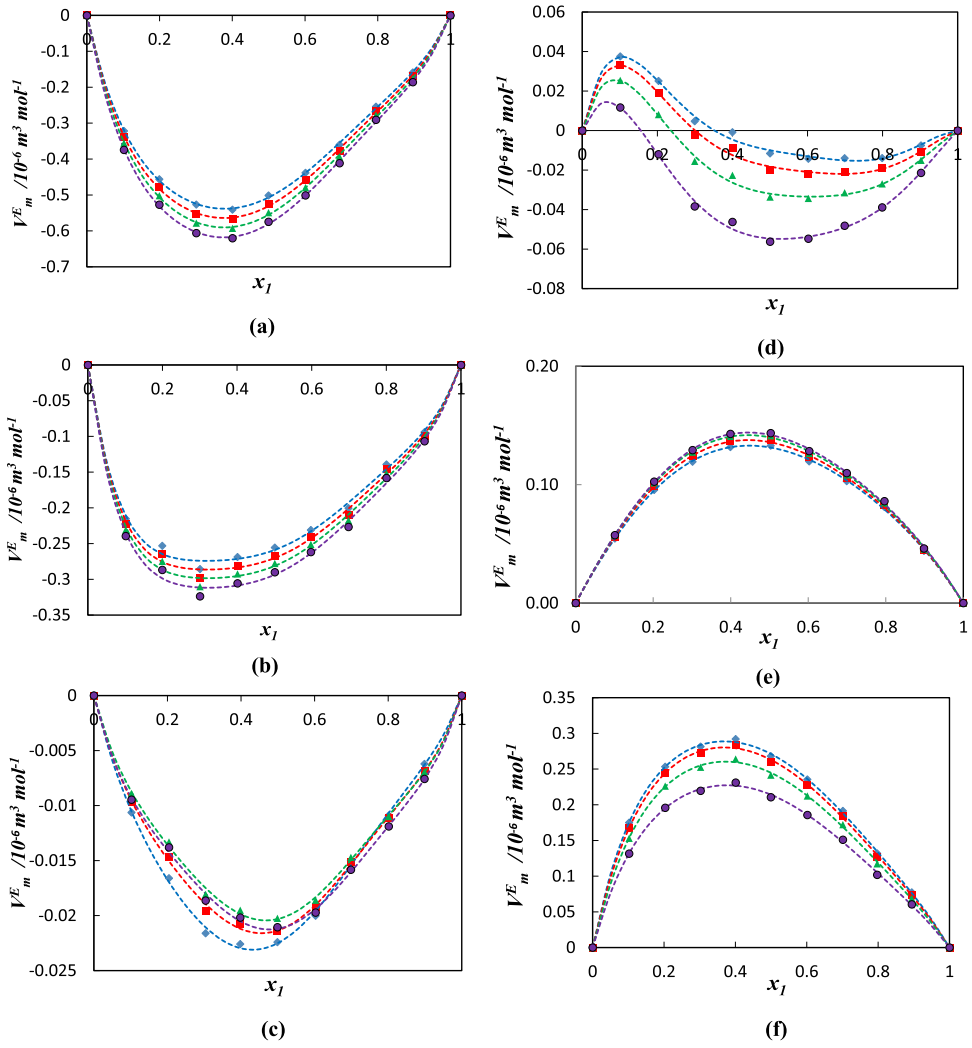

Figure 4. Plot of excess molar volumes, V^E_m, for the binary mixtures: (a) {22MEE (1) + methanol (2)}, (b) {22MEE (1) + ethanol (2)}, (c) {22MEE (1) + propan-1-ol (2)}, (d) {22MEE (1) + propan-2-ol (2)}, (e) {22MEE (1) + butan-1-ol (2)}, and (f) {22MEE (1) + butan-2-ol (2)} as a function of the composition expressed in the mole fraction of 22MEE at 293.15 K (blue ◆), 303.15 K (red ■), 313.15 K (green ▲), and 323.15 K (violet ●). The dotted lines were generated using Redlich−Kister polynomial curve fitting.

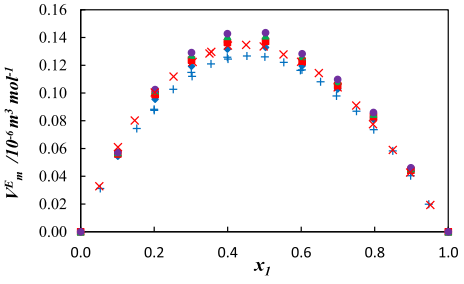

Figure 5. Plot of excess molar volumes, V^E_m, for the binary mixtures {22MEE (1) + butan-1-ol (2)} at 293.15 K (blue ◆), 303.15 K (red ■), 313.15 K (green ▲), and 323.15 K (violet ●) together with the literature data[7] at 293.15 K (blue +) and 303.15 K (red ×).

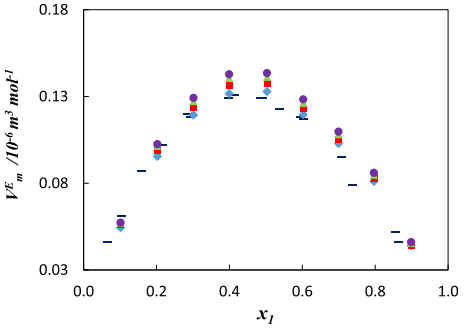

Figure 6. Plot of excess molar volumes, V^E_m, for the binary mixtures {22MEE (1) + butan-1-ol (2)} at 293.15 K (blue ◆), 303.15 K (red ■), 313.15 K (green ▲), and 323.15 K (violet ●) together with the literature data[8] at 298.15 K (dark blue —).

are presented in Table 3. As the results show, increasing temperature from (293.15 to 323.15) K decreases the values of ρ, u, and n_D for all binary systems.

The experimental data of the binary mixtures of 22MEE with methanol, ethanol, propan-2-ol, and butan-2-ol measured here cannot be compared to the data in the literature because, to the best of our knowledge, these systems apparently were not previously measured.

In Figure 1, the experimental density values for the binary system {22MEE (1) + propan-1-ol (2)} at temperatures of (293.15, 303.15, 313.15, and 323.15) K and those reported by Pal and Kumar[6] at temperatures of (298.15, 308.15, and 318.15) K are compared and show a good agreement.

https://dx.doi.org/10.1021/acs.jced.0c00330
J. Chem. Eng. Data XXXX, XXX, XXX−XXX

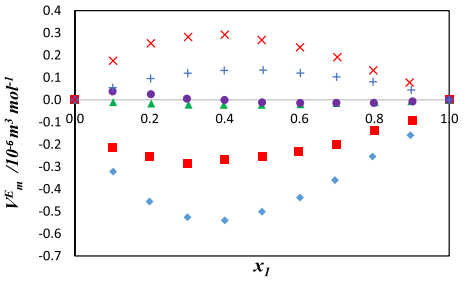

Figure 7. Plot of excess molar volumes, V^E_m, for the binary mixtures of 22MEE with methanol (blue ◆), ethanol (red ■), propan-1-ol (green ▲), propan-2-ol (violet ●), butan-1-ol (blue +), and butan-2-ol (red ×) at 293.15.

In Figure 2, the plot of deviation in density between the experimental density values and those reported by Mozo et al.[7] for the binary system {22MEE (1) + butan-1-ol (2)} at temperatures of (293.15 and 303.15) K shows a good agreement and the maximum deviation was found to be within the experimental error as reported.

Speed of sound, u, for the binary mixture {22MEE (1) + butan-1-ol (2)} at temperatures of (293.15 and 303.15) K together with the literature data reported by Mozo et al.[7] at

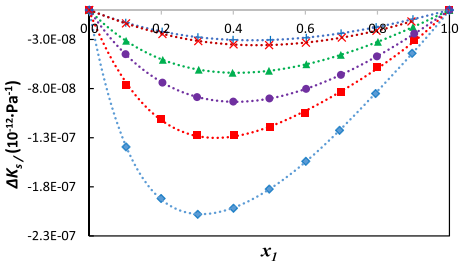

Figure 9. Plot of deviation in isentropic compressibility, $\Delta\kappa_s$, for the binary mixtures of 22MEE with methanol (blue ◆), ethanol (red ■), propan-2-ol (violet ●), propan-1-ol (green ▲), butan-2-ol (red ×), and butan-1-ol (blue +) at 293.15 K.

(293.15 and 303.15) K are plotted in Figure 3 for a comparison purpose. From Figure 3, it can be seen that the experimental, u, values are in a good accordance with those reported by Mozo et al.[7]

3.2. Excess Molar Volumes. The excess molar volumes, V^E_m, for the studied systems were calculated from densities of the pure liquids and their mixtures using standard equation given elsewhere.[51] The corresponding V^E_m values of all the mixtures measured at different temperatures are presented in Table S1 and plotted against the mole fraction of 22MEE in

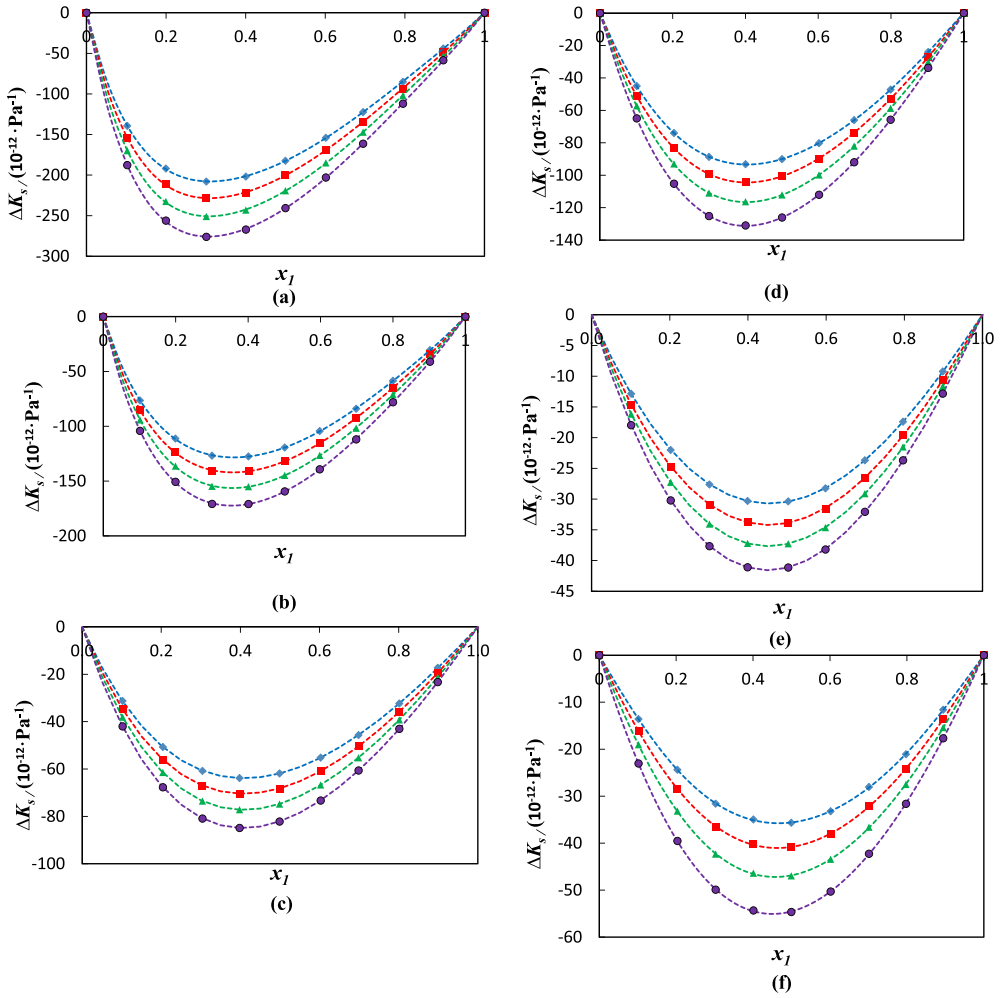

Figure 8. Plot of deviation in isentropic compressibility, $\Delta\kappa_s$, for the binary mixtures: (a) {22MEE (1) + methanol (2)}, (b) {22MEE (1) + ethanol (2)}, (c) {22MEE (1) + propan-1-ol (2)}, (d) {22MEE (1) + propan-2-ol (2)}, (e) {22MEE (1) + butan-1-ol (2)}, and (f) {22MEE (1) + butan-2-ol (2)} as a function of the composition expressed in the mole fraction of 22MEE at 293.15 K (blue ◆), 303.15 K (red ■), 313.15 K (green ▲), and 323.15 K (violet ●). The dotted lines were generated using Redlich−Kister polynomial curve fitting.

https://dx.doi.org/10.1021/acs.jced.0c00330
J. Chem. Eng. Data XXXX, XXX, XXX−XXX

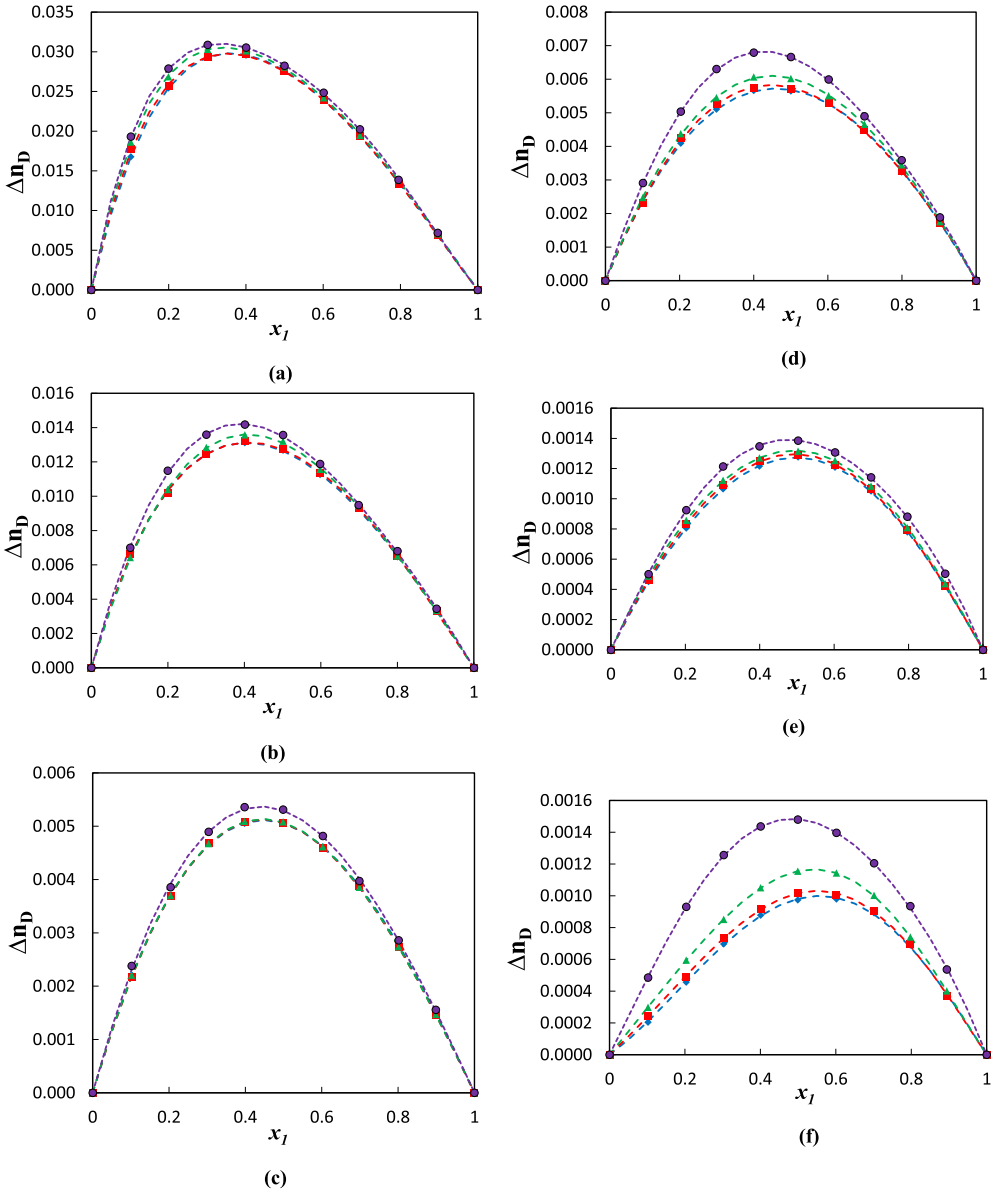

Figure 10. Plot of deviation in the refractive index, Δn_D, for the binary mixtures: (a) {22MEE (1) + methanol (2)}, (b) {22MEE (1) + ethanol (2)}, (c) {22MEE (1) + propan-1-ol (2)}, (d) {22MEE (1) + propan-2-ol (2)}, (e) {22MEE (1) + butan-1-ol (2)}, and (f) {22MEE (1) + butan-2-ol (2)} as a function of the composition expressed in the mole fraction of 22MEE at 293.15 K (blue ◆), 303.15 K (red ■), 313.15 K (green ▲), and 323.15 K (violet ●). The dotted lines were generated using Redlich−Kister polynomial curve fitting.

Figure 4a−f. For the binary mixture of (22MEE + methanol or + ethanol or + propan-1-ol), the negative values of V_m^E are observed. The V_m^E values of the 22MEE + methanol mixture are more negative than those observed for the (22MEE + ethanol) and (22MEE + propan-1-ol) mixtures. For the mixtures of (22MEE with butan-1-ol or butan-2-ol), the positive V_m^E values increase systematically in the order stated for the liquids. Both positive and negative V_m^E values are observed for the (22MEE + propan-2-ol) system, which has a sinusoidal shape.

The molecules of the alkoxyalkanols are self-associated as the alcohols.[1] The effect of the simultaneous presence of etheric and alcoholic oxygen atoms in the same molecule of alkoxyalkanol and the presence of the etheric oxygen improve the ability of the −OH group[2] to form hydrogen bonds in the alkoxyalkanol molecules. As already mentioned below, the V_m^E values are negative over the complete composition range in the case of methanol, ethanol, and propan-1-ol systems and positive for the butan-1-ol and butan-2-ol systems. These results may be explained by the depolymerization of self-associated alkoxyalkanols by the alcohols and self-associated alcohols by the alkoxyalkanols, which contribute to the expansion of volume and the hydrogen bond formation between alkoxyalkanols and alcohols leading to volume contraction.[81] According to the V_m^E results, we can suggest that expansion of volume is dominant in butan-1-ol and butan-2-ol systems, while the contraction in volume is dominant in methanol, ethanol, and propan-1-ol systems. The positive deviations are mostly because of H-bond breaking, while negative could be because of weak specific interactions between unlike molecules.[81] The V_m^E values decrease with an increase of temperature for (22MEE + methanol, or +ethanol, or +propan-2-ol, or +butan-2-ol) binary mixtures may be because of a decrease of packing efficiency between 22MEE and methanol, or +ethanol, or +propan-2-ol, or +butan-2-ol, and

https://dx.doi.org/10.1021/acs.jced.0c00330
J. Chem. Eng. Data XXXX, XXX, XXX−XXX

Table 4. Coefficients A_i, and Standard Deviations, σ, Obtained for the Binary Systems Studied in This Work at Different Temperatures and at Pressure p = 0.1 MPa Using the Redlich−Kister Equation[a]

	T (K)	A_1	A_2	A_3	A_4	A_5	σ
			{22MEE (1) + Methanol (2)}				
$V_m^E/(10^{-6} \times m^3 \cdot mol^{-1})$	293.15	−2.027	1.009	−0.154	0.184	−1.165	0.006
	303.15	−2.123	1.064	−0.159	0.178	−1.265	0.006
	313.15	−2.220	1.121	−0.161	0.183	−1.364	0.006
	323.15	−2.322	1.182	−0.166	0.195	−1.475	0.007
$\Delta\kappa_s/(10^{-12} \times Pa^{-1})$	293.15	−729.92	473.34	−291.41	280.55	−202.02	0.68
	303.15	−801.21	521.42	−321.13	311.62	−241.36	0.78
	313.15	−877.87	574.27	−354.98	348.54	−271.80	0.89
	323.15	−963.58	633.17	−392.78	392.99	−309.34	1.02
Δn_D	293.15	0.111	−0.058	0.029	−0.014		0.0001
	303.15	0.110	−0.056	0.034	−0.027		0.0002
	313.15	0.112	−0.060	0.042	−0.029		0.0002
	323.15	0.113	−0.059	0.047	−0.041		0.0002
			{22MEE (1) + Ethanol (2)}				
$V_m^E/(10^{-6} \times m^3 \cdot mol^{-1})$	293.15	−1.036	0.384	−0.276	0.653	−1.134	0.010
	303.15	−1.081	0.406	−0.297	0.651	−1.158	0.010
	313.15	−1.126	0.427	−0.317	0.664	−1.173	0.011
	323.15	−1.175	0.452	−0.336	0.672	−1.195	0.011
$\Delta\kappa_s/(10^{-12} \times Pa^{-1})$	293.15	−478.16	239.34	−116.14	105.97	−99.73	0.40
	303.15	−528.08	266.79	−133.81	118.40	−116.90	0.43
	313.15	−580.17	295.78	−150.74	131.85	−127.60	0.48
	323.15	−638.73	328.37	−169.36	147.57	−141.02	0.54
Δn_D	293.15	0.051	−0.019	0.006	−0.003		0.0001
	303.15	0.051	−0.018	0.005	−0.005		0.0001
	313.15	0.052	−0.021	0.002	0.001		0.0001
	323.15	0.054	−0.025	0.007	0.002		0.0001
			{22MEE (1) + Propan-1-ol (2)}				
$V_m^E/(10^{-6} \times m^3 \cdot mol^{-1})$	293.15	−0.090	0.035	0.031	−0.010	−0.053	0.001
	303.15	−0.085	0.022	0.037	−0.007	−0.069	0.001
	313.15	−0.081	0.016	0.040	−0.006	−0.074	0.001
	323.15	−0.085	0.011	0.039	0.001	−0.080	0.001
$\Delta\kappa_s/(10^{-12} \times Pa^{-1})$	293.15	−247.44	87.27	−29.61	12.12		0.08
	303.15	−272.63	96.01	−36.79	12.73		0.03
	313.15	−298.84	106.01	−40.35	13.85		0.02
	323.15	−328.39	117.42	−44.90	15.45		0.03
Δn_D	293.15	0.020	−0.004	0.001	0.001		0.0001
	303.15	0.020	−0.005	−0.001	0.001		0.0001
	313.15	0.020	−0.005	−0.001	0.001		0.0001
	323.15	0.021	−0.005	0.001	0.001		0.0001
			{22MEE (1) + Propan-2-ol (2)}				
$V_m^E/(10^{-6} \times m^3 \cdot mol^{-1})$	293.15	−0.040	−0.073	0.066	−0.368	0.399	0.003
	303.15	−0.073	−0.074	0.073	−0.358	0.364	0.002
	313.15	−0.128	−0.060	0.069	−0.344	0.343	0.003
	323.15	−0.219	−0.028	0.054	−0.316	0.315	0.003
$\Delta\kappa_s/(10^{-12} \times Pa^{-1})$	293.15	−360.10	134.47	−51.35	7.15	20.90	0.12
	303.15	−402.62	151.07	−56.36	12.38	6.17	0.13
	313.15	−448.80	170.79	−63.65	14.71	5.49	0.14
	323.15	−504.45	195.52	−73.49	19.04	2.99	0.15
Δn_D	293.15	0.023	−0.004	0.001	−0.001		0.0001
	303.15	0.023	−0.005	0.001	0.002		0.0001
	313.15	0.024	−0.005	0.001	0.001		0.0001
	323.15	0.027	−0.009	0.001	0.003		0.0001
			{22MEE (1) + Butan-1-ol (2)}				
$V_m^E/(10^{-6} \times m^3 \cdot mol^{-1})$	293.15	0.526	−0.109	0.035	0.069		0.002
	303.15	0.544	−0.121	0.027	0.077		0.002
	313.15	0.560	−0.129	0.021	0.090		0.002
	323.15	0.569	−0.131	0.014	0.097		0.002
$\Delta\kappa_s/(10^{-12} \times Pa^{-1})$	293.15	−121.85	22.53	0.21	4.41		0.05
	303.15	−135.68	25.07	−4.41	4.51		0.06
	313.15	−149.30	28.32	−4.96	4.87		0.05

https://dx.doi.org/10.1021/acs.jced.0c00330
J. Chem. Eng. Data XXXX, XXX, XXX−XXX

Table 4. continued

	T (K)	A_1	A_2	A_3	A_4	A_5	σ
			{22MEE (1) + Butan-1-ol (2)}				
	323.15	−164.72	31.90	−6.15	6.39		0.06
Δn_D	293.15	0.005	0.001	0.001	0.001		0.0001
	303.15	0.005	0.001	0.001	0.001		0.0001
	313.15	0.005	0.001	0.001	0.001		0.0001
	323.15	0.006	−0.001	0.001	0.001		0.0001
			{22MEE (1) + Butan-2-ol (2)}				
$V_m^E/(10^{-6} \times m^3 \cdot mol^{-1})$	293.15	1.085	−0.520	0.186	−0.270	0.388	0.004
	303.15	1.052	−0.513	0.176	−0.235	0.335	0.004
	313.15	0.979	−0.475	0.146	−0.198	0.303	0.004
	323.15	0.856	−0.414	0.110	−0.151	0.262	0.004
$\Delta\kappa_s/(10^{-12} \times Pa^{-1})$	293.15	−142.36	19.55	−0.25	−5.90	17.25	0.12
	303.15	−163.20	24.45	−2.12	−6.74	11.72	0.12
	313.15	−187.41	32.04	−4.22	−6.09	11.60	0.13
	323.15	−218.11	42.96	−8.92	−4.25	11.47	0.14
Δn_D	293.15	0.004	0.001	−0.001	0.001		0.0001
	303.15	0.004	0.001	−0.001	0.001		0.0001
	313.15	0.005	0.001	−0.001	−0.001		0.0001
	323.15	0.006	0.001	−0.001	0.001		0.0001

[a]Standard uncertainties u are $u(T)$ = 0.02 K and $u(p)$ = 0.04 MPa and the combined expanded uncertainty U_c in mole fraction, density, speed of sound, and refractive index were $U_c(x)$ = 0.0006, $U_c(\rho)$ = 0.005 g·cm^{-3}, $U_c(u)$ = 1.33 m·s^{-1}, and $U_c(n)$ = 0.004, respectively (0.95 level of confidence).

vice versa for (22MEE + propan-1-ol, or+ butan-1-ol) binary mixtures where increases.

The excess molar volumes, V_m^E, for the binary mixtures {22MEE (1) + butan-1-ol (2)} at temperatures of (293.15, 303.15, 313.15, and 323.15) K together with literature data reported by Mozo et al.[7] at (293.15 and 303.15) K and those reported by Cobos et al.[8] at (298.15 K) are plotted in Figures 5 and 6 respectively, for the comparison purpose. From these figures, it can be observed that the experimental, V_m^E, values are in good accordance with the literature data reported by Mozo et al.[7] and by Cobos et al.[8] respectively.

In Figure 7, experimental, V_m^E, values of each system at 293.15 K are plotted, which shows that excess molar volumes, V_m^E, increase as the chain length of alcohol increases at the same temperature. However, 22MEE interacts more strongly with methanol. The difference in the size of unlike molecules is an important factor.

3.3. Isentropic Compressibility and Deviation in Isentropic Compressibility. Isentropic compressibility κ_s and deviations in isentropic compressibility, $\Delta\kappa_s$, were determined from experimental densities, ρ, and speeds of sound, u, using the standard equations given elsewhere.[51] The isentropic compressibility, κ_s, values for studied mixtures at (293.15, 303.15, 313.15, and 323.15) K are given in Table 3. Table 3 indicates that isentropic compressibility, κ_s, values increase with an increase in temperature at a fixed composition for all investigated systems owing to an increase in thermal agitation, which makes the solution more compressible.[82] In addition, the κ_s values decrease with the decrease in the concentration of 22MEE at a fixed temperature for all binary mixtures.

The calculated $\Delta\kappa_s$ values for the selected binary mixtures are also listed in Table S1. The change of this property with the mole fraction of 22MEE is shown in Figure 8a−f. It is evident from Figure 8a−f and Table S1 that the $\Delta\kappa_s$ values are negative over the entire mole fraction range and become more negative with increasing temperature for all binary mixtures.

In Figure 9, experimental, $\Delta\kappa_s$, values of each system at 293.15 K are plotted, which indicate that the $\Delta\kappa_s$ values increases with the increasing chain length of the alcohols. The values of $\Delta\kappa_s$ in terms of negativity are enhanced in the following order: methanol > ethanol > propan-2-ol > propan-1-ol > butan-2-ol > butan-1-ol. These results indicate that the (22MEE + butan-1-ol) mixture is the most compressible, which confirms weaker interactions in the mixtures containing higher alcohols.[83−86]

3.4. Deviation in Refractive Index. Refractive index deviations, Δn_D, were calculated using standard equation given elsewhere.[51] The Δn_D data for the studied systems (22MEE + methanol or + ethanol or + propan-1-ol or + propan-2-ol or + butan-1-ol or + butan-2-ol) at (293.15, 303.15, 313.15, and 323.15) K are listed in Table S1 and plotted versus the mole fraction of 22MEE in Figure 10a−f. It can be seen that the changes in the refractive index of all mixtures are positive throughout the entire composition range; while the chain length of the alkanol decreases the change in the refractive index becomes more positive. The same can be said about the change in refractive indices of these mixtures at higher temperatures, which were slightly more positive than they were at 293.15 K.

3.5. Correlation of Derived Properties. The results of excess molar volume, V_m^E, deviations in isentropic compressibility, $\Delta\kappa_s$, and changes of refractive index, Δn_D, of the (22MEE + methanol or + ethanol or + propan-1-ol or + propan-2-ol or + butan-1-ol or + butan-2-ol) mixtures have been fitted to the Redlich−Kister polynomial equation.[5] In each case, the optimum number of coefficients was ascertained from an examination of the variation of standard deviation, (σ).[5] Table 4 presents the values of the fitting parameters A_i together with the standard deviation, σ. The values of V_m^E, $\Delta\kappa_s$, and Δn_D as well as the plots of the Redlich−Kister model are displayed in Figures 4a−f, 8a−f and 10a−f, respectively. The agreement between the experimental data and those calculated using the Redlich−Kister equation was satisfactory at the investigated temperatures for all the systems.

4. CONCLUSIONS

The investigated mixtures were chosen in order to discuss the nature of interactions between their components. In this work, density, speed of sound, and refractive index have been

https://dx.doi.org/10.1021/acs.jced.0c00330
J. Chem. Eng. Data XXXX, XXX, XXX−XXX

measured at (293.15, 303.15, 313.15, and 323.15) K for six binary mixtures (22MEE + methanol), (22MEE + ethanol), (22MEE + propan-1-ol), (22MEE + propan-2-ol), (22MEE + butan-1-ol), and (22MEE + butan-2-ol). These data have been used to calculate the excess molar volumes, isentropic compressibility, deviation in isentropic compressibility, and deviation in refractive indices. According to the obtained results, it may be concluded that the lower alkanols were found to associate more strongly with 22MEE molecules as compared with the higher ones.

■ ASSOCIATED CONTENT

Supporting Information

The Supporting Information is available free of charge at https://pubs.acs.org/doi/10.1021/acs.jced.0c00330.

Excess molar volume, V_m^E, deviation in refractive index, Δn_D, and deviation in isentropic compressibility, $\Delta\kappa_s$, for the binary systems {22MEE (1) + methanol (2) or ethanol (2) or propan-1-ol (2) or propan-2-ol (2) or butan-1-ol (2) or butan-2-ol (2)} at (293.15, 303.15, 313.15, and 323.15) K and at p = 0.1 MPa (PDF)

■ AUTHOR INFORMATION

Corresponding Author

Latifa Negadi − *LATA2M, Laboratoire de Thermodynamique Appliquée et Modélisation Moléculaire, University of Tlemcen, Tlemcen 13000, Algeria; Thermodynamics Research Unit, School of Engineering, University of KwaZulu-Natal, Durban 4041, South Africa;* orcid.org/0000-0003-1977-8229; Email: latifa.negadi@univ-tlemcen,dz, latifanegadi@yahoo,fr

Authors

Djazia Belhadj − *LATA2M, Laboratoire de Thermodynamique Appliquée et Modélisation Moléculaire, University of Tlemcen, Tlemcen 13000, Algeria*

Indra Bahadur − *Chemistry Department, Faculty of Natural and Agricultural Sciences, North-West University, Mmabatho 2735, South Africa;* orcid.org/0000-0003-2906-473X

Amina Negadi − *LATA2M, Laboratoire de Thermodynamique Appliquée et Modélisation Moléculaire, University of Tlemcen, Tlemcen 13000, Algeria*

Natalia Muñoz-Rujas − *Departamento de Ingeniería Electromecánica, Universidad de Burgos, Escuela Politécnica Superior, Burgos 09006, Spain;* orcid.org/0000-0003-2185-1392

Eduardo Montero − *Departamento de Ingeniería Electromecánica, Universidad de Burgos, Escuela Politécnica Superior, Burgos 09006, Spain;* orcid.org/0000-0001-9948-3767

Complete contact information is available at: https://pubs.acs.org/10.1021/acs.jced.0c00330

Notes

The authors declare no competing financial interest.

■ ACKNOWLEDGMENTS

The authors (L.N.) and (A.N.) acknowledge funding from DGRSDT (Algeria).

■ REFERENCES

(1) Barbés, B.; García, I.; González, J. A.; Cobos, J. C.; Casanova, C. Excess properties of (an n-alkoxyethanol + an organic solvent) VI. VEm{xCH3(CH2)-1O(CH2)2O(CH2)2OH + (1 - x)C6H5CH3} for v = 1, 2, and 4 at the temperature 298.15 K. *J. Chem. Thermodyn.* **1994**, *26*, 791−795.

(2) Buckley, P.; Brochu, M. Microwave Spectrum, Dipole Moment, and Intramolecular Hydrogen Bond of 2-Methoxyethanol. *Can. J. Chem.* **1972**, *50*, 1149−1156.

(3) Zéberg-Mikkelsen, C. K.; Lugo, L.; García, J.; Fernández, J. Volumetric properties under pressure for the binary system ethanol +toluene. *Fluid Phase Equilib.* **2005**, *235*, 139−151.

(4) Csikos, R.; Pallay, I.; Laky, J. Low-lead fuel with MTBE and C alcohols. *Hydrocarbon Process.* **1976**, *55*, 121−125.

(5) Redlich, O.; Kister, A. T. Algebraic Representation of Thermodynamic Properties and the Classification of Solutions. *Ind. Eng. Chem.* **1948**, *40*, 345−348.

(6) Pal, A.; Kumar, A. Excess molar volumes and viscosities of binary liquid mixtures of 1-propanol+ ethylene glycol monomethyl ether, + diethylene glycol monomethyl ether, and+ triethylene glycol monomethyl ether at (298.15, 308.15 and 318.15) K. *J. Indian Chem. Soc.* **2004**, *81*, 375−383.

(7) Mozo, I.; García de la Fuente, I.; González, J. A.; Cobos, J. C. Thermodynamics of Mixtures Containing Alkoxyethanols. XXIV. Densities, Excess Molar Volumes, and Speeds of Sound at (293.15, 298.15, and 303.15) K and Isothermal Compressibilities at 298.15 K for 2-(2-Alkoxyethoxy)ethanol + 1-Butanol Systems. *J. Chem. Eng. Data* **2007**, *52*, 2086−2090.

(8) Cobos, J. C.; Garcia, I.; Casanova, C.; Roux-Desgranges, G.; Grolier, J.-P. E. Excess properties of mixtures of some n-alkoxyethanols with organic solvents. *Thermochim. Acta* **1988**, *131*, 73−78.

(9) Kim, J.; Kim, M. Excess Molar Enthalpies and Excess Molar Volumes for the Binary Mixtures {1, 2-dichloropropane+ 2-(2-methoxyethoxy) ethanol, and+ 2-(2-ethoxyethoxy) ethanol} at 298.15 K. *Korean Chem. Eng. Res.* **2006**, *44*, 444−452.

(10) Kinart, C. M.; Nowak, K.; Kinart, W. J. Volumetric properties of binary mixtures of alkoxyethanols with ethyl tert-butyl ether at various temperatures. *J. Chem. Thermodyn.* **2005**, *37*, 423−429.

(11) Riddick, J. A.; Bunger, W. B.; Sakano, T. K. *Organic Solvents: Physical Properties and Methods of Purification*, 4th ed.; Wiley: United States, 1986.

(12) Pal, A.; Singh, Y. P. The speed of sound and isentropic functions of {xH(CH2)ν(OC2H4)2OH + (1−x)(C4H9)O} (ν = 1, 2, and 4) at the temperature 298.15 K. *J. Chem. Thermodyn.* **1996**, *28*, 1197−1205.

(13) Carmona, F. J.; González, J. A.; García de la Fuente, I.; Cobos, J. C. Thermodynamic Properties of N-Alkoxyethanols + Organic Solvent Mixtures. X. Liquid−Liquid Equilibria of Systems Containing 2-Methoxyethanol, 2-(2-Methoxyethoxy)ethanol or 2-(2-Ethoxyethoxy)ethanol, and Selected Alkanes. *J. Chem. Eng. Data* **1999**, *44*, 892−895.

(14) Pal, A.; Bhardwaj, R. K. Speeds of sound and isentropic compressibilities of (n-alkoxyethanols+ toluene) at T= 298.15 K. *J. Chem. Thermodyn.* **2002**, *34*, 1157−1171.

(15) Comelli, F.; Francesconi, R.; Castellari, C. Excess molar enthalpies of binary mixtures containing propylene carbonate + some n-alkoxy- and n-alkoxyethoxy-ethanols at 288.15, 298.15, and 313.15 K. *Thermochim. Acta* **2000**, *354*, 89−97.

(16) Douhéret, G.; Lajoie, P.; Davis, M. I.; Ratliff, J. L.; Ulloa, J.; Høiland, H. Volumetric properties of binary mixtures of water with methoxy(ethoxy)ethanols. *J. Chem. Soc., Faraday Trans.* **1995**, *91*, 2291−2298.

(17) Pal, A.; Kumar, H.; Kumar, A.; Dass, G. Excess molar volumes and viscosities of mixtures of some n-alkoxyethanols with dialkyl carbonates at 298.15 K. *Fluid Phase Equilib.* **1999**, *166*, 245−258.

(18) Carmona, F. J.; Antonio González, J.; García de la Fuente, I.; Carlos Cobos, J. Thermodynamic properties of n-alkoxyethanols +organic solvent mixtures. *Thermochim. Acta* **2004**, *409*, 169−175.

(19) Francesconi, R.; Castellari, C.; Comelli, F. Excess Molar Enthalpies and Excess Molar Volumes of Diethyl Carbonate + Somen-

Alkoxyethanols at (298.15 and 313.15) K. *J. Chem. Eng. Data* **1999**, *44*, 1373−1378.
(20) Pal, A.; Sharma, S. Viscosities and Densities of Somen-Alkoxyethanols with Trichloroethylene and Tetrachloroethylene at 298.15 K. *J. Chem. Eng. Data* **1998**, *43*, 21−24.
(21) Cobos, J. A. *Int. DATA Ser., Sel. Data Mixtures, Ser. A* **1988**, *2*, 87−89.
(22) Pal, A.; Singh, Y. P. Excess molar volumes and apparent molar volumes of {xH(CH2)vO(CH2)2O(CH2)2OH + (1 - x)H2O} at the temperature 298.15 K. *J. Chem. Thermodyn.* **1994**, *26*, 1063−1070.
(23) Gong, Y.-h.; Shen, C.; Lu, Y.-z.; Meng, H.; Li, C.-x. Viscosity and Density Measurements for Six Binary Mixtures of Water (Methanol or Ethanol) with an Ionic Liquid ([BMIM][DMP] or [EMIM][DMP]) at Atmospheric Pressure in the Temperature Range of (293.15 to 333.15) K. *J. Chem. Eng. Data* **2012**, *57*, 33−39.
(24) Negadi, L.; Feddal-Benabed, B.; Bahadur, I.; Saab, J.; Zaoui-Djelloul-Daouadji, M.; Ramjugernath, D.; Negadi, A. Effect of temperature on density, sound velocity, and their derived properties for the binary systems glycerol with water or alcohols. *J. Chem. Thermodyn.* **2017**, *109*, 124−136.
(25) Ortega, J. Densities and refractive indices of pure alcohols as a function of temperature. *J. Chem. Eng. Data* **1982**, *27*, 312−317.
(26) Djojoputro, H.; Ismadji, S. Density and Viscosity of Binary Mixtures of Ethyl-2-methylbutyrate and Ethyl Hexanoate with Methanol, Ethanol, and 1-Propanol at (293.15, 303.15, and 313.15) K. *J. Chem. Eng. Data* **2005**, *50*, 1343−1347.
(27) Wilson, W.; Bradley, D. Speed of Sound in Four Primary Alcohols as a Function of Temperature and Pressure. *J. Acoust. Soc. Am.* **1964**, *36*, 333−337.
(28) Rodríguez, A.; Canosa, J.; Tojo, J. Density, Refractive Index, and Speed of Sound of Binary Mixtures (Diethyl Carbonate + Alcohols) at Several Temperatures. *J. Chem. Eng. Data* **2001**, *46*, 1506−1515.
(29) González, B.; Calvar, N.; Gómez, E.; Domínguez, Á. Density, dynamic viscosity, and derived properties of binary mixtures of methanol or ethanol with water, ethyl acetate, and methyl acetate at T=(293.15, 298.15, and 303.15)K. *J. Chem. Thermodyn.* **2007**, *39*, 1578−1588.
(30) Aralaguppi, M. I.; Jadar, C. V.; Aminabhavi, T. M. Density, Viscosity, Refractive Index, and Speed of Sound in Binary Mixtures of Acrylonitrile with Methanol, Ethanol, Propan-1-ol, Butan-1-ol, Pentan-1-ol, Hexan-1-ol, Heptan-1-ol, and Butan-2-ol. *J. Chem. Eng. Data* **1999**, *44*, 216−221.
(31) Nikam, P. S.; Jadhav, M. C.; Hasan, M. Density and Viscosity of Mixtures of Nitrobenzene with Methanol, Ethanol, Propan-1-ol, Propan-2-ol, Butan-1-ol, 2-Methylpropan-1-ol, and 2-Methylpropan-2-ol at 298.15 and 303.15 K. *J. Chem. Eng. Data* **1995**, *40*, 931−934.
(32) Aminabhavi, T. M.; Banerjee, K. Density, Viscosity, Refractive Index, and Speed of Sound in Binary Mixtures of 2-Chloroethanol with Alkanols (C1−C6) at 298.15, 303.15, and 308.15 K. *J. Chem. Eng. Data* **1998**, *43*, 509−513.
(33) Francesconi, R.; Comelli, F. Excess Enthalpies and Excess Volumes of the Liquid Binary Mixtures of Propylene Carbonate + Six Alkanols at 298.15 K. *J. Chem. Eng. Data* **1996**, *41*, 1397−1400.
(34) Noda, K.; Ohashi, M.; Ishida, K. Viscosities and densities at 298.15 K for mixtures of methanol, acetone, and water. *J. Chem. Eng. Data* **1982**, *27*, 326−328.
(35) Varfolomeev, M. A.; Zaitseva, K. V.; Rakipov, I. T.; Solomonov, B. N.; Marczak, W. Marczak' W. Speed of Sound, Density, and Related Thermodynamic Excess Properties of Binary Mixtures of Butan-2-one with C1−C4 n-Alkanols and Chloroform. *J. Chem. Eng. Data* **2014**, *59*, 4118−4132.
(36) Cao, Q.; Lu, X.; Wu, X.; Guo, Y.; Xu, L.; Fang, W. Density, Viscosity, and Conductivity of Binary Mixtures of the Ionic Liquid N-(2-Hydroxyethyl)piperazinium Propionate with Water, Methanol, or Ethanol. *J. Chem. Eng. Data* **2015**, *60*, 455−463.
(37) Diaz Peña, M.; Tardajos, G. Isothermal compressibilities of n-1-alcohols from methanol to 1-dodecanol at 298.15, 308.15, 318.15, and 333.15 K. *J. Chem. Thermodyn.* **1979**, *11*, 441−445.
(38) Orge, B.; Iglesias, M.; Rodríguez, A.; Canosa, J. M.; Tojo, J. Mixing properties of (methanol, ethanol, or 1-propanol) with (n-pentane, n-hexane, n-heptane and n-octane) at 298.15 K. *Fluid Phase Equilib.* **1997**, *133*, 213−227.
(39) Nikam, P. S.; Mahale, T. R.; Hasan, M. Density and Viscosity of Binary Mixtures of Ethyl Acetate with Methanol, Ethanol, Propan-1-ol, Propan-2-ol, Butan-1-ol, 2-Methylpropan-1-ol, and 2-Methylpropan-2-ol at (298.15, 303.15, and 308.15) K. *J. Chem. Eng. Data* **1996**, *41*, 1055−1058.
(40) Ritzoulis, G.; Fidantsi, A. Relative Permittivities, Refractive Indices, and Densities for the Binary MixturesN,N'-Dimethylacetamide with Methanol, Ethanol, 1-Butanol, and 2-Propanol at 298.15 K. *J. Chem. Eng. Data* **2000**, *45*, 207−209.
(41) Nikam, P. S.; Shirsat, L. N.; Hasan, M. Density and Viscosity Studies of Binary Mixtures of Acetonitrile with Methanol, Ethanol, Propan-1-ol, Propan-2-ol, Butan-1-ol, 2-Methylpropan-1-ol, and 2-Methylpropan-2-ol at (298.15, 303.15, 308.15, and 313.15) K. *J. Chem. Eng. Data* **1998**, *43*, 732−737.
(42) Won, Y. S.; Chung, D. K.; Mills, A. F. Density, viscosity, surface tension, and carbon dioxide solubility and diffusivity of methanol, ethanol, aqueous propanol, and aqueous ethylene glycol at 25 °C. *J. Chem. Eng. Data* **1981**, *26*, 140−141.
(43) Wu, J.-Y.; Chen, Y.-P.; Su, C.-S. Density and Viscosity of Ionic Liquid Binary Mixtures of 1-n-Butyl-3-methylimidazolium Tetrafluoroborate with Acetonitrile, N,N-Dimethylacetamide, Methanol, and N-Methyl-2-pyrrolidone. *J. Solution Chem.* **2014**, *44*, 395−412.
(44) Pikkarainen, L. Excess volumes of binary solvent mixtures of N,N-diethylmethanesulfonamide with aliphatic alcohols. *J. Chem. Eng. Data* **1987**, *32*, 429−431.
(45) Bendiaf, L.; Negadi, A.; Mokbel, I.; Negadi, L. Isothermal vapor−liquid equilibria of binary systems containing green solvents derived from biomass: (Furfuryl alcohol+toluene), (furfuryl alcohol +ethanol), or (furfural+toluene). *Fuel* **2014**, *122*, 247−253.
(46) Bendiaf, L.; Bahadur, I.; Negadi, A.; Naidoo, P.; Ramjugernath, D.; Negadi, L. Effects of alkyl group and temperature on the interactions between furfural and alcohol: Insight from density and sound velocity studies. *Thermochim. Acta* **2015**, *599*, 13−22.
(47) Zaoui-Djelloul-Daouadji, M.; Negadi, A.; Mokbel, I.; Negadi, L. (Vapor-liquid) equilibria and excess Gibbs free energy functions of (ethanol+glycerol), or (water+glycerol) binary mixtures at several temperatures. *J. Chem. Thermodyn.* **2014**, *69*, 165−171.
(48) Mokhtarani, B.; Sharifi, A.; Mortaheb, H. R.; Mirzaei, M.; Mafi, M.; Sadeghian, F. Density and viscosity of 1-butyl-3-methylimidazolium nitrate with ethanol, 1-propanol, or 1-butanol at several temperatures. *J. Chem. Thermodyn.* **2009**, *41*, 1432−1438.
(49) Jiménez, E.; Casas, H.; Segade, L.; Franjo, C. Surface Tensions, Refractive Indexes and Excess Molar Volumes of Hexane + 1-Alkanol Mixtures at 298.15 K. *J. Chem. Eng. Data* **2000**, *45*, 862−866.
(50) Lee, M.-J.; Lin, T.-K. Density and Viscosity for Monoethanolamine + Water, + Ethanol, and + 2-Propanol. *J. Chem. Eng. Data* **1995**, *40*, 336−339.
(51) Makhlouf, H.; Muñoz-Rujas, N.; Aguilar, F.; Belhachemi, B.; Montero, E. A.; Bahadur, I.; Negadi, L. Density, speed of sound and refractive index of mixtures containing 2-phenoxyethanol with propanol or butanol at various temperatures. *J. Chem. Thermodyn.* **2019**, *128*, 394−405.
(52) Paez, S.; Contreras, M. Densities and viscosities of binary mixtures of 1-propanol and 2-propanol with acetonitrile. *J. Chem. Eng. Data* **1989**, *34*, 455−459.
(53) Gupta, M.; Vibhu, I.; Shukla, J. P. Optical and volumetric study of molecular interactions in binary mixtures of tetrahydrofuran with 1-propanol and 2-propanol. *Phys. Chem. Liq.* **2003**, *41*, 575−582.
(54) Jiménez, E.; Cabanas, M.; Segade, L.; García-Garabal, S.; Casas, H. Excess volume, changes of refractive index and surface tension of binary 1,2-ethanediol + 1-propanol or 1-butanol mixtures at several temperatures. *Fluid Phase Equilib.* **2001**, *180*, 151−164.
(55) Pang, F.-M.; Seng, C.-E.; Teng, T.-T.; Ibrahim, M. H. Densities and viscosities of aqueous solutions of 1-propanol and 2-propanol at

https://dx.doi.org/10.1021/acs.jced.0c00330
J. Chem. Eng. Data XXXX, XXX, XXX−XXX

temperatures from 293.15 K to 333.15 K. *J. Mol. Liq.* **2007**, *136*, 71−78.
(56) Resa, J. M.; González, C.; Goenaga, J. M. Density, Refractive Index, Speed of Sound at 298.15 K, and Vapor−Liquid Equilibria at 101.3 kPa for Binary Mixtures of Propanol + 2-Methyl-1-butanol and Propanol + 3-Methyl-1-butanol. *J. Chem. Eng. Data* **2006**, *51*, 73−78.
(57) Ali, A.; Nain, A. K.; Chand, D.; Ahmad, R. Volumetric, ultrasonic and viscometric studies of molecular interactions in binary mixtures of aromatic+aliphatic alcohols at different temperatures. *Phys. Chem. Liq.* **2005**, *43*, 205−224.
(58) González, B.; Calvar, N.; González, E.; Domínguez, Á. Density and Viscosity Experimental Data of the Ternary Mixtures 1-Propanol or 2-Propanol + Water + 1-Ethyl-3-methylimidazolium Ethylsulfate. Correlation and Prediction of Physical Properties of the Ternary Systems. *J. Chem. Eng. Data* **2008**, *53*, 881−887.
(59) Lee, M.-J.; Lin, T.-K.; Pai, Y.-H.; Lin, K.-S. Density and Viscosity for Monoethanolamine + 1-Propanol, + 1-Hexanol, and + 1-Octanol. *J. Chem. Eng. Data* **1997**, *42*, 854−857.
(60) Iloukhani, H.; Almasi, M. Densities, viscosities, excess molar volumes, and refractive indices of acetonitrile and 2-alkanols binary mixtures at different temperatures: Experimental results and application of the Prigogine−Flory−Patterson theory. *Thermochim. Acta* **2009**, *495*, 139−148.
(61) Pereiro, A. B.; Rodríguez, A. Ternary (liquid+liquid) equilibria of the azeotrope (ethyl acetate+2-propanol) with different ionic liquids at T=298.15K. *J. Chem. Thermodyn.* **2007**, *39*, 1608−1613.
(62) Pereiro, A. B.; Rodríguez, A. Binary mixtures containing OMIM PF6: density, speed of sound, refractive index and LLE with hexane, heptane and 2-propanol at several temperatures. *Phys. Chem. Liq.* **2008**, *46*, 162−174.
(63) Kao, Y.-C.; Tu, C.-H. Densities, viscosities, refractive indices, and surface tensions for binary and ternary mixtures of 2-propanol, tetrahydropyran, and 2,2,4-trimethylpentane. *J. Chem. Thermodyn.* **2011**, *43*, 216−226.
(64) Ku, H.-C.; Wang, C.-C.; Tu, C.-H. Densities, Viscosities, Refractive Indexes, and Surface Tensions for Binary and Ternary Mixtures of Tetrahydofuran, 2-Propanol, and 2,2,4-Trimethylpentane. *J. Chem. Eng. Data* **2008**, *53*, 566−573.
(65) Bahadur, I.; Deenadayalu, N.; Tywabi, Z.; Sen, S.; Hofman, T. Volumetric properties of ternary (IL+2-propanol or 1-butanol or 2-butanol+ethyl acetate) systems and binary (IL+2-propanol or 1-butanol or 2-butanol) and (1-butanol or 2-butanol+ethyl acetate) systems. *J. Chem. Thermodyn.* **2012**, *49*, 24−38.
(66) Farhan, A. M.; Awwad, A. M. Relative Permittivities, Refractive Indices, and Densities of Dihydrofuran-2(3H)-one + Butan-1-ol and + Butan-2-ol atT= (293.15, 298.15, 303.15, and 313.15) K. *J. Chem. Eng. Data* **2010**, *55*, 1035−1038.
(67) Troncoso, J.; Carballo, E.; Cerdeiriña, C. A.; González, D.; Romaní, L. Systematic Determination of Densities and Speeds of Sound of Nitroethane + Isomers of Butanol in the Range (283.15−308.15) K. *J. Chem. Eng. Data* **2000**, *45*, 594−599.
(68) Zorębski, E.; Waligóra, A. Densities, Excess Molar Volumes, and Isobaric Thermal Expansibilities for 1,2-Ethanediol + 1-Butanol, or 1-Hexanol, or 1-Octanol in the Temperature Range from (293.15 to 313.15) K. *J. Chem. Eng. Data* **2008**, *53*, 591−595.
(69) Zorębski, E.; Góralski, P.; Godula, B.; Zorębski, M. Thermodynamic and acoustic properties of binary mixtures of 1-butanol with 1,2-butanediol. The comparison with the results for 1,3-, and 1,4-butanediol. *J. Chem. Thermodyn.* **2014**, *68*, 145−152.
(70) da Silva, J. L.; Aznar, M. Thermophysical properties of 2,5-dimethylfuran and liquid−liquid equilibria of ternary systems water +2,5-dimethylfuran+alcohols (1-butanol or 2-butanol or 1-hexanol). *Fuel* **2014**, *136*, 316−325.
(71) Dubey, G. P.; Sharma, M. Temperature and Composition Dependence of the Densities, Viscosities, and Speeds of Sound of Binary Liquid Mixtures of 1-Butanol with Hexadecane and Squalane. *J. Chem. Eng. Data* **2008**, *53*, 1032−1038.
(72) Valén, A.; López, M. C.; Urieta, J. S.; Royo, F. M.; Lafuente, C. Thermodynamic study of mixtures containing oxygenated compounds. *J. Mol. Liq.* **2002**, *95*, 157−165.
(73) Gascón, I.; Martín, S.; Cea, P.; López, M. C.; Royo, F. M. Density and Speed of Sound for Binary Mixtures of a Cyclic Ether with a Butanol Isomer. *J. Solution Chem.* **2002**, *31*, 905−915.
(74) Giner, B.; Artigas, H.; Carrión, A.; Lafuente, C.; Royo, F. M. Excess thermodynamic properties of isomeric butanols with 2-methyltetrahydrofuran. *J. Mol. Liq.* **2003**, *108*, 303−311.
(75) Ali, A.; Nain, A. K.; Lal, B.; Chand, D. Densities, Viscosities, and Refractive Indices of Binary Mixtures of Benzene with Isomeric Butanols at 30°C. *Int. J. Thermophys.* **2004**, *25*, 1835−1847.
(76) Papari, M. M.; Ghodrati, H.; Fadaei, F.; Sadeghi, R.; Behrouz, S.; Rad, M. N. S.; Moghadasi, J. Volumetric and ultrasonic study of mixtures of 2-phenylethanol with 1-butanol, 2-butanol, and 2-methyl-1-butanol at T=(298.15−323.15) K and atmospheric pressure: Measurement and prediction. *J. Mol. Liq.* **2013**, *180*, 121−128.
(77) Laavi, H.; Zaitseva, A.; Pokki, J.-P.; Uusi-Kyyny, P.; Kim, Y.; Alopaeus, V. Vapor−Liquid Equilibrium, Excess Molar Enthalpies, and Excess Molar Volumes of Binary Mixtures Containing Methyl Isobutyl Ketone (MIBK) and 2-Butanol, tert-Pentanol, or 2-Ethyl-1-hexanol. *J. Chem. Eng. Data* **2012**, *57*, 3092−3101.
(78) Resa, J. M.; González, C.; Juez, M.; Ortiz de Landaluce, S. Density, refractive index and speed of sound for mixtures of ethyl acetate with 2-butanol and 3-methyl-1-butanol. *Fluid Phase Equilib.* **2004**, *217*, 175−180.
(79) Fortin, T. J.; Laesecke, A.; Freund, M.; Outcalt, S. Advanced calibration, adjustment, and operation of a density and sound speed analyzer. *J. Chem. Thermodyn.* **2013**, *57*, 276−285.
(80) Joint Committee for Guides in Metrology. *Evaluation of Measurement Data—Guide to the Expression of Uncertainty in Measurement (GUM)*; JCGM, 2008, p 100.
(81) Ramana Reddy, K.V.; Rambabu, K.; Devarajulu, T.; Krishnaiah, A. Excess Volumes of (2-Ethoxyethanol + Alcohols) at 308.15 K. *Phys. Chem. Liq.* **1996**, *31*, 9−13.
(82) Zafarani-Moattar, M. T.; Shekaari, H. Apparent molar volume and isentropic compressibility of ionic liquid 1-butyl-3-methylimidazolium bromide in water, methanol, and ethanol at T=(298.15 to 318.15)K. *J. Chem. Thermodyn.* **2005**, *37*, 1029−1035.
(83) Choudary, N. V.; Naidu, P. R. Sound velocities and isentropic compressibilities of mixtures of 1, 2-dichloroethane with alkanols. *Chem. Scr.* **1982**, *19*, 89−92.
(84) Dharmaraju, G.; Venkateswarlu, P.; Raman, G. K. Ultrasonic studies in binary-liquid mixtures of associated liquids (cyclohexylamine+ alcohol). *Chem. Scr.* **1982**, *19*, 140−142.
(85) Benson, G. C.; Handa, Y. P. Ultrasonic speeds and isentropic compressibilities for (decan-1-ol + n-alkane) at 298.15 K. *J. Chem. Thermodyn.* **1981**, *13*, 887−896.
(86) Naorem, H.; Suri, S. K. Thermodynamic studies on the binary liquid mixtures containing furan derivatives: Furfural + Aliphatic Ketones. *J. Mol. Liq.* **1991**, *50*, 39−52.

https://dx.doi.org/10.1021/acs.jced.0c00330
J. Chem. Eng. Data XXXX, XXX, XXX−XXX

Journal of Molecular Liquids 330 (2021) 115436

Contents lists available at ScienceDirect

Journal of Molecular Liquids

journal homepage: www.elsevier.com/locate/molliq

Density, speed of sound, refractive index and related derived/excess properties of binary mixtures (furfural + dimethyl sulfoxide), (furfural + acetonitrile) and (furfural + sulfolane) at different temperatures

Djazia Belhadj [a], Amina Negadi [a], Pannuru Venkatesu [b], Indra Bahadur [c], Latifa Negadi [a,d,*]

[a] LATA2M, Laboratoire de Thermodynamique Appliquée et Modélisation Moléculaire, University of Tlemcen, Post Office Box 119, Tlemcen 13000, Algeria
[b] Department of Chemistry, University of Delhi, Delhi 110 007, India
[c] Department of Chemistry, School of Physical and Chemical Sciences, Faculty of Natural and Agricultural Sciences, North-West University (Mafikeng Campus), Private Bag X2046, Mmabatho 2735, South Africa
[d] Thermodynamics Research Unit, School of Engineering, University of KwaZulu-Natal, Howard College Campus, King George V Avenue, 4041 Durban, South Africa

ARTICLE INFO

Article history:
Received 29 July 2020
Received in revised form 16 November 2020
Accepted 18 January 2021
Available online 22 January 2021

Keywords:
Thermodynamic properties
Furfural
DMSO
Acetonitrile
Sulfolane

ABSTRACT

In this work, experimental densities (ρ), speed of sound (u) and refractive indices (n_D) were measured over the entire composition range for the binary mixtures containing furfural with dimethyl sulfoxide (DMSO) or acetonitrile at (293.15, 303.15, 313.15 and 323.15) K whereas for sulfolane mixture at (303.15, 313.15 and 323.15) K and at pressure of 0.1 MPa. Further, the measured data has been utilized to compute isentropic compressibility (κ_s), intermolecular free length(L_f), specific acoustic impedance(Z), relative association(R_A), relaxation strength (r) and Rao's molar sound function(R). The excess/derived properties on mixing were also derived from values of measured properties for all studied mixtures under the same experimental conditions. The correlation of excess/derived properties was made by help of the Redlich-Kister polynomial equation and found to be satisfactory. The experimental and calculated results were interpreted from the viewpoint of intermolecular interactions that occur between the components of the investigated systems.

1. Introduction

Liquid mixtures have found applications in different fields rather than single liquid as they provide a wide choice of solvent mixtures with appropriate properties [1]. Thermophysical properties of binary liquid mixtures can be contributed to clarification of the various intermolecular interactions existing between the different species found in solution. Obviously, the reliable knowledge of these properties of pure compounds and mixtures is of great importance in many fields of research as well as in industrial practice [2–4]. Studying the concentration and temperature dependence of thermophysical and thermodynamics properties contributes to our understanding of intermolecular interactions in liquids, liquid mixtures and solutions [2–5]. Intermolecular interactions in binary mixtures modify the structural arrangements which lead to change the shape of the molecule [6]. The investigation of molecular interactions is therefore crucial in elucidation of the structural changes in the mixtures.

The present paper is focused on a study of thermophysical and thermodynamic properties of three binary systems formed by dimethyl sulfoxide (DMSO) or acetonitrile or sulfolane with furfural as a common compound. Furfural is one of the furan derivatives produced from the hemicellulosic fraction of lignocellulosics, which is considered a promising commodity bio-based chemical because of the possibility of its use in the production of several products as paints, fertilizers, fuel additives and many others products [5,7,8]. Once furfural has many applications, investigation of its properties in different mixtures is important. In this regard and as a continuation of our research program on thermodynamic and thermophysical properties of binary mixtures containing solvents derived from biomass [9–13], we report here experimental results of density (ρ), speed of sound (u) and refractive index (n_D) for the binary systems mentioned above over the whole miscibility range at different temperatures and at pressure of 0.1 MPa. These properties have been used to determine isentropic compressibility(κ_s), intermolecular free length(L_f), specific acoustic impedance(Z), relative association(R_A), relaxation strength (r) and Rao's molar sound function (R) and also the deviation parameters. The significance of these results has been

* Corresponding author at: LATA2M, Laboratoire de Thermodynamique Appliquée et Modélisation Moléculaire, University of Tlemcen, Post Office Box 119, Tlemcen 13000, Algeria.
E-mail address: latifa.negadi@univ-tlemcen.dz (L. Negadi).

https://doi.org/10.1016/j.molliq.2021.115436
0167-7322/

Table 1
CAS #, suppliers, molar mass and purities of chemicals used in this study.

Chemical name	CAS #	Supplier	Lot #	Molar mass/(g.mole^{-1})	Mass fraction purity (as stated by the supplier)
Furfural	98–01-1	Sigma-Aldrich	SHBG2086V	96.08	99.0%
DMSO	67–68-5	Sigma-Aldrich	BCBC5164	78.13	99.5%
Acetonitrile	75–05-8	Sigma-Aldrich	SZBE040V	41.05	99.9%
Sulfolane	126–33-0	Sigma-Aldrich	MKBH1265V	120.17	99.0%

Table 2
Comparison of experimental density, ρ, speed of sound, u, and refractive indices, n_D, of the pure component with the corresponding literature values at different temperatures and at pressure of 0.1 MPa.

Component	T/(K)	ρ/(g.cm^{-3})		u/ (m.s^{-1})		n_D	
		Exp.	Lit.	Exp.	Lit.	Exp.	Lit.
Furfural	293.15	1.15999	1.15933 [14] 1.160 [15] 1.160128 [17]	1458.20	1458.8 [14] 1460 [16] 1458.52 [17]	1.52637	1.5261 [7] 1.526168 [17] 1.5252 [9]
	298.15	1.15467	1.157 [15] 1.15493 [18] 1.1545 [19] 1.154805 [17]	1440.17	1440.19 [17]	1.52375	1.5236 [18] 1.52345 [19] 1.5235 [7] 1.523577 [17]
	303.15	1.14935	1.14869 [14] 1.151 [15] 1.149766 [20] 1.149478 [17]	1422.02	1422.5 [14] 1422.05 [17]	1.52123	1.5206 [20] 1.520969 [17]
	313.15	1.13866	1.13801 [14] 1.138793 [17]	1386.01	1386.5 [14] 1385.97 [17]	1.51615	1.515740 [17]
	323.15	1.12792	1.128061 [17]	1350.29	1350.20 [17]	1.51112	1.510486 [17]
DMSO	293.15	1.10033	1.100 [21] 1.100865 [22] 1.10073 [25] 1.10053 [24] 1.100 [23]	1503.63	1503.9 [21] 1504.7 [23]	1.47829	1.479 [21] 1.4795 [24] 1.479 [23]
	298.15	1.09531	1.095 [21] 1.09574 [25] 1.09537 [27] 1.0954 [29] 1.096107 [26] 1.09537 [28] 1.0960 [31]	1486.81	1486.8 [21] 1495.29 [26] 1496 [28]	1.47695	1.477 [21] 1.4768 [25] 1.4768 [29] 1.4770 [30] 1.4769 [31]
	303.15	1.09030	1.090 [21] 1.090812 [22] 1.09074 [25] 1.09049 [24] 1.090 [23] 1.0949 [32] 1.091140 [26] 1.09241 [28] 1.0949 [33] 1.09054 [34] 1.09135 [35]	1469.88	1469.9 [21] 1471.0 [23] 1475 [27] 1478.83 [26] 1472 [28] 1490.9 [33] 1477 [34]	1.47493	1.475 [21] 1.4733 [25] 1.4752 [24] 1.475 [23]
	313.15	1.08026	1.080 [21] 1.080770 [22] 1.08075 [25] 1.08032 [24] 1.080 [23] 1.081443 [26]	1436.28	1436.3 [21] 1437.4 [23] 1445.56 [26]	1.47033	1.470 [21] 1.4694 [25] 1.4700 [24] 1.470 [23]
	323.15	1.07023	1.070 [21] 1.070728 [22] 1.07159 [37] 1.07019 [36]	1403.00	1403.0 [21]	1.46606	1.466 [21] 1.4659 [36]
Acetonitrile	293.15	0.78196	0.782 [23] 0.7821 [38] 0.78204 [40] 0.78204 [39]	1299.20	1299.7 [23] 1298.8 [39] 1299 [41]	1.34387	1.344 [23] 1.3436 [40]
	298.15	0.77657	0.7762 [42] 0.7754 [43] 0.77661 [45] 0.7771 [44] 0.7766 [38] 0.77664 [40] 0.77666 [39]	1279.40	1271.3 [43] 1278.9 [45] 1288 [44] 1279.0 [39] 1284 [41]	1.34150	1.3407 [44] 1.34140 [30] 1.3411 [40] 1.3413 [31]

Table 2 (*continued*)

Component	T/(K)	$\rho/(g.cm^{-3})$		$u/(m.s^{-1})$		n_D	
		Exp.	Lit.	Exp.	Lit.	Exp.	Lit.
			0.7765 [31]				
	303.15	0.77113	0.771 [23]	1259.27	1258.8 [23]	1.33906	1.339 [23]
			0.77080 [42]		1251.9 [43]		1.3391 [44]
			0.7699 [43]		1258.8 [39]		1.3390 [40]
			0.7715 [44]		1268 [41]		
			0.77145 [30]				
			0.7710 [38]				
			0.77121 [40]				
			0.77124 [39]				
	313.15	0.76018	0.760 [23]	1218.56	1218.4 [23]	1.33423	1.334 [23]
			0.75942 [42]		1218.5 [39]		1.3342 [46]
			0.7602 [38]		1229 [41]		1.3348 [47]
			0.76029 [39]				
	323.15	0.74910	0.7491 [38]	1178.67	1189 [41]	1.32931	1.3297 [47]
			0.74957 [47]				
Sulfolane	303.15	1.26171	1.2620 [48]	1583.52	1588 [49]	1.48171	1.48143 [48]
			1.2618 [49]		1593.56 [50]		1.4818 [51]
			1.26080 [52]				1.4817 [53]
			1.26140 [51]				
			1.26196 [54]				
			1.26202 [55]				
			1.26080 [56]				
			1.2621 [53]				
	313.15	1.25292	1.2532 [48]	1552.30	1558 [49]	1.47823	1.47800 [48]
			1.2532 [57]				
			1.2516 [49]				
			1.25190 [52]				
			1.25317 [55]				
			1.2545 [53]				
	323.15	1.24416	1.2442 [48]	1520.73	–	1.47478	1.47440 [48]
			1.24336 [52]				
			1.24421 [55]				
			1.24336 [56]				

Standard uncertainties u are $u(T) = \pm 0.02$ K, $u(p) = \pm 0.04$ MPa and the combined expanded uncertainty Uc in mole fraction, density, sound velocity and refractive index were $Uc(x) = \pm 0.0007$, $Uc(\rho) = \pm 0.004$ g/cm^3, $Uc(u) = \pm 1.35$ m/s and $Uc(n) = \pm 0.006$, respectively, (0.95 level of confidence).

Table 3
Densities, ρ, speed of sound, u, and refractive indices, n_D, for the binary systems (furfural + DMSO, or acetonitrile, or sulfolane) at different temperatures and at pressure of 0.1 MPa.

x_1	$\rho/(g.cm^{-3})$	$u/(m.s^{-1})$	n_D
{Furfural (1) + DMSO (2)}			
$T = 293.15$ K			
0.0000	1.10033	1503.63	1.47829
0.1047	1.10667	1494.58	1.48400
0.2024	1.11272	1488.10	1.48922
0.3008	1.11877	1482.42	1.49429
0.4017	1.12502	1477.36	1.49932
0.5009	1.13106	1473.20	1.50412
0.6011	1.13712	1469.41	1.50882
0.7008	1.14303	1466.18	1.51335
0.7989	1.14873	1463.35	1.51769
0.8971	1.15427	1460.62	1.52193
1.0000	1.15999	1458.20	1.52637
$T = 303.15$ K			
0.0000	1.09030	1469.88	1.47493
0.1047	1.09664	1461.00	1.48049
0.2024	1.10269	1454.62	1.48555
0.3008	1.10871	1448.88	1.49043
0.4017	1.11490	1443.67	1.49528
0.5009	1.12088	1439.24	1.49990
0.6011	1.12687	1435.13	1.50442
0.7008	1.13270	1431.50	1.50878
0.7989	1.13828	1428.28	1.51292
0.8971	1.14374	1425.09	1.51700
1.0000	1.14935	1422.02	1.52123
$T = 313.15$ K			
0.0000	1.08026	1436.28	1.47033
0.1047	1.08661	1427.53	1.47584
0.2024	1.09264	1421.18	1.48091
0.3008	1.09863	1415.40	1.48581
0.4017	1.10477	1410.01	1.49068
0.5009	1.11069	1405.33	1.49528

(*continued on next page*)

Table 3 (*continued*)

x_1	$\rho/(g.cm^{-3})$	$u/(m.s^{-1})$	n_D
0.6011	1.11660	1400.92	1.49975
0.7008	1.12234	1396.91	1.50404
0.7989	1.12783	1393.25	1.50811
0.8971	1.13318	1389.62	1.51205
1.0000	1.13866	1386.01	1.51615
$T = 323.15$ K			
0.0000	1.07023	1403.00	1.46606
0.1047	1.07657	1394.40	1.47158
0.2024	1.08258	1388.04	1.47653
0.3008	1.08853	1382.20	1.48135
0.4017	1.09462	1376.63	1.48615
0.5009	1.10047	1371.71	1.49068
0.6011	1.10630	1366.99	1.49508
0.7008	1.11195	1362.61	1.49930
0.7989	1.11734	1358.48	1.50327
0.8971	1.12257	1354.43	1.50714
1.0000	1.12792	1350.29	1.51112
{Furfural (1) + Acetonitrile (2)}			
T = 293.15 K			
0.0000	0.78196	1299.20	1.34387
0.1030	0.84199	1315.78	1.37272
0.2016	0.89309	1332.62	1.39760
0.3079	0.94218	1351.28	1.42140
0.4006	0.98044	1367.19	1.43974
0.4978	1.01700	1383.78	1.45724
0.5975	1.05094	1400.10	1.47360
0.6949	1.08113	1415.41	1.48816
0.7961	1.10973	1430.35	1.50190
0.8969	1.13584	1444.61	1.51452
1.0000	1.15999	1458.20	1.52637
T = 303.15 K			
0.0000	0.77113	1259.27	1.33906
0.1030	0.83110	1276.77	1.36801
0.2016	0.88218	1293.85	1.39297
0.3079	0.93128	1313.08	1.41678
0.4006	0.96956	1329.44	1.43510
0.4978	1.00615	1346.35	1.45271
0.5975	1.04014	1363.01	1.46881
0.6949	1.07036	1379.03	1.48334
0.7961	1.09900	1393.79	1.49692
0.8969	1.12515	1408.26	1.50957
1.0000	1.14935	1422.02	1.52123
T = 313.15 K			
0.0000	0.76018	1218.56	1.33423
0.1030	0.82008	1236.90	1.36373
0.2016	0.87117	1255.10	1.38860
0.3079	0.92029	1274.92	1.41228
0.4006	0.95860	1291.72	1.43059
0.4978	0.99523	1309.03	1.44800
0.5975	1.02926	1326.02	1.46405
0.6949	1.05953	1341.88	1.47848
0.7961	1.08822	1357.33	1.49184
0.8969	1.11442	1372.02	1.50462
1.0000	1.13866	1386.01	1.51615
T = 323.15 K			
0.0000	0.74910	1178.67	1.32931
0.1030	0.80895	1197.59	1.35896
0.2016	0.86004	1216.54	1.38405
0.3079	0.90920	1236.99	1.40789
0.4006	0.94755	1254.25	1.42655
0.4978	0.98422	1271.95	1.44402
0.5975	1.01831	1289.30	1.45999
0.6949	1.04865	1305.44	1.47396
0.7961	1.07739	1321.19	1.48747
0.8969	1.10364	1336.12	1.49961
1.0000	1.12792	1350.29	1.51112
{Furfural (1) + Sulfolane (2)}			
T = 303.15 K			
0.0000	1.26171	1583.52	1.48171
0.1012	1.25224	1566.49	1.48561
0.1990	1.24293	1550.40	1.48938
0.3018	1.23256	1533.72	1.49337
0.4013	1.22214	1517.87	1.49726
0.5005	1.21126	1502.57	1.50116
0.5991	1.20002	1486.42	1.50507

Table 3 (*continued*)

x_1	$\rho/(g.cm^{-3})$	$u/(m.s^{-1})$	n_D
0.7006	1.18805	1470.37	1.50912
0.8014	1.17567	1454.36	1.51317
0.9002	1.16306	1438.56	1.51717
1.0000	1.14935	1422.02	1.52123
T = 313.15 K			
0.0000	1.25292	1552.30	1.47823
0.1012	1.24328	1534.62	1.48196
0.1990	1.23381	1518.22	1.48557
0.3018	1.22327	1501.21	1.48940
0.4013	1.21268	1485.00	1.49313
0.5005	1.20162	1468.87	1.49687
0.5991	1.19020	1452.71	1.50062
0.7006	1.17803	1436.16	1.50451
0.8014	1.16544	1419.61	1.50840
0.9002	1.15262	1403.21	1.51225
1.0000	1.13866	1386.01	1.51615
T = 323.15 K			
0.0000	1.24416	1520.73	1.47478
0.1012	1.23433	1503.09	1.47834
0.1990	1.22469	1486.40	1.48179
0.3018	1.21397	1469.05	1.48546
0.4013	1.20320	1452.48	1.48903
0.5005	1.19197	1435.92	1.49262
0.5991	1.18036	1419.36	1.49621
0.7006	1.16799	1402.30	1.49994
0.8014	1.15519	1385.20	1.50367
0.9002	1.14213	1368.18	1.50737
1.0000	1.12792	1350.29	1.51112

Standard uncertainties u are $u(T) = \pm 0.02$ K, $u(p) = \pm 0.04$ MPa and the combined expanded uncertainty Uc in mole fraction, density, sound velocity and refractive index were $Uc(x) = \pm 0.0007$, $Uc(\rho) = \pm 0.004$ g/cm^3, $Uc(u) = \pm 1.35$ m/s and $Uc(n) = \pm 0.006$, respectively, (0.95 level of confidence).

Table 4
Isentropic compressibility (κ_s), intermolecular free length (L_f), specific acoustic impedance (Z), relative association (R_A), relaxation strength (r) and Rao's molar sound function (R) for the binary systems (furfural + DMSO, or acetonitrile, or sulfolane) at different temperatures and at pressure of 0.1 MPa.

x_1	$\kappa_s/(TPa^{-1})$	$L_f/(10^{-12}\ m)$	$Z/(10^5\ kg\ m^{-2}\ s^{-1})$	R_A	r	$R/(10^{-3}\ m^{(10/3)}\ mol^{-1}\ s^{(-1/3)})$
{furfural (1) + DMSO (2)}						
T = 293.15 K						
0.0000	401.97	40.862	16.545	1.0000	0.1168	0.8135
0.1047	404.52	40.991	16.540	1.0078	0.1274	0.8266
0.2024	405.83	41.057	16.558	1.0148	0.1350	0.8389
0.3008	406.74	41.103	16.585	1.0216	0.1416	0.8513
0.4017	407.26	41.129	16.621	1.0285	0.1474	0.8640
0.5009	407.37	41.135	16.663	1.0350	0.1522	0.8764
0.6011	407.29	41.131	16.709	1.0414	0.1566	0.8890
0.7008	406.97	41.115	16.759	1.0476	0.1603	0.9016
0.7989	406.52	41.092	16.810	1.0535	0.1635	0.9139
0.8971	406.09	41.070	16.859	1.0592	0.1666	0.9263
1.0000	405.43	41.037	16.915	1.0651	0.1694	0.9393
T = 303.15 K						
0.0000	424.51	42.764	16.026	1.0000	0.1560	0.8148
0.1047	427.20	42.900	16.022	1.0079	0.1662	0.8279
0.2024	428.60	42.970	16.040	1.0149	0.1735	0.8402
0.3008	429.65	43.022	16.064	1.0218	0.1800	0.8525
0.4017	430.36	43.058	16.096	1.0287	0.1859	0.8651
0.5009	430.70	43.075	16.132	1.0353	0.1909	0.8776
0.6011	430.87	43.083	16.172	1.0418	0.1955	0.8901
0.7008	430.83	43.081	16.215	1.0481	0.1995	0.9025
0.7989	430.65	43.072	16.258	1.0541	0.2031	0.9149
0.8971	430.51	43.065	16.299	1.0599	0.2067	0.9272
1.0000	430.27	43.053	16.344	1.0659	0.2101	0.9401
T = 313.15 K						
0.0000	448.74	44.762	15.516	1.0000	0.1942	0.8160
0.1047	451.60	44.905	15.512	1.0079	0.2040	0.8291
0.2024	453.13	44.981	15.528	1.0150	0.2110	0.8413
0.3008	454.35	45.041	15.550	1.0220	0.2174	0.8536
0.4017	455.29	45.087	15.577	1.0290	0.2234	0.8662
0.5009	455.88	45.117	15.609	1.0357	0.2285	0.8786
0.6011	456.33	45.139	15.643	1.0423	0.2334	0.8911
0.7008	456.60	45.152	15.678	1.0486	0.2378	0.9035
0.7989	456.77	45.161	15.713	1.0547	0.2417	0.9157
0.8971	456.99	45.172	15.747	1.0606	0.2457	0.9280
1.0000	457.17	45.180	15.782	1.0666	0.2496	0.9408
T = 323.15 K						

(*continued on next page*)

Table 4 (*continued*)

x_1	$\kappa_s/(\mathrm{TPa}^{-1})$	$L_f/(10^{-12}\ \mathrm{m})$	$Z/(10^5\ kg\ m^{-2}\ s^{-1})$	R_A	r	$R/(10^{-3}\ \mathrm{m}^{(10/3)}\ \mathrm{mol}^{-1}\ \mathrm{s}^{(-1/3)})$
0.0000	474.69	46.855	15.015	1.0000	0.2311	0.8173
0.1047	477.73	47.005	15.012	1.0080	0.2405	0.8303
0.2024	479.44	47.089	15.027	1.0152	0.2474	0.8425
0.3008	480.86	47.159	15.046	1.0222	0.2537	0.8548
0.4017	482.06	47.217	15.069	1.0293	0.2597	0.8673
0.5009	482.95	47.261	15.095	1.0360	0.2650	0.8796
0.6011	483.72	47.299	15.123	1.0427	0.2701	0.8920
0.7008	484.36	47.330	15.152	1.0491	0.2747	0.9044
0.7989	484.96	47.360	15.179	1.0553	0.2791	0.9166
0.8971	485.59	47.390	15.204	1.0613	0.2834	0.9288
1.0000	486.26	47.423	15.230	1.0674	0.2878	0.9415
{furfural (1) + acetonitrile (2)}						
T = 293.15 K						
0.0000	757.64	56.098	10.159	1.0000	0.3407	0.5728
0.1030	686.01	53.380	11.079	1.0722	0.3237	0.6080
0.2016	630.51	51.176	11.901	1.1325	0.3063	0.6425
0.3079	581.26	49.137	12.732	1.1892	0.2867	0.6805
0.4006	545.66	47.608	13.404	1.2327	0.2698	0.7142
0.4978	513.51	46.184	14.073	1.2735	0.2520	0.7500
0.5975	485.40	44.902	14.714	1.3109	0.2343	0.7870
0.6949	461.70	43.792	15.302	1.3437	0.2174	0.8234
0.7961	440.45	42.773	15.873	1.3744	0.2008	0.8616
0.8969	421.87	41.861	16.408	1.4021	0.1848	0.8998
1.0000	405.43	41.037	16.915	1.4274	0.1694	0.9393
T = 303.15 K						
0.0000	817.77	59.354	9.711	1.0000	0.3806	0.5749
0.1030	738.11	56.389	10.611	1.0728	0.3632	0.6098
0.2016	677.14	54.010	11.414	1.1337	0.3461	0.6441
0.3079	622.78	51.797	12.228	1.1910	0.3265	0.6819
0.4006	583.56	50.139	12.890	1.2348	0.3096	0.7155
0.4978	548.30	48.601	13.546	1.2760	0.2919	0.7512
0.5975	517.50	47.216	14.177	1.3137	0.2743	0.7881
0.6949	491.27	46.004	14.761	1.3466	0.2571	0.8245
0.7961	468.39	44.920	15.318	1.3778	0.2412	0.8625
0.8969	448.15	43.939	15.845	1.4057	0.2253	0.9006
1.0000	430.27	43.053	16.344	1.4313	0.2101	0.9401
T = 313.15 K						
0.0000	885.91	62.894	9.263	1.0000	0.4200	0.5768
0.1030	797.03	59.655	10.144	1.0734	0.4024	0.6115
0.2016	728.69	57.041	10.934	1.1348	0.3847	0.6456
0.3079	668.51	54.634	11.733	1.1925	0.3651	0.6833
0.4006	625.21	52.835	12.382	1.2367	0.3482	0.7168
0.4978	586.38	51.168	13.028	1.2783	0.3306	0.7523
0.5975	552.56	49.671	13.648	1.3164	0.3132	0.7891
0.6949	524.16	48.377	14.218	1.3497	0.2966	0.8254
0.7961	498.78	47.192	14.771	1.3810	0.2803	0.8634
0.8969	476.68	46.135	15.290	1.4092	0.2647	0.9014
1.0000	457.17	45.180	15.782	1.4349	0.2496	0.9408
T = 323.15 K						
0.0000	960.89	66.664	8.829	1.0000	0.4573	0.5789
0.1030	861.91	63.137	9.688	1.0742	0.4398	0.6133
0.2016	785.65	60.279	10.463	1.1361	0.4219	0.6472
0.3079	718.80	57.657	11.247	1.1943	0.4023	0.6847
0.4006	670.86	55.702	11.885	1.2390	0.3855	0.7181
0.4978	628.01	53.893	12.519	1.2809	0.3680	0.7535
0.5975	590.76	52.271	13.129	1.3193	0.3507	0.7902
0.6949	559.57	50.872	13.689	1.3530	0.3343	0.8263
0.7961	531.74	49.591	14.234	1.3845	0.3181	0.8643
0.8969	507.56	48.450	14.746	1.4130	0.3026	0.9022
1.0000	486.26	47.423	15.230	1.4390	0.2878	0.9415
{furfural (1) + sulfolane (2)}						
T = 303.15 K						
0.0000	316.08	36.901	19.979	1.0000	0.0205	1.1101
0.1012	325.43	37.442	19.616	0.9961	0.0414	1.0919
0.1990	334.71	37.973	19.270	0.9921	0.0610	1.0744
0.3018	344.91	38.547	18.904	0.9874	0.0811	1.0563
0.4013	355.15	39.115	18.550	0.9824	0.1000	1.0391
0.5005	365.67	39.690	18.200	0.9770	0.1181	1.0223
0.5991	377.16	40.309	17.837	0.9714	0.1369	1.0056
0.7006	389.33	40.954	17.469	0.9652	0.1555	0.9887
0.8014	402.13	41.622	17.098	0.9586	0.1738	0.9720
0.9002	415.47	42.306	16.731	0.9518	0.1916	0.9559
1.0000	430.27	43.053	16.344	0.9442	0.2101	0.9401
T = 313.15 K						
0.0000	331.23	38.457	19.449	1.0000	0.0587	1.1105
0.1012	341.53	39.051	19.080	0.9961	0.0801	1.0923

Table 4 (*continued*)

x_1	$\kappa_s/(\mathrm{TPa}^{-1})$	$L_f/(10^{-12}\ \mathrm{m})$	$Z/(10^5\ kg\ m^{-2}\ s^{-1})$	R_A	r	$R/(10^{-3}\ \mathrm{m}^{(10/3)}\ \mathrm{mol}^{-1}\ \mathrm{s}^{(-1/3)})$
0.1990	351.63	39.624	18.732	0.9921	0.0996	1.0748
0.3018	362.74	40.245	18.364	0.9873	0.1197	1.0568
0.4013	373.94	40.861	18.008	0.9823	0.1386	1.0396
0.5005	385.71	41.500	17.650	0.9769	0.1572	1.0228
0.5991	398.13	42.162	17.290	0.9712	0.1756	1.0062
0.7006	411.56	42.868	16.918	0.9649	0.1943	0.9893
0.8014	425.77	43.601	16.545	0.9583	0.2128	0.9727
0.9002	440.62	44.355	16.174	0.9514	0.2309	0.9566
1.0000	457.17	45.180	15.782	0.9438	0.2496	0.9408
T = 323.15 K						
0.0000	347.55	40.092	18.920	1.0000	0.0966	1.1107
0.1012	358.59	40.724	18.553	0.9960	0.1175	1.0926
0.1990	369.57	41.343	18.204	0.9919	0.1370	1.0752
0.3018	381.70	42.016	17.834	0.9870	0.1570	1.0572
0.4013	393.95	42.685	17.476	0.9820	0.1759	1.0401
0.5005	406.89	43.380	17.116	0.9766	0.1946	1.0233
0.5991	420.54	44.101	16.753	0.9708	0.2131	1.0067
0.7006	435.39	44.874	16.379	0.9645	0.2319	0.9899
0.8014	451.15	45.679	16.002	0.9578	0.2505	0.9733
0.9002	467.73	46.510	15.626	0.9509	0.2688	0.9573
1.0000	486.26	47.423	15.230	0.9432	0.2878	0.9415

Standard uncertainties u are $u(T) = \pm 0.02$ K, $u(p) = \pm 0.04$ MPa and the combined expanded uncertainty Uc in mole fraction, density, sound velocity and refractive index were $Uc(x) = \pm 0.0007$, $Uc(\rho) = \pm 0.004$ g/cm^3, $Uc(\mathrm{u}) = \pm 1.35$ m/s and $Uc(n) = \pm 0.006$, respectively, (0.95 level of confidence).

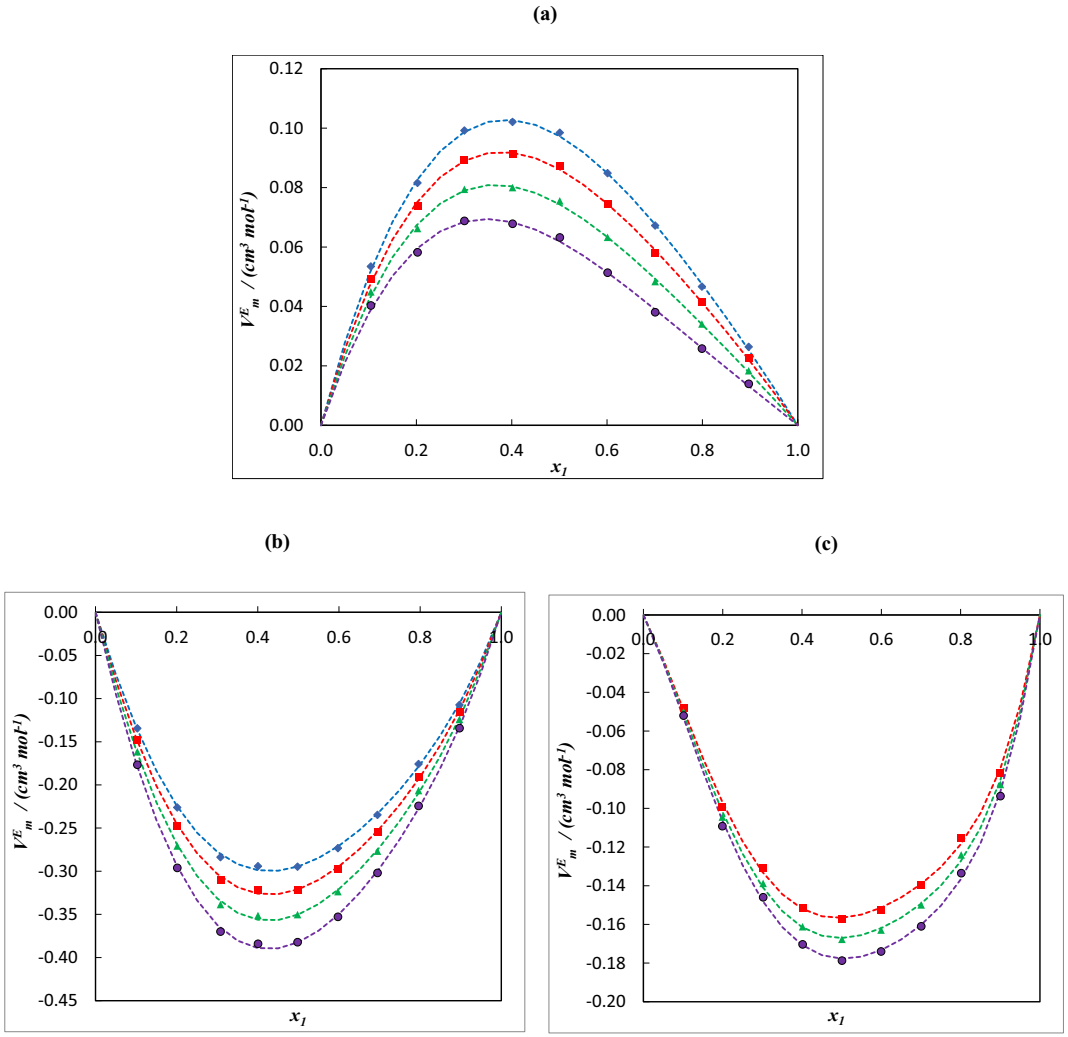

Fig. 1. Plot of excess molar volumes V^E_m for the binary mixtures: (a) {furfural (1) + DMSO (2)}, (b) {furfural (1) + acetonitrile (2)}, (c) {furfural (1) + sulfolane (2)} as function of the composition expressed in the mole fraction of furfural at 293.15 K (◆), 303.15 K (■), 313.15 K (▲) and 323.15 K (●). The dotted lines were generated using Redlich-Kister polynomial curve-fitting.

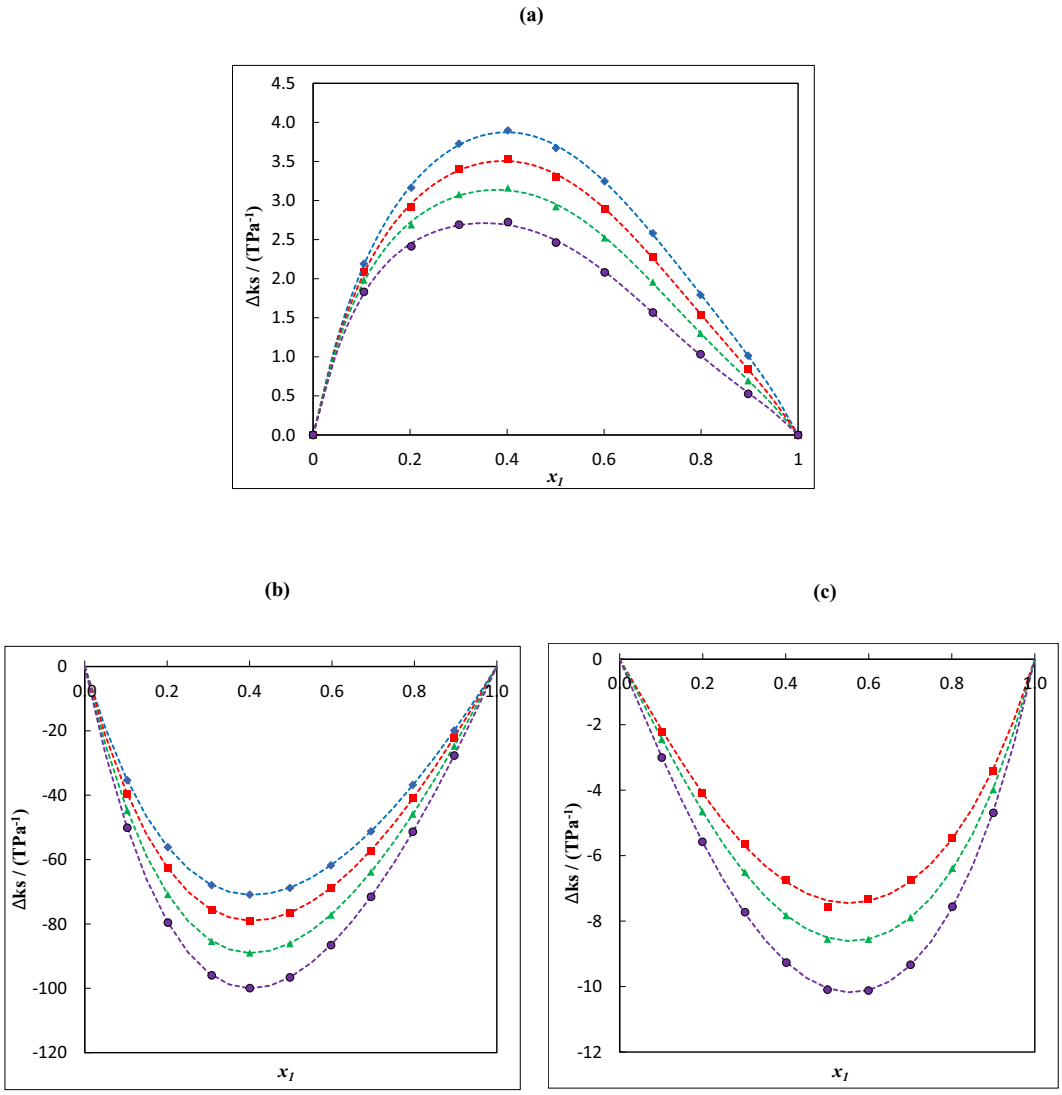

Fig. 2. Plot of deviations in isentropic compressibility $\Delta\kappa_s$ for the binary mixtures: (a) {furfural (1) + DMSO (2)}, (b) {furfural (1) + acetonitrile (2)}, (c) {furfural (1) + sulfolane (2)} as function of the composition expressed in the mole fraction of furfural at 293.15 K (◆), 303.15 K (■), 313.15 K (▲) and 323.15 K (●). The dotted lines were generated using Redlich-Kister polynomial curve-fitting.

emphasized in understanding the intermolecular interactions between components of the mixtures. To the best of our knowledge, the studied conduct in the present work is novel because there is no studies reported in literatures of thermophysical properties for studied mixtures.

2. Experimental procedure

2.1. Chemicals

Furfural, dimethyl sulfoxide (DMSO), acetonitrile and sulfolane were obtained from Sigma-Aldrich, Germany, all with minimum purities of 99%. The specifications and sources of all chemicals are summarized in Table 1. The purities of the chemicals were also checked by comparing the experimental ρ, u and n_D values of the pure components at various temperatures with those available in literature [7,9,14–57] and found to be in good agreement for ρ, u and n_D values, respectively, and are collected in Table 2. No further purification of these chemicals was required. Before carrying out the experiments, pure liquids and each mixture were degassed using an ultrasonic bath (Branson, model 3510E-MTH).

2.2. Apparatus and procedure

Binary mixtures of furfural with DMSO, acetonitrile and sulfolane were prepared by weight using an OHAUS, EX124 US analytical balance that was accurate to within ±0.0001 g. The average uncertainty in the mole fraction of the mixtures was estimated to be less than 0.0007. The values of ρ and u of pure liquids and their mixtures were measured at different temperatures and at pressure of 0.1 MPa using a digital vibrating tube densimeter and sound velocity analyzer Anton Paar (DSA 5000 M) with a temperature accuracy of ±0.02 K.The uncertainty in ρ and u measurements were ± 0.004 g.cm^{-3} and ± 1.35 m.s^{-1}, respectively. The u values were measured using a propagation time technique with frequency around 3 MHz [58].

Refractive indices for the sodium D-line were determined by the Anton Paar Abbemat 300 digital refractometer with an uncertainty in the experimental measurements of ± 0.006. The refractometer was

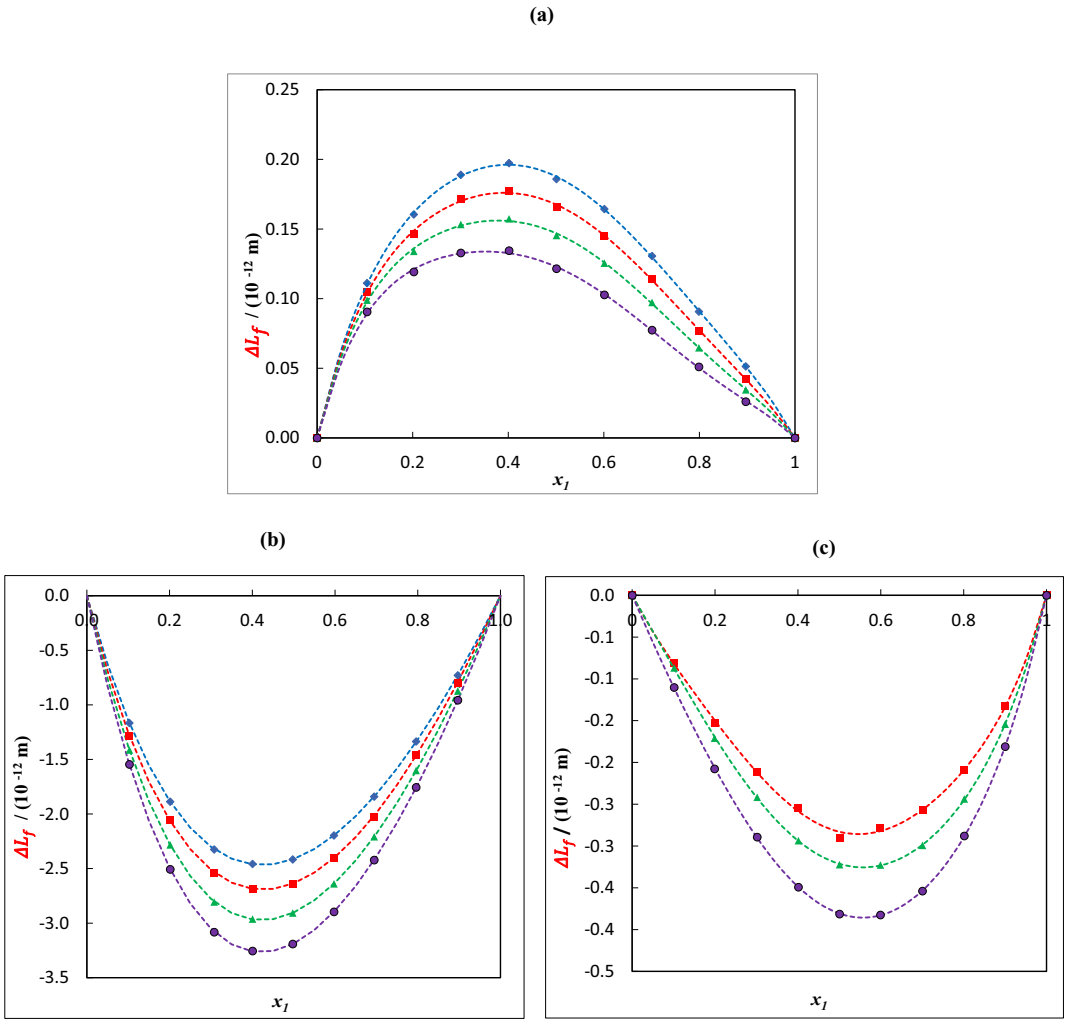

Fig. 3. Plot of deviations in intermolecular free length ΔL_f for the binary mixtures: (a) {furfural (1) + DMSO (2)}, (b) {furfural (1) + acetonitrile (2)}, (c) {furfural (1) + sulfolane (2)} as function of the composition expressed in the mole fraction of furfural at 293.15 K (◆), 303.15 K (■), 313.15 K (▲) and 323.15 K (●). The dotted lines were generated using Redlich-Kister polynomial curve-fitting.

calibrated with water before each temperature and each series of measurements and checked for pure liquids with known refractive indices. Reproducibility of the results was confirmed by performing a minimum five independent readings for each sample. All measurements were performed at the specified temperature range with a temperature accuracy of ±0.02 K.

2.3. Calculations of the empirical equations

From the experimental data of density, speed of sound and refractive indices, various thermodynamic acoustical and optical properties were calculated using the following relations employed in previous studies [59–65]. The isentropic compressibility (κ_s) is calculated directly from the measured values of u and the ρ using Newton–Laplace equation as

$$\kappa_s = 1/(\rho u^2) \tag{1}$$

Where ρ and u are the density and speed of sound of the mixtures respectively.

The u and the ρ of the medium using Newton–Laplace equation give the intermolecular free length (L_f) as

$$L_f = \kappa_{jacob} \times (\kappa_s)^{1/2} \tag{2}$$

Where, κ_{jacob} is the Jacobson's temperature-dependent constant which is equal to $\kappa_{jacob} = (93.875 + 0.375\ T) \times 10^{-8}$ [1].

The specific acoustic impedance was calculated using the following relation:

$$Z = \rho \times u \tag{3}$$

The relative association (R_A) is given by:

$$R_A = (\rho/\rho_0) \times (u_0/u)^{1/3} \tag{4}$$

Where ρ_0 and u_0 are the density and speed of sound of the pure solvents, respectively.

The relaxation strength (r) was calculated according to the following equation:

$$r = 1 - (u/u_\infty)^2 \tag{5}$$

Where u_∞ is speed of sound at infinity and its value is 1600 m.s^{-1}.

Rao's molar sound function (R) is given by:

$$R = (M/\rho) \times u^{1/3} \quad (6)$$

Where M is the molecular weight of the mixture.

Thermodynamic excess functions are very sensitive toward mutual interactions between the component molecules of the binary mixtures. The sign and the extent of deviation of the functions from ideality depend on the strength of interactions between unlike molecules [66,67]. Excess molar volume (V_m^E), deviations in isentropic compressibility ($\Delta\kappa_s$), deviations in intermolecular free length (ΔL_f), deviations in acoustic impedance (ΔZ), deviations in speed of sound (Δu) and deviation of refractive index (Δn_D) are calculated using the general relation:

$$Y^E = Y - (x_1 Y_1 + x_2 Y_2) \quad (7)$$

where Y represents V_m, κ_s, L_f, Z, u or n_D of the mixture. x is the mole fraction, and subscripts 1 and 2 refer to furfural and (DMSO or acetonitrile or sulfolane), respectively.

3. Results and discussion

3.1. Thermophysical properties of the binary mixtures (furfural + DMSO), (furfural + acetonitrile) and (furfural + sulfolane)

The values of ρ for the binary mixtures (furfural + DMSO) and (furfural + acetonitrile) at (293.15, 303.15, 313.15 and 323.15) K and at pressure of 0.1 MPa and for (furfural + sulfolane) at (303.15, 313.15 and 323.15) K are listed as a function of the mole fraction of furfural in Table 3. The plots of density at investigated temperatures are represented in Fig. 1S(a-c). It is evident from the results reported in Table 3 that the ρ values decrease by increasing the temperature for all binary systems at the same concentration. This can be explained by the molecular agitations in binary mixtures with increase in temperature which causes weakened molecular interactions resulting in decreasing ρ values [5]. Also, the ρ values increase with composition of furfural for the (furfural + DMSO) and (furfural + acetonitrile) systems whereas decrease for the (furfural + sulfolane) system. Obviously, sulfolane is much denser than furfural comparing to DMSO and acetonitrile which have density values lower than furfural.

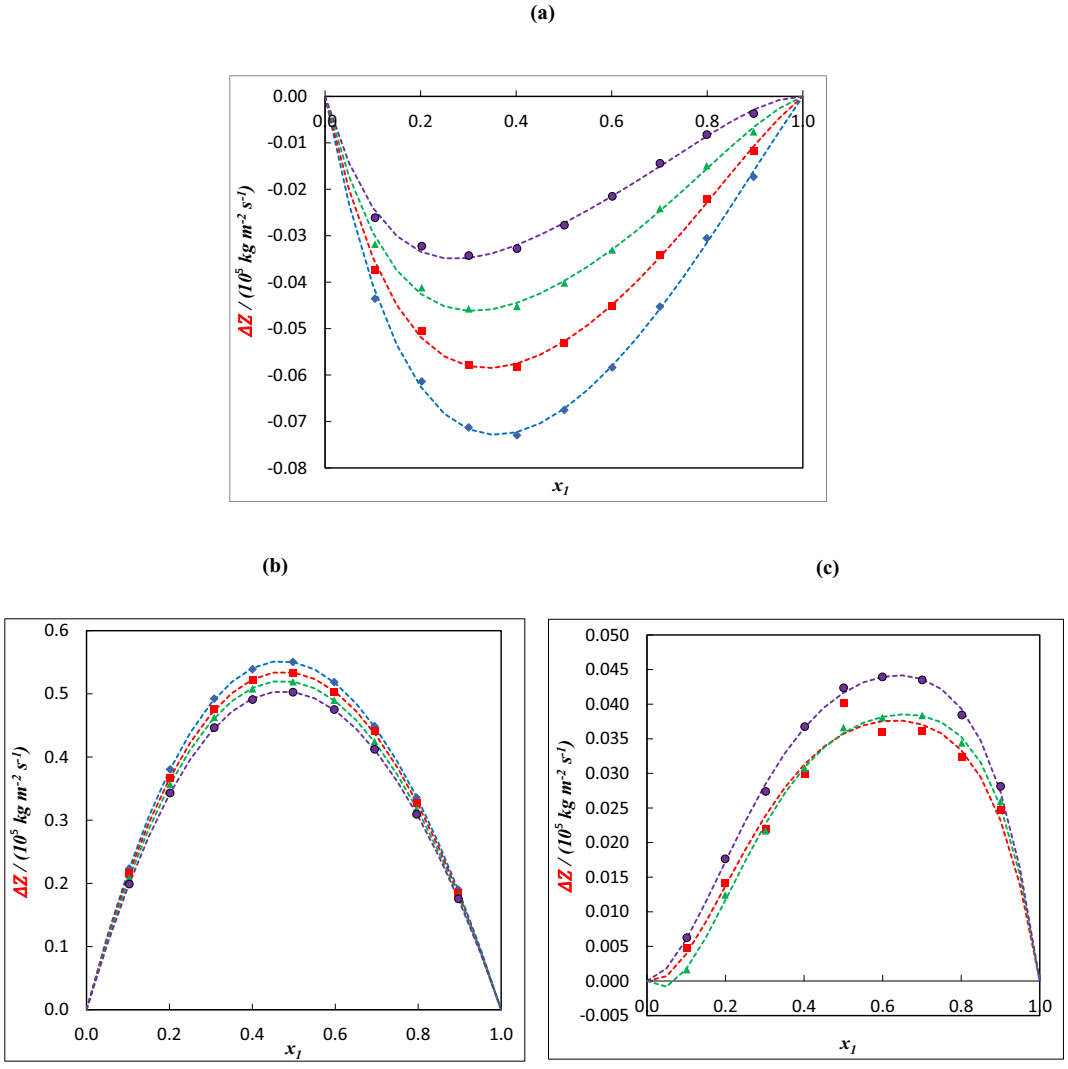

Fig. 4. Plot of deviations in acoustic impedance ΔZ for the binary mixtures: (a) {furfural (1) + DMSO (2)}, (b) {furfural (1) + acetonitrile (2)}, (c) {furfural (1) + sulfolane (2)} as function of the composition expressed in the mole fraction of furfural at 293.15 K (◆), 303.15 K (■), 313.15 K (▲) and 323.15 K (●). The dotted lines were generated using Redlich-Kister polynomial curve-fitting.

Later, u data provides information about (solvent + solvent), (solute + solvent) and (solute + solute) interactions in mixtures [68]. Table 3 reveals that the u values decrease with an increase in temperature for all binary mixtures which can be explained by the fact that with an increase in the temperature, the free spaces in molecules increase [5]. With increasing temperature, the thermal energy causes the breaking of the bonds and it weakens the molecular forces which decrease the speed of sound [63]. The decrease in u signifies that the interaction between solute and solvent is becoming less dominant [1]. The values of u were found to increase with increasing composition of furfural for the (furfural + acetonitrile) system whereas this decreases with increasing composition for the (furfural + DMSO) and (furfural + sulfolane) system at all temperatures. The speed of sound results are plotted in Fig. 2S(a-c).

Refractive indices (n_D) were measured for all the studied binary mixtures at the same experimental conditions and are included in Table 3 and presented in Fig. 3S(a-c). From these results, it can be seen that the n_D values decrease with an increase in temperature and increase as the concentration increases for all binary systems. The experimentally determined ρ, u and n_D values for the studied systems at the investigated temperatures cannot be compared to data in the literature because these systems apparently are not reported previously.

3.1.1. Excess and derived properties of the binary mixtures (furfural + DMSO), (furfural + acetonitrile) and (furfural + sulfolane)

The values of κ_s, L_f, Z, R_A, r and R for studied mixtures at investigated temperatures are provided in Table 4 and plotted against the mole fraction of furfural in Figs. 4S (a-c), 5S (a-c), 6S (a-c), 7S (a-c), 8S (a-c) and 9S (a-c). The isentropic compressibility κ_s results for studied mixtures and as shown in Figs. 4S (a-c), κ_s increases with an increase in temperature at a fixed composition for all investigated systems. An increase in isentropic compressibility κ_s indicates a change in the arrangement of the solvent molecules around the solute molecule undergoing conformational change, which results in weakening of the solute/solvent interactions [1]. This makes the solution more compressible [58].

Also, κ_s decreases with increase in concentration for the (furfural + acetonitrile) system which is an indicative of the fact that intermolecular forces are increasing which conducts the molecules to a closer packing resulting into a decrease in intermolecular free length [6]. As the concentration is increasing, κ_s increases for the (furfural + sulfolane) system inversely to (furfural + DMSO) which is not really affected by the concentration. Figs. 5S(a-c) show the variation of intermolecular free length L_f with mole fraction. From Figs. 5S(a-c), it is clear that L_f gives a similar behavior as reflected by κ_s. Intermolecular free length and isentropic compressibility are directly related to each other.

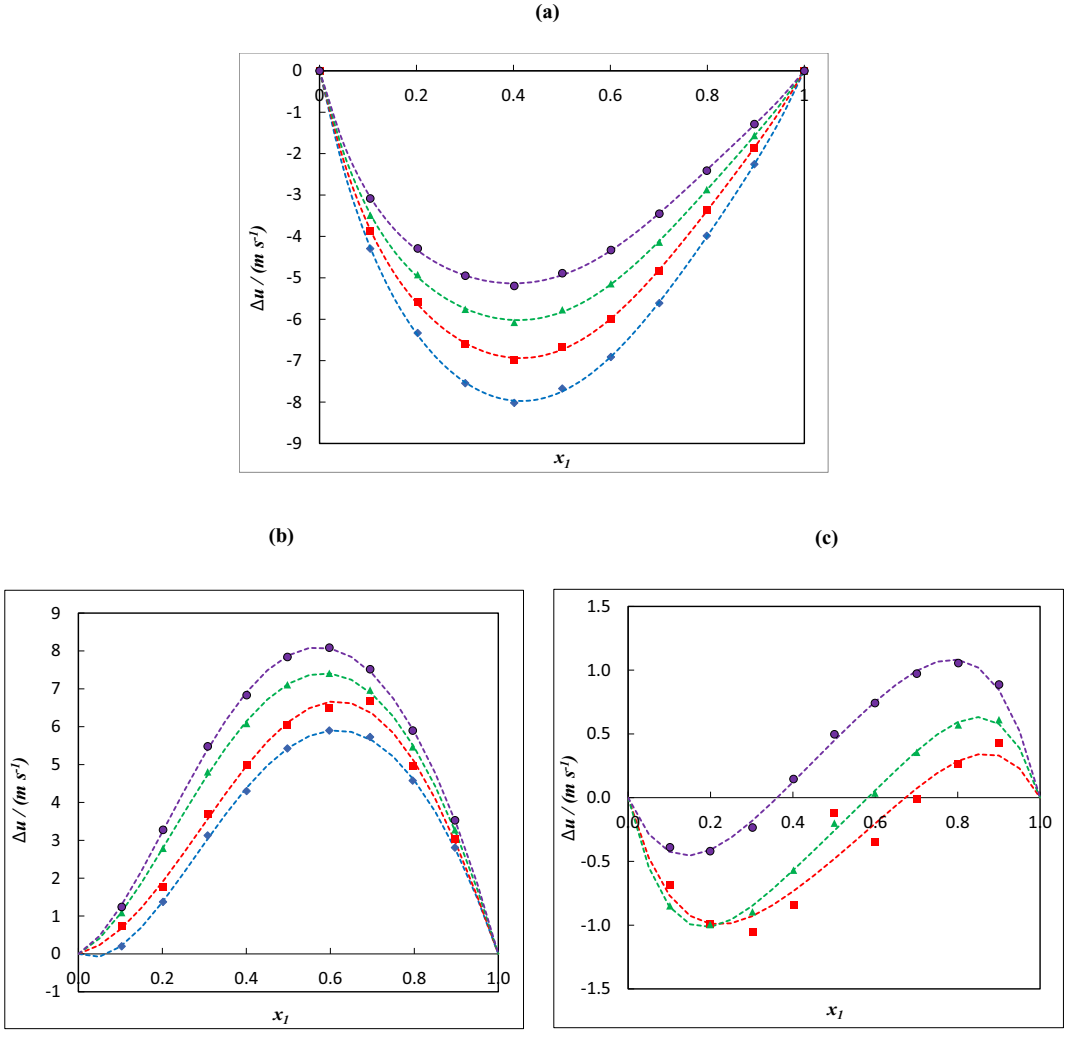

Fig. 5. Plot of deviations in speed of sound Δu for the binary mixtures: (a) {furfural (1) + DMSO (2)}, (b) {furfural (1) + acetonitrile (2)}, (c) {furfural (1) + sulfolane (2)} as function of the composition expressed in the mole fraction of furfural at 293.15 K (◆), 303.15 K (■), 313.15 K (▲) and 323.15 K (●). The dotted lines were generated using Redlich-Kister polynomial curve-fitting.

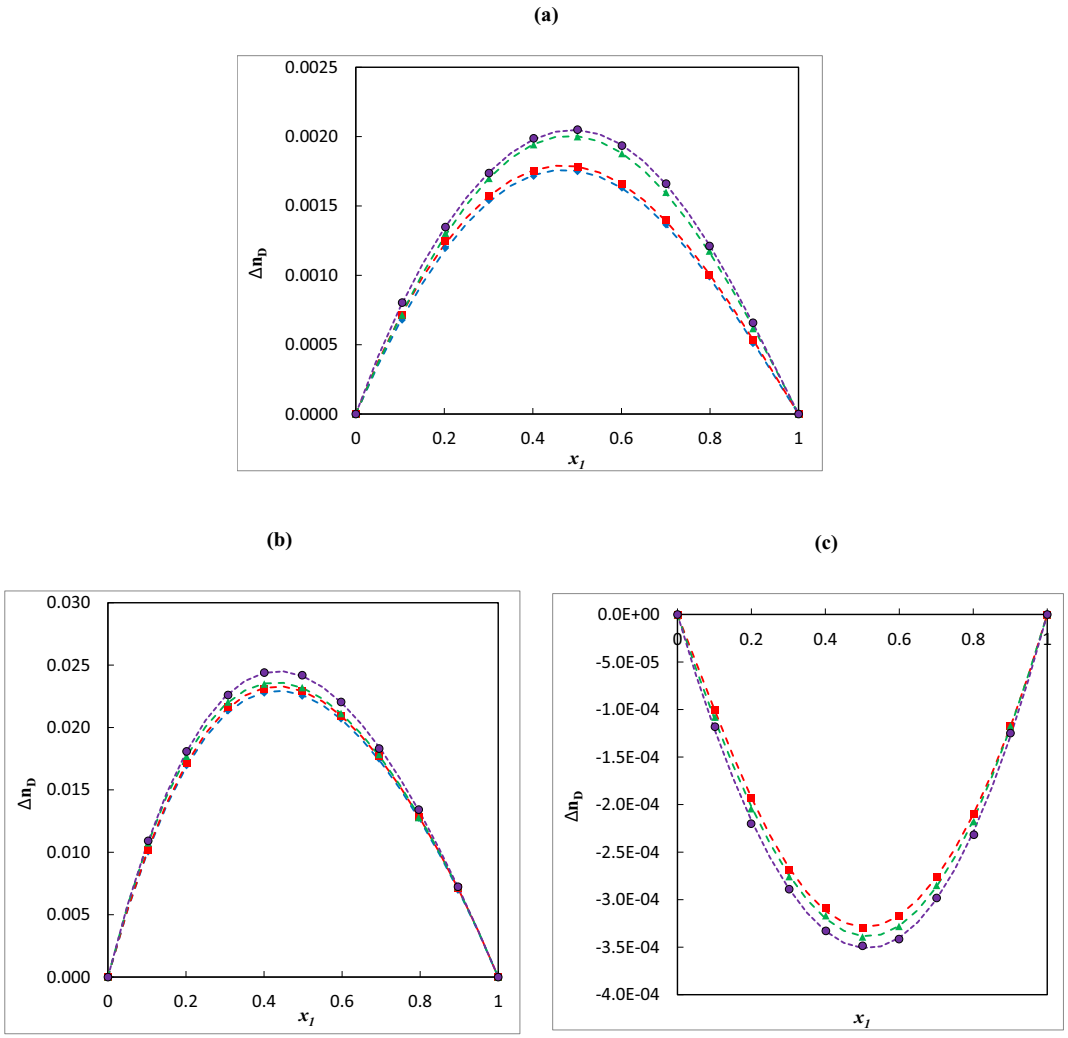

Fig. 6. Plot of changes of refractive index Δn_D for the binary mixtures: (a) {furfural (1) + DMSO (2)}, (b) {furfural (1) + acetonitrile (2)}, (c) {furfural (1) + sulfolane (2)} as function of the composition expressed in the mole fraction of furfural at 293.15 K (◆), 303.15 K (■), 313.15 K (▲) and 323.15 K (●). The dotted lines were generated using Redlich-Kister polynomial curve-fitting.

Hence, the isentropic compressibility increases with an increase in intermolecular free length. The stronger intermolecular interactions result in a tightly packed liquid structure which leads to the decrease in isentropic compressibility and intermolecular free length [1]. The formation of weaker intermolecular interaction leads to an increase in isentropic compressibility and intermolecular free length.

Moreover, intermolecular free length is a predominant factor in determining the variation of speed of sound in solutions. The inter dependence of L_f and u has been evolved from a model for sound propagation proposed by Eyring and Kincaid [69] speed of sound should decrease if the intermolecular free length increases and vice versa as a result of mixing of components. The specific acoustic impedance Z is the parameter related to the inertial and elastic properties of the medium [61]. Therefore, it is important to analyze specific acoustic impedance in relation to concentration and temperature. The dependence of Z on the concentration of furfural is presented in Fig. 6S(a-c). As shown in Fig. 6S(a-c), the specific acoustic impedance of the two binary systems (furfural + DMSO) and (furfural + acetonitrile) increases by increasing the concentration and decreases for (furfural + sulfolane) mixture. Z exhibits a decreasing trend with temperature for all investigated mixtures.

The variation of relative association R_A for all binary mixtures is presented in Fig. 7S(a-c). The higher values of R_A are indicated by the breaking up of solvent-solvent interaction whereas the lower values by the solvation of solute [70]. The dependence of the relaxation strength r on the concentration of the solute at different temperatures is shown graphically in Fig. 8S(a-c). Relaxation strength is found to decrease with increase in concentration for (furfural + acetonitrile) system and increase for both systems (furfural + DMSO) and (furfural + sulfolane). At a fixed concentration, it increases with temperature. The increase in r suggests the predominance of solute-solute interactions whereas the decrease in r values confirms the presence of solute-solvent interactions [62,71].

Fig. 9S (a-c) illustrates the results of Rao's molar sound function R. From Figs. 9S (a-c), it can be seen that the variation in R is linearly increasing with the concentration for both systems (furfural + acetonitrile) and (furfural + DMSO) and decreasing for (furfural + sulfolane). Also, the R values are independent of temperature for all binary mixtures.

Excess values of molar volume (V_m^E), deviations in isentropic compressibility ($\Delta\kappa_s$), deviations in intermolecular free length (ΔL_f), deviations in acoustic impedance (ΔZ), deviations in speed of sound (Δu)

Table 5
Coefficients A_i, and standard deviations, σ, obtained for the binary systems studied in this work at different temperatures and at pressure of 0.1 MPa for the Redlich–Kister equation.

	T (K)	A_1	A_2	A_3	A_4	A_5	σ
{Furfural (1) + DMSO (2)}							
$V^E_m/(cm^3\ mol^{-1})$	293.15	0.389	−0.186	0.043	0.011	–	0.001
	303.15	0.345	−0.179	0.049	0.012	–	0.001
	313.15	0.298	−0.178	0.051	0.009	–	0.001
	323.15	0.248	−0.176	0.051	0.006	–	0.001
$\Delta\kappa_s/(\mathrm{TPa}^{-1})$	293.15	14.8	−6.4	−0.3	−2.1	6.2	0.0
	303.15	13.4	−6.1	−0.5	−3.3	6.4	0.0
	313.15	11.8	−6.0	−0.5	−3.8	7.0	0.0
	323.15	10.0	−6.0	−0.2	−4.0	7.0	0.0
$\Delta L_f/(10^{-12}\ \mathrm{m})$	293.15	0.751	−0.327	−0.012	−0.107	0.313	0.002
	303.15	0.670	−0.309	−0.022	−0.167	0.321	0.002
	313.15	0.588	−0.301	−0.024	−0.193	0.350	0.002
	323.15	0.492	−0.297	−0.009	−0.198	0.345	0.002
$\Delta Z/(10^5\ kg\ m^{-2}\ s^{-1})$	293.15	−0.269	0.147	−0.068	0.043	–	0.001
	303.15	−0.211	0.129	−0.061	0.062	–	0.001
	313.15	−0.159	0.117	−0.061	0.066	–	0.001
	323.15	−0.109	0.107	−0.061	0.063	–	0.001
$\Delta u/(m/s)$	293.15	−31.0	10.8	0.1	4.1	−10.4	0.1
	303.15	−26.9	9.5	0.6	5.9	−10.0	0.1
	313.15	−23.3	8.6	0.6	6.3	−10.2	0.1
	323.15	−19.7	7.9	0.0	6.0	−9.3	0.0
Δn_D	293.15	0.0070	−0.0009	−0.0008	−0.0003	–	0.0000
	303.15	0.0071	−0.0010	−0.0005	−0.0004	–	0.0000
	313.15	0.0080	−0.0006	−0.0011	0.0001	–	0.0000
	323.15	0.0082	−0.0003	−0.0006	−0.0009	–	0.0000
{Furfural (1) + acetonitrile (2)}							
$V^E_m/(cm^3\ mol^{-1})$	293.15	−1.178	0.301	−0.205	−0.147	–	0.003
	303.15	−1.284	0.336	−0.218	−0.145	–	0.003
	313.15	−1.401	0.378	−0.233	−0.157	–	0.004
	323.15	−1.529	0.417	−0.247	−0.163	–	0.004
$\Delta\kappa_s/(\mathrm{TPa}^{-1})$	293.15	−274.6	97.9	−37.6	12.7	–	0.1
	303.15	−305.7	107.7	−43.6	20.1	–	0.2
	313.15	−343.7	126.2	−49.6	17.0	–	0.1
	323.15	−385.7	143.7	−55.0	15.7	–	0.1
$\Delta L_f/(10^{-12}\ \mathrm{m})$	293.15	−9.649	2.832	−0.940	0.263	–	0.003
	303.15	−10.541	3.011	−1.076	0.530	–	0.007
	313.15	−11.611	3.502	−1.180	0.331	–	0.003
	323.15	−12.751	3.894	−1.246	0.226	–	0.004
$\Delta Z/(10^5\ kg\ m^{-2}\ s^{-1})$	293.15	2.201	−0.250	0.055	0.022	–	0.001
	303.15	2.135	−0.201	0.057	−0.038	–	0.002
	313.15	2.077	−0.219	0.043	0.027	–	0.001
	323.15	2.012	−0.201	0.027	0.052	–	0.001
$\Delta u/(m/s)$	293.15	21.8	15.8	−8.8	2.7	–	0.1
	303.15	24.5	17.9	−7.6	−3.6	–	0.2
	313.15	28.5	13.1	−7.8	2.5	–	0.1
	323.15	31.5	11.9	−8.7	5.2	–	0.1
Δn_D	293.15	0.0903	−0.0233	0.0040	0.0031	–	0.0001
	303.15	0.0916	−0.0242	0.0037	0.0044	–	0.0001
	313.15	0.0926	−0.0258	0.0064	0.0015	–	0.0001
	323.15	0.0964	−0.0254	0.0025	0.0006	–	0.0001
{Furfural (1) + Sulfolane (2)}							
$V^E_m/(cm^3\ mol^{-1})$	303.15	−0.626	0.021	−0.134	−0.369	–	0.002
	313.15	−0.668	0.011	−0.137	−0.396	–	0.002
	323.15	−0.711	−0.011	−0.140	−0.406	–	0.003
$\Delta\kappa_s/(\mathrm{TPa}^{-1})$	303.15	−29.5	−6.0	−1.5	−3.7	–	0.1
	313.15	−34.0	−7.5	−2.0	−5.1	–	0.0
	323.15	−40.2	−8.9	−3.1	−4.7	–	0.0
$\Delta L_f/(10^{-12}\ \mathrm{m})$	303.15	−1.132	−0.242	0.180	−0.188	−0.433	0.005
	313.15	−1.285	−0.299	0.016	−0.263	−0.153	0.001
	323.15	−1.523	−0.347	−0.011	−0.231	−0.205	0.001
$\Delta Z/(10^5\ kg\ m^{-2}\ s^{-1})$	303.15	0.143	0.061	0.012	0.114	–	0.003
	313.15	0.143	0.071	0.010	0.144	–	0.001
	323.15	0.167	0.072	0.029	0.118	–	0.001
$\Delta u/(m/s)$	303.15	−1.9	5.4	−0.8	3.4	–	0.2
	313.15	−1.0	6.3	−0.8	5.7	–	0.0
	323.15	1.8	6.4	0.9	3.8	–	0.0
Δn_D	303.15	−0.0013	0.0000	0.0002	−0.0001	–	0.0000
	313.15	−0.0014	−0.0001	0.0001	0.0000	–	0.0000
	323.15	−0.0014	−0.0001	0.0000	0.0000	–	0.0000

Standard uncertainties u are $u(T) = \pm 0.02$ K, $u(p) = \pm 0.04$ MPa and the combined expanded uncertainty Uc in mole fraction, density, sound velocity and refractive index were $Uc(x) = \pm 0.0007$, $Uc(\rho) = \pm 0.004$ g/cm^3, $Uc(\mathrm{u}) = \pm 1.35$ m/s and $Uc(n) = \pm 0.006$, respectively, (0.95 level of confidence).

and changes in refractive index (Δn_D) were also calculated and presented in Table 1S. Figs. 1-6(a-c) show that the excess values of V_m, κ_s, L_f, Z, u and n_D are positive/negative and nonlinear throughout the concentration range.

Inspection of Figs. 1 (a-c) reveals that the excess molar volume V_m^E values are positive over the complete composition range for the system (furfural + DMSO) and negative for both (furfural + acetonitrile) and (furfural + sulfolane) systems. It's well known that the furfural molecules are dipolar associate in the pure state [72], these dipolar associates are breaking by the addition of polar solvents. The positive values of V_m^E are due to mutual breaking of hydrogen-bonding structures in the mixtures resulting in expansion in volume [73]. The predominance of hydrogen bond interactions between the unlike molecules over the dissociation effects in the mixtures is indicated by the negative values of V_m^E [74–76]. The magnitudes of V_m^E values follow the sequence: (furfural + DMSO) > (furfural + sulfolane) > (furfural + acetonitrile), from these results it's clear that the interaction of furfural with acetonitrile is stronger than furfural with sulfolane than furfural with DMSO.

The deviation in isentropic compressibility $\Delta\kappa_s$ over the entire composition range of furfural for all mixtures is plotted in Figs. 2 (a-c). It can be seen from Figs. 2 (a-c), that the $\Delta\kappa_s$ values are positive for (furfural + DMSO) system indicating weaker interactions between solute and solvent molecules resulting from the disruption of molecular association [1]. The observed negative values of $\Delta\kappa_s$ of (furfural + acetonitrile) and (furfural + sulfolane) systems can be explained by the presence of specific interactions between molecules in mixtures which provides decreasing in the free- space [77–79]. As shown in Table 1S, increasing temperature for all mixtures at a fixed composition of furfural leads to a decrease in $\Delta\kappa_s$ values.

The results shown in Figs. 3-4(a-c) indicate that ΔL_f values are positive over the entire mole fraction range for (furfural + DMSO) while ΔZ shows opposite trend which indicates that the physical interaction due to dispersion forces or weak dipole–dipole interaction [80]. Inversely to (furfural + acetonitrile) and (furfural + sulfolane) systems which reveal negative values of ΔL_f and positive values of ΔZ at all investigated temperatures. This may be due to the chemical interaction consisting of charge transfer forces, formation of H bonds and other complex forming interactions [80].

The dependence of deviations in speed of sound Δu on mole fraction of furfural is presented in Figs. 5 (a-c). The Δu values are negative for (furfural + DMSO) and positive for (furfural + acetonitrile) system. Both positive and negative Δu values are observed for (furfural + sulfolane) system, which has a sinusoidal shape.

The Δn_D data for studied systems are also listed in Table 1S and plotted versus the mole fraction of furfural in Fig. 6(a-c). As shown, the changes in refractive index are positive for both (furfural + DMSO) and (furfural + acetonitrile) system, these values increase with temperature. (furfural + sulfolane) system presents negative values of Δn_D which decrease with increasing temperature.

3.2. Correlation of derived properties

The excess functions V_m^E, $\Delta\kappa_s$, ΔL_f, ΔZ, Δu and Δn_D were fitted to Redlich–Kister [81] polynomial equation of the type

$$X = x_1 x_2 \sum_{i=1}^{k} A_i (1-2x_1)^{i-1} \quad (9)$$

where $X = V_m^E$ or $\Delta\kappa_s$ or ΔL_f or ΔZ or Δu or Δn_D.

A_i are the fitting parameters obtained by least-square method.

In each case, the optimum number of coefficients was ascertained from an examination of the variation of standard deviation, σ, with:

$$\sigma(X) = \left[\frac{\sum_{i=1}^{N} (X_{expt} - X_{calc})^2}{(N-k)}\right]^{1/2} \quad (10)$$

where $X_{expt.}$ and $X_{calc.}$ are the experimental and calculated values of the property X, respectively, and N and k are the number of experimental points and number of coefficients used in the Redlich-Kister equation. Table 5 presents the values of the fitting parameters A_i together with the standard deviation, σ. The values of V_m^E, $\Delta\kappa_s$, ΔL_f, ΔZ, Δu and Δn_D as well as the plots of the Redlich-Kister model are displayed in Figs. 1 (a-c), 2 (a-c), 3 (a-c), 4 (a-c), 5 (a-c) and 6 (a-c), respectively. The agreement between the experimental data and those calculated using Redlich–Kister equation was satisfactory at the investigated temperatures for all the systems.

4. Conclusions

In the present investigation, the density, speed of sound and refractive index were measured at different temperatures and at pressure of 0.1 MPa for binary mixtures containing furfural as a common component with DMSO or acetonitrile or sulfolane as the other component. Out of these measured data the isentropic compressibility (κ_s), intermolecular free length (L_f), specific acoustic impedance (Z), relative association (R_A), relaxation strength (r) and Rao's molar sound function (R) have been calculated. The obtained results show that the increase in temperature for all binary mixtures leads to a decrease in density, speed of sound and refractive index values. Also, the calculated parameters depend on the temperature and/or on the composition of the mixture. Deviation parameters have been also computed and correlated by a Redlich–Kister type polynomial equation to derive the coefficients and standard deviation. Both negative and positive deviations were observed for all deviation parameters, which is indicative of the presence of molecular interactions. The results have been discussed in terms of the interactions between the participating components of the mixtures.

Declaration of Competing Interest

The authors declare that they have no known competing financial interests or personal relationships that could have appeared to influence the work reported in this paper.

Acknowledgements

The authors (L.N.) and (A.N.) acknowledge funding from DGRSDT (Algeria).

Appendix A. Supplementary data

Supplementary data to this article can be found online at https://doi.org/10.1016/j.molliq.2021.115436.

References

[1] B. Thanuja, G. Nithya, C.C. Kanagam, Ultrasonic studies of intermolecular interactions in binary mixtures of 4-methoxy benzoin with various solvents: excess molar functions of ultrasonic parameters at different concentrations and in different solvents, Ultrason. Sonochem. 19 (6) (2012) 1213–1220.
[2] K. Tamura, T. Sonoda, S. Murakami, Thermodynamic properties of aqueous solution of 2-Isopropoxyethanol at 25°C, J. Solut. Chem. 28 (6) (1999) 777–789.
[3] B. García, R. Alcalde, J.M. Leal, J.S. Matos, Solute−solvent interactions in amide −water mixed Solvents, J. Phys. Chem. B 101 (40) (1997) 7991–7997.
[4] P. Venkatesu, Thermophysical contribution of N,N-dimethylformamide in the molecular interactions with other solvents, Fluid Phase Equilib. 298 (2010) 173–191.
[5] R. Umapathia, C.N. Rao, P. Naidoo, I. Bahadur, D. Ramjugernath, P. Venkatesua, Effect of temperature on molecular interactions between ri(butyl)methylphosphonium methylsulfate and furfural, J. Chem. Thermodyn. 149 (2020) 106150.

[6] P.K. Pandey, A. Awasthi, A. Awasthi, Intermolecular interactions in binary mixtures of 2-Chloroethanol with 2-Dimethylaminoethanol and 2-Diethylaminoethanol at different temperatures, Chem. Phys. 423 (2013) 119–126.
[7] K. Yan, G. Wu, T. Lafleur, C. Jarvis, Production, properties and catalytic hydrogenation of furfural to fuel additives and value-added chemicals, Renew. Sust. Energ. Rev. 38 (2014) 663–676.
[8] J.K. Raman, E. Gnansounou, Furfural production from empty fruit bunch – A biorefinery approach, Ind. Crop. Prod. 69 (2015) 371–377.
[9] L. Bendiaf, A. Negadi, I. Mokbel, L. Negadi, Isothermal vapor–liquid equilibria of binary systems containing green solvents derived from biomass (Furfuryl alcohol +toluene), (furfuryl alcohol+ethanol), or (furfural+toluene), Fuel 122 (2014) 247–253.
[10] M. Zaoui-Djelloul-Daouadji, L. Bendiaf, I. Bahadur, A. Negadi, D. Ramjugernath, E.E. Ebenso, L. Negadi, Volumetric and acoustic properties of binary systems (furfural or furfuryl alcohol+toluene) and (furfuryl alcohol+ethanol) at different temperatures, Thermochim. Acta 611 (2015) 47–55.
[11] L. Kara Zaitri, L. Negadi, I. Mokbel, N. Msakni, J. Jose, Liquid–vapor equilibria of binary systems containing alcohols (1-butanol, or 2-butanol or 1-hexanol) present in the production by chemical process of 2,5-dimethyl furan from biomass, Fuel 95 (2012) 438–445.
[12] L. Negadi, I. Mokbel, N. Chiali-Baba-Ahmed, L. Kara Zaitri, Phase equilibrium properties of binary mixtures containing 2,5-dimethylfuran and furfuryl alcohol or methyl isobutyl ketone at several temperatures, J. Chem. Thermodyn. 70 (2014) 233–238.
[13] L. Negadi, B. Feddal-Benabed, I. Bahadur, J. Saab, M. Zaoui-Djelloul-Daouadji, D. Ramjugernath, A. Negadi, Effect of temperature on density, sound velocity, and their derived properties for the binary systems glycerol with water or alcohols, J. Chem. Thermodyn. 109 (2017) 124–136.
[14] L. Bendiaf, I. Bahadur, A. Negadi, P. Naidoo, D. Ramjugernath, L. Negadi, Effects of alkyl group and temperature on the interactions between furfural and alcohol: insight from density and sound velocity studies, Thermochim. Acta 599 (2015) 13–22.
[15] R.W. Stephenson, M. Van Winkle, Modification of relative volatilities by addition of solvent, J. Chem. Eng. Data 7 (4) (1962) 510–516.
[16] M. Baccaredda, P. Pino, La Velocita degli Ultrasuoni in Alcuni Composti Carbonilici e Carbossilici, Gazz. Chim. Ital 81 (1951) 205–211.
[17] L. Lomba, B. Giner, I. Bandrés, C. Lafuente, M.R. Pino, Physicochemical properties of green solvents derived from biomass, Green Chem. 13 (8) (2011) 2062–2070.
[18] H. Naorem, S.K. Suri, Excess molar enthalpies for binary liquid mixtures of furfural with some aromatic hydrocarbons, J. Solut. Chem. 18 (5) (1989) 493–497.
[19] J.A. Riddick, W.B. Bunger, Solvents, Organic, Techniques of Organic Chemistry, Wiley-Interscience, New York, 1970.
[20] B.F. de Almeida, T.M. Waldrigui, T.D.C. Alves, L.H. de Oliveira, M. Aznar, Experimental and calculated liquid–liquid equilibrium data for water+furfural+solvents, Fluid Phase Equilib. 334 (2012) 97–105.
[21] F. Ouaar, A. Negadi, I. Bahadur, R. Phadagi, B. Feddal-Benabed, L. Negadi, Volumetric, acoustic and transport properties of mixtures containing dimethyl sulfoxide and some amines or alkanolamines: measurement and correlation, J. Chem. Thermodyn. 121 (2018) 187–198.
[22] X. Wang, F. Yang, Y. Gao, Z. Liu, Volumetric properties of binary mixtures of dimethyl sulfoxide with amines from (293.15 to 363.15)K, J. Chem. Thermodyn. 57 (2013) 145–151.
[23] F. Ouaar, A. Negadi, I. Bahadur, L. Negadi, Thermophysical approach to understand the nature of molecular interactions and structural factor between methyl isobutyl ketone and organic solvents mixtures, J. Chem. Thermodyn. 113 (2017) 291–300.
[24] N.G. Tsierkezos, A.E. Kelarakis, M.M. Palaiologou, Densities, viscosities, refractive indices, and surface tensions of dimethyl sulfoxide + butyl acetate mixtures at (293.15, 303.15, and 313.15) K, J. Chem. Eng. Data 45 (2) (2000) 395–398.
[25] O. Ciocirlan, O. Iulian, Vapor pressure, density, viscosity and refractive index of dimethyl sulfoxide+ 1, 4-dimethylbenzene system, J. Serbian Chem. Soc. 73 (1) (2008) 73–85.
[26] B. Naseem, A. Jamal, A. Jamal, Influence of sodium acetate on the volumetric behavior of binary mixtures of DMSO and water at 298.15 to 313.15K, J. Mol. Liq. 181 (2013) 68–76.
[27] M. Radhamma, P. Venkatesu, M.P. Rao, M.J. Lee, H.M. Lin, Excess molar volumes and ultrasonic studies of dimethylsulphoxide with ketones at T=303.15K, J. Chem. Thermodyn. 40 (3) (2008) 492–497.
[28] V. Govinda, P. Attri, P. Venkatesu, P. Venkateswarlu, Thermophysical properties of dimethylsulfoxide with ionic liquids at various temperatures, Fluid Phase Equilib. 304 (1) (2011) 35–43.
[29] J.G. Baragi, M.I. Aralaguppi, T.M. Aminabhavi, M.Y. Kariduraganavar, A.S. Kittur, Density, viscosity, refractive index, and speed of sound for binary mixtures of anisole with 2-chloroethanol, 1,4-dioxane, tetrachloroethylene, tetrachloroethane, DMF, DMSO, and diethyl oxalate at (298.15, 303.15, and 308.15) K, J. Chem. Eng. Data 50 (3) (2005) 910–916.
[30] A.H. Absood, M.S. Tutunji, K.Y. Hsu, H.L. Clever, The density and enthalpy of mixing of solutions of acetonitrile and of dimethyl sulfoxide with several aromatic hydrocarbons, J. Chem. Eng. Data 21 (3) (1976) 304–308.
[31] T.M. Aminabhavi, B. Gopalakrishna, Density, viscosity, refractive index, and speed of sound in aqueous mixtures of N,N-dimethylformamide, dimethyl sulfoxide, N, N-dimethylacetamide, acetonitrile, ethylene glycol, diethylene glycol, 1,4-dioxane, tetrahydrofuran, 2-methoxyethanol, and 2-ethoxyethanol at 298.15 K, J. Chem. Eng. Data 40 (4) (1995) 856–861.
[32] K. Tiwari, C. Patra, S. Padhy, V. Chakravortty, Molecular interaction study on binary mixtures of dimethyl Sulphoxide + isobutyl methyl ketone (IBMK), + Acetylacetone and + tri-N-Butylphosphate (TBP) from the excess properties of ultrasonic velocity, viscosity and density, Phys. Chem. Liq. 32 (3) (1996) 149–157.
[33] A. Ali, K. Tewari, A.K. Nain, V. Chakravortty, Study of intermolecular interaction in dimethylsulphoxide + 1-alkanols (1-butanol, 1-hexanol, 1-octanol) at 303.15 K, Phys. Chem. Liq. 38 (4) (2000) 459–473.
[34] S.L. Oswal, N.B. Patel, Speeds of sound, isentropic compressibilities, and excess volumes of binary mixtures of acrylonitrile with organic solvents, J. Chem. Eng. Data 45 (2) (2000) 225–230.
[35] V. Syamala, K. Siva Kumar, P. Venkateswarlu, Volumetric, ultrasonic and viscometric studies of binary mixtures of dimethyl sulphoxide with chloro and nitro substituted aromatic hydrocarbons at T=303.15K, J. Chem. Thermodyn. 38 (12) (2006) 1553–1562.
[36] O. Ciocirlan, O. Iulian, Density, viscosity and refractive index of the dimethyl sulfoxide+ o-xylene system, J. Serbian Chem. Soc. 74 (3) (2009) 317–329.
[37] S.A. Markarian, A.M. Asatryan, A.L. Zatikyan, Volumetric properties of aqueous solutions of diethylsulfoxide at temperatures from 298.15 K to 343.15 K, J. Chem. Thermodyn. 37 (8) (2005) 768–777.
[38] S. Paez, M. Contreras, Densities and viscosities of binary mixtures of 1-propanol and 2-propanol with acetonitrile, J. Chem. Eng. Data 34 (4) (1989) 455–459.
[39] S. Singh, I. Bahadur, G.G. Redhi, D. Ramjugernath, E.E. Ebenso, Density and speed of sound measurements of imidazolium-based ionic liquids with acetonitrile at various temperatures, J. Mol. Liq. 200 (2014) 160–167.
[40] H. Iloukhani, M. Almasi, Densities, viscosities, excess molar volumes, and refractive indices of acetonitrile and 2-alkanols binary mixtures at different temperatures: experimental results and application of the Prigogine–Flory–Patterson theory, Thermochim. Acta 495 (1) (2009) 139–148.
[41] F. Chen, Z. Yang, Z. Chen, J. Hu, C. Chen, J. Cai, Density, viscosity, speed of sound, excess property and bulk modulus of binary mixtures of γ-butyrolactone with acetonitrile, dimethyl carbonate, and tetrahydrofuran at temperatures (293.15 to 333.15) K, J. Mol. Liq. 209 (2015) 683–692.
[42] P.S. Nikam, L.N. Shirsat, M. Hasan, Density and viscosity studies of binary mixtures of acetonitrile with methanol, ethanol, propan-1-ol, propan-2-ol, butan-1-ol, 2-methylpropan-1-ol, and 2-methylpropan-2-ol at (298.15, 303.15, 308.15, and 313.15) K, J. Chem. Eng. Data 43 (5) (1998) 732–737.
[43] K. Rajagopal, S. Chenthilnath, Study on excess thermodynamic parameters and theoretical estimation of ultrasonic velocity using scaled particle theory in binary liquid mixtures of 2-methyl-2-propanol and nitriles at different temperatures, Chin. J. Chem. Eng. 18 (5) (2010) 804–816.
[44] M.I. Aralaguppi, C.V. Jadar, T.M. Aminabhavi, Density, refractive index, viscosity, and speed of sound in binary mixtures of 2-ethoxyethanol with dioxane, acetonitrile, and tetrahydrofuran at (298.15, 303.15, and 308.15) K, J. Chem. Eng. Data 41 (6) (1996) 1307–1310.
[45] M.A. Varfolomeev, I.T. Rakipov, B.N. Solomonov, W. Marczak, Speed of sound, density, and related thermodynamic excess properties of binary mixtures of 2-Pyrrolidone and N-Methyl-2-pyrrolidone with acetonitrile and chloroform, J. Chem. Eng. Data 61 (3) (2016) 1032–1046.
[46] G. Moumouzias, D.K. Panopoulos, G. Ritzoulis, Excess properties of the binary liquid system propylene carbonate + acetonitrile, J. Chem. Eng. Data 36 (1) (1991) 20–23.
[47] X. Yang, H. Song, J. Wang, W. Zou, Temperature and composition dependence of the density, viscosity and refractive index of binary mixtures of a novel gemini ionic liquid with acetonitrile, RSC Adv. 6 (35) (2016) 29172–29181.
[48] M. Vahidi, B. Moshtari, Dielectric data, densities, refractive indices, and their deviations of the binary mixtures of N-methyldiethanolamine with sulfolane at temperatures 293.15–328.15K and atmospheric pressure, Thermochim. Acta 551 (2013) 1–6.
[49] M.K. Patwari, R.K. Bachu, S. Boodida, S. Nallani, Densities, viscosities, and speeds of sound of binary liquid mixtures of sulfolane with ethyl acetate, n-propyl acetate, and n-butyl acetate at temperature of (303.15, 308.15, and 313.15) K, J. Chem. Eng. Data 54 (3) (2009) 1069–1072.
[50] C.M. Kinart, M. Maj-Rudnicka, W.J. Kinart, A. Ćwiklińska, Z. Kinart, Studies on intermolecular interactions in sulfolane+alkoxyethanol binary mixtures by speed of sound and 1H NMR measurements at T=303.15K, J. Mol. Liq. 186 (2013) 28–32.
[51] A.M. Awwad, A.H. Al-Dujaili, H.E. Salman, Relative permittivities, densities, and refractive indices of the binary mixtures of sulfolane with ethylene glycol, diethylene glycol, and poly(ethylene glycol) at 303.15 K, J. Chem. Eng. Data 47 (3) (2002) 421–424.
[52] C. Yang, W. Yu, P. Ma, Densities and viscosities of binary mixtures of Ethylbenzene + N-Methyl-2-pyrrolidone, Ethylbenzene + Sulfolane, and styrene + octane from (303.15 to 353.15) K and atmospheric pressure, J. Chem. Eng. Data 50 (4) (2005) 1197–1203.
[53] L. Mohammadi, A. Omrani, Volumetric and optical properties of sulfolane (TMS)+1, 5-pentanediol binary solutions, J. Mol. Liq. 241 (2017) 163–172.
[54] C.M. Kinart, M. Maj, A. Ćwiklińska, W.J. Kinart, Densities, viscosities and relative permittivities of some n-alkoxyethanols with sulfolane at T=303.15 K, J. Mol. Liq. 139 (1) (2008) 1–7.
[55] M.A. Saleh, M. Shamsuddin Ahmed, S.K. Begum, Density, viscosity and thermodynamic activation for viscous flow of water+sulfolane, Phys. Chem. Liq. 44 (2) (2006) 153–165.
[56] C. Yang, P. Ma, Q. Zhou, Excess molar volumes and viscosities of binary mixtures of Sulfolane with benzene, toluene, Ethylbenzene, p-xylene, o-xylene, and m-xylene at 303.15 and 323.15 K and atmospheric pressure, J. Chem. Eng. Data 49 (4) (2004) 881–885.
[57] G.S. Chen, H. Knapp, Densities and excess molar volumes for sulfolane plus ethylbenzene, sulfolane plus 1-methylnaphthalene, water plus N,N-dimethylformamide, water plus methanol, water plus N-formylmorpholine, and water plus N-methylpyrrolidone, J. Chem. Eng. Data 40 (4) (1995) 1001–1004.
[58] M.T. Zafarani-Moattar, H. Shekaari, Apparent molar volume and isentropic compressibility of ionic liquid 1-butyl-3-methylimidazolium bromide in water,

methanol, and ethanol at T=(298.15 to 318.15)K, J. Chem. Thermodyn. 37 (10) (2005) 1029–1035.
[59] A. Awasthi, M. Rastogi, J.P. Shukla, Ultrasonic and IR study of molecular association process through hydrogen bonding in ternary liquid mixtures, Fluid Phase Equilib. 215 (2) (2004) 119–127.
[60] M. Rastogi, A. Awasthi, M. Gupta, J.P. Shukla, Molecular association of aliphatic ketones and phenol in a nonpolar solvent-ultrasonic and IR study, J. Mol. Liq. 107 (1) (2003) 185–204.
[61] A. Awasthi, J.P. Shukla, Ultrasonic and IR study of intermolecular association through hydrogen bonding in ternary liquid mixtures, Ultrasonics 41 (6) (2003) 477–486.
[62] S. Azhagiri, S. Jayakumar, R. Padmanaban, S. Gunasekaran, S. Srinivasan, Acoustic and thermodynamic properties of binary liquid mixtures of Benzaldehyde in hexane and cyclohexane, J. Solut. Chem. 38 (4) (2009) 441–448.
[63] I. Ion, F. Sirbu, A.C. Ion, Density, refractive index, and ultrasound speed in mixtures of active carbon and exfoliated graphite nanoplatelets dispersed in N,N-dimethylformamide at temperatures from (293.15 to 318.15) K, J. Chem. Eng. Data 58 (5) (2013) 1212–1222.
[64] S.K. Dash, S.K. Pradhan, B. Dalai, L. Moharana, B.B. Swain, Studies on molecular interaction in binary mixtures of diethyl ether with some alkanols – an acoustic approach, Phys. Chem. Liq. 50 (6) (2012) 735–749.
[65] S. Bagchi, S.K. Nema, R.P. Singh, Ultrasonic and viscometric investigation of ISRO polyol in various solvents and its compatibility with polypropylene glycol, Eur. Polym. J. 22 (10) (1986) 851–857.
[66] J.S. Sandhu, A.K. Sharma, R.K. Wadi, Excess molar volumes of n-alkanol (C1-C5) binary mixtures with acetonitrile, J. Chem. Eng. Data 31 (2) (1986) 152–154.
[67] B. García, R. Alcalde, J.M. Leal, J.S. Matos, Formamide–(C1–C5) alkan-1-ols solvent systems, journal of the chemical society, Faraday Trans. 92 (18) (1996) 3347–3352.
[68] M.N. Roy, D. Ekka, R. Dewan, Physico-chemical studies of some bio-active solutes in pure methanoic acid, Acta Chim. Slov. 58 (4) (2011) 792–796.
[69] J.F. Kincaid, H. Eyring, Free volumes and free angle ratios of molecules in liquids, J. Chem. Phys. 6 (10) (1938) 620–629.
[70] R.J. Fork, W.R.M, Trans Faraday Sco 61 (1965) 2105.
[71] S. Baluja, S. Oza, Ultrasonic studies of some derivatives of sulphonamide in dimethylformamide, Fluid Phase Equilib. 200 (1) (2002) 11–18.
[72] V.G. Kulnevich, Y.M. Shapiro, Electronic spectroscopy of solutions of heterocyclic-compounds in H2SO4. 1. Study of stability of furan compounds in H2SO4, Khim. Geterotsikl. Soedin. 12 (1972) 1594–1596.
[73] A. Ali, A.K. Nain, D. Chand, R. Ahmad, Volumetric, ultrasonic and viscometric studies of molecular interactions in binary mixtures of aromatic+aliphatic alcohols at different temperatures, Phys. Chem. Liq. 43 (2) (2005) 205–224.
[74] N. Radojković, A. Tasić, D. Grozdanić, B. Djordjević, D. Malić, Excess volumes of acetone + benzene, acetone + cyclohexane, and acetone + benzene + cyclohexane at 298.15 K, J. Chem. Thermodyn. 9 (4) (1977) 349–356.
[75] J. Homer, M.C. Cooke, Molecular complexes. Part 9.—Studies by a phase distribution procedure which employs nuclear magnetic resonance spectroscopy for quantitative measurements, J. Chem. Soc. Faraday Trans. 1: Phys. Chem. Condensed Phases 69 (1973) 1990–1994.
[76] J.P.E. Grolier, G.C. Benson, P. Picker, Enthalpies of mixing of organic liquids measured directly as a function of composition by means of scanning dynamic flow microcalorimetry, J. Chem. Thermodyn. 7 (1) (1975) 89–95.
[77] N.V. Choudary, P.R. Naidu, Sound velocities and isentropic compressibilities of mixtures of 1, 2-dichloroethane with alkanols, Chem. Scr. 19 (2) (1982) 89–92.
[78] G. Dharmaraju, P. Venkateswarlu, G.K. Raman, Ultrasonic studies in binary-liquid mixtures of associated liquids (cyclohexylamine+ alcohol), Chem. Scr. 19 (3) (1982) 140–142.
[79] G.C. Benson, Y.P. Handa, Ultrasonic speeds and isentropic compressibilities for (decan-1-ol + n-alkane) at 298.15 K, J. Chem. Thermodyn. 13 (9) (1981) 887–896.
[80] V.K. Misra, I. Vibhu, R. Singh, M. Gupta, J.P. Shukla, Ultrasonic velocity, viscosity, density and excess properties of binary mixture of dimethyl sulphoxide with propanoic acid and n-butyric acid, J. Mol. Liq. 135 (1) (2007) 166–169.
[81] O. Redlich, A.T. Kister, Algebraic representation of thermodynamic properties and the classification of solutions, Ind. Eng. Chem. 40 (2) (1948) 345–348.

J. Chem. Thermodynamics 172 (2022) 106820

Contents lists available at ScienceDirect

The Journal of Chemical Thermodynamics

journal homepage: www.journals.elsevier.com/the-journal-of-chemical-thermodynamics

A study on mixing properties of binary mixtures of 1-hexene with alkoxyethanols at different temperatures

Djazia Belhadj [a], Amina Negadi [a], Ariel Hernández [b], Ilham Mokbel [c,d], Indra Bahadur [e,*], Latifa Negadi [a,f,*]

[a] LATA2M, Laboratoire de Thermodynamique Appliquée et Modélisation Moléculaire, University of Tlemcen, Post Office Box 119, Tlemcen 13000, Algeria
[b] Departamento de Ingeniería Industrial, Facultad de Ingeniería, Universidad Católica de la Santísima Concepción, Alonso de Ribera 2850, Concepción, Chile
[c] LMI-UMR 5615, Laboratoire Multimatériaux et Interfaces, Université Claude Bernard lyon1, 43 bd du 11 Novembre 1918, Villeurbanne, France
[d] Université Jean Monnet, F-42023 Saint Etienne, France
[e] Department of Chemistry, Faculty of Natural and Agricultural Sciences, North-West University (Mafikeng Campus), Private Bag X2046, Mmabatho 2735, South Africa
[f] Thermodynamics Research Unit, School of Engineering, University of KwaZulu-Natal, Howard College Campus, King George V Avenue, 4041 Durban, South Africa

ARTICLE INFO

Keywords:
1-hexene
Alkoxyethanols
Density
Speed of sound
Refractive index
PC-SAFT EoS

ABSTRACT

Blends of 1-hexene with alkoxyethanols have been studied in terms of intermolecular interactions. The investigated alkoxyethanols were 2-methoxyethanol or 2-ethoxyethanol or 2-butoxyethanol. This study was based on measurements of densities, ρ, speeds of sound, u, and refractive indices, n_D, throughout the full range of composition. With the help of measured data, some derived/excess properties have been computed such as excess molar volume, V_m^E, isentropic compressibility, κ_s, deviation in isentropic compressibility, $\Delta\kappa_s$, and deviation in refractive indices, Δn_D and these properties were fitted to a Redlich−Kister equation. Furthermore, PC-SAFT equation of state (PC-SAFT EoS) were used to correctly modeled the density of pure fluids and mixtures whereas the Nomoto's relation modeled the speed of sound for the binary mixtures with the least deviation, while for the refractive index of all the mixtures, Laplace mixing rule was the best approach..

1. Introduction

Continuation of our research on the thermophysical properties of binary liquids mixtures, this paper reported the new experimental data of densities, ρ, speeds of sound, u, and refractive indices, n_D, for binary systems constituted by 2-methoxyethanol or 2-ethoxyethanol or 2-butoxyethanol with 1-hexene as a common compound at different temperatures. The selected solvent in the present study are important chemicals for industry and have found their used in widespread. Alkenes and alkoxyethanols are more and more used to improve the octane ratings of blended gasolines [1–3]. The presence of the (–O– group) and (–OH group) in the same molecule of alkoxyethanols attribute to the formation of intra- and inter molecular hydrogen bonds between these groups [3–5].

Densities, speeds of sound, and refractive indices properties of 1-hexene and alkoxyethanols binary mixtures provide information about intra and inter molecular interactions that exist between 1-hexene and alkoxyethanols which are then utilized in the development of predictive/correlative models. Above mention properties are also important for engineering applications regarding heat transfer, mass transfer, and fluid flow. Generally, the knowledge of these properties are required in chemical design and chemical process industries, as material is treated in fluid form.

To the best of our knowledge, literature review shows that the mixing properties of (1-hexene + 2-methoxyethanol or 2-ethoxyethanol or 2-butoxyethanol) binary mixtures have not been reported. Therefore, there is a need to carry out these measurements for the above mention mixtures. The obtained results have been utilized to determine excess molar volumes, isentropic compressibility, deviation in isentropic compressibility and deviation in refractive indices and have been fitted to the Redlich–Kister equation [6] to obtain the binary coefficients and standard deviations.

The prediction or correlation of thermodynamic properties (as density, refractive index, speed of sound, among others) and phase equilibria with equations of state (EoSs) remains an important goal in chemical and related industries [7]. One of the best known molecular-

* Corresponding authors at: LATA2M, Laboratoire de Thermodynamique Appliquée et Modélisation Moléculaire, University of Tlemcen, Post Office Box 119, Tlemcen 13000, Algeria (L. Negadi).
E-mail addresses: bahadur.indra@nwu.ac.za (I. Bahadur), latifa.negadi@univ-tlemcen.dz (L. Negadi).

https://doi.org/10.1016/j.jct.2022.106820
Received 20 February 2022; Received in revised form 6 May 2022; Accepted 8 May 2022
Available online 10 May 2022

based equations of state is perturbed chain statistical associating fluid theory (PC-SAFT). This EoS provides a practical and rigorous thermodynamic framework to model thermodynamic properties of many systems [7–9]. According to the literature, few studies have been performed in predicting vapor–liquid equilibria and liquid–liquid equilibria behavior of 2-alkoxyethanol systems [10]. Besides, few investigations related with the applicability of SAFT type equation of state to surfactant mixtures can be found in the literature [11]. In this work, the density of pure fluids and binary mixtures will be modeled with PC-SAFT EoS. On the other hand, the speed of sound for the mixtures will be modeled with the following approaches; Schaaff's collision factor theory (SCFT) [12] and Nomoto's relation (NR) [13], and different mixing rules [14] will be used for modeling the refractive index of the mixtures. Furthermore, the results have been used to describe the nature of intermolecular interactions.

2. Experimental procedure

2.1. Chemicals

The chemicals used in this study are 1-hexene, 2-methoxyethanol, 2-ethoxyethanol and 2-butoxyethanol, they were supplied by Sigma-Aldrich and TCI. The detailed information of the chemicals such as abstracts registry number (CAS number), the stated purity by the suppliers and sources are given in Table 1. Pure liquids and each mixture were degassed by ultrasonic bath (Branson, model 3510E-MTH) just before the experiment. All liquids were used without further purification, their purity was ascertained by comparing experimental values of density, speed of sound and refractive index with those reported in the literature as presented in Table 2.

2.2. Apparatus and procedure

The mixtures of various compositions were prepared just before use by mixing appropriate volumes of the components and weighed in an OHAUS, EX124 US analytical balance with a precision of 0.0001 g. The uncertainty in the mole fractions is 0.0007. An Anton Paar (DSA 5000 M) digital vibrating tube densimeter and a sound velocity analyser with a temperature uncertainty of 0.02 K are used to measure the density ρ and speed of sound u of the pure liquids and their mixtures at (293.15, 298.15 and 303.15) K and at pressure of 0.1 MPa. Anton Paar DSA 5000 M can measure at the same time density in the range of (0 to 3) $\times 10^3$ kg.m^{-3} and speed of sound from (1000 to 2000) m.s^{-1} in a temperature range of (273.15 to 343.15) K with a pressure variation from (0 to 0.3) $\times 10^5$ Pa. The speed of sound u values were measured using a propagation time technique with frequency around 3 MHz [15]. The expanded uncertainty in density ρ and speed of sound u were 0.0008 g.cm^{-3} and 3.03 m.s^{-1}, respectively with a level confidence of 0.95. The calibration for the DSA 5000 M was done with ultrapure water and dry air at T = 293.15 K.

Refractive indices of pure components and their binary mixtures were measured using an Anton Paar Abbemat 300 digital refractometer with an uncertainty of 0.02 K in temperature. The refractive index values were obtained using sodium D-line. The expanded uncertainty in the measured values is 0.0009 with a level confidence of 0.95. The calibration for the Anton Paar Abbemat 300 digital refractometer was done by measuring the refractive index of ultrapure water at T = 293.15 K.

3. Theoretical models

3.1. PC-SAFT EoS

This EoS has an ideal gas contribution (id), a hard-chain contribution (hc), attractive interactions of dispersion forces (disp), and association contribution (assoc), which can be expressed as sum of different parts of Helmholtz energy (A). PC-SAFT EoS is given by Eq. (1) [7,8]:

$$A = A^{id} + A^{hc} + A^{disp} + A^{assoc} \tag{1}$$

where A^{id} can be obtained as Eq. (2):

$$A^{id} = RT\left[\ln(\rho RT) + \sum_{i=1}^{n_c}\frac{\rho_i}{\rho}\ln\left(\frac{\rho_i}{\rho}\right)\right] \tag{2}$$

In the previous equation, R is the universal gas constant, T is the absolute temperature, ρ is the molar density of the mixture, ρ_i is the molar density of component i in the mixture, and n_c is the number of components.

The hard-chain contribution of the Helmholtz energy is described by Eq. (3):

$$A^{hc} = RT\left[\overline{m}A^{hs} - \sum_{i=1}^{n_c}\frac{\rho_i}{\rho}(m_i - 1)\ln(g_{ii}^{hs})\right] \tag{3}$$

where $\overline{m}$ is the average length of the chain, m_i is the effective number of segments, A^{hs} is the hard-sphere contribution of the Helmholtz energy, and g_{ii}^{hs} is the radial distribution function of the hard-sphere.

The average length of the chain and g_{ii}^{hs} can be obtained by Eqs. (4) and (5), respectively:

$$\overline{m} = \sum_{i=1}^{n_c}\frac{\rho_i}{\rho}m_i \tag{4}$$

$$g_{ii}^{hs} = \frac{1}{1-\zeta_3} + \frac{d_i}{2}\frac{3\zeta_2}{(1-\zeta_3)^2} + \frac{d_i^2}{4}\frac{2\zeta_2^2}{(1-\zeta_3)^3} \tag{5}$$

where the temperature-dependent segment diameter (d_i) is given by Eq. (6):

$$d_i = \sigma_i\left[1 - 0.12\exp\left(\frac{-3\varepsilon_i/k_B}{T}\right)\right] \tag{6}$$

where σ_i is the segment diameter and k_B is the Boltzmann constant.

ζ_n is given by Eq. (7):

$$\zeta_n = \frac{\pi}{6}N_A\rho\sum_{i=1}^{n_c}\frac{\rho_i}{\rho}m_i d_i^n, n\in\{0,1,2,3\} \tag{7}$$

with N_A, the Avogadro constant.

The Helmholtz energy of the hard-spheres from Eq. (8):

$$A^{hs} = \frac{1}{\zeta_0}\left[\frac{3\zeta_1\zeta_2}{1-\zeta_3} + \frac{\zeta_2^3}{\zeta_3(1-\zeta_3)^2} + \left(\frac{\zeta_2^3}{\zeta_3^2} - \zeta_0\right)\ln(1-\zeta_3)\right] \tag{8}$$

The dispersion contribution of the Helmholtz energy is expressed by

Table 1
CAS #, molar mass, purities and suppliers of pure liquids used in this study.

Chemical name	CAS #	Molar mass/(g.mole^{-1})	Mass fraction purity (as stated by the supplier	Supplier
1-Hexene	592–41-6	84.16	0.970	Sigma-Aldrich
2-Methoxyethanol	109–86-4	76.09	≥0.995	Sigma-Aldrich
2-Ethoxyethanol	110–80-5	90.12	≥0.990	TCI
2-Butoxyethanol	111–76-2	118.18	≥0.990	TCI

All liquids were used without further purification.

Table 2
Comparison of experimental density, ρ, speed of sound, u, and refractive indices n_D of the pure liquid component with the corresponding literature values at (293.15, 298.15 and 303.15) K and at pressure $p = 0.1$ MPa.

Component	T/(K)	$\rho/(g.cm^{-3})$		$u/(m.s^{-1})$		n_D	
		Exp.	Lit.	Exp.	Lit.	Exp.	Lit.
1-Hexene	293.15	0.6735	0.6733 [21] 0.6732 [22] 0.6732 [23] 0.6728 [24]	1088.81	–	1.3880	1.3899 [22] 1.3879 [23]
	298.15	0.6688	0.6685 [22] 0.66901 [25] 0.66805 [27] 0.6684 [23] 0.6685 [26]	1066.46	1066.06 [25] 1065.8 [26]	1.3852	1.3870 [22] 1.3850 [23] 1.3850 [26]
	303.15	0.6640	–	1044.01	–	1.3824	–
2-Methoxyethanol	293.15	0.9646	0.96488 [28] 0.9647 [16] 0.9646 [20]	1359.64	1358 [20]	1.4023	1.4020 [20]
	298.15	0.9600	0.9597 [29] 0.96029 [28] 0.9603 [17] 0.9602 [16] 0.9601 [30] 0.9603 [31]	1342.49	1339.4 [29] 1340.2 [17] 1340.2 [31]	1.4004	1.4002 [17] 1.40046 [30]
	303.15	0.9554	0.95577 [28] 0.9555 [16] 0.9553 [20] 0.95577 [32]	1325.15	1322 [20] 1332 [32] 1324.41 [33]	1.3984	1.3970 [20]
2-Ethoxyethanol	293.15	0.9294	0.9295 [16] 0.9296 [20]	1319.87	1328 [20] 1321 [34]	1.4080	1.4080 [20] 1.408 [34]
	298.15	0.9249	0.9256 [17] 0.9250 [16] 0.9250 [31] 0.925327 [36] 0.9258 [37]	1302.33	1302.8 [17] 1302.8 [31] 1302.51 [36] 1300 [37]	1.4059	1.4051 [17] 1.4054 [35] 1.4056 [37]
	303.15	0.9204	0.9205 [16] 0.920572 [36] 0.9210 [37]	1284.61	1286 [20] 1284.35 [33] 1286 [34]	1.4039	1.4037 [37] 1.404 [34]
2-Butoxyethanol	293.15	0.9004	0.9004 [16] 0.90119 [38]	1322.98	1323.9 [38]	1.4196	1.4196 [39]
	298.15	0.8962	0.8966 [17] 0.8962 [16] 0.8965 [31] 0.896122 [36]	1306.11	1303.4 [17] 1303.2 [31] 1305.84 [36]	1.4176	1.4176 [17]
	303.15	0.8920	0.8920 [16] 0.892172 [36] 0.89235 [38]	1289.04	1292.44 [33] 1290.6 [38]	1.4156	1.4157 [39]

Standard uncertainties u are $u(T) = 0.02$ K, $u(p) = 0.04$ MPa and the combined expanded uncertainty Uc in mole fraction, density, sound velocity and refractive index were $Uc(x) = 0.0007$, $Uc(\rho) = 0.0008$ g/cm^3, $Uc(u) = 3.03$ m/s and $Uc(n) = 0.0009$, respectively, (0.95 level of confidence).

Eq. (9):

$$A^{disp} = -RT(\pi N_A \rho)\left[2I_1\overline{m^2\varepsilon\sigma^3} + \overline{m}C_1 I_2 \overline{m^2\varepsilon^2\sigma^3}\right] \quad (9)$$

with I_1 and I_2, integrals of the perturbation theory, which can be obtained by Eqs. (10) and (11), respectively:

$$I_1 = \sum_{i=0}^{6} a_i \zeta_3{}^i \quad (10)$$

$$I_2 = \sum_{i=0}^{6} b_i \zeta_3{}^i \quad (11)$$

where a_i and b_i are defined by Eqs. (12) and (13), respectively:

$$a_i = a_{0i} + \frac{\overline{m}-1}{\overline{m}} a_{1i} + \frac{(\overline{m}-1)}{\overline{m}} \frac{(\overline{m}-2)}{\overline{m}} a_{2i} \quad (12)$$

$$b_i = b_{0i} + \frac{\overline{m}-1}{\overline{m}} b_{1i} + \frac{(\overline{m}-1)}{\overline{m}} \frac{(\overline{m}-2)}{\overline{m}} b_{2i} \quad (13)$$

where a_{ki} and b_{ki} for $k = 0, 1, 2$ and $i = 0, \cdots, 6$, are universal constant that are published in the literature [7].

The terms $\overline{m^2\varepsilon\sigma^3}$, $\overline{m^2\varepsilon^2\sigma^3}$, and C_1 parameters are defined by Eqs. (14), (15), and (16), respectively:

$$\overline{m^2\varepsilon\sigma^3} = \sum_{i=1}^{n_c}\sum_{j=1}^{n_c} \frac{\rho_i}{\rho}\frac{\rho_j}{\rho} m_i m_j \frac{\varepsilon_{ij}}{k_B T}\sigma_{ij}{}^3 \quad (14)$$

$$\overline{m^2\varepsilon^2\sigma^3} = \sum_{i=1}^{n_c}\sum_{j=1}^{n_c} \frac{\rho_i}{\rho}\frac{\rho_j}{\rho} m_i m_j \left(\frac{\varepsilon_{ij}}{k_B T}\right)^2 \sigma_{ij}{}^3 \quad (15)$$

$$C_1 = \left[1 + \overline{m}\frac{8\zeta_3 - 2\zeta_3{}^2}{(1-\zeta_3)^4} + (1-\overline{m})\frac{20\zeta_3 - 27\zeta_3{}^2 + 12\zeta_3{}^3 - 2\zeta_3{}^4}{[(1-\zeta_3)(2-\zeta_3)]^2}\right]^{-1} \quad (16)$$

The last term of Eq. (1) is the Helmholtz energy contribution due to the association, which is expressed by Eq. (17):

$$A^{assoc} = \frac{RT}{\rho}\sum_{i=1}^{n_c}\rho_i\left[\sum_{A_i}\left(\ln X^{A_i} - \frac{X^{A_i}}{2}\right) + \frac{M_i}{2}\right] \quad (17)$$

where M_i is the number of association sites on molecule i and X^{A_i} is the fraction of component i that is not bonded at site A_i, which can be obtained by Eq. (18):

$$X^{A_i} = \left(1 + \sum_{j=1}^{n_c}\rho_j\sum_{B_j}X^{B_j}\Delta^{A_iB_j}\right)^{-1} \quad (18)$$

The association strength ($\Delta^{A_iB_j}$) is defined by Eq. (19):

$$\Delta^{A_iB_j} = N_A\sigma_{ij}{}^3\kappa^{A_iB_j}g_{ij}{}^{hs}\left[\exp\left(\frac{\varepsilon^{A_iB_j}}{k_BT}\right) - 1\right] \quad (19)$$

where $\varepsilon^{A_iB_j}$ and $\kappa^{A_iB_j}$ is the cross-association energy and cross-association volume, respectively, and $g_{ij}{}^{hs}$ can be obtained by Eq. (20):

$$g_{ij}{}^{hs} = \frac{1}{1-\zeta_3} + \frac{d_id_j}{d_i+d_j}\frac{3\zeta_2}{(1-\zeta_3)^2} + \left(\frac{d_id_j}{d_i+d_j}\right)^2\frac{2\zeta_2{}^2}{(1-\zeta_3)^3} \quad (20)$$

For each pure fluid, PC-SAFT EoS requires the following parameters: the number of segments (m), the segment diameter (σ), the depth of pair potential energy (ε/k_B), the association energy of interaction (ε^{AB}/k_B), and the effective volume of interaction (κ^{AB}) between site A and B on molecule. When the fluids are non-associating, $\frac{\varepsilon^{AB}}{k_B} = \kappa^{AB} = 0$. In this work, 1-hexene was considered as pure component with no association sites and for the case of 2-alkoxyethanol, Nguyen Huynh et al. [10] proposes to use a 2B scheme, i.e., one site being on the hydrogen and the other site on the oxygen of the hydroxyl groups. Furthermore, the authors state that the participation of -O- group in association might be ignored with respect to –OH group, it means no intramolecular association will be considered.

For the mixtures, the following mixing rules are required:

$$\sigma_{ij} = \frac{1}{2}(\sigma_i + \sigma_j) \quad (21)$$

$$\varepsilon_{ij} = \sqrt{\varepsilon_i\varepsilon_j}(1 - k_{ij}) \quad (22)$$

$$\varepsilon^{A_iB_j} = \frac{1}{2}(\varepsilon^{A_iB_i} + \varepsilon^{A_jB_j}) \quad (23)$$

$$\kappa^{A_iB_j} = \sqrt{\kappa^{A_iB_i}\kappa^{A_jB_j}}\left[\frac{\sqrt{\sigma_i\sigma_j}}{(\sigma_i+\sigma_j)/2}\right]^3 \quad (24)$$

where k_{ij} is the binary interaction parameter.

3.2. Approaches for the speed of sound

In this work, the speed of sound (u) for the binary mixtures can be modeled with Schaaff's collision factor theory (SCFT) [12] and Nomoto's relation (NR) [13].

From SCFT, the speed of sound is given by Eq. (25):

$$u = \rho u_\infty(x_1s_1 + x_2s_2)(x_1B_1 + x_2B_2) \quad (25)$$

where ρ is the molar density of the mixture, which can be obtained from PC-SAFT EoS, $u_\infty = 1600$ m/s, s_i ($i = 1,2$) is the space filling factor of component i in the mixture and can be compute using Eq. (25), experimental speed of sound of the pure fluid, and molar density of the pure fluid obtained with PC-SAFT EoS. x_i ($i = 1,2$) is the liquid mole fraction, and B_i ($i = 1, 2$) is the actual volume of the molecule per mole of component i, which is given by Eq. (26):

$$B_i = N_A m_i\frac{\pi}{6}d_i^3 \quad (26)$$

On the other hand, from NR, the speed of sound is given by Eq. (27):

$$u = \left(\frac{x_1D_1 + x_2D_2}{\frac{x_1}{\rho_1} + \frac{x_2}{\rho_2}}\right)^3 \quad (27)$$

where D_i stand the molar speed of sound and can be obtained by Eq. (28):

$$D_i = \frac{1}{\rho_i}u_i{}^{1/3} \quad (28)$$

Also, ρ_i is the molar density of the pure fluid obtained with PC-SAFT EoS and u_i is the experimental speed of sound of the pure fluid.

It is important to mention that NR is a simpler calculation method than SCFT, because NR does not require density data for the binary mixture.

3.3. Refractive index mixing rules

The refractive index of the binary mixture (n_{DM}) can be predicted [14] by Eq. (29):

$$\left(\frac{1}{\rho}\right)f(n_{DM}) = \left(\frac{w_1}{\rho_1}\right)f(n_{D1}) + \left(\frac{w_2}{\rho_2}\right)f(n_{D2}) \quad (29)$$

where w_1 and w_2 are the weight fraction of 1-hexene and 2-alkoxyethanol, respectively, and $f(n_D)$ is a function of the refractive index. The density of the pure fluids and the binary mixture can be obtained by application of PC-SAFT EoS. The following mixing rules were used; Lorentz-Lorenz (LL), Gladstone-Dale (GD), Laplace (LP), and Eykman (EK). These mixing rules are given by Eqs. ((30)–(33)):

$$LL: f(n_D) = \frac{n_D{}^2 - 1}{n_D{}^2 + 2} \quad (30)$$

$$GD: f(n_D) = n_D - 1 \quad (31)$$

$$LP: f(n_D) = n_D{}^2 - 1 \quad (32)$$

$$EK: f(n_D) = \frac{n_D{}^2 - 1}{n_D + 0.4} \quad (33)$$

4. Results and discussion

4.1. Density, speed of sound and refractive indices

The experimental data of density, speed of sound and refractive indices at temperatures (293.15, 298.15 and 303.15) K and at pressure p = 0.1 MPa for the binary systems (1-hexene + 2-methoxyethanol), (1-hexene + 2-ethoxyethanol) and (1-hexene + 2-butoxyethanol) over the whole composition range are listed as a function of the mole fraction of 1-hexene in Table 3. The influence of temperature and concentration of 1-hexene on density, speed of sound and refractive indices is presented in Figs. S1-S3(a-c). It can be seen from Table 3 that the density values at a specific temperature of pure chemicals in the present work are in the order: 2-methoxyethanol > 2-ethoxyethanol > 2-butoxyethanol > 1-hexene. It is clear from Table 3 that the values of density, speed of sound and refractive indices decrease with an increase in temperature for all binary mixtures. Also, the elevation of concentration leads to a decrease of density, speed of sound and refractive indices values.

4.2. Excess molar volumes

The excess molar volumes $V_m{}^E$ of the binary mixtures has been calculated from the experimental density values of pure liquids and their mixtures by applying the following equation:

Table 3
Densities, ρ, speed of sound, u, isentropic compressibility,κs, and refractive indices, $n_{D,}$ for liquid binary systems (1-hexene (x_1) + 2-methoxyethanol, or 2-ethoxyethanol, or 2-butoxyethanol (x_2) at (293.15, 298.15 and 303.15) K and at pressure $p = 0.1$ MPa.

x_1	$P/(g.cm^{-3})$	$u/(m.s^{-1})$	$\kappa_s/(TPa^{-1})$	n_D
{1-hexene (x_1) + 2-methoxyethanol (x_2)}				
		T = 293.15 K		
0.0000	0.9646	1359.64	561	1.4023
0.1008	0.9209	1298.49	644	1.4004
0.2037	0.8805	1245.87	732	1.3984
0.3016	0.8458	1205.08	814	1.3966
0.4023	0.8134	1171.85	895	1.3948
0.5020	0.7843	1146.55	970	1.3932
0.5995	0.7585	1127.34	1037	1.3918
0.6960	0.7350	1112.70	1099	1.3906
0.7996	0.7119	1100.96	1159	1.3895
0.8980	0.6919	1092.84	1210	1.3885
1.0000	0.6735	1088.81	1253	1.3880
		T = 298.15 K		
0.0000	0.9600	1342.49	578	1.4004
0.1008	0.9162	1281.10	665	1.3983
0.2037	0.8758	1227.58	758	1.3962
0.3016	0.8410	1186.26	845	1.3943
0.4023	0.8086	1152.50	931	1.3924
0.5020	0.7795	1126.96	1010	1.3907
0.5995	0.7537	1106.93	1083	1.3892
0.6960	0.7302	1091.79	1149	1.3879
0.7996	0.7070	1079.51	1214	1.3867
0.8980	0.6870	1070.96	1269	1.3856
1.0000	0.6688	1066.46	1315	1.3852
		T = 303.15 K		
0.0000	0.9554	1325.15	596	1.3984
0.1008	0.9116	1262.89	688	1.3963
0.2037	0.8710	1209.12	785	1.3942
0.3016	0.8362	1167.25	878	1.3922
0.4023	0.8037	1132.96	969	1.3902
0.5020	0.7746	1106.59	1054	1.3883
0.5995	0.7488	1086.35	1132	1.3866
0.6960	0.7252	1070.72	1203	1.3851
0.7996	0.7021	1057.94	1273	1.3838
0.8980	0.6822	1048.95	1332	1.3828
1.0000	0.6640	1044.01	1382	1.3824
{1-hexene (x_1) + 2-ethoxyethanol (x_2)}				
		T = 293.15 K		
0.0000	0.9294	1319.87	617.61	1.4080
0.1018	0.8971	1277.43	683.08	1.4058
0.2034	0.8663	1239.53	751.27	1.4035
0.3022	0.8380	1207.40	818.59	1.4013
0.4038	0.8101	1178.77	888.36	1.3990
0.5018	0.7845	1155.22	955.22	1.3968
0.5989	0.7604	1135.79	1019.42	1.3948
0.6981	0.7369	1119.27	1083.20	1.3928
0.8004	0.7140	1105.67	1145.64	1.3909
0.8970	0.6935	1095.68	1201.04	1.3893
1.0000	0.6735	1088.81	1252.51	1.3880
		T = 298.15 K		
0.0000	0.9249	1302.33	637.46	1.4059
0.1018	0.8925	1259.45	706.33	1.4036
0.2034	0.8617	1221.08	778.32	1.4013
0.3022	0.8333	1188.47	849.64	1.3990
0.4038	0.8054	1159.36	923.77	1.3967
0.5018	0.7797	1135.32	995.07	1.3944
0.5989	0.7556	1115.43	1063.70	1.3922
0.6981	0.7321	1098.40	1132.17	1.3901
0.8004	0.7092	1084.30	1199.36	1.3881
0.8970	0.6887	1073.86	1259.06	1.3864
1.0000	0.6688	1066.46	1314.75	1.3852
		T = 303.15 K		
0.0000	0.9204	1284.61	658.41	1.4039
0.1018	0.8879	1241.27	730.96	1.4014
0.2034	0.8570	1202.44	807.02	1.3990
0.3022	0.8285	1169.36	882.66	1.3965
0.4038	0.8006	1139.77	961.51	1.3940
0.5018	0.7748	1115.27	1037.59	1.3917
0.5989	0.7507	1094.88	1111.15	1.3895
0.6981	0.7272	1077.39	1184.64	1.3873
0.8004	0.7043	1062.81	1256.98	1.3853
0.8970	0.6839	1051.93	1321.40	1.3836
1.0000	0.6640	1044.01	1381.71	1.3824
{1-hexene (x_1) + 2-butoxyethanol (x_2)}				
		T = 293.15 K		
0.0000	0.9004	1322.98	634.55	1.4196
0.1038	0.8788	1293.40	680.18	1.4171
0.2055	0.8571	1264.62	729.58	1.4144
0.3001	0.8364	1238.41	779.57	1.4117
0.4053	0.8130	1210.36	839.64	1.4084
0.5053	0.7902	1184.92	901.29	1.4052
0.6023	0.7678	1161.75	964.98	1.4019
0.7017	0.7445	1139.94	1033.63	1.3985
0.7980	0.7216	1120.85	1103.07	1.3951
0.8977	0.6977	1103.64	1176.66	1.3916
1.0000	0.6735	1088.81	1252.51	1.3880
		T = 298.15 K		
0.0000	0.8962	1306.11	654.08	1.4176
0.1038	0.8746	1276.11	702.13	1.4150
0.2055	0.8527	1246.86	754.31	1.4123
0.3001	0.8320	1220.21	807.23	1.4096
0.4053	0.8085	1191.66	870.98	1.4062
0.5053	0.7857	1165.68	936.65	1.4029
0.6023	0.7632	1142.00	1004.65	1.3995
0.7017	0.7399	1119.63	1078.20	1.3959
0.7980	0.7169	1099.98	1152.84	1.3924
0.8977	0.6930	1082.14	1232.23	1.3888
1.0000	0.6688	1066.46	1314.75	1.3852
		T = 303.15 K		
0.0000	0.8920	1289.04	674.68	1.4156
0.1038	0.8703	1258.64	725.30	1.4130
0.2055	0.8484	1228.93	780.46	1.4102
0.3001	0.8276	1201.85	836.52	1.4072
0.4053	0.8040	1172.79	904.25	1.4038
0.5053	0.7812	1146.30	974.24	1.4004
0.6023	0.7586	1122.12	1046.90	1.3969
0.7017	0.7352	1099.19	1125.81	1.3933
0.7980	0.7122	1078.96	1206.16	1.3897
0.8977	0.6882	1060.51	1291.90	1.3861
1.0000	0.6640	1044.01	1381.71	1.3824

Standard uncertainties u are $u(T) = 0.02$ K, $u(p) = 0.04$ MPa and the combined expanded uncertainty Uc in mole fraction, density, sound velocity and refractive index were $Uc(x) = 0.0007$, $Uc(\rho) = 0.0008$ g/cm^3, $Uc(u) = 3.03$ m/s and $Uc(n) = 0.0009$, respectively, (0.95 level of confidence).

$$V_m^E = \frac{x_1M_1 + x_2M_2}{\rho} - \frac{x_1M_1}{\rho_1} - \frac{x_2M_2}{\rho_2} \quad (34)$$

where x_1 and x_2 are mole fractions, M_1 and M_2 denote molar masses; ρ_1 and ρ_2 are the densities; where 1 refers to 1-hexene and 2 refers to 2-methoxyethanol or 2-ethoxyethanol or 2-butoxyethanol, and ρ is the density of the mixtures.

The calculated data of V_m^E for all the three binary systems at different temperatures are presented in Table S1, and the representative curves are shown in Fig.1(a-c). Both positive and negative V_m^E values are observed for all the studied mixtures at all temperatures. Positive values of V_m^E are due to H-bond breaking while negative are mostly because of weak specific interactions between the mixing components [16,17]. Alkoxyalkanols molecules are self-associated, the presence of

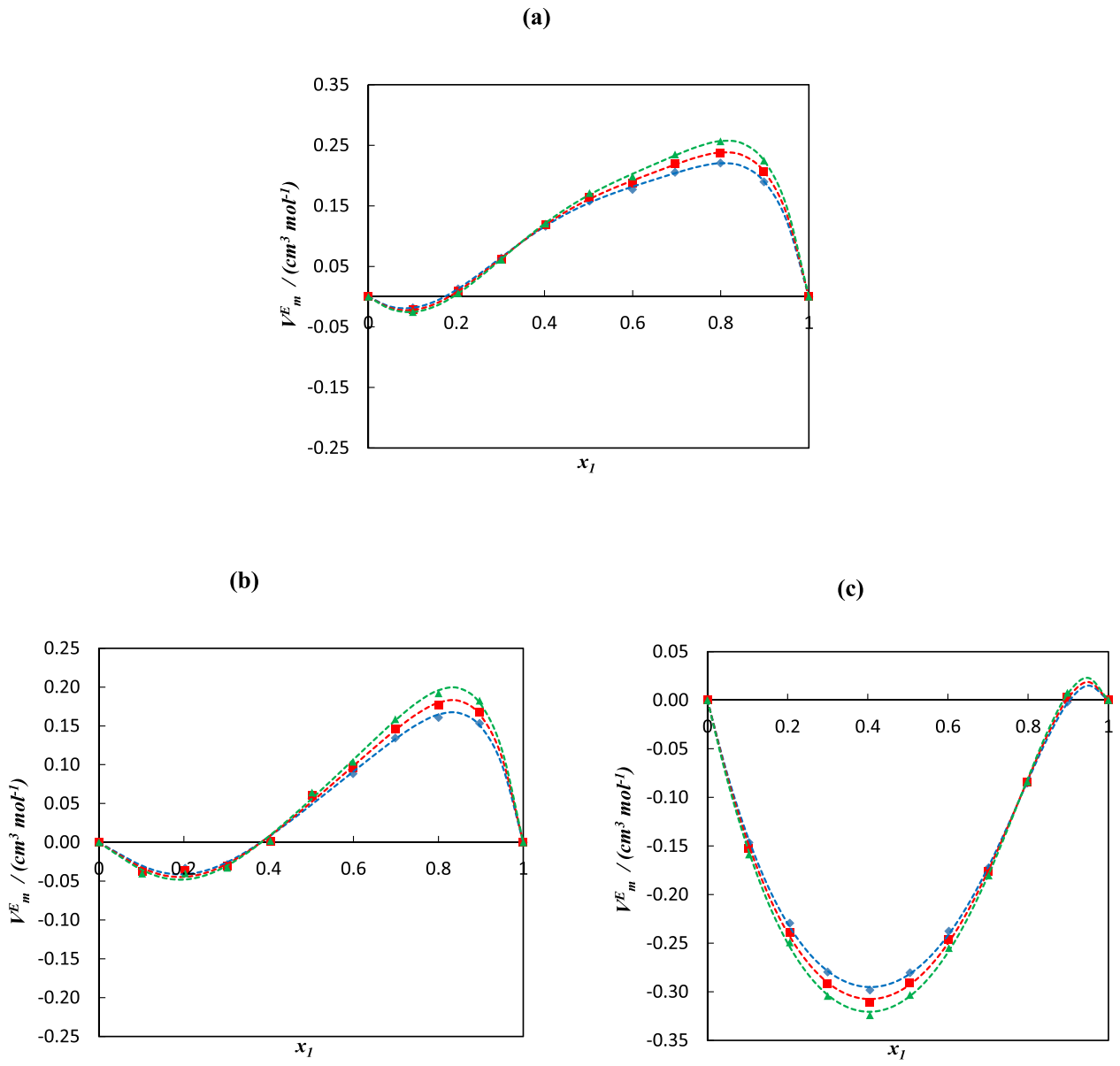

Fig. 1. Plot of excess molar volumes, V^E_m, for the binary mixtures: (a) {1-hexene (x_1) + 2-methoxyethanol (x_2)}, (b) {1-hexene (x_1) + 2-ethoxyethanol (x_2)}, (c) {1-hexene (x_1) + 2-butoxyethanol (x_2)} as function of the composition expressed in the mole fraction of 1-hexene at 293.15 K (◆), 298.15 K (■), and 303.15 K (▲). The dotted lines were generated using Redlich-Kister polynomial curve fitting.

etheric and alcoholic oxygen atoms in the same molecule and the presence of the etheric oxygen lead to hydrogen bonds formation in the alkoxyalkanols molecules [4,5]. For the binary mixtures (1-hexene + 2-methoxyethanol or 2-ethoxyethanol) $V_m{}^E$ values shifted from negative to positive at lower concentration of 1-hexene while the binary mixture (1-hexene + 2-butoxyethanol) shows negative values at the higher concentration of 1-hexene at mole fraction $x_1 = 0.9$ for all temperatures and over the whole range of mole fractions. The negative $V_m{}^E$ values of lower and higher concentration of 1-hexene for (1-hexene + 2-methoxyethanol or 2-ethoxyethanol) and (1-hexene + 2-butoxyethanol) suggest a minimal interaction between alkoxyalkanols with 1-hexene depending on the amount of each constituent is available in the solution. The negative values also because of the formation of the hydrogen bonding between alkoxyalkanols and 1-hexene.

4.3. Isentropic compressibility, and deviation in isentropic compressibility

The isentropic compressibility κ_s is calculated directly from the measured values of u and the ρ using Newton–Laplace equation as

$$\kappa_s = \frac{1}{\rho u^2} \tag{35}$$

While, $\Delta\kappa_s$ was determined by using the following expression:

$$\Delta\kappa_s(x) = \kappa_s - \sum_{i=1}^{2} x_i \kappa_{s,i} \tag{36}$$

where $\kappa_{s,i}$ and x_i are the isentropic compressibility and mole fractions of the pure component i, respectively.

The isentropic compressibility, κ_s, data of the studied binary mixtures at (293.15, 298.15 and 303.15) K are presented in Table 3 and the curves are shown in Fig. S4(a-c). It is noticeable from Table 3 that increasing the temperature from 293.15 to 303.15 K led to the augmentation of κ_s values at a fixed composition for all investigated systems. Additionally, the κ_s values increases with an increase in the concentration of 1-hexene at a fixed temperature for all binary mixtures.

The calculated values of $\Delta\kappa_s$ for the selected binary mixtures at

(293.15, 298.15 and 303.15) K are included in Table S1 and the plots are shown in Fig. 2(a-c). The values of $\Delta\kappa_s$ are all positive for the first and the second binary mixtures (1-hexene + 2-methoxyethanol) and (1-hexene + 2-ethoxyethanol) at all temperatures except at the mole fraction $x_1 = 0.1$ of the second binary mixtures where the $\Delta\kappa_s$ values are negative at 298.15 and 303.15 K. Positive deviation indicates weak interactions between component molecules [18,19]. For the third binary mixture (1-hexene + 2-butoxyethanol), the values of $\Delta\kappa_s$ are all negative at all temperatures which is an indication of specific interactions providing a decrease in the free- space [20].

4.4. Deviation in refractive index

Refractive index deviations Δn_D was determined using the following expression:

$$\Delta n_D = n_{D,M} - x_1 n_{D1} - x_2 n_{D2} \tag{37}$$

where n_{D1} and n_{D2} are the refractive index of pure components and $n_{D,M}$ is the refractive index of the mixtures.

The Δn_D data for the studied systems (1-hexene + 2-methoxyethanol), (1-hexene + 2-ethoxyethanol) and (1-hexene + 2-butoxyethanol) at (293.15, 298.15 and 303.15) K are presented in Table S1 and plotted versus the mole fraction of 1-hexene in Fig. 3(a-c). The values of Δn_D are negative for the binary mixtures (1-hexene + 2-methoxyethanol) and (1-hexene + 2-ethoxyethanol) over the whole range of composition and at all the temperatures. In the case of the binary mixture (1-hexene + 2-butoxyethanol), the results show a positive values throughout the entire composition range and at all the temperatures.

4.5. Correlation of derived properties

For each mixture, the excess or deviation properties (V_m^E, $\Delta\kappa_s$, and Δn_D) were fitted to the Redlich-Kister [6] polynomial equation.

$$X = x_1 x_2 \sum_{i=1}^{k} A_i (1 - 2x_1)^{i-1} \tag{38}$$

where $X = V_m^E$ or $\Delta\kappa_s$ or Δn_D.

A_i are the fitting parameters obtained by least-square method.

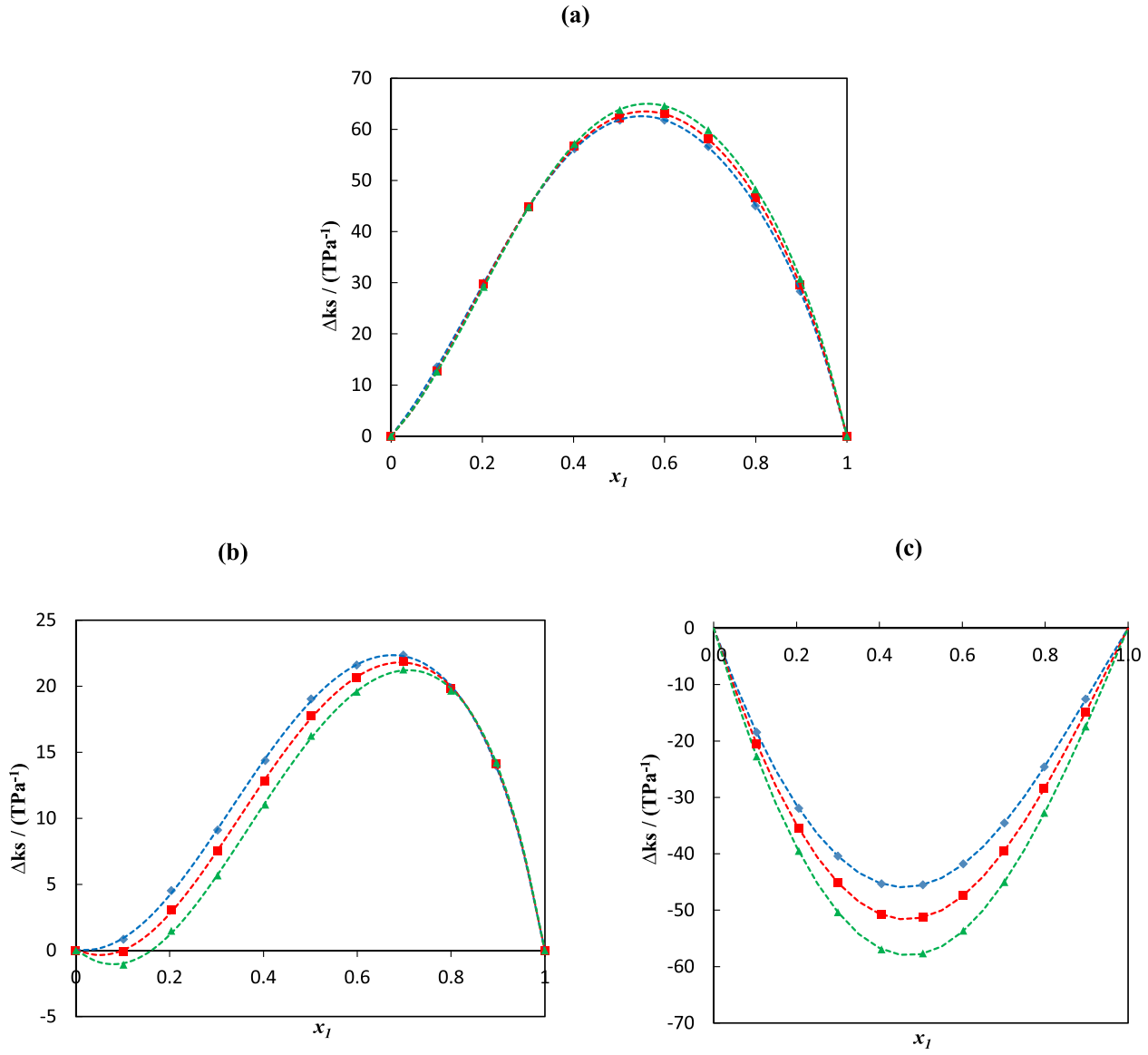

Fig. 2. Plot of deviation in isentropic compressibility, $\Delta\kappa_s$, for the binary mixtures: (a) {1-hexene (x_1) + 2-methoxyethanol (x_2)}, (b) {1-hexene (x_1) + 2-ethoxyethanol (x_2)}, (c) {1-hexene (x_1) + 2-butoxyethanol (x_2)} as function of the composition expressed in the mole fraction of 1hexene at 293.15 K (◆), 298.15 K (■), and 303.15 K (▲). The dotted lines were generated using Redlich-Kister polynomial curve fitting.

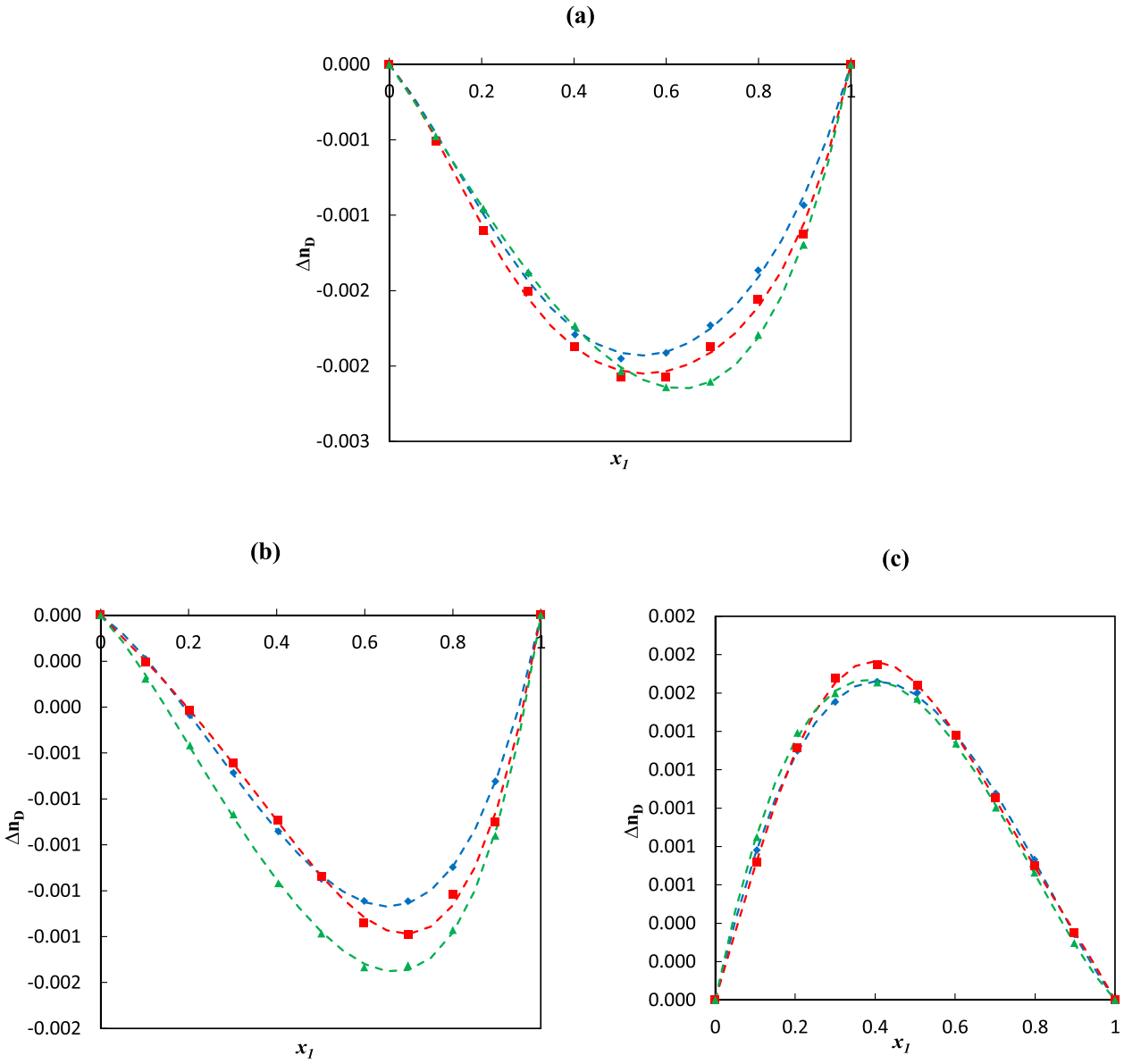

Fig. 3. Plot of deviation in refractive index, Δn_D, for the binary mixtures: (a) {1-hexene (x_1) + 2-methoxyethanol (x_2)}, (b) {1-hexene (x_1) + 2-ethoxyethanol (x_2)}, (c) {1-hexene (x_1) + 2-butoxyethanol (x_2)} as function of the composition expressed in the mole fraction of 1-hexene at 293.15 K (◆), 298.15 K (■), and 303.15 K (▲). The dotted lines were generated using Redlich-Kister polynomial curve fitting.

In each case, the optimum number of coefficients was ascertained from an examination of the variation of standard deviation, σ, with

$$\sigma(X) = \left[\frac{\sum_{i=1}^{N}(X^{exp} - X^{calc})^2}{N-k}\right]^{1/2} \tag{39}$$

where X^{exp} and X^{calc} are the experimental and calculated values of the property X, respectively, and N and k are the number of experimental points and number of coefficients used in the Redlich-Kister equation.

Table 4 records the values of the fitting parameters A_i together with the standard deviation, σ.

The data of ${V_m}^E$, $\Delta\kappa_s$, and Δn_D as well as the graphic representation of the Redlich-Kister model are shown in Figs. 1-3(a-c), respectively.

Finally, it can be concluded that the equations used for interpolating the experimental data measured in this study gave good results, as the σ values for the ${V_m}^E$, $\Delta\kappa_s$, data fitted to the Redlich-Kister polynomial equation were in the range from 0.003 to 0.008, 0.0 to 0.3, respectively and for Δn_D data was 0.000. These results indicate that the fit is quite satisfactory.

4.6. Modeling density with PC-SAFT EoS

All pure-fluid parameters of PC-SAFT EoS have been listed in Table 5. Table 6 indicates the deviations in liquid density for the fluids obtained in the range of 293.15 to 303.15 K. The experimental liquid density has been obtained from the results published in this work. The absolute average deviation for liquid density ($AAD\rho$%) of pure fluid was obtained using Eq. (40):

$$AAD\rho\% = \frac{100}{n}\sum_{i=1}^{n}\frac{|\rho_i^{exp} - \rho_i^{theo}|}{\rho_i^{exp}} \tag{40}$$

where n is the number of experimental points, *exp* and *theo* are experimental and theoretical value, respectively.

From Table 6 it can be seen that PC-SAFT EoS was able of correctly modeling the liquid density of 1-hexene and 2-alkoxyethanols with a deviation of less than 0.463%. The highest deviation was obtained for 1-

Table 4
Coefficients A_i, and standard deviations, σ, obtained for liquid binary systems studied in this work at (293.15, 298.15 and 303.15) K and at pressure $p = 0.1$ MPa for the Redlich–Kister equation.

	T (K)	A_1	A_2	A_3	A_4	A_5	σ
{1-hexene (x_1) + 2-methoxyethanol (x_2)}							
$V_m^E/(cm^3\ mol^{-1})$	293.15	0.618	0.638	0.012	1.254	0.784	0.003
	298.15	0.642	0.717	0.038	1.348	0.859	0.003
	303.15	0.670	0.802	0.049	1.445	0.971	0.003
$\Delta\kappa_s/(\mathrm{TPa}^{-1})$	293.15	247.4	58.6	−54.0	64.6	39.2	0.1
	298.15	250.2	66.4	−44.1	72.3	21.4	0.3
	303.15	255.2	76.9	−56.4	72.4	43.7	0.1
Δn_D	293.15	−0.008	−0.002	0.001	−0.002	–	0.000
	298.15	−0.008	−0.002	−0.001	−0.004	–	0.000
	303.15	−0.008	−0.004	−0.002	−0.001	–	0.000
{1-hexene (x_1) + 2-ethoxyethanol (x_2)}							
$V_m^E/(cm^3\ mol^{-1})$	293.15	0.192	0.854	0.283	0.603	0.704	0.007
	298.15	0.206	0.926	0.331	0.675	0.751	0.008
	303.15	0.221	1.003	0.380	0.740	0.799	0.008
$\Delta\kappa_s/(\mathrm{TPa}^{-1})$	293.15	75.2	75.4	−8.2	19.8	25.8	0.2
	298.15	70.0	81.9	−6.6	21.1	25.9	0.2
	303.15	64.0	89.3	−5.1	21.5	26.4	0.2
Δn_D	293.15	−0.005	−0.003	−0.001	−0.001	–	0.000
	298.15	−0.005	−0.004	−0.002	0.000	–	0.000
	303.15	−0.006	−0.004	−0.002	−0.001	–	0.000
{1-hexene (x_1) + 2-butoxyethanol (x_2)}							
$V_m^E/(cm^3\ mol^{-1})$	293.15	−1.132	0.527	0.308	0.672	0.358	0.003
	298.15	−1.177	0.568	0.349	0.716	0.387	0.004
	303.15	−1.225	0.606	0.385	0.777	0.433	0.004
$\Delta\kappa_s/(\mathrm{TPa}^{-1})$	293.15	−182.5	33.1	22.7	8.8	–	0.0
	298.15	−205.5	31.8	22.7	7.3	–	0.1
	303.15	−231.2	30.0	22.9	6.8	–	0.1
Δn_D	293.15	0.006	−0.003	0.000	0.000	–	0.000
	298.15	0.007	−0.004	−0.001	0.002	–	0.000
	303.15	0.006	−0.003	0.000	−0.001	–	0.000

Standard uncertainties u are $u(T) = 0.02$ K, $u(p) = 0.04$ MPa and the combined expanded uncertainty Uc in mole fraction, density, sound velocity and refractive index were $Uc(x) = 0.0007$, $Uc(\rho) = 0.0008$ g/cm^3, $Uc(\mathrm{u}) = 3.03$ m/s and $Uc(n) = 0.0009$, respectively, (0.95 level of confidence).

Table 5
PC-SAFT EoS parameters for the liquids considered in this work.

Fluid	m	σ/(Å)	ε/k_B/(K)	ε^{AB}/k_B/(K)	κ^{AB}	Ref.
1-hexene	2.98530	3.77530	236.81000	-	-	[7]
2-methoxyethanol	2.98978	3.28153	212.80925	2245.71	0.15184	[10]
2-ethoxyethanol	3.18626	3.48657	248.08295	1685.00	0.10455	[10]
2-butoxyethanol	4.62892	3.38648	249.99083	1183.37	0.01865	[10]

Table 6
Statistical deviation of the density for the pure liquids using PC-SAFT EoS and experimental density data obtained in this work.

Fluid	$AAD\rho$%
1-hexene	0.463
2-methoxyethanol	0.075
2-ethoxyethanol	0.255
2-butoxyethanol	0.100

hexene (0.463 %) and the lowest deviation was obtained for 2-methoxyethanol (0.075 %). Therefore, the presence of two sites on each 2-alkoxyethanol molecule correctly models the association due the interactions of hydrogen bonding between the oxygen atom and the hydrogen atom.

In this work, the PC-SAFT EoS was used to describe the liquid density at 293.15 K, 298.15 K, and 303.15 K of the following mixtures; 1-hexene + 2-methoxyethanol, 1-hexene + 2-ethoxyethanol, and 1-hexene + 2-butoxyethanol. The only parameter of PC-SAFT that needs to be adjusted for binary mixtures is the binary interaction parameter, which were determined by minimizing the objective function given by Eq. (41):

$$FO = \sum_{i=1}^{n} \left(\frac{\rho_i^{exp} - \rho_i^{theo}}{\rho_i^{exp}} \right)^2 \tag{41}$$

where ρ_i^{exp} is the experimental density information of the mixture published in this work, and ρ_i^{theo} is the density value of the mixture obtained from PC-SAFT EoS. The binary interaction parameters obtained were 0, −0.028, and −0.016 for the 1-hexene + 2-methoxyethanol, 1-hexene + 2-ethoxyethanol, and 1-hexene + 2-butoxyethanol mixtures, respectively. It can be seen that the binary parameter is a constant value for the studied temperature range. Therefore, PC-SAFT EoS could be used predictively for these mixtures and using other temperatures. Besides, according to our results, PC-SAFT EoS does not require non-zero k_{ij} to model the density of the 1-hexene + 2-methoxyethanol (see Table 7), i.e., it can be used predictively for all the range of temperature.

From Table 7, it is observed that PC-SAFT EoS correctly models the liquid density of the mixtures with the binary interaction parameters obtained in this work. The highest average $AAD\rho$% was obtained for 1-hexene + 2-ethoxyethanol mixture (0.427%) and the lowest average

Table 7
Statistical deviation for the density of the liquid mixtures using PC-SAFT EoS and different mixing rules.

Mixture	T / (K)	$AAD\rho$%
1-hexene + 2-methoxyethanol	293.15	0.393
	298.15	0.383
	303.15	0.373
	Average	0.383
1-hexene + 2-ethoxyethanol	293.15	0.428
	298.15	0.426
	303.15	0.426
	Average	0.427
1-hexene + 2-butoxyethanol	293.15	0.411
	298.15	0.382
	303.15	0.354
	Average	0.382

$AAD\rho$% was obtained for 1-hexene + 2-butoxyethanol mixture (0.382%). Fig. 4 (a-c) show that the theoretical approach used correctly models the variation of the density of the mixtures with the liquid molar fraction of 1-hexene. The correct representation of the self-association of the alkoxyethanol molecules and the non-cross-association with the 1-hexene molecules is able to achieve good results in density modeling with PC-SAFT EoS.

4.7. Modeling the speed of sound

SCFT and NR approaches were compared in modeling the speed of sound for the binary mixtures. The absolute average deviation for speed of sound ($AADu$%) of the mixtures was obtained using Eq. (42):

$$AADu\% = \frac{100}{n}\sum_{i=1}^{n}\frac{|u_i^{exp} - u_i^{theo}|}{u_i^{exp}} \quad (42)$$

The deviations with both models are published in Table 8 and it can be seen that NR best models the speed of sound for all the mixtures. The lowest average $AADu$% is reached for the 1-hexene + 2-butoxyethanol

Table 8
Statistical deviation for the speed of sound for liquid mixtures using SCFT and NR.

Mixture	T/(K)	$AADu$%	
		SCFT	NR
1-hexene (x_1) + 2-methoxyethanol (x_2)	293.15	4.027	2.131
	298.15	4.086	2.118
	303.15	4.159	2.115
	Average	4.091	2.121
1-hexene (x_1) + 2-ethoxyethanol (x_2)	293.15	2.802	1.554
	298.15	2.838	1.543
	303.15	2.876	1.533
	Average	2.839	1.543
1-hexene (x_1) + 2-butoxyethanol (x_2)	293.15	1.486	0.909
	298.15	1.489	0.886
	303.15	1.493	0.861
	Average	1.489	0.885

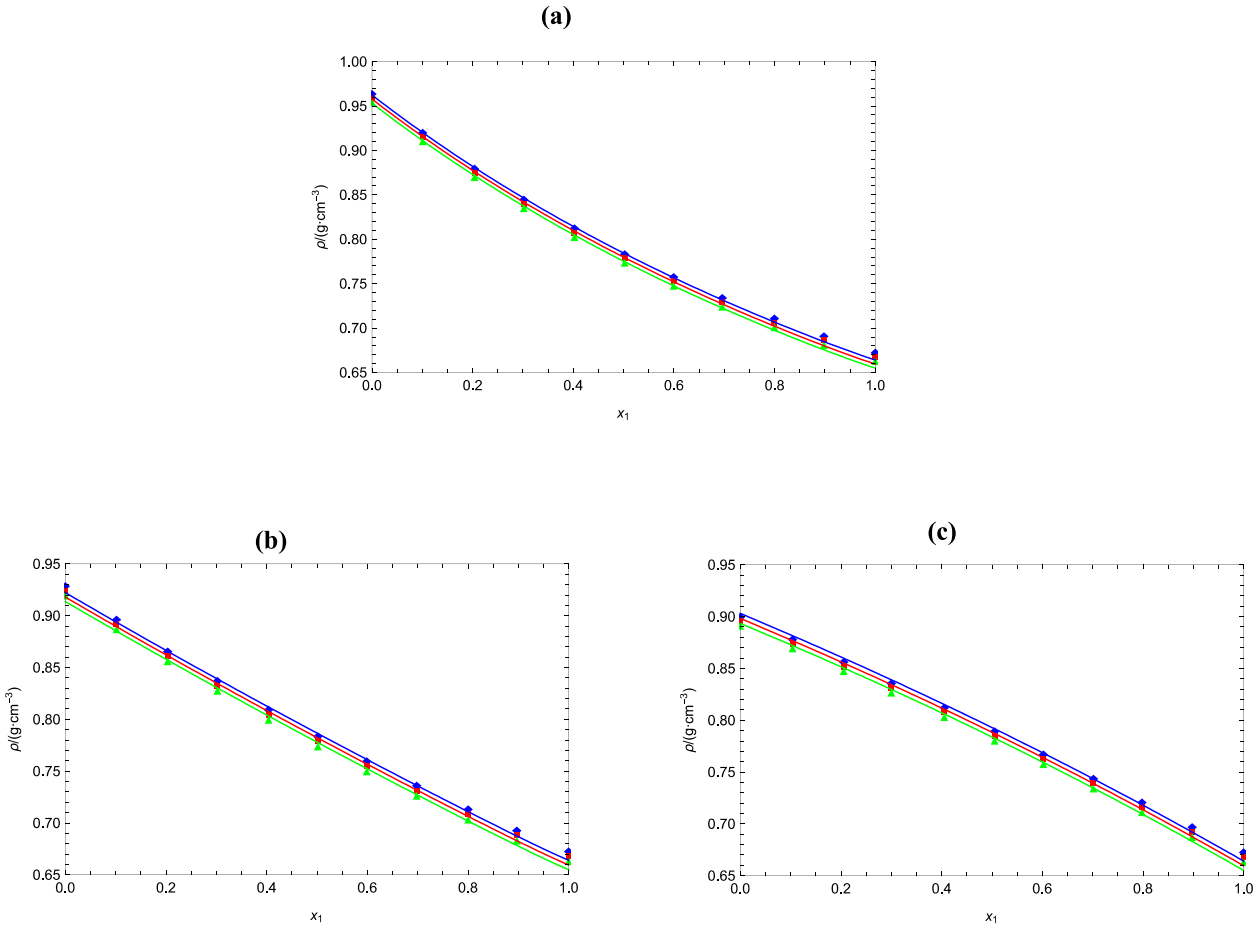

Fig. 4. Comparison between experimental and calculated density using PC-SAFT for the binary mixtures: (a) {1-hexene (x_1) + 2-methoxyethanol (x_2)}, (b) {1-hexene (x_1) + 2-ethoxyethanol (x_2)}, (c) {1-hexene (x_1) + 2-butoxyethanol (x_2)} as function of the composition expressed in the mole fraction of 1-hexene at 293.15 K (◆), 298.15 K (■), and 303.15 K (▲). The straight lines represent the calculated density values using PC-SAFT.

(0.885 %) using NR and the highest average *AADu*% is reached for the 1-hexene + 2-methoxyethanol (4.091 %) using SCFT. A simple equation like NR approach better represents the speed of sound behavior. This can be explained because the assumptions of linearity in the molar speed of sound and in the molar volume are close to the results obtained experimentally. As NR was the best approach for modeling the speed of sound, Fig. 5(a-c) show the behavior obtained. According to these figures, it is observed that NR over predicts the speed of sound for all the mixtures and the two best predictions are for the 1-hexene + 2-ethoxyethanol and 1-hexene + 2-butoxyethanol mixtures; this can be explained by an approximately linear density dependence for these mixtures (see Fig. 4b and c).

4.8. Modeling refractive indices

As described in the theoretical section, four mixing rules together with the density results obtained with PC-SAFT EoS, were used to model the refractive index of the mixtures.

The absolute average deviation for refractive index ($AADn_D$%) of the mixtures was obtained using Eq. (43):

$$AADn_D\% = \frac{100}{n}\sum_{i=1}^{n}\frac{\left|{n_{D,i}}^{exp} - {n_{D,i}}^{theo}\right|}{{n_{D,i}}^{exp}} \tag{43}$$

Table 9 shows the deviations obtained in the refractive index of the mixtures and can be observed that the theoretical calculations with different mixing rules are good agree with the experimental information published in this work, however, the best mixing rule was Laplace (LP) with deviations less than 0.198%. The best modeling was for the 1-hexene + 2-butoxyethanol mixture (average $AADn_D = 0.093\%$). Fig. 6 (a-c) illustrate the experimental data and theoretical behavior of the refractive index obtained with Laplace mixing rule, because was the best model (see Table 9). From these figures, it is seen that LP over predicts the refractive index for all mixtures. Therefore, the low deviation obtained does not correctly represent what is observed in Fig. 6(a-c), because a low deviation is also attributed to the fact that the refractive index range between the components of the mixture is very small. On the other hand, the study of some adjustment parameter in Eq. (29) or a new mixing rule could perhaps improve the results obtained.

Table 9
Statistical for the refractive index of the liquid mixtures using PC-SAFT EoS and different mixing rules.

Mixture	T/(K)	$AADn_D$%			
		LL	GD	LP	EK
1-hexene (x_1) + 2-methoxyethanol (x_2)	293.15	0.146	0.131	0.115	0.138
	298.15	0.152	0.137	0.120	0.144
	303.15	0.151	0.135	0.118	0.142
	Average	0.150	0.134	0.118	0.141
1-hexene (x_1) + 2-ethoxyethanol (x_2)	293.15	0.240	0.213	0.183	0.225
	298.15	0.245	0.217	0.187	0.230
	303.15	0.256	0.228	0.198	0.241
	Average	0.247	0.219	0.189	0.232
1-hexene (x_1) + 2-butoxyethanol (x_2)	293.15	0.126	0.108	0.088	0.117
	298.15	0.131	0.112	0.092	0.121
	303.15	0.138	0.119	0.098	0.128
	Average	0.142	0.113	0.093	0.122

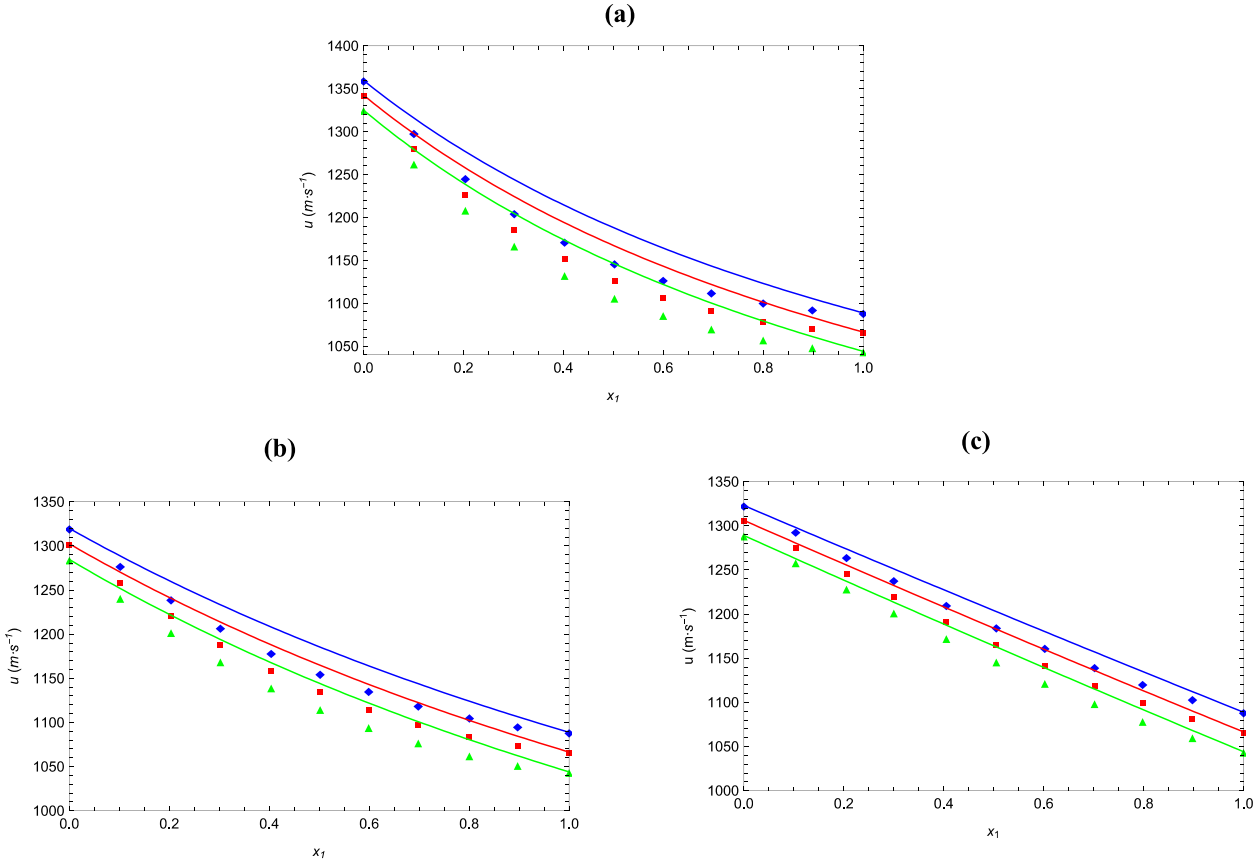

Fig. 5. Comparison between experimental and calculated speeds of sound using Nomoto's relation for the binary mixtures: (a) {1-hexene (x_1) + 2-methoxyethanol (x_2)}, (b) {1-hexene (x_1) + 2-ethoxyethanol (x_2)}, (c) {1-hexene (x_1) + 2-butoxyethanol (x_2)} as function of the composition expressed in the mole fraction of 1-hexene at 293.15 K (◆), 298.15 K (■), and 303.15 K (▲). The straight lines represent the calculated speeds of sound values using Nomoto's relation.

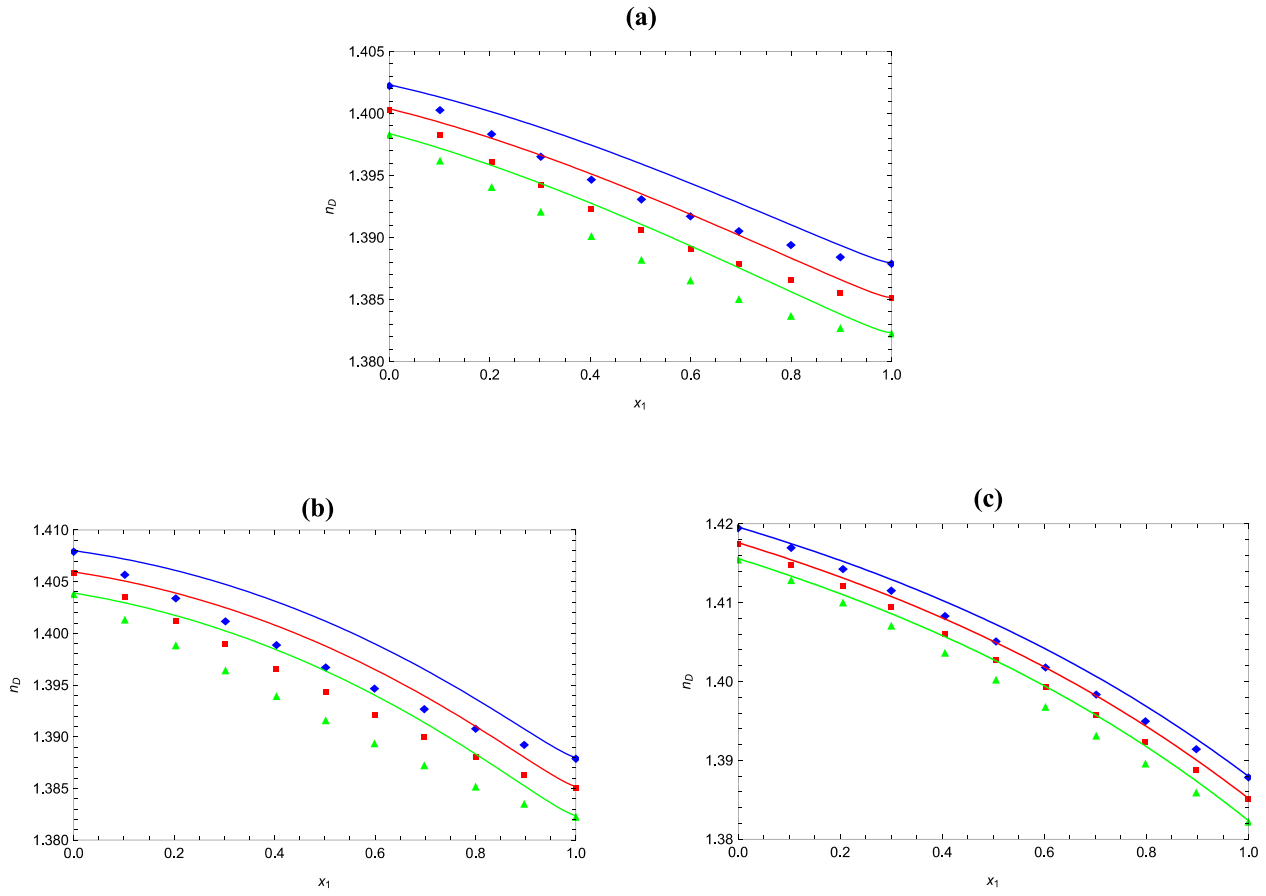

Fig. 6. Comparison between experimental and calculated refractive indices using Laplace mixing rule for the binary mixtures: (a) {1-hexene (x_1) + 2-methoxyethanol (x_2)}, (b) {1-hexene (x_1) + 2-ethoxyethanol (x_2)}, (c) {1-hexene (x_1) + 2-butoxyethanol (x_2)} as function of the composition expressed in the mole fraction of 1-hexene at 293.15 K (◆), 298.15 K (■), and 303.15 K (▲). The straight lines represent the calculated refractive indices values using Laplace mixing rule.

5. Conclusion

The present study reports new measured data of density, speed of sound and refractive index over the entire composition range at (293.15, 298.15 and 303.15) K and at pressure p = 0.1 MPa for three binary mixtures composed by 1-hexene with 2-methoxyethanol or 2-ethoxyethanol or 2-butoxyethanol. Deviation parameters including excess molar volumes, isentropic compressibility, deviation in isentropic compressibility and deviation in refractive indices have been also computed and correlated by a Redlich–Kister type polynomial equation to derive the coefficients and standard deviation. The agreement between the experimental data and those calculated using the Redlich−Kister equation was satisfactory at the investigated temperatures for all the binary systems. PC-SAFT EoS was used as a theoretical approach to model the density of pure fluids and mixtures with an average deviation of 0.223% considering all fluids and an average deviation of 0.397 % considering all the mixtures. From our work it is concluded that PC-SAFT EoS can be used predictively in these binary mixtures studied, using $k_{ij} = 0$ for the 1-hexene + 2-methoxyethanol mixture at any temperature, and using the binary interaction parameter published in this work for the other two mixtures for other temperatures (different from those used in this work). The advantage of using an equation of state model is that the density results were used in the speed of sound and the refractive index calculations. Besides, an approximately linear dependence for the density of the 1-hexene + 2-ethoxyethanol and 1-hexene + 2-butoxyethanol mixtures allowed the best speed of sound results with NR. Finally, of the different mixing rules for the refractive index, with LP mixing rule the smallest average deviation was obtained (0.133 % considering all the mixtures).

Declaration of Competing Interest

The authors declare that they have no known competing financial interests or personal relationships that could have appeared to influence the work reported in this paper.

Acknowledgements

L.N. and A.N. acknowledge funding from DGRSDT (Algeria).

The present work has been done in the framework of the Algerian-French bilateral project Tassili (Ref. 21MDU318).

Appendix A. Supplementary data

Supplementary data to this article can be found online at https://doi.org/10.1016/j.jct.2022.106820.

References

[1] Z. Wang, G.C. Benson, B.C.Y. Lu, J. Chem. Eng. Data 49 (2) (2004) 311–312.
[2] R.P. Csikos, I. Laky, J. Hydrocarbon Process. 55 (1976) 121–125.
[3] D. Belhadj, I. Bahadur, A. Negadi, N. Muñoz-Rujas, E. Montero, L. Negadi, J. Chem. Eng. Data 65 (11) (2020) 5192–5209.
[4] B.G. Barbés, I. González, J.A. Cobos, J.C. Casanova, J. Chem. Thermodyn. 26 (8) (1994) 791–795.
[5] P.B.M. Buckley, Canadian J. Chem. 50 (8) (1972) 1149–1156.
[6] O. Redlich, A.T. Kister, Ind. Eng. Chem. 40 (2) (1948) 345–348.
[7] J. Gross, G. Sadowski, Ind. Eng. Chem. Res. 40 (4) (2001) 1244–1260.
[8] J. Gross, G. Sadowski, Ind. Eng. Chem. Res. 41 (22) (2002) 5510–5515.
[9] R. Tahery, A. Hernández, J. Chem. Thermodyn. (2022), 106723.
[10] D. NguyenHuynh, T.T. Nguyen, T.T.X. Nguyen, Fluid Phase Equilib. 7 (20) (2017) 434.

[11] N.M. Garrido, G.K. Folas, G.M. Kontogeorgis, Fluid Phase Equilib. 273 (1–2) (2008) 11–20.
[12] W. Schaaffs, Acta Acustica United with Acustica 33 (4) (1975) 272–276.
[13] O. Nomoto, J. Phys. Soc. Japan 13 (12) (1958) 1528–1532.
[14] B. Giner, C. Lafuente, A. Villares, M. Haro, M.C. Lopez, J. Chem. Thermodyn. 39 (1) (2007) 148–157.
[15] M.T. Zafarani-Moattar, H. Shekaari, J. Chem. Thermodyn. 37 (10) (2005) 1029–1035.
[16] X. Shi, C. Li, H. Guo, S. Shen, J. Chem. Eng. Data 64 (9) (2019) 3960–3970.
[17] L. Sarkar, M.N. Roy, J. Chem. Eng. Data 54 (12) (2009) 3307–3312.
[18] B. Thanuja, G.N ithya, C.C. Kanagam, Ultrasonics Sonochemistry. 19(6) (2012) 1213-1220.
[19] D. Belhadj, A. Negadi, P. Venkatesu, I. Bahadur, L. Negadi, J. Mol. Liq. 330 (2021), 115436.
[20] R. Singh, M. Yasmin, H. Agarwal, V.K. Shukla, M. Gupta, J.P. Shukla, Phys. Chem. Liq. 51 (5) (2013) 606–620.
[21] D. Vega-Maza, M.C. Martín, J.M. Trusler, J.J. Segovia, J. Chem. Thermodyn. 57 (2013) 550–557.
[22] R.K. Burkat, A.J. Richard, J. Chem. Thermodyn. 7 (3) (1975) 271–277.
[23] T.W. Mears, A. Fookson, P. Pomerantz, E.H. Rich, C.S. Dussinger, F.L. Howard, J. Res. Natl. Bur. Stand. 44 (3) (1950) 299–304.
[24] G.A. Torín-Ollarves, J.J. Segovia, M.C. Martín, M.A. Villamañán, J. Chem. Eng. Data 58 (10) (2013) 2717–2723.
[25] G. Tardajos, M. Diaz Pena, A. Lainez, E. Aicart, J. Chem. Eng. Data 31 (4) (1986) 492–493.
[26] M. Lifi, J. Lorenzo, F. Aguilar, N. Muñoz-Rujas, E.A. Montero, Y. Chhiti, F.E.M. H. Alaoui, J. Chem. Thermodyn. 153 (2021), 106306.
[27] E. Aicart, E. Junquera, T.M. Letcher, J. Chem. Eng. Data 40 (6) (1995) 1225–1227.
[28] C.M. Kinart, M. Klimczak, A. Ćwiklińska, W.J. Kinart, J. Mol. Liq. 135 (1–3) (2007) 192–195.
[29] M.N. Roy, B.K. Sarkar, R. Chanda, J. Chem. Eng. Data 52 (5) (2007) 1630–1637.
[30] L. Albuquerque, C. Ventura, R. Gonçalves, J. Chem. Eng. Data 41 (4) (1996) 685–688.
[31] M.N. Roy, B. Sinha, V.K. Dakua, J. Mol. Liq. 136 (1–2) (2007) 128–137.
[32] K.M. Krishna, K. Rambabu, P. Venkateswarlu, G.K. Raman, J. Chem. Eng. Data 40 (1) (1995) 132–135.
[33] C.M. Kinart, J. Mol. Liq. 186 (2013) 28–32.
[34] N.L. Benkelfat-Seladji, F. Ouaar, A. Hernández, I. Bahadur, N. Muñoz-Rujas, S. K. Singh, E. Montero, N. Chiali-Baba Ahmed, L. Negadi, J. Chem. Thermodyn. (2022) (106762).
[35] T.M. Aminabhavi, B. Gopalakrishna, J. Chem. Eng. Data 40 (3) (1995) 632–641.
[36] K. Tamura, A. Osaki, S. Murakami, B. Laurent, J.P.E. Grolier, Fluid Phase Equilib. 173 (2) (2000) 285–296.
[37] M.I. Aralaguppi, C.V. Jadar, T.M. Aminabhavi, J. Chem. Eng. Data 41 (6) (1996) 1307–1310.
[38] A. Ćwiklińska, C.M. Kinart, J. Chem. Thermodyn. 43 (3) (2011) 420–429.
[39] D.R. Chiou, S.Y. Chen, L.J. Chen, J. Chem. Eng. Data 55 (2) (2010) 1012–1016.

Abstract

The present thesis is part of a general program of research concerning the thermophysical and thermodynamic properties of binary mixtures containing molecules of industrial and environmental interest.

The first part presents the experimental results of densities, speeds of sound and refractive indices measurements of twelve (12) binary mixtures at different temperatures and at pressure of 0.1 MPa. The measured data has been utilized to compute isentropic compressibility, intermolecular free length, specific acoustic impedance, relative association, relaxation strength and Rao's molar sound function. The excess/deviation properties such as excess molar volume, deviations in isentropic compressibility, deviations in intermolecular free length, deviations in acoustic impedance, deviations in speed of sound and deviation of refractive index were also calculated for all studied mixtures under the same experimental conditions. The correlation of excess properties was made by help of the Redlich-Kister polynomial equation.

The second part contains vapor-liquid equilibrium data of three binary mixtures measured by means of a static apparatus at several temperatures. The obtained results were correlated with the Antoine equation. From these data, the excess Gibbs function and the vapor phase composition were evaluated using the Barker's method. The activity coefficients of the components in binary mixtures were also estimated. Additionally, the experimental data were correlated by using three activity coefficient models NRTL, UNIQUAC and Modified UNIFAC (Dortmund).

Keywords: Thermophysical properties, Derived/Excess properties, Redlich-Kister polynomial equation, Vapor-liquid equilibrium, NRTL, UNIQUAC and Modified UNIFAC (Dortmund).

Résumé

La présente thèse rentre dans un programme général de recherche concernant les propriétés thermophysiques et thermodynamiques des mélanges binaires contenant des molécules d'intérêt industriel et environnemental.

La première partie présente les résultats expérimentaux des mesures de densité, de vitesse du son et d'indice de réfraction de douze (12) mélanges binaires à différentes températures et à une pression de 0,1 MPa. Les résultats obtenus ont été utilisés pour calculer le facteur de compressibilité isentropique, la longueur intermoléculaire, l'impédance acoustique, l'association relative, la force de relaxation et la fonction du son de Rao's. Les propriétés d'excès telles que le volume molaire d'excès, la déviation de la compressibilité isentropique, la déviation de la longueur intermoléculaire, la déviation de l'impédance acoustique, la déviation de la vitesse du son et la déviation de l'indice de réfraction ont été calculées également pour tous les mélanges étudiés dans les mêmes conditions expérimentales. L'équation polynomiale de Redlich-Kister a été utilisée pour la corrélation des grandeurs d'excès.

La deuxième partie contient les résultats d'équilibre liquide-vapeur de trois mélanges binaires mesurés à plusieurs températures à l'aide d'un appareil statique. Les résultats

obtenus ont été ajustés en utilisant l'équation d'Antoine. A partir de ces données, L'enthalpie libre d'excès ainsi que la fraction molaire de la phase vapeur ont été déterminées par la méthode de Barker. Les coefficients d'activité des composants dans les mélanges binaires ont été également estimés. Les données expérimentales obtenues ont été corrélées à l'aide de trois modèles de coefficients d'activité NRTL, UNIQUAC et Modified UNIFAC (Dortmund).

Mots clés : Propriétés thermophysiques, Propriétés dérivées/d'excès, Equation polynomiale de Redlich-Kister, Equilibre liquide-vapeur, NRTL, UNIQUAC et UNIFAC modifiée (Dortmund).

ملخص

الاطروحة الحالية هي جزء من برنامج عام للبحث المتعلق بالخصائص الفيزيائية الحرارية والديناميكية الحرارية للمخاليط الثنائية التي تحتوي على جزيئات ذات أهمية صناعية وبيئية.

يعرض الجزء الأول النتائج التجريبية لقياسات الكثافة وسرعات الصوت ومعاملات الانكسار لاثني عشر (12) مزيجًا ثنائيًا عند درجات حرارة مختلفة وضغط 0.1 ميجا باسكال. تم استخدام البيانات المقاسة لحساب الانضغاط المتساوي، والطول الحر بين الجزيئات، والمقاومة الصوتية المحددة، والارتباط النسبي، وقوة الاسترخاء، ووظيفة الصوت المولي لراو. تم حساب الخصائص الزائدة / الانحراف مثل الحجم المولي الزائد، الانحراف في الانضغاط المتساوي، الانحراف في الطول الحر بين الجزيئات، الانحراف في المقاومة الصوتية، الانحراف في سرعة الصوت وانحراف معامل الانكسار لجميع المخاليط المدروسة تحت نفس الظروف التجريبية. تم الربط بين الخصائص الزائدة بمساعدة معادلة ريدليش-كيستار متعددة الحدود.

يحتوي الجزء الثاني على نتائج توازنات سائل-بخار لثلاثة مخاليط ثنائية مقاسة بواسطة جهاز ثابت عند درجات حرارة متعددة. تم ضبط النتائج المتحصل عليها باستعمال معادلة انطوان. من هذه البيانات، تم حساب الطاقة الزائدة لجيبس بالإضافة إلى الجزء المولي للطور المتبخر باستخدام طريقة باركر.
كما تم تقدير معاملات النشاط للمكونات في الخلائط الثنائية. بالإضافة إلى ذلك، تم ربط البيانات التجريبية باستخدام ثلاثة نماذج معامل النشاط NRTL، UNIQUAC و UNIFAC المعدلة (دورتموند).

الكلمات المفتاحية: الخواص الفيزيائية الحرارية، الخواص المشتقة / الزائدة، معادلة ريدليش-كيستار متعددة الحدود، توازنات سائل-بخار، NRTL، UNIQUAC، UNIFAC المعدلة (دورتموند).